SJC

British Journal of Pharmacology

July 1991

Volume 103 Number 3 pages 1621–1834

Br. J. Pharmacol. (1991), **103**, 1623–1625

SPECIAL REPORT

© Macmillan Press Ltd, 1991

Ketamine potentiates 5-HT_3 receptor-mediated currents in rabbit nodose ganglion neurones

John A. Peters, Hilary M. Malone & [1]Jeremy J. Lambert

Neuroscience Research Group, Department of Pharmacology & Clinical Pharmacology, Ninewells Hospital & Medical School, University of Dundee, Dundee, DD1 9SY

The interaction of ketamine with the 5-HT_3 receptor of rabbit nodose ganglion neurones is described. Ketamine (3–30 μM) enhanced 5-HT_3 receptor-mediated currents recorded under voltage-clamp conditions. This action did not appear to be related to the known effect of ketamine of inhibiting 5-HT uptake.

Keywords: 5-HT_3 receptors; ketamine; rabbit nodose ganglion neurones

Introduction In some neurones of the peripheral and central nervous system, 5-HT_3 receptor activation elicits a membrane depolarization mediated by the opening of cation selective ion channels (Peters *et al.*, 1991). The dissociative anaesthetic, ketamine, voltage-dependently blocks both nicotinic (Maleque *et al.*, 1981) and N-methyl-D-aspartate (NMDA) -activated cation conducting channels (MacDonald *et al.*, 1987). Here, the actions of ketamine upon 5-HT_3 receptor-mediated currents recorded from isolated nodose ganglion neurones of the rabbit were examined. We now report that in contrast to its action on nicotinic and NMDA-activated ion channels, ketamine produces a dose-dependent potentiation of the 5-HT_3 receptor-mediated current.

Methods Adult New Zealand rabbits (3.5–6.0 kg) were anaesthetized with halothane, killed by exsanguination, and the nodose ganglia excised. Ganglia were enzymatically dissociated into a single cell suspension by the method of Ikeda *et al.* (1986), with minor modifications. The cells were maintained for 1–7 days in a culture medium comprising: Dulbecco's Modified Eagle's Medium (90% vol/vol) and heat inactivated foetal calf serum (10% vol/vol), supplemented with penicillin (5×10^4 iu l^{-1}), streptomycin (50 mg l^{-1}) and nerve growth factor (50 ng ml^{-1}). Agonist-evoked membrane currents were recorded at room temperature (17–22°C) under voltage-clamp conditions by use of a patch pipette in conjunction with either a List Electronics L/M EPC-7 converter headstage and amplifier or an Axoclamp 2A amplifier in discontinuous single electrode voltage-clamp mode (switching frequency 8–13 kHz). Cells were continuously superfused (2–4 ml min^{-1}) with a recording medium containing (in mM): NaCl 140, KCl 2.8, $CaCl_2$ 1.0, $MgCl_2$ 2.0 and HEPES 10 (pH 7.2). In some experiments LiCl totally replaced NaCl in the extracellular medium. The patch pipette solution comprised (in mM): CsCl (or KCl) 140, $MgCl_2$ 2.0, $CaCl_2$ 0.1, EGTA, 1.1 and HEPES 10 (pH 7.2). Agonists were applied either by pressure ejection (1.4×10^5 Pa, 5–20 ms duration, 0.1 Hz) from a second patch pipette, or by inclusion within the superfusate. All other compounds were applied by the latter route. Quantitative results are expressed as the arithmetic mean ± the standard error of the mean. The drugs used were obtained from the following sources: DL-2-aminophosphonovaleric acid (APV), 5-hydroxytryptamine (5-HT) creatinine sulphate complex (Sigma); 2-methyl-5-HT, ondansetron (Glaxo); ICS 205-930 ((3α-tropanyl)-1H-indole-3-carboxylic acid ester), methysergide (Sandoz); 1-phenylbiguanide (RBI); MK-801 ((+)-5-methyl-10,11-dihydro-5H-dibenzo[a,d]cyclohepten-5,10-imine maleate (Merck Sharp and Dohme); ketanserin (Janssen), ketamine (Parke-Davis), citalopram (Lundbeck) and paroxetine (SmithKline Beecham).

[1] Author for correspondence.

Results In neurones voltage-clamped at a holding potential of −60 mV, 5-HT (10 μM) applied by pressure ejection evoked a transient inward current response associated with an increase in membrane conductance. Such currents were little affected by either bath applied methysergide (1 μM; $n = 6$) or ketanserin (1 μM; $n = 7$) but were reduced to 3.1 ± 0.8% ($n = 3$) and 0.3 ± 0.3% ($n = 6$) of control by ICS 205-930 (1 nM) and ondansetron (1 nM) respectively. Bath-applied ketamine reversibly and concentration-dependently potentiated the amplitude of submaximal inward currents evoked by pressure applied 5-HT (Figure 1a,b). Over the concentration range 3–30 μM, potentiation was well maintained throughout the period of ketamine application, but higher concentrations (100–300 μM) of the drug produced a complex effect consisting of an initial potentiation which was succeeded by a fall in current amplitude toward, or below, control values. Upon washout of high concentrations of ketamine (300 μM), a second phase of potentiation was often observed (Figure 1a). Potentiation by ketamine (30 μM) occurred at all holding potentials examined (−80 to +40 mV) and the drug had no effect upon the reversal potential (approx. −3.0 mV) of the 5-HT-induced response (Figure 1c,d). In neurones where ketamine (10–30 μM) produced a clear potentiation of 5-HT, APV (30 μM) had no effect ($n = 3$) whereas MK-801 (30 μM) slightly reduced the response to 93.3 ± 3.2% ($n = 3$) of control.

In cells sequentially challenged with rapidly superfused 5-HT (1 μM), 2-methyl-5-HT (3 μM) and 1-phenylbiguanide (30 μM), ketamine (10 μM) potentiated the amplitude of the inward current response evoked by each agonist (Figure 2a). Citalopram (0.01–1 μM) had no effect upon responses to pressure applied 5-HT ($n = 3$; Figure 2b). Neither the addition of citalopram (1 μM) or paroxetine (30 nM) to the bathing medium, nor the total replacement of extracellular Na^+ by Li^+, prevented the potentiating action of ketamine (10–30 μM; Figure 2b,c).

Discussion The dissociative anaesthetic, ketamine, blocks the cation-conducting channels activated by nicotine and NMDA (Maleque *et al.*, 1981; MacDonald *et al.*, 1987). In contrast, ketamine (3–30 μM) enhanced the 5-HT_3 receptor-mediated current of rabbit nodose ganglion neurones. Qualitatively, ketamine (30 μM) produced a similar effect in mouse nodose ganglion neurones, although the magnitude of the potentiation was much less than that of the rabbit and was often succeeded by an antagonism of the response (Malone, preliminary observations). Species differences in the properties of 5-HT_3 receptors (see Peters *et al.*, 1991) may account for this discrepancy. The effect of ketamine in the rabbit was not restricted to 5-HT, as currents evoked by the 5-HT_3 receptor agonists, 2-methyl-5-HT and 1-phenylbiguanide, were similarly potentiated. The ketamine-induced potentiation was not mimicked by the competitive NMDA receptor antagonist, APV, or by the NMDA ion channel blocker, MK-801.

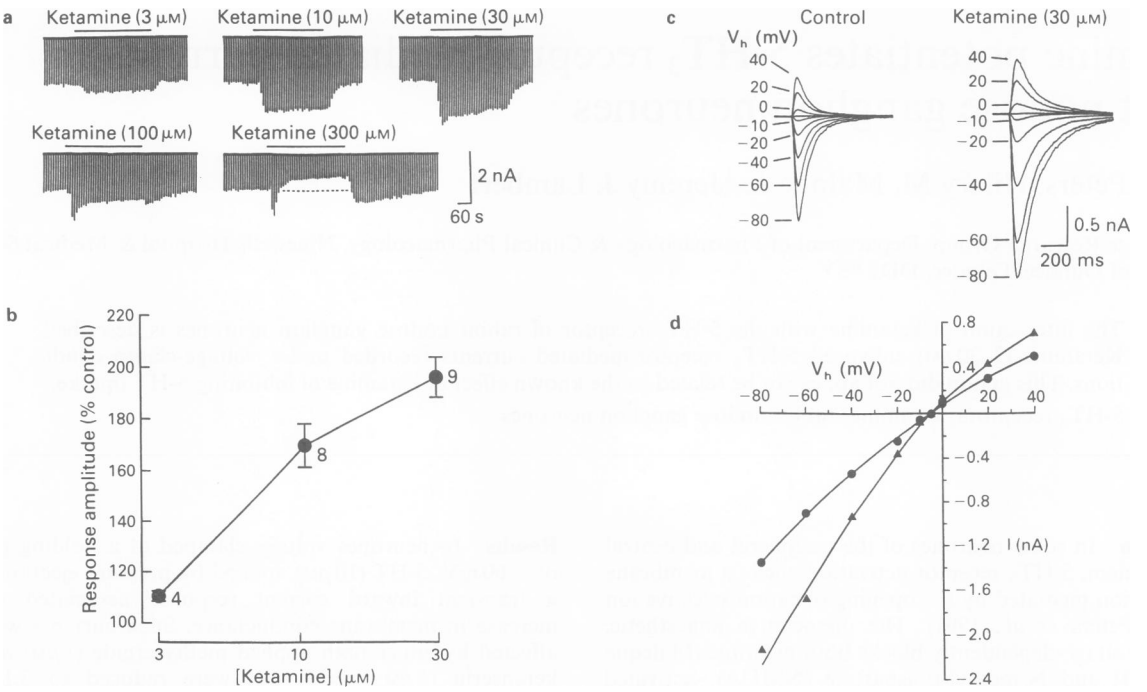


Figure 1 Ketamine potentiates 5-HT_3 receptor-mediated membrane currents in rabbit nodose ganglion neurones. (a) Traces illustrating the potentiation of responses to pressure applied 5-hydroxytryptamine (5-HT, 10 μM, 1.4×10^5 Pa, 0.1 Hz, Pa, 0.1 Hz, 10 ms duration) by bath-applied ketamine. Note that potentiation in response to high concentrations of ketamine (100–300 μM) is not maintained throughout the period of superfusion and is succeeded by blockade of the response in the case of 300 μM ketamine. A second phase of potentiation occurs upon washout of 300 μM ketamine. Currents were recorded at a holding potential of −60 mV and low pass filtered at 0.5 kHz. (b) Graph illustrating the concentration-dependence of the ketamine induced potentiation of currents evoked by 5-HT. Response amplitude, as a percentage of control, is plotted against the logarithm of ketamine concentration in the medium on a logarithmic scale. Each data point represents the mean of 4–9 observations performed on separate neurones. Vertical lines represent s.e.mean. (c) Traces illustrating the transmembrane current in response to pressure applied 5-HT, recorded at various holding potentials (V_h), and the influence of ketamine (30 μM) on such responses. Note that the leakage currents have been subtracted. (d) Graph representing the data from (c) shows the relationship between the amplitude of the 5-HT-induced current and holding potential under control conditions (●) and in the presence of 30 μM ketamine (▲). Note that the potentiation by ketamine occurs at all holding potentials, without influencing the $I_{5\text{-HT}}$ reversal potential (approx. −3 mV).

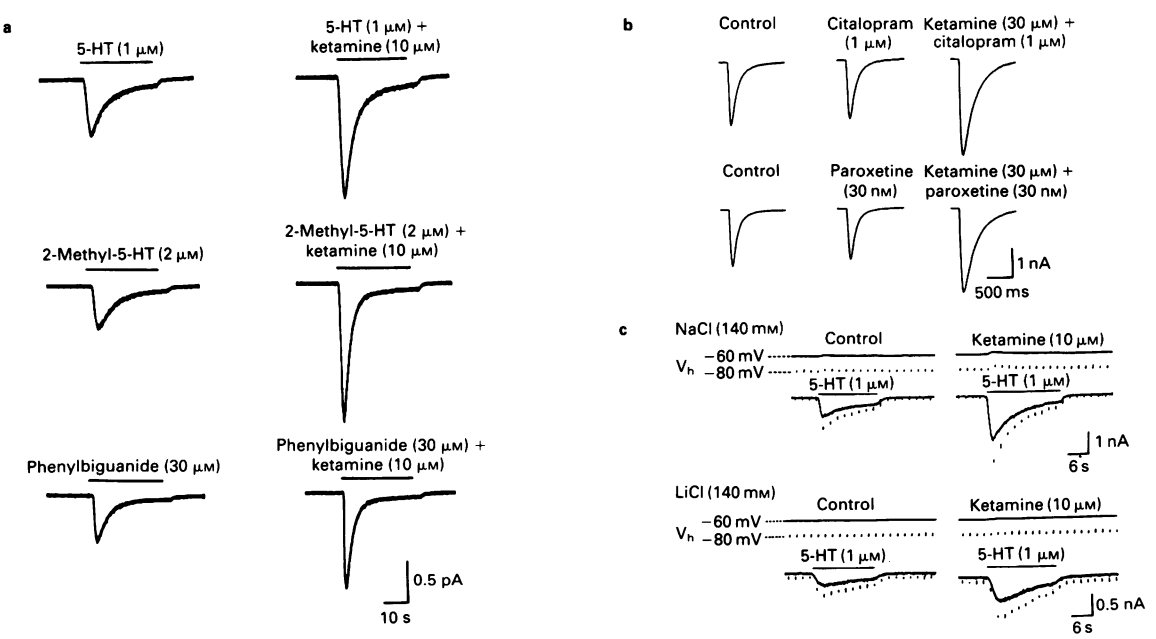


Figure 2 The action of ketamine is not mediated by inhibition of Na^+-dependent 5-hydroxytryptamine (5-HT) uptake. (a) Traces depicting the potentiation by ketamine (10 μM) of inward current responses to 5-HT (1 μM), 2-methyl-5-HT (3 μM) and 1-phenylbiguanide (30 μM) applied by rapid superfusion. All currents were recorded from the same neurone which was voltage-clamped at a holding potential of −60 mV. (b) Traces depicting responses to pressure applied 5-HT (10 μM, 1.4×10^5 Pa, 0.1 Hz, 12 ms duration) in control conditions and following the superfusion of citalopram (1 μM) or paroxetine (30 nM) for 5 min. Note that the uptake inhibitors neither enhance 5-HT-evoked currents, nor prevent the potentiation occurring to ketamine applied in their presence. Each trace is the computer-generated average of 4 responses to 5-HT recorded at a holding potential of −60 mV. (c) Replacement of extracellular Na^+ by Li^+ does not prevent ketamine-induced potentiation of responses to rapidly superfused 5-HT. The upper of each pair of traces represent holding potential (V_h), which was transiently stepped from −60 mV to −80 mV for 100 ms at a rate of 0.5 Hz. Lower traces depict membrane current in response to 5-HT and the voltage steps. Note that, in extracellular media containing either Na^+ or Li^+ as the predominant cation, ketamine (10 μM) potentiates both the amplitude of the 5-HT-evoked current and the increase in membrane conductance which underlies the response.

Ketamine, at concentrations similar to those used here, blocks the uptake of 5-HT into rat brain synaptosomes and inhibits the binding of the 5-HT uptake inhibitor, paroxetine, to rat brain membranes (Martin *et al.*, 1990). However, in our experiments the 5-HT uptake blockers, citalopram and paroxetine, did not enhance the 5-HT-induced current or prevent its potentiation by ketamine. The neuronal uptake of 5-HT is a sodium-dependent process which cannot be supported by lithium (Wood, 1987). However, ketamine was equieffective in potentiating 5-HT-induced currents in a sodium or lithium based extracellular solution. Collectively, these observations suggest that an inhibition of 5-HT uptake is unlikely to explain the effects of ketamine reported here. The molecular mechanism of the ketamine-induced potentiation is as yet unknown. The 5-HT_3 receptor-mediated current in rabbit nodose ganglion neurones desensitizes rapidly, and the method by which known concentrations of agonist were applied in the present study is likely to result in some degree of desensitization occurring prior to the attainment of a peak current response. In view of this complication, no attempt was made to examine the influence of ketamine upon the 5-HT concentration-effect relationship and we are unable to distinguish between the enhancement of the maximal effect of 5-HT, or an enhancement of its potency, as potential mechanisms underlying the action of ketamine. Clearly, the possibility that ketamine binds to a distinct site on the 5-HT_3 receptor protein to enhance the interaction of agonist and receptor, in a manner analogous to positive allosteric modulators at other ligand-gated ion channels, requires further investigation.

This work was supported by the Wellcome Trust and a Dundee University Research Initiative Grant.

References

IKEDA, S.R., SCHOFIELD, G.G. & WEIGHT, F.F. (1986). Na^+ and Ca^{2+} currents of acutely isolated adult rat nodose ganglion cells. *J. Neurophysiol.*, **55**, 527–539.

MALEQUE, M.A., WARNICK, J.E. & ALBUQUERQUE, E.X. (1981). The mechanism and site of action of ketamine on skeletal muscle. *J. Pharmacol. Exp. Ther.*, **219**, 638–645.

MACDONALD, J.F., MILJKOVIC, Z. & PENNEFATHER, P. (1987). Use-dependent block of excitatory amino acid currents in cultured neurones by ketamine. *J. Neurophysiol.*, **58**, 251–266.

MARTIN, D.C., INTRONA, R.P. & ARONSTAM, R.S. (1990). Inhibition of neuronal 5-HT uptake by ketamine, but not halothane, involves disruption of substrate recognition by the transporter. *Neurosci. Lett.*, **112**, 99–103.

PETERS, J.A., LAMBERT, J.J. & MALONE, H.M. (1991). Physiological and pharmacological aspects of 5-HT_3 receptor function. In *Aspects of Synaptic Transmission.* ed. Stone, T. London: Taylor & Francis (in press).

WOOD, M.D. (1987). Examination of the relationship between the uptake site for 5-hydroxytryptamine and the high affinity binding site for [^{3}H] imipramine II. The role of sodium ions. *Neuropharmacology*, **26**, 1081–1085.

(Received March 15, 1991
Accepted April 10, 1991)

Br. J. Pharmacol. (1991), **103**, 1626–1628 © Macmillan Press Ltd, 1991

Prostaglandin E_1 decreases the low-density-lipoprotein entry into rabbit arterial wall

[1]H. Sinzinger, Irene Virgolini, [2]Graziana Lupattelli, *E. Molinari, *A. Gerakakis & †P. Angelberger

Atherosclerosis Research Group (ASF) Vienna, Atherosclerosis Research Group of the Austrian Academy of Sciences (ATK), *Research Department Immuno AG, Vienna, and †3 Chemical Institute, Research Center Seibersdorf, Austria

1 In 72 male rabbits fed a 1% cholesterol supplemented diet the effect of a 4 weeks daily infusion of prostaglandin E_1 (PGE_1, 20 $\mu g\,kg^{-1}\,min^{-1}$ over 2 h) on [^{125}I]-low density lipoprotein (LDL) accumulation (10 μCi; 0.5 mg protein ml^{-1}) was examined versus sham-treatment after removal of the endothelium of the abdominal aorta by a Fogarthy catheter.

2 The uptake of [^{125}I]-LDL was significantly ($P < 0.01$) higher in endothelium-free aortic segments (showing the highest peak maximum at around 12 h after ^{125}I-injection) as compared to aortic segments with endothelium intact (showing the lowest uptake of [^{125}I]-LDL with the peak maximum at 48 h, last control time). Segments with the endothelium restored showed a similar LDL-retention curve to segments with endothelium however, being again significantly ($P < 0.01$) higher.

3 PGE_1-treatment caused reduction in LDL-accumulation, being significantly ($P < 0.001$) pronounced in segments without endothelium and in segments with endothelium restored.

4 The findings indicate a beneficial effect of PGE_1 in lipid metabolism by decreasing the LDL-influx into the arterial wall *in-vivo*.

Keywords: prostaglandin E_1; rabbit arterial wall; low-density lipoprotein (LDL)-entry; experimental atherosclerosis

Introduction

Atherosclerotic arteries accumulate cholesterol and cholesterol ester (Newman & Zilversmit, 1962; Peloffo *et al.*, 1983) and produce decreased amounts of antiaggregatory prostaglandins *in vitro*. Beneficial effects of therapeutic application of prostacyclin (PGI_2) and prostaglandin E_1 (PGE_1) (for review see: Sinzinger *et al.*, 1989a) have been reported in advanced human atherosclerosis. It has been demonstrated that PGE_1 reduces the net arterial cholesterol content by increasing mobilisation and diminishing cholesterol esterification (for review see: Willis *et al.*, 1986). In addition, a direct effect of PGE_1 on low-density-lipoprotein (LDL)-receptor activity has been demonstrated quite recently (Sinzinger *et al.*, 1989b). Since radiolabelling of LDL is proven to be a useful technique for quantification of cholesterol content in human (Lees *et al.*, 1983; Kaliman *et al.*, 1985; Sinzinger *et al.*, 1986) and animal tissue (Bratzler *et al.*, 1977; Alavi & Moore, 1985; Vallabhajosula *et al.*, 1988) we have examined the effect of a 4 weeks i.v. PGE_1 therapy on [^{125}I]-LDL entry in segments with endothelium, without endothelium and with endothelium restored of the abdominal aorta in rabbits fed a 1%-cholesterol diet.

Methods

Isolation of low-density lipoprotein

Polyclonal anti-apo-B-antibodies were obtained by immunizing sheep with pure LDL. Gamma-globulins were precipitated from sheep plasma with ammonium sulphate (390 $g\,l^{-1}$; Sanabo, Vienna, Austria) to a final concentration of 35% and further purified by immunoaffinity chromatography. For this purpose 3 g of pure LDL was coupled to 400 ml of BrCN-activated Sepharose Cl 4B (Pharmacia, Uppsala, Sweden) by standard techniques. The immuno-purified antibodies were themselves coupled to CNBr-activated Sepharose Cl 4B and used to isolate apo-B-containing lipoproteins (LDL, VLDL) from rabbit plasma: 10 ml of anti-LDL-sepharose Cl 4B gel was placed in a glass column (22 × 2 cm). The gel was thereafter extensively washed with 500 ml of isotonic NaCl solution; 10 ml of rabbit (overnight fast for at least 14 h) citrated (3.8% sodium citrate, 1:10) plasma were recirculated for 30 min over the column at a flow rate of 10 $ml\,min^{-1}$. The column was then washed with isotonic saline solution until it was protein-free (E 260/280 nm < 0.002). Lipoproteins were desorbed from the column with 2 bed volumes of 0.2 M glycine/HCl, pH 3.0, and dialyzed overnight against 5 l of isotonic saline. The solution was then concentrated by ultrafiltration on Amicon XM 100 filters (Vienna, Austria) to a final concentration of 10 mg LDL ml^{-1}. This preparation was then ready for radiolabelling.

Labelling of low-density lipoprotein

LDL were labelled with ^{125}I by the iodine monochloride (ICl) technique (MacFarlane, 1958). An ICl-stock solution (34 $\mu mol\,ml^{-1}$ 6 M HCl) was purified before labelling by means of 3 extractions with $CHCl_3$ and diluted 1:100 with 2 M NaCl. To a microvial kept at 4°C approximately 1 mg LDL, 1 M glycine buffer, pH 10, about 1 mCi [^{125}I]-NaI and freshly diluted ICl-solution were added to give a molar ratio ICl/apoprotein of 10/1. The reaction mixture (0.5–1 ml) was slowly stirred for 10 min at 4°C and sterile filtered into a dialysis bag which was kept in dialysis buffer (0.15 M CaCl, 0.01 M PO, pH 7.5, 0.2 mM EDTA) at 4°C until used for *in vivo* studies. Analysis for radiochemical purity (>96%) was determined by TCA-precipitation and poly-acrylamid gel electrophoresis.

Experimental studies

In 72 male rabbits, aged 6 months, fed normal chow and allowed water *ad libitum*, the abdominal aortic endothelium was abraded by means of a Fogarthy catheter (Sinzinger *et al.*, 1979). The animals were then fed a 1% cholesterol supplemented diet for one month. In order to study the effect of PGE_1 on endothelial lining and LDL-uptake, the animals were divided into 2 groups: group A ($n = 36$ animals) received infusion of 2 μg PGE_1 kg^{-1}, i.v. (Prostavasin; Schwarz

[1] Author for correspondence: Atherosclerosis Research Group (ASF) Vienna, Nadlergasse 1, A-1090 Vienna, Austria.
[2] Permanent address: 2nd Department of Medicine, Ospedale Monteluce, University of Perugia, Italy.

Pharma, Monheim, Germany) daily for 2 h; group B ($n = 36$ animals) received the vehicle only. After one treatment month, 10 μCi [^{125}I]-LDL (1 ml, 0.5 mg protein) was injected intravenously and the animals killed by decapitation at various time intervals (1, 3, 6, 12, 24, 48 h) after the injection. Morphological examination (including Sudan III-staining) and classification of surface lining (intact endothelium, endothelium restored, without endothelium) was performed. The tracer-uptake in abdominal aortic segments was quantified per surface area.

Statistical analysis

Values are presented as $\bar{x} \pm$ s.d. Calculation for significance was performed by the Student's t test for paired data.

Results

Aortic segments with endothelium intact

The uptake of ^{125}I-labelled LDL by abdominal aortic segments of the rabbit continuously increased with time. In the control-group with intact endothelium, the total [^{125}I]-LDL-entry into aortic segments was lowest reaching 709 $\pm$ 31 c.p.m. after 48 h (Figure 1). PGE$_1$-treatment moderately ($P < 0.065$) decreased the entry of LDL (654 $\pm$ 34 c.p.m. after 48 h).

Aortic segments with endothelium removed

Aortic segments without endothelium demonstrated the highest uptake of [^{125}I]-LDL into rabbit arterial wall. The peak maximum uptake (10548 $\pm$ 1160 c.p.m.) was reached at around 12 h after injection of autologous [^{125}I]-LDL (Figure 2). PGE$_1$ significantly ($P < 0.001$) decreased the peak-entry (7524 $\pm$ 754 c.p.m.) and showed a sustained effect on [^{125}I]-LDL retention.

Aortic segments with restored endothelium

Aortic segments with restored endothelium showed a continuous increase of [^{125}I]-LDL-uptake (peak-maximum 5097 $\pm$ 181 c.p.m. at 48 h after injection). The total tracer-uptake was significantly ($P < 0.001$) higher than in segments with intact endothelial lining at the different control times. PGE$_1$ significantly reduced the LDL-entry ($P < 0.01$) reaching 3875 $\pm$ 338 c.p.m. at 48 h after injection (Figure 3).

Discussion

As enhanced lipid accumulation in the rabbit arterial wall was demonstrated by Anitschkow (1933) after experimental fat feeding. Cholesterol and LDL-accumulation in the arterial wall are key events, both in experimental animal and human atherogenesis. Some prostaglandins have been claimed to be effective in decreasing this increased entry. In rabbit aortic smooth muscle cells (Hajjar *et al.*, 1982) a protection against cholesterol and cholesterol ester accumulation via a decreased cholesterol influx into the cells, a diminished cholesterol biosynthesis and an increased cholesterol ester mobilization (enhanced cholesterol ester hydrolase activity; Hajjar & Weksler, 1983) induced by PGI$_2$ have been postulated.

In isolated monocytes, 10 μM PGE$_1$ caused a 61% decrease of cholesterol biosynthesis and a 70% drop in cholesterol accumulation (Hajjar, 1985). However, it has not been determined so far whether the administration of prostaglandins or stable analogues are able to reduce cholesterol accumulation in atherosclerotic arteries *in vivo*.

The findings reported here indicate for the first time that PGE$_1$, given on a long-term basis, may act as a hypolipidaemic substance at the vascular wall level. PGE$_1$ seems to affect mainly the second part of the LDL kinetic curve, which has been shown to be an indicator for cellular cholesterol content (Virgolini *et al.*, 1989). Furthermore, the total entry of apo-B-containing lipoprotein was significantly depressed. This net decrease in cholesterol content induced by PGE$_1$ which has been shown in smooth muscle cells (St. Clair, 1976), monocytes (Krone *et al.*, 1985) and *in vivo* in rabbits and in 2 patients (Sinzinger *et al.*, 1987) may be one major mechanism of action of this compound on a long-term basis.

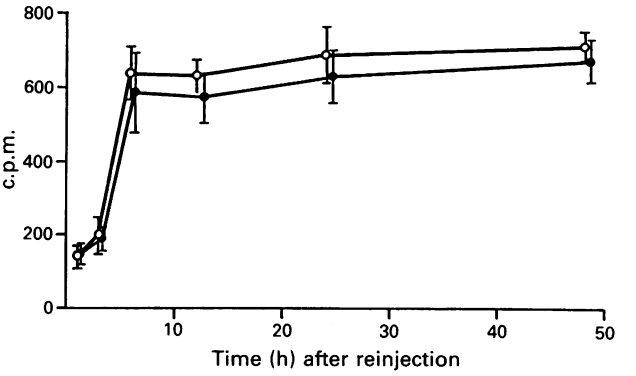


Figure 1 Effect of prostaglandin E$_1$ (PGE$_1$) on low-density lipoprotein (LDL)-entry into segments with endothelium intact of the rabbit abdominal aorta at different time intervals after injection of autologous [^{125}I]-LDL: (○) Control group; (●) PGE$_1$ group.

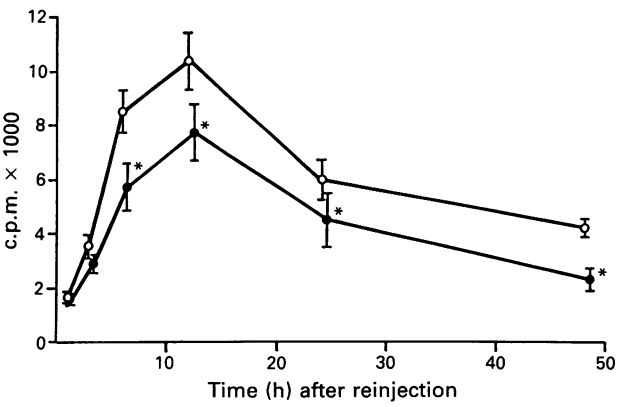


Figure 2 Effect of prostaglandin E$_1$ (PGE$_1$) on low-density lipoprotein (LDL)-entry into segments with endothelium removed of the rabbit abdominal aorta measured at various time intervals: (○) control group; (●) PGE$_1$ group. * $P < 0.001$.

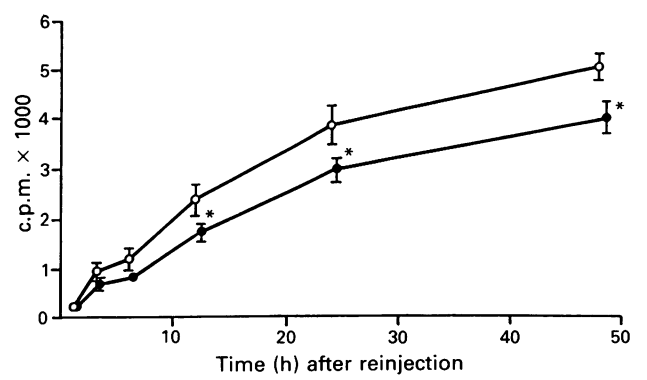


Figure 3 Effect of prostaglandin E$_1$ (PGE$_1$) on low-density lipoprotein (LDL)-entry into segments with endothelium restored of the rabbit abdominal aorta up to 48 h after LDL reinjection: (○) Control group; (●) PGE$_1$ group. * $P < 0.001$.

The PGE$_1$ used in this study was kindly provided by Dr Waltraud Rogatti, Schwarz-Pharma GmbH, Monheim, FRG. The authors gratefully acknowledge the valuable technical help of Gabriele Cafourek and Susanne Granegger and are grateful to Eva Unger for preparing and typing the manuscript.

References

ALAVI, M. & MOORE, S. (1985). Measurement of 125-I-LDL entry into ballooned rabbit aorta using average plasma value. *Arteriosclerosis*, **5**, 413.

ANITSCHKOW, N.N. (1933). Experimental arteriosclerosis in animals. In *Arteriosclerosis: a Survey of the Problem*. ed. Cowdry, E.C. pp. 271–322. New York: MacMillan.

BRATZLER, R.L., CHISOLM, G.M., COLTON, C.K., SMITH, K.A. & LEES, R.S. (1977). The distribution of labeled low density lipoproteins across the rabbit thoracic aorta *in vivo*. *Atherosclerosis*, **28**, 289–307.

HAJJAR, D.P. (1985). Prostaglandins and cyclic nucleotides. Modulators of arterial cholesterol metabolism. *Biochem. Pharmacol.*, **34**, 295–300.

HAJJAR, D.P. & WEKSLER, B.B. (1983). Metabolic activity of cholesteryl-esters in aortic smooth muscle cells is altered by prostaglandin I2 and E2. *J. Lipid Res.*, **24**, 1176–1185.

HAJJAR, D.P., WEKSLER, B.B., FALCONE, D.J., HEFTON, J.M., TACK-GOLDMAN, K. & MINICK, C.R. (1982). Prostacyclin modulates cholesteryl ester hydrolytic activity by its effect on cyclic adenosine monophosphate in rabbit aortic smooth muscle cells. *J. Clin. Invest.*, **70**, 479–488.

KALIMAN, J., SINZINGER, H., BERGMANN, H. & KOLBE, C. (1985). Value of 123I-low density lipoproteins (LDL) in the diagnosis of human atherosclerotic lesions. *Circulation*, **72**, 163.

KRONE, W., KACZMARCZYK, P., MÜLLER-WIELAND, D. & GRETEN, H. (1985). The prostacyclin analogue iloprost and prostaglandin E_1 suppress sterol synthesis in freshly isolated human mononuclear leukocytes. *Biochim. Biophys. Acta*, **835**, 154–157.

LEES, R.S., LEES, A.M. & STRAUSS, H.W. (1983). External imaging of human atherosclerosis. *J. Nucl. Med.*, **24**, 154–156.

MACFARLANE, A.S. (1958). Efficient tracer labelling of proteins with iodine. *Nature*, **182**, 53.

NEWMAN, H.A.I. & ZILVERSMIT, D.B. (1962). Quantitative aspects of cholesterol flux in rabbit atheromatous lesions. *J. Biol. Chem.*, **237**, 2078–2085.

PELOFFO, R.O., NERVI, A.M., GONZALEZ, S. & BRENNER, R.R. (1983). Turnover of low density lipoproteins in normal and atherosclerotic rabbits. *Acta Physiol. Latinoam.*, **33**, 33–44.

SINZINGER, H., BERGMANN, H., KALIMAN, J. & ANGELBERGER, P. (1986). Imaging of human atherosclerotic lesions using 123-I-low-density lipoprotein. *Eur. J. Nucl. Med.*, **12**, 291–292.

SINZINGER, H., FITSCHA, P. & KALIMAN, J. (1987). Wirkmechanismen von PGE_1 bei Atherosklerose. *VASA*, **20**, 189–191.

SINZINGER, H., SILBERBAUER, K. & WINTER, M. (1979). Effects of experimental atherosclerosis on prostacyclin (PGI_2) generation in arteries of miniature swine. *Artery*, **5**, 448–462.

SINZINGER, H., VIRGOLINI, I., LI, S., LUPATTELLI, G. & ROGATTI, W. (1989b). Effect of prostaglandin E_1 (PGE_1) on ^{123}I-low density lipoprotein (LDL) Apo-B,E-receptor binding. *Physiologist*, **32**, 171.

SINZINGER, H., VIRGOLINI, I. & O'GRADY, J. (1989a). Clinical trials of PGE_1, PGI_2 and mimetics in patients with peripheral vascular disease. In *Prostaglandins in Clinical Research: Cardiovascular System*. ed. Schrör, K. & Sinzinger, H. pp. 85–96. New York: Alan R. Liss Inc.

ST. CLAIR, R.W. (1976). Metabolism of the arterial wall and atherosclerosis. In *Atherosclerosis Reviews*. ed. Paoletti, R. & Gotto, A.M. pp. 61–177. New York: Raven Press.

VALLABHAJOSULA, S., PAIDI, M., BADIMON, J.J., LE, N.A., GOLDSMITH, S.J., FUSTER, V. & GINSBERG, H.N. (1988). Radiotracers for low density lipoprotein biodistribution studies *in vivo*: technetium-99 m low density lipoprotein versus radioiodinated low density lipoprotein preparations. *J. Nucl. Med.*, **7**, 1237–1245.

VIRGOLINI, I., ANGELBERGER, P., LUPATTELLI, G., PIDLICH, J. & SINZINGER, H. (1989). *In vivo* Einstrom autologer radioaktiv markierter Low-density-Lipoproteine (LDL) in menschliche Gefäße. *Wr. klin. Wschr.*, **101**, 798–805.

WILLIS, A.L., SMITH, D.L. & VIGO, C. (1986). Suppression of principal atherosclerotic mechanisms by prostacyclin and other eicosanoids. *Prog. Lipid Res.*, **48**, 1–22.

(Received September 17, 1990
Revised January 25, 1991
Accepted February 21, 1991)

Br. J. Pharmacol. (1991), **103**, 1629–1632 © Macmillan Press Ltd, 1991

Possible role of leukotrienes in hypoxic contraction of canine isolated basilar artery

*Mai Gu, *Douglas A. Elliott, *†Bill Y. Ong & *†#[1]Deepak Bose

Departments of *Pharmacology & Therapeutics, †Anesthesia and #Internal Medicine, Faculty of Medicine, University of Manitoba, Winnipeg, Man., Canada, R3E 0W3

1 Hypoxia reversibly increased isometric tension in unstimulated canine isolated basilar artery rings.

2 Nordihydroguaiaretic acid (NDGA; 5×10^{-6} M), an inhibitor of lipoxygenase and quinacrine (10^{-5} M), which blocks the release of arachidonic acid from phospholipids by inhibiting the enzyme phospholipase A_2, blocked hypoxia-induced contractions.

3 The preferential leukotriene D_4 (LTD_4) antagonist, L-660,711, also inhibited the hypoxia-induced contractions in concentrations ranging from 10^{-8} M to 10^{-5} M. The effects seen were statistically significant ($P < 0.05$). Two components of inhibition were seen.

4 Arachidonic acid ($5\,\mu g\,ml^{-1}$) caused contraction of the isolated basilar artery rings. This response was inhibited by NDGA (5×10^{-6} M) and L-660,711 (10^{-5} M).

5 The LTD_4 (10^{-8} M–10^{-7} M)-induced contraction was relaxed by L-660,711 in a dose-dependent manner. Both the contraction caused by LTD_4 as well as that caused by hypoxia were relaxed by 5×10^{-6} M adenosine.

6 Leukotriene(s) may be involved in hypoxia-induced contraction of canine isolated basilar artery. However, they may not be the sole mediator(s).

Keywords: Blood vessel; cerebral blood flow; contraction; hypoxia; smooth muscle

Introduction

Previously, we have shown that hypoxia causes a reversible contraction of canine isolated basilar artery (Mallick *et al.*, 1987), which is not due to rigor of the metabolically impaired smooth muscle cells. Instead it is a Ca^{2+}-dependent process, because it can be blocked by the Ca^{2+} ion chelator, EGTA, and by the Ca^{2+} channel blocker, methoxyverapamil (D600) (Mallick *et al.*, 1987). It is not reduced by α-adrenoceptor blockade (phentolamine), muscarinic receptor blockade (atropine) or by combined histamine and 5-hydroxytryptamine receptor blockade (methysergide). Indomethacin, which blocks the production of prostaglandins by inhibiting cyclo-oxygenase, also does not have an effect on the hypoxic contraction of the canine basilar artery (Mallick *et al.*, 1987).

In the present study, we examined the role of leukotrienes in hypoxia-induced contractions of canine isolated basilar artery. Leukotrienes are able to contract cerebral blood vessels (Jancar *et al.*, 1987; Nishiye *et al.*, 1988) and are produced in relatively large amounts during cerebral ischaemia (Suzuki *et al.*, 1983; Moskowitz *et al.*, 1984; Kiwak *et al.*, 1985). In addition, a possible clinical implication is that the synthesis of leukotrienes can be greatly increased if the competitive pathway for arachidonate utilization, i.e. synthesis of prostaglandins, is blocked by cyclo-oxygenase inhibitors (e.g. non-steroidal antiinflammatory drugs). These drugs may be used in the treatment of some cerebral vascular disorders, e.g. transient ischaemic attack (Reilly *et al.*, 1988). The role of leukotrienes in mediating changes in cerebral arterial tone under pathological conditions, therefore, deserves consideration.

Methods

Isolated basilar arteries were obtained from mongrel dogs (7–15 kg) of either sex. The dogs were anaesthetized with intravenously administered pentobarbitone sodium ($30\,mg\,kg^{-1}$). The posterior part of the skull was opened with a bone cutter. The brain stem with the attached basilar artery was carefully removed and placed in oxygenated, cool (4°C) Krebs-Henseleit solution. The basilar artery was dissected clear from the surrounding brain and meninges and then cut transversely into rings 1–1.5 cm long. The external diameter of the rings was less than 1 mm. After dissection, two stainless-steel wires (AWG 32) were inserted carefully into the lumen of the ring, causing minimal trauma. One of the wires was connected to a force transducer (Grass FT-03), the other to a micromanipulator. The latter was used to adjust the preload on the vascular ring. The preparations were kept in 20 ml organ baths filled with Krebs-Henseleit solution with the following composition (in mM): NaCl 118, KCl 4.7, KH_2PO_4 1.4, $MgSO_4$ 1.2, $CaCl_2$ 2.5, $NaHCO_3$ 25 and dextrose 11. The solution was bubbled with a mixture of 95% O_2:5% CO_2 to maintain a pH of 7.4. Maximum contraction of the isolated vessel ring was usually obtained at a preload of about 2 g. The integrity of the endothelium was verified by the application of acetylcholine to the ring, after precontracting it with 5-hydroxytryptamine (2.5×10^{-7} M). A prompt and reversible relaxation of 0.10 g or more indicated that functional endothelium was present. The vessel was allowed to equilibrate for 30–60 min at an ambient temperature of 37°C while the resting tension was continuously adjusted until it became stable at 2 g. KCl (60 mM) was used to verify the contractile response of the vessel.

Hypoxia was produced by bubbling the bathing solution with a mixture of 95% N_2:5% CO_2. During the hypoxic period, Po_2 in the organ bath decreased from 600 mmHg to 25 mmHg. The duration of hypoxia was 10–15 min. The tension of the vessel started to increase after 1–2 min of hypoxia and then either remained at this high level or tended to gradually relax towards prehypoxic level. At the end of hypoxia, normoxia was restored by bubbling 95% O_2:5% CO_2. This caused a rapid reduction in tension followed by recovery to the pre-hypoxic level. Various pharmacological agents were added to the bath 30–60 min after the initial hypoxic contraction. Sixty minutes later, the muscle was made hypoxic again for 10–15 min followed by normoxia. The tissue was then washed 2–3 times with fresh Krebs-Henseleit solution and after a rest period of 30–60 min, the tissue was subjected to another episode of hypoxia. At the end of each

[1] Author for correspondence at: Department of Pharmacology & Therapeutics, University of Manitoba, 770 Bannatyne Avenue, Winnipeg, MB, Canada, R3E 0W3.

experiment, KCl (60 mM) was added to the organ bath to assess vascular reactivity.

Stock solutions of nordihydroguiairetic acid (NDGA) and 5,8,11,14 eicosatetraenoic acid (ETYA) were made in 20% v/v aqueous ethanol and arachidonic acid (AA) was dissolved in 60% v/v aqueous ethanol. Volumes added to the organ bath resulted in final concentrations of ethanol less than 0.1%, which were shown not to affect the resting tension or the responsiveness to contractile agents and hypoxia. Quinacrine, L-660,711 (3-(3-(2-(7-chloro-2-quinolinyl)ethenyl)phenyl) ((3-dimethylamino-3-oxopropyl)thio)methyl)thio)propanoic acid, and leukotriene D_4 were dissolved in distilled water. NDGA, AA and quinacrine were obtained from Sigma Chemicals (St. Louis, MI, U.S.A.). The leukotriene antagonist (L-660,711) and leukotriene D_4 (LTD_4) were kind gifts from Dr A.W. Ford-Hutchinson (Merck-Frosst Canada).

Results have been expressed as mean ± s.e.mean. Differences between various treatments were analyzed for statistical significance by the paired t test in the case of self controlled experiments with a single treatment or by repeated Analysis of Variance with Tukey's test where there were two or more treatments. A P value of <0.05 was considered to be statistically significant. A commercial computer programme (SYSTAT) was used for the statistical analyses.

Results

Effects of NDGA, quinacrine and leukotriene antagonists on hypoxia-induced contraction of canine isolated basilar artery

Hypoxia produced a contraction of the canine isolated basilar artery which was reversed by reoxygenation (Figure 1a). The reproducibility of hypoxia-induced contractions was verified by repeating hypoxia every 60 min. In five such experiments, the consecutive hypoxic contractions, 120 min apart, were 0.77 ± 0.18 g and 0.80 ± 0.13 g ($P = 0.35$). Hypoxic contractions were blocked by NDGA (5×10^{-6} M), being significantly decreased from 0.79 ± 0.31 g to 0.05 ± 0.04 g (Figure 2). In previous experiments it was found that ETYA (2–5 mM), which inhibits both lipoxygenase and cyclo-oxygenase, had the same effect as NDGA in reducing hypoxic contraction (data not shown). Quinacrine (10^{-5} M) also reduced hypoxic-contraction from 0.97 ± 0.14 g to 0.16 ± 0.06 g (Figure 2). The inhibition by L-660,711, a specific LTD_4 antagonist, was dose-related in that at 10^{-8} M the hypoxic contraction was inhibited from

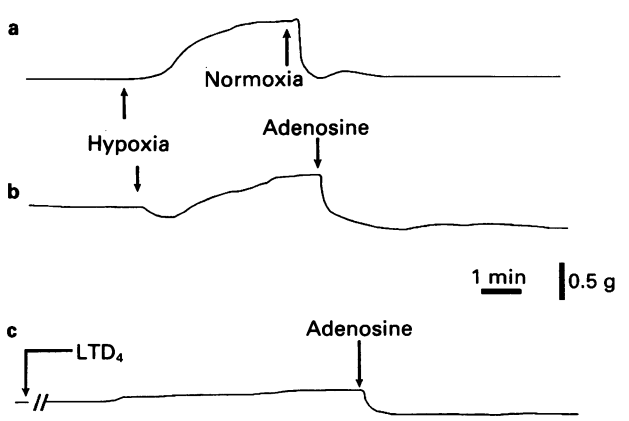


Figure 1 Effect of adenosine on contractions of canine isolated basilar artery induced by hypoxia or leukotriene D_4 (LTD_4). After stabilization of the muscle, hypoxia caused a gradual increase in tension after 1–2 min. Restoration of normoxia caused a prompt reduction in tension followed by recovery to control level. Adenosine (5×10^{-6} M) resulted in a rapid decrease in tension induced by (b) hypoxia or (c) LTD_4 ($10^{-8} - 10^{-7}$ M). Results are typical of 5 experiments.

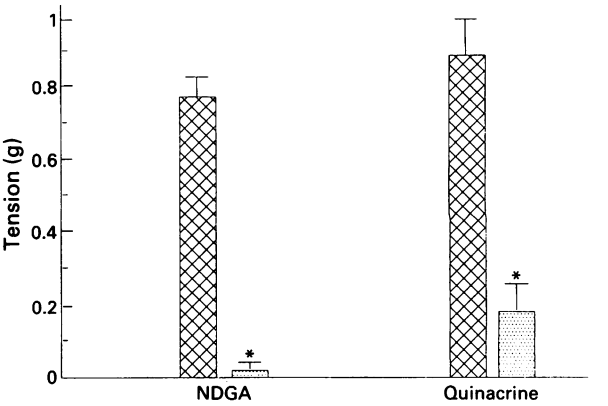


Figure 2 Effects of nordihydroguaiaretic acid (NDGA, 5×10^{-6} M; $n = 5$) and quinacrine (10^{-5} M; $n = 7$) on hypoxia-induced contractions of canine isolated basilar artery. Hatched columns represent tension change during hypoxia while stippled columns represent that after the addition of the agents. Both agents blocked hypoxia-induced contraction significantly at the $P < 0.05$ level (paired t test) as indicated by asterisks.

1.06 ± 0.14 g to 0.62 ± 0.13 g (a 42% inhibition, $P = 0.01$), while at 10^{-7} M, 10^{-6} M and 10^{-5} M, the contractions were reduced to 0.51 ± 0.12 g, 0.48 ± 0.12 g and 0.06 ± 0.03 g, respectively (Figure 3).

The specificity of these agents on hypoxia-induced contractions was tested by assessing their effects on responses of the vessels to KCl (60 mM). Contractions of the vascular rings to KCl were not decreased significantly by addition of NDGA (5×10^{-6} M) (from 1.64 ± 0.29 g to 1.44 ± 0.18 g). However, after quinacrine (1×10^{-5} M), the response to KCl was decreased from 1.55 ± 0.1 g to 0.73 ± 0.2 g. L-660,711 (10^{-6} M) increased the response to KCl from 1.46 ± 0.28 g to 1.82 ± 0.25 g, but this difference did not attain statistical significance. These results indicate that NDGA and the leukotriene antagonist were not having a direct relaxant effect on hypoxic tissues. However, the effect of quinacrine cannot be interpreted unambiguously as being due to inhibition of phospholipase A_2.

Effects of arachidonic acid and leukotriene D_4 on canine isolated basilar artery and inhibition by NDGA and L-660,711

Arachidonic acid (5 μg ml^{-1}) caused an immediate contraction of isolated arteries in 6 separate experiments. The active

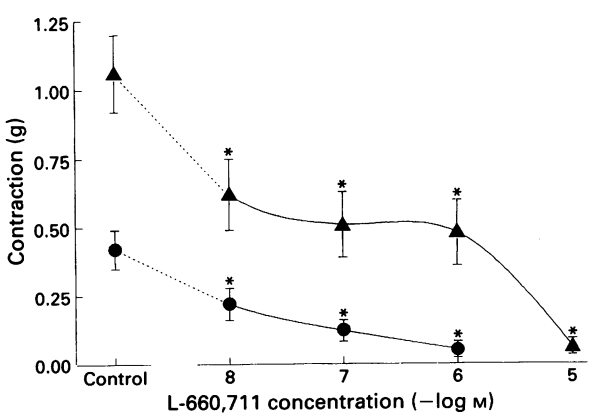


Figure 3 Inhibition of hypoxic contraction (▲) and leukotriene D_4 (LTD_4)-induced contraction (●) by L-660,711. Various concentrations of L-660,711 were added cumulatively ($n = 8$) and incubated for 60 min prior to initiation of hypoxia. In the case of LTD_4-induced contractions, L-660,711 was added cumulatively (10^{-8} to 10^{-6} M), 30 min after the tension had reached a plateau ($n = 7$). The relaxation by L-660,711 was noted 60 min after each addition. Asterisks denote significant difference ($P < 0.05$) compared to control tension before addition of L-660,711.

tension of the rings was increased by an average of 0.67 ± 0.14 g. This contraction was inhibited by NDGA (5×10^{-6} M; from 0.67 ± 0.14 g to 0.25 ± 0.13 g, $n = 6$) as well as by L-660,711 (10^{-5} M; from 0.59 ± 0.15 g to 0.29 ± 0.11 g, $n = 5$). Leukotriene D_4 (10^{-8}–10^{-7} M) caused a gradual and sustained increase in tension of the artery. The tension increased by an average of 0.28 ± 0.05 g, 0.41 ± 0.05 g, 0.73 ± 0.13 g and 0.75 ± 0.14 g after 30, 60, 120 and 180 min, respectively. L-660,711 relaxed this increased tension in a dose-dependent manner, the dose-response curve being monophasic and achieving full inhibition at 10^{-6} M (Figure 3). In contrast, this antagonist appeared to inhibit hypoxic contraction in at least two steps. An initial phase of inhibition was seen with a concentration of 10^{-8} M L-660,711 (from 1.06 ± 0.14 g to 0.62 ± 0.13 g). The effect reached a plateau at concentrations of 10^{-7} M (0.51 ± 0.12 g) and 10^{-6} M (0.48 ± 0.12 g) before showing a second phase of inhibition at 10^{-5} M L-660,711 (0.06 ± 0.03 g). The change in tension produced by each concentration of L-660,711 was statistically significant at $P < 0.05$ (Repeated Analysis of Variance with Tukey's test).

Effects of adenosine on hypoxia- and leukotriene D_4-induced contractions of canine isolated basilar artery

Canine basilar artery rings contracted by hypoxia were completely relaxed by exposure to 5×10^{-6} M adenosine by 92% ($n = 6$, Elliott, 1989) (Figure 1b). Pretreatment with adenosine also attenuated hypoxic contraction in a dose-dependent manner (Elliott, 1989). The increase in tension caused by LTD_4 (10^{-8} M–10^{-7} M) was also reduced rapidly by adenosine (5×10^{-6} M) from 0.87 ± 0.13 g to 0.19 ± 0.07 g ($P = 0.001$ by paired t test; $n = 6$; Figure 1c).

Discussion

Hypoxia caused contraction of the canine isolated basilar artery. Previous studies have shown that this hypoxia-induced contraction was not due to adrenergic, muscarinic, histaminergic or 5-hydroxytryptaminergic mechanisms, nor was it due to the release of prostaglandins (Mallick *et al.*, 1987). Our present experiments now suggest that leukotrienes may play a role in mediating hypoxic contraction.

Leukotrienes are components of the slow reacting substance of anaphylaxis and are products of metabolism of arachidonic acid via the 5-lipoxygenase pathway. Recently leukotrienes have been shown to be potent vasoconstrictors, particularly in coronary (Kito *et al.*, 1981; Michelassi *et al.*, 1982; Kopia *et al.*, 1987) and cerebral arteries of several species including man (Tagari *et al.*, 1983; Rosenblum, 1985; Busija *et al.*, 1986; Jancar *et al.*, 1987; Nishiye *et al.*, 1988). In agreement with other authors, we have also noted the constrictor effect of leukotrienes on canine isolated basilar artery rings. This supports the notion that leukotrienes may be involved in regulating cerebral vascular tone under certain pathological conditions, e.g. hypoxia and/or ischaemia, in which their production has been shown to be increased (Moskowitz *et al.*, 1984; Kiwak *et al.*, 1985; Ban *et al.*, 1989).

NDGA, an inhibitor of lipoxygenase, blocked hypoxia-induced smooth muscle contraction in this study. Although indomethacin, a cyclo-oxygenase inhibitor, has no effect on these contractions, ETYA, an inhibitor of both lipoxygenase and cyclo-oxygenase, abolished them in previous experiments (Elliott, 1989). These results indicate that leukotrienes may be involved in the generation of vascular tone during hypoxia. The release of arachidonic acid from phospholipids is facilitated by phospholipase A_2. Quinacrine, which is reputed to inhibit phospholipase A_2 (Viga *et al.*, 1980), blocked hypoxia-induced contractions. This evidence is important because quinacrine acts at a different site along the arachidonate metabolic pathway from NDGA and both steps are crucial in the production of leukotrienes.

Our hypothesis that leukotrienes are involved in hypoxia-induced contractions was further supported by the ability of a leukotriene antagonist to inhibit hypoxia-induced contractions. We used the selective LTD_4 receptor antagonist L-660,711 (Jones *et al.*, 1988) and found that low concentrations inhibited both hypoxia- and LTD_4-induced contraction, supporting the possibility that LTD_4 may play an important role in hypoxic contraction. However, the apparent resistance of part of the hypoxic contraction to L-660,711 suggests that other mediators may be involved. Further studies are needed to clarify this question.

Hypoxic contractions were usually larger than LTD_4-induced contractions. The size of post-hypoxic contraction may depend upon the amount of endogenously produced leukotriene(s) and also on the sensitivity of the vessel. In coronary artery, the hypoxic response was antagonized by inhibitors of lipoxygenase but not inhibitors of cyclo-oxygenase (Vanhoutte *et al.*, 1985). It was proposed that under hypoxic conditions, endogenous arachidonic acid was shunted through the lipoxygenase pathway, leading to increased production of leukotrienes which open calcium channels. Enhanced entry of calcium may result in activation of phospholipase A_2, release of more arachidonic acid and its metabolism by the lipoxygenase pathway to leukotriene(s), causing contractile activation of the vascular smooth muscle. However, in the above study this point was not actually determined and it was not stated how hypoxia could selectively inhibit cyclo-oxygenase and spare lipoxygenase. Additionally, leukotrienes produced endogenously during hypoxia may have a greater access to the receptors than when administered exogenously. Another explanation for the larger contraction during hypoxia could be that the action of leukotriene(s) may be potentiated by hypoxia. This is a possibility which needs further study.

Arachidonic acid caused contraction of the smooth muscle as has also been observed by others (Koide *et al.*, 1981; Jancar *et al.*, 1987) and this may be attributable to metabolites of the cyclo-oxygenase and the lipoxygenase pathways that have vasoconstrictor properties. However, Koide *et al.* (1981) and Jancar *et al.* (1987) found that arachidonic acid-induced contraction was not significantly inhibited by cyclo-oxygenase inhibitors, e.g. indomethacin and acetylsalicylic acid, while NDGA, BW755C (which inhibits both lipoxygenase and cyclo-oxygenase pathways) and FPL 55712 (which blocks LTC_4 receptors; Rosenblum, 1985) inhibited the contraction induced by arachidonic acid, implying that leukotrienes, but not prostaglandins, mediate contractions induced by arachidonic acid. In our studies, both NDGA and L-660,711 inhibited the arachidonic acid-induced contractions, further confirming that arachidonic acid-induced contractions are mediated by the lipoxygenase metabolites.

The possibility that hypoxic contractions could be through an effect on the endothelium has been previously examined by us in the canine isolated basilar artery (Elliott *et al.*, 1989). It was shown that the hypoxic contraction of canine basilar artery was only partially blocked after mechanical and chemical removal of the endothelium. The present study was done in vessels with intact endothelium. In a preliminary study the effect of hypoxia on endothelium-derived relaxing factor (EDRF) was examined and it was found that the release of EDRF by acetylcholine is not impaired during hypoxia (Gu, Ong & Bose, unpublished findings). Thus, a significant amount of hypoxic contraction, presumably due to leukotriene(s), is independent of the endothelium.

Constriction of cerebral vessels is seen under certain pathological circumstances (e.g. ischaemia followed by reperfusion), resulting in impaired cerebral blood flow (Todd *et al.*, 1986). The mechanism of this phenomenon is not well understood. Our present experiments are of interest because it is possible that hypoxia-induced constriction may be responsible for cerebral vascular constriction induced by ischaemia/reperfusion (Todd *et al.*, 1986). However, *in vivo* experiments

have consistently shown an increase in cerebral blood flow during hypoxia followed by a decrease upon reoxygenation (Pulsinelli *et al.*, 1982; Todd *et al.*, 1986). This has been explained on the basis of increased production of a potent vasodilator, adenosine, by the brain parenchyma during hypoxia, *in vivo* (Winn *et al.*, 1981). The production of leukotrienes has also been shown to be increased during hypoxia, *in vivo* (Kiwak *et al.*, 1985). In our *in vitro* experiments, hypoxia caused vasoconstriction because the action of the vasoconstrictor mediator was not antagonized by adenosine, as is the case *in vivo*. The finding that adenosine does antagonize hypoxia- as well as leukotriene-induced constriction, *in vitro*, supports the hypothesis that the constrictor effect of leukotriene(s) may be antagonized *in vivo* by adenosine released from brain cells. We have found that rat pial arterioles, *in vivo*, dilate when subjected to hypoxia. However during reoxygenation they exhibit a phase of vasoconstriction (Gu *et al.*, unpublished observations). This delayed vasoconstriction may be a result of the washout of adenosine followed by a more sustained action of the leukotrienes released during hypoxia. However, in order to prove our hypothesis, the interactions between leukotrienes and adenosine needs to be studied *in vivo*.

In conclusion, our data show that leukotrienes may be involved in hypoxia-induced contraction of canine isolated basilar artery. Since a component of the hypoxic contraction is less sensitive to blockade by L-660,711, the role of other mediator(s), including other products of the lipoxygenase pathway, cannot be excluded. The possible role of this phenomenon in delayed vasoconstriction during global cerebral ischaemia, *in vivo*, needs to be evaluated.

This work was supported by grants-in-aid from the Medical Research Council of Canada and the Manitoba Heart and Stroke Foundation. M.G. received a studentship from the Manitoba Health Research Council.

References

BAN, M., TONAI, T., KOHNO, T., MATSUMOTO, K., HORIE, T., YAMAMOTO, S., MOSKOWITZ, M.A. & LEVINE, L. (1989). A flavinoid inhibitor of 5-lipoxygenase inhibits leukotriene production following ischemia in gerbil brain. *Stroke*, **20**, 248–252.

BUSIJA, D.W., LEFFLER, C.W. & BEASLEY, D.G. (1986). Effects of leukotrienes C_4, D_4 and E_4 on cerebral arteries of newborn pigs. *Pediatr. Res.*, **20**, 973–976.

ELLIOTT, D.A. (1989). Role of endothelium, lipoxygenase products and membrane depolarizing factors in hypoxic contraction of the canine isolated basilar artery. *M.Sc. Thesis, University of Manitoba.*

ELLIOTT, D.A., ONG, B.Y., BRUNI, J.E. & BOSE, D. (1989). Role of endothelium in hypoxic contraction of canine basilar artery. *Br. J. Pharmacol.*, **96**, 949–955.

JANCAR, S., SCHULZ, R., KRUEGER, C. & COOK, D.A. (1987). Mechanisms of arachidonic acid-induced contractions of canine cerebral arteries. *Eur. J. Pharmacol.*, **136**, 345–352.

JONES, T.R., ZAMNONI, R., BELLEY, M., CHAMPION, E., CHARETTE, L., FORD-HUTCHINSON, A.W., FRENETTE, R., GAUTHIER, J-Y., LEGER, S., MASSON, P., McFARLANE, C.S., PIECHUTA, H., ROKACH, J., WILLIAM, H., YOUNG, R.N., DEHAVEN, R.N. & PONG, S.S. (1988). Pharmacology of L-660,711 (MK-571): a novel potent and selective leukotriene D_4 receptor antagonist. *Can. J. Physiol. Pharmacol.*, **67**, 17–28.

KITO, G., OKUDA, H., OHKAWA, S., TERAO, S. & KIKUCHI, K. (1981). Contractile activities of leukotriene C_4 and D_4 on vascular strips from rabbits. *Life Sci.*, **29**, 1325–1332.

KIWAK, K.J., MOSKOWITZ, M.A. & LEVINE, L. (1985). Leukotriene production in gerbil brain after ischemic insult, subarachnoid hemorrhage and concussive injury. *J. Neurosurg.*, **62**, 865–869.

KOIDE, T., NODA, Y., HATA, S., SUGIOKA, K., KOBAYASHI, S. & NAKANO, M. (1981). Contraction of canine basilar artery following linoleic acid, arachidonic acid, 13-hydroxyperoxylinoleic or 15-hydroxyperoxy arachidonic acid. *Proc. Soc. Exp. Biol. Med.*, **168**, 399.

KOPIA, G.A., VALOCIK, R.E., TORPHY, T.J., CIESLINKSI, L.B., SARAV, H.M., FOLEY, J.J. & WASSERMAN, M.A. (1987). Inhibition of leukotriene D_4-induced coronary vasoconstriction by leukotriene antagonists in anesthetized dog. *J. Pharmacol. Exp. Ther.*, **241**, 174–180.

MALLICK, B.A., BOSE, D., CHAU, T. & ONG, B.Y. (1987). Mechanism of impaired myogenic response in cerebral blood vessels during posthypoxic recovery. *Can. J. Physiol. Pharmacol.*, **65**, 159–164.

MICHELASSI, F., LANDA, L., HILL, R.D., LOWENSTEIN, E., WATKINS, W.D., PETKAU, A.J. & ZAPOL, W.M. (1982). Leukotriene D_4: a potent coronary artery vasoconstrictor associated with impaired ventricular contraction. *Science*, **217**, 841–843.

MOSKOWITZ, M.A., KIWAK, K.J., HEKIMIAN, K. & LEVINE, L. (1984). Synthesis of compounds with properties of leukotriene C_4 and D_4 in gerbil brains after ischemia and reperfusion. *Science*, **224**, 886–889.

NISHIYE, E., ITOH, T. & KURIYAMA, H. (1988). Some effects of leukotriene D_4 on the mechanical properties of the guinea-pig basilar artery. *Br. J. Pharmacol.*, **93**, 591–600.

PULSINELLI, W.A., LEVY, D.E. & DUFFY, T.E. (1982). Regional cerebral blood flow and glucose metabolism following transient forebrain ischemia. *Ann. Neurol.*, **11**, 499–509.

REILLY, I.A.G. & FITZGERALD, G.A. (1988). Aspirin in cardiovascular disease. *Drugs*, **35**, 154–176.

ROSENBLUM, W.I. (1985). Constricting effect of leukotrienes on cerebral arterioles of mice. *Stroke*, **16**, 262–263.

SUZUKI, N., NAKAMURA, T., IMABAYASHI, S., ISHIKAWA, Y., SASAKI, T. & ASANO, T. (1983). Identification of 5-hydroxyeicosatetraenoic acid in cerebrospinal fluid after subarachnoid hemorrhage. *J. Neurochem.*, **41**, 1186–1189.

TAGARI, P., DU BOULAY, G.H., AITKEN, V. & BOULLIN, D.J. (1983). Leukotriene D_4 and cerebral vasculature *in vivo* and *in vitro*. *Prostaglandins, Leukot. Med.*, **11**, 281–297.

TODD, N.V., PICOZZI, P. & CROCKARD, H.A. (1986). Quantitative measurement of cerebral blood flow and cerebral blood volume after cerebral ischemia. *J. Cereb. Blood Flow Metab.*, **6**, 338–341.

VANHOUTTE, P.M., RIMELE, T.J. & FLAVAHAN, N.A. (1985). Lipoxygenase and calcium entry in vascular smooth muscle. *J. Cardiovasc. Pharmacol.*, **7** (Suppl.), S47–S52.

VIGO, C., LEWIS, G.P. & PIPER, P.J. (1980). Mechanisms of inhibition of phospholipase A_2. *Biochem. Pharmacol.*, **29**, 623–627.

WINN, H.R., RUBIO, R. & BERNE, R.M. (1981). Brain adenosine concentration during hypoxia in rats. *Am. J. Physiol.*, **241**, H235–H242.

(Received November 26, 1990
Revised January 25, 1991
Accepted February 14, 1991)

Br. J. Pharmacol. (1991), **103**, 1633–1640 © Macmillan Press Ltd, 1991

Pharmacological modulation of endothelin-induced contraction of guinea-pig isolated airways and thromboxane release

[1]János G. Filep, Bruno Battistini & Pierre Sirois

Department of Pharmacology, Faculty of Medicine, University of Sherbrooke, Sherbrooke, P.Q., Canada, J1H 5N4

1 The aim of the present experiments was to study the possible involvement of known bronchoconstrictor substances in mediating the myotropic action of endothelin-1 (ET-1, human-porcine endothelin) in guinea-pig isolated airways.

2 ET-1 (1–100 nM) caused a dose-dependent contraction of guinea-pig trachea, upper bronchus and parenchyma. The contractions developed slowly, reaching maximal values 4–6 min after addition of the peptide.

3 The contractile action of ET-1 was significantly attenuated by indomethacin (10 μM), a cyclo-oxygenase blocker, BM 13505 (5 μM), a thromboxane receptor antagonist, FPL 55712 (19 μM) and YM 16638 (1 μM), antagonists of the sulphidopeptide leukotrienes, BN 52021 (10 μM) and WEB 2086 (1 μM), platelet-activating factor receptor antagonists in all three tissue preparations studied.

4 Pretreatment of the airway tissues with compound U 75302 (3 μM), a selective leukotriene B_4 receptor antagonist, or with a mixture of antagonists containing methysergide (0.75 μM), phentolamine (0.4 μM), propranolol (13 μM), atropine (0.4 μM) and diphenhydramine (0.45 μM) did not modify the myotropic action of ET-1.

5 ET-1, 10 and 100 nM induced three, and nine fold increases in thromboxane A_2 release from lung parenchymal strips.

6 ET-1-induced thromboxane A_2 release was completely abolished by indomethacin, and was significantly attenuated by BN 52021, WEB 2086 and FPL 55712. Neither BM 13505 nor YM 16638 exerted a significant effect on thromboxane release.

7 The present findings show that contraction of guinea-pig airway smooth muscle by ET-1 is mediated, in part, by the release of thromboxane A_2, sulphidopeptide leukotrienes and platelet-activating factor, and suggest that the increased thromboxane A_2 release following ET-1 is partly a consequence of enhanced synthesis of sulphidopeptide leukotrienes and platelet-activating factor.

Keywords: Endothelin; thromboxane release; leukotrienes; PAF; bronchoconstriction; isolated airways (guinea-pig)

Introduction

Endothelin-1 (ET-1, porcine or human endothelin) is a potent vasoconstrictor peptide of 21 amino acids, originally identified in the culture medium of aortic endothelial cells (Yanagisawa *et al.*, 1988). Recently, the release of ET-1 by cultured tracheal epithelial cells has also been reported (Black *et al.*, 1989). Its production in the vicinity of airway smooth muscle suggests that ET-1 could affect adjacent local airway tone. *In vitro* and *in vivo* studies indicate that ET-1 exerts a potent contractile effect on guinea-pig and human isolated bronchial and tracheal tissues (Uchida *et al.*, 1988; Maggi *et al.*, 1989; Borges *et al.*, 1989; Advenier *et al.*, 1990; Battistini *et al.*, 1990). Furthermore, intravenous or aerosol administration of ET-1 to anaesthetized guinea-pigs evoked sustained bronchoconstriction (Payne & Whittle, 1988; Lagente *et al.*, 1989; Macquin-Mavier *et al.*, 1989). The slow onset of the contractile action of ET-1 raises the possibility that its effects are, in part, mediated by release of secondary mediators. Experimental evidence supporting this hypothesis is derived from the studies where intravenous administration of different cyclo-oxygenase blockers (Payne & Whittle, 1988; Lagente *et al.*, 1989; Macquin-Mavier *et al.*, 1989) or pretreatment of isolated airway tissues with thromboxane receptor antagonists (Battistini *et al.*, 1990) resulted in a significant inhibition of airway responses to ET-1. Although these findings suggest an important role for cyclo-oxygenase products, especially thromboxane A_2 (TxA_2) in the pulmonary actions of ET-1, they do not exclude the possibility that ET-1 could release other bronchoconstrictor mediators. The present experiments were designed to study this latter possibility by employing specific receptor antagonists of known bronchoconstrictor agents, including leukotrienes, platelet-activating factor (PAF), histamine, 5-hydroxytryptamine (5-HT) and acetylcholine. Since some of these mediators are also capable of enhancing pulmonary TXA_2 formation (Piper & Samhoun, 1981; Ueno *et al.*, 1982; Lefort *et al.*, 1984; Chung *et al.*, 1986), the effects of their antagonists on ET-1-induced TXA_2 release were also studied.

[1] Author for correspondence.

Methods

Tissue preparation

Male Dunkin-Hartley guinea-pigs weighing 400–560 g were killed by cervical dislocation and rapidly bled. The trachea, upper bronchi and lung parenchyma were rapidly excised, placed in Krebs-Henseleit buffer solution and delicately trimmed of excess connective tissue and fat. The tracheae were cut into two equal segments. Then the tracheal segments and the left and right upper bronchi were cut in spirals of approximately 2.8 mm wide × 30 mm long and 1.5 mm wide × 1.5 cm long, respectively. Two strips of peripheral parenchyma (approximately 2 × 3 × 22 mm) were also prepared from the anterior surface of lower lung lobes. Tissues were mounted separately in 5 ml organ baths and were connected to isotonic force-displacement transducers (Grass model FTO3C) under an initial tension of 1.5 g. Tissues were equilibrated for 60 min in oxygenated (95% O_2 and 5% CO_2) Krebs-Henseleit solution (composition, mM: NaCl 118, KCl 4.7, $CaCl_2$ 2.5, KH_2PO_4 1.18, $NaHCO_3$ 25, $MgSO_4 . 7H_2O$ 1.18 and glucose 11.1) at 37°C, pH 7.0. Changes in tension were recorded continuously on a Grass 7D polygraph.

Experimental protocol

Following the equilibration period, pairs of tissues were preincubated with one of the following drugs or its vehicle: indomethacin (10 μM); the thromboxane receptor antagonist, BM 13505 (5 μM) (Patscheke *et al.*, 1987); U 75302 (3 μM), a selective leukotriene (LT) B_4 receptor antagonist (Lawson *et al.*, 1989); FPL 55712 (19 μM) and YM 16638 (1 μM), sulphidopeptide leukotriene receptor antagonist (Augstein *et al.*, 1973; Tomioka *et al.*, 1988); the PAF receptor antagonists, BN 52021 (10 μM) (Braquet *et al.*, 1985; Földes-Filep *et al.*, 1987) and WEB 2086 (1 μM) (Casals-Stenzel *et al.*, 1987); diphenhydramine (0.45 μM), a H_1-histamine receptor antagonist; methysergide (0.75 μM), a 5-HT antagonist; propranolol (13 μM), a β-adrenoceptor antagonist; phentolamine (0.4 μM), an α-adrenoceptor antagonist and atropine (0.4 μM), an anticholinoceptor drug. The preincubation time was 10 min, except for FPL 55712, when it was 2 min. Following preincubation, cumulative concentrations of synthetic ET-1 (1–100 nM) were added to the organ baths, the next concentration being added when the effect of the preceding one had reached a steady state level. Previous studies had indicated that 100 nM ET-1 evoked near maximal contraction in all three tissues studied (Uchida *et al.*, 1988; Maggi *et al.*, 1989; Battistini *et al.*, 1990). Thus in the present study, higher concentrations of ET-1 were not studied because of the limited availability of the peptide. In each experiment only one drug was used and only one concentration-response curve for ET-1 was recorded. To minimize variations between tissues, endothelin-induced responses are expressed as the percentage of the contraction evoked by 4.5 μM of histamine.

Endothelin-1-induced thromboxane A_2 release from the lung parenchyma

In another set of experiments the effects of the above mentioned drugs on ET-1-induced TXA_2 formation were also studied. Lung parenchyma strips were incubated under the same conditions as described above. Following a control incubation period of 4 min, tissues were treated for 10 min at 37°C with one of the following drugs: indomethacin (10 μM), BM 13505 (5 μM), FPL 55712 (19 μM), YM 16638 (1 μM), BN 52021 (10 μM) or WEB 2086 (1 μM). Then tissues were stimulated with two consecutive concentrations of ET-1 (10 and 100 nM). Following an incubation period of 4 min, an aliquot of the medium was removed and stored at −20°C until analysis of TXB_2, the stable metabolite of TXA_2. Only one drug was tested in each parenchymal strip.

TXB_2 concentrations were measured by an enzyme immunoassay according to the method of Pradelles *et al.* (1985). The detection limit of the assay was 0.3 pg/tube. Intraassay and interassay coefficients of variation were 4.3% ($n = 6$) and 6.1% ($n = 8$), respectively. The TXB_2 antiserum (Cayman Labs, Ann Arbor, MI, U.S.A.) had less than 1% cross reactivity with other prostanoids.

Statistical analysis

All values are expressed as means ± s.e.mean. Statistical analysis of the data was performed by a Dunn multiple contrast hypothesis test (Dunn, 1964) or by a Mann-Whitney U test, as appropriate. A $P < 0.05$ level was considered significant for all tests.

Drugs

Endothelin-1 (Peninsula Labs, Belmont, CA, U.S.A.) was dissolved in distilled water and stored in aliquots at −20°C. Other drugs were freshly prepared each day and included indomethacin (Merck, Sharp & Dohme, Canada), BM 13505 (4-[2-(4-chlorobenzene sulphonylamino)ethyl] benzene acetic acid, Boehringer-Mannheim GmbH, FRG); FPL 55712 (sodium 7-[3-(4-acetyl-3-hydroxy-2-propylphenoxy)-2-hydroxypropoxy]-4-oxo-8-propyl-4H-1-benzopyran-2-carboxylate, Fisons Pharmaceuticals, Loughborough, England); YM 16638 ([[5-[[3-(4-acetyl-3-hydroxy-2-propylphenoxy)-propyl] thio]-1,3,4-thiadiazol-2-yl]thio]acetic acid, Yamanouchi Pharmaceuticals, Tokyo, Japan); U 75302 (6-(6-[3-hydroxy-1E,5Z-undecadienyl]-2-pyridinyl)-1,5-hexanediol, Upjohn Co., Kalamazoo, MI); BN 52021 (ginkgolide B, Institut Henri Beaufour, Le Plessis Robinson, France); WEB 2086 (3-[4-(2-chlorphenyl) -9-methyl-6H-thienol [3,2-f] [1,2,4] triazolo-[4,3-a] [1,4]-diazepine-2-yl]-1-(4-morpholinyl)-1-propanon, Boehringer-Ingelheim KG, FRG); phentolamine hydrochloride (CIBA-Geigy, Basel, Switzerland); methysergide hydrogen maleate (Sandoz Ltd, Basel, Switzerland); propranolol hydrochloride (Ayerst Labs, Montreal, Canada) diphenhydramine hydrochloride and atropine sulphate (Sigma Chemical Co., St. Louis, MO, U.S.A.). Drugs were dissolved in distilled water except BN 52021, U 75302 and YM 16638, which were dissolved in dimethylsulphoxide; BM 13505, indomethacin and FPL 55712 were dissolved in ethanol, and were diluted further with Krebs-Henseleit solution as appropriate. The final concentration of ethanol or dimethylsulphoxide in the organ bath never exceeded 0.1% (vol/vol).

Results

Pharmacological modulation of endothelin-1-induced contraction

ET-1 (1–100 nM) evoked a concentration-dependent, slowly developing, tonic contraction of guinea-pig isolated trachea, bronchus and parenchyma. The contraction reached a plateau 4–6 min after addition of the peptide to the organ bath. The threshold concentration of ET-1 for eliciting contraction was 1–5 nM in all three tissue preparations. Pretreatment of the tissues with the cyclo-oxygenase blocker, indomethacin (10 μM) significantly attenuated the contractile response to ET-1 over the entire concentration-range studied (Figure 1). Similarly, the concentration-response curves for ET-1 were shifted to the right in the presence of BM 13505 (5 μM), a specific thromboxane receptor antagonist (Figure 1). The inhibitory effects of indomethacin and BM 13505 were similar in parenchyma and trachea, whereas BM 13505 appeared to be slightly more potent in the upper bronchus (Figure 1).

The concentration-response curves obtained in the presence of FPL 55712 (19 μM), a sulphidopeptide leukotriene receptor antagonist were markedly depressed at lower concentrations (1–10 nM) of ET-1 (53–95% inhibition in all three tissues), but a slight, 10–36% inhibition was observed at higher ET-1 concentrations (50–10 nM) (Figure 2). However, these latter changes were also statistically significant. Similar tendencies were observed when tracheal and bronchial strips were pretreated with the other sulphidopeptide leukotriene receptor antagonist, YM 16638 (1 μM). In the parenchyma, the contractile action of ET-1, even at concentrations as low as 1–10 nM, was weakly antagonized by compound YM 16638 (10–18% inhibition versus 40–93% inhibition in the trachea and bronchus) (Figure 2). In contrast to sulphidopeptide leukotriene antagonism, blockade of the leukotriene B_4 (LTB_4) receptors by compound U 75302 (3 μM) did not affect significantly the myotropic effect of ET-1 in all three tissue preparations (Figure 3).

When isolated airway tissues were pretreated with the PAF receptor antagonist, BN 52021 (10 μM) or WEB 2086 (1 μM), ET-1-induced contractions were significantly attenuated over the entire concentration-range studied (Figure 4). At the concentrations employed, BN 52021 and WEB 2086 appeared to exert similar inhibition in all three tissues (Figure 4).

Preliminary experiments showed that in the presence of methysergide (0.75 μM), propranolol (13 μM), phentolamine (0.4 μM), atropine (0.4 μM) or diphenhydramine (0.45 μM) the contractile response of isolated airways to ET-1 was not significantly affected. Similarly, when these five drugs were com-

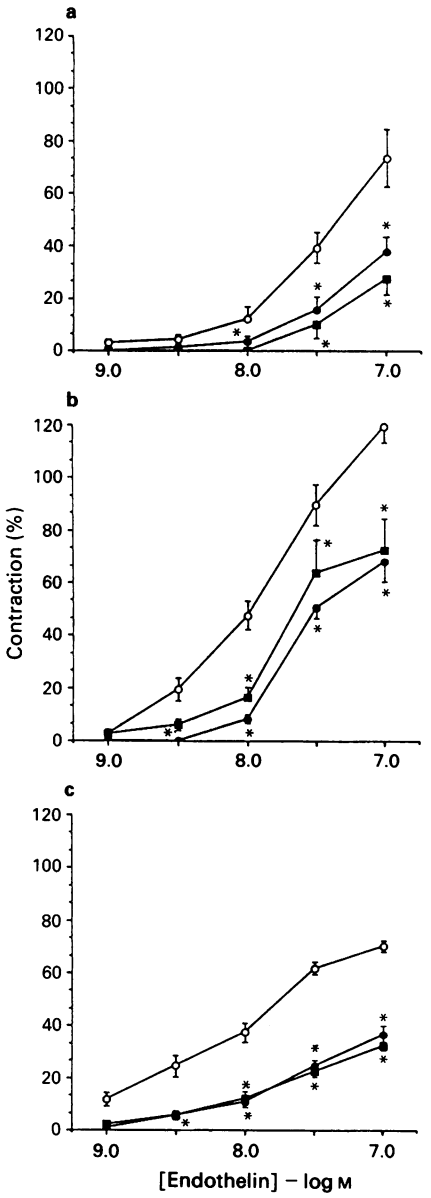


Figure 1 Inhibition by thromboxane receptor antagonist, BM 13505 (●) and indomethacin (■) of endothelin-1-induced contraction of guinea-pig isolated trachea (a), external bronchus (b) and lung parenchyma (c); control (○). Pairs of tissues were preincubated with BM 13505 (5 μM), indomethacin (10 μM) or their vehicle for 10 min. Number of experiments: in (a), (b) and (c) control $n = 9$; in (a) and (c) BM 13505 $n = 4$, and in (b) $n = 3$; in (a) indomethacin $n = 5$ and in (b) and (c), $n = 6$. Results are expressed as the percentage of the maximal response to 4.5 μM histamine, and are means with s.e.mean shown by vertical bars. * $P < 0.05$ (compared to control by Mann-Whitney U test).

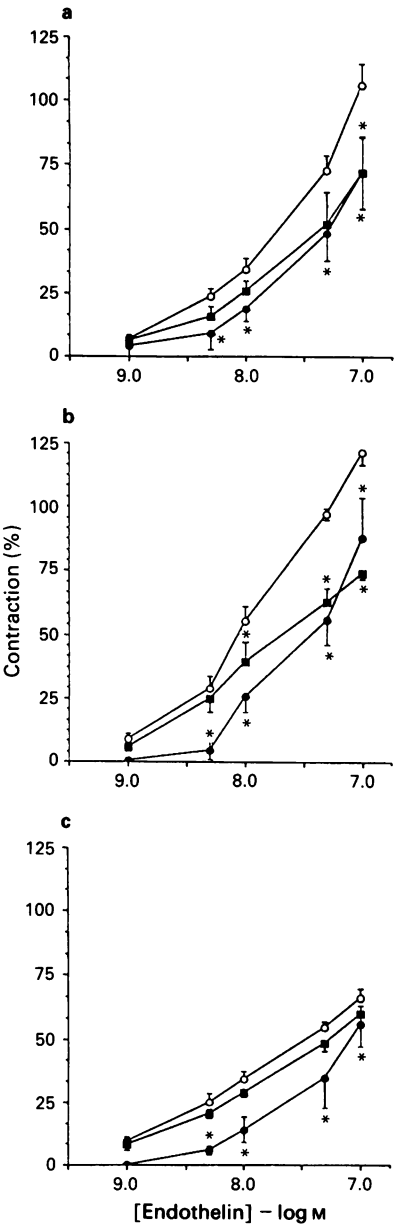


Figure 2 Effects of sulphidopeptide leukotriene receptor antagonists on endothelin-1-induced contraction of guinea-pig isolated trachea (a), external bronchus (b) and lung parenchyma (c). Pairs of tissues were preincubated with FPL 55712 (19 μM) (●), YM 16638 (1 μM) (■) or their vehicle (○) for 2 and 10 min, respectively. Number of experiments: in (a), (b) and (c), control $n = 9$; in (b) and (c) FPL 55712 $n = 4$, in (a) $n = 5$; in (b) and (c) YM 16638 $n = 5$, in (a) $n = 4$. Results are expressed as the percentage of the maximal response to 4.5 μM histamine, and are means with s.e.mean shown by vertical bars. * $P < 0.05$ (compared to appropriate control by Mann-Whitney U test).

bined, the concentration-response curves for ET-1 did not differ significantly from the control ones (Figure 5).

Ethanol or dimethylsulphoxide by itself, up to a concentration of 0.1%, neither affected the basal tone nor modified the response to ET-1 in all three tissue preparations (data not shown).

Inhibition of endothelin-1-induced thromboxane A_2 release

In another set of experiments the effects of ET-1 on thromboxane production by lung parenchymal strips were also studied. Analysis of the incubation medium showed that the basal release of TXA_2 was in the 150–300 pg range (Table 1). Consecutive addition of 10 and 100 nM ET-1 caused about three, and nine fold increases of thromboxane release, respectively (Table 1). Indomethacin (10 μM) treatment reduced basal TXA_2 release by more than 80%, and completely abolished the rise in TXA_2 release in response to ET-1 (Table 1). Neither basal nor ET-1-stimulated TXA_2 formation was affected by the thromboxane receptor antagonist, BM 13505 (5 μM) (Table 1).

The increase in TXA_2 formation following 10 and 100 nM ET-1 was significantly attenuated by FPL 55712 (19 μM). Although the other sulphidopeptide leukotriene antagonist, YM 16638 (1 μM) inhibited ET-1-induced TXA_2 release by more than 10%, these changes did not reach statistical significance (Table 1).

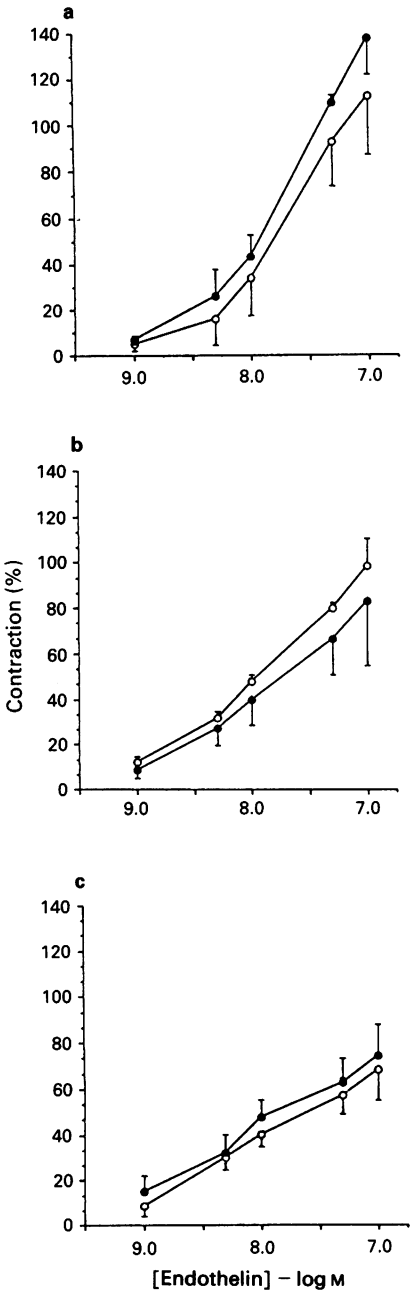


Figure 3 Endothelin-1-induced contraction of guinea-pig isolated trachea (a), bronchus (b) or lung parenchyma (c) in the absence and presence of a leukotriene B_4 receptor antagonist U 75302. Pairs of tissues were preincubated with compound U 75302 (3 μM) or its vehicle (○) for 10 min. Results are expressed as the percentage of the maximal response to 4.5 μM histamine, and are means with s.e.mean shown by vertical bars. In (a), (b) and (c) $n = 3$ for control and for U75302.

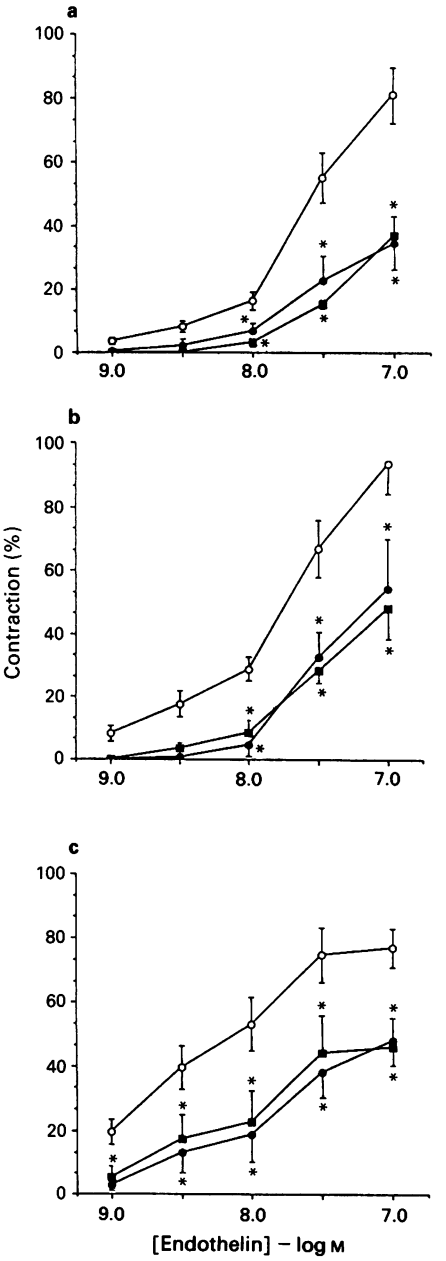


Figure 4 Inhibition by platelet-activating factor receptor antagonists of endothelin-1-induced contraction of guinea-pig isolated trachea (a), external bronchus (b) and lung parenchyma (c). Pairs of tissues were preincubated with WEB 2086 (1 μM) (●), BN 52021 (10 μM) (■) or their vehicle (○) for 10 min. Number of experiments: in (a), (b) and (c) control $n = 9$; in (a) and (c) WEB 2086 $n = 5$, in (b) $n = 4$; in (b) and (c) BN 52021 $n = 5$, in (a) $n = 4$. Results are expressed as the percentage of the maximal response to 4.5 μM histamine, and are means with s.e.mean shown by vertical bars. * $P < 0.05$ (compared to control by Mann-Whitney U test).

Table 1 Pharmacological modulation of endothelin-1 (ET-1)-induced thromboxane release from guinea-pig lung parenchymal strips

	In the absence of antagonist	*In the presence of antagonist*		
		Saline	ET-1 (10 nM)	ET-1 (100 nM)
Control ($n = 6$)	218 ± 27	190 ± 29	587 ± 38	2040 ± 160
Indomethacin ($n = 3$)	212 ± 32	29 ± 4**	16 ± 3**	35 ± 6**
BM 13505 ($n = 3$)	226 ± 43	211 ± 37	478 ± 25	2001 ± 55
FPL 55712 ($n = 3$)	254 ± 26	185 ± 28	306 ± 59*	963 ± 233*
YM 16638 ($n = 3$)	215 ± 23	231 ± 47	505 ± 61	1834 ± 170
WEB 2086 ($n = 3$)	238 ± 34	165 ± 11	349 ± 43*	1274 ± 52*
BN 52021 ($n = 3$)	194 ± 29	141 ± 20	394 ± 48*	1312 ± 114*

After a control period of 4 min, lung parenchymal strips were preincubated for 10 min with one of the drugs as indicated. Then tissues were challenged consecutively with saline (vehicle of ET-1), and 10 and 100 nM ET-1. Following an incubation period of 4 min, an aliquot was removed for determination of thromboxane B_2 (see Methods). Values are means ± s.e.mean and are referred to 100 mg of tissue (wet weight). Multiple comparisons were performed by Dunn's multiple contrast hypothesis test using ranks. * $P < 0.05$; ** $P < 0.01$.

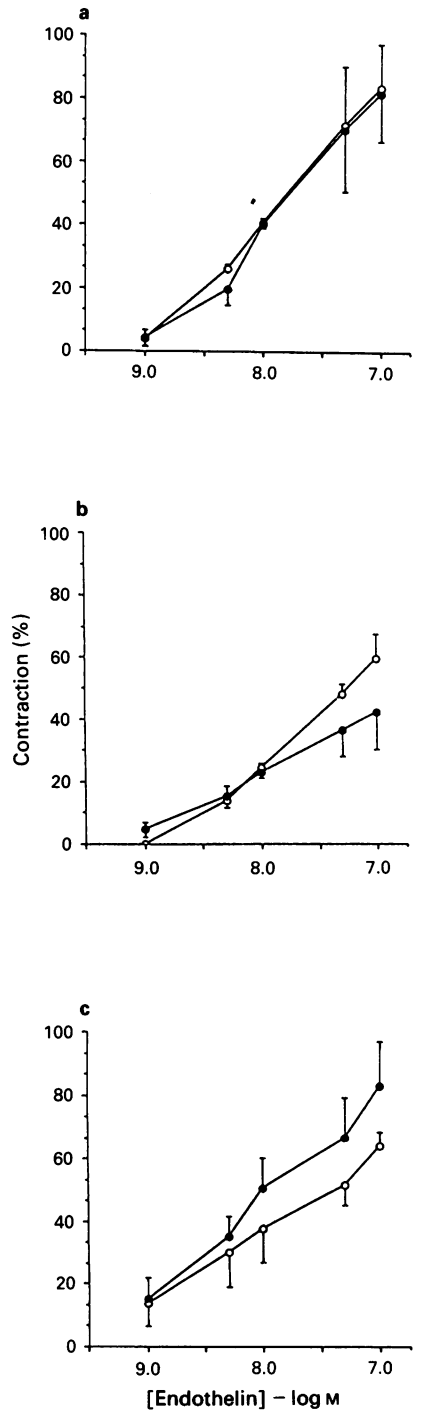


Figure 5 Endothelin-1-induced contraction of guinea-pig isolated trachea (a), bronchus (b) or lung parenchyma (c) in the absence (○) or presence (●) of a mixture of antagonists (MPPAD) containing methysergide (0.75 μM), phentolamine (0.4 μM), propranolol (13 μM), atropine (0.4 μM) and diphenhydramine (0.45 μM). Pairs of tissues were preincubated with the antagonists for 10 min. Results are expressed as mean with s.e.mean shown by vertical bars of 3 independent experiments.

Pretreatment of the lung parenchymal strips with PAF receptor antagonists was highly effective in reducing the effect of ET-1. TXA_2 release evoked by 10 and 100 nM ET-1 was inhibited by more than 30 and 40% by BN 52021 (10 μM) and WEB 2086 (1 μM), respectively (Table 1).

Preincubation of the tissues with compound U 75302 (3 μM), methysergide (0.75 μM), propranolol (13 μM), phentolamine (0.4 μM), atropine (0.4 μM) or diphenhydramine (0.45 μM) failed to interfere with ET-1-stimulated TXA_2 release (data not shown).

Discussion

The present findings provide evidence supporting the theory that TXA_2, sulphidopeptide leukotrienes and PAF may play an important role in mediating the myotropic action of ET-1 in guinea-pig isolated airways. The cyclo-oxygenase inhibitor, indomethacin (10 μM) significantly attenuated the contractile response to ET-1 in the trachea, bronchus and parenchyma. These findings are consistent with the data obtained *in vivo* in the guinea-pig, where indomethacin (10 mg kg^{-1}) or meclofenamate (0.5 to 2 mg kg^{-1}) suppressed the bronchoconstriction evoked by intravenous or aerosol administration of ET-1 (Payne & Whittle, 1988; Lagente *et al.*, 1989; Macquin-Mavier *et al.*, 1989). Others have reported that indomethacin (5 μM) depresses markedly the contractile response to lower concentrations of ET-1 (1–10 nM), whereas no significant inhibition was seen at higher ET-1 concentrations (50–300 nM) in the guinea-pig trachea *in vitro* (Maggi *et al.*, 1989). Recently, indomethacin (5 μM) has been reported to enhance the myotropic action of ET-1 in the guinea-pig trachea (Hay, 1990; Henry *et al.*, 1990). The reasons for this discrepancy are unclear at present, but it might be attributed to differences in tissue preparations (use of tracheal rings or segments in the previous studies versus zig-zag strips in the experiments of Maggi *et al.*, 1989, and helical strips in the present study) and/or to differences in the experimental protocols (lower initial load, different incubation buffers and exposure of the tissues to high concentrations of KCl or carbachol before studying the effects of ET-1 in the previous experiments) in addition to the different strains of guinea-pig used. ET-1 appeared to be more potent in our tracheal preparations (estimated EC_{50} 24.4 nM) than was previously reported (estimated EC_{50} values of 50–60 nM in the experiments of Hay, 1990 and Henry *et al.*, 1990). Another possibility might be that inhibition of prostaglandin synthesis by indomethacin is heterogeneous in lung tissue as was previously reported for the kidney (Attallah & Stahl, 1980). Since regional differences in prostanoid synthesis have also been demonstrated in pulmonary tissues (Raeburn, 1990), one may speculate that the cells which synthesize TXA_2 are more sensitive to indomethacin than those which produce relaxant prostanoids such as prostaglandin E_2 (PGE_2) and PGI_2. At low concentrations, indomethacin could potentiate whereas at high concentrations it could inhibit the myotropic response to ET-1. ET-1 has been shown to induce prostacyclin and TXA_2 release from pulmonary tissues both *in vivo* (De Nucci *et al.*, 1988) and *in vitro* (Filep *et al.*, 1990). Recent reports of the dose-related effects of indomethacin on basal prostanoid formation by intact guinea-pig trachea may lend further support to the above hypothesis. Indomethacin at a concentration of 2.8 μM inhibited prostacyclin release by about 80%, while it did not affect PGE_2 release (Bramley *et al.*, 1990). At a higher concentration (10 μM), indomethacin inhibited basal release of prostacyclin, TXA_2 (Filep *et al.*, 1990 and the present study) and PGE_2 release (Filep *et al.*, unpublished observations) by more than 75%.

Further evidence supporting a role for cyclo-oxygenase metabolites, especially TXA_2 is derived from the experiments with BM 13505, a specific thromboxane receptor antagonist (Patscheke *et al.*, 1987). Compound BM 13505 significantly attenuated the contractile response to ET-1 over the entire concentration-range studied in all three tissue preparations. Since neither basal nor ET-1-stimulated TXA_2 formation was affected by BM 13505, it is unlikely that it inhibited cyclo-oxygenase activity. Furthermore, at 5 μM, BM 13505 did not interfere with the biological responses to other bronchoconstrictor agents, including PAF, 5-HT (Patscheke *et al.*, 1987) and histamine (Battistini *et al.*, 1990). These findings indicate that the inhibitory action of BM 13505 can be attributed to antagonism of thromboxane receptors. Since at the concentrations employed; indomethacin and BM 13505 inhibited ET-1-induced contractions to a similar degree, one may assume that the effect of indomethacin may be largely the con-

sequence of inhibition of thromboxane synthesis. Before concluding, however, that TXA_2 is the sole mediator of the bronchoconstrictor action of ET-1, one should keep in mind that indomethacin reduced ET-1-induced airway contraction by about 50%, while it completely inhibited ET-1-induced TXA_2 release. Recently it has been reported that the thromboxane receptor antagonist, SQ 29 548 did not inhibit the myotropic response to ET-1 in the guinea-pig trachea (Hay, 1990). In this latter study, the sensitivity of tissues to ET-1 was lower than in our preparation (see above). Although the reasons for the different sensitivity are not known, it might be that the ability of ET-1 to induce thromboxane formation varies from tissue preparation to preparation, which might also explain the discordant results obtained with compounds BM 13 505 and SQ 29 548.

Preincubation of guinea-pig isolated airways with compound U 75302, a selective LTB_4 receptor antagonist (Lawson et al., 1989) did not modify significantly the myotropic action of ET-1. At a concentration of 3 μM, compound U 75302 completely abolished the contractile response of the guinea-pig parenchyma to 1–100 nM LTB_4 (Lawson et al., 1989). Since under the same experimental conditions, compound U 75302 exerted a slight partial agonist effect (Lawson et al., 1989), it is not clear at present whether or not some of its antagonist activity was due to desensitization of the LTB_4 receptors. In contrast to LTB_4 receptor blockade, antagonism of sulphidopeptide leukotriene receptors was effective in inhibiting the contractile response to ET-1. The inhibitory action of compounds YM 16638 (1 μM) and FPL 55712 (19 μM) was similar in the trachea and bronchus, while compound YM 16638 was less potent in the parenchyma. The reason for this latter finding is not clear, but it might be related to the different effects of FPL 55712 and YM 16638 on ET-1-induced TXA_2 formation (see below). At present it is not known whether FPL 55712 or YM 16638 can be used to distinguish between LTC_4 and LTD_4 receptors. Indeed, FPL 55712 has been described as a selective LTC_4 (Bach et al., 1979) or LTD_4 receptor antagonist (Casey et al., 1983), while others have failed to find a selective antagonism (Letts & Piper, 1982; Filep et al., 1987). YM 16638 was reported to be a 3 to 6 times more potent antagonist of LTC_4 than LTD_4 (Tomioka et al., 1988). In contrast to the present findings, ET-1-induced contractions of guinea-pig tracheal smooth muscle were not altered by the leukotriene receptor antagonist, SKF 104 353 (Hay, 1990). However, these latter and the present experiments are not easily comparable, since Hay's experiments were performed in the presence of 5 μM indomethacin. Cyclooxygenase inhibition is thought to decrease basal smooth muscle tone but not all studies record this effect (Raeburn, 1990). The compound SKF 104 353 was shown to interact with the effects of U-44069, a thromboxane A_2-mimetic (Bramley et al., 1990). This effect may have been non-specific and might be a consequence of further alteration of basal smooth muscle tone by SKF 104 353. The decreased basal tone can lead to an apparent increase in maximal response to the agonist (Raeburn, 1990), which, in turn, might have overshadowed the inhibitory effect of the leukotriene receptor blockade.

To study the possible involvement of PAF in mediating the contractile effect of ET-1, guinea-pig isolated airways were pretreated with the specific PAF receptor antagonists, BN 52021 (Braquet et al., 1985; Földes-Filep et al., 1987) or WEB 2086 (Casals-Stenzel et al., 1987). At concentrations of 10 μM and 1 μM, respectively, which have previously been shown to inhibit the pulmonary actions of exogenous PAF (Desquand et al., 1986; Pretolani et al., 1987), both BN 52021 and WEB 2086 significantly diminished the myotropic action of ET-1. These two structurally unrelated PAF receptor antagonists exerted similar inhibitory actions in isolated airways. These findings suggest the possible involvement of PAF in the contractile action of ET-1 on the airway. This hypothesis is further supported by the *in vivo* effectiveness of BN 52021 (10 mg kg^{-1}) in diminishing bronchoconstriction evoked by aerosol administration of ET-1 (Lagente et al., 1989) and ET-1-induced contraction of isolated glomeruli and mesangial cells (López-Farré et al., 1990). Furthermore, in this latter study ET-1 was found to increase PAF production by mesangial cells in a dose-dependent fashion (López-Farré et al., 1990). This speculation should, however, be tempered by the fact that studies examining the effects of PAF on guinea-pig isolated large airways and parenchymal strips resulted in conflicting data, as both contractions and relaxations were reported (reviewed by Halonen et al., 1990). Thus it remains disputable whether the *in vivo* bronchoconstrictor action of ET-1 is mediated via a direct or indirect mechanism (Barnes, 1988). Nevertheless, it is possible that PAF applied to different preparations of isolated airways may be bound and/or metabolized to various extents by the exterior surface of the tissues, and consequently, in certain preparations PAF cannot reach the contractile tissues that might be less accessible (Halonen et al., 1990).

The constrictor action of ET-1 was not modified by pretreatment of the isolated airway tissues with methysergide or with diphenhydramine. This latter observation is in keeping with the lack of histamine release from guinea-pig isolated perfused lung stimulated with ET-1 (Touvay et al., 1990). Furthermore, ET-1-induced contractions were similar in the absence and presence of atropine, propranolol and phentolamine. In contrast, enhanced bronchoconstriction following intravenous administration of ET-1 was reported in propranolol-treated guinea-pigs (Macquin-Mavier et al., 1989; Touvay et al., 1990). Since the bronchopulmonary responses to ET-1 were not potentiated by propranolol when ET-1 was administered by aerosol (Lagente et al., 1989), it may be concluded that propranolol possesses a systemic rather than a local airway activity, which may not be related to β-adrenoceptor blockade (Ney et al., 1983).

Although in the present study the actions of ET-1 on lung parenchymal strips in the presence of various inhibitors closely resembled its effects on large airways, it should be remembered that the peripheral lung parenchymal strips are complex tissues and cannot be interpreted only as peripheral airways. The contractile elements of the lung parenchyma include both small airway and vascular smooth muscle cells and contractile cells located in the alveolar septa (Goldie et al., 1984). Therefore, the observed effects of ET-1 are likely to be the result of its combined action on these elements. Numerous papers have demonstrated the potent contractile action of ET-1 in most vascular beds (for recent review see Yanagisawa & Masaki, 1989). For example, ET-1 was found to be a more potent myotropic agent in the rat aorta than in the guinea-pig trachea (Hay, 1990). The maximal responses to ET-1 in the rat aorta were significantly reduced by indomethacin (1 μM) or a thromboxane receptor antagonist (Eglen et al., 1989). These findings are similar to our observations in the parenchyma. Interestingly, ET-1 was reported to dilate the rat pulmonary vascular bed (Hasunuma et al., 1990). Thus, if ET-1 could induce relaxation of pulmonary small blood vessels, contraction of the isolated parenchyma would have been the result of its action on the airway and/or interstitial contractile cells.

ET-1-induced contraction of lung parenchymal strips was associated with a dose-dependent release of TXA_2. Previously ET-1 has been shown to be able to induce prostanoid, including TXA_2 release from perfused guinea-pig lungs (De Nucci et al., 1988). Since the myotropic action of ET-1 can be attenuated by sulphidopeptide leukotriene and PAF receptor antagonists, and the contractile activity of these mediators in the guinea-pig lung is thought to depend on TXA_2 formation (Engineer et al., 1978; Piper & Samhoun, 1981; Ueno et al., 1982; Hamasaki et al., 1984; Lefort et al., 1984; Chung et al., 1986; Jancar et al., 1989), it is reasonable to assume that the enhanced TXA_2 formation in response to ET-1 might be, in part, a consequence of increased synthesis of PAF and sulphidopeptide leukotrienes. Indeed, preincubation of the parenchymal strips with the PAF receptor antagonists, BN 52021 and WEB 2086 or with FPL 55712 significantly diminished

TXA_2 release following addition of ET-1. Previous studies have demonstrated that none of the PAF antagonists used are capable of inhibiting cyclo-oxygenase activity at the concentrations employed (Braquet *et al.*, 1985; H. Heuer, personal communication). On the other hand, it is uncertain at present whether FPL 55712 could affect cyclo-oxygenase activity as suggested by Krell *et al.* (1981). In contrast, others have concluded that FPL 55712 at the same concentrations as those used by Krell *et al.* (1981) probably exerts its inhibitory action at the receptor site (Engineer *et al.*, 1978; Piper & Samhoun, 1981; Sirois *et al.*, 1983). In addition, FPL 55712 failed to modify the contractile response to LTB_4 in the guinea-pig parenchyma, where the myotropic action of LTB_4 is almost entirely dependent on thromboxane formation (Sirois *et al.*, 1983). In the present experiments, FPL 55712 significantly attenuated both ET-1-induced TXA_2 release and contraction, whereas the other sulphidopeptide leukotriene antagonist, YM 16638 was only slightly active in inhibiting both TXA_2 release and contraction. Therefore, it may be concluded that the more potent inhibitory action of FPL 55712 could be related to decreased TXA_2 formation. One possibility might be that FPL 55712, but not compound YM 16638, interfered with cyclo-oxygenase activity. However, in the present study FPL 55712 did not inhibit basal TXA_2 release, thus making this explanation unlikely. Since compound YM 16638 is a more potent antagonist of LTC_4 than LTD_4 receptors (Tomioka *et al.*, 1988), TXA_2 release may be assumed to be mediated through LTD_4 receptors.

The present data give no information on the cellular source of TXA_2, PAF and sulphidopeptide leukotrienes. Intense endothelin-like immunoactivity has been detected in the majority of airway epithelial (secretory and Clara cells, type II pneumocytes) as well as in airway smooth muscle cells (Turner *et al.*, 1989; Rozengurt *et al.*, 1990). Most of these cells are capable of synthesizing various eicosanoids (Robidoux *et al.*, 1988) and probably PAF (Prevost *et al.*, 1988). Thus, one or more of them might be responsible for the enhanced production of these mediators.

In conclusion, the present data demonstrate that the contractile action of ET-1 in guinea-pig isolated airways is, in part, mediated by generation of secondary mediators like thromboxane A_2, sulphidopeptide leukotrienes and PAF, but it is independent of the release of histamine, 5-HT and acetylcholine. These findings also suggest that ET-1 can induce TXA_2 release directly through its specific receptors and/or indirectly through enhancing formation of sulphidopeptide leukotrienes and PAF.

We thank Drs P. Braquet (Institut Henri Beaufour, Le Plessis Robinson, France), H. Heuer (Boehringer-Ingelheim KG, FRG), I.M. Richards (The Upjohn Co., Kalamazoo, MI), P. Sheard (Fisons Pharmaceuticals, Loughborough, England), K. Stegmeier (Boehringer-Mannheim GmbH, F.R.G.) and K. Tomioka (Yamanouchi Pharmaceuticals, Tokyo, Japan) for generously providing us with BN 52021, WEB 2086, U 75302, FPL 55712 and YM 16638, respectively. The authors thank the Medical Research Council of Canada for financial support and Ms Solange Cloutier for technical assistance. J.G.F. and P.S. are in receipt of a Medical Research Council Fellowship and a Scientist Award, respectively.

References

ADVENIER, C., SARRIA, B., NALINE, E., PUYBASSET, L. & LAGENTE, V. (1990). Contractile activity of three endothelins (ET-1, ET-2 and ET-3) on the human isolated bronchus. *Br. J. Pharmacol.*, **100**, 168–172.

ATTALLAH, A. & STAHL, R. (1980). Inhibition of renal PGE_2 biosynthesis *in vivo*: regional differences. *Prostaglandins*, **19**, 649–650.

AUGSTEIN, J., FARMER, J.B., LEE, T.B., SHEARD, P. & TATTERSALL, M.L. (1973). Selective inhibition of slow reacting substance of anaphylaxis. *Nature*, **245**, 215–217.

BACH, M.K., BRASHLER, J.R., BROOKS, C.D. & NEERKEN, A.J. (1979). Slow-reacting substances: comparison of some properties of human lung SRS-A and two distinct fractions from ionophore-induced rat mononuclear cell SRS. *J. Immunol.*, **122**, 160–165.

BARNES, P.J. (1988). Platelet-activating factor and asthma. *J. Allergy Clin. Immunol.*, **81**, 152–160.

BATTISTINI, B., FILEP, J. & SIROIS, P. (1990). Potent thromboxane-mediated *in vitro* bronchoconstrictor effect of endothelin in the guinea-pig. *Eur. J. Pharmacol.*, **178**, 141–142.

BLACK, P.N., GHATEI, M.A., TAKAHASHI, K., BRETHERTON-WATT, D., KRAUSZ, T., DOLLERY, C.T. & BLOOM, S.R. (1989). Formation of endothelin by cultured airway epithelial cells. *FEBS Lett.*, **255**, 129–132.

BORGES, R., VON GRAFEINSTEIN, H. & KNIGHT, D.E. (1989). Tissue selectivity of endothelin. *Eur. J. Pharmacol.*, **165**, 223–230.

BRAMLEY, A.M., SAMHOUN, M.N. & PIPER, P.J. (1990). The role of the epithelium in modulating the responses to guinea-pig trachea induced by bradykinin *in vitro*. *Br. J. Pharmacol.*, **99**, 762–766.

BRAQUET, P., SPINNEWYN, B., BRAQUET, M., BOURGAIN, R.H., TAYLOR, J.E., NUNEZ, D. & DRIEU, K. (1985). BN 52021 and related compounds: A new series of highly specific PAF-acether receptor antagonists isolated from Ginkgo biloba. *Blood Vessels*, **16**, 559–572.

CASALS-STENZEL, J., MUACEVIC, G. & WEBER, K.H. (1987). Pharmacological actions of WEB 2086, a new specific antagonist of platelet-activating factor. *J. Pharmacol. Exp. Ther.*, **241**, 974–981.

CASEY, F.B., APPLEBY, B.J. & BUCK, C.D. (1983). Selective inhibition of the lipoxygenase metabolic pathway of arachidonic acid by the SRS-A antagonist, FPL 55712. *Prostaglandins*, **25**, 1–11.

CHUNG, K.F., AIZAWA, H., LEIKAUF, G.D., UEKI, I.F., EVANS, T.W. & NADEL, J.A. (1986). Airway hyperresponsiveness induced by platelet-activating factor: role of thromboxane generation. *J. Pharmacol. Exp. Ther.*, **236**, 580–584.

DE NUCCI, G., THOMAS, R., D'ORLEANS-JUSTE, P., ANTUNES, E., WALDER, C., WARNER, T.D. & VANE, J.R. (1988). Pressor effects of circulating endothelin are limited by its removal in the pulmonary circulation and by the release of prostacyclin and endothelium-derived relaxing factor. *Proc. Natl. Acad. Sci. U.S.A.*, **85**, 9797–9800.

DESQUAND, S., TOUVAY, C., RANDON, J., LAGENTE, V., VILAIN, B., MARIDONNEAU-PARINI, I., ETIENNE, A., LEFORT, J., BRAQUET, P. & VARGAFTIG, B.B. (1986). Interference of BN 52021 (Ginkgolide B) with the bronchopulmonary effects of PAF-acether in the guinea-pig *Eur. J. Pharmacol.*, **127**, 83–95.

DUNN, O.J. (1964). Multiple comparisons using rank sums. *Technometrics*, **6**, 241–252.

EGLEN, R.M., MICHEL, A.D., SHARIF, N.A., SWANK, S.R. & WHITING, R.L. (1989). The pharmacological properties of the peptide endothelin. *Br. J. Pharmacol.*, **97**, 1297–1307.

ENGINEER, D.M., MORRIS, H.R., PIPER, P.J. & SIROIS, P. (1978). The release of prostaglandins and thromboxanes from guinea-pig lung by slow reacting substance of anaphylaxis, and its inhibition. *Br. J. Pharmacol.*, **64**, 211–218.

FILEP, J.G., BATTISTINI, B. & SIROIS, P. (1990). Endothelin induces thromboxane release and contraction of isolated guinea-pig airways. *Life Sci.*, **47**, 1845–1850.

FILEP, J., FÖLDES-FILEP, E. & FRÖLICH, J.C. (1987). Vascular responses to leukotriene B_4, C_4 and D_4 following FPL 55712, indomethacin, saralasin, phentolamine and verapamil in the conscious rat. *Br. J. Pharmacol.*, **90**, 431–439.

FÖLDES-FILEP, E., BRAQUET, P. & FILEP, J. (1987). Inhibition by BN 52021 (Ginkgolide B) of the specific binding of [^{3}H]-platelet-activating factor to human neutrophil granulocytes. *Biochem. Biophys. Res. Commun.*, **148**, 1412–1417.

GOLDIE, R.G., BERTRAM, J.F., PAPADIMITRIOU, J.M. & PATERSON, J.W. (1984). The lung parenchyma strip. *Trends Pharmacol. Sci.*, **5**, 7–9.

HALONEN, M., DUNN, A.M., PALMER, J.D. & McMANUS, L.M. (1990). Anatomic basis for species differences in peripheral lung strip contraction to PAF. *Am. J. Physiol.*, **259**, L81–L86.

HAMASAKI, Y., MOJARAD, M., SAGA, T., TAI, H. & SAID, S.I. (1984). Platelet-activating factor raises airway and vascular pressure and induces edema in lungs perfused with platelet-free solution. *Am. Rev. Resp. Dis.*, **129**, 742–746.

HASUNUMA, K., RODMAN, D.M., O'BRIEN, R.F. & McMURTRY, I.F. (1990). Endothelin-1 causes pulmonary vasodilation in rats. *Am. J. Physiol.*, **259**, H48–H54.

HAY, D.W.P. (1990). Mechanism of endothelin-induced contraction in guinea-pig trachea: comparison with rat aorta. *Br. J. Pharmacol.*, **100**, 383–392.

HENRY, P.J., RIGBY, P.J., SELF, G.J., PREUSS, J.M. & GOLDIE, R.G.

(1990). Relationship between endothelin-1 binding site densities and constrictor activities in human and animal airway smooth muscle. *Br. J. Pharmacol.*, **100**, 786–792.

JANCAR, S., THERIAULT, P., LAUZIERE, M., BRAQUET, P. & SIROIS, P. (1989). PAF-induced release of spasmogens from guinea-pig lungs. *Br. J. Pharmacol.*, **96**, 153–162.

KRELL, R.D., OSBORN, R., VICKERY, L., FALCONE, K., O'DONNELL, M.D., GLAESON, J., KINZIG, C. & BRYAN, D. (1981). Contraction of isolated airway smooth muscle by synthetic leukotrienes C_4 and D_4. *Prostaglandins*, **22**, 387–409.

LAGENTE, V., CHABRIER, P.E., MENCIA-HUERTA, J.M. & BRAQUET, P. (1989). Pharmacological modulation of the bronchopulmonary action of the vasoactive peptide, endothelin, administered by aerosol in the guinea-pig. *Biochem. Biophys. Res. Commun.*, **158**, 625–632.

LAWSON, C.F., WISHKA, D.G., MORRIS, J. & FITZPATRICK, F.A. (1989). Receptor antagonism of leukotriene B_4 myotropic activity by the 2,6 disubstituted pyridine analog U-75302: characterization on lung parenchyma strips. *J. Lipid Med.*, **1**, 3–12.

LEFORT, J., ROTILIO, D. & VARGAFTIG, B.B. (1984). The platelet-independent release of TXA_2 by PAF-acether from guinea-pig lungs involves mechanisms distinct from those of leukotrienes. *Br. J. Pharmacol.*, **82**, 565–575.

LETTS, L.G. & PIPER, P.J. (1982). The actions of leukotrienes C_4 and D_4 on guinea-pig isolated hearts. *Br. J. Pharmacol.*, **76**, 169–176.

LÓPEZ-FARRÉ, A., GÓMEZ-GARRE, D., BERNABEU, F., MONTAÑES, I., MILLÁS, I. & LÓPEZ-NOVOA, J.M. (1990). Platelet-activating factor (PAF): A mediator of renal effect and mesangial cell contraction induced by endothelin (ET) (abstract). *J. Lipid. Med.*, **2**, 189.

MACQUIN-MAVIER, I., LEVAME, M., ISTIN, N. & HARF, A. (1989). Mechanism of endothelin-mediated bronchoconstriction in the guinea-pig. *J. Pharmacol. Exp. Ther.*, **250**, 740–745.

MAGGI, C.A., PATACCHINI, R., GIULIANI, S. & MELI, A. (1989). Potent contractile effect of endothelin on isolated guinea-pig airways. *Eur. J. Pharmacol.*, **160**, 179–182.

NEY, U.M. (1983). Propranolol-induced airway hyperreactivity in guinea-pigs. *Br. J. Pharmacol.*, **79**, 1003–1009.

PATSCHEKE, H., STEGMEIER, K., HORNBERGER, W., STAIGER, C.H. & NEUGEBAUER, G. (1987). Inhibition of platelet activation by the novel thromboxane receptor antagonist BM 13505 (abstract). *Thromb. Haemostasis*, **58**, 182.

PAYNE, A.N. & WHITTLE, B.J.R. (1988). Potent cyclo-oxygenase-mediated bronchoconstrictor effect of endothelin in the guinea-pig *in vivo*. *Eur. J. Pharmacol.*, **158**, 303–304.

PIPER, P.J. & SAMHOUN, M.N. (1981). The mechanism of action of leukotriene C_4 and D_4 on isolated lung and parenchyma strips of guinea-pig, rabbit and rat. *Prostaglandins*, **21**, 793–804.

PRADELLES, P., GRASSI, J. & MACLOUF, J. (1985). Enzyme immunoassays of eicosanoids using acetylcholinesterase as label: an alternative to radioimmunoassay. *Anal. Chem.*, **57**, 1170–1173.

PRETOLANI, M., LEFORT, J., MALANCHERE, E. & VARGAFTIG, B.B. (1987). Interference of the novel PAF-acether antagonist WEB 2086 with the bronchopulmonary responses to PAF-acether and to active and passive anaphylactic shock in guinea-pigs. *Eur. J. Pharmacol.*, **140**, 311–321.

PREVOST, M.C., CARIVEN, C. & CHAP, H. (1988). Possible origins of PAF-acether and lyso-PAF-acether in rat lung alveoli secondary to hypoxia. *Biochem. Biophys. Acta*, **962**, 354–361.

RAEBURN, D. (1990). Eicosanoids, epithelium and airway reactivity. *Gen. Pharmacol.*, **21**, 11–16.

ROBIDOUX, C., PELE, J.P., MACLOUF, J., PRADELLES, P. & SIROIS, P. (1988). Stimulation of release of prostaglandins and thromboxanes from isolated guinea pig lung cells by bradykinin, f-Met-Leu-Phe, phorbol myristate, ionophore A23187, and leukotrienes. *Inflammation*, **12**, 285–295.

ROZENGURT, N., SPRINGALL, D.R. & POLAK, J.M. (1990). Localization of endothelin-like immunoreactivity in airway epithelium of rats and mice. *J. Pathol.*, **160**, 5–8.

SIROIS, P., ROY, S. & BORGEAT, P. (1983). Specificity of receptors for leukotrienes A_4, B_4, C_4, D_4, E_4 and histamine on the guinea-pig lung parenchyma. Effect of FPL 55712 and desensitization of the myotropic activity. *Prostaglandins*, **26**, 91–101.

TOMIOKA, K., YAMADA, T., MASE, T., HARA, H. & MURASE, K. (1988). Pharmacological properties of the orally active leukotriene antagonist [[5-[[3-(4-acetyl-3-hydroxy-2-propylphenoxy)-propyl] thio]-1,2,3-thiadiazol-2-yl] thio acetic acid. *Arzneim. Forsch./Drug Res.*, **38**, 682–685.

TOUVAY, C., VILLAIN, B., PONS, F., CHABRIER, P.E., MENCIA-HUERTA, J.M. & BRAQUET, P. (1990). Bronchopulmonary and vascular effects of endothelin in the guinea-pig. *Eur. J. Pharmacol.*, **176**, 23–33.

TURNER, N.C., POWER, R.F., POLAK, J.M., BLOOM, S.R. & DOLLERY, C.T. (1989). Endothelin-induced contraction of tracheal smooth muscle and identification of specific endothelin binding sites in the trachea of the rat. *Br. J. Pharmacol.*, **98**, 361–366.

UCHIDA, Y., NINOMIYA, H., SAOTOME, M., NOMURA, A., OHTSUKA, M., YANAGISAWA, M., GOTO, K., MASAKI, T. & HASEGAWA, S. (1988). Endothelin, a novel vasoconstrictor peptide, as a potent bronchoconstrictor. *Eur. J. Pharmacol.*, **154**, 227–228.

UENO, A., KUNIO, T. & KATORI, M. (1982). Possible involvement of thromboxane in bronchoconstrictive and hypertensive effects of LTC_4 and LTD_4 in guinea pigs. *Prostaglandins*, **23**, 865–880.

YANAGISAWA, M., KURIHARA, M., KIMURA, S., TOMOBE, Y., KOBAYASHI, M., MITSUI, Y., YAZAKI, Y., GOTO, T. & MASAKI, T. (1988). A novel potent vasoconstrictor peptide produced by vascular endothelial cells. *Nature*, **332**, 411–415.

YANAGISAWA, M. & MASAKI, T. (1989). Endothelin, a novel endothelium-derived peptide. Pharmacological activities, regulation and possible roles in cardiovascular control. *Biochem. Pharmacol.*, **38**, 1877–1883.

(Received July 19, 1990
Revised January 30, 1991
Accepted February 14, 1991)

Br. J. Pharmacol. (1991), **103**, 1641–1648 © Macmillan Press Ltd, 1991

Action of nicorandil on ATP-sensitive K^+ channel in guinea-pig ventricular myocytes

†Keiko Nakayama, *Zheng Fan, †Fumiaki Marumo, *Tohru Sawanobori & *[1]Masayasu Hiraoka

*Department of Cardiovascular Diseases, Medical Research Institute and †Second Department of Internal Medicine, Tokyo Medical and Dental University, Yushima, Bunkyo-ku, Tokyo, Japan

1 Patch-clamp techniques were used to study the effects of nicorandil (2-nicotinamiodethyl nitrate) on the adenosine 5'-triphosphate (ATP)-sensitive K^+ channel current ($I_{K.ATP}$) in guinea-pig ventricular myocytes.

2 Nicorandil activated the time-independent outward current. This effect was dependent on intracellular ATP concentration ($[ATP]_i$) showing a larger effect at 2 mM than at 10 mM $[ATP]_i$. The nicorandil-induced outward current was inhibited by application of 0.3 μM glibenclamide.

3 In the inside-out patch configuration, 0.3–1.0 mM nicorandil increased the open-state probability of $I_{K.ATP}$ without a change in its conductance value (about 90pS). This effect was inhibited by glibenclamide. Analysis of the open and closed time distributions showed that nicorandil had no effect on open and closed distributions shorter than 5 ms. On the other hand, nicorandil increased the life time of bursts and decreased the interburst intervals.

4 The inward rectifier K^+ channel current was not influenced by internal application of nicorandil.

5 Therefore, we conclude that $I_{K.ATP}$ is the only K^+ current activated by nicorandil, and the main effect of nicorandil is on the kinetics of the $I_{K.ATP}$ bursting behaviour. These actions are similar to that of pinacidil on this preparation.

Keywords: Nicorandil; ATP-sensitive K^+ channel; guinea-pig ventricular myocytes

Introduction

The vasodilators, cromakalim, nicorandil and pinacidil have the ability to relax vascular smooth muscle and to hyperpolarize the membrane potential (Hamilton *et al.*, 1986). Hyperpolarization is considered to be caused by activation of certain types of K^+ channels. Because of their hyperpolarizing action, these vasodilators are claimed to be K^+ channel openers (Cook, 1988). The K^+ channel openers shorten action potential duration (APD) and sometimes hyperpolarize the resting membrane potential of heart muscle (Yanagisawa & Taira, 1981; Imanishi *et al.*, 1983; Taira, 1987; Smallwood & Steinberg, 1988). Recently, the target of the K^+ channel openers in the heart has been clarified by use of the single channel recording technique. A common action of the three agents, cromakalim, nicorandil and pinacidil was shown to be activation of the ATP-sensitive K^+ channel ($I_{K.ATP}$) in the heart (Escande *et al.*, 1988; 1989; Sanguinetti *et al.*, 1988; Osterrieder, 1988; Hiraoka & Fan, 1989; Arena & Kass, 1989a,b; Fan *et al.*, 1990). Standen *et al.* (1989) subsequently demonstrated the existence of $I_{K.ATP}$ in arterial smooth muscle cells and showed that cromakalim actually opened this channel.

In the previous study (Hiraoka & Fan, 1989), we demonstrated that nicorandil activated an outward K^+ current dependent on intracellular ATP concentration ($[ATP]_i$) and showed the current activated by nicorandil was $I_{K.ATP}$ at the single channel level in mammalian ventricular myocytes. However, the detailed action of nicorandil on $I_{K.ATP}$ remained unclarified. We subsequently studied the action of another K^+ channel opener, pinacidil on $I_{K.ATP}$ at the single channel level (Fan *et al.*, 1990; Nakayama *et al.*, 1990). Pinacidil activated the $I_{K.ATP}$ current in a dose-dependent and $[ATP]_i$-dependent manner. Kinetic analysis of the channel transitions revealed that pinacidil and $[ATP]_i$ act antagonistically on the opening and closing behaviour of $I_{K.ATP}$. To obtain further insight into the activation mechanism of $I_{K.ATP}$ of the heart by the K^+ channel openers, we have studied the actions of nicorandil on the whole cell current at various $[ATP]_i$ quantitatively and on the kinetics of single channel currents in guinea-pig ventricular myocytes. Part of this study was presented as an abstract (Hiraoka *et al.*, 1990).

[1] Author for correspondence.

Methods

Single myocytes were isolated enzymatically from guinea-pig ventricles as described elsewhere (Hirano & Hiraoka, 1988).

Solutions

In the whole cell configuration the bath solution was Tyrode solution, the composition of which was (mM): NaCl 144, NaH_2PO_4 0.33, KCl 4.0, $CaCl_2$ 1.8, $MgCl_2$ 0.53, glucose 5.5 and HEPES 5.0; the pH was adjusted to 7.3–7.4 by addition of NaOH. The composition of the pipette solution was (mM): KCl 120, K_2ATP (Sigma Chemical Co., St. Louis, MO, U.S.A.) 5.0, HEPES 5.0 and K_4BAPTA (Dojin Co., Kumamoto, Japan) 5.0; the pH was adjusted to 7.2 with KOH. In pipette solutions with different ATP contents, the concentration of KCl was varied so as to maintain the final K^+ concentration constant at 150 mM.

In the case of single-channel recordings, the bath solution (intracellular solution) contained (mM): KCl 140, glucose 5.5, EGTA 2 and HEPES 5; the pH was adjusted to 7.3 with KOH. The drug was dissolved in the bath solution at the concentration indicated in the text. The composition of the pipette solution (extracellular medium) was (mM): KCl 140, $CaCl_2$ 1.8, $MgCl_2$ 0.53, glucose 5.5 and HEPES 5; the pH was adjusted to 7.3 by addition of KOH.

Whole-cell experiments

The whole cell configuration of the patch-clamp technique (Hamill *et al.*, 1981) was used to record membrane currents with a patch-clamp amplifier (Model 8900, Dagan Corp., Min-

neapolis, MN, U.S.A.). The recording technique and the data acquisition systems have been described previously (Hirano & Hiraoka, 1988). When the ramp voltage-clamp method was employed, an intelligent arbitrary function synthesizer (Model 1731, NF Inst., Yokohama, Japan) was used to supply the command pulse.

The temperature of the bath chamber was maintained at 34–35°C. Before contacts of the electrode and the cell, the junction potential was adjusted to zero at the level of the bath solution. At the end of each experiment the junction potential was checked again and, if the differences between the 1st and the 2nd measurements exceeded more than ±2 mV, the value of the membrane potential was corrected accordingly.

Measurements of cell surface area

The area of the cell surface was estimated from the cell capacitance assuming a specific membrane capacitance of 1 μF cm^{-2}. The cell capacitance was calculated from current responses induced by 1 mV depolarizing pulse from a holding potential of −90 mV (Lindar & Neher, 1988).

Single-channel recordings

Single-channel current recordings were made at room temperature in the inside-out patch configuration (Hamill *et al.*, 1981) with the same patch-clamp amplifier as in the whole-cell experiments. The current signals were stored on a video cassette recorder (BR-6400, Victor, Tokyo, Japan) through a PCM converter system (RP-882, NF Inst., Yokohama, Japan) at a conversion rate of 40 kHz. The recorded signals were filtered off-line through an 8-pole Bessel filter (48 dB/octave, FV-665, NF Inst., Yokohama, Japan) and digitized at 30 kHz on the disc of a computer (IBM-PS/2) using an analog-to-digital converter (TL-1 DMA interface, Axon Inst., Burlingame, CA, U.S.A.).

Single channel data analysis

Single channel records were analysed by the programme of the software package, pCLAMP 5.5 on a computer (IBM-PS/2). Briefly, the unitary current amplitude of $I_{K.ATP}$ channel was measured from the all point histograms through Gaussian fitting. When the inward rectifier K^+ current (I_{K1}) was induced together with $I_{K.ATP}$ at a potential negative to 0 mV (Trube & Hescheler, 1984), $I_{K.ATP}$ was identified by larger amplitude, current fluctuation during channel opening, and blockade by increased $[ATP]_i$. Each apparent distribution of open time, burst duration or closed time was formed using different cut-off frequencies (f_c) of the filter and bin-widths as described in the text and figure legends. At first, for measurement of the lifetime of the open- and closed state, 10 kHz f_c was used for detecting all events. From these data, mean open time and the shortest closed time constants were obtained. Then a burst duration and closed-state distribution were analysed using 0.1 kHz f_c. Under this f_c, almost all the fast closing events less than 1.6 ms which appeared under the 10 kHz f_c were filtered out leaving the open state, that is burst (Yellen, 1984). On the other hand, when the closed-time distribution analyses were carried out using the 0.1 kHz f_c, less than 5% of gaps between bursts were underestimated. Finally, a critical closed-time of 600 ms was chosen to separate one cluster from another.

Data were expressed as mean ± s.e. statistical comparison was made using non-paired or paired t test. A P value of less than 0.05 was considered significant.

Drugs

Nicorandil (2-nicotinamidoethyl nitrate; a gift from Chugai Pharmaceutical Co., Tokyo, Japan) was freshly prepared before every experiment and diluted into the test solution to obtain the final concentrations indicated in the text. Glibenclamide (a gift from Hoechst Japan, Tokyo) was dissolved as 0.2 mM stock solution in 2% dimethyl sulphoxide (DMSO) and diluted into the test solution appropriately before study. The final concentration of DMSO contained in the test solution was less than 0.01%. Our recent study confirmed that DMSO, at this concentration, had no effect on $I_{K.ATP}$ (Nakayama *et al.*, 1990).

Results

Effect of internal ATP concentration on nicorandil-activated outward current

We have already reported that nicorandil activates a time-independent outward current and this is suppressed by increasing $[ATP]_i$ (Hiraoka & Fan, 1989). Therefore, we examined quantitatively the nicorandil-activated current in different $[ATP]_i$. A ramp voltage clamp method was used to produce a slow depolarization (200 mV. 30 s^{-1}) from −120 mV to 80 mV. Figure 1 presents typical results obtained under

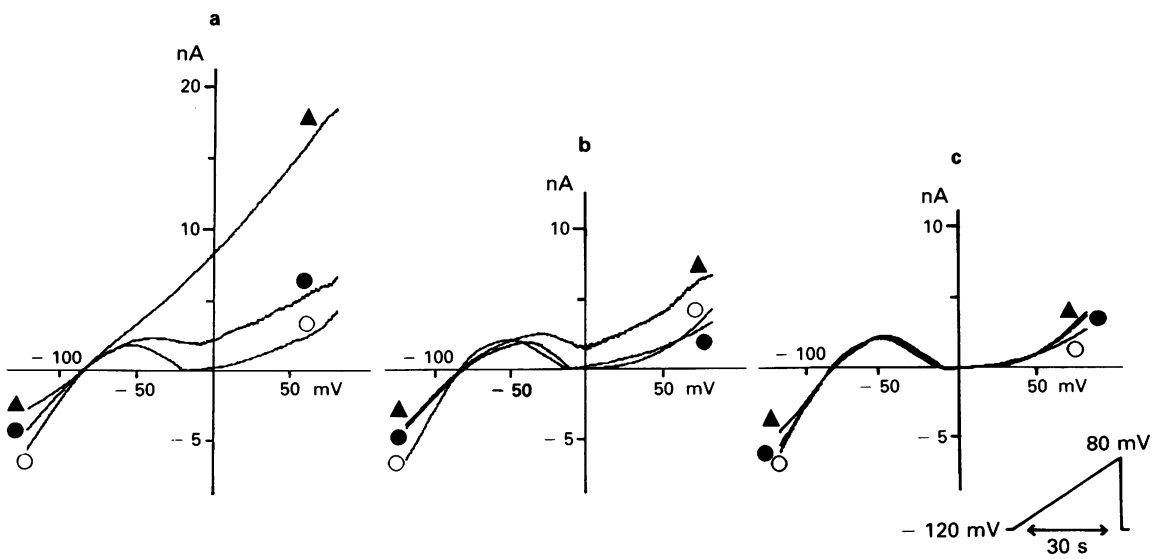


Figure 1 Effects of nicorandil on the background current induced by a 30 s depolarizing ramp voltage clamp pulse from −120 mV to +80 mV at different intracellular ATP concentrations ($[ATP]_i$). $[ATP]_i$ was 2 mM in (a); 5 mM in (b); and 10 mM in (c). (○) Control current before the application of nicorandil; (●) current in the presence of 0.3 mM nicorandil; (▲) current in the presence of 1.0 mM nicorandil.

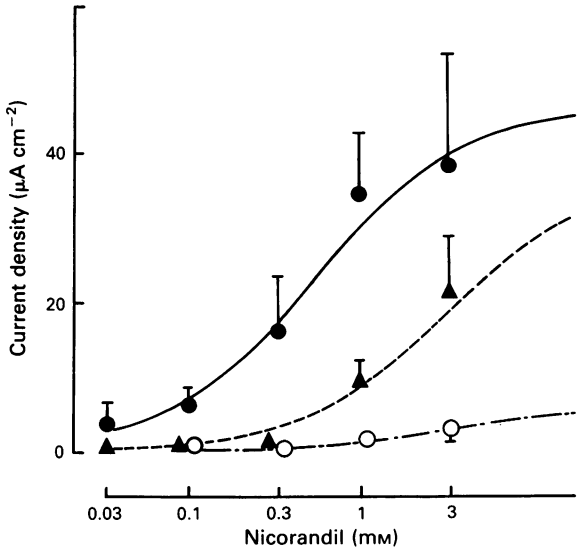


Figure 2 Dose-response curves of the nicorandil-activated current at different $[ATP]_i$. The ordinate scale indicates current density and the abscissa scale, the nicorandil concentration. Current density was calculated from the background current values at 0 mV. Each value represents a mean of four or five measurements from different preparations; bars indicate ±s.e. (●) 2 mM $[ATP]_i$; (▲) 5 mM $[ATP]_i$; (○) 10 mM $[ATP]_i$. A sigmoidal curve was fitted to the equation: $I = I_{max}/(1 + (Kd/[Nico])^n)$ where I = current density, I_{max} = maximum current density, K_d = apparent dissociation constant, n = slope parameter (Hill's coefficient) = 1, using a least squares method. Values of K_d were 0.5 mM, 2.3 mM and 2.9 mM for 2, 5 and 10 mM $[ATP]_i$, respectively.

conditions of different $[ATP]_i$. Nicorandil dose-dependently produced an increased outward current at voltages positive to −80 mV, and decreased the inward current negative to this voltage (see Discussion). These effects were most prominent at 2 mM $[ATP]_i$, while nicorandil had almost no effect on the outward current at 10 mM $[ATP]_i$. A quantitative estimation of the nicorandil-activated outward current was achieved by expressing the dose-response curve as current density compensating cell surface area (Figure 2). The current density was calculated using the current level at 0 mV from the type of experiments shown in Figure 1, since it was near zero during the control. At 2 mM $[ATP]_i$, the current density showed a sigmoidal dependence on the nicorandil concentration and was nearly saturated at 3 mM ($37.9 \pm 17.4\,\mu A\,cm^{-2}$, $n = 4$). At 5 mM $[ATP]_i$, the current density activated by nicorandil was decreased in comparison to 2 mM $[ATP]_i$ ($21.3 \pm 5.5\,\mu A\,cm^{-2}$ at 3 mM nicorandil; $n = 4$). At 10 mM $[ATP]_i$, the effect of nicorandil was further decreased to $3.06 \pm 1.61\,\mu A\,cm^{-2}$ at 3 mM nicorandil ($n = 4$). We did not examine the effects of nicorandil at concentrations higher than 3 mM, because such high concentrations could not be dissolved in the test solution.

Block of the nicorandil-activated current by glibenclamide

The effect of glibenclamide, a specific blocker of $I_{K.ATP}$ (Fosset *et al.*, 1988) on the nicorandil-activated current was examined. Since we have shown that nicorandil activates $I_{K.ATP}$ at the single channel level (Hiraoka & Fan, 1989), the nicorandil-activated outward current should be blocked by glibenclamide. Figure 3 shows a complete block by 0.3 μM glibenclamide of the nicorandil-activated current. The wash-out of glibenclamide caused a slow recovery and it took more than 10 min partially to reverse the effect. The effects of glibenclamide were confirmed in three myocytes.

Effect of nicorandil on the single channel current

The effects of nicorandil on the single channel current were examined by the inside-out patch configuration (Figure 4).

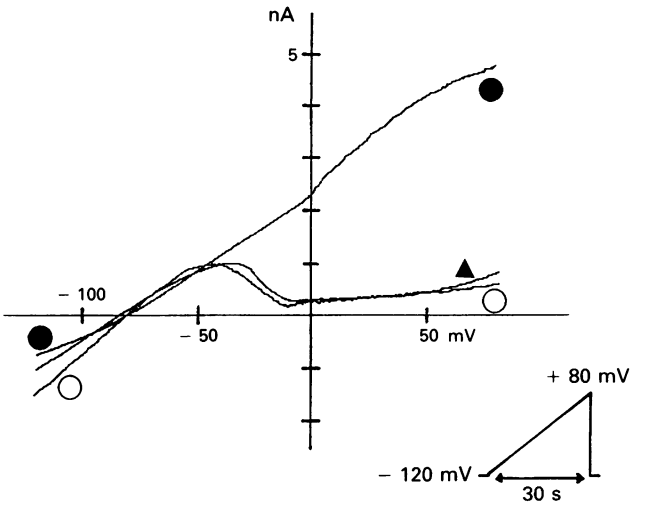


Figure 3 Effect of glibenclamide on the nicorandil-activated background current. Current was induced by 30 s depolarizing ramp pulse from −120 to +80 mV. $[ATP]_i$ was 2 mM. Note that 0.3 μM glibenclamide (▲) completely suppressed the nicorandil-activated background current (●); (○) control.

When the intracellular solution did not contain ATP, the channel stayed in the open state almost all the time (open-state probability (P_{open}) was 0.94) (Figure 4a). The P_{open} was decreased to 0.32 when 0.5 mM ATP was applied to the intracellular solution (Figure 4b), while addition of 1 mM nicorandil increased P_{open} to 0.54 without apparent changes in the unitary current amplitude (Figure 4c). The increased channel activity was largely inhibited by 0.3 μM glibenclamide, the P_{open} decreased to 0.07 (Figure 4d). The effect of glibenclamide, however, was not easily reversed and incomplete recovery was seen during the wash-out period of more than 10 min. In nine out of twelve examined patches, application of 1 mM nicorandil caused channel activation similar to that shown in Figure 4c. The effects of nicorandil did not last long and, 5–10 min after application, the increased channel activity gradually declined. Furthermore, $I_{K.ATP}$ activity decreased with time in the low $[ATP]_i$, the process known as 'run-down' of the channel (Ashcroft, 1988). Once the channels were completely inactivated in the low $[ATP]_i$ due to run-down, nicorandil up to 3 mM could not restore the channel activity as reported recently ($n = 10$; data not shown) (Takano & Noma, 1990). Therefore, we assume that the patches in which nicorandil did not activate the channels, contained no $I_{K.ATP}$ channels or these channels were completely inactivated.

The conductance properties of the nicorandil-activated channel were examined in more detail (Figure 5). Amplitude histogram analysis of all the data points observed in 0.5 mM ATP solution, and 0.5 mM ATP plus 1 mM nicorandil solution showed that there was one Gaussian peak distribution at positive voltages. When the membrane potential was held at negative voltages, there were two peaks of amplitude histogram observed. The smaller amplitude channel showed long-lasting openings, had a single channel conductance of 30 pS and was not recorded at positive voltages probably due to inward rectification. Because of the magnitude of conductance and strong inward-rectification, this channel was identified as I_{K1} (Kameyama *et al.*, 1983; Sakmann & Trube, 1984). The other channel had a larger amplitude, and showed rapid opening and closing behaviour and it was sensitive to ATP applied intracellularly. Application of 1 mM nicorandil increased the open-state probability of this larger amplitude current. The current-voltage relationship (I–V) of this channel is shown in Figure 5B. The current recorded in the presence of 0.5 mM ATP had a reversal potential of −2.8 mV. The I–V curve at negative voltages was linear with a slope conductance of 92.9 pS ($n = 5$). On the basis of the slope conductance, the reversal potential and ATP sensitivity, the current recorded at 0.5 mM ATP was identified as $I_{K.ATP}$. The nicorandil-activated

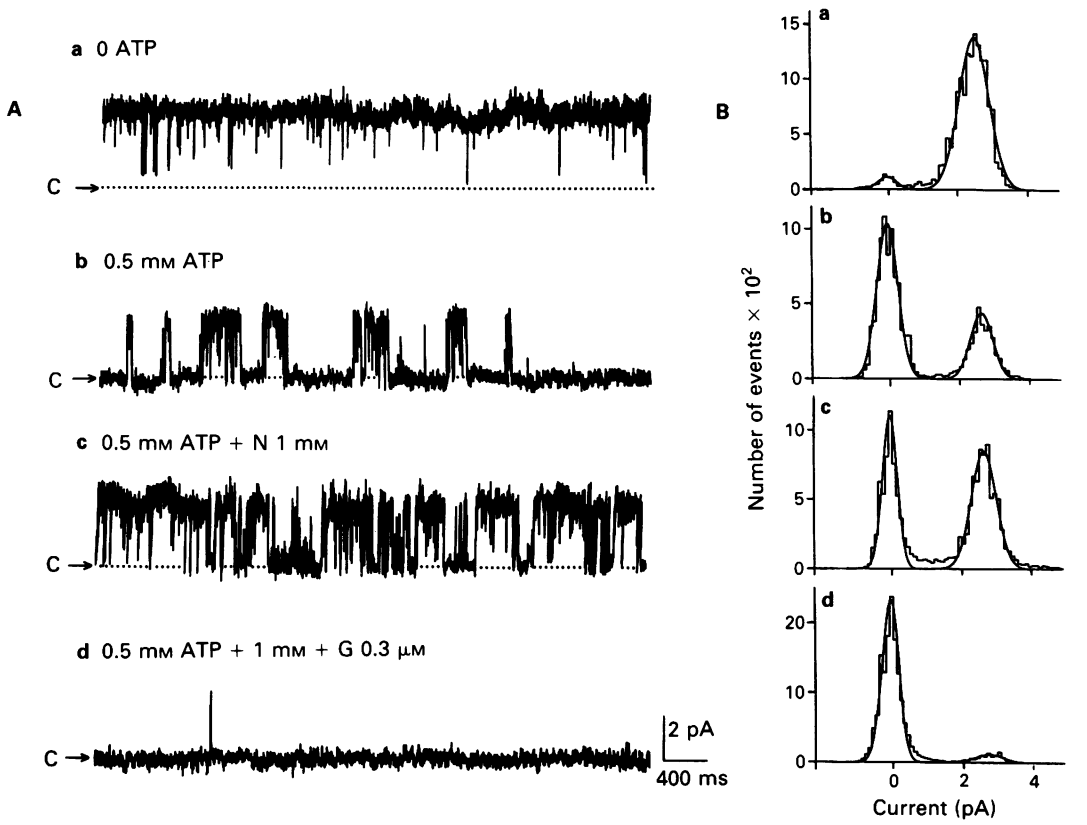


Figure 4 Effect of nicorandil (N) and glibenclamide (G) on the ATP-sensitive single-channel current. (A) Current traces recorded from a single patch. Membrane potential was held at +40 mV in the inside-out patch configuration. C, Closed level. (a) Channel activity in the absence of ATP (0 ATP) in the intracellular solution. There were marked openings of the channel, so that the channel mostly stayed at the open state (P_{open} = 0.94). (b) Presence of 0.5 mM ATP in the intracellular solution. P_{open} was decreased to 0.32. (c) Application of 0.5 mM ATP and 1 mM nicorandil in the intracellular solution. Marked openings of the channel were again observed (P_{open} = 0.54). (d) Further application of 0.3 μM glibenclamide in the internal solution, resulted in suppression of channel activity (P_{open} = 0.07). (B) Amplitude histograms recorded from the same patch in panel (A) in the corresponding conditions of (a)–(d).

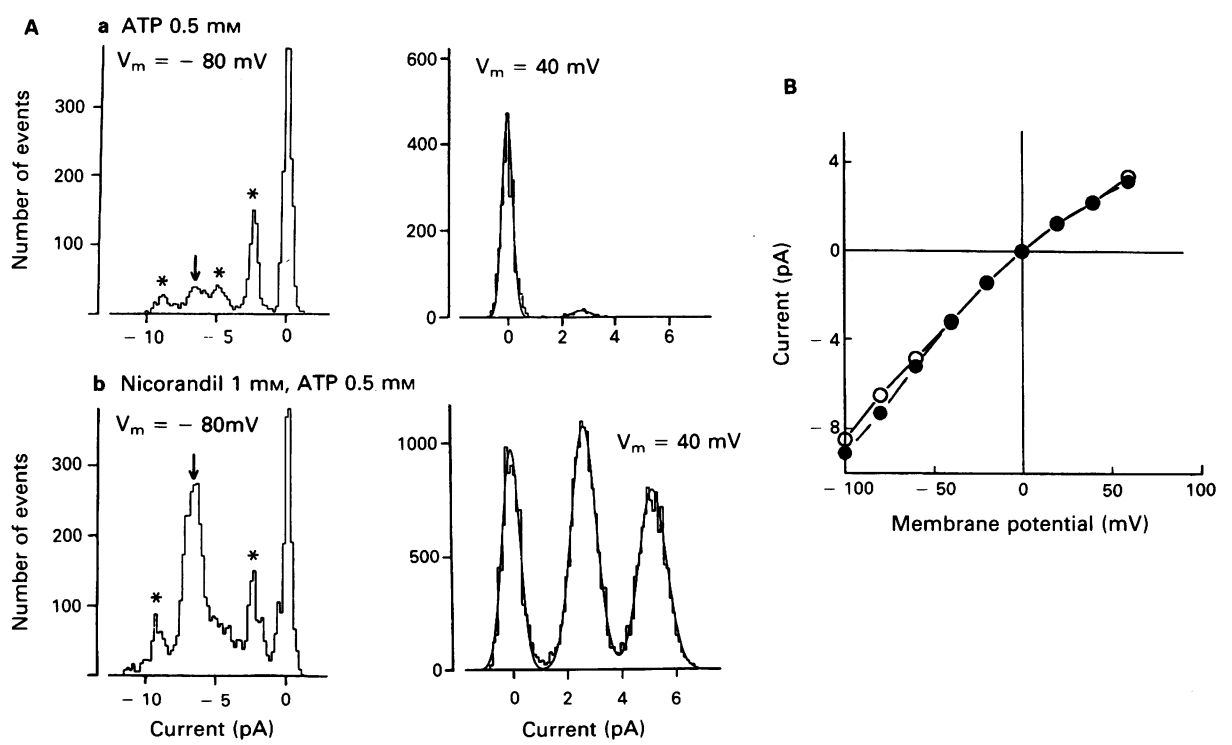


Figure 5 Effects of nicorandil on activation of ATP-sensitive K^+ channel currents recorded from an inside-out membrane patch. (A) (a) Amplitude histograms of the single-channel current at V_m = −80 mV (left panel) and V_m = +40 mV (right panel) obtained in the solution containing 0.5 mM ATP. (A) (b) Amplitude histograms of the single-channel current at V_m = −80 mV (left panel) and V_m = +40 mV (right panel) obtained in a solution containing 1 mM nicorandil and 0.5 mM ATP. In (A) ↓: ATP sensitive K^+ channel; *: the inward rectifier K^+ channel. Note that the amplitude of both channels was not changed by nicorandil, but the numbers of events of the larger amplitude (↓) were increased at V_m = −80 mV. (B) Current-voltage relationship (*I*–V) and the effect of nicorandil on it. Nicorandil did not change the conductance of this channel current.

current had a reversal potential of −2.3 mV and a slope conductance of 88.9 pS (n = 4). There was no significant difference in the reversal potential or slope conductance between $I_{K.ATP}$ and the nicorandil-activated current. The linearity of the I–V curves in both cases was lost at voltages positive to +40 mV, indicating weak inward rectification at high positive voltages.

Modulation of channel kinetics by nicorandil

The open and closed time distributions were analysed to determine the action of nicorandil on the kinetic properties of $I_{K.ATP}$. Probability density histograms of the open and closed times measured at −80 mV are shown in Figures 6 and 7. The

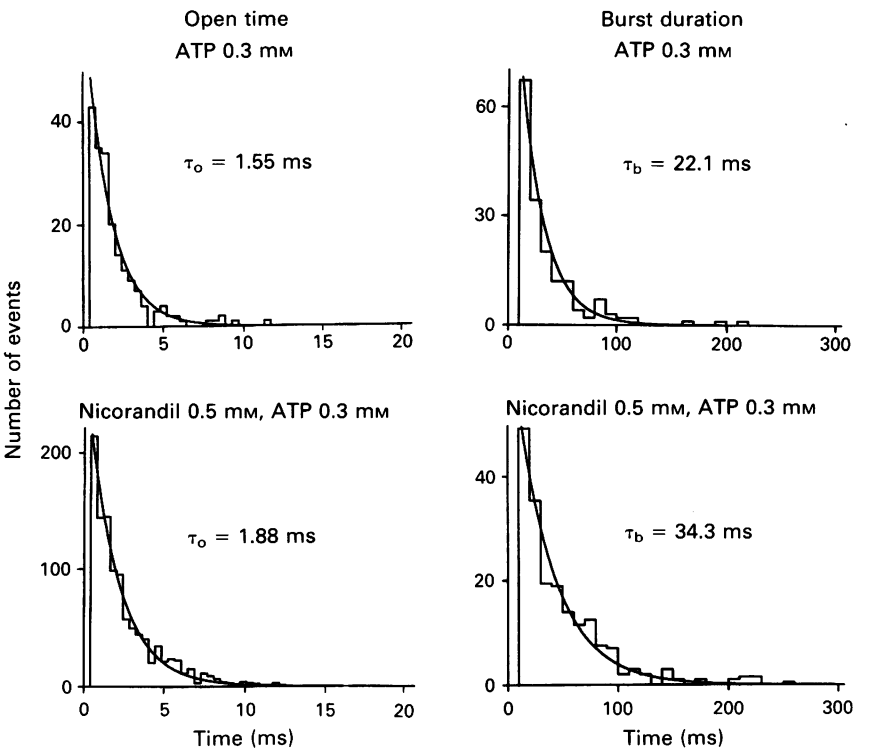


Figure 6 Effects of nicorandil on the open time of the ATP-sensitive single-channel current recorded from an inside-out patch membrane. Histograms of open time, analysed with high f_c = 10 kHz (left column) and histogram of life-time of bursts analysed with low f_c = 0.1 kHz (right column), with 0.3 mM ATP (upper panel) and 0.5 mM nicorandil plus 0.3 mM ATP (lower panel) in the internal solution. The time constants (τ_0) of the open time and that of the bursts (τ_b) obtained under the two different conditions were best expressed by single exponentials. Nicorandil increased τ_b without affecting τ_0.

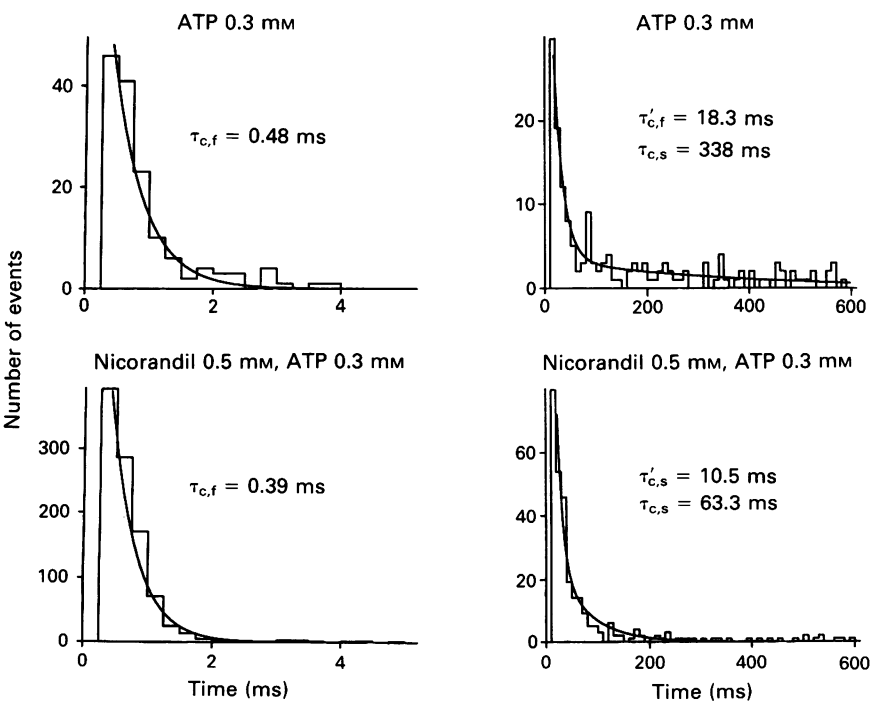


Figure 7 Effects of nicorandil on closed time distributions of the ATP-sensitive channel current recorded from an inside-out patch membrane. The left panel shows analysis of closed time shorter than 5 ms at an f_c of 10 kHz and the right panel shows the analysis of those up to 600 ms at an f_c of 0.1 kHz. The presence of nicorandil did not alter the time constants of the fast components ($\tau_{c,f}$ or $\tau'_{c,f}$) in distributions of short (left panel) or long (right panel) closed times. The time constant of the slow component ($\tau_{c,s}$) in the distribution of long closed times (right panel) was shortened by nicorandil. Data obtained from same patch as Figure 6 showing only a single level of channel activity throughout the two conditions.

open time histogram, which was analysed from the current record filtered at f_c of 10 kHz, revealed a single exponential distribution with a time constant of 1.55 ms in 0.3 mM ATP. In 0.3 mM ATP plus 0.5 mM nicorandil, the open time constant did not differ substantially from that in the control condition (τ_0 = 1.88 ms). The life time of a burst was defined as an opening period observed in the records filtered at f_c of 0.1 kHz (see, Methods). The histogram of burst duration consisted of a single exponential distribution. Its time constant, designated as τ_b was markedly prolonged by nicorandil.

The histogram of closed time within bursts was best fitted to a single exponential function. This analysis was performed with closed times longer than 5 ms to be discarded, and filtered at f_c of 10 kHz. The time constant of the closed time within bursts was designated at $\tau_{c,f}$. The value of $\tau_{c,f}$ was not changed markedly by application of nicorandil. The closed time histogram analysis using records filtered at f_c of 0.1 kHz and discarding closed times longer than 600 ms consisted of two exponentials with time constants of a fast ($\tau'_{c,f}$) and a slow component ($\tau_{c,s}$). $\tau'_{c,f}$ was equivalent to $\tau_{c,f}$ filtered at f_c of 10 kHz which was distorted by heavy filtering. The value of $\tau'_{c,f}$ was not influenced by nicorandil. $\tau_{c,s}$ represented the time constant of the interburst durations. The value of $\tau_{c,s}$ was 338 ms in 0.3 mM ATP. This value was markedly decreased to 63.3 ms by application of 0.5 mM nicorandil. These findings suggest that nicorandil increases the open-state probability of $I_{K.ATP}$ by an increase in burst durations and a decrease in interburst intervals. Similar results were obtained from three other patches at different concentrations of nicorandil and $[ATP]_i$. In a previous study (Fan *et al.*, 1990), we analysed the effects of $[ATP]_i$ and pinacidil on the clusters separated by longer closed times than 600 ms. In the present study, however, as the frequencies of such clusters were relatively low and the nicorandil effects were short-lived as stated above, we did not examine the drug actions on the clusters separated by closed times longer than 600 ms.

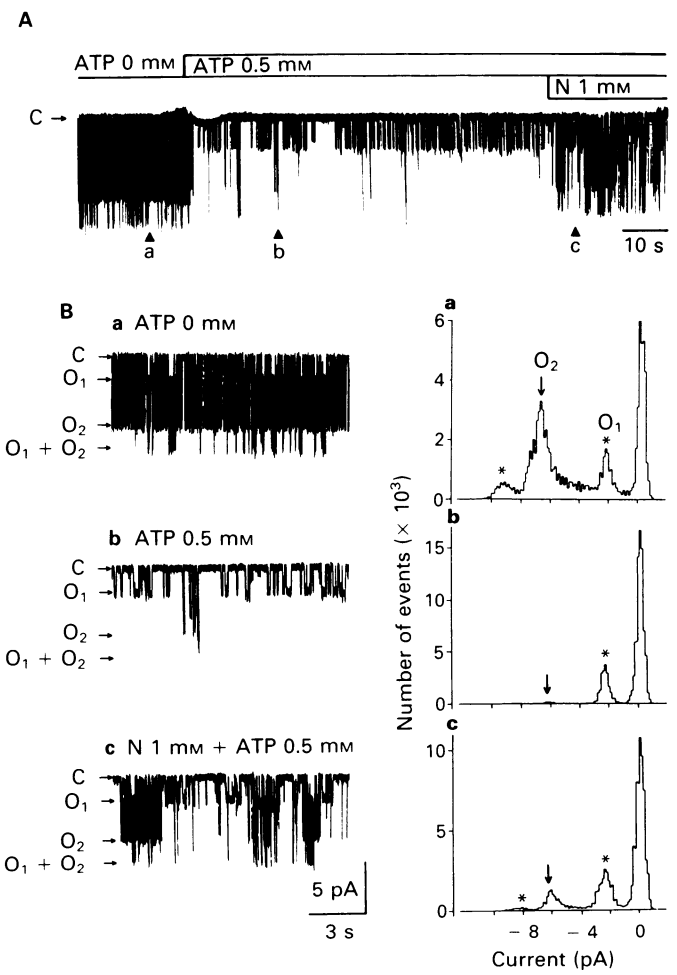


Figure 8 Effects of nicorandil on the inward rectifier K^+ channel current recorded from an inside-out patch membrane. (A) Continuous record at a holding potential of −80 mV. At the top, the ATP concentration and application time of nicorandil in the internal solution are shown. (B) Expansions of the records (left panel) and amplitude histograms (right panel) at the times marked by (▲) are shown. O_2 (↓) represents the ATP-sensitive K^+ channel current and O_1(*) represents the inward rectifier K^+ channel current. Note that the inward rectifier K^+ channel current was not influenced by nicorandil and no other current was activated by the drug under these recording conditions.

Effect of nicorandil on the inward rectifier K^+ channel

Kakei *et al.* (1986) reported nicorandil activated a small-conductance, time-independent K^+ channel (4.6 ± 1.7 pS) estimated from the relation between the variance and the mean of whole-cell current in guinea-pig ventricular myocytes. Therefore, we examined the effects on a K^+ channel other than $I_{K.ATP}$ present in these cells. Figure 8 shows a typical example for estimation of the nicorandil effect on a single I_{K1} channel in an inside-out patch. At a holding potential of −80 mV, two kinds of channels were observed, $I_{K.ATP}$ and I_{K1} as already revealed in Figure 5. $I_{K.ATP}$ was suppressed by 0.5 mM ATP and activated by 1 mM nicorandil. On the other hand, the open-state probability (P_0) of the I_{K1} channel was 23.7 ± 8.4% at 0 mM ATP (n = 3), and was not changed by 0.5 mM ATP (P_0 = 21.7 ± 5.2%) and 1 mM nicorandil (P_0 = 28.6 ± 8.6%). Neither ATP nor nicorandil had any effects on the unitary amplitude of I_{K1}. We did not see any channel activity having a unitary current amplitude smaller than those of $I_{K.ATP}$ and I_{K1} in the presence of 0.5 mM ATP and of nicorandil up to 1 mM in 15 patches examined.

Discussion

The present study shows that a coronary vasodilator, nicorandil, activates the time-independent outward current in ventricular myocytes, in a manner dependent on $[ATP]_i$. The dose-response curve of nicorandil had a sigmoid dependence on $[ATP]_i$ and the curve was shifted to the right with increasing $[ATP]_i$. The nicorandil-activated outward current was inhibited by application of glibenclamide. Single channel current recordings confirmed an activation of $I_{K.ATP}$ by nicorandil without changing the unitary amplitude of the current. The mode of the channel activation was to prolong the burst duration and to shorten the interburst interval. Therefore, in ventricular myocytes nicorandil activates $I_{K.ATP}$ channel by increasing its open probability via modification of the bursting behaviour of the channels.

Direct evidence for $I_{K.ATP}$ as a target of K^+ channel openers was first described in cardiac myocytes at the single channel level (Escande *et al.*, 1988; 1989; Hiraoka & Fan, 1989; Arena & Kass, 1989b). Recently, several studies have indicated that the target is also $I_{K.ATP}$ in vascular smooth muscle cells (Standen *et al.*, 1989) and pancreatic β cells (Dunne, 1990). Therefore, K^+ channel openers seem to have a common target in different tissues, although effectiveness and sensitivity to these openers were not equal among different preparations. In addition, conflicting reports have been presented as to the target of the K^+ channel openers in vascular smooth muscle cells at the single channel level (Standen *et al.*, 1989; Gelband *et al.*, 1989; Inoue *et al.*, 1989; Kajioka *et al.*, 1990). It is not known whether these conflicting results represent the diversity of K^+ channels in vascular smooth muscles from different organs, species differences or any other unspecified reasons. At present, it is not known whether, or not, the K^+ channel activated by the K^+ channel openers in vascular smooth muscles is identical to $I_{K.ATP}$ in the heart and pancreatic β cells.

The general characteristics of the target of K^+ channel openers in the heart and pancreatic β cells are similar. For example, the target channel is inhibited by increased $[ATP]_i$ and by glibenclamide and has a single channel conductance of

60–90 pS under symmetrical K^+ conditions (Escande *et al.*, 1988; 1989; Arena & Kass, 1989a; Fan *et al.*, 1990; Dunne, 1990). These characteristics are similar to those of $I_{K.ATP}$ reported by others (see, Ashcroft, 1988).

The properties of $I_{K.ATP}$ described in cardiac and skeletal muscles, and in pancreatic β cells are similar to those recorded in the present study (Ashcroft, 1988). The single channel conductance recorded during control experiments using a low (0.5 mM) ATP concentration is about 93 pS, a little larger than that of our previous report (about 80 pS; Fan *et al.*, 1990). This difference may arise from different systems of the patch clamp amplifiers used and somewhat different sampling frequencies of the low-pass filter in both experiments.

There is general agreement that at least one or two open states and two closed states are required to account for $I_{K.ATP}$ channel kinetics (Ashcroft, 1988). In our previous report (Fan *et al.*, 1990), we proposed the following channel kinetic scheme for $I_{K.ATP}$:

$$C_3 \underset{k_{-3}}{\overset{k_3}{\rightleftharpoons}} C_2 \underset{k_{-2}}{\overset{k_2}{\rightleftharpoons}} O \underset{k_{-1}}{\overset{k_1}{\rightleftharpoons}} C_1$$

where the rate constant k_{-1} was considered to be much faster than k_{-2}. For the present analysis, we used different f_c values and discarded the critical times to discriminate the different states, as we did in a previous report (Fan *et al.*, 1990). A single open state was proposed, because the open time distribution was best fitted to a single exponential function when data were collected using an f_c value of 10 kHz. When f_c was set at 0.1 kHz, the briefer closures than 1.6 ms were filtered out so that the transition from state O to state C_2 could be observed, i.e. the burst duration. For closed time analysis, we also employed different f_c value and divided the shut time events of the channel into different time scales. Using an f_c value of 10 kHz and the closed time duration up to 5 ms, the transition from state C_1 to state O was analysed. When f_c was reduced to 0.1 kHz and the closed time durations up to 600 ms were included, the histogram was best fitted to two exponentials which were considered to reflect the transitions from C_1 to O and C_2 to O. The closed time longer than 600 ms was taken to separate clusters of bursts from one another. This revealed another closed state, C_3 (see, Fan *et al.*, 1990).

The transitions between state O and C_1 are insensitive to nicorandil. Nicorandil seems to affect the transition between state O and C_2, that is increases in burst duration. This effect of nicorandil on $I_{K.ATP}$ kinetics was similar to that of pinacidil and opposite to increasing the ATP concentration (Fan *et al.*, 1990), although the nicorandil effect on the transition between C_2 and C_3 was not evaluated. Gillis *et al.* (1989) analysed the effects of sulphonamides on $I_{K.ATP}$ kinetics in β cells. They showed that glibenclamide and tolbutamide shortened the $I_{K.ATP}$ burst duration and lengthened the closed time between the bursts, and this effect is similar to increasing the concentration of extracellular glucose recorded in cell-attached patch. From all of these data, many $I_{K.ATP}$ modulators, including ATP, influence the same aspect of channel kinetics.

Nicorandil has been shown to shorten APD and to hyperpolarize depolarized resting membrane potentials (Yanagisawa & Taira, 1981; Imanishi *et al.*, 1983). It was suggested that the mechanism responsible for these findings was activation of the background K^+ conductance (Taira, 1987) and delayed outward K^+ current (I_K) (Imanishi *et al.*, 1983). In our previous report, we ruled out the possible involvement of I_K in drug-induced outward current. In the present study we have excluded the effect of nicorandil on I_{K1} at the single channel level using an inside-out patch, and did not see any evidence for activation of a small conductance K^+ channel as described by Kakei *et al.* (1986). We also showed the complete block of nicorandil-activated outward current by glibenclamide, a specific $I_{K.ATP}$ blocker (Fosset *et al.*, 1988). So far, $I_{K.ATP}$ seems to be the only K^+ current activated by nicorandil. In the whole current configuration, nicorandil decreased the inward current at potentials negative to −90 mV, a finding that does not agree with the explanation of $I_{K.ATP}$ as the only K^+ current affected by nicorandil. The most likely explanation for this is that nicorandil has an inhibitory action on I_{K1} from the outer surface of the membrane, since it did not affect I_{K1} with the internal application (Figure 8). Further studies are necessary to understand the whole drug effects on ventricular cells including outside-out membranes patches.

This work was supported by a grant from the Ministry of Education, Science and culture of Japan to M.H.

The authors thank Ms N. Fujita for her secretarial assistance.

References

ARENA, J.P. & KASS, R.S. (1989a). Enhancement of potassium-sensitive current in heart cells by pinacidil: Evidence for modulation of the ATP-sensitive potassium channel. *Circ. Res.*, **65**, 436–445.

ARENA, J.P. & KASS, R.S. (1989b). Activation of ATP-sensitive K channels in heart cells by pinacidil: Dependence on ATP. *Am. J. Physiol.*, **257**, H2092–H2096.

ASHCROFT, F.M. (1988). Adenosine 5'-triphosphate-sensitive potassium channels. *Annu. Rev. Neurosci.*, **11**, 97–118.

COOK, N.S. (1988). The pharmacology of potassium channels and their therapeutic potential. *Trends Pharmacol. Sci.*, **9**, 21–28.

DUNNE, M.J. (1990). Effects of pinacidil, RP 49356 and nicorandil on ATP-sensitive potassium channels in insulin-secreting cells. *Br. J. Pharmacol.*, **99**, 487–492.

ESCANDE, D., THURINGER, D., LE GUERN, S. & CAVERO, I. (1988). The potassium channel opener cromakalim (BRL 34915) activates ATP-dependent K^+ channels in isolated cardiac myocytes. *Biochim. Biophys. Res. Commun.*, **154**, 620–625.

ESCANDE, D., THURINGER, D., LE GUERN, S., COURTEIX, J., LAVILLE, M. & CAVERO, I. (1989). Potassium channel openers act through an activation of ATP-sensitive K^+ channels in guinea-pig cardiac myocytes. *Pflügers Arch.*, **414**, 669–675.

FAN, Z., NAKAYAMA, K. & HIRAOKA, M. (1990). Pinacidil activates the ATP-sensitive K^+ channel in inside-out and cell-attached patch membranes of guinea-pig ventricular myocytes. *Pflügers Arch.*, **415**, 387–394.

FOSSET, M., DE WEILLE, J.R., GREEN, R.D. & SCHMID-ANTOMARCHI, H. (1988). Antidiabetic sulphonylurea control action potential properties in heart cells via high affinity receptors that are linked to ATP-dependent K^+ channels. *J. Biol. Chem.*, **263**, 7933–7938.

GELBAND, C.H., LODGE, N.J. & VAN BREEMEN, C. (1989). A Ca^{2+}-activated K^+ channel from rabbit aorta: modulation by cromakalim. *Eur. J. Pharmacol.*, **167**, 201–210.

GILLIS, K.D., GEE, W.M., HAMMOUD, A., McDANIEL, M.L., FALKE, L.C. & MISLER, S. (1989). Effects of sulfonamides on a metabolite-regulated ATP_i-sensitive K^+ channel in rabbit pancreatic B-cells. *Am. J. Physiol.*, **257**, C1119–C1127.

HAMILL, O.P., MARTY, A., NEHER, E., SACKMANN, B. & SIGWORTH, F. (1981). Improved patch-clamp techniques for high-resolution current recordings from cells and cell-free membrane patches. *Pflügers Arch.*, **351**, 85–100.

HAMILTON, T.C., WEIR, S.W. & WESTON, A.H. (1986). Comparison of the effects of BRL 34915 and verapamil on electrical and mechanical activity in rat portal vein. *Br. J. Pharmacol.*, **88**, 103–111.

HIRANO, Y. & HIRAOKA, M. (1988). Barium-induced automatic activity in isolated ventricular myocytes from guinea-pig hearts. *J. Physiol.*, **395**, 455–472.

HIRAOKA, M. & FAN, Z. (1989). Activation of ATP-sensitive outward K^+ current by nicorandil (2-nicotinamidoethyl nitrate) in isolated ventricular myocytes. *J. Pharmacol. Exp. Ther.*, **250**, 278–285.

HIRAOKA, M., FAN, Z. & NAKAYAMA, K. (1990). Modulations of ATP-sensitive K^+ channel current of the heart by nicorandil and pinacidil. *Eur. J. Pharmacol.*, **183**, 1125.

IMANISHI, S., ARITA, M., KIYOSUE, T. & AOMINE, M. (1983). Effects of SG-75 (nicorandil) on electrical activity of canine cardiac Purkinje fibers: Possible increase in potassium conductance. *J. Pharmacol. Exp. Ther.*, **229**, 198–205.

INOUE, I., NAKAYA, Y., NAKAYA, S. & MORI, H. (1989). Extracellular Ca^{2+}-activated K channel in coronary artery smooth muscle cells and its role in vasodilatation. *FEBS Lett.*, **255**, 281–284.

KAJIOKA, S., OIKE, M. & KITAMURA, K. (1990). Nicorandil opens a calcium-dependent potassium channel in smooth muscle cells of the rat portal vein. *J. Pharmacol. Exp. Ther.*, **254**, 905–913.

KAKEI, M., YOSHINAGA, M., SAITO, K. & TANAKA, H. (1986). The potassium current activated by 2-nicotinamidoethyl nitrate (nicorandil) in single ventricular cells of guinea pigs. *Proc. R. Soc. B.*, **229**, 331–343.

KAMEYAMA, M., KIYOSUE, T. & SOEJIMA, M. (1983). Inward rectifier K channel in the rabbit ventricular cells. *Jpn. J. Physiol.*, **33**, 1039–1056.

LINDAR, M. & NEHER, E. (1988). Patch-clamp techniques for time-resolved capacitance measurements in single cells. *Pflügers Arch.*, **411**, 137–146.

NAKAYAMA, K., FAN, Z., MARUMO, F. & HIRAOKA, M. (1990). Interrelation between pinacidil and intracellular ATP concentrations on activation of the ATP-sensitive K^+ current in guinea-pig ventricular myocytes. *Circ. Res.*, **67**, 1124–1133.

OSTERRIEDER, W. (1988). Modification of K^+ conductance of heart cell membrane by BRL 34915. *Naunyn-Schmeidebergs Arch. Pharmacol.*, **337**, 93–97.

SAKMANN, B. & TRUBE, G. (1984). Conductance properties of single inwardly rectifying potassium channels in ventricular cells from guinea-pig hearts. *J. Physiol.*, **347**, 641–657.

SANGUINETTI, M.C., SCOTT, A.L., ZINGARO, G.J. & SIEGEL, P.K. (1988). BRL 34915 (cromakalim) activates ATP-sensitive K^+ current in cardiac muscle. *Proc. Natl. Acad. Sci. U.S.A.*, **85**, 8360–8364.

SMALLWOOD, J.K. & STEINBERG, M.I. (1988). Cardiac electrophysiological effects of pinacidil and related pyridylcyanoguancidine: Relationship to antihypertensive activity. *J. Cardiovasc. Pharmacol.*, **12**, 102–109.

STANDEN, N.B., QUAYLE, J.M., DAVIES, N.W., BRAYDEN, J.E., HUANG, Y. & NELSON, M.T. (1989). Hyperpolarizing vasodilators activate ATP-sensitive K^+ channels in arterial smooth muscle. *Science*, **245**, 177–180.

TAIRA, N. (1987). Similarity and dissimilarity in the mode and mechanism of action between nicorandil and classical nitrates: An overview. *J. Cardiovasc. Pharmacol.*, **10**, Suppl. 8, S1–S9.

TAKANO, M. & NOMA, A. (1990). Selective modulation of the ATP-sensitive K^+ channel by nicorandil in guinea-pig cardiac cell membrane. *Naunyn-Schmiedebergs Arch. Pharmacol.*, **342**, 592–597.

TRUBE, G. & HESCHELER, J. (1984). Inward-rectifying channels in isolated patches of the heart cell membrane: ATP-dependence and comparison with cell-attached patches. *Pflügers Arch.*, **401**, 178–184.

YELLEN, G. (1984). Ionic permeation and blockade in Ca^{2+}-activated K^+ channels of bovine chromaffin cells. *J. Gen. Physiol.*, **84**, 157–186.

YANAGISAWA, T. & TAIRA, N. (1980). Effect of 2-nicotinamidoethyl nitrate (SG-75) on the membrane potential of left atrial muscle fibres of the dog. Increase in potassium conductance. *Arch. Pharmacol.*, **312**, 69–76.

(Received December 6, 1990
Revised February 19, 1991
Accepted February 26, 1991)

Br. J. Pharmacol. (1991), **103**, 1649–1656 © Macmillan Press Ltd, 1991

Regulation of transepithelial ion transport and intracellular calcium by extracellular ATP in human normal and cystic fibrosis airway epithelium

S.J. Mason, A.M. Paradiso & R.C. Boucher

Department of Medicine, University of North Carolina Chapel Hill, North Carolina 27599, U.S.A.

1 The role of extracellular nucleotides in regulation of ion transport activities (short circuit current, I_{sc}) of human respiratory epithelia was studied.

2 Application of nucleotides to the apical or basolateral membrane of human nasal epithelium induced a concentration-dependent increase in I_{sc}.

3 The rank order of potency of purine- or pyrimidine-induced changes in I_{sc} of normal human nasal epithelium when applied to the apical membrane (UTP $\geqslant$ ATP > ATPγS > 2MeSATP > ADPβS $\gg$ $\beta\gamma$MeATP $\geqslant$ $\alpha\beta$MeATP) or basolateral membrane (2MeSATP > UTP > ATP > ATPγS > $\alpha\beta$MeATP > $\beta\gamma$MeATP) is consistent with involvement of a P_2 purinoceptor. A similar rank order of potencies was observed for nucleotide effects on intracellular calcium measured by Fura-2 fluorescence using microspectrofluorimetry.

4 Similar nucleotide potency in the regulation of ion transport and intracellular calcium in cystic fibrosis (CF) airway epithelium (UTP $\geqslant$ ATP) was observed, suggesting purinoceptors might be used to stimulate ion transport processes that would promote hydration of airway secretions and facilitate their clearance from CF lungs.

5 These data provide evidence for the regulation of ion transport by P_2 purinoceptors in normal and cystic fibrosis human airway epithelium.

Keywords: Epithelium; adenosine triphosphate; purinoceptors; airway epithelium; cystic fibrosis; ion transport; purine nucleotide; pyrimidine nucleotide; calcium release

Introduction

Extracellular adenosine triphosphate (ATP) has been shown to regulate a variety of biological processes including non-vascular smooth muscle contraction (Maguire & Satchell, 1979; Brown & Burnstock, 1981) and vascular tone (Burnstock & Kennedy, 1986; Haeussinger *et al.*, 1987), platelet aggregation (Born & Kratzer, 1984), neurotransmission (Burnstock, 1971; Burnstock & Sneddon, 1985), and cellular ion transport (Burgess *et al.*, 1979; Gallacher, 1982) and secretory activities (Chapal & Loubatières-Mariani, 1981; Pearson *et al.*, 1983). These effects are mediated by specific purinoceptors which respond to ATP or other nucleotides present in the extracellular millieu (Gordon, 1986).

Purinoceptors have been functionally identified in rat pulmonary epithelia in studies of regulation of alveolar Type II surfactant phospholipid secretion (Rice & Singleton, 1986). To our knowledge these receptors have not been described in human airway epithelial cells. Because ion transport appears to be regulated by purinoceptor stimulation in other eipthelia (Burgess *et al.*, 1979; Gallacher, 1982), we investigated several features of the effect of extracellular nucleotides on the ion transport activities of human airway epithelium.

Purinoceptor regulation of ion transport might have potential therapeutic benefit in lung diseases characterized by abnormalities in epithelial ion transport, e.g., cystic fibrosis. In cystic fibrosis (CF) the airway epithelial dysfunction is expressed in part by defective regulation of Cl^- ion transport by secretagogues that regulate the apical cell membrane Cl^- channel by adenosine 3′ : 5′-cyclic monophosphate (cyclic AMP)-dependent or protein kinase C-dependent mechanisms (Boucher *et al.*, 1986, 1989; Riordan *et al.*, 1989; Rommens *et al.*, 1989). Induction of Cl^- secretion by CF airway epithelia *in vivo* would be expected to help liquify the relatively dehydrated, thick airway surface liquid that characterizes this disease. We therefore tested whether nucleotides would bypass regulatory defects in CF airway epithelia and induce Cl^- secretion at rates similar to those of normal airway cells. Consequently, this study could suggest a new class of therapeutic agents for the treatment of CF.

Methods

Cell culture

Freshly excised human nasal epithelium from normal or cystic fibrosis subjects was grown in primary culture in F-12, hormone-supplemented medium as previously described (Wu *et al.*, 1985). For $[Ca^{2+}]_i$ measurements, cultures were grown on non-fluorescent vitrogen substrates on glass coverslips. Cultures for electrophysiological studies were grown to confluence on permeable collagen matrix supports (CMS), allowing addition of agonists to the basolateral or apical surface of the epithelial sheet.

Biolectric studies

Confluent monolayers of primary human nasal epithelium were mounted in modified Ussing chambers (Knowles *et al.*, 1983; Boucher *et al.*, 1988). The studies were performed under short circuit current conditions at 37°C, and in some studies, amiloride was added to the apical bath (10^{-4} M) to block transepithelial sodium transport. Changes in transepithelial potential difference (V_t), resistance (R_t) and short circuit current (I_{sc}) were measured in response to addition of various nucleotides. Each cultured preparation was exposed to only one concentration of an agonist on either the basolateral or apical surface to avoid the tachyphylaxis observed in preliminary cumulative dose-response studies. To construct concentration-effect relationships of responses to nucleotides, we assumed that the same maximum response to an agonist could be induced from each tissue culture preparation from the same individual (see Statistics).

Measurements of intracellular calcium

Primary human nasal epithelial cells grown to confluence on vitrogen coated coverslips were loaded with a final concentration of 3 μM Fura-2/AM at 37°C for 30 min. The cells were then washed in NaCl Ringer and mounted in a chamber for measurements of fluorescence. To reduce the rate of leakage of Fura-2 from the cell into the extracellular space and avoid time-dependent compartmentalization of the probe, all measurements of $[Ca^{2+}]_i$ were performed at 25°C. At this temperature, no vesicular bright spots indicative of compartmentalization of the probe were observed.

Measurements of $[Ca^{2+}]_i$ in single human nasal epithelial cells were obtained with a modular microspectrofluorimeter (SPEX Industries, Inc., Edison, NJ, U.S.A.) attached to a Zeiss Axiovert IM 35 microscope. The system was equipped with a xenon lamp, beam splitter, two monochromators and a rotating chopper mirror that permitted excitation of cell fluorescence at alternating wavelengths of 340 and 380 nm (emission $\geqslant$ 450 nm). The fluorescent signal from a single cell was measured with a photometer equipped with a pinhole (spot diameter of 3–5 μm) that excluded signals from adjacent cells.

After agonist was added, the fluorescent signal was quenched by a NaCl Ringer solution containing 1.5×10^{-4} M digitonin and 10^{-3} M $MnCl_2$. The remaining signal at each excitation wavelength, equivalent to the background fluorescence in non-loaded cells, was subtracted from data from Fura-2/AM loaded cells before the ratio (340 nm/380 nm) was taken. The 340 nm/380 nm ratio was converted to an actual $[Ca^{2+}]_i$ measurement by using the external calibration standards and the formula derived by Grynkiewicz et al. (1985) used with dual wavelength measurements: $[Ca^{2+}]_i = K[(R_x - R_o)/(R_s - R_x)]$, with R_o and R_s representing the ratios at 0 Ca^{2+} and saturating Ca^{2+}, respectively. R_x represents the experimental ratio. K is $K_d(F_o/F_s)$, with $K_d = 1.57 \times 10^{-7}$ M at 25°C as the effective dissociation constant for Fura-2, and F_o and F_s represent the fluorescence intensities at 380 nm with 0 and saturating Ca^{2+}, respectively.

Statistical methods

A relatively large variability in the maximal responses was observed in tissues from different donors. However, the responses (I_{sc} or $[Ca^{2+}]_i$) within preparations from a single donor were more homogeneous. To control for inter-donor tissue variability, tissues from a single donor were used for the entire concentration-range of a nucleotide agonist. Only tissues with transepithelial potential difference greater than -5 mV and transepithelial resistance greater than 100 ohms cm^{-2} were used in the studies. For comparing effectiveness of ATP administered to the luminal versus basolateral surface of normal and CF preparations, the absolute changes in I_{sc} from basal levels are plotted. For comparison of rank orders of potency for nucleotides, the percentage change in I_{sc} from basal levels is shown. For measurements of $[Ca^{2+}]_i$, only absolute changes from basal levels are plotted. To estimate a representative variance for the response to agonists, we (1), determined the absolute response to the maximum agonist concentration; (2) calculated the percentage of the maximal response yielded by each lower agonist concentration (normalized maximum percentage response); and (3) calculated the variance of the normalized responses for each agonist concentration in preparations from different donors. Rank orders of potency of the agonists were obtained by comparing EC_{50}s of each agonist.

Chemicals and solutions

ATP, UTP, ATPγS, CTP, GTP, ITP, adenylyl-imidodiphosphate (AMPPNP), β,γ-methylene ATP (β,γ-MeATP), ADPβS, ADP, AMP, UDP, 5-BrUTP, UMP, ATPαS and dipyridamole were obtained from Boehringer Mannheim Biochemicals (Indianapolis, IN, U.S.A.). α,β-Methylene ATP (α,β-MeATP) and amiloride were obtained from Sigma Chemicals (St. Louis, MO, U.S.A.). 2-Methylthio ATP (2MeSATP) was purchased from Research Biochemicals Inc. (Natick, MA, U.S.A.).

Bioelectric properties were measured with confluent monolayers bathed by Ham's F-12 culture solution without hormone supplements (Gibco, Grand Island, NY, U.S.A.).

The acetoxymethylester of Fura-2 (Fura-2/AM) and the pentapotassium salt Fura-2 were purchased from Molecular Probes (Eugene, OR, U.S.A.). To obtain external calibration standards for the dye, the pentapotassium salt Fura-2 was used at 15 μM in solution with 150 mM KCl, 20 mM NaCl, 10 mM 4-(2-hydroxyethyl)-1-piperazineethanesulphonic acid (HEPES), and either 5 mM $CaCl_2$ or 2 mM EGTA.

For intracellular calcium studies, NaCl Ringer solution at 25°C was employed, containing the following (in mM): NaCl 150, KCl 5, D-glucose 5, HEPES 10, $CaCl_2$ 2, $MgCl_2$ 2, adjusted to pH 7.4. For studies to determine the ionic form of ATP active at the receptor, $MgCl_2$ was varied in the above NaCl Ringer between nominally Mg^{2+}-free, 2 mM and 5 mM Mg^{2+}. For studies with solutions free of calcium, 2 mM EGTA replaced the $CaCl_2$.

Results

Normal human nasal epithelium-ion transport

The effects of extracellular ATP on normal human nasal epithelium were investigated employing biolectric measurements of ion transport activity when the nucleotide was applied to either the apical or basolateral membrane. Representative tracings obtained after application of ATP to cultured sheets of human nasal epithelium mounted in Ussing chambers are illustrated in Figure 1. Figure 1(a) and (b) represents the I_{sc} response when ATP is applied to the apical or basolateral membrane of tissues in the basal, Na^+ absorptive mode (Boucher et al., 1986). ATP rapidly stimulated an increase in I_{sc} when applied to either surface. In general, the change in I_{sc} induced by application of ATP to the apical or the basolateral side returned to baseline or below within 5 min after addition of agonist. Oscillations in I_{sc} following ATP were frequently observed. Apical pretreatment with amiloride (10^{-4} M) removes active Na^+ absorption as a component of the I_{sc} so that the residual I_{sc} reflects a Cl^- secretory current (Boucher et al., 1986; Willumsen et al., 1989). Figure 1(c) and (d) represent the typical Cl^- secretory response of human nasal epithelium when ATP is applied to amiloride-pretreated tissues. Following the initial peak, the ATP induced increase in I_{sc} after basolateral addition to amiloride-pretreated tissues returned to baseline within 5 min (Figure 1d). In contrast, most tissues (91% of those followed for 10 min) treated with ATP on the apical surface following amiloride pretreatment exhibited prolonged (> 10 min) increases in I_{sc} above baseline levels (Figure 1c).

The concentration-effect relationship of ATP applied to normal human nasal epithelium under basal conditions is shown in Figure 2. Comparisons were made between responses of tissues from different donors based on the peak change in I_{sc} following ATP application (see Figure 1). The curve describes the mean peak change in I_{sc} in response to increasing log concentrations of ATP applied to the apical or basolateral surface. The effectiveness of the nucleotide is approximately equal when applied to the apical or basolateral surface between 10^{-7} and 10^{-4} M. A large increase in I_{sc} is seen with 10^{-3} M ATP applied to the basolateral membrane that is not seen with apical application.

Figure 3 illustrates concentration-effect relationships for ATP applied to the apical or basolateral membrane of amiloride-pretreated tissues. Again, the effect of ATP on ion transport is shown as the mean peak change in I_{sc} after ATP application. The change in ion transport induced by ATP in

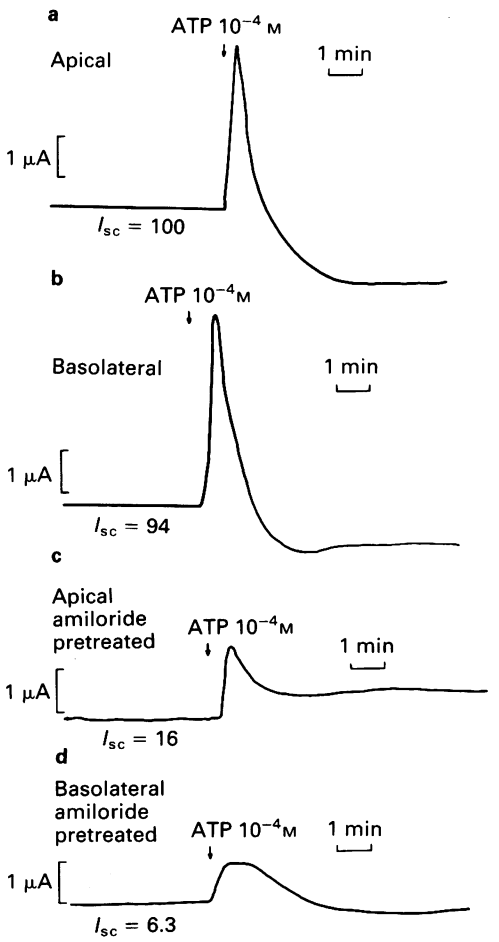


Figure 1 Representative tracings of effect on I_{sc} of extracellular ATP (10^{-4} M) applied to the apical or basolateral membrane of human nasal epithelium. (a) Response of human nasal epithelium in basal transport mode (primarily Na^+ absorptive) to ATP applied to the apical surface (basal I_{sc} = 100 μA cm^{-2}). (b) Response of human nasal epithelium in basal mode to ATP applied to the basolateral surface (basal I_{sc} = 94 μA cm^{-2}). (c) Cl^- secretory response to ATP applied to apical surface of amiloride-pretreated tissue (post-amiloride I_{sc} = 16 μA cm^{-2}). (d) Cl^- secretory response to ATP applied to the basolateral surface of amiloride-pretreated tissue (post-amiloride I_{sc} = 6 μA cm^{-2}).

amiloride-pretreated tissues is routinely smaller than that observed in tissues in the basal state (Figure 2). The potency and effectiveness of ATP in amiloride-treated tissues are similar whether applied to the apical or basolateral membrane and the log concentration-effect curves are sigmoidal in character, with EC_{50} values of approximately 1–2 × 10^{-5} M.

The purinoceptor subtype(s) linked to regulation of ion transport of human nasal epithelium were characterized by obtaining concentration-effect relationships for a variety of purine and pyrimidine agonists in preparations derived from normal and CF patients. We characterized receptor subtype(s) on the basolateral surface by measuring nucleotide effect on basal Na^+ transport rates. Because therapies designed to induce Cl^- secretion might best be delivered by the aerosol route, receptor subtype characterization on the apical barrier was performed in the presence of amiloride. The effect of extracellular nucleotides on ion transport is shown as the percentage change in I_{sc} from control values when applied to the basolateral or apical surface of the culture. Basal pre-agonist currents were similar for tissues in each concentration group (see Figure legends).

Under the culture conditions employed in these studies, the P_1 receptor agonist adenosine, following preincubation of tissues with dipyridamole (10^{-6} M) to block adenosine uptake, induced only small and variable changes in I_{sc} compared to

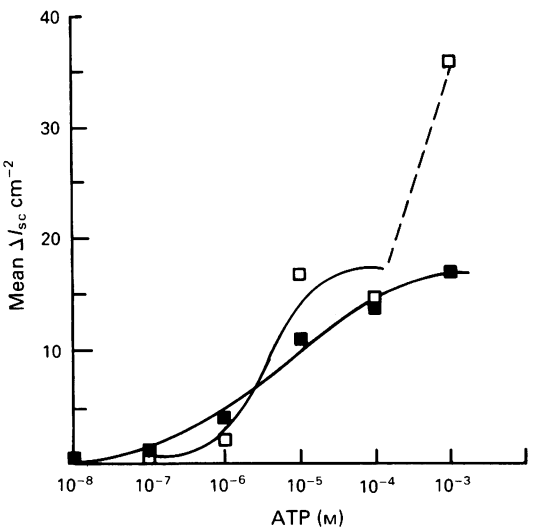


Figure 2 Log concentration-effect relationship (mean change in I_{sc} from basal levels) of ATP applied to the apical (■) or basolateral (□) surface of human nasal epithelium without amiloride-pretreatment. Mean I_{sc} of tissues in basal mode for range of ATP concentrations tested were (in μA cm^{-2}): apical ATP 80 ± 2, range 16–150, n = 3–9 at each agonist concentration; basolateral ATP 68 ± 5, range 17–138, n = 3–13 at each agonist concentration. S.e.mean of each data point is ≤12% of the normalized maximum response.

ATP (compare with Figures 4 and 5, below). Addition of adenosine to the apical surface of amiloride-pretreated human nasal epithelium at 10^{-5} M (n = 7) or 10^{-4} M (n = 8) induced an increase of 10 ± 7 or 10 ± 6%, respectively, whereas addition of the same doses to the basolateral barrier (n = 8, each dose) raised I_{sc} by less than 5%. These findings suggest that the activation of P_1 receptors contributes little to the measured effects of extracellularly applied ATP on ion transport. Therefore, we focused on agonists that interact with P_2 receptors in the regulation of ion transport and $[Ca^{2+}]_i$ mobilization in human nasal epithelium.

Figure 4 illustrates the concentration-effect relationships of agonists applied to the basolateral surface of airway epithe-

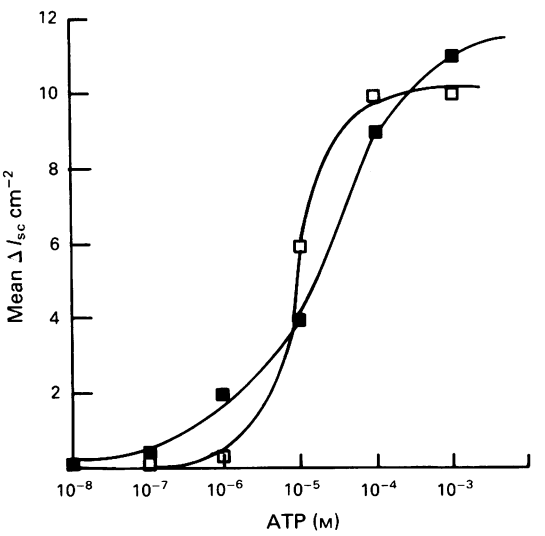


Figure 3 Log concentration-effect relationships (mean change in I_{sc} over basal levels) of ATP applied to the apical (■) or basolateral (□) membrane of amiloride-pretreated (10^{-4} M) human nasal epithelium. Mean I_{sc} of amiloride-pretreated tissues for the range of ATP concentrations tested were (in μA cm^{-2}): apical ATP, 13 ± 1, range 9–16, n = 3–11 at each agonist concentration; basolateral ATP, 14 ± 1, range 8–28, n = 3–6 at each agonist concentration. S.e.mean of each data point is ≤12% of the normalized maximum response.

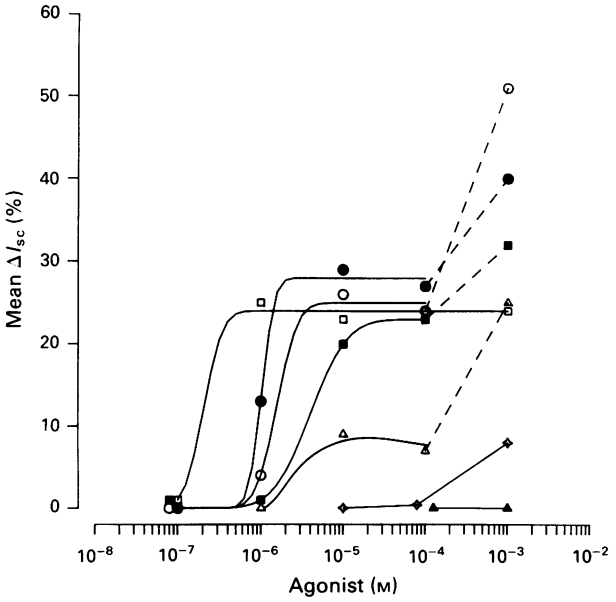


Figure 4 Log concentration-effect curves (percentage change in I_{sc} from basal levels) of nucleotides applied to the basolateral surface of normal human nasal epithelium. Mean basal I_{sc} in each set of experiments were (in $\mu A\,cm^{-2}$): ATP (○), 69 ± 5, range 55–80, $n = 5$ ($n = 3$–11 at each agonist concentration); UTP (●), 66 ± 9, range 21–158, $n = 9$ ($n = 3$–23); 2MeSATP (□), 48 ± 6, range 35–65, $n = 6$ ($n = 3$–17); ATPγS (■), 47 ± 8, range 28–72, $n = 3$ ($n = 3$); ADPβS (△), 49 ± 6, range 36–65, $n = 3$ ($n = 3$); αβMeATP (◇), 51 ± 12, range 28–66, $n = 3$ ($n = 3$); βγMeATP (▲), 79 ± 21, range 59–100, $n = 3$ ($n = 3$). S.e.mean of each data point is ≤15% of the normalized maximum response.

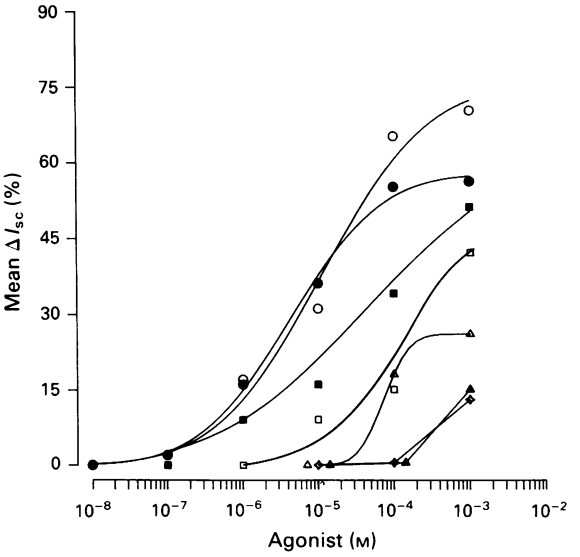


Figure 5 Log concentration-effect curves (percentage change in I_{sc} from basal levels) of nucleotides applied to the apical surface of human nasal epithelium pretreated with amiloride (10^{-4} M). Mean post-amiloride I_{sc} in each set of experiments were (in $\mu A\,cm^{-2}$): ATP (○), 13 ± 1, range 9–16, $n = 8$ ($n = 3$–11 at each agonist concentration); UTP (●), 12 ± 1, range 11–15, $n = 5$ ($n = 3$–17); ATPγS (■), 12 ± 1, range 8–15, $n = 3$ ($n = 3$); 2MeSATP (□), 16 ± 2, range 12–21, $n = 3$; ($n = 3$–7); ADPβS (△), 15 ± 1, range 13–16, $n = 3$ ($n = 3$) βγMeATP (▲), 14 ± 0, range 8–19, $n = 3$ ($n = 3$); αβMeATP (◇), 11 ± 0, range 7–14, $n = 3$ ($n = 3$). S.e.mean of each data point is ≤13% of the normalized maximum response.

lium. Compared to the concentration-effect curve of ATP, agonists that stimulate P_{2x} receptors (αβMeATP and βγMeATP) induced little change in ion transport rates. The observed rank order of potency for agonists that significantly increased I_{sc} was 2MeSATP > UTP ⩾ ATP > ATPγs > ADP > ADPβS. At concentrations of ATP, UTP, ATPγS or ADPβS between 10^{-7} and 10^{-4} M, the relationship between log agonist concentration and observed responses was a curve of sigmoidal character. The concentration-effect curve of these agonists was biphasic in character when the effect on I_{sc} of 10^{-3} M drug was considered.

The concentration-effect relationships for nucleotides added to the apical surface of amiloride-pretreated tissues are shown in Figure 5. Compounds reported to be effective P_{2x} receptor agonists produced little change in ion transport by airway epithelium. Those reported to be effective P_{2y} or UTP-sensitive receptor agonists stimulated Cl^- secretion with the following rank order of potency: ATP ⩾ UTP > ATPγS > ADP > 2MeSATP > ADPβS.

In an attempt to test whether multiple P_2 receptor types are expressed on each membrane, or a single novel receptor subtype is expressed on either barrier, additivity studies were performed using two ligands that supposedly interact with separate receptor subtypes, UTP and 2MeSATP. Co-addition of saturating concentrations of 2MeSATP (10^{-4} M) and UTP (10^{-4} M) on the basolateral membrane induced an effect that was about twice that induced by each of the agonists alone in sets of tissue preparations obtained from three separate donors. The mean increase in I_{sc} for UTP alone was 4.6 ± 0.5 $\mu A\,cm^{-2}$, and for 2MeSATP alone was 4.3 ± 0.9 $\mu A\,cm^{-2}$, whereas current increased 10 ± 1 $\mu A\,cm^{-2}$ in response to the combination of UTP and 2MeSATP ($n = 3$). The additivity observed suggests each ligand interacts with a separate receptor on the basolateral membrane. When the two agonists were applied to the apical surface singly and in combination following amiloride, no additive effects were evident.

Normal human nasal epithelium-intracellular calcium

Based on studies in other epithelia indicating that regulation of $[Ca^{2+}]_i$ by purinoceptors initiates changes in ion transport rates (Kimmich & Randles, 1982), we investigated whether ATP regulated $[Ca^{2+}]_i$ in single human nasal epithelial cells using an intracellular Ca^{2+}-sensitive fluorescent dye. Extracellular application of ATP induced an immediate increase in $[Ca^{2+}]_i$ levels that decreased over 1 to 2 min to a prolonged plateau (Figure 6a). Exposure to ATP in Ca^{2+}-free medium resulted in an initial sharp increase in $[Ca^{2+}]_i$ which returned to baseline over a 2 min period with no plateau phase observed (Figure 6b). Return of the cells to a Ca^{2+}-containing solution resulted in restoration of the plateau phase in the Ca^{2+} response to ATP.

To investigate whether changes in $[Ca^{2+}]_i$ might be related to regulation of ion transport, receptor characterization was performed by measuring changes in $[Ca^{2+}]_i$ in response to a number of nucleotide drugs. Concentration-effect curves for angonists active at P_{2x}, P_{2y} subtype or UTP-sensitive receptors and other purine or pyrimidine receptor agonists were generated, measuring mean change in $[Ca^{2+}]_i$ in response to agonist concentration (Figure 7). ATP, UTP and ATPγS were the most effective agonists. Classical P_{2x} (αβMeATP and βγMeATP) and P_{2y} (2MeSATP and ADPβS) receptor agonists had little effect (Figure 7a) as did other analogues of ATP and ADP (Figure 7b). 5BrUTP was essentially as effective as UTP for stimulation of Ca^{2+} mobilization (Figure 7c).

To characterize the chemical form of ATP interacting with the purinoceptor on human nasal epithelium, fluorescence measurements of single cell $[Ca^{2+}]_i$ response to ATP (10^{-3} to 10^{-8} M) were obtained with various levels of Mg^{2+} in the extracellular medium. Increasing $[Mg^{2+}]$ resulted in a shift to the right of the dose-response curve: the EC_{50} values for ATP were 5×10^{-6} M in solutions nominally Mg^{2+}-free; 2×10^{-5} M in solutions containing 2 mM Mg^{2+}; and 1×10^{-4} M in solutions containing 5 mM Mg^{2+} ($n = 4$ for each Mg^{2+} concentration). These shifts suggest that the free acid form ATP^{4-} is the active form at human airway P_2 receptors

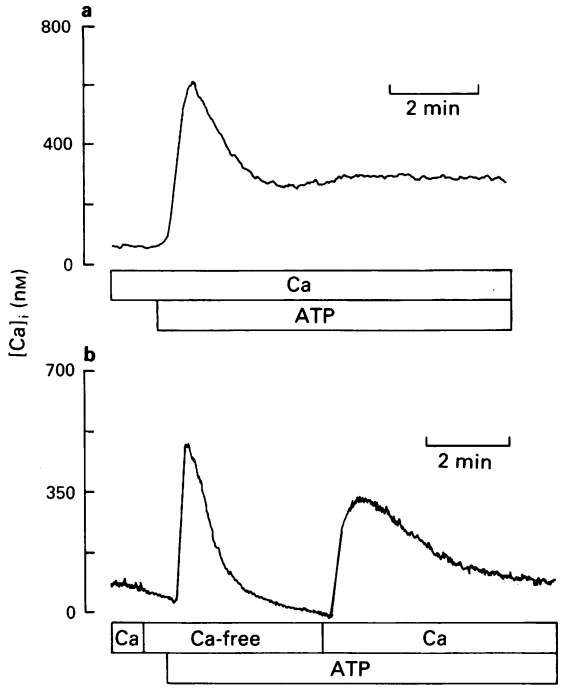


Figure 6 The effect of ATP (10^{-4} M) on the concentration of intracellular calcium $[Ca^{2+}]_i$ in single human nasal epithelial cells with (a) and without (b) 2 mM Ca^{2+} in the bathing medium. In (b) external Ca^{2+} was restored to the culture medium after the peak response to ATP, resulting in a plateau level above baseline. The increase in $[Ca^{2+}]_i$ is calculated from the change in fluorescence due to increased binding of free Ca^{2+} by the dye Fura-2 (30 min preincubation with culture at 37°C at 3 μM concentration). (a) and (b) are representative of 9 experiments performed on separate tissues from 8 patients. Mean basal $[Ca^{2+}]_i$ = 70 ± 5 nM, maximum mean change in $[Ca^{2+}]_i$ = 739 ± 171 nM.

rather than $MgATP^{2-}$, the ionic form more prevalent under most physiological conditions. The EC_{50} value of bradykinin, another agent which increases $[Ca^{2+}]_i$ in human nasal epithelial cells via a non-purinoceptor (Paradiso *et al.*, 1989), was not altered by varying $[Mg^{2+}]$ in the extracellular medium.

Cystic fibrosis nasal epithelium

Availability of CF tissues is limited, and our investigation of effects of nucleotides was restricted to examining regulation of Cl^- secretion rates and $[Ca^{2+}]_i$ levels by ATP and UTP. Only small changes in Cl^- secretion (amiloride-resistant I_{sc}) were observed in CF tissues following basolateral addition of ATP (14 ± 3 maximum mean % change in I_{sc}, n = 6) compared with normal tissues (51 ± 8 maximum mean % change in I_{sc}, n = 6). Apical administration of ATP following blockade of Na^+ absorption with amiloride resulted in two distinct patterns of response in tissues from CF subjects (Figures 8 and 9). Most tissues exhibited an increase in I_{sc} over basal levels after ATP (Figure 8a), suggesting stimulation of Cl^- secretion. However, approximately 30% of CF tissues tested responded with a change to opposite polarity of I_{sc} following ATP (Figure 8b), suggesting a secretion dominated by cations in these preparations (Bean & Friel, 1990). UTP applied to the apical surface routinely stimulated increases in Cl^- secretion in CF tissues (Figure 8c). Mean peak change in I_{sc} from post-amiloride basal levels in response to ATP or UTP application was measured in individual CF tissues to obtain the concentration-effect relationships illustrated in Figure 9.

Increases in $[Ca^{2+}]_i$ in CF tissues were also observed after addition of ATP or UTP (Figure 10). The similar potency and effectiveness of ATP and UTP in these tissues suggests the presence of a P_2 receptor type sensitive to UTP on CF epithelium.

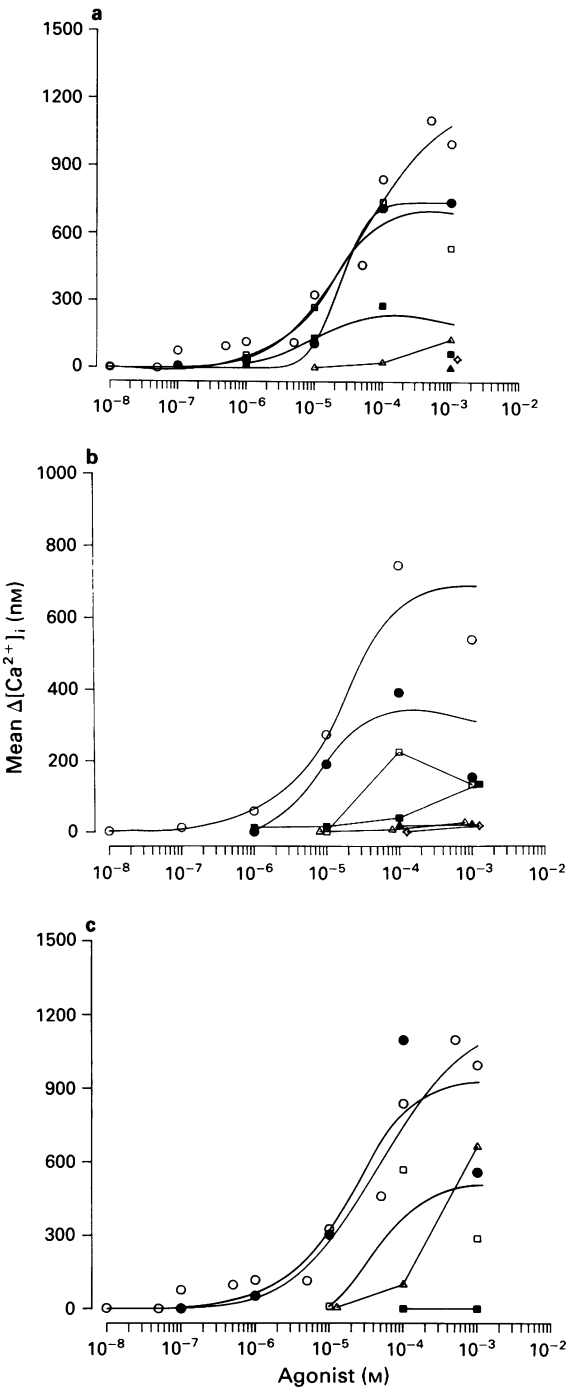


Figure 7 Log concentration-effect relationships of purine and pyrimidine compounds on $[Ca^{2+}]_i$ (mean change in $[Ca^{2+}]_i$ over basal levels). (a) comparison of agonists which bind to P_{2x}, P_{2y} or UTP-sensitive receptors, mean basal $[Ca^{2+}]_i$ in each set of experiments were (in nM): UTP (○), 81 ± 8, range 48–113, n = 5 (n = 3–6 at each agonist concentraion); ATPγS (●), 116 ± 11, range 85–151, n = 4 (n = 3–6); ATP (□), 61 ± 3, range 51–70, n = 8 (n = 3–8); 2MeSATP (■), 123 ± 19, range 95–180, n = 3 (n = 3); ADPβS (△), 91 ± 17, range 74–107, n = 3 (n = 3); αβMeATP (◇), 82 ± 16, range 50–99, n = 3 (n = 3); βγMeATP (▲), 68 ± 4, range 61–74, n = 3 (n = 3). (b) Comparison of other purine agonists with response stimulated by ATP (○). Mean basal $[Ca^{2+}]_i$ in each set of experiments were (nM): GTP (●), 117 ± 13, range 92–153, n = 3 (n = 3); AMPPNP (□), 137 ± 50, range 74–235, n = 3 (n = 3); ITP (■), 103 ± 10, range 85–121, n = 3 (n = 3); ADP (△), 94 ± 16, range 75–127, n = 3 (n = 2–3); AMP (▲), 111 ± 28, range 69–189, n = 3 (n = 3); ATPαS (◇), 89 ± 2, range 87–91, n = 1 (n = 2). (c) Comparison of UTP (○) with other pyrimidine agonists, mean basal $[Ca^{2+}]_i$ (in nM): 5BrUTP (●), 110 ± 13, range 82–152, n = 3 (n = 2–3); UDP (□), 89 ± 2, range 84–92, n = 3 (n = 3); CTP (△), 83 ± 10, range 69–102, n = 3 (n = 3); UMP (■), 78 ± 14, range 64–91, n = 2 (n = 2). S.e.mean of each data point is ⩽12% of the normalized maximum response.

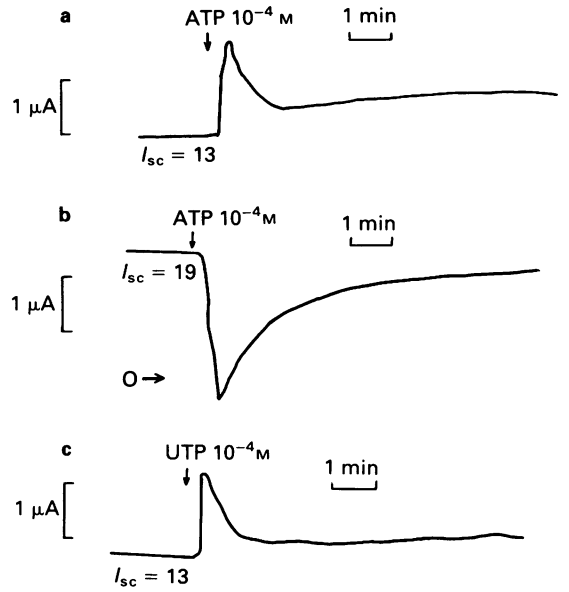


Figure 8 Representative bioelectric tracings of effect on I_{sc} of extracellular ATP (10^{-4} M) or UTP (10^{-4} M) applied to the apical surface of amiloride-pretreated (10^{-4} M) CF human nasal epithelium. (a) Cl^- secretion in response to ATP (post-amiloride $I_{sc} = 13\,\mu A\,cm^{-2}$). (b) I_{sc} response to ATP of opposite polarity (post-amiloride $I_{sc} = 19\,\mu A\,cm^{-2}$). (c) Cl^- secretory response to UTP (post-amiloride $I_{sc} = 5\,\mu A\,cm^{-2}$).

Discussion

We have demonstrated that ATP modulates ion transport rates when added to either the apical or basolateral surface of human airway epithelium. These effects appear to be mediated by cell surface receptors that respond to ATP by regulating ion transport rates, which may be related to release of Ca^{2+} from internal stores and extracellular Ca^{2+} influx.

The ion transport activities measured in this study are believed to be important in regulation of the volume and composition of secretions produced by human airway cells (Yankaskas *et al.*, 1985). Inflammatory mediators like bradykinin and histamine probably alter the water content of luminal secretions through their effects on ion flow and thus affect the rate of clearance of these secretions within the airways. Our characterization of the effects of nucleotide receptors on human nasal epithelial transport rates has led to insights into the functional effects of activation of these receptors on the metabolism of airway secretions. For example, ATP applied to the basolateral surface of the epithelium induces a large increase in ion transport rate (I_{sc}), reflecting a component of increased absorption of Na^+ in response to ATP. The increase in Na^+ absorption results in increased water movement across the epithelium, likely acting to deplete the volume of airway surface liquid. Amiloride blocks Na^+ absorption and stimulates Cl^- secretion in human nasal epithelium, probably reversing the direction of water flow. Consequently, addition of ATP to the luminal surface of the epithelium during amiloride treatment would probably accelerate this rate of Cl^- secretion and water movement.

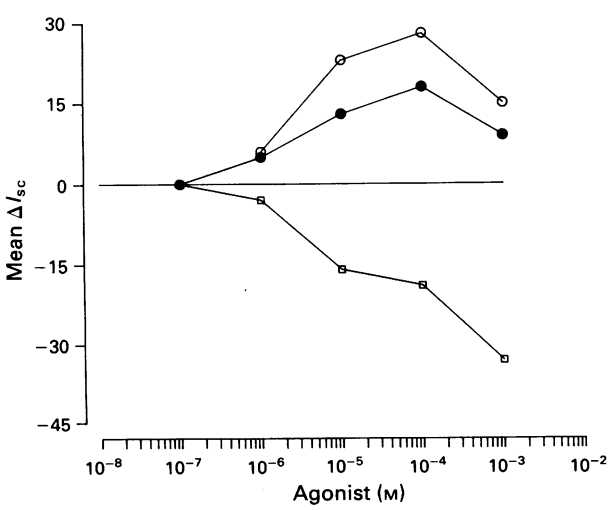


Figure 9 Log concentration-effect curves for changes in I_{sc} from basal levels when ATP or UTP are applied to the apical surface of amiloride-pretreated (10^{-4} M) cystic fibrosis tissues. Mean post-amiloride I_{sc} in each set of experiments were (in $\mu A\,cm^{-2}$): ATP [Group A (●), Group B (□)], 13 ± 1, range 3–31, $n = 4$ ($n = 4$–13 at each agonist concentration); UTP (○), 12 ± 2, range 8–14, $n = 3$ ($n = 3$). S.e.mean of each data point is ⩽13% of the normalized maximum response.

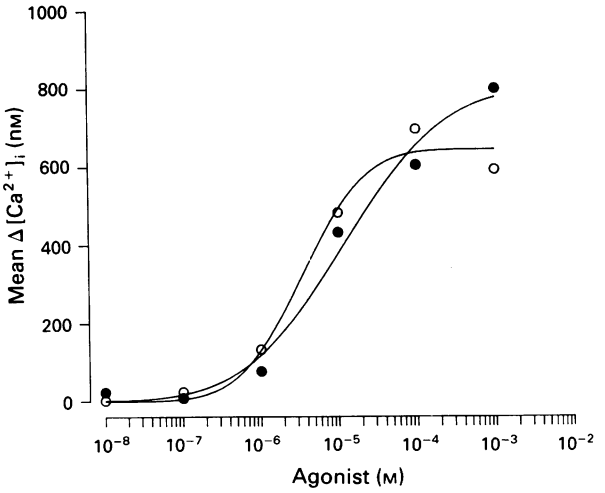


Figure 10 Log concentration-effect relationships of the effect of ATP and UTP on $[Ca^{2+}]_i$ (change from basal levels) in single cystic fibrosis nasal epithelial cells. Mean basal $[Ca^{2+}]_i$ (in nM): ATP (○), 65 ± 6, range 44–86, $n = 3$ ($n = 3$ at each agonist concentration); UTP (●), 67 ± 3, range 56–79, $n = 3$ ($n = 3$–4). S.e.mean of each data point is ⩽8% of the normalized maximum response.

Our ion transport data suggest the presence of at least one of the several reported P_2 receptor subtypes (Burnstock & Kennedy, 1985) on both the apical and basolateral membrane. The receptor on either membrane that initiates the ion transport responses is clearly not of the P_{2x} subtype as basal I_{sc} shows little or no change in response to the potent P_{2x} agonists $\alpha\beta$MeATP and $\beta\gamma$MeATP. The rank orders of potency and efficacy for agonists applied to the apical surface of human nasal epithelium were: ATP ⩾ UTP > ATPγS > 2MeSATP > ADPβS. This relationship is suggestive of the presence of a receptor sensitive to UTP and not of the typical P_{2y} subtype, which interacts most potently with 2MeSATP and ADPβS. A putative P_2 receptor responding with approximately equal potency to UTP and ATP has been reported in a number of cell types, including human neutrophils (Seifert *et al.*, 1989; Cockcroft & Stutchfield, 1989; Kuroki & Minakami, 1989), HL60 cells (Cockcroft & Stutchfield, 1989), fibroblasts (Fine *et al.*, 1989), amnion cells (Vander Kooy *et al.*, 1989), Ehrlich ascites tumour cells (Dubyak & De Young, 1985), pituitary cells (Davidson *et al.*, 1990), A431 epidermoid carcinoma cells (Hosoi & Edidin, 1989), J774 mouse macrophage cells (Greenberg *et al.*, 1988) and perfused rat liver (Haeussinger *et al.*, 1988). Controversy exists at present about whether UTP responsiveness implies the existence of a separate pyrimidine receptor (Haeussinger *et al.*, 1987; von Kuegelgen *et al.*, 1987; Seifert & Schultz, 1989; Stutchfield & Cockcroft, 1990; Pfeilschifter, 1990).

Rank orders of potency of nucleotides added to the basolateral membrane suggest that the P_2 receptor(s) found there are

also not of the P_{2x} or P_{2y} subtype, and are sensitive to UTP. The I_{sc} rank order of potency (2MeSATP > UTP > ATP > ATPγS > ADPβS) for nucleotide additions to the basolateral membrane does raise the possibility that two receptor subtypes may be required to account for the observed functional responses. The potency of the prototype P_{2y} receptor agonist, 2MeSATP, was greater than that of the other agonists tested. However, the lack of effect of another classical P_{2y} agonist, ADPβS, compared to 2MeSATP in human nasal epithelium makes it unlikely that the receptor mediating I_{sc} response is the usual P_{2y} receptor subtype. No currently accepted P_2 receptor subtype fits this potency profile. Additive studies with 2MeSATP and UTP suggest that two receptor subtypes rather than a single receptor may be required to account for this profile. Similar studies on the apical membrane did not suggest the presence of two receptor subtypes, but the failure to detect additivity could reflect limitations of the maximal response measured in this assay (Cl^- secretion), as compared to that of basolateral addition (Na^+ absorption). Rigorous identification of the presence of more than one P_2 receptor subtype on either membrane of human nasal epithelium will require antagonist compounds not currently available.

The concentration-effect relationship of potent agonists added to the basolateral membrane was biphasic in character when the I_{sc} response to 10^{-3} M drug is considered (Figure 4). However, in experiments in which ATP was added to the basolateral surface in the presence of amiloride, the relationship was sigmoidal (Figure 3), suggesting that a process that regulates the rate of Na^+ absorption is responsible for the large increment of I_{sc} at millimolar drug concentrations. Because increased Na^+ absorption is probably the transport process that contributes to the change in I_{sc} at lower nucleotide concentrations, the biphasic response may indicate linkage of purinoceptors to two effector systems that regulate Na^+ transport rates.

As in the I_{sc} studies, changes in cell $[Ca^{2+}]_i$ induced by nucleotides cannot be explained by a P_2 receptor of the P_{2x} subtype. Rank orders of potency of agonists (UTP ≥ ATP > ATPγS > 2MeSATP > ADPβS) suggest the presence of a UTP-sensitive receptor. Sensitivity of this receptor to the presence of Mg^{2+} ions suggests that it is activated by the free acid form ATP^{4-}. It is not possible to speculate about the nature of receptors on the apical and basolateral membranes because agonists may have access to both sides of cells grown on coverslips. Ongoing studies of polarized epithelial preparations specially configured for fluorescent $[Ca^{2+}]_i$ measurements should help to elucidate the receptor type(s) present on each membrane.

The ion transport and $[Ca^{2+}]_i$ data suggest that human airway epithelium responds to various extracellular nucleotides via a receptor-mediated mechanism. By analogy to other epithelia, this mechanism probably involves phospholipase C-mediated breakdown of membrane phospholipids to inositol phosphates, coupled with release of Ca^{2+} from internal stores. Preliminary studies in normal primary human nasal epithelium and CF cell lines in which inositol phosphate production in response to nucleotides was measured, support phospholipid breakdown as the mediator of calcium release (H. Alex Brown, personal communication). The similar EC_{50}s for the I_{sc} response and Ca^{2+} response to various nucleotide agonists also support a link between these two phenomena.

The effectiveness of extracellular nucleotides in stimulating Cl^- secretion by amiloride-pretreated normal human airway epithelium raises the question of therapeutic uses for these compounds in diseases of epithelial dysfunction like cystic fibrosis. Although regulatory pathways that involve cyclic AMP and Ca^{2+} phospholipid-dependent protein kinases are defective in CF airway epithelium (Boucher *et al.*, 1986), a recent report indicates that Ca^{2+}-dependent Cl^- secretory regulatory mechanisms are retained by CF epithelia (Boucher *et al.*, 1989). Our data show $[Ca^{2+}]_i$ was increased and Cl^- secretion stimulated by ATP and UTP in CF airway epithelial cells pretreated with amiloride. In a recent pilot study, amiloride administered by the aerosol route was reported to slow but not abolish the progression of CF lung disease (Knowles *et al.*, 1990). The mode of action is probably via a reduction of the excessive rate of Na^+ absorption that also characterizes this disease and, consequently, conservation of liquid on the airway surface. ATP or UTP combined with amiloride and administered to target the airway epithelium might act to induce Cl^- secretion toward the airway lumen, further increasing the water content of secretions and increasing their rate of clearance from the respiratory system. Thus, by combining purinoceptor agonists as a new class of therapeutic agents with amiloride, it may be possible to abolish the loss of lung function consequent to this disease.

We appreciate the thoughtful criticism of this manuscript by Dr J. Gatzy and Dr K. Harden, the technical assistance of Ms T. Mace, and the secretarial assistance of Ms L. Brown. This work was supported by the National Institutes of Health grants HL34322 and HL42384, and the Cystic Fibrosis Foundation grant RO15.

References

BEAN, B.P. & FRIEL, D.D. (1990). ATP-activated channels in excitable cells. In *Ion Channels*, Vol. 2, ed. Narahashi, T. pp. 169–203. New York: Plenum Publishing Corporation.

BORN, G.V.R. & KRATZER, M.A.A. (1984). Source and concentration of extracellular adenosine triphosphate during haemostasis in rats, rabbits and man. *J. Physiol.*, **354**, 419–429.

BOUCHER, R.C., CHENG, E.H.C., PARADISO, A.M., STUTTS, M.J., KNOWLES, M.R. & EARP, H.S. (1989). Chloride secretory response of cystic fibrosis human airway epithelia: Preservation of calcium but not protein kinase C- and A-dependent mechanisms. *J. Clin. Invest.*, **84**, 1424–1431.

BOUCHER, R.C., COTTON, C.U., GATZY, J.T., KNOWLES, M.R. & YANKASKAS, J.R. (1988). Evidence for reduced Cl^- and increased Na^+ permeability in cystic fibrosis human primary cell cultures. *J. Physiol.*, **405**, 77–103.

BOUCHER, R.C., STUTTS, M.J., KNOWLES, M.R., CANTLEY, L. & GATZY, J.T. (1986). Na^+ transport in cystic fibrosis respiratory epithelia. Abnormal basal rate and response to adenylate cyclase activation. *J. Clin. Invest.*, **78**, 1245–1252.

BROWN, C.M. & BURNSTOCK, G. (1981). The structural conformation of the polyphosphate chain of the ATP molecule is critical for its promotion of prostaglandin biosynthesis. *Eur. J. Pharmacol.*, **69**, 81–86.

BURGESS, G.M., CLARET, M. & JENKINSON, D.H. (1979). Effects of catecholamines, ATP and ionophore A23187 on potassium and calcium movements in isolated hepatocytes. *Nature*, **279**, 544–546.

BURNSTOCK, G. (1971). Neural nomenclature. *Nature*, **229**, 282–283.

BURNSTOCK, G. & KENNEDY, C. (1985). Is there a basis for distinguishing two types of P_2-purinoceptor? *Gen. Pharmacol.*, **16**, 433–440.

BURNSTOCK, G. & KENNEDY, C. (1986). A dual function for adenosine 5'-triphosphate in the regulation of vascular tone. *Circ. Res.*, **58**, 319–330.

BURNSTOCK, G. & SNEDDON, P. (1985). Evidence for ATP and noradrenaline as cotransmitters in sympathetic nerves. *Clin. Sci.*, **68** (Suppl. 10), 89s–92s.

CHAPAL, J. & LOUBATIERES-MARIANI, M.-M. (1981). Effects of phosphate-modified adenine nucleotide analogues on insulin secretion from perfused rat pancreas. *Br. J. Pharmacol.*, **73**, 105–110.

COCKCROFT, S. & STUTCHFIELD, J. (1989). ATP stimulates secretion in human neutrophils and HL60 cells via a pertussis toxin-sensitive guanine nucleotide-binding protein coupled to phospholipase C. *FEBS Lett.*, **245**, 25–29.

DAVIDSON, J.S., WAKEFIELD, I.K., SOHNIUS, U., VAN DER MERWE, P.A. & MILLAR, R.P. (1990). A novel extracellular nucleotide recep-

tor coupled phosphoinositidase-C in pituitary cells. *Endocrinology*, **126**, 80–87.

DUBYAK, G.R. & DE YOUNG, M.B. (1985). Intracellular Ca^{2+} mobilization activated by extracellular ATP in Ehrlich ascites tumor cells. *J. Biol. Chem.*, **260**, 10653–10661.

FINE, J., COLE, P. & DAVIDSON, J.S. (1989). Extracellular nucleotides stimulate receptor-mediated calcium mobilization and inositol phosphate production in human fibroblasts. *Biochem. J.*, **263**, 371–376.

GALLACHER, D.V. (1982). Are there purinergic receptors on parotid acinar cells? *Nature*, **296**, 83–86.

GORDON, J.L. (1986). Extracellular ATP: effects, sources and fate. *Biochem. J.*, **233**, 309–319.

GREENBERG, S., DI VIRGILIO, F., STEINBERG, T.H. & SILVERSTEIN, S.C. (1988). Extracellular nucleotides mediate Ca^{2+} fluxes in J774 macrophages by two distinct mechanisms. *J. Biol. Chem.*, **263**, 10337–10343.

GRYNKIEWICZ, G., POENIE, M. & TSIEN, R.Y. (1985). A new generation of Ca indicators with greatly improved fluorescence properties. *J. Biol. Chem.*, **260**, 3440–3450.

HAEUSSINGER, D., BUSSHARDT, E., STEHLE, T., STOLL, B., WETTSTEIN, M. & GEROK, W. (1988). Stimulation of thromboxane release by extracellulaf UTP and ATP from perfused rat liver. *Eur. J. Biochem.*, **178**, 249–256.

HAEUSSINGER, D., STEHLE, T. & GEROK, W. (1987). Actions of extracellular UTP and ATP in perfused rat liver. *Eur. J. Biochem.*, **167**, 65–71.

HOSOI, K. & EDIDIN, M. (1989). Exogenous ATP and other nucleoside phosphates modulate epidermal growth factor receptors of A-431 epidermoid carcinoma cells. *Proc. Natl. Acad. Sci. U.S.A.*, **86**, 4510–4514.

KIMMICH, G.A. & RANDLES, J. (1982). An ATP- and Ca^{2+}-regulated Na^+ channel in isolated intestinal epithelial cells. *Am. J. Physiol.*, **243**, C116–C123.

KNOWLES, M.R., CHURCH, N.L., WALTNER, W.E., YANKASKAS, J.R., GILLIGAN, P.H., KING, M., EDWARDS, L.J., HELMS, R.W. & BOUCHER, R.C. (1990). A pilot study of aerosolized amiloride for the treatment of cystic fibrosis lung disease. *N. Engl. J. Med.*, **322**, 1189–1194.

KNOWLES, M.R., STUTTS, M.J., SPOCK, A., FISCHER, N., GATZY, J.T. & BOUCHER, R.C. (1983). Abnormal ion permeation through cystic fibrosis respiratory epithelium. *Science*, **221**, 1067–1070.

KUROKI, M. & MINAKAMI, S. (1989). Extracellular ATP triggers superoxide production in human neutrophils. *Biochem. Biophys. Res. Commun.*, **162**, 377–380.

MAGUIRE, M.H. & SATCHELL, D.G. (1979). The contribution of adenosine to the inhibitory actions of adenine nucleotides on the guinea-pig *taenia coli*: studies with phosphate-modified adenine nucleotide analogs and dipyridamole. *J. Pharmacol. Exp. Ther.*, **211**, 626-631.

PARADISO, A.M., YANKASKAS, J.R. & BOUCHER, R.C. (1989). Regulation of cytosolic Ca in human nasal epithelium by receptor gated mechanisms. *FASEB J.*, **3**, A1297.

PEARSON, J.D., SLAKEY, L.L. & GORDON, J.L. (1983). Stimulation of prostaglandin production through purinoceptors on cultured porcine endothelial cells. *Biochem. J.*, **214**, 273–276.

PFEILSCHIFTER, J. (1990). Comparison of extracellular ATP and UTP signalling in rat renal mesangial cells. *Biochem. J.*, **272**, 469–472.

RICE, W.R. & SINGLETON, F.M. (1986). P_2-purinoceptors regulate surfactant secretion from rat isolated alveolar Type II cells. *Br. J. Pharmacol.*, **89**, 485–491.

RIORDAN, J.R., ROMMENS, J.M., KEREM, B-T., ALON, N., ROZMAHEL, R., GRZELCZAK, Z., ZIELENSKI, J., LOK, S., PLAVSIC, N., CHOU, J-L., DRUMM, M.L., IANNUZZI, M.C., COLLINS, F.S. & TSUI, L-C. (1989). Identification of the cystic fibrosis gene: Cloning and characterization of complementary DNA. *Science*, **245**, 1066–1073.

ROMMENS, J.M., IANNUZZI, M.C., KEREM, B-T., DRUMM, M.L., MELMER, G., DEAN, M., ROZMAHEL, R., COLE, J.L., KENNEDY, D., HIDAKA, N., ZSIGA, M., BUCHWALD, M., RIORDAN, J.R., TSUI, L-C. & COLLINS, F.S. (1989). Identification of the cystic fibrosis gene: chromosome walking and jumping. *Science*, **245**, 1059–1065.

SEIFERT, R. & SCHULTZ, G. (1989). Involvement of pyrimidinoceptors in the regulation of cell functions by uridine and by uracil nucleotides *Trends Pharmacol. Sci.*, **10**, 365–369.

SEIFERT, R., WENZEL, K., ECKSTEIN, F. & SCHULTZ, G. (1989). Purine and pyrimidine nucleotides potentiate activation of NADPH oxidase and degranulation by chemotactic peptides and induce aggregation. *Eur. J. Biochem.*, **181**, 277–285.

STUTCHFIELD, J. & COCKCROFT, S. (1990). Undifferentiated HL60 cells respond to extracellular ATP and UTP by stimulating phospholipase C activation and exocytosis. *FEBS Lett.*, **262**, 256–258.

VANDER KOOY, D., DUBYAK, G.R., MOORE, R.M. & MOORE, J.J. (1989). Adenosine triphosphate activates the phospholipase-C cascade system in human amnion cells without increasing prostaglandin production. *Endocrinology*, **124**, 2005–2012.

VON KUEGELGEN, I., HAEUSSINGER, D. & STARKE, K. (1987). Evidence for a vasoconstriction-mediating receptor for UTP, distinct from the P_2 purinoceptor, in rabbit ear artery. *Naunyn Schmiedebergs Arch. Pharmacol.*, **336**, 556–560.

WILLUMSEN, N.J., DAVIS, C.W. & BOUCHER, R.C. (1989). Intracellular Cl^- activity and cellular pathways in cultured human airway epithelium. *Am. J. Physiol.*, **256**, C1033–C1044.

WU, R., YANKASKAS, J., CHENG, E., KNOWLES, M.R. & BOUCHER, R. (1985). Growth and differentiation of human nasal epithelial cells in culture. Serum-free, hormone-supplemented medium and proteoglycan synthesis. *Am. Rev. Respir. Dis.*, **132**, 311–320.

YANKASKAS, J.R., COTTON, C.U., KNOWLES, M.R., GATZY, J.T. & BOUCHER, R.C. (1985). Culture of human nasal epithelial cells on collagen matrix supports. *Am. Rev. Respir. Dis.*, **132**, 1281–1287.

(Received November 6, 1990
Revised February 11, 1991
Accepted February 27, 1991)

Br. J. Pharmacol. (1991), **103**, 1657–1662 © Macmillan Press Ltd, 1991

The effect of streptozotocin-induced diabetes on cholinergic motor transmission in the rat urinary bladder

G.N. Luheshi & [1]M.A. Zar

The Department of Pharmacological Sciences, The Medical School, Framlington Place, Newcastle Upon Tyne, NE2 4HH

1 The effect of streptozotocin (STZ)-induced diabetes on cholinergic motor transmission in the rat urinary bladder was investigated by recording contractile activity of detrusor strips *in vitro*.

2 The Ca^{2+}-channel antagonist, nifedipine, was found to be more effective in blocking the non-cholinergic motor transmission than P_2-purinoceptor desensitization by α,β-methylene ATP.

3 The neurogenic contractile responses to electrical field stimulation in the presence of nifedipine (cholinergic) were larger in the diabetic detrusor than in the non-diabetic controls. The potentiation of the cholinergic transmission was more evident at higher frequencies.

4 Concentration-response curves for acetylcholine were identical in detrusors from diabetic and non-diabetic animals, thus excluding a postsynaptic supersensitivity to acetylcholine being responsible for the potentiation of cholinergic motor transmission.

5 It is concluded that the potentiation of cholinergic motor transmission is due to enhanced release of acetylcholine in diabetic detrusor. Possible reasons for this enhancement are discussed in relation to diabetes.

Keywords: Streptozotocin; diabetes mellitus; urinary bladder; nifedipine; cholinergic transmission

Introduction

Dysfunction of urinary bladder is of common occurrence in human diabetics and is believed to be the result of diabetic autonomic neuropathy (Faerman *et al.*, 1971; Buck *et al.*, 1974; Ellenberg, 1980). Since the motor transmission of the mammalian urinary bladder, including that of man, is dual in nature comprising an atropine-sensitive (cholinergic) and an atropine-resistant (non-cholinergic) component (Ambache & Zar, 1970; Burnstock *et al.*, 1972; Hoyle *et al.*, 1989; Luheshi & Zar, 1990a), it is clearly of some interest to determine which of these two components is the principal target of diabetic autonomic neuropathy leading to the bladder dysfunction. An earlier investigation conducted on streptozotocin (STZ)-induced diabetic rats, an animal model for human diabetes, showed a marked decline in the non-cholinergic motor transmission, probably caused by a reduced release of the non-cholinergic motor transmitter in the diabetic animals (Luheshi & Zar, 1990b). Lincoln *et al.* (1984) reported that the cholinergic component of the motor transmission in rats was unaffected by diabetes. These workers had used atropine in their investigation to determine the cholinergic contribution, as have several other researchers in diabetic and non-diabetic animals (Sibley, 1984; Luheshi & Zar, 1987). The use of atropine for this purpose is based upon the tacit assumption that the two transmissions have identical time courses, so that the total nerve-mediated response represents the algebraic summation of the two components; therefore the elimination of the cholinergic by atropine, not only enables the non-cholinergic contribution to be accurately estimated but also allows the accurate assessment of the cholinergic contribution. However, there is no evidence to support this assumption. Indeed, a comparison of the records of contractions to electrical field stimulation (EFS) reveals a divergence in the time-course of the contraction in the presence of atropine from that in its absence (Luheshi, 1990; Zar *et al.*, 1990). Clearly these considerations make it imperative that a drug other than a muscarinic receptor antagonist should be employed to estimate the cholinergic element in the motor transmission of the detrusor. Two further procedures, namely purinoceptor desensitization and Ca^{2+}-channel inactivation by nifedipine are available for assessing the cholinergic transmission in the urinary bladder. Both procedures have been employed in the experiments to be described, in order to judge their suitability in estimating the cholinergic contribution of the nerve-evoked response in diabetic detrusor. Recent work (Luheshi & Zar, 1990c), has confirmed the earlier finding of Choo & Mitchelson (1980) that purinoceptor desensitization impairs but does not abolish the non-cholinergic motor transmission in rat isolated urinary bladder, thus casting doubt on the suitability of this procedure for assessing the cholinergic transmission in rat detrusor. The Ca^{2+}-channel antagonist, nifedipine, on the other hand has been demonstrated to block fully the non-cholinergic component while sparing the cholinergic component of transmission in the rat detrusor (Zar *et al.*, 1990). A similar conclusion was arrived at by Iacovou *et al.* (1990), using guinea-pig detrusor.

Methods

Animals

All experiments were performed on young adult male Wistar rats, 8 weeks old and weighing 210–240 g at the start of the experiment. The animals were randomly allocated to two experimental groups, a diabetic one and a corresponding control. The animals in both groups were maintained for a period of 12 weeks under precisely the same conditions. Both groups were kept in a temperature controlled room (22 ± 2°C), artificially lit from 06 h 00 min–18 h 00 min each day. The animals were fed standard laboratory diet and provided water *ad libitum*. After taking the initial weights, each rat was routinely weighed once a week and the weight recorded up to the end of the study (12 weeks).

Induction of diabetes

The rats to be made diabetic were fasted overnight and their blood glucose levels estimated. Diabetes was induced by administering a single intraperitoneal injection of 75 mg kg^{-1} STZ to each rat. Three days after the STZ treatment, the animals were fasted for 2 h before obtaining another blood sample from each animal in order to estimate the blood glucose level. This was to ensure that diabetes had been

[1] Author for correspondence.

induced. Animals with blood glucose levels $\geqslant 16.6\,mmol\,l^{-1}$ were deemed to be diabetic and therefore suitable for the study. The blood glucose levels of the diabetic rats were thereafter monitored at regular intervals. The control animals were treated in an identical fashion except that saline was injected instead of STZ. Both groups of animals were then maintained for 12 weeks.

Experimental procedures

At the end of the allocated period for maintenance (12 weeks) the animals were killed by concussion and decapitation. Final blood samples were collected for estimation of their glucose contents.

Preparation of the detrusor strip The strip was prepared according to the procedure of Ambache & Zar (1970), as subsequently modified by Zar *et al.* (1990). After killing the animal the lower abdomen was opened and the bladder exposed. The urine present in the bladder was withdrawn into a 5 ml syringe and its volume recorded. The bladder was then held at its apex slightly stretched and the investing layers of serosal coat, connective tissue and accompanying blood vessels were cut away as close as possible from the outer surface of the bladder wall. The bladder was excised by a cut above the trigone and rapidly weighed. The bladder was then placed in a Petri dish and washed with several changes of Krebs-Henseleit solution. The bladder was opened by two lateral incisions and then unfolded to give a rectangular sheet of tissue. The unfolded tissue was laid on Krebs-soaked tissue paper and strips of bladder 1–1.5 cm long and 0.2 cm wide were cut with a pair of fine scissors. The strip preparation of the detrusor was suspended in a 1 ml jacketed organ bath between built-in vertical platinum electrodes, at a resting tension of 0.5 g. The resting tension was kept constant at 0.5 g throughout the experiment by appropriate adjustments whenever needed. The preparation was maintained at 37°C in Krebs-Henseleit solution gassed in the reservoir and in the organ bath with 95% O_2 plus 5% CO_2 mixture. Indomethacin 10 μM was present in the Krebs solution throughout the experiment in order to minimize the spontaneous activity of the isolated preparation. For recording the tension of the detrusor muscle, the preparation was connected to an isometric transducer and a potentiometric recorder. An equilibration period of 30 min was allowed before the start of further experimentation (see below); during this period the preparation was repeatedly washed with fresh Krebs solution.

Experiments on isolated detrusor strips In each experiment, isolated detrusor strips were used to obtain contractile responses to two types of stimuli: electrical field stimulation and acetylcholine (ACh). The two types of stimuli were not delivered to the same strip. One, or if necessary, more strips were reserved for each type of stimulus.

Electrical field stimulation The strips reserved for electrical field stimulation (EFS) were treated with either α,β-methylene ATP (α,β-MeATP) following the method of Luheshi & Zar (1990a) in order to produce purinoceptor desensitization or with nifedipine following the method of Zar *et al.* (1990). The parameters of EFS were as follows: trains of pulses: pulse duration of 0.1 ms: train duration, 10 s: frequency of 1, 2, 4, 8, 16, 32 and 64 Hz; interval between two trains of 60 s: voltage, supramaximal for evoking maximal contraction at each frequency. In experiments where the strips were treated with α,β-MeATP the maximum frequency of stimulation used was 16 Hz. The choice of parameters for EFS was based upon the satisfaction of two criteria: first, reproducibility of the response at each frequency of stimulation and second, total abolition of the response by tetrodotoxin, 0.5 μM. Fulfilment of both criteria was deemed to imply that EFS was supramaximal and the EFS-evoked responses were neurogenic. In experiments using nifedipine, EFS was started after allowing a 30 min exposure to nifedipine and during its continued presence for the rest of the experiment. The chosen concentration of nifedipine (1 μM) was based upon previous observations (Zar *et al.*, 1990) where the responses to EFS were maximally depressed by nifedipine 1 μM and nifedipine in higher concentrations was no more effective than nifedipine 1 μM.

Construction of dose-response curves to acetylcholine The object of the experiments was to compare the ability of nifedipine-treated detrusor strips from the two groups of animals, diabetic and control, to generate tension in response to ACh. The strips were exposed to nifedipine 1 μM for 30 min before obtaining concentration-response relationships for ACh. ACh was added to the bath in a concentration range of 10^{-8}–10^{-3} M, in a non-cumulative manner. Exposure to a dose of ACh was maintained until the maximal response to that concentration was obtained. The preparation was then repeatedly washed with several changes of nifedepine containing Krebs-solution. The preparation was allowed to relax fully before exposing it to the next higher concentration of ACh.

Statistics

At the end of each experiment, the bladder strip was detached from the recording set up, blotted dry and weighed. In order to render the results comparable from one strip to another and from strips of different animals, the tension generated by the strip and the weight of the strip were used to calculate the tension per 100 mg bladder tissue.

All values are expressed as mean ± s.e.mean and the statistical significance was calculated by Student's t test.

Materials

The drugs used and their sources were: nifedipine (Bayer), physostigmine sulphate (Burroughs Wellcome), tetrodotoxin (Sankyo), acetylcholine chloride, atropine sulphate, indomethacin, streptozotocin, α,β-MeATP (Sigma). Solutions of drugs were made fresh on the day of their use with the exception of tetrodotoxin the stock solution of which was stored at −20°C.

Preparation of drug solutions

Streptozotocin: this was dissolved immediately prior to its injection in 50 mM sodium citrate buffer and titrated to pH 4.5 with HCl. The drug solution was kept on ice at all times before use.

Nifedipine: this drug was dissolved in absolute ethanol to make a solution of 10^{-3} M.

Indomethacin: absolute ethanol was also used to dissolve this drug to make a solution of 10^{-2} M.

All other drugs were dissolved in distilled water.

Nifedipine is very light-sensitive, specially in solution and is degraded to inactive metabolites when exposed to light of wavelength less than 450 nm which covers daylight and ordinary fluorescent laboratory light. All experiments involving this drug were therefore carried out in a laboratory illuminated solely with a sodium vapour lamp.

Composition of Krebs-Henseleit solution

The composition in mM was: NaCl 118, KCl 4.7, $CaCl_2$ 2.5, $MgSO_4$ 1.2, $NaHCO_3$ 25, KH_2PO_4 1.2 and glucose 11.

Estimation of blood glucose level

Periodic routine estimation was carried out by taking a drop of blood from the tail vein of the rat and estimating its glucose level with BM-Test-Glycemie strips (Boehringer-Manheim).

Table 1 Body weight, blood glucose concentration, weight of bladder and volume of residual urine in diabetic and control rats

	Controls	*Diabetic*
Body weight (g)		
Initial	219 ± 8	215 ± 8
Final	387 ± 15	182 ± 9***
Blood glucose ($mmol\,l^{-1}$)	4 ± 0.2	27 ± 2.1***
Residual urine in bladder (ml)	0.5 ± 0.08	3.9 ± 0.3***
Bladder weight (mg)	91 ± 7	805 ± 42***

All values are means ± s.e.mean ($n = 8$). The values in diabetic animals have been compared with their corresponding controls and the level of significant difference is indicated by *** $P < 0.001$. Volume of residual urine represents the volume of urine present in the bladder immediately after exsanguination of the animal.

The final estimate of blood glucose was carried out after the animal had been killed. Blood samples and glucose standards (50 μl) were collected into ice cold 0.016% uranyl acetate (1 ml). The mixture was agitated, centrifuged at 800 g and the supernatant assayed for glucose spectrophotometrically by the standard glucose oxidase method with the 'GOD-PAP' assay kit (Boehringer-Ingelheim, London).

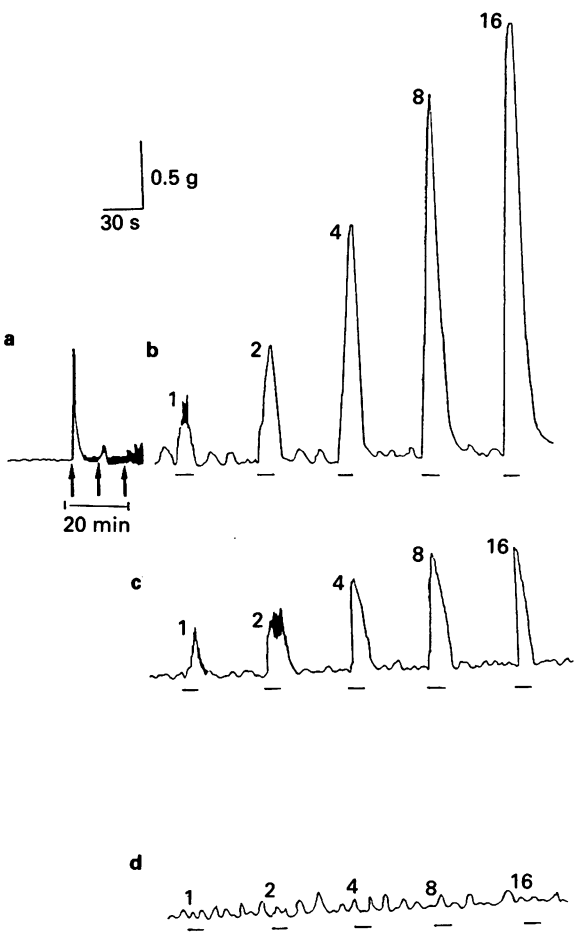


Figure 1 Isolated detrusor from a streptozotocin (STZ)-diabetic rat: a typical experiment showing responses to electrical field stimulation following desensitization to the contractile action of α,β-methylene ATP (α,β-ATP) first without any drugs (b) and then in the presence of atropine (c) followed by atropine 3 μM + tetrodotoxin (TTX) 0.5 μM (d). Atropine was introduced into the bath 20 min before (c) and TTX 5 min before (d). Electrical field stimulation: 10 s bursts of stimuli, duration indicated by bars and frequency (1–16 Hz) by subscripts. Desensitization to α,β-MeATP was obtained by three administrations of the drug (marked by arrows) in 10 μM concentrations (a).

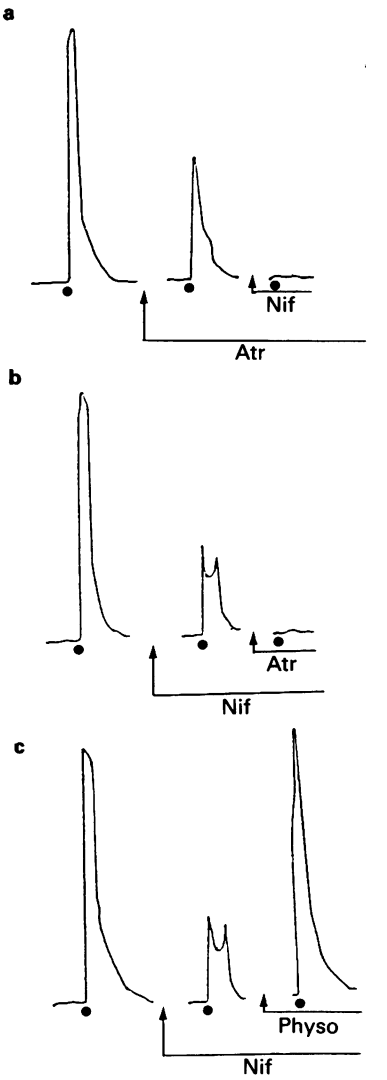


Figure 2 Isolated detrusor of diabetic rat: contractile responses of three detrusor strips, (a), (b) and (c) from the same animal to electrical field stimulation (●, 10 s bursts of stimuli at 8 Hz). In each strip, the response in the left panel represents the control response, the response in the middle panel was obtained following 30 min exposure to atropine, 3 μM (Atr) or nifedipine 1 μM (Nif) while the response in the right panel was evoked following a 30 min exposure to nifedipine (a), atropine (b) or physostigmine 1 μM (Phys; c).

Results

Body weight and blood glucose levels

The animals in the diabetic group, in contrast to their corresponding controls showed no gain in weight over the course of the investigation. The control animals made significant weight gains during the same period (Table 1).

As was to be expected, the blood glucose levels in the STZ-treated diabetic animals were extremely high when compared to the untreated control rats (Table 1) and remained so throughout the duration of the investigation.

Bladder weight and residual urine

By the end of the investigation the weight of the whole urinary bladder in the diabetic group was significantly higher than in

controls. Similarly, the volume of residual urine (VRU) i.e. the volume of urine present in the bladder after the death of the animal was also considerably higher in the diabetic animals (Table 1).

Contractile responses to electrical field stimulation

Two sets of preliminary experiments, one employing purinoceptor-desensitized detrusor strips and the second using the calcium channel antagonist nifedipine, were conducted to determine the optimal method for eliminating the non-cholinergic motor transmission.

Purinoceptor desensitized preparations In these experiments the effectiveness of purinoceptor desensitization in abolishing the non-cholinergic motor transmission of the diabetic detrusor was investigated. The record of one such experiment is shown in Figure 1. Following desensitization of the detrusor strip to the contractile action of α,β-MeATP (Figure 1a), the strip was subjected to EFS at frequencies of 1, 2, 4, 8 and 16 Hz. The field stimulation evoked slow, sustained and frequency-dependent contractions which were maintained throughout the duration of the electrical stimulus (Figure 1b). Repeating the cycle of stimulation following exposure to atropine 3 μM for 30 min and in its continued presence resulted in the partial suppression of the contractile responses but at no frequency of stimulation was the response completely abolished (Figure 1c). The responses, resistant to α,β-MeATP desensitization and to atropine were completely abolished by exposure to TTX (0.5 μM) indicating that such responses were neurogenic (Figure 1d).

Nifedipine-treated preparations In the second set of preliminary experiments, nifedipine was used to test whether it would totally abolish the non-cholinergic component of the motor transmission in bladder strips from diabetic rats, as it did in detrusor strips from normal animals (Zar *et al.*, 1990). These experiments involved stimulating the preparations with 10 s bursts of stimuli at 8 Hz. Records from a typical experiment are shown in Figure 2. The results show that nifedipine 1 μM completely abolished the atropine-resistant component of the motor transmission (Figure 2a); nifedipine partially blocked the EFS-evoked response of the non-atropinized preparation and the nifedipine-resistant component was fully blocked by atropine, 3 μM (Figure 2b). The nifedipine-resistant component was greatly augmented by physostigmine 1 μM (Figure 2c).

The effect of diabetes on cholinergic motor transmission in the rat detrusor in presence of nifedipine in order to eliminate non-cholinergic transmission

In light of the results of the foregoing preliminary experiments, the detrusor strips from diabetic and control animals were contracted with 10 s bursts of stimuli at frequencies of 1, 2, 4, 8, 16, 32 and 64 Hz in the presence of nifedipine 1 μM. The field stimulation produced responses which increased with increasing frequency in the detrusor strips taken from both diabetic as well as control rats. Figure 3 is the record of two typical experiments showing the tension generated by the detrusor strips in response to EFS from a control (a) and a diabetic (c) animal following incubation with nifedipine 1 μM. The electrical stimulus was then repeated at the same frequencies, this time in the presence of atropine (3 μM) as well as nifedipine. As can be seen from Figure 3 (b and d) the introduction of atropine completely abolished the nifedipine resistant response confirming its cholinergic nature.

When compared to the tensions generated by detrusor strips from the control animals, the nifedipine-resistant

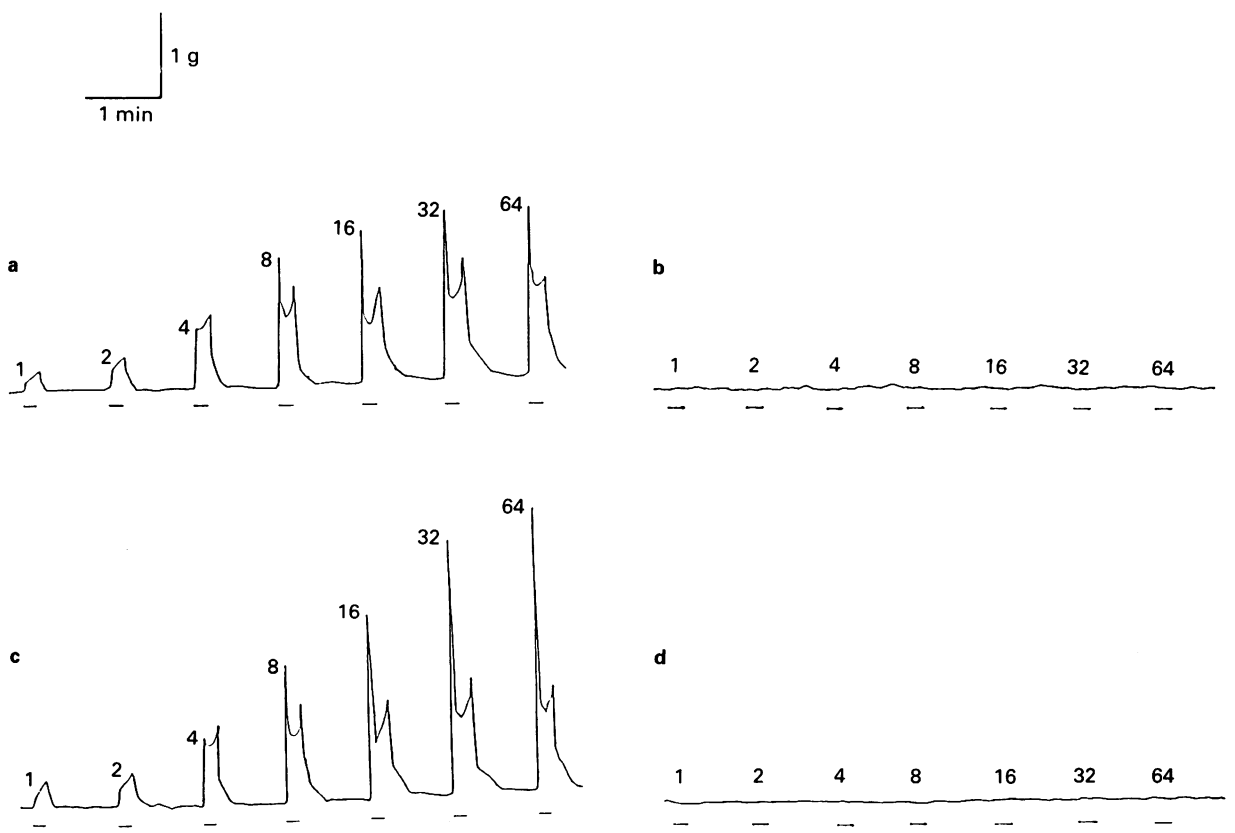


Figure 3 Isolated detrusor strips from a control (above) and diabetic (below) rat: two typical experiments showing contractile responses to electrical field stimulation in the presence of nifedipine, 1 μM. The frequency of pulses within each train is given by the subscripts (1–64 Hz) and the duration of each stimulus burst is indicated by a horizontal bar. The responses to electrical field stimuli were evoked in the absence (a, c) or presence of atropine 3 μM. Note that the peak tension generated by the 'diabetic' detrusor was substantially greater than the control detrusor and both were blocked by atropine.

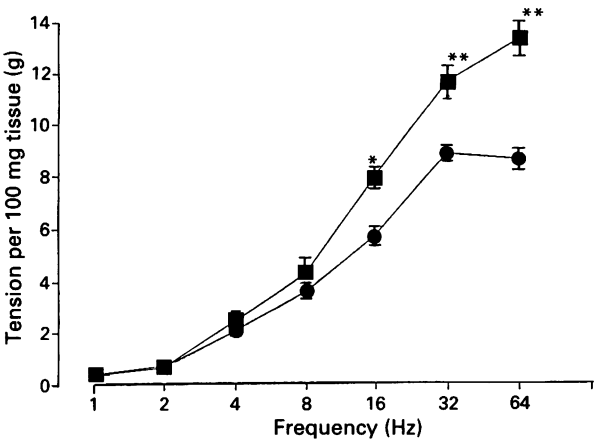


Figure 4 Cholinergic contractile responses of detrusor from diabetic (■) and non-diabetic control (●) rats to electrical field stimulation. All values are means (s.e.mean shown by vertical bars; $n = 8$). Nifedipine 1 μM was present throughout the duration of each experiment. * $P \leq 0.05$ and ** $P \leq 0.01$ indicate the degree of significant difference from the non-diabetic control value.

(cholinergic) components in strips from STZ-diabetic animals generated greater tension (Figure 3). This difference was statistically significant at frequencies of 16 Hz and above and was most evident at the highest two frequencies, 32 and 64 Hz, (Figure 4). In addition to the difference in the magnitude of tension generated, the responses of the strips from the control animals tended to peak at a frequency of 32 Hz while those produced by the strips from the diabetic animals continued to rise up to the maximum frequency of 64 Hz used in this investigation.

Contractile response to acetylcholine

ACh, 10^{-7}–10^{-3} M produced contractions that increased with increase in the dose of the drug. The tension generated by the detrusor strips from both sets of animals in response to ACh was very similar in magnitude and there was no significant difference evident between the 2 groups of animals at any concentration of ACh (Figure 5).

Discussion

There are sound reasons to believe that the animals treated with STZ in the present investigation were fully diabetic. Thus the data shown in Table 1 demonstrating the failure of the STZ-treated rats to gain weight coupled with the highly significant rise in blood glucose levels in these animals are strongly indicative of the successful induction of diabetes. Similarly the increase in bladder weight and in the volume of residual urine observed in the STZ-treated animals when compared to the controls (Table 1) is also consistent with changes observed by other workers using STZ-treated rats as animal models for human diabetes (Kolta *et al.*, 1985; Longhurst & Belis, 1986; Moss *et al.*, 1987; Santicioli *et al.*, 1987; Steers *et al.*, 1990). These changes in the bladder mass of diabetic animals parallel a rise in protein concentration (Longhurst & Bellis, 1985) and have been previously attributed to diuresis (Goss *et al.*, 1973), or to damage of sensory or motor nerves (Buck *et al.*, 1974; Ekstrom & Uvelius, 1981).

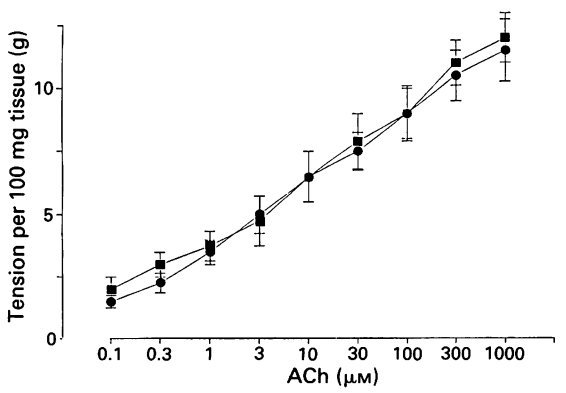


Figure 5 Concentration-response curves of acetylcholine (ACh) in detrusor strips from diabetic (■) and non-diabetic control (●) rats. All values are means and vertical bars indicate s.e.mean ($n = 8$). Nifedipine 1 μM was present throughout the duration of each experiment. Note that there is no significant difference between the two curves at any concentration of ACh.

It is quite obvious from the results of experiments with α,β-MeATP that purinoceptor desensitization as a method for isolating the cholinergic component of the motor transmission in the diabetic detrusor is less than satisfactory. The results of an earlier investigation on detrusor from non-diabetic rats had also led to a similar conclusion regarding the ineffectiveness of purinoceptor desensitization in inducing a full extinction of non-cholinergic transmission in this organ (Luheshi & Zar, 1990c). In the non-diabetic detrusor, nifedipine, unlike purinoceptor desensitization, has been shown to be highly effective in its selective inhibition of the non-cholinergic motor transmission (Zar *et al.*, 1990). From the results obtained in the present study, there seems to be little reason to doubt that the effect of nifedipine on motor transmission is the same in the STZ-diabetic detrusor as in the non-diabetic one. As was shown in the detrusor strips taken from the bladders of non-diabetic rats (Zar *et al.*, 1990), treatment with nifedipine drastically reduced the amplitude of the EFS-evoked response in the diabetic detrusor as well. Also in common with the findings in non-diabetic detrusor, the nifedipine-resistant response of the diabetic detrusor was potentiated by the anticholinesterase physostigmine and was abolished by atropine. It seems, therefore, reasonable to conclude that the nifedipine-resistant response of the diabetic detrusor to EFS was mediated entirely through cholinergic mechanisms.

The finding that the EFS-evoked cholinergic response generated significantly greater tension in diabetic detrusor compared to the control is unexpected, as well as puzzling, since clinical diabetes mellitus is frequently associated with a 'failing' detrusor function (Fagerberg *et al.*, 1967; Kahan *et al.*, 1970; Buck *et al.*, 1974; Bradley, 1980; Ellenberg, 1980). In theory, the enhanced nerve-mediated cholinergic response of the diabetic detrusor must have originated in either an augmented sensitivity of the detrusor to released ACh, or to an augmented ACh release, or to a combination of both of these factors. That this apparent 'good health' of the cholinergic response in the diabetic detrusor is not attributable to a postsynaptic exaggerated responsiveness or supersensitivity to ACh is shown by a lack of any significant change in the ACh concentration-response curve in diabetic detrusor compared to the control. This conclusion seems to be broadly in line with the findings of other workers regarding ACh responsiveness of the diabetic detrusor which have been somewhat variable, with reports of increased contractile responses (Kolta *et al.*, 1985), decreased contractile responses (Longhurst & Belis, 1986), or no change in contractile responses (Lincoln *et al.*, 1984). It seems likely that such differences in the reported ACh responsiveness might be a reflection of the state of innervation of the detrusor which in its turn would depend upon the severity and duration of experimental diabetes.

Having thus disposed of the possibility of a postsynaptic mechanism underpinning the enhanced cholinergic response to EFS, one is left with the unavoidable conclusion that the concentration of ACh in the synaptic cleft following EFS was higher in detrusor preparations from diabetic rats. The single most important factor determining the transmitter-concentration in the synaptic cleft is, without doubt, the quantum of the neurotransmitter released in response to the stimulus. Another factor contributing to a rise in transmitter-

concentration within the synaptic cleft might be a diminished rate of ACh inactivation in and around the synaptic cleft in the detrusor of diabetic animals. The latter possibility seems unlikely since tissue cholinesterase activity in diabetic bladder is reported to be higher than in controls (Lincoln *et al.*, 1984). Also the fact that the sensitivity to ACh remained unaltered, speaks against a diminution of cholinesterase activity in the diabetic detrusor. It follows therefore that the likeliest cause of the enhanced nerve-mediated cholinergic response in the diabetic detrusor is a greater than normal release of ACh in response to EFS. The results of the present investigation do not throw any light on the mechanism responsible for this enhanced release of transmitter in response to EFS. However it may be hypothesized that this phenomenon is an early sign of the onset of degenerative changes in the cholinergic nerves initiated by diabetes and that these pathological changes may cause the nerves to lose their normal control over the quantum of transmitter released in response to EFS. An alternative explanation could be that the increase in the cholinergic response is a result of a hypothetical compensatory mechanism by the cholinergic component for the progressive failure of the non-cholinergic component of the motor transmission in diabetic detrusor, evidence of which was presented earlier (Luheshi & Zar, 1990b). It seems rational therefore to assume that the cholinergic and the non-cholinergic components of the motor transmission in the detrusor act in concert with each other so that a partial failure of one (in this case the non-cholinergic) would trigger a compensatory enhancement of the other (the cholinergic).

In conclusion, the present study has shown that the Ca^{2+}-channel antagonist, nifedipine is more effective than purinoceptor-desensitization by α,β-MeATP in abolishing the non-cholinergic motor transmission of the diabetic rat detrusor. Furthermore, induction of diabetes causes a presynaptically-mediated augmentation of the cholinergic motor transmission in rat detrusor.

References

AMBACHE, N. & ZAR, M.A. (1970). Non-cholinergic transmission by post-ganglionic motor neurons in the mammalian bladder. *J. Physiol.*, **210**, 761–783.

BRADLEY, W.E. (1980). Diagnosis of urinary bladder dysfunction in diabetes mellitus. *Ann. Int. Med.*, **92**, 323–326.

BUCK, A.C., McRAE, C.U., REER, P.I. & CHISHOLM, G.D. (1974). The diabetic bladder. *Proc. R. Soc. Med.*, **67**, 81–83.

BURNSTOCK, G., DUMSDAY, B. & SMYTHE, A. (1972). Atropine resistant excitation of the urinary bladder: the possibility of transmission via nerves releasing a purine nucleotide. *Br. J. Pharmacol.*, **44**, 451–461.

CHOO, L.K. & MITCHELSON, F. (1980). The effect of indomethacin and adenosine 5'-triphosphate on excitatory innervation of the rat urinary bladder. *Can. J. Physiol. Pharmacol.*, **58**, 1042–1048.

EKSTROM, J. & UVELIUS, B. (1981). Length-tension relations of smooth muscle from normal and denervated rat urinary bladders. *Acta Physiol. Scand.*, **112**, 443–447.

ELLENBERG, M. (1980). Development of urinary bladder dysfunction in diabetes mellitus. *Ann. Intern. Med.*, **92**, 321–323.

FAERMAN, I., MALER, M., JADZINSKY, M., FOX, D., ALVAREZ, E., ZILVERBARG, J., CIBEIRA, J.B. & COLINAS, R. (1971). Asymptomatic neurogenic bladder in juvenile diabetics. *Diabetologia*, **7**, 168–172.

FAGERBERG, S.E., KOCK, N.G., PETERSEN, J. & STENER, J. (1967). Urinary bladder disturbances in diabetics. I. A comparative study of male diabetes and controls aged between 20 and 50 years. *Scand. J. Urol. Nephrol.*, **1**, 19–27.

GOSS, R.J., LIANG, M.B., WEISHOLTZ, S.J. & PELTZER, T.J. (1973). The physiological basis of urinary bladder hypertrophy. *Proc. Soc. Exp. Biol. Med.*, **142**, 1332–1335.

HOYLE, C.H.V., CHAPPLE, C. & BURNSTOCK, G. (1989). Isolated human bladder: evidence for an adenine dinucleotide acting on P_{2X}-purinoceptors and for purinergic transmission. *Eur. J. Pharmacol.*, **174**, 115–118.

IACOVOU, J.W., HILL, S.J. & BIRMINGHAM, A.T. (1990). Agonist-induced contraction and accumulation of inositol phosphates in the guinea-pig detrusor: evidence that muscarinic and purinergic receptors raise intracellular calcium by different mechanisms. *J. Urol.*, **144**, 775–779.

KAHAN, M., GOLDBERG, P.D. & MANDEL, E.E. (1970). Neurogenic vesical dysfunction and diabetes mellitus. *N.Y. J. Med.*, **2**, 2448–2455.

KOLTA, M.G., WALLACE, L.J. & GERALD, M.C. (1985). Streptozotocin-induced diabetes affects rat urinary bladder response to autonomic agents. *Diabetes*, **34**, 917–921.

LINCOLN, J., CROCKETT, M., HAVEN, A.J. & BURNSTOCK, G. (1984). Rat bladder in the early stages of streptozotocin-induced diabetes: adrenergic and cholinergic innervation. *Diabetologia*, **26**, 81–87.

LONGHURST, P.A. & BELIS, J.A. (1986). Abnormality of rat bladder contractility in streptozotocin-induced diabetes mellitus. *J. Pharmacol. Exp. Ther.*, **238**, 773–777.

LUHESHI, G.N. (1990). Diabetes in the rat and postganglionic neuromuscular transmission. *Ph.D. Thesis, University of Newcastle Upon Tyne.*

LUHESHI, G.N. & ZAR, M.A. (1987). Motor transmission in urinary bladder of streptozotocin-induced diabetic rats. *Br. J. Pharmacol.*, **92**, 528P.

LUHESHI, G.N. & ZAR, M.A. (1990a). Presence of non-cholinergic motor transmission in isolated human bladder. *J. Pharm. Pharmacol.*, **42**, 223–224.

LUHESHI, G.N. & ZAR, M.A. (1990b). Inhibitory effect of streptozotocin-induced diabetes on non-cholinergic motor transmission in rat detrusor and its prevention by sorbinil. *Br. J. Pharmacol.*, **101**, 411–417.

LUHESHI, G.N. & ZAR, M.A. (1990c). Purinoceptor desensitization impairs but does not abolish the non-cholinergic motor transmissions in rat isolated urinary bladder. *Eur. J. Pharmacol.*, **185**, 205–208.

MOSS, H.E., LINCOLN, J. & BURNSTOCK, G. (1987). A study of bladder dysfunction during streptozotocin-induced diabetes in the rat using an in vitro whole bladder preparation. *J. Urol.*, **138**, 1279–1284.

SANTICIOLI, P., GAMSE, R., MAGGI, C.A. & MELI, A. (1987). Cystometric changes in the early phase of streptozotocin-induced diabetes in rats: evidence for sensory changes not correlated to diabetic neuropathy. *Naunyn-Schmiedebergs Arch. Pharmacol.*, **335**, 580–587.

SIBLEY, G.N.A. (1984). A comparison of spontaneous and nerve-mediated activity in bladder muscle from man, pig and rabbit. *J. Physiol.*, **354**, 431–443.

STEERS, W.D., MACKWAY, A.M., CIAMBOTTI, J. & DEGROAT, W.C. (1990). Effects of streptozotocin induced diabetes on bladder function in the rat. *J. Urol.*, **143**, 1032–1036.

ZAR, M.A., IRAVANI, M.M. & LUHESHI, G.N. (1990). Effect of nifedipine on the contractile responses of the isolated rat bladder. *J. Urol.*, **143**, 835–839.

(Received December 3, 1990
Revised March 1, 1991
Accepted March 4, 1991)

Br. J. Pharmacol. (1991), **103**, 1663–1668 © Macmillan Press Ltd, 1991

Excretion of metabolites of prostacyclin and thromboxane by rats with nephrotoxic nephritis: effects of interleukin-1

[1]Paul S. Ward, Richard W. Fuller, [2]James M. Ritter, *Stephen J. Cashman, *Andrew J. Rees & *Colin T. Dollery

Departments of Clinical Pharmacology and *Medicine, Royal Postgraduate Medical School, Hammersmith Hospital, Du Cane Road, London W12 0NN

1 To obtain direct evidence of abnormal eicosanoid biosynthesis in rats injected with anti-glomerular-basement-membrane antibodies (a-GBM), products derived from thromboxane A_2 (TXA_2) and prostacyclin (PGI_2) were measured in 24 h urine collections before and after a-GBM.

2 Administration of a-GBM (9.5 mg) caused albuminuria, decreased creatinine clearance, increased numbers of intra-glomerular neutrophils and increased excretion of TXB_2, 2,3-dinor-TXB_2 (products of TXA_2) and 6-oxo-$PGF_{1\alpha}$ and 2,3-dinor-6-oxo-$PGF_{1\alpha}$ (products of PGI_2) at 24 h.

3 Interleukin-1 (IL-1_β; 5 μg) alone caused an increase in PGI_2 metabolite excretion but had no effect on TXA_2 metabolites. It had no effect on creatinine clearance but increased numbers of glomerular neutrophils by approximately 4–5 fold compared to a-GBM.

4 Pretreatment of rats with IL-1_β before a-GBM synergistically increased albumin excretion but only additively increased eicosanoid excretion. Numbers of intra-glomerular neutrophils and creatinine clearance were unchanged compared to IL-1_β alone.

5 The cyclo-oxygenase inhibitor, ibuprofen (10 mg kg^{-1} i.p., twice daily for 4 days) inhibited both serum TXB_2 production and urinary prostaglandin excretion. It also caused an almost complete attenuation of albumin excretion. Creatinine clearance and glomerular neutrophils remained unchanged after a-GBM/IL-1_β.

6 We conclude that the 50% inhibition of thromboxane production induced by ibuprofen does not modify the fall in creatinine clearance of accumulation of neutrophils in the glomerulus caused by the a-GBM. This degree of inhibition of eicosanoid production was associated with a striking decrease in proteinuria, but this may reflect a haemodynamic rather than a disease modifying action.

Keywords: Prostacyclin; thromboxane A_2; interleukin-1; nephritis; anti-glomerular-basement-membrane antibodies

Introduction

Intravenous administration of heterologous antibody to glomerular basement membrane (nephrotoxic globulin, a-GBM) causes neutrophil-dependent glomerular injury characterized by albuminuria (Unanue & Dixon, 1967). Several biochemical mediators have been implicated in the pathophysiology of the ensuing nephrotoxic nephritis which, however, remains incompletely understood. Indirect evidence based on measurements of eicosanoid production by isolated glomeruli *ex vivo*, and on the effects of various inhibitors of the arachidonic acid cascade on renal function in nephrotoxic nephritis (NTN) has pointed to a role for increased eicosanoid formation. During the first 2 to 3 h after administration of a-GBM, the glomerular filtration rate has been shown to fall (Lianos *et al.*, 1983), and this may be mediated via increased production of the vasoconstrictor thromboxane A_2 (TXA_2); in the later stages of the disease (by 24 h) the glomerular filtration rate has returned to normal, perhaps because of increased synthesis of vasodilator prostaglandins (PGE_2 and/or PGI_2) (Stork & Dunn, 1985). Direct evidence of altered eicosanoid formation in NTN *in vivo* is lacking.

Intercurrent bacterial infections can cause relapse of glomerulonephritis in man (reviewed by Heptinstall, 1983). Bacterial endotoxin stimulates production of several cytokines, including interleukin-1 (IL-1_β; Werber *et al.*, 1987). We recently found that parenteral injections of small doses of human recombinant IL-1_β substantially increased albuminuria caused by a-GBM (Tomosugi *et al.*, 1989). IL-1_β has been shown to be capable of stimulating prostaglandin synthesis *in vitro* (Mizel *et al.*, 1981; Rossi *et al.*, 1985; Conti *et al.*, 1986; Levine & Xiao, 1986) so it is possible that altered eicosanoid biosynthesis mediates or otherwise influences the effect of these cytokines on the course of NTN.

The objects of our present study were to seek direct evidence of abnormal eicosanoid formation in NTN and to investigate the effects of IL-1_β on eicosanoid biosynthesis in this condition. Thromboxanes and prostaglandins are readily formed in response to trauma during tissue isolation of blood sampling (Dollery *et al.*, 1984; Granström *et al.*, 1985). The least invasive way of investigating eicosanoid biosynthesis is by measurement of eicosanoid derived products in urine (Roberts *et al.*, 1981). We therefore measured hydrolysis products and metabolites of TXA_2 and PGI_2 in urine, to provide measures of biosynthesis of these eicosanoids *in vivo*. Cyclo-oxygenase-inhibition has been shown to be beneficial in reducing proteinuria in patients with nephrotic syndrome (Donker *et al.*, 1978; Velosa & Torres, 1986; Vriesendorp *et al.*, 1986). To study the role of prostaglandins in NTN, we have also studied the effect of ibuprofen, a cyclo-oxygenase inhibitor. This drug has previously been shown to be effective in protecting against haemodynamic alterations induced in glomerulonephritis in the rat by Takahashi *et al.* (1990), and a similar dosing regimen was used as in this study.

Methods

Animals

Male Sprague-Dawley rats were purchased from Olac, U.K. They were given free access to food and water until they were 180–200 g, when they were selected at random for the following experiments.

[1] Author for correspondence.
[2] Present address: Department of Clinical Pharmacology, UMDS, Guys Hospital, London Bridge, London SE1 9RT.

Protocol

Induction of nephrotoxic nephritis Rats were housed individually in metabolism cages which facilitated the collection of their urine. They were allowed to acclimatize overnight before starting the experiments. Water was still supplied *ad libitum* but food was withdrawn for the whole period of the urine collections.

Urine collection commenced at 9 h 00 min on day 0. Next day the urine was removed and a second 24 h collection started. The animals were lightly anaesthetized with ether, and injected via the dorsal tail vein with 1 ml of vehicle (0.9% saline), a-GBM (9.5 mg), IL-1_β (Biogen, Geneva; 5 μg $\equiv 5 \times 10^7$ units) or a-GBM with IL-1_β ($n = 6$ for each of the four groups). a-GBM was prepared as described previously (El Nahas *et al.*, 1985). On day 2, the animals were again anaesthetized, the peritoneum opened, and the animals exsanguinated via the abdominal aorta. The left kidney was removed and preserved in 10% neutral-buffered formalin for histological analysis.

Cyclo-oxygenase inhibition In a separate experiment, 2 groups of 6 rats were injected intra-peritoneally twice-daily with 1 ml of vehicle (0.9% saline) or ibuprofen (Sigma Chemical Co, Poole, Dorset; 10 mg kg^{-1}) a dose previously determined to be effective at inhibiting serum TXB_2 production by >95%, for the whole period of the experiment. After four days, nephritis was induced with a-GBM + IL-1_β, as above.

Assay procedures

Urinary prostaglandins were assayed by the Barrow *et al.* (1989) modification of the method of Chiabrando *et al.* (1987). Briefly, urine volume was measured and deuterated internal standard (5 ng) of each prostaglandin to be measured added. Phosphate buffer (0.1 M, pH 8.4, 10 ml) was added and the samples left to equilibrate for at least one week at −20°C. They were then defrosted, centrifuged, and extracted on Sephadex-4B immuno-affinity columns containing immobilized antibodies raised against thromboxane B_2 and 6-oxo-$PGF_{1\alpha}$. These cross-reacted with the respective 2,3-dinor-metabolites. The columns were washed with Milli-Q grade water (Millipore Corp.) and eluted with acetone:water (95:5) v/v, 3 × 0.5 ml. This was blown to dryness and the samples derivatised and analysed on a Finnigan-MAT 4500 gas-chromatograph/mass spectrometer, using electron-capture detection. Inter- and intra-assay variations were each <10%, and recovery through the extraction was >60%.

Serum TXB_2 was measured by radio-immunoassay (Fuller *et al.*, 1984). Albuminuria was measured by gel rocket-immuno-electrophoresis (Laurell, 1972). The gels were run at 2 V cm^{-1} overnight, washed, and stained with Coomassie Blue. Creatinine clearance was determined from measurement of serum and urine creatinine concentrations.

Morphology

Specimens for light microscopy were fixed in neutral-buffered formalin, embedded in wax, and sections cut at 3 μm. These were stained for neutrophils with chloroacetate esterase. Severity of infiltration was assessed as numbers of positive-staining cells in 50 sequential glomeruli per section. Slides were randomized and coded before counting.

Statistical analysis

Data from the initial induction experiments were analysed by analysis of variance, and from the ibuprofen study with an unpaired t test. Comparisons were made between rats on different treatment limbs on day 2 of the protocol. Data are expressed as mean ± s.e.mean and differences considered significant when $P < 0.05$.

Results

The results of the renal morphology and functional studies are summarised in Table 1. a-GBM alone decreased creatinine clearance by 68% at 24 h. IL-1_β had no effect, but in combination caused some attenuation of the a-GBM-induced fall, though this was neither statistically different from either the saline control group, or the a-GBM alone treated group. Neutrophil infiltration into the glomerulus occurred following a-GBM ($P < 0.05$). Both IL-1_β and a-GBM/IL-1_β caused a significantly greater influx ($P < 0.001$), with no difference between these two treatments. Rats given a-GBM alone displayed a small but significant ($P < 0.05$) albuminuria (Figure 1), consistent with earlier findings. Whilst IL-1_β alone had no effect, when given in conjunction with a-GBM it resulted in a very large and highly significant ($P < 0.001$) synergistic

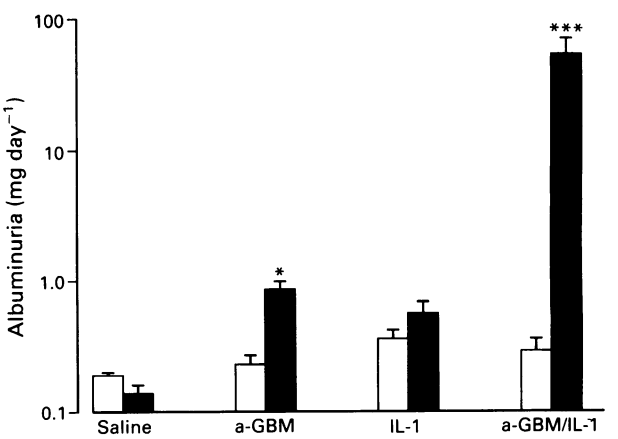


Figure 1 Urinary excretion of albumin following saline, anti-glomerular-basement-membrane antibodies (a-GBM, 9.5 mg), interleukin-1 (IL-1_β, 5 μg) or a-GBM/IL-1_β (9.5 mg; 5 μg). Results are mean (vertical bars show s.e.mean) for 24 h pre- (open columns) and post-treatment (solid columns), $n = 6$ for all groups. There were no differences in excretion rate between any of the groups on the pretreatment day. Excretion rate is shown on a $\log_{10}$ scale. * $P < 0.05$; *** $P < 0.001$ vs pretreatment day.

Table 1 Effect of anti-glomerular-basement-membrane antibodies (a-GBM) and/or interleukin-1_β (IL-1_β) on creatinine clearance and numbers of infiltrating glomerular neutrophils

	Saline	*a-GBM*	IL-1_β	*a-GBM/IL*
CCr (ml min^{-1})	1.55 ± 0.37	0.49 ± 0.09**	1.78 ± 0.48	0.91 ± 0.41
Neutrophils	1.67 ± 0.61	6.5 ± 1.43*	34.5 ± 10.5***	23.5 ± 1.98***

All measurements were made 24 h post-treatment. CCr = creatinine clearance; Neutrophils = infiltrating glomerular neutrophils/50 glomeruli. a-GBM (9.5 mg) and IL-1_β (5 μg) were given intravenously in 1.0 ml of 0.9% saline. Data are mean ± s.e.mean, $n = 6$ for all groups. *** $P < 0.001$; ** $P < 0.01$; * $P < 0.05$ vs. saline control.

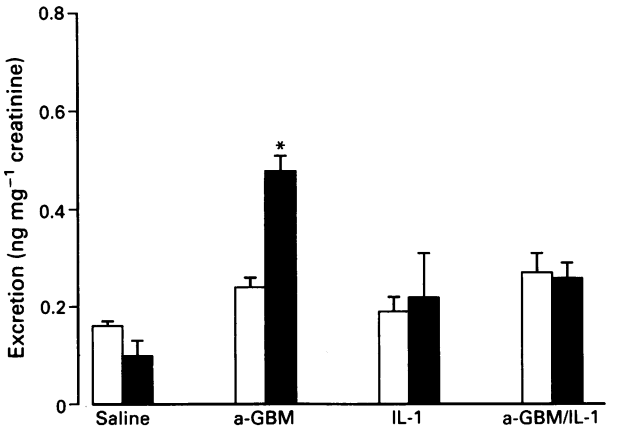


Figure 2 Urinary excretion of thromboxane B_2 (TXB_2) following saline, anti-glomerular-basement-membrane antibodies (a-GBM, 9.5 mg), interleukin-1 (IL-1_β, 5 μg) or a-GBM/IL-1_β (9.5 mg; 5 μg). Results are mean (vertical bars show s.e.mean) for 24 h pre- (open columns) and post-treatment (closed columns), $n = 6$ for all groups. There were no differences in excretion rate between any of the groups on the pretreatment day. * $P < 0.05$ vs. pretreatment day.

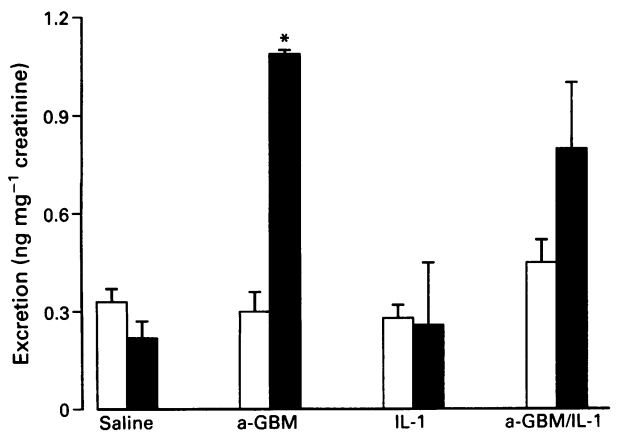


Figure 3 Urinary excretion of 2,3-dinor-thromboxane B_2 (2,3-dinor-TXB_2) following saline, anti-glomerular-basement-membrane antibodies (a-GBM, 9.5 mg), interleukin-1 (IL-1_β, 5 μg) or a-GBM/IL-1_β (9.5 mg; 5 μg). Results are mean (vertical bars show s.e.mean) for 24 h pre- (open columns) and post-treatment (solid columns), $n = 6$ for all groups. There were no differences in excretion rate between any of the groups on the pretreatment day. * $P < 0.05$ vs. pretreatment day.

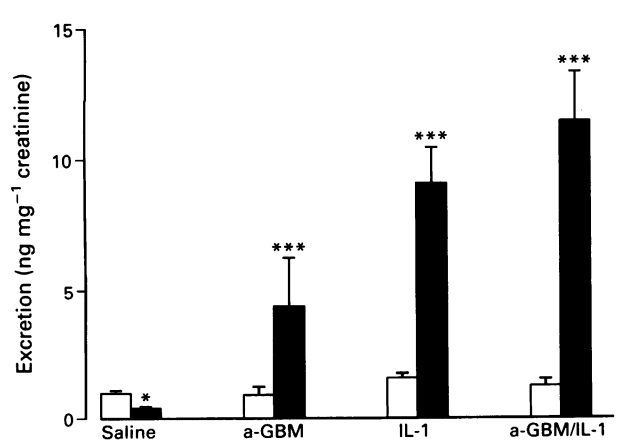


Figure 4 Urinary excretion of 6-oxo-prostaglandin $F_{1\alpha}$ (6-oxo-$PGF_{1\alpha}$) following saline, anti-glomerular-basement-membrane antibodies (a-GBM, 9.5 mg), interleukin-1 (IL-1_β, 5 μg) or a GBM/IL-1_β (9.5 mg; 5 μg). Results are mean (vertical bars show s.e.mean) for 24 h pre- (open columns) and post-treatment (solid columns), $n = 6$ for all groups. There were no differences in excretion rate between any of the groups on the pretreatment day. * $P < 0.05$; *** $P < 0.001$ vs. pretreatment day.

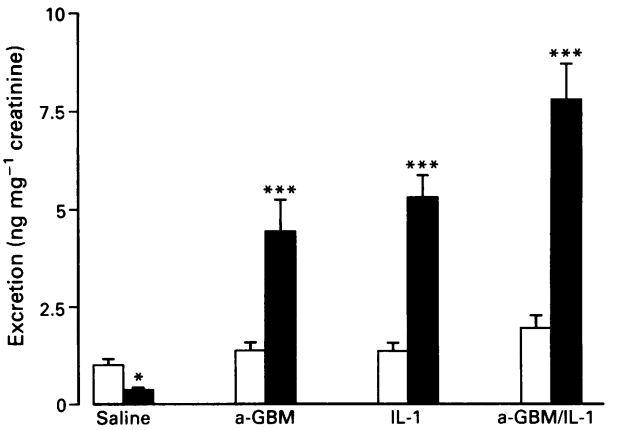


Figure 5 Urinary excretion of 2,3-dinor-6-oxo-prostaglandin $F_{1\alpha}$ (2,3-dinor-6-oxo-$PGF_{1\alpha}$) following saline, anti-glomerular-basement-membrane antibodies (a-GBM, 9.5 mg), interleukin-1 (IL-1_β, 5 μg) or a-GBM/IL-1_β (9.5 mg; 5 μg). Results are mean (vertical bars show s.e.mean) for 24 h pre- (open columns) and post-treatment (solid columns), $n = 6$ for all groups. There were no differences in excretion rate between any of the groups on the pretreatment day. * $P < 0.05$; *** $P < 0.001$ vs. pretreatment day.

increase in albuminuria, from 0.29 ± 0.07 to 54.6 ± 16.1 mg day^{-1}.

The results of the prostaglandin analysis are displayed in Figures 2–5. TXB_2 excretion was moderately elevated following a-GBM alone (Figure 2; 0.24 ± 0.02 vs. 0.48 ± 0.03 ng mg^{-1} creatinine; $P < 0.05$). Excretion of 2,3-dinor-TXB_2 was more markedly elevated following a-GBM alone (Figure 3; 0.3 ± 0.06 vs. 1.09 ± 0.01 ng mg^{-1} creatinine; $P < 0.05$). IL-1_β alone had no effect on excretion of either TXB_2 or 2,3-dinor-TXB_2. Following the combination of a-GBM/IL-1_β, 2,3-dinor-TXB_2 excretion was increased. Although this did not achieve statistical significance, it should be noted that excretion of 2,3-dinor-TXB_2 on pretreatment day was higher than for the other treatment groups. Excretion of 6-oxo-$PGF_{1\alpha}$ (Figure 4) and 2,3-dinor-6-oxo-$PGF_{1\alpha}$ (Figure 5) was substantially and highly significantly raised after a-GBM alone, IL-1_β alone, and to an even greater extent by the two given in combination. The effects of a-GBM and IL-1_β were approximately additive compared to either treatment alone.

Effect of cyclo-oxygenase inhibition

Pretreatment of animals with ibuprofen reduced serum TXB_2 to less than 5% of the value for non-ibuprofen treated animals post a-GBM/IL-1_β. The reductions in prostanoid excretion were less than the reduction in serum TXB_2 (Table 2). This is probably partly a reflection of the timing of collection: blood for serum TXB_2 was taken near the presumed peak of ibuprofen inhibition, whilst the urine collections provided an integrated measure over 24 h. Following treatment with a-GBM/IL-1_β there was marked albuminuria (around 50 mg day^{-1}). Ibuprofen attenuated this to a level approaching that found in control non-nephritic animals (Figure 6). Ibuprofen had no detectable effect on creatinine clearance, either with or without a-GBM/IL-1_β. No glomerular thrombi were seen in any of the treatment groups. Glomerular neutrophils were not affected by ibuprofen pretreatment, though there was a trend towards increased numbers in the ibuprofen-treated group compared to control ($P < 0.08$).

Discussion

These experiments provide the first direct evidence that eicosanoid synthesis is increased in nephrotoxic nephritis *in vivo* in rats. Depending on the metabolite measured, there was a 2 to

Table 2 Effect of pretreatment with the cyclo-oxygenase inhibitor ibuprofen ($10\,mg\,kg^{-1}$) on serum thromboxane B_2 (TXB_2) and markers of renal damage and urinary prostaglandin excretion after anti-glomerular-basement-membrane antibodies and interleukin-1_β (a-GBM/IL-1_β)

	– Ibuprofen	*+ Ibuprofen*
Serum TXB_2 ($ng\,ml^{-1}$)	43.9 ± 17.2	2.05 ± 0.41***
Creatinine clearance	0.35 ± 0.02	0.35 ± 0.05
Albumin ($mg\,day^{-1}$)	29.51 ± 7.2	1.85 ± 0.41***
Glomerular neutrophils	9.83 ± 2.1	15.9 ± 2.8
Glomerular thrombi	<1	<1
TXB_2	0.32 ± 0.04	0.18 ± 0.02
2,3-dinor-TXB_2	0.93 ± 0.19	0.57 ± 0.21
6-oxo-$PGF_{1\alpha}$	9.74 ± 1.54	4.55 ± 1.59*
2,3-dinor-6-oxo-$PGF_{1\alpha}$	17.0 ± 3.25	9.08 ± 1.49*

Creatinine clearance = $ml\,min^{-1}$, glomerular neutrophils and thrombi = per 50 glomeruli, prostaglandin excretion = $ng\,mg^{-1}$ creatinine. a-GBM (9.5 mg) and IL-1_β (5 μg) were given intravenously in 1.0 ml of 0.9% saline. Ibuprofen was injected intraperitoneally, twice daily for 4 days before induction of nephritic injury. All measurements were made 24 h after a-GBM/IL-1_β. *** $P < 0.001$; * $P < 0.05$, both – ibuprofen vs. + ibuprofen.

4.7 fold increase in eicosanoid excretion with a-GBM alone, compared with the same animal under control conditions. This corroborates evidence based on measurements of eicosanoid production by isolated glomeruli from rats with NTN (Lianos *et al.*, 1983; Stork & Dunn, 1985). Excretion rates of 6-oxo-$PGF_{1\alpha}$ and 2,3-dinor-6-oxo-$PGF_{1\alpha}$ were increased to a similar extent by a-GBM, implying that PGI_2 biosynthesis is increased by a-GBM. Evidence from other groups has suggested that primary hydrolysis products of both eicosanoids are of renal origin, whereas the 2,3-dinor-metabolites are of extra-renal and probably systemic origin (Fitzgerald *et al.*, 1981; reviewed in Fitzgerald *et al.*, 1987). In man, we gave TXB_2 both by inhalation and by mouth (Taylor *et al.*, 1991) and demonstrated an increase in excretion of both TXB_2 (3–4 fold) and 2,3-dinor-TXB_2 (5–7 fold) suggesting that TXB_2 is not exclusively renally derived. Consistent with this evidence of extra-renal cyclo-oxygenase activation is histological evidence of damage in organs other than the kidney, notably the lung. Macroscopic pulmonary haemorrhages were noted in animals with NTN and never in vehicle-injected animals (data not shown). Capillary thrombi have been noted within the glomeruli of nephritic animals only when pretreated with bacterial lipopolysaccharide, IL-1_β or tumour necrosis factor (Tomosugi *et al.*, 1988), and platelets in these would be expected to be a rich source of thromboxane.

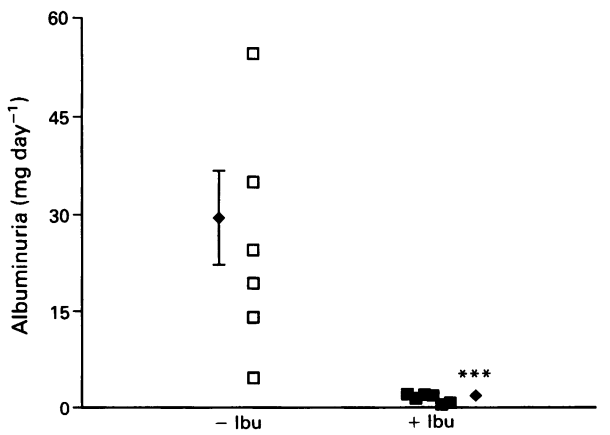


Figure 6 Urinary excretion of albumin following anti-glomerular-basement-membrane antibodies (a-GBM, 9.5 mg), interleukin-1 (IL-1_β, 5 μg): effect of pretreatment with ibuprofen ($10\,mg\,kg^{-1}$). Data represent values for individual animals either with (■; + Ibu) or without (□; – Ibu) pretreatment with ibuprofen. The mean excretion rate (vertical bars show s.e.mean if greater than symbol size) is also shown, offset from the individual data points. *** $P < 0.001$.

IL-1_β increased excretion of PGI_2- but not TXA_2-derived products, consistent with selective stimulation of PGI_2 synthesis. IL-1_β is well known to stimulate PGE_2 synthesis *in vitro* (Albrightson *et al.*, 1985; Beasley *et al.*, 1987; Kohan, 1989), but its effects on PGI_2 synthesis have been much less studied. Levine & Xiao (1985) demonstrated that IL-1_β stimulates 6-oxo-$PGF_{1\alpha}$ production by rat liver cells and Rossi *et al.* (1985) showed the same in vascular endothelial cells. We cannot identify the cellular site of the PGI_2 synthesis in the present experiments but this may well be vascular endothelial cells of the kidney and other organs, such as the lungs. The lack of effect of IL-1_β on TXA_2 biosynthesis was unexpected, since macrophages and polymorphonuclear leucocytes exhibit enhanced thromboxane synthesis after treatment with IL-1_β *in vitro* (Conti *et al.*, 1986). Increased TXA_2 production *in vivo* would have been a possible mechanism for the amplification by IL-1_β of the injurious effect of a-GBM, but our results do not support this hypothesis. On the contrary, the effect of IL-1_β on PGI_2 synthesis was additive with the effect of a-GBM itself, but IL-1_β attenuated the increase in TXB_2 and 2,3-dinor-TXB_2 excretion caused by a-GBM. A possible explanation is that increased PGI_2 synthesis caused by IL-1_β reduces platelet or white cell activation, resulting in reduced thromboxane formation. Despite an apparently favourable change in the balance of eicosanoid production, histological damage to the kidney and albuminuria were both increased by IL-1_β. A possible explanation is that the source of the increased prostacyclin production lay outside the kidney. It must be noted that histological damage to the glomeruli was assessed only by light microscopy and not by electron-microscopy of the membrane.

Nephrotoxic nephritis is a neutrophil-dependent injury and the results from this series of experiments show that injury is associated with increased numbers of neutrophils seen in the glomeruli. At 24 h post-induction of injury however, the numbers of infiltrating neutrophils is less than that seen at 2–4 h (Tomosugi *et al.*, 1989). It is not possible though to measure reliably prostaglandin excretion in rats over this period without cannulation of the bladder, a procedure which itself would increase prostaglandin production and therefore negate the 'non-invasive' advantage of urinary prostaglandin measurement over circulating plasma levels. It is interesting to note that in the group given IL-1 alone there was a significant increase in neutrophils seen in the glomerulus at 24 h but that there was no increase in albuminuria and no capillary thrombi seen. Both tumour necrosis factor (which has many overlapping, multiple specificities with IL-1; reviewed by Le & Vilcek, 1987) and bacterial lipopolysaccharide (which causes release of IL-1; Werber *et al.*, 1987) cause increased adhesiveness of neutrophils for endothelium *in vitro* (Gamble *et al.*, 1985). This increase has been noted before (Cashman *et al.*, 1989) and the lack of evidence of glomerular injury is presumed to be a reflection of the state of activation of these cells. Indeed, even under the electron microscope, where neutrophils were firmly adherent to underlying endothelium, there was no evidence of neutrophil granule release, and the endothelium appeared intact (S.J. Cashman, unpublished observation).

When animals were pretreated with the cyclo-oxygenase inhibitor ibuprofen, this decreased serum TXB_2 generation and excretion of urinary prostaglandin metabolites. Interestingly, it did not prove possible to inhibit urinary excretion of these products by more than 50%, despite a >95% inhibition of serum TXB_2. This is however in agreement with data from other groups working in man, and presumably is a reflection of the rate of recovery of cyclo-oxygenase activity following a given dose of drug (Fitzgerald *et al.*, 1983; Frazer & Ritter, 1987). Ibuprofen pretreatment reduced a-GBM/IL-1_β-induced albuminuria to levels comparable to those seen following a-GBM alone. This experiment does not therefore, tell us whether ibuprofen is reducing damage due to binding of

the a-GBM antibodies, or whether it is interfering with the synergism between this and IL-1_β.

The most likely explanation of the reduced proteinuria following ibuprofen is reduction of the intra-glomerular pressure. Two possible mechanisms have been proposed. The first is reduction of renin release and in consequence, a fall in angiotensin-II and diminished vasoconstrictor effect upon the efferent arteriole (Eriksson *et al.*, 1990). The second is reduced production of the vasodilator prostanoid, prostacyclin and resulting vasoconstriction of the afferent arteriole (Golbetz *et al.*, 1989). Our results tend to suggest that ibuprofen does not protect against injury *per se*, but inhibits net flux of albumin across equally damaged glomerular capillar walls. Consistent with this, work on angiotensin converting enzyme inhibitors showed that the ability of these drugs to inhibit proteinuria in patients with nephrotic syndrome is related to effects on filtration fraction (Heeg *et al.*, 1987). As the filtration fraction falls, proteinuria decreases, suggesting that the fall in proteinuria is related to reduction of intra-glomerular pressure. Similarly, ibuprofen is probably not protecting against the direct effects of the a-GBM, which is the primary cause of injury, but rather is attenuating the synergism between this and IL-1_β. Many of the effects of IL-1_β are known to be mediated through increased prostaglandin production and it could be that cyclo-oxygenase inhibition reduces interactions between neutrophils and endothelium, both potential sources of increased PGI_2 production.

In conclusion, we have confirmed *in vivo* previous *ex vivo* experiments suggesting that prostaglandin synthesis is elevated following injury due to anti-GBM antibodies, and also that IL-1_β is capable of causing increased prostacyclin synthesis. Inhibition of prostaglandin synthesis with the cyclo-oxygenase inhibitor ibuprofen reduced renal injury, as assessed by increased albumin excretion, but surprisingly had no effect on creatinine clearance. It has been proposed that increased thromboxane production contributes to the glomerular injury caused by a-GBM.

Although we have demonstrated increased production of thromboxane, the experiments with ibuprofen suggest that a 50% reduction in thromboxane production does not modify the glomerular injury (judged by creatinine clearance and glomerular neutrophil count), although it greatly reduces albuminuria. It is possible that a much greater degree of inhibition of thromboxane production might have modified the renal injury but it is difficult to achieve a very high degree of blockade of eicosanoid production *in vivo* with non-toxic doses of cyclo-oxygenase inhibitors.

This work was supported by the Medical Research Council.

References

ALBRIGHTSON, C.R., BAENZIGER, N.L. & NEEDLEMAN, P. (1985). Exaggerated human vascular cell prostaglandin biosynthesis mediated by monocytes: role of monokines and interleukin-1. *J. Immunol.*, **135**, 1872–1877.

BARROW, S.E., WARD, P.S., SLEIGHTHOLME, M.A., RITTER, J.M. & DOLLERY, C.T. (1989). Cigarette smoking: profiles of thromboxane and prostacyclin derived products in human urine. *Biochim. Biophys. Acta*, **993**, 121–127.

BEASLEY, D., DINARELLO, C.A. & CANNON, J.G. (1987). Interleukin-1 induces natriuresis in conscious rats: Role of renal prostaglandins. *Kidney Int.*, **33**, 1059–1065.

CASHMAN, S.J., KOSHINO, Y., TOMOSUGI, N. & REES, A.J. (1989). Effects of lipopolysaccharide and tumour necrosis factor on neutrophil counts and interleukin-1 gene expression. *Nephrol. Dial. Transplant*, **4**, 315.

CHIABRANDO, C., BENINI, A., PICCINELLI, A., CARMANATI, C., COZZI, E., REMUZZI, G. & FANELLI, R. (1987). Antibody-mediated extraction/negative-ion chemical ionization mass spectrometric measurement of thromboxane B_2 and 2,3,-dinor-thromboxane B_2 in human and rat urine. *Anal. Biochem.*, **163**, 255.

CONTI, P., CIFONE, M.G., ALESSE, E., REALE, M., IESCHI, C. & DINARELLO, C.A. (1986). *In vitro* enhanced thromboxane B_2 release by polymorphonuclear leukocytes and macrophages after treatment with human recombinant interleukin-1. *Prostaglandins*, **32**, 111–115.

DOLLERY, C.T., BARROW, S.E., BLAIR, I.A., LEWIS, P.J., MACDERMOT, J., ORCHARD, M.A., RITTER, J.M., ROBINSON, C., SHEPHERD, G.L. & ALLINSON, M. (1984). In *Atherosclerosis: Mechanisms and Approaches to Therapy*. ed. Miller, N.E. pp. 105–123. New York: Raven Press.

DONKER, A.J., BRENTJENS, J.R., VAN DER HEM, G.K. & ARISA, L. (1976). Treatment of the nephrotic syndrome with indomethacin. *Nephron*, **22**, 374–381.

EL NAHAS, A.M., LECHLER, R., ZOOB, S.N. & RESS, A.J. (1985). Progression to renal failure after nephrotoxic nephritis in rats studied by renal transplantation. *Clin. Sci.*, **68**, 15–27.

ERIKSSON, L.O., STURFELT, G., THYSELL, H. & WOLLHEIM, F.A. (1990). Effects of sulindac and naproxen on prostaglandin excretion in patients with impaired renal function and rheumatoid arthritis. *Am. J. Med.*, **89**, 313–321.

FITZGERALD, G.A., BRASH, A.R., FALARDEAU, P. & OATES, J.A. (1981). Estimated rate of prostacyclin secretion into the circulation of normal men. *J. Clin. Invest.*, **68**, 1271–1276.

FITZGERALD, G.A., HEALY, C. & DAUGHERTY, J. (1987). Thromboxane A_2 biosynthesis in health and disease. *Fed. Proc.*, **46**, 154–158.

FITZGERALD, G.A., OATES, J.A., HAWIGER, M., MAAS, R.L., JACKSON ROBERTS II, L., LAWSON, J.A. & BRASH, A.R. (1983). Endogenous biosynthesis of prostacyclin and thromboxane and platelet function during chronic aspirin administration in man. *J. Clin. Invest.*, **71**, 676–688.

FRAZER, C.E. & RITTER, J.M. (1987). Recovery of prostacyclin synthesis by rabbit aortic endothelium and other tissues after inhibition by aspirin. *Br. J. Pharmacol.*, **91**, 251–256.

FULLER, R.W., KELSEY, C.R., COLE, P.J., DOLLERY, C.T. & McDERMOTT, J. (1984). Dexamethasone inhibits the production of thromboxane B_2 and leukotriene B_4 by human abd peritoneal macrophages in culture. *Clin. Sci.*, **67**, 635–656.

GAMBLE, J.R., HARLAN, J.M., KLEBANOFF, S.J. & VADAS, M.A. (1985). Stimulation of adherence of neutrophils to umbilical vein endothelium by recombinant tumour necrosis factor. *Proc. Natl. Acad. Sci. U.S.A.*, **82**, 8667–8671.

GOLBETZ, H., BLACK, V., SHEMESH, O. & MYERS, B. (1989). Mechanism of the antiproteinuric effect of indomethacin in nephrotic humans. *Am. J. Physiol.*, **256**, F44–F51.

GRANSTRÖM, E., WESTLUND, P., KUMLIN, M. & NORDENSTRÖM, A. (1985). Monitoring thromboxane production *in vivo*: metabolic and analytical aspects. *Adv. Prost. Throm. Leuk. Res.*, Vol. 15, pp. 67–70. New York: Raven Press.

HEPTINSTALL, R.H. (1983). *Pathology of the Kidney*, 3rd edition. Chapter 12. Boston; Little Brown.

HEEG, J.E., DE JONG, P.E., VAN DER HEM, G.K. & DE ZEEUW, D. (1987). Reduction of proteinuria by angiotensin-converting enzyme inhibition. *Kidney Int.*, **32**, 78–83.

KOHAN, D.E. (1989). Interleukin-1 regulation of prostaglandin E_2 synthesis by the papillary collecting duct. *J. Lab. Clin. Med.*, **114**, 717–723.

LAURELL, C.B. (1972). Electroimmunoassay. *Scand. J. Clin. Lab. Invest.*, **29**, (Suppl 124), 265–275.

LE, J. & VILCEK, J. (1987). Biology of disease. Tumour necrosis factor and interleukin-1: cytokines with multiple overlapping biological activities. *Lab. Invest.*, **56**, 234–248.

LEVINE, L. & XIAO, D.-M. (1985). The stimulations of arachidonic acid metabolism by recombinant murine interleukin-1 and tumor producers or 1-oleoyl-2-acetyl-glycerol are synergistic. *J. Immunol.*, **135**, 3430–3433.

LIANOS, E.A., ANDRES, G.A. & DUNN, M.J. (1983). Glomerular prostaglandin and thromboxane synthesis in rat nephrotoxic serum nephritis. *J. Clin. Invest.*, **72**, 1439–1448.

MIZEL, S.B., DAYER, J.M., KRANE, S.M. & MERGENHAGEN, S.E. (1981). Stimulation of rheumatoid synovial cell collagenase and prostaglandin production by partially purified lymphocyte-activating factor (interleukin-1). *Proc. Natl. Acad. Sci. U.S.A.*, **78**, 2474–2477.

ROBERTS, L.J. II, SWEETMAN, B.J. & OATES, J.A. (1981). Metabolism of thromboxane B_2 in man. *J. Biol. Chem.*, **256**, 8384–8393.

ROSSI, V., BREVIARIO, E.F., GHEZZI, P., DEJANA, E. & MANTOVANI, A. (1985). Interleukin-1 induces prostacyclin in vascular cells. *Science*, **229**, 1174–1177.

STORK, J.E. & DUNN, M.J. (1985). Haemodynamic roles of thromboxane A_2 and prostaglandin E_2 in glomerulonephritis. *J. Pharmacol. Exp. Ther.*, **233**, 672–678.

TAKAHASHI, K., SCHREINER, G.F., YAMASHITA, K., CHRISTMAN, B.W., BLAIR, I.A. & BADR, K.F. (1990). Predominant functional roles for thromboxane A_2 and prostaglandin E_2 during late nephrotoxic serum glomerulonephritis in the rat. *J. Clin. Invest.*, **85**, 1974–1982.

TAYLOR, I.K., WARD, P.S., O'SHAUGHNESSY, K.M., DOLLERY, C.T., BLACK, P.B., BARROW, S.E., TAYLOR, G.W. & FULLER, R.W. (1991). Thromboxane A_2 biosynthesis in acute asthma and following antigen challenge. *Am. Rev. Resp. Dis.*, **143**, 119–125.

TOMOSUGI, N., CASHMAN, S.J., HAY, H., PUSEY, C.D., EVANS, D.J., SHAW, A. & REES, A.J. (1989). Modulation of antibody mediated injury *in vivo* by bacterial lipopolysaccharide, tumor necrosis factor and interleukin-1. *J. Immunol.*, **142**, 3083–3090.

UNANUE, E.R. & DIXON, F.J. (1967). Experimental glomerulonephritis: immunological events and pathogenetic mechanisms. *Adv. Immunol.*, **6**, 1–90.

VELOSA, J.A. & TORRES, V.E. (1986). Benefits and risks of nonsteroidal antiinflammatory drugs in steroid resistant nephrotic syndrome. *Am. J. Kidney Dis.*, **8**, 345–350.

VRIESENDORP, R., DONKER, J.M., DE ZEEUW, D., DE JONG, P.E., VAN DER HEM, G.K. & BRENTJENS, J.R.H. (1986). Effect of nonsteroidal antiinflammatory drugs on proteinuria. *Am. J. Med.*, **81**, 84–94.

WERBER, H.I., EMANCIPATOR, S.N., TYKOCINSKI, M.L. & SEDOR, J.R. (1987). The interleukin-1 gene is expressed by rat glomerular mesangial cells and is augmented in immune complex glomerulonephritis. *J. Immunol.*, **138**, 3207–3212.

(Received November 27, 1990
Revised February 28, 1991
Accepted March 3, 1991)

Br. J. Pharmacol. (1991), **103**, 1669–1676 © Macmillan Press Ltd, 1991

Chronic dihydropyridine treatment can reverse the behavioural consequences of and prevent adaptations to, chronic ethanol treatment

M.A. Whittington, *S.J. Dolin, *T.L. Patch, R.J. Siarey, A.R. Butterworth & [1]H.J. Little

Pharmacology Department, The Medical School, University Walk, Bristol, BS8 1TD and *Clinical Pharmacology Unit, Addenbrooks Hospital, Cambridge, CB2 2QQ

1 Chronic treatment with the dihydropyridine calcium channel antagonist, nitrendipine, given concurrently with ethanol, prevented the ethanol withdrawal syndrome in mice, even though the chronic nitrendipine treatment was stopped 24 h or 48 h before the withdrawal testing.

2 This effect was seen in two strains of mice with different methods of ethanol administration. Nitrendipine was effective when given for two weeks but not after only two days' treatment.

3 Two other dihydropyridine calcium antagonists, nimodipine and PN 200-110, given chronically with ethanol, also prevented the withdrawal syndrome. The tests were again made 24 h after the last administration of dihydropyridine.

4 The chronic nitrendipine treatment also prevented the rise in the number of central dihydropyridine binding sites that occurs on chronic ethanol administration.

5 Chronic administration of nitrendipine alone did not cause any withdrawal behaviour.

6 Chronic nitrendipine treatment did not affect the seizure threshold to bicuculline in mice that were not given ethanol.

7 Whole brain concentration measurements showed that the effects were not due to residual nitrendipine in the CNS at the time of withdrawal testing or to differences in central ethanol concentrations during the treatment.

8 It is suggested that the results provide evidence for a functional role for dihydropyridine-sensitive calcium channels in ethanol dependence.

Keywords: Ethanol withdrawal; dihydropyridines; calcium; chronic ethanol treatment

Introduction

The neurochemical basis of dependence on ethanol is uncertain. Ethanol affects a wide range of biochemical functions and many different neurotransmitters. Its effects may be due to actions on membrane lipids (Goldstein, 1986), which could result in the observed alterations in neuronal transmission. Tolerance occurs to many of its effects on long term treatment and adaptations have been demonstrated in many different systems. However, so far no single action or adaptation has been shown to be responsible for ethanol-dependence.

Withdrawal from chronic ethanol intake results in a hyperexcitability syndrome, seen in animals as tremor, hyperreflexia and convulsions, described by Goldstein & Pal (1971). In man similar symptoms occur, plus confusional states and hallucinations. Drugs that have similar actions to ethanol, such as the benzodiazepines or barbiturates, will substitute for ethanol in withdrawal, and are used therapeutically to control the syndrome. However, these compounds possess dependence liability of their own and do not appear to alter the underlying changes responsible for ethanol-dependence.

We have found that chronic administration of ethanol *in vivo* increases the number of dihydropyridine binding sites in the central nervous system (Dolin *et al.*, 1987). When a single strain of rodents was used, inbred for either ethanol withdrawal sensitivity or resistance, the increase in dihydropyridine binding sites after ethanol treatment correlated well with withdrawal severity (Brennan *et al.*, 1990). These binding sites show a high affinity for dihydropyridine calcium channel antagonists, such as nifedipine or nitrendipine, and the calcium channel activators, such as Bay K 8644 (Littleton & Little, 1987), but their physiological role is uncertain (Miller, 1985). They may to correspond to the 'L' subtype of neuronal calcium channel, described in cultured cells of neuronal origin (Nowycky *et al.*, 1985), although the selectivity for this subtype may not be as clear in mammalian neurones (Akaike *et al.*, 1989; Takahashi *et al.*, 1989; Takahashi & Akaike, 1990). Dihydropyridine calcium channel antagonists have few overt behavioural actions in normal circumstances, although high affinity binding sites have been identified in the CNS (Murphy *et al.*, 1982; Schoemaker *et al.*, 1983). They were originally thought to have little effect on neurones, but actions on central neurones are being increasingly reported (Middlemiss & Spedding, 1986; Raeburn & Gonzales, 1988; Grover & Teyler, 1990). The increase in binding site number found after chronic ethanol administration was accompanied by increases in the actions of the dihydropyridines on transmitter release and on inositol phospholipid breakdown (Dolin *et al.*, 1987), suggesting a functional change caused by the ethanol.

Calcium channel antagonists, given acutely at the start of ethanol withdrawal, decreased the ethanol withdrawal syndrome (Little *et al.*, 1986). This action was stereospecific (Littleton *et al.*, 1990), being seen with the (+)-isomer of PN 200-110, but not with the (−)-isomer that does not block calcium channels (Hof *et al.*, 1986). The effect appeared to be selective for the ethanol withdrawal syndrome as dihydropyridines, such as nitrendipine and nimodipine, were found to provide little protection against other convulsive states (Dolin *et al.*, 1988a). We have found no anticonvulsant action against the $GABA_A$ antagonist, bicuculline (Dolin *et al.*, 1990). When administered with ethanol, dihydropyridine calcium channel antagonists potentiated the actions of ethanol (Dolin & Little, 1986).

From these results we put forward the hypothesis that some of the changes that occur on chronic ethanol intake could be due to the increase in number and function of dihydropyridine binding sites (Littleton *et al.*, 1988; Dolin & Little, 1989). If

[1]Author for correspondence.

this hypothesis were correct, then prevention of the increase in number of dihydropyridine-sensitive sites should prevent the adaptations to chronic ethanol intake. In 1985, Panza et al. reported that chronic administration of a dihydropyridine calcium channel antagonist resulted in a decrease in the number of central dihydropyridine binding sites. The present study was designed to determine whether chronic administration of a dihydropyridine would alter the adaptations to long term ethanol administration, as manifest by the ethanol withdrawal syndrome. Comparison was made with the effects of such chronic dihydropyridine treatment on seizure thresholds to bicuculline, in order to determine the selectivity of protection against the ethanol withdrawal seizure activity.

Some of these results have been presented in abstract form to the British Pharmacological Society (Dolin et al., 1988b).

Methods

Chronic drug administration

Two methods of chronic ethanol administration were used, and two strains of mice. This avoided any influence of the method of administration or the rodent strain on the results. Male mice, C57 strain (22–27 g at the start of the treatment) were given ethanol, 24% v/v in tap water, as sole fluid for twelve weeks. Nitrendipine was given either by injection (see below) or dissolved in the drinking fluid at 1.77 mM. This concentration was the highest that would remain in solution in the drinking bottles. Nitrendipine was added to the drinking fluid either for the whole of the twelve weeks ethanol treatment period or for the last two weeks of this period. The amount of fluid drunk by each treatment group in every experiment was measured three times a week. No significant differences were found between the amount of ethanol drunk by mice receiving concurrent nitrendipine and those given ethanol alone. The ethanol intake values when nitrendipine was dissolved in the ethanol throughout the treatment period, for example, were: ethanol alone, $13.5 \pm 0.4\,g\,kg^{-1}$ daily and ethanol plus nitrendipine, $13.3 \pm 0.3\,g\,kg^{-1}$ daily (mean ± s.e.mean, 11 mice in each group). In both studies, nitrendipine was removed from the drinking fluid 24 h before withdrawal of ethanol and behavioural rating (see below). Controls drank tap water. The dose of nitrendipine received by this method of administration was $51 \pm 5\,mg\,kg^{-1}$ daily (mean ± s.e.mean for both experiments, 23 mice).

In the second method, male mice of the TO strain (25–30 g) were kept in inhalational chambers for two weeks in an atmosphere of $12–18\,g\,l^{-1}$ ethanol. The ethanol concentrations in the chambers were measured twice daily. Groups of mice that were to undergo comparison in behavioural experiments were always kept in the same chamber. Controls were kept in the same environment, outside the chambers.

Nitrendipine was suspended in Tween 80, 0.5%, and sonicated well before use. As the drug is photosensitive, it was protected from light at all times by use of a red safe-light and dark bottles. In the injection schedules, mice were given injections, i.p., twice daily (10 h 00 min and 22 h 00 min) of either nitrendipine, $50\,mg\,kg^{-1}$ or $10\,mg\,kg^{-1}$, or the vehicle, Tween 80, 0.5%. The choice of doses of nitrendipine was based on our previous work on the interactions between ethanol and nitrendipine (Dolin & Little, 1989) and the effects of nitrendipine in the ethanol withdrawal syndrome (Littleton et al., 1990). The last injections were given 24 h before the testing of the withdrawal syndrome, unless otherwise stated.

All groups of animals remained healthy throughout the treatments. They were weighed at regular intervals during the treatments and there were no significant differences between the weight gains of the different groups. The numbers of mice in each treatment group were between 7 and 12.

The details of the duration of the nitrendipine treatments are given in each results section. In all cases the nitrendipine treatment was stopped at least 24 h before the withdrawal testing. For the drinking schedules, the nitrendipine was removed from the drinking fluid 24 h before the withdrawal of ethanol; for the injection schedules the last injections were given at this 24 h interval. This was because the intention of the experiments was to study the effects of the chronic treatments, not the acute action of nitrendipine on the withdrawal syndrome.

The effects of two weeks' administration of nitrendipine, $50\,mg\,kg^{-1}$ twice daily, by injections, in the absence of ethanol was examined in the TO strain of mice. It was not possible in the C57 mice, where the ethanol was given in the drinking fluid, to make a direct comparison with the effects of nitrendipine alone dissolved in the drinking fluid, because nitrendipine was not sufficiently soluble to dissolve in water without ethanol.

In separate experients the effects on the ethanol withdrawal syndrome of chronic treatment with two other dihydropyridine compounds were examined. Nimodipine was given twice daily at $50\,mg\,kg^{-1}$ and (±)-PN 200-110 twice daily at $4\,mg\,kg^{-1}$. In each case the last injection was given 24 h before withdrawal of ethanol.

The ethanol withdrawal syndrome

The ethanol withdrawal syndrome was measured by ratings of convulsive behaviour (Goldstein & Pal, 1971; Littleton et al., 1990). This method measures both tremor and clonic convulsions. The mice were removed from the ethanol between 09 h 00 min and 09 h 30 min. Behavioural ratings were made once an hour on all mice for 12 h.

The observer who carried out the ratings was unaware of the prior drug treatment. The ratings of the withdrawal syndrome were compared by nonparametric analysis of variance, using a format designed for repeat measurements on the same samples and multiple comparisons with controls (Meddis, 1984). Statistical comparisons were made on the ratings at between 3 h and 12 h from the start of withdrawal. During the first 2 h the withdrawal syndrome was beginning, but was not seen clearly until about 3 h.

Dihydropyridine binding

Central dihydropyridine receptor binding was measured by the method of Glossman & Ferry (1985), using [^{3}H]-nimodipine (specific activity $130\,Ci\,mmol^{-1}$). The tissues were homogenized in Tris buffer, 50 mM and centrifuged (45,000 *g*, 15 min) and washed with the buffer three times. Tissue aliquots were incubated (25°C, 45 min) with [^{3}H]-nimodipine, 0.125 nM to 4 nM, then filtered (Whatman GF/B glass filters) and counted. All measurements were made in triplicate. Non-specific binding was estimated with 1 μM nitrendipine. The protein content of the tissues was measured with Folin's reagent. The results were subjected to Scatchard analysis to give the receptor density, B_{max}, in $fmol\,mg^{-1}$ protein, and the dissociation constant, K_d in nM.

The measurements of [^{3}H]-nimodipine binding were made in whole brains of C57 mice and in cerebral cortex of TO mice. The C57 tissues were taken at 5 h from ethanol withdrawal, when the effects of the drug treatment were evident in the parallel behavioural tests. Nitrendipine was given by i.p. injection at $50\,mg\,kg^{-1}$, twice daily, for the last two weeks of the ethanol drinking period. Animals receiving ethanol alone and controls were given vehicle injections. The TO mice received two weeks inhalation of ethanol, as described above, with injections of nitrendipine, $50\,mg\,kg^{-1}$, or vehicle, twice daily. In both studies the last injections were given 24 h before removal of tissues.

Measurement of seizure threshold to bicuculline

For comparison with the ethanol withdrawal experiments, seizure thresholds to bicuculline were determined after two

weeks treatment with nitrendipine, twice daily as above, in TO mice that did not receive ethanol. The amount of bicuculline required to cause the first signs of clonic convulsion was measured, by the tail vein infusion method of Nutt *et al.* (1980). The mice were humanely killed immediately the first sign of a seizure was seen. These measurements were made between 30 h and 32 h after the last of the chronic treatment injections, to correspond to the time at which a clear drug effect was seen in the ethanol withdrawal studies. The *n* values were 7 for the controls and 9 for the nitrendipine treatment.

Measurement of central nitrendipine concentrations

Measurements were made of the concentrations of nitrendipine in brains removed from animals receiving the chronic treatment. The brains were removed, following cervical dislocation, from C57 mice, that had been drinking the ethanol and nitrendipine solution for 12 weeks as described above. Tissues were taken at the end of the chronic treatment (at 10 h 00 min before removal of the nitrendipine) and 32 h after removal of nitrendipine from the drinking fluid, i.e. 8 h after withdrawal of ethanol, to correspond with the peak drug effect in the withdrawal testing. Comparison was made with the brain concentrations 2 h and 8 h after acute injections of nitrendipine, in C57 mice that had been drinking 24% ethanol alone for twelve weeks.

Whole brain nitrendipine concentrations were measured by gas/liquid chromatography. Electron capture detection was used to analyse samples separated with a 25 meter capillary column coated with SE30. The temperature programming for the analysis was as follows: injector 280°C, detector 320°C, oven started at 180°C for 2 min then ramped up to 290°C at 16°C min^{-1} and left at this temperature for 10 min. Helium carrier gas at 6 p.s.i. was used to ensure the flow of sample along the column at the optimum speed for separation. The sample was flushed from the end of the capillary column into the detector with nitrogen make-up gas at 20 p.s.i.

The brains were homogenized in 10 M NaOH, 1 ml per 50 mg wet weight, and the proteins precipitated with sodium tungstate and sulphuric acid. The samples were centrifuged at 4000 r.p.m. for 10 min, then the nitrendipine was extracted by shaking with the same volume of toluene. The organic layer was removed and dried with anhydrous $MgSO_4$; then the samples were evaporated to dryness and reconstituted in 100 μl toluene, with 1 μM nimodipine as internal standard.

Brain concentrations of ethanol

The brain concentrations of ethanol were measured at times corresponding to the peak drug effect in the behavioural tests to ensure that the chronic treatments did not alter the pharmacokinetics of ethanol. The samples were taken at 2 h from ethanol withdrawal for the C57 strain (drinking ethanol or ethanol plus nitrendipine) and 5 h from withdrawal for the TO strain (ethanol inhalation, with and without nitrendipine injections), after the chronic treatment schedules described above.

Ethanol concentrations were measured by gas-liquid chromatography, with flame ionization detection, Pye type 104 dual column. Whole brains were homogenized in 150 mM NaCl, diluted 1:3, and the internal standard, n-propanol (100 $\mu g\,ml^{-1}$) added. Proteins were precipitated with sodium tungstate and sulphuric acid. The areas under the curves were compared; recovery of ethanol was 100%.

Brain concentrations of ethanol, the results from the binding studies and the ethanol consumption of the groups of C57 mice, were compared by Student's *t* test.

Drugs used

Nitrendipine and nimodipine were kindly donated by Bayer A/G. (±)-PN 200-110 (isopropyl-4- (2,1,3-benzoxadiazol-4-yl-1,4-dihydro-2,6-dimethyl-5-methoxy-carbonyl-pyridine-3-carboxylate) was given by Sandoz.

Results

Effects of nitrendipine on the withdrawal syndrome in C57 mice drinking ethanol

Nitrendipine given in the drinking fluid for 12 weeks Removal of ethanol resulted in the appearance of a clear ethanol withdrawal syndrome, beginning approximately 2–3 h after withdrawal (Figures 1a and b). When nitrendipine was given for the 12 week ethanol drinking period, this withdrawal syndrome was not seen (Figure 1a). The ratings of convulsive behaviour were significantly lower than those for animals given ethanol alone ($P < 0.005$) and were not significantly different from control values, i.e. from ratings of animals which did not receive any ethanol ($P > 0.1$).

Nitrendipine dissolved in the drinking fluid for 2 weeks of the 12 week drinking period When nitrendipine was given for the last 2 weeks only of the 12 weeks of ethanol drinking there was a significant decrease in the withdrawal ratings ($P < 0.05$), compared with those for animals given ethanol alone, but the syndrome was not completely abolished (Figure 1b). The ratings for mice given ethanol plus nitrendipine were significantly higher ($P < 0.05$) than those of control animals that were not given ethanol.

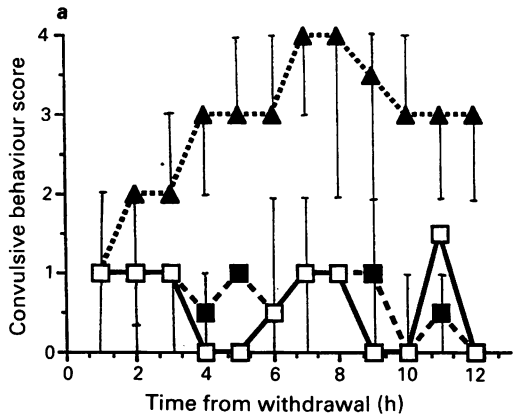
Nitrendipine given by injection for 2 weeks to C57 mice drinking ethanol The ethanol withdrawal syndrome was also prevented when nitrendipine was given to C57 mice by injection (50 mg kg^{-1}, twice daily) for the last 2 weeks of the 12 week drinking period, up until the last 24 h of ethanol treatment (data not shown). The ratings of withdrawal after the nitrendipine treatment were significantly lower ($P < 0.001$) after nitrendipine plus ethanol than after ethanol alone, and were not significantly different from control values ($P > 0.1$).

Effects of nitrendipine on TO mice given ethanol by inhalation

Nitrendipine given twice daily for 2 weeks at 50 mg kg^{-1} Removal of mice from the ethanol inhalational chamber resulted in the appearance of a withdrawal syndrome similar to that seen in the C57 mice, although the ratings were slightly lower. Injections of nitrendipine for the whole 2 weeks of the ethanol administration abolished the syndrome (Figure 2a). The difference between the ratings for animals given ethanol alone and those given ethanol plus nitrendipine was significant ($P < 0.001$) and the latter ratings were not different from control values ($P > 0.1$). In this experiment the last injection of nitrendipine was made 24 h before the withdrawal testing. When the last injection was made 48 h before the withdrawal the effect of nitrendipine was still seen (Figure 2b) ($P < 0.001$ for comparison between ethanol alone and ethanol plus nitrendipine).

Effect of duration of nitrendipine administration In a separate experiment, nitrendipine was given, at 50 mg kg^{-1}, to TO mice for 2 days only, during the 48 h preceding the 24 h interval before the withdrawal of ethanol (i.e. four injections, the last being given 24 h before withdrawal). In this study there was no effect of nitrendipine ($P > 0.1$) on the withdrawal syndrome (Figure 3a).

Dose-dependency of nitrendipine action The administration of nitrendipine at 10 mg kg^{-1} twice daily during the 2 week ethanol administration period caused a significant decrease in



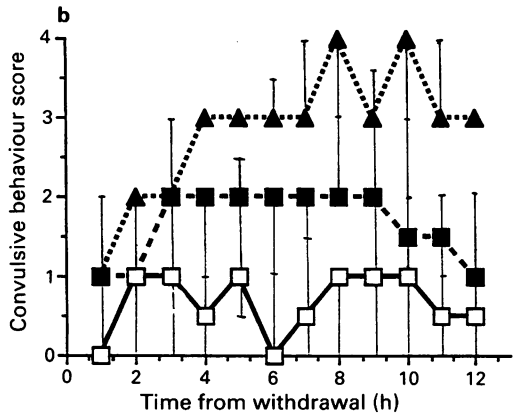
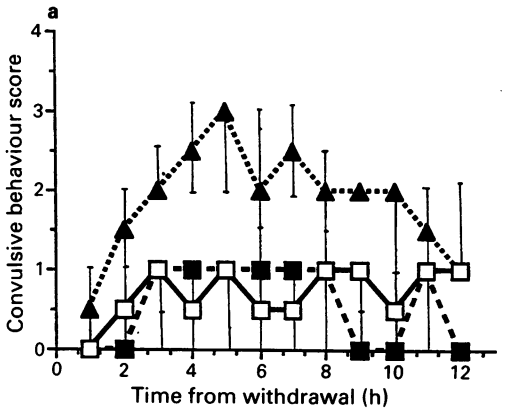


Figure 1 (a) The effects of either ethanol alone or ethanol plus nitrendipine (1.77 mM) given to C57 mice in the drinking fluid for 12 weeks. The addition of nitrendipine abolished the withdrawal syndrome, even though little drug remained in the CNS at the time of testing. Results in this and subsequent figures are median values (± interquartile ranges) for 7–12 mice. The ratings of convulsive behaviour were significantly lower in animals given nitrendipine injections than those for animals given ethanol alone ($P = 0.005$) and were not significantly different from control values, i.e. from ratings of animals which did not receive any ethanol ($P < 0.1$). Comparisons made between 3 h and 12 h of the testing period: (▲) ethanol plus Tween vehicle injections; (■) ethanol plus nitrendipine injections; (□) controls. (b) Nitrendipine dissolved in the drinking fluid for the last 2 weeks of the 12 week drinking period decreased with withdrawal syndrome in C57 mice. There was a significant decrease in the withdrawal ratings ($P < 0.05$), for animals given nitrendipine compared with those for animals given ethanol alone. The ratings for mice given ethanol plus nitrendipine were significantly higher ($P < 0.05$) than those of control animals not given ethanol: (▲) ethanol alone; (■) ethanol plus nitrendipine; (□) controls.



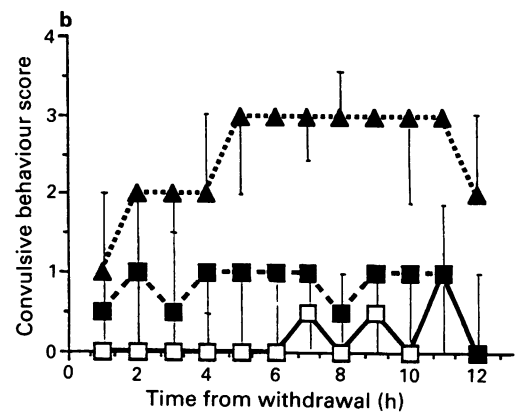


Figure 2 Nitrendipine given twice daily at 50 mg kg^{-1} for the 2 week period of ethanol inhalation abolished the withdrawal syndrome in the TO strain of mice. The difference between the ratings for animals given ethanol alone and those given ethanol plus nitrendipine was significant ($P < 0.001$) and the latter ratings were not different from control values ($P > 0.1$). The last injections were given 24 h before the tests were commenced: (▲) ethanol plus Tween vehicle injections; (■) ethanol plus nitrendipine injections; (□) controls. (b) As in (a) except that the last injections were made 48 h before the withdrawal. The effect of nitrendipine was still seen, $P < 0.001$ for comparison between ethanol alone and ethanol plus nitrendipine: (▲) ethanol plus Tween vehicle injections; (■) ethanol plus nitrendipine injections; (□) controls.

the withdrawal ratings, compared with mice given ethanol alone, $P < 0.001$ (Figure 3b). However, the withdrawal syndrome was not completely abolished, as had been seen with the 50 mg kg^{-1} dose of nitrendipine, as the ratings were significantly higher than those of control animals, given no ethanol, $P < 0.001$.

The effects of chronic treatment with the dihydropyridines nimodipine and PN 200-110 Chronic nimodipine treatment also prevented the withdrawal syndrome to ethanol (Figure 4a). The ratings after ethanol plus nimodipine were significantly lower than those after ethanol alone ($P = 0.005$), and were not significantly different from control values. A similar, but smaller, effect was seen with PN 200-110 (Figure 4b). In this case the ratings after ethanol plus PN 200-110 were significantly lower than those after ethanol alone ($P < 0.01$), but were higher than the control values ($P < 0.05$).

Nitrendipine in the absence of ethanol treatment The administration of nitrendipine at 50 mg kg^{-1}, twice daily, did not result in the appearance of any withdrawal signs in mice that did not receive any ethanol, in either the TO strain or the C57 strain (not illustrated). The ratings of convulsive behaviour were not significantly different from those of mice that were given vehicle injections, $P > 0.1$.

Central dihydropyridine binding

The values for dihydropyridine binding are given in Table 1. In tissues from both C57 mice and the TO strain there was a significant increase in the B_{max} values when comparison was made between ethanol treatment and controls ($P < 0.05$), but this difference was not significant ($P < 0.1$) when the B_{max} values for ethanol plus nitrendipine treatment were compared with controls. The same pattern was therefore seen in both sets of binding data even though different strains of mice were

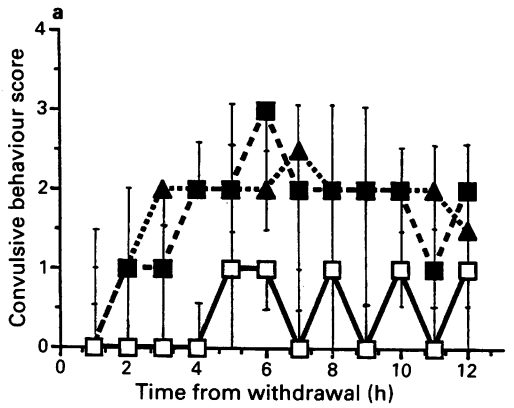


Figure 3 (a) When nitrendipine was given to TO mice for the last 2 days only of the 2 week ethanol administration period, at 50 mg kg^{-1}, there was no effect on the withdrawal syndrome, $P > 0.1$ for comparison between ethanol alone and ethanol plus nitrendipine: (▲) ethanol plus Tween vehicle injections; (■) ethanol plus nitrendipine injections; (□) controls. (b) The administration of nitrendipine at 10 mg kg^{-1} twice daily during the 2 week ethanol administration period caused a significant decrease in the withdrawal ratings, compared with mice given ethanol alone, $P < 0.001$. Ratings for ethanol plus nitrendipine treatment were higher than those of control animals, given no ethanol, $P < 0.001$: (▲) ethanol plus Tween vehicle injections; (■) ethanol plus nitrendipine injections; (□) controls.

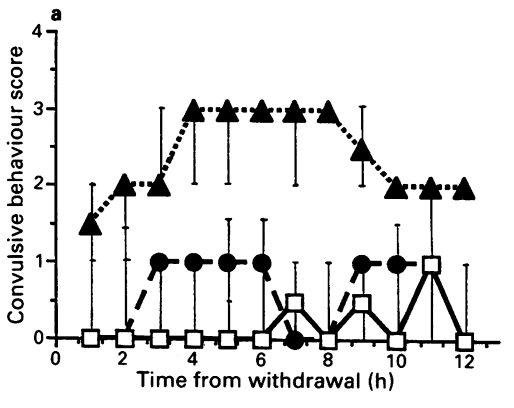


Figure 4 (a) Nimodipine, twice daily at 50 mg kg^{-1}, for the 2 week period of ethanol inhalation, prevented the withdrawal syndrome in the TO strain of mice. The difference between the ratings for animals given ethanol alone and those given ethanol plus nimodipine was significant ($P < 0.005$) and the latter ratings were not different from control values ($P > 0.1$). The last injections were given 24 h before the tests were commenced: (▲) ethanol plus Tween vehicle injections; (●) ethanol plus nimodipine injections; (□) controls. (b) PN 200-110, at 4 mg kg^{-1}, twice daily for the 2 week period of ethanol inhalation, abolished the withdrawal syndrome in the TO mice. The ratings for animals given ethanol plus PN 200-110 were significantly different from those following ethanol alone ($P < 0.01$) and from control values ($P < 0.05$). The last injections were given 24 h before the tests were commenced: (▲) ethanol plus Tween vehicle injections; (●) ethanol plus nitrendipine injections; (□) controls.

used, different areas (whole brain and cerebral cortex) and the tissues were removed at different time periods (5 h from ethanol withdrawal and immediately on withdrawal). There were no significant differences in K_d values.

Table 1 B_{max} and K_d values for [^{3}H]-nimodipine binding in C57 and TO mice, taken 5 h and 0 h, respectively, from withdrawal of ethanol

Chronic treatment	B_{max} (fmol mg^{-1})	K_d (nM)
(i) C57 mice, 5 h from ethanol withdrawal		
Controls, vehicle injections (11)	232 ± 10	0.67 ± 0.07
Ethanol alone, 12 weeks (9)	277* ± 16	0.74 ± 0.07
Ethanol, 12 weeks, plus 2 weeks injections nitrendipine (7)	249 ± 17	0.74 ± 0.04
(ii) TO mice, 0 h from withdrawal		
Controls, vehicle injections (5)	230 ± 20	0.99 ± 0.27
Ethanol alone, vehicle injections (5)	300* ± 18	0.93 ± 0.09
Ethanol plus nitrendipine injections for the whole 2 weeks (5)	253 ± 18	0.79 ± 0.06
Nitrendipine injections alone (5)	210 ± 21	0.67 ± 0.04

Values are mean ± s.e.mean; n is given in parentheses.
* $P < 0.05$, Student's t test, compared with control values.

Lack of effect of nitrendipine treatment on seizure thresholds to bicuculline

The chronic nitrendipine treatment had no effect on the seizure thresholds to bicuculline in naive mice, i.e. animals that were not given any ethanol ($P > 0.1$). The thresholds were 0.32 ± 0.07 mg kg^{-1} bicuculline for the controls and 0.35 ± 0.09 mg kg^{-1} bicuculline for the group given nitrendipine treatment. The time of measurement of these thresholds after the end of the chronic treatment schedule corresponded to the peak drug effect in the ethanol withdrawal studies.

Central nitrendipine concentrations

The whole brain concentrations of nitrendipine are given in Table 2. The concentrations at the time of clear drug effects in the withdrawal testing (8 h withdrawal from ethanol, 32 h withdrawal from nitrendipine) were considerably lower than those achieved following acute injections of nitrendipine.

Table 2 A Brain concentrations of nitrendipine in C57 mice after 12 weeks drinking ethanol plus 1.77 mM nitrendipine

Time	*Nitrendipine concentration* ($ng\,g^{-1}$ wet wt.)
(a) During treatment	248 ± 32 (6)
(b) Prior to withdrawal	64 ± 11 (6)
(c) During withdrawal	55 ± 11 (6)

Tissues were taken: (a) At the end of the chronic treatment, before removal of nitrendipine from the drinking fluid; (b) Just before withdrawal from the ethanol, 24 h after removal of nitrendipine from the drinking fluid; (c) At a time corresponding to a clear drug effect on the withdrawal syndrome, 32 h after removal of nitrendipine from the drinking fluid and 8 h from ethanol withdrawal.

B Brain nitrendipine concentrations in C57 mice after acute injections of nitrendipine, given immediately on withdrawal from twelve weeks drinking ethanol.

Nitrendipine dose	*Time from injection*	
	2 h	*8 h*
$10\,mg\,kg^{-1}$	576 ± 133	139 ± 64
$50\,mg\,kg^{-1}$	1514 ± 171	416 ± 85

All values are mean ± s.e.mean (*n*); $ng\,g^{-1}$ wet wt. tissue.

During the chronic treatment the values were of similar magnitude to those found 8 h after the acute injections, but lower than those found 2 h after injection.

Whole brain ethanol concentrations

Table 3 shows the whole brain concentrations of ethanol in groups of TO mice 5 h after withdrawal from ethanol treatment and in C57 mice 2 h after withdrawal. There was no significant difference between the concentrations following administration of ethanol alone and ethanol plus nitrendipine, in either strain, $P > 0.1$.

Discussion

Concurrent chronic administration of the dihydropyridine calcium channel antagonists, nitrendipine, nimodipine or PN 200-110, prevented the occurrence of the ethanol withdrawal syndrome. This effect was seen when 24 h was left between the removal of nitrendipine or the last injections of the chronic treatments and was still evident when a 48 h period was given between the last injections of nitrendipine and the withdrawal testing. The chronic treatment did not affect seizure thresholds to bicuculline in mice that were not given ethanol, indicating that it was not having a general, nonselective, anticonvulsant action.

We have found previously that administration of calcium channel antagonists acutely at the beginning of withdrawal from ethanol provided protection from the ethanol withdrawal syndrome (Little *et al.*, 1986; Littleton *et al.*, 1990). However, the effects of the dihydropyridines described in the present results did not appear to be due to such acute actions. The brain nitrendipine concentrations at the time of withdrawal were longer than those in the CNS following acute administration of $10\,mg\,kg^{-1}$ nitrendipine. The $10\,mg\,kg^{-1}$ dose, given acutely on withdrawal, was ineffective, although $50\,mg\,kg^{-1}$ provided protection (Littleton *et al.*, 1990). When nitrendipine was given for the last 2 days only of the 2 week ethanol administration period, there was no effect on the withdrawal syndrome, suggesting that it was necessary to give the dihydropyridine for a certain length of time before the effects are seen. Two weeks administration was effective in both strains of mice.

Table 3 Whole brain concentrations of ethanol ($mg\,100\,g^{-1}$)

(i) *TO strain, 5 h after withdrawal from ethanol* (*n*)	
Chronic treatment:	
Ethanol + vehicle injections	16.6 ± 10.5 (6)
Ethanol + nitrendipine, $50\,mg\,kg^{-1}$	14.5 ± 5.9 (7)
(ii) *C57 strain, 2 h after withdrawal from ethanol* (*n*)	
Chronic treatment:	
Ethanol alone	48.1 ± 21.2 (7)
Ethanol + nitrendipine	41.8 ± 12.8 (9)

$P > 0.1$, comparisons between ethanol alone and ethanol plus nitrendipine, for each set of results (Student's *t* test).

The action of nitrendipine, given chronically, in preventing the ethanol withdrawal syndrome, parallels the effect of this compound in preventing development of tolerance to ethanol (Little & Dolin, 1987; Wu *et al.*, 1987; Dolin & Little, 1989). In the latter study we demonstrated that concurrent injections of nitrendipine, $50\,mg\,kg^{-1}$ i.p. once daily, in rats prevented the tolerance to the ataxic actions of ethanol that were seen after two weeks ethanol administration. The $10\,mg\,kg^{-1}$ dose of nitrendipine was ineffective in that study. We also showed that such concurrent nitrendipine administration prevented the increase in the number of dihydropyridine-sensitive binding sites in the cerebral cortex found after the chronic ethanol administration.

The action of nitrendipine in the present study was seen in both C57 and TO strains of mice, when different methods of ethanol administration were used and occurred whether nitrendipine was injected or dissolved in the drinking fluid. The effect was dose-dependent, $10\,mg\,kg^{-1}$ nitrendipine having less action than $50\,mg\,kg^{-1}$ when tested in the TO strain. Administration of ethanol to C57 mice for shorter periods than 12 weeks (for example, 5 weeks; unpublished observations) causes a pronounced withdrawal syndrome on cessation of treatment. The prevention of such a syndrome, despite the long period of ethanol administration, therefore suggests that 2 weeks' administration of nitrendipine reversed the changes in the CNS responsible for withdrawal hyperexcitability.

The action of nitrendipine was to decrease the ratings of convulsive behaviour. These measurements were made on a continuous rating scale, rather than being separated into tremor and convulsions, as it was apparent from the behaviour that there was a continuous gradation of severity, with no clear separation of the two signs (Littleton *et al.*, 1990). The effects of nitrendipine were not due to alterations in central ethanol concentrations or to differences in ethanol intake. We have previously shown that nitrendipine does not alter brain ethanol concentrations when given concurrently (Dolin, 1988, data quoted in Dolin & Little, 1989).

The doses of dihydropyridines used in this study were similar to those which have been demonstrated to be required for other actions on the central nervous system. Supervilai & Karobath (1984) showed that $10\,mg\,kg^{-1}$ of PN 200-110, i.p., was required to cause full displacement of *in vivo* dihydropyridine binding from rat brain. The doses of nitrendipine were the same as those found to prevent the development of tolerance to ethanol (Dolin & Little, 1989) and slightly lower than those required to prevent ethanol withdrawal when given acutely (Little *et al.*, 1986).

It is now recognised that there is a difference between the concentrations required for effects on central neurones and those effective on smooth muscle. This is thought to be due to the fact that dihydropyridines bind selectively to the inactivated form of the receptor (Bean, 1984). The effective concentrations are therefore dependent on the time the channels in different tissues spend in the inactivated state. One factor involved in this tissue selectivity could be the generally more hyperpolarized nature of neurones compared to smooth muscle cells, since the inactivation of the dihydropyridine-sensitive calcium channel involves membrane depolarization.

We suggest that the selective action of nitrendipine described in the present results was, at least in part, due to an effect on the adaptive response of dihydropyridine-sensitive calcium channels to the chronic ethanol treatment. The measurements of dihydropyridine binding (Table 1) show that the increase in dihydropyridine receptor number caused by the ethanol was decreased by the concurrent nitrendipine treatment, the same effect being seen in both sets of experiments. This follows a similar pattern to that seen in our study on the effects of nitrendipine on ethanol tolerance (Dolin & Little, 1989) and to that found by Brennan & Littleton (1990) in a cultured cell line grown in ethanol.

We have demonstrated by electrophysiological studies (Whittington & Little, 1989a,b; Whittington & Little, 1991b) that nitrendipine prevented the evidence of neuronal hyperexcitability seen in isolated hippocampal slices following chronic ethanol administration *in vivo*. This action of nitrendipine was seen whether the compound was added to the perfusion medium during the electrophysiological recording or given to the animals during the chronic ethanol treatment, as in the present study. This shows that the behaviour seen after ethanol and nitrendipine chronic treatments was likely to be due to an action on central neurones. Prevention of withdrawal-induced hyperexcitability in the hippocampal slice by addition of the dihydropyridine calcium channel antagonist, PN 200-110, to the bathing medium showed the same stereospecificity as the actions of this compound on calcium channels (Whittington & Little, 1990; 1991a).

The results provide evidence that the ethanol withdrawal syndrome may involve increases in central dihydropyridine-sensitive calcium channels. We suggest that the effect was due to an adaptive response to the long-term presence of the dihydropyridine, involving prevention, or reversal, of the ethanol-induced increase in dihydropyridine-sensitive calcium channels. Nitrendipine did not cause any withdrawal syndrome when given chronically in the absence of ethanol. This action of dihydropyridines may therefore provide a new approach to ethanol dependence, that could alter the neuronal adaptations to chronic ethanol intake, rather than simply substituting for ethanol, as do the drugs in current use.

We thank the Wellcome Trust, the Brewers' Society and the East Anglian Health Authority for financial support. H.J.L. is a Wellcome Trust Senior Lecturer.

References

AKAIKE, N., KOSTYUK, P.G. & OSIPCHUCK, Y.V. (1989). Dihydropyridine-sensitive low-threshold calcium channels in isolated rat hypothalamic neurones. *J. Physiol.*, **412**, 181–195.

BEAN, B. (1984). Nitrendipine block of cardiac calcium channels: high affinity binding to the inactivated site. *Proc. Natl. Acad. Sci. U.S.A.*, **81**, 6388–6392.

BRENNAN, C.H. & LITTLETON, J.M. (1990). Second messengers involved in genetic regulation of the number of calcium channels in bovine adrenal chromaffin cells in culture. *Neuropharmacology*, **29**, 689–693.

BRENNAN, C.H., CRABBE, J. & LITTLETON, J.M. (1990). Genetic upregulation of dihydropyridine-sensitive calcium channels in brain may determine susceptibility to physical dependence on alcohol. *Neuropharmacology*, **29**, 429–432.

DOLIN, S.J. (1988). The effects of calcium antagonists on sedative drug action in rodents; anaesthesia, physical dependence and tolerance. *PhD Thesis, University of London.*

DOLIN, S.J., GRANT, A.J., HUNTER, A.B. & LITTLE, H.J. (1988a). Anticonvulsant profile and whole brain concentrations of nitrendipine and nimodipine. *Eur. J. Pharmacol.*, **152**, 19–27.

DOLIN, S.J. & LITTLE, H.J. (1986). Augmentation by calcium channel antagonists of general anaesthetic potency in mice. *Br. J. Pharmacol.*, **88**, 909–914.

DOLIN, S.J. & LITTLE, H.J. (1989). Are changes in neuronal calcium channels involved in ethanol tolerance? *J. Pharmacol. Exp. Ther.*, **250**, 985–991.

DOLIN, S.J., LITTLE, H.J., HUDSPITH, M., PAGONIS, C. & LITTLETON, J.M. (1987). Increased dihydropyridine calcium channels in rat brain may underlie ethanol physical dependence. *Neuropharmacology*, **26**, 270–275.

DOLIN, S.J., PATCH, T.L., WHITTINGTON, M.A., SIAREY, R.J. & LITTLE, H.J. (1988b). Evidence for the importance of dihydropyridine-sensitive calcium channels in ethanol tolerance and dependence. *Br. J. Pharmacol.*, **95**, 877P.

DOLIN, S.J., PATCH, T., RABBANI, M., SIAREY, R.J., BOWHAY, A.R. & LITTLE, H.J. (1990). Nitrendipine decreases benzodiazepine withdrawal seizures but not the development of benzodiazepine tolerance or withdrawal signs. *Br. J. Pharmacol.*, **101**, 691–697.

GOLDSTEIN, D.B. (1986). The alcohol withdrawal syndrome. A view from the laboratory. *Recent Dev. Alcoholism*, **4**, 231–240.

GOLDSTEIN, D.B. & PAL, N. (1971). Alcohol dependence produced in mice by inhalation of ethanol: grading the withdrawal reaction. *Science*, **172**, 288–290.

GLOSSMAN, H. & FERRY, D.R. (1985). Assays for calcium channels. *Methods Enzymol.*, **109**, 513–550.

GROVER, L.M. & TEYLER, T.L. (1990). Two components of long-term transmission induced by different patterns of afferent activation. *Nature*, **347**, 477–479.

HOF, R.P., HOF, A., RUEGG, U., COOK, N.S. & VOGEL, A.J. (1986). Stereoselectivity at the calcium channel; different profiles of the hemodynamic activity of the enantiomers of the dihydropyridine PN 200-110. *Cardiovasc. Pharmacol.*, **8**, 221–226.

LITTLE, H.J. & DOLIN, S.J. (1987). Lack of tolerance to ethanol after concurrent administration of nitrendipine. *Br. J. Pharmacol.*, **92**, 606P.

LITTLE, H.J., DOLIN, S.J. & HALSEY, M.J. (1986). Calcium channel antagonists decrease the ethanol withdrawal syndrome. *Life Sci.*, **39**, 2059.

LITTLETON, J.M., HARPER, J.H., HUDSPITH, M., PAGONIS, C., DOLIN, S.J. & LITTLE, H.J. (1988). Adaptation in neuronal calcium channels may cause alcohol physical dependence. In *The Psychopharmacology of Addiction.* British Association for Psychopharmacology Monograph. ed: Lader, M. pp. 60–72, Oxford: University Press.

LITTLETON, J.M. & LITTLE, H.J. (1987). Dihydropyridines and the ethanol withdrawal syndrome; stereospecificity and the effects of Bay K 8644. *Br. J. Pharmacol.*, **92**, 663P.

LITTLETON, J.M., WHITTINGTON, M.A. & LITTLE, H.J. (1990). Effects of dihydropyridine calcium channel antagonists in ethanol withdrawal; doses required, stereospecificity and actions of Bay K 8644. *Psychopharmacology*, **100**, 387–392.

MEDDIS, R. (1984). *Statistics Using Ranks, A Unified Approach.* Oxford and New York: Basil Blackwell.

MIDDLEMISS, D.N. & SPEDDING, M. (1985). A functional correlate for the dihydropyridine binding site in rat brain. *Nature*, **314**, 94–96.

MILLER, R.J. (1985). Multiple calcium channels and neuronal function. *Science*, **235**, 46–52.

MURPHY, K.M.M., GOULD, R.J. & SNYDER, S.H. (1982). Autoradiographic visualisation of [^{3}H]-nitrendipine binding sites in rat brain: localisation to synaptic zones. *Eur. J. Pharmacol.*, **81**, 517–519.

NOWYCKY, M.C., FOX, A.P. & TSIEN, R.W. (1985). Three types of neuronal calcium channel with different calcium agonist sensitivity. *Nature*, **316**, 440–443.

NUTT, D.J., COWEN, P.J. & GREEN, A.R. (1980). On the measurement in rats of the convulsive effect of drugs and the changes which follow electroconvulsive shock. *Neuropharmacology*, **19**, 1017–1021.

PANZA, G., GREBB, J.A., SANNA, E., WRIGHT, A.G. & HANDBAUER, F.I. (1985). Evidence for down-regulation of [^{3}H]-nitrendipine recognition sites in mouse brain after long-term treatment with nifedipine or verapamil. *Neuropharmacology*, **24**, 1113–1117.

RAEBURN, D. & GONZALES, R.A. (1988). CNS disorders and calcium antagonists. *Trends Pharmacol. Sci.*, **9**, 117–118.

SCHOEMAKES, H., LEE, K., ROESKE, W.R. & YAMAMURA, H.I. (1983). *In vivo* identification of antagonist binding sites using [^{3}H]-nitrendipine. *Eur. J. Pharmacol.*, **88**, 275–276.

SUPERVILAI, P. & KAROBATH, M. (1984). The interaction of [^{3}H]-PY 108-068 and of [^{3}H]-PN 200–110 with calcium channel binding sites in the rat brain. *J. Meural Transm.*, **60**, 149–167.

TAKAHASHI, K. & AKAIKE, N. (1990). Nicergoline inhibits T-type

calcium channels in rat isolated hippocampal CA1 pyramidal neurones. *Br. J. Pharmacol.*, **100**, 705–710.

TAKAHASHI, B., WAKAMORI, M. & AKAIKE, N. (1989). Hipocampal CA1 pyramidal cells of rats have four voltage-dependent calcium conductances. *Neurosci. Lett.*, **104**, 229–234.

WHITTINGTON, M.A. & LITTLE, H.J. (1989a). Nitrendipine decreases the electrophysiological changes which follow chronic ethanol treatment in vivo. *Br. J. Pharmacol.*, **96**, 137P.

WHITTINGTON, M.A. & LITTLE, H.J. (1989b). Electrophysiological changes following chronic ethanol treatment in vivo. *Br. J. Pharmacol.*, **97**, 435 P.

WHITTINGTON, M.A. & LITTLE, H.J. (1990). Stereospecificity of the actions of PN 200-110 on the changes due to ethanol withdrawal in hippocampal field potentials. *Br. J. Pharmacol.*, **98**, 923 P.

WHITTINGTON, M.A. & LITTLE, H.J. (1991a). A calcium channel antagonist stereoselectively decreases hyperexcitability induced in isolated hippocampal slices by ethanol withdrawal, but not that due to bicuculline. *Br. J. Pharmacol.* (in press).

WHITTINGTON, M.A. & LITTLE, H.J. (1991b) Nitrendipine, given chronically during drinking, decreases the electrophysiological changes seen in the isolated hippocampal slice during ethanol withdrawal. *Br. J. Pharmacol.*, **103**, 1677–1684.

WU, P.H., PHAM, T. & NARANJO, C.A. (1987). Nifedipine delays the acquisition of ethanol tolerance. *Eur. J. Pharmacol.*, **139**, 233–236.

(Received December 12, 1990
Revised February 25, 1991
Accepted March 7, 1991)

Br. J. Pharmacol. (1991), **103**, 1677–1684 © Macmillan Press Ltd, 1991

Nitrendipine, given during drinking, decreases the electrophysiological changes in the isolated hippocampal slice, seen during ethanol withdrawal

M.A. Whittington & [1]H.J. Little

Department of Pharmacology, The Medical School, University Walk, Bristol, BS8 1TD

1 Extracellular recordings were made from mouse isolated hippocampal slices prepared after chronic treatment *in vivo* with either ethanol or ethanol plus the dihydropyridine calcium channel antagonist, nitrendipine.

2 The withdrawal of ethanol caused a variety of changes in the field potentials, as previously reported, including decreases in the thresholds for eliciting single and multiple population spikes, increases in paired pulse potentiation and shifts to the left of the input/output curves.

3 The addition of nitrendipine to the drinking mixture in the chronic ethanol treatment significantly decreased all the changes in the field potentials that were seen after ethanol withdrawal.

4 Addition of nitrenedipine to the perfusion medium also decreased the signs of hyperexcitability seen in the hippocampal slices during ethanol withdrawal.

5 The results provide further evidence that neuronal calcium channels may be involved in ethanol dependence and that the adaptive changes caused by chronic ethanol treatment can be modulated by alterations at dihydropyridine-sensitive sites.

Keywords: Ethanol withdrawal; hippocampus; dihydropyridines; Ca^{2+}.

Introduction

The results in the preceding paper (Whittington *et al.*, 1991) showed that a dihydropyridine calcium channel antagonist, nitrendipine, given concurrently with ethanol, during chronic ethanol administration, prevented the ethanol withdrawal syndrome. This was considered to be an adaptive response, as it was seen when the dihydropyridine treatment was stopped 24 h or 48 h before the testing of withdrawal and the CNS concentrations of nitrendipine at the time of testing were too low to produce an acute effect on the withdrawal syndrome. In addition, nitrendipine, given concurrently with ethanol in chronic treatment, has been found to prevent the development of tolerance to ethanol (Little & Dolin, 1987; Dolin & Little, 1989). The increase in the number of dihydropyridine binding sites that occurred after chronic ethanol administration, was also prevented, suggesting a possible causal relationship between the binding site changes and development of ethanol tolerance (Dolin *et al.*, 1988; Dolin & Little, 1989). We have put forward the theory that the effects of concurrently administered calcium channel antagonists on ethanol dependence are due to the prevention of the upregulation of voltage-sensitive calcium channels (Dolin *et al.*, 1988; Dolin & Little, 1989; Littleton & Little, 1989).

Ethanol has been known for some time to affect neuronal calcium mechanisms. It decreased the fast phase of depolarization-induced calcium flux into neurones, an effect to which tolerance developed on chronic treatment (Harris & Hood, 1980; Friedman *et al.*, 1980). Ethanol decreased calcium spikes in cultured neurones (Stokes & Harris, 1982). Carlen *et al.* (1982) reported that ethanol (5–20 mM) increased both inhibitory and excitatory postsynaptic potentials in the isolated rat hippocampus and the hyperpolarization that followed the eliciting of calcium spikes. They concluded that ethanol increased both pre- and postsynaptic calcium-mediated mechanisms.

Only a few electrophysiological studies have been carried out on the effects of chronic ethanol treatment. Acute tolerance was seen to the depression of orthodromically evoked CA1 field potentials occurring at bath concentrations of up to 100 mM ethanol (Durand *et al.*, 1981). Three weeks after withdrawal from chronic ethanol treatment, Durand & Carlen (1984) found decreased after-hyperpolarizations and decreased spike frequency adaptation to depolarizing current in CA1 neurones in rat isolated hippocampal slices. These authors also reported decreased inhibitory postsynaptic potentials (i.p.s.ps) in dentate granule and CA1 neurones. However, when the same measurements were made 24 h after ethanol withdrawal, a different pattern was seen, with increased after-hyperpolarizations (Reynolds *et al.*, 1990). We have described changes in field potentials in the isolated hippocampal slice after chronic ethanol treatment (Whittington & Little, 1990; 1991). These changes included decreased thresholds for eliciting population spikes, following both orthodromic and antidromic stimulation, and increased paired pulse potentiation. They followed different time courses during the withdrawal period, suggesting different origins of the forms of hyperexcitability.

In the present study we have measured the effects of the dihydropyridine calcium channel antagonist, nitrendipine, on these changes in field potentials in the hippocampal slice following chronic ethanol treatment. Nitrendipine was given either during the chronic ethanol treatment *in vivo* or added to the perfusion medium. We have used a treatment schedule for nitrendipine *in vivo* that prevented the behavioural manifestations of ethanol withdrawal (see Whittington *et al.*, 1991). The aim was to see whether or not the nitrendipine treatment affected the changes in neuronal activity, as measured by extracellular field potentials, that occur following ethanol withdrawal. The chronic treatment schedules were chosen to parallel our behavioural and receptor binding measurements (see Whittington *et al.*, 1991).

Some of these results have been presented in abstract form to the British Pharmacological Society.

Methods

Chronic drug treatment

Male mice, C57 strain, 25–30 g, were given ethanol, 24% v/v, as sole fluid, for 12 weeks. The mouse was chosen for these

[1] Author for correspondence.

studies in order to provide a direct comparison with our earlier behavioural studies. For the chronic nitrendipine treatment the compound was dissolved in the drinking fluid at 1.77 mM. This did not alter the ethanol intake; the mean daily intakes were $15.0 \pm 0.9\,g\,kg^{-1}$ daily ($n = 9$) for ethanol alone and $14.4 \pm 0.1\,g\,kg^{-1}$ daily ($n = 12$) for ethanol plus nitrendipine. Mice were selected at random from these groups for preparation of the slices. Nitrendipine intake was $56.4 \pm 3.8\,mg\,kg^{-1}$ daily. The nitrendepine was removed from the drinking fluid 24 h before the experiments (the ethanol remaining) so that the effects of chronic nitrendipine treatment, rather than any acute action, could be studied. The mice were weighed at regular intervals during the chronic treatment and there were no significant differences between the weights of any of the treatment groups.

Controls drank water only. In separate experiments, nitrendipine was included in the perfusion medium (see below). Owing to the low aqueous solubility of nitrendipine it was not possible to treat animals by this method with nitrendipine in the absence of ethanol. Chronic treatment with nitrendipine alone, by injection, had no effect on the behaviour of mice, as measured by responses to handling (see Whittington *et al.*, 1991).

Hippocampal slices were prepared between 09 h 00 min and 10 h 00 min and perfused with standard Ringer solution. The animals were not withdrawn from the ethanol before preparation of the slices, so ethanol would have been gradually washed out of the slices during the beginning of the recording period.

Electrophysiological recordings

Dissections were made in HEPES medium (see below) and 400 μm slices of hippocampus were cut on a McIlwain chopper. The slices were maintained in recording chambers on nylon mesh and lens tissue, superfused with Krebs solution (see below) at 30°C ± 0.5°C and $1.5\,ml\,min^{-1}$. Extracellular recordings from stratum pyramidale in area CA1 were started 30 min after the slices were placed in the perfusion bath, that is 45 min from removal of tissues.

Orthodromic stimulation of Schaffer collateral/commissural fibres was given, with paired pulses, constant current, 50 μs duration and 0.1 Hz. The stimulating electrodes consisted of two silver insulated wires, 0.2 mm in diameter, passed through 1 mm diameter silicon tubing. Recording electrodes were made from 1.2 mm diameter electrode glass and filled with 2 M KCl; the resistances were between 5 and 15 MΩ. A 70 ms interval was used for the paired pulses because preliminary experiments showed that it gave the maximum paired pulse potentiation in normal mouse hippocampal slices. A stimulation level of 1.25 times the threshold stimulation for eliciting a single population spike was used in the studies on paired pulse potentiation.

The thresholds for the production of population spikes, and paired pulse potentiation, were measured every 15 min and input/output curves determined at 1, 3, 5 and 7 h from removal of tissues, i.e. from the start of ethanol withdrawal. Measurements were made of the thresholds for elicitation of single population spikes and multiple population spikes (see Figure 1b). The former threshold was the minimum stimulating current required to produce a single population spike superimposed on the excitatory postsynaptic potential (e.p.s.p.) produced by the first of the paired stimuli, as discerned by eye. The threshold for multiple population spikes was established by the minimum stimulating current required to produce a second population spike, seen after the first but superimposed on the same e.p.s.p. (see Figure 2c).

In the studies on the acute actions of nitrendipine, the compound was dissolved in dimethylsulphoxide (DMSO) and then added to the bathing medium at 10 μM. The final DMSO concentration of 0.02%, did not alter the field potentials. (We have not found any action of DMSO on the field potentials at concentrations up to 0.5%). The effects of nitrendipine added to the bathing medium were studied on control slices and following chronic ethanol administration *in vivo*. In each case the compound was present during the entire recording period, rather than being added after control responses were established. The reason for this was that we wished to study the effects of nitrendipine on the various changes that occur in the field potentials from the beginning of ethanol withdrawal. Comparison was therefore made between rather than within slices.

At the completion of every day's experiments the perfusion chamber was washed through with distilled water for at least 30 min, and washed through every 5 days with 500 mM sodium hydroxide followed by 100 mM citric acid in order to prevent residual drug build up on the sides of the perfusion tubing.

Statistical analysis

The areas of the population spikes were measured by Acorn computer analysis. In every case a minimum of three responses were averaged for each stimulus. The results in the Figures are expressed as mean ± s.e.mean for each of the different treatments. Five tissues from five different animals were used for each treatment group. Comparisons were made between results from tissues following the different treatments by analysis of variance. The times given in the results section are all from the removal of the tissues. This corresponded with the withdrawal of ethanol.

Input/output relationships were derived from population spike area, and e.p.s.p. slope data. Non-linear regression was used to produce sigmoidal curves, to enable calculation of the stimulus required to produce half-maximal responses. Comparisons of data from these curves were made between different tissues, following the various treatments, by use of Student's nonpaired t test.

Certain precautions were taken to ensure that valid comparisons could be made between the field potentials from tissues from different treatment groups (Whittington & Little, 1990). The order of testing and the distribution of the various treatments between the two recording chambers were carefully balanced. The positions of the stimulating and recording electrodes were determined in every tissue by using the ends of the arc of granular cells in the dentate gyrus and the apex of the CA3 region above the fimbria as common reference points between slices.

Composition of solutions

The composition of the perfusion fluid was (mM): NaCl 124, KCl 3.25, NaH_2PO_4 1.25, $NaHCO_3$ 20.0, $MgSO_4$ 2.0, $CaCl_2$ 2.0, and D-glucose 10.0. The pH was 7.2 at 30°C. The composition of the HEPES buffered perfusion medium was (mM): NaCl 120, KCl 2.0, KH_2PO_4 1.25, $NaHCO_3$ 20.0, $MgSO_4$ 2.0, $CaCl_2$ 2.0, D-glucose 10.0 HEPES acid 7.0 and NaHEPES 2.6. The pH was 7.2 at 23°C.

Results

Thresholds for elicitation of population spikes

Chronic nitrendipine treatment The chronic ethanol treatment caused decreases in the threshold for eliciting both single and multiple population spikes, from 3 h onwards, compared with control tissues ($P < 0.005$ and 0.001 respectively). These decreases were smaller after the chronic nitrendipine treatment *in vivo* (Figures 1a and 2a). Examples of some of the traces obtained during measurement of multiple population spike thresholds are shown in Figure 2c. Analysis of variance over the 4 h–7 h period (inclusive) showed significant differences ($P < 0.005$ for eliciting single and $P < 0.001$ for multiple population spikes) when tissues from animals treated with ethanol alone were compared with those from mice treated with ethanol plus nitrendipine. Although the effect of the ethanol treatment did not appear to be completely abolished,

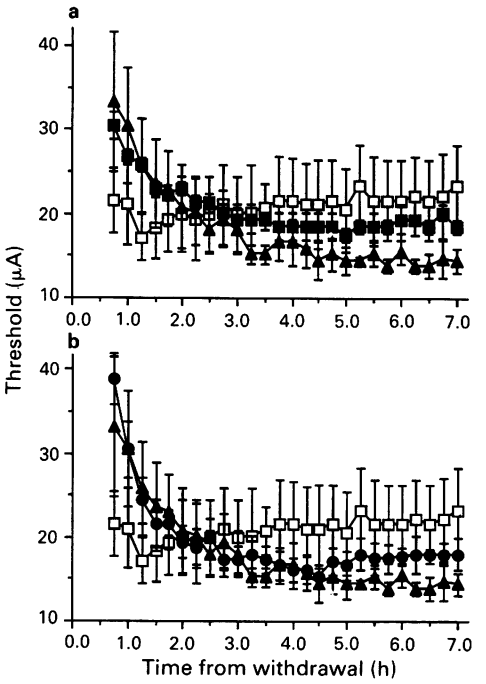


Figure 1 (a) The effect of chronic treatment with nitrendipine on the decrease in thresholds for eliciting single population spikes caused by withdrawal from chronic ethanol treatment. The chronic nitrendipine treatment was stopped 24 h before the ethanol withdrawal. Times given are all from preparation of tissues. This was also the time of ethanol withdrawal (time zero on the horizontal axis). The thresholds in slices from mice treated with ethanol were significantly different from those in slices from mice treated with ethanol and nitrendipine (comparison from 3 h to 7 h inclusive $P < 0.005$). Thresholds are in μA, mean with s.e.mean shown by vertical bars: (□) controls; (▲) chronic ethanol-treatment; (■) chronic ethanol plus nitrendipine treatment. (b) The effect of bath application of nitrendipine on the decrease in thresholds for eliciting single population spikes caused by withdrawal from chronic ethanol treatment. Nitrendipine, 10 μM, was present in the bathing medium from the start of recording. The thresholds measured when nitrendipine was added after ethanol withdrawal were significantly different from those when vehicle was added to slices prepared after ethanol treatment *in vivo* ($P < 0.005$). Thresholds are in μA, mean with s.e.mean shown by vertical bars. Times given are all from preparation of tissues. (□) Controls; (▲) chronic ethanol treatment; (●) chronic ethanol treatment, nitrendipine, 10 μM, in perfusion medium.

comparison of the results for the tissues following chronic treatment with ethanol plus nitrendipine were not significantly different from those from control tissues ($P > 0.1$).

Acute addition of nitrendipine to the bathing medium The decreases in thresholds for eliciting single and multiple population spikes seen after chronic ethanol treatment were reduced when nitrendipine, 10 μM, was added to the bathing medium (Figures 1b and 2b). Analysis of variance over the 4 h to 7 h period (inclusive) showed significant differences between data from slices from ethanol-treated mice recorded with and without nitrendipine in the bathing medium ($P < 0.005$ for both single population spike thresholds and multiple spike thresholds). The extent of protection from the effects of ethanol withdrawal afforded by the acute addition of nitrendipine appeared smaller than that due to chronic nitrendipine intake (compare Figures 1a and 1b and Figures 2a and 2b). The thresholds for eliciting multiple population spikes (Figure 2b) were still significantly different from control values when nitrendipine was perfused in the bathing medium after ethanol withdrawal ($P < 0.001$), but this difference was not significant for the single spike thresholds ($P > 0.1$).

Paired pulse potentiation

Chronic nitrendipine treatment Hippocampal slices from animals that received chronic ethanol treatment showed a transient increase in paired pulse potentiation, seen only between 2 and 4 h from the start of recording, as reported previously (Whittington & Little, 1990; 1991). This effect was also decreased by chronic nitrendipine administration (Figure 3a). The difference between the paired pulse potentiation for controls and ethanol treatment, between 1–4 h from the start of recording, was significant ($P < 0.001$). The difference between ethanol and ethanol plus chronic nitrendipine treatments was also significant ($P < 0.001$), although the paired pulse potentiation after ethanol plus nitrendipine was still higher than the control values ($P < 0.001$).

Acute addition of nitrendipine to the bathing medium The addition of nitrendipine to the medium, at 10 μM, (Figure 3b) also reduced the increase in paired pulse potentiation seen after chronic ethanol treatment ($P < 0.001$ for comparison between ethanol alone and ethanol plus nitrendipine), although there was still a significant difference between ethanol plus nitrendipine and control treatments ($P < 0.001$).

Input/output curves

Chronic nitrendipine treatment The input/output curves showed that the chronic ethanol treatment caused a shift to the left, at the 5 h and 7 h intervals, of the lines for population spike area against stimulus intensity, without changes in the gradient of the line or the maximum responses (Figure 4a). The decrease in the stimulus intensity required to produce half maximal population spikes (S_{50}) was almost completely abolished by the chronic nitrendipine treatment ($P < 0.005$ for comparison of this value for ethanol alone and for ethanol plus nitrendipine, at both 5 h and 7 h after withdrawal), indicating a reduction in the shift to the left of these curves during ethanol withdrawal. After treatment with ethanol plus nitrendipine, the position of the input/output curve and its gradient were not significantly different from the control curve.

Acute addition of nitrendipine to the bathing medium Nitrendipine added to the bathing medium at 10 μM, caused a small, but significant, decrease in the shift to the left of the input/output curve for population spike area caused by the chronic ethanol treatment (Figure 4b). The effect of the ethanol treatment on the stimulation level required to produce half-maximal responses (S_{50}) was significantly decreased by the addition of nitrendipine ($P < 0.01$ at 5 h and 7 h), but the S_{50} remained significantly lower than the control value ($P < 0.01$). The gradient of the line after addition of nitrendipine to the bathing medium was significantly lower than either the line for slices prepared after ethanol treatment or for controls.

Input/output curves for the slopes of the field e.p.s.ps

Chronic nitrendipine treatment The plots of field e.p.s.p. slope against stimulus intensity showed that the ethanol treatment decreased both the slope and the maximum value for this measurement at the 5 h and 7 h time intervals, and shifted the lower part of the curves to the left (Figure 5a). This indicated a greater response of the pyramidal cells for a given stimulus intensity at the lower end of the stimulation range, but smaller responses at higher levels of stimulation.

Figure 5a shows that chronic nitrendipine treatment had a clear effect on the decrease in maximal response caused by the chronic ethanol treatment. The protective effect of nitrendipine on the maximal responses (calculated from the sigmoid curves) was significant at the 7 h time interval ($P < 0.01$, comparison between ethanol alone and ethanol plus nitrendipine).

When the gradients of the sigmoid curves for e.p.s.p. slope against stimulus intensity were compared, the ethanol treatment was found to cause significant decreases in these values

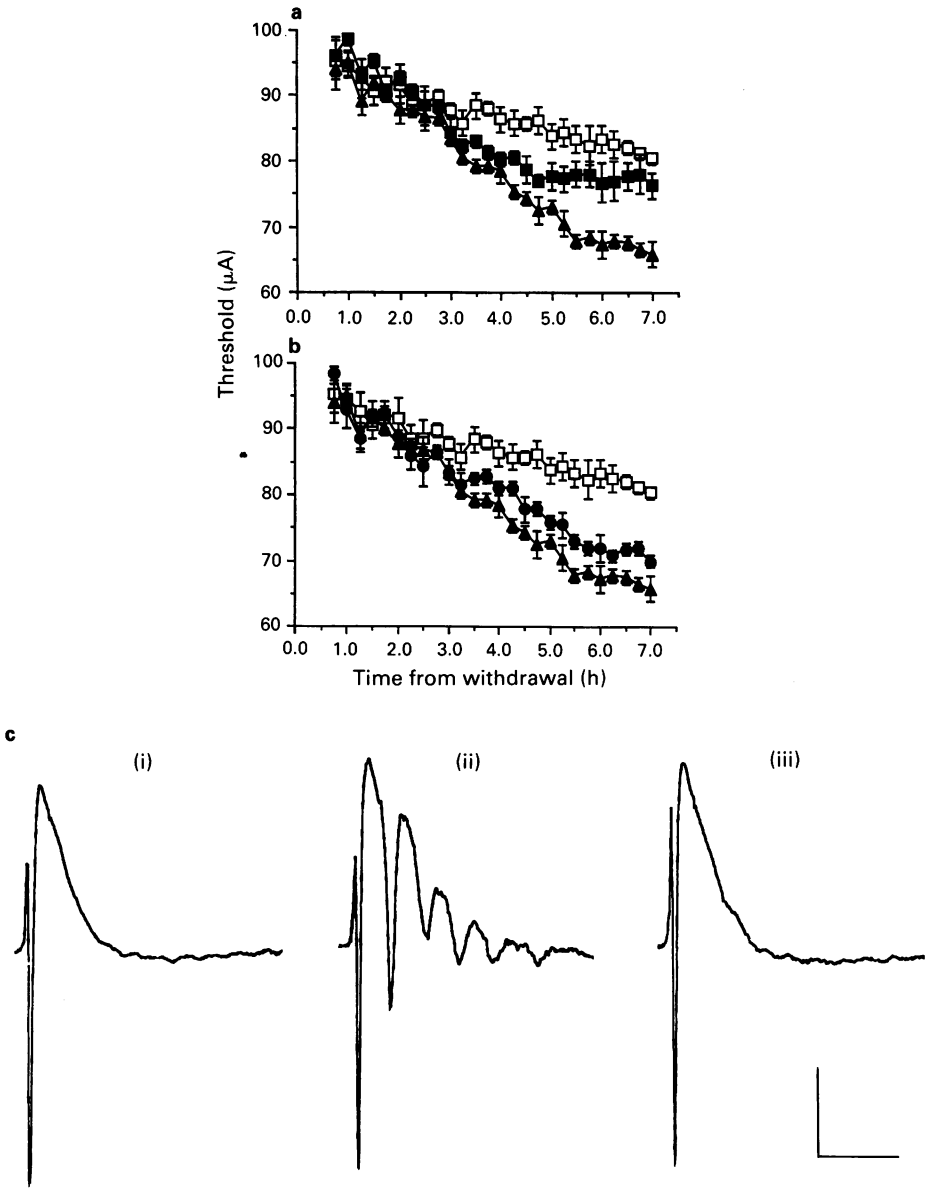


Figure 2 (a) The effect of chronic treatment with nitrendipine on the decrease in thresholds for eliciting multiple population spikes caused by withdrawal from chronic ethanol treatment. Times given are all from preparation of tissues, as described in Figure 1(a). The thresholds in slices from mice treated with ethanol were significantly different from those in slices from mice treated with ethanol plus nitrendipine, from 3 h to 7 h inclusive ($P < 0.001$). Thresholds are in μA, mean with s.e.mean shown by vertical bars. (□) Controls; (▲) chronic ethanol treatment; (■) chronic ethanol plus nitrendipine treatment. (b) The effect of bath application of nitrendipine on the decrease in thresholds for eliciting multiple population spikes caused by withdrawal from chronic ethanol treatment. Nitrendipine, 10 μM, was present in the bathing medium from the start of recording. The thresholds when nitrendipine was added after ethanol treatment were significantly different from those when vehicle was added ($P < 0.005$). Thresholds are in μA, mean with s.e.mean shown by vertical bars. Times given are all from preparation of tissues. (□) Controls; (▲) chronic ethanol treatment; (●) chronic ethanol treatment, nitrendipine, 10 μM, in perfusion medium. (c) Examples of traces recorded from slices during eliciting of multiple population spikes. These recordings were made 7 h after preparation of tissues, that is 7 h from ethanol withdrawal. The stimulation level was 70 μA, for all three slices. The scale bar is 2 mV, 20 ms. (i) Control; (ii) chronic treatment with ethanol; (iii) chronic treatment with ethanol plus nitrendipine

at the 3 h and 5 h intervals ($P < 0.01$, comparison between chronic ethanol treatment and controls), whereas the values were not significantly changed after chronic administration of ethanol plus nitrendipine ($P > 0.1$, comparison between controls and ethanol plus nitrendipine). This reflects the prevention by nitrendipine of the decrease, caused by the ethanol treatment, in the maximal responses.

The stimulus intensities required to produce half maximal field e.p.s.p. slopes do not give a good indication of the changes when, as in this instance, the maximum values and gradients of the curves are altered, although when these S_{50} values were calculated, the chronic nitrendipine prevented the decreases due to the chronic ethanol treatment ($P < 0.05$, comparison between ethanol and ethanol plus nitrendipine-treated groups). The shift to the left of the lower part of the curves appeared to be less affected by the nitrendipine treatment.

Acute addition of nitrendipine to the bathing medium The acute action of nitrendipine on the changes in the field e.p.s.p. slopes showed a qualitatively similar pattern to that of the chronic nitrendipine treatment (Figure 5b). The effect of the ethanol treatment on the maxima of the sigmoid curves for field e.p.s.p. slope against stimulus intensity was completely prevented when nitrendipine was added to the bathing medium, at 10 μM ($P < 0.01$ for comparison between addition

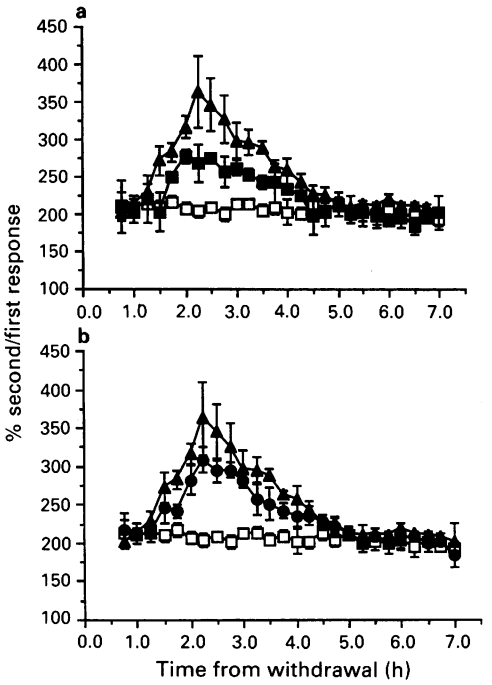


Figure 3 (a) The effect of concurrent chronic treatment with nitrendipine on the increase in paired pulse potentiation caused by withdrawal from chronic ethanol treatment. Times given are all from preparation of tissues, as described in Figure 1(a). The paired pulse potentiation in slices from mice treated with ethanol was significantly different from that in slices from mice treated with ethanol and nitrendipine (1 h to 4 h inclusive, $P < 0.001$). Thresholds are in μA, mean with s.e.mean shown by vertical bars. (□) Controls; (▲) chronic ethanol treatment; (■) chronic ethanol plus nitrendipine treatment. (b) The effect of bath application of nitrendipine on the increase in paired pulse potentiation caused by withdrawal from chronic ethanol treatment. Nitrendipine, 10 μM, was present in the bathing medium from the start of recording. The potentiation when nitrendipine was added after ethanol withdrawal was significantly different from that when vehicle was added after ethanol withdrawal ($P < 0.001$). Thresholds are in μA, mean with s.e.mean shown by vertical bars. Times given are all from preparation of tissues. (□) Controls; (▲) chronic ethanol treatment; (●) chronic ethanol treatment, nitrendipine, 10 μM, in perfusion medium.

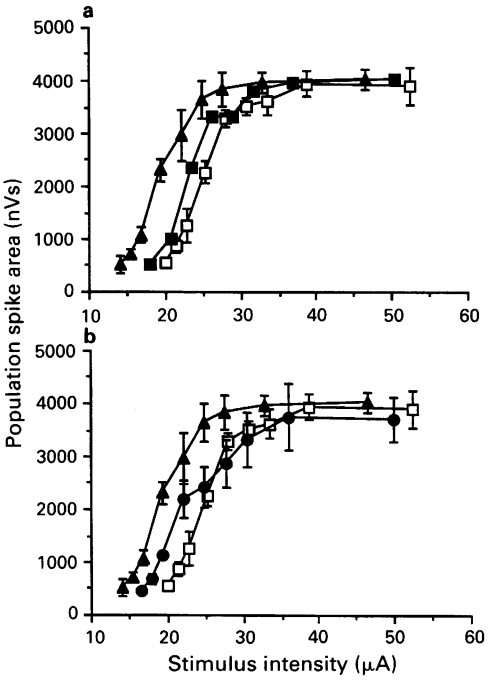


Figure 4 (a) The effect of concurrent chronic treatment with nitrendipine on the shift to the left in input/output curves derived from population spike measurements caused by withdrawal from chronic ethanol treatment. The diagram illustrates the changes in input/output curves 5 h after ethanol withdrawal. The stimulus intensities required to produce half maximal population spikes were significantly different when recordings from slices from mice treated with ethanol were compared with those from slices from mice treated with ethanol and nitrendipine ($P < 0.005$). Data are given as mean with s.e.mean shown by vertical bars. (□) Controls; (▲) chronic ethanol treatment; (■) chronic ethanol plus nitrendipine treatment. (b) The effect of bath application of nitrendipine, 10 μM, on the shift to the left in input/output curves derived from population spike measurements caused by withdrawal from chronic ethanol treatment. The diagram illustrates the changes in input/output curves 5 h after ethanol withdrawal. After the ethanol treatment, the stimulus intensities required to produce half maximal population spikes when nitrendipine was added to the bathing medium were significantly different from the results when vehicle was added ($P < 0.01$). Data shown as mean with s.e.mean shown by vertical bars. (□) Controls; (▲) chronic ethanol treatment; (●) chronic ethanol treatment, nitrendipine, 10 μM, in perfusion medium.

of nitrendipine and addition of vehicle, at 5 h and 7 h into withdrawal).

Nitrendipine, 10 μM, also decreased the changes in the gradient of these curves that were seen 5 h and 7 h after ethanol withdrawal ($P < 0.05$, comparison between slices from mice treated with ethanol, recorded with or without nitrendipine in the bathing medium). However, the effect of the chronic ethanol treatment in causing a shift of the lower part of the curve to the left appeared to be less affected by the nitrendipine.

Lack of effect of nitrendipine in control tissues

The addition of nitrendipine to the purfusion medium at 10 μM did not alter any aspect of the field potentials recorded from control slices, $P > 0.1$ (Figures 6a and b). There were no changes in either the gradient or the maxima of the input/output curves ($P < 0.01$, not illustrated). Nitrendipine added to the perfusion medium at 10 μM had no effect on paired pulse potentiation in control tissues (Figure 6c).

Discussion

All the changes in the field potentials in the mouse isolated hippocampal slice preparation caused by ethanol withdrawal were significantly smaller when the dihydropyridine calcium channel antagonist, nitrendipine, was given chronically with the ethanol, even though the amount of ethanol drunk was unaltered. The effects of the *in vivo* ethanol treatment were also reduced when nitrendipine was added to the bathing medium. No significant effects of bath-applied nitrendipine were seen in slices from control animals on the thresholds for eliciting population spikes, paired pulse potentiation or input/output data for population spike area, amplitude and e.p.s.p. slope. Chronic administration of ethanol therefore appeared to alter the actions of ntirendipine on the field potentials.

These results parallel the effects of nitrendipine treatment on the behavioural manifestations of withdrawal (Whittington & Little, 1988; Whittington *et al.*, 1991). We have previously demonstrated that concurrent nitrendipine treatement also prevented the development of ethanol tolerance (Dolin & Little, 1989). Such treatment also prevented the increase in central dihydropyridine binding caused by chronic ethanol administration (Dolin *et al.*, 1988; Dolin & Little, 1989). Chronic administration of nitrendipine therefore decreased the results of long-term ethanol administration as seen by three different techniques: behaviour, field potential recording and receptor binding. In addition, Brennan *et al.* (1990) showed a correlation between the sensitivity of mouse strains to ethanol withdrawal and the extent of the increases in dihydropyridine binding. Changes in neuronal dihydropyridine-sensitive

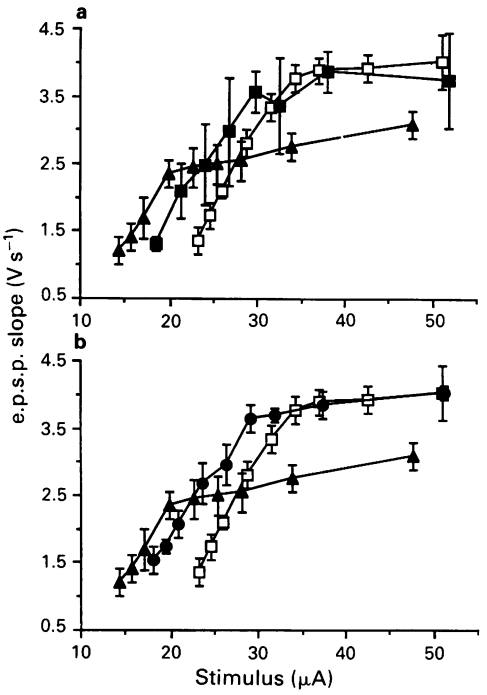


Figure 5 (a) The effects of chronic nitrendipine treatment on the changes caused by withdrawal from chronic ethanol treatment *in vivo*, in input/output curves for field excitatory postsynaptic potentials (e.p.s.p.) slope against stimulus intensity. The graph illustrates the changes seen 7 h after ethanol withdrawal. The chronic nitrendipine treatment prevented the decrease in maximum response seen after ethanol withdrawal at this time. Data expressed as mean with s.e.mean shown by vertical bars. (□) Controls; (▲) chronic ethanol treatment; (■) chronic ethanol plus nitrendipine treatment. (b) Effects of bath application of nitrendipine, 10 μM, on changes, caused by withdrawal from chronic ethanol treatment, in input/output curves for field e.p.s.p. slope against stimulus intensity. The graph illustrates the changes seen 7 h after ethanol withdrawal. Nitrendipine prevented the decrease in maximum response seen after ethanol withdrawal at this time. Data expressed as mean with s.e.mean shown by vertical bars. (□) Controls; (▲) chronic ethanol treatment; (●) chronic ethanol treatment, nitrendipine, 10 μM, in perfusion medium.

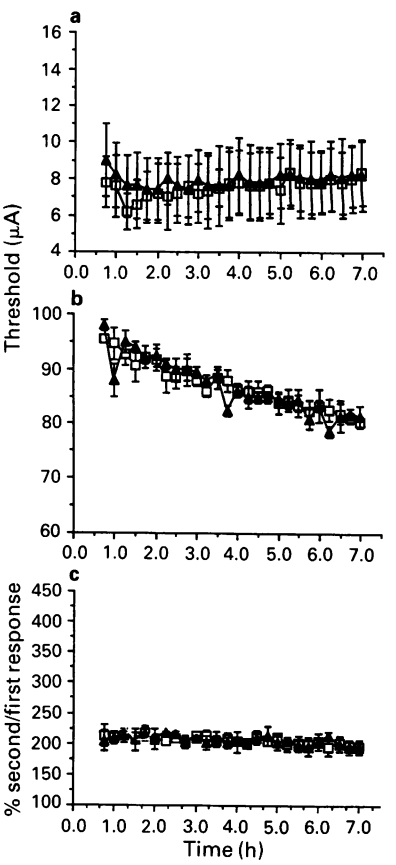


Figure 6 (a) Lack of effect of nitrendipine, 10 μM applied in the perfusion medium, on single population spike thresholds in tissues from control animals (mean with s.e.mean shown by vertical bars). Nitrendipine did not cause any changes in the thresholds for eliciting single population spikes ($P > 0.01$). (□) Controls plus vehicle; (▲) controls plus nitrendipine. (b) Lack of effect of nitrendipine, 10 μM applied in the perfusion medium, on multiple population spike thresholds in tissues from control animals (mean with s.e.mean shown by vertical bars). Nitrendipine did not cause any changes in the thresholds for eliciting multiple population spikes ($P > 0.01$). (□) Controls plus vehicle; (▲) controls plus nitrendipine. (c) Lack of effect of nitrendipine, 10 μM applied in the perfusion medium, on paired pulse potentiation in tissues from control animals (mean with s.e.mean shown by vertical bars). Nitrendipine did not cause any changes in paired pulse potentiation ($P > 0.1$). (□) Controls plus vehicle; (●) controls plus nitrendipine.

calcium channels may therefore be involved in ethanol dependence.

The actions of nitrendipine in decreasing all the changes in the field potentials appeared to be qualitatively similar whether it was given chronically during the ethanol treatment or 'acutely' in the bathing medium, although the effects of the latter were rather small. We have previously shown that the calcium channel antagonist, PN 200-110, added to the perfusion medium, completely prevented the changes in the hippocampal slices after chronic ethanol treatment, in a stereospecific manner (Whittington & Little, 1989; 1991). The brain concentrations of nitrendipine, measured during the chronic treatment (Whittington *et al.*, 1991), were in the range 200–260 nM (this is an approximate calculation assuming equal distribution throughout the CNS). The effects of chronic and acute treatment cannot be compared directly as the action of chronic nitrendipine appears to involve an adaptive response. It is unlikely that the action of the chronically administered nitrendipine was due to the presence of the compound in the tissue at the time of recording because the nitrendipine was removed from the drinking fluid 24 h before the preparation of the slices and very little was present in the brain at the time of preparation of the tissues (Whittington *et al.*, 1991).

In our previous study of the changes in field potentials in the hippocampal slice during ethanol withdrawal, we concluded that possible mechanisms for these changes could include decreases in feedback inhibition, increased ability of pyramidal cells to generate action potentials for a given field e.p.s.p. size and possibly changes in intracellular calcium concentrations (Whittington & Little, 1990). The present study suggests that alterations in dihydropyridine-sensitive calcium channels might be the underlying cause of these changes. It is appreciated, however, that intracellular measurements will be necessary before definitive conclusions can be drawn concerning the selectivity of the doses and concentrations of nitrendipine used in the present study. These are currently in progress.

We suggest therefore that the effects of chronically administered nitrendipine were due to an adaptive response to the presence of the compound in the central nervous system, preventing the action of ethanol on the dihydropyridine-sensitive channels. Panza *et al.* (1985) demonstrated that the long term intake of a dihydropyridine calcium channel antagonist could result in down-regulation of central dihydropyridine-sensitive binding sites. This study used considerable higher doses (280 mg kg^{-1} daily) than the present experiments. We have found that doses in the range that we use (50 mg kg^{-1} daily) did not cause down-regulation of dihydropyridine-sensitive sites when given alone, but did prevent the up-regulation caused by chronic ethanol adminis-

tration (Dolin *et al.*, 1988; 1989; Whittington & Little, 1991; Whittington *et al.*, 1991).

Although high affinity binding sites have been demonstrated on neurones in the CNS (Glossman *et al.*, 1982), calcium channel antagonists have only weak effects on normal mammalian neurones. The results in the present paper demonstrating a lack of effect of nitrendipine on any aspect of the field potentials in hippocampal slices from control animals are in agreement with the literature. Some actions of dihydropyridines on neurones have been demonstrated by voltage clamp techniques, for example, Docherty & Brown (1986) showed that nimodipine at 0.05–10 μM decreased calcium currents in hippocampal CA1 pyramidal cells. Nifedipine at 1 μM to 10 μM did not modify presynaptic calcium entry in hippocampal slices, but decreased the calcium concentration changes thought to be associated with postsynaptic responses (Louvel *et al.*, 1986; Jones & Heinemann, 1987). Low micromolar concentrations of dihydropyridines have been shown to affect subtypes of calcium channels other than the 'L' subtype for which they were originally thought to be selective (Takahashi *et al.*, 1989; Takahashi & Akaike, 1990). Grover & Teyler (1990) have demonstrated a dihydropyridine-sensitive component of transmission in CA1 pyramidal cells, seen only at very high frequency stimulation.

The extent of the protective action of nitrendipine differed slightly for the various electrophysiological measurements. The decreases in the thresholds for eliciting population spikes after chronic ethanol treatment were only partially prevented by the chronic nitrendipine treatment, but the shifts to the left of the input/output curves were almost completely abolished. The initial increase in population spike threshold, seen in slices from ethanol-treated mice was not affected by nitrendipine treatment. This increase may indicate that residual levels of ethanol were present in the slice during the initial stages of recording, or that the presence of ethanol in the brain during dissection affected the re-establishment of synaptic activity in the slice during the first minutes of the recording period.

The decreases in maximal field e.p.s.p. slopes, after chronic ethanol treatment, were completely prevented by nitrendipine. This effect of ethanol withdrawal may indicate a decrease in maximum e.p.s.p. size at the site of generation on apical dendrites. Alternatively, the maximum e.p.s.p. size may have been reduced by alteration in the shape of the field potential, i.e. whether or not a population spike was present. In the latter case, the changes would have been produced by effects at the recording site, the cell soma. The increases in field e.p.s.p. slope in response to lower levels of stimulation seen after the ethanol treatment were little affected by nitrendipine.

The nitrendipine treatment schedule used in this study totally prevented the behavioural withdrawal syndrome (see Whittington *et al.*, 1991, preceding paper). Comparable amounts of ethanol were taken in during both sets of experiments, so the severity of withdrawal would be expected to be similar. These results suggest that the input/output curves may be a better model of the withdrawal syndrome than the thresholds and there may be different components to the changes in field e.p.s.p. slope at low stimulation levels than in the responses to the rest of the stimulation range.

The hippocampal slice was chosen for this study because of the extent of knowledge about the neuronal pathways and the demonstration of high concentrations of dihydropyridine binding sites (Glossman *et al.*, 1982). It is possible, however, that the first stages of the behavioural withdrawal syndrome occur lower in the brainstem (Hunter & Walker, 1978). Many of the changes seen after chronic ethanol could be explained by increased numbers of dihydropyridine-sensitive calcium channels. These sites have recently been shown to be located on cell bodies and dendrites of hippocampal pyramidal CA1 pyramidal cells and are found in high density at the base of major dendrites (Westenbroek *et al.*, 1990). They are thought to contribute to the large local calcium currents in this area. These currents will play a part in controlling the transmission of stimuli from dendrites to soma. Increases in their number would be likely to increase this transmission, thus causing hyperexcitability.

It is not yet certain whether the chronic ethanol treatment used in this study caused any anatomical neuronal damage. This is currently under investigation. Longer ethanol treatment schedules have been shown to cause neuronal loss (Lee *et al.*, 1981). While the decreases in the maximum field e.p.s.p. responses could have been explained by loss of neurones, it seems unlikely that this could have been reversed by the bath application of nitrendipine, as was seen.

Littleton and co-workers, using cell cultures, have recently shown that the upregulation of calcium channels after chronic ethanol treatment may involve the inositol lipid-protein kinase C system (Brennan & Littleton, 1990) and that the synthesis of new protein is required (Harper *et al.*, 1989). The prevention of this upregulation by chronic dihydropyridine treatment, demonstrated in our studies, was seen also in the cell cultures. Our results therefore show that chronic ethanol treatment causes an increase in the number of dihydropyridine binding sites and an enhanced functional activity of neuronal calcium channels, and that this, in whole or in part, is the cause of withdrawal hyperexcitability and can be prevented by concurrent dihydropyridine administration.

We thank the Wellcome Trust and the Brewers' Society for financial support. H.J.L. is a Wellcome Trust Senior Lecturer. Some of these results have been presented in abstract form to the British Pharmacological Society.

References

BRENNAN, C.H. & LITTLETON, J.M. (1990). Second messengers involved in genetic regulation of the number of calcium channels in bovine adrenal chromaffin cells in culture. *Neuropharmacology*, **29**, 689–693.

BRENNAN, C.H., CRABBE, J. & LITTLETON, J.M. (1990). Genetic regulation of dihydropyridine-sensitive calcium channels may determine susceptibility to alcohol physical dependence. *Neuropharmacology*, **29**, 429–432.

CARLEN, P.L., GUREVICH, N. & DURAND, D. (1982). Ethanol in low doses augments calcium-mediated mechanisms measured intracellularly in hippocampal neurones. *Science*, **215**, 306–309.

DOCHERTY, R.J. & BROWN, D.A. (1986). Interaction of 1,4-dihydropyridines with somatic Ca2+ currents in hippocampal CA1 neurones of the guinea pig in vitro. *Neurosci. Lett.*, **70**, 106–109.

DOLIN, S.J. & LITTLE, H.J. (1989). Are changes in neuronal calcium channels involved in ethanol tolerance. *J. Pharmacol. Exp. Ther.*, **250**, 985–991.

DOLIN, S.J., PATCH, T., SIAREY, R.J., WHITTINGTON, M.A. & LITTLE, H.J. (1988). Evidence for the involvement of dihydropyridine-sensitive calcium channels in ethanol dependence. *Br. J. Pharmacol.*, **95**, 877P.

DURAND, D. & CARLEN, P.L. (1984). Decreased neuronal inhibition in vitro after long-term administration of ethanol. *Science*, **224**, 1359–1361.

DURAND, D., CORRIGALL, W.A., KUITAN, P. & CARLEN, P.L. (1981). Effects of low concentrations of ethanol on CA1 hippocampal neurones in vitro. *J. Physiol. Pharmacol.*, **59**, 979–984.

FRIEDMAN, M.B., ERICKSON, C.K. & LESLIE, S.W. (1980). Effects of acute and chronic ethanol administration on whole mouse brain synaptosomal calcium influx. *Biochem. Pharmacol.*, **29**, 1903–1908.

GLOSSMAN, H., FERRY, D.R., LUBBECKE, F., MEWES, R. & HOFMANN, F. (1982). Calcium channels; direct identification with radioligand binding sites. *Trends Pharmacol. Sci.*, **3**, 431–437.

GROVER, L.M. & TEYLER, T.M. (1990). Two components of long-term potentiation induced by different patterns of afferent activation. *Nature*, **347**, 477–479.

HARPER, J.C., BRENNAN, C.H. & LITTLETON, J.M. (1989). Genetic upregulation of calcium channels in a cellular model of ethanol dependence. *Neuropharmacology*, **28**, 1299–1302.

HARRIS, R.A. & HOOD, W.F. (1980). Inhibition of synaptosomal calcium uptake by ethanol. *J. Pharmacol. Exp. Ther.*, **213**, 562–568.

HUNTER, B.E. & WALKER, D.E. (1978). Ethanol-dependence in the rat: role of extrapyramidal motor systems in the withdrawal reaction. *Exp. Neurol.*, **62**, 374–393.

JONES, R.S. & HEINEMANN, U.H. (1987). Differential effects of calcium entry blockers on pre- and postsynaptic influx of calcium in the rat hippocampus in vitro. *Brain Res.*, **416**, 257–266.

LEE, K., DUNWIDDIE, T., DEITRICH, R., LYNCH, G. & HOFFER, B. (1981). Chronic ethanol consumption and hippocampal neuron dendritic spines: a morphimetric and physiological analysis. *Exp. Neurol.*, **71**, 541–540.

LITTLE, H.J. & DOLIN, S.J. (1987). Lack of tolerance to ethanol after concurrent administration of nitrendipine. *Br. J. Pharmacol.*, **92**, 606P.

LITTLETON, J.M. & LITTLE, H.J. (1989). Adaptation in neuronal calcium channels as a common basis for physical dependence on central depressant drugs. In *Psychoactive Drugs; Tolerance and Sensitisation*. ed.: Goudie, A.J. & Emmett-Oglesby, M., pp. 461–518. Humana Press.

LOUVEL, J., ABBES, S. & GODFRAIND, J.M. (1986). Effect of organic calcium dependent processes. *Exp. Brain Res.*, **14**, 375–385.

PANZA, G., GREBB, J.A., SANNA, E., WRIGHT, A.G. & HANBAUER, L. (1985). Evidence for down regulation of ^{3}H-nitrendipine recognition sites in mouse brain after long term treatment with nifedipine or verapamil. *Neuropharmacology*, **24**, 1113–1117.

REYNOLDS, J.N., WU, P.H., KHANNA, J.M. & CARLEN, P.L. (1990). Ethanol tolerance in hippocampal neurons: adaptive changes in cellular responses to ethanol measured in vitro. *J. Pharmacol. Exp. Ther.*, **252**, 265–271.

STOKES, J.A. & HARRIS, R.A. (1982). Alcohol and synaptosomal calcium transport. *Mol. Pharmacol.*, **22**, 99–104.

TAKAHASHI, K. & AKAIKE, N. (1900). Nicergoline inhibits T-type calcium channels in rat isolated hippocampal CA1 pyramidal neurones. *Br. J. Pharmacol.*, **100**, 705–710.

TAKAHASHI, K., WAKAMORI, M. & AKAIKE, N. (1989). Hippocampal CA1 pyramidal cells of rats have four voltage-dependent calcium conductances. *Neurosci. Lett.*, **104**, 229–234.

WESTENBROEK, R.E., AHLIJANIAN, M.K. & CATTERALL, W.A. (1990). Clustering of L-type calcium channel at the base of major dendrites in hippocampal pyramidal neurones. *Nature*, **347**, 281–284.

WHITTINGTON, M.A. & LITTLE, H.J. (1988). Nitrendipine prevents the ethanol withdrawal syndrome, when administered chronically with ethanol, prior to withdrawal. *Br. J. Pharmacol.*, **94**, 885P.

WHITTINGTON, M.A. & LITTLE, H.J. (1989). Stereospecificity of the actions of PN 200-110 on the changes due to ethanol withdrawal in hippocampal field potentials. *Br. J. Pharmacol.*, **98**, 923P.

WHITTINGTON, M.A. & LITTLE, H.J. (1990). Patterns of changes in field potentials in the isolated hippocampal slice on withdrawal from chronic ethanol treatment of mice in vivo. *Brain Res.*, **523**, 237–244.

WHITTINGTON, M.A. & LITTLE, H.J. (1991). A calcium channel antagonist stereoselectively decreases hyperexcitability induced in isolated hippocampal slices by ethanol withdrawal, but not that due to bicuculline. *Br. J. Pharmacol.* (in press).

WHITTINGTON, M.A., DOLIN, S.J., PATCH, T.L., SIAREY, R.J., BUTTERWORTH, A.R. & LITTLE, H.J. (1991). Chronic dihydropyridine treatment can reverse the behavioural adaptations to ethanol. *Br. J. Pharmacol.*, **103**, 1669–1676.

(Received December 20, 1990
Revised February 25, 1991
Accepted March 7, 1991)

Br. J. Pharmacol. (1991), **103**, 1685–1690 © Macmillan Press Ltd, 1991

Different sensitivities of rabbit isolated blood vessels exhibiting co-transmission to the slow calcium channel blocker, nifedipine

[1]J.M. Bulloch, [2]A. MacDonald & J.C. McGrath

Autonomic Physiology Unit, Institute of Physiology, University of Glasgow, Glasgow G12 8QQ

1 Antagonist drugs were used to separate the purinergic and adrenergic contributions as well as the adrenoceptor sub-types involved in the sympathetic vasoconstrictor responses produced by electrical field stimulation in rabbit isolated ileocolic and proximal saphenous arteries. Blocking drugs were applied either alone or in various combinations and sequences.

2 Nifedipine attenuated vasoconstrictor responses to sympathetic nerve stimulation both in the presence and in the absence of α-adrenoceptor blocking agents. However in the presence of α,β-methylene ATP, nifedipine produces at best only a small attenuation of the vasoconstrictor response.

3 These results suggest that the purinergic component of the response to sympathetic nerve stimulation, at least in these tissues, can be antagonized by nifedipine, whereas the α_1-adrenoceptor-mediated response is relatively resistant.

Keywords: rabbit blood vessels; purinergic nerve stimulation; co-transmission; nifedipine

Introduction

There is strong evidence for co-transmission involving a purine most likely adenosine 5'-triphosphate (ATP), as well as noradrenaline at sympathetic nerve terminals in the vas deferens (Sneddon *et al.*, 1983; Sneddon & Burnstock, 1984a; Stjärne & Astrand, 1984; 1985) and in blood vessels *in vitro* (Sneddon & Burnstock, 1984b; Ishikawa, 1985; Kennedy *et al.*, 1986; Muramatsu, 1986; Burnstock & Warland, 1987) as well as *in vivo* (Bulloch & McGrath, 1986; 1988a,b).

An interesting feature of the earlier studies on vas deferens was that the non-adrenergic component, subsequently shown to be purinergic (Sneddon & Burnstock, 1984a), was blocked by the calcium channel blocking agent, nifedipine, an effect shown to be due to blockade of the propagation of the action potential in the smooth muscle (Blakeley *et al.*, 1981). Later studies also showed a preferential blocking effect of nifedipine on the purinergic component of the vasopressor response to stimulation of the sympathetic outflow in the pithed rat (Bulloch & McGrath, 1988b). The aim of the present study was to test whether vascular smooth muscle *in vitro* also shows differential susceptibility of the purinergic component to nifedipine.

For this study we have chosen blood vessels where the purinergic contribution to sympathetic nerve stimulation has been demonstrated to varying degrees, for example; the ileocolic artery (von Kügelgen & Starke, 1985; Bulloch & Starke, 1988; 1990) where the purinergic component of the sympathetic nerve-mediated response is dominant; the saphenous artery (Burnstock & Warland, 1987) which also exhibits a large purinergic component but where a large α_1-adrenoceptor-mediated component is also evident.

A preliminary communication of these results has been published (Bulloch *et al.*, 1988).

Methods

New Zealand White rabbits, of either sex (2–3 kg) were killed by stunning and exsanguination, and the blood vessels to be studied were dissected out and cleared of fatty tissue.

The proximal segment of the saphenous artery was cut into four 4 mm rings. A thin wire (upper) support was inserted through the lumen of the ring taking care not to damage the endothelial cell lining. A second wire (lower) support, attached to an electrode assembly, was also threaded through the lumen and the tissue was then suspended between the two supports. The upper support was connected by thread to a Grass FT03c transducer for isometric recording. Individual electrode assemblies were then mounted in 30 ml organ baths containing physiological salt solution (PSS) maintained at 37°C, and gassed with 95% O_2:5% CO_2. Tissues were placed under an initial resting tension of 1.0 g and left for 1 h to reach an eventual resting tone of approximately 0.5 g. Sections from the ileocolic artery were similarly prepared.

For perfusion studies, the proximal section of the largest ramus arteriae ileocolicae was dissected out and cleared of fatty tissue. Side branches were tied off and the arteries were cannulated at both ends before being mounted vertically in a 4 ml organ bath. They were then perfused at a constant rate of flow (2.7 ml min^{-1}) in such a way that the perfusate did not mix with the bathing fluid.

Electrical stimulation (parameters and protocol)

Ring segments taken from the saphenous artery and ileocolic artery were electrically stimulated at various frequencies for 1 s duration (35–40 V, at frequencies of 4, 8, 16, 32 and 64 Hz, pulse width 0.1–0.3 ms) to produce isometric contractions. Additional stimuli of 4 Hz for 10 s, or 5 Hz and 10 Hz for 20 s, were used in some preparations as examples of long duration stimuli. The interval between trains of pulses, during frequency response curves (FRC), was 5 min.

In the perfused ileocolic artery, vasoconstriction produced by electrical field stimulation (platinum electrodes: 0.3 ms pulse width; supramaximal current strength of 200 mA; variable frequencies and train lengths) was observed as an increase in perfusion pressure (monitored by a Statham P23 Db pressure transducer).

Drugs and solutions

The composition of the PSS used for the saphenous artery was (mM): NaCl 118.4, KCl 4.7, $CaCl_2$ 2.5, $MgSO_4.7H_2O$ 1.2, $NaHCO_3$ 24.9, KH_2PO_4 1.2 and glucose 11.1. Na_2 EDTA, 23 μM, was included in all the above experiments to prevent oxidative degradation of NA. The composition of the PSS used for the ileocolic artery was (mM): NaCl 118, KCl 4.8, $CaCl_2$ 2.5, $NaHCO_3$ 25, KH_2PO_4 0.9, glucose 11, Na_2 EDTA

[1] Author for correspondence.
[2] Present address: Department of Biological Sciences, Glasgow College, Glasgow G4 0BA.

0.03 and ascorbic acid 0.3. The medium was saturated with 95% O_2: 5% CO_2 and maintained at 37°C.

The following drugs were used: prazosin HCl (Pfizer); rauwolscine HCl (Roth); α,β-methylene ATP (Sigma); nifedipine (Bayer); yohimbine HCl (Roth).

The blocking drugs were applied at least 20 min before starting each series of stimulations, either alone or in various combinations and sequences. The choice of these agents and concentrations used were based on their selectivity of blockade in previous analyses on vas deferens and isolated blood vessels (see Bulloch & Starke, 1990; McGrath *et al.*, 1990); prazosin, post-junctional α_1-adrenoceptors (Cambridge *et al.*, 1977); rauwolscine, pre- and post-junctional α_2-adrenoceptors (Weitzell *et al.*, 1979); α,β-methylene ATP (α,β-MeATP), post-junctional P_{2x}-purinoceptors (Sneddon & Burnstock, 1984a,b); nifedipine, postjunctional blockade of transmission propa gated by action potentials sustained by slow Ca^{2+} channels (Blakeley *et al.*, 1981).

All drugs were dissolved in distilled water and added to the organ baths in a volume of 30 μl or less, except nifedipine which was dissolved in ethanol and water (1:4) before being added to the organ bath.

The means and standard error of the means were calculated and compared by a paired or unpaired t test. P values of 0.05 or less were considered to be signficant; n is the number of preparations.

Results

The perfused ileocolic artery

Stimulation of the isolated perfused ileocolic arteries, produced reproducible vasoconstrictions, observed as increases in perfusion pressure, which were pulse number- and frequency-dependent.

Short periods of electrical stimulation (1 s) elicted monophasic vasoconstriction, whereas longer periods (20 s) produced biphasic vasoconstriction of which the first component was mainly mediated by ATP (selectively inhibited by α,β-MeATP) whereas the second component although still mainly purinergic, had a large noradrenergic component (antagonized by prazosin) (see Bulloch & Starke, 1990).

Electrically evoked vasopressor responses of the isolated perfused ileocolic artery (5 Hz, 50 V, 10 and 100 pulses), were not significantly affected by the addition of nifedipine (10 μmol l^{-1}) on its own to the bathing medium (Figure 1a). In the presence of prazosin (0.3 μmol l^{-1}) (Figure 1b) the effect of nifedipine (10 μmol l^{-1}) was more variable between tissues but did show a significant attenuation at 10 Hz 100 pulses.

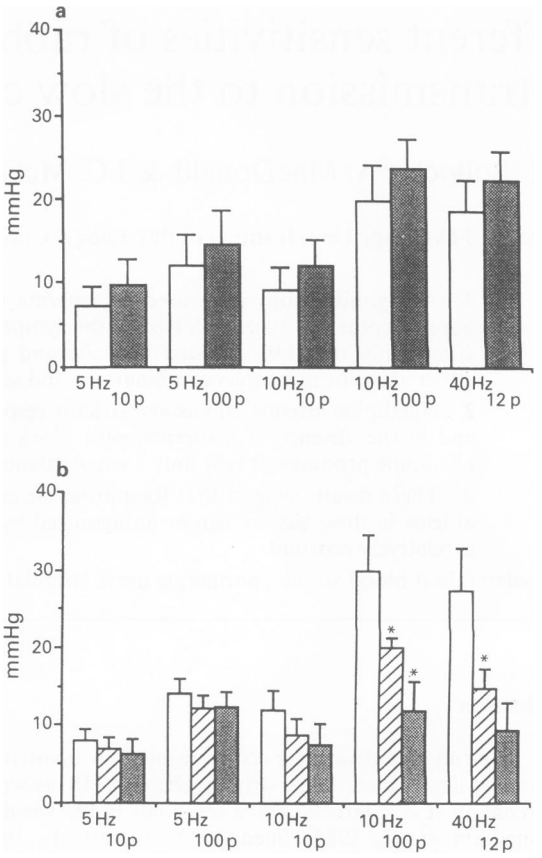


Figure 1 The effect of nifedipine on responses at different frequencies and pulse trains in the isolated perfused ileocolic artery of the rabbit is illustrated (a) in the absence of prazosin and (b) in the presence of prazosin (0.3 μmol l^{-1}). Arteries were stimulated electrically at various frequencies and pulse durations in the order shown in the figure to produce vasopressor responses. Additional stimuli of 1 Hz, 5 Hz and 10 Hz for 20 s, were also performed 30 min before the start of each experiment. The interval between trains of pulses was 5 min. Arteries were stimulated, first before the addition of drugs (open columns), then after (a) nifedipine (10 μmol l^{-1}) (solid columns); or (b) after prazosin (0.3 μmol l^{-1}) (hatched columns) and subsequently after nifedipine (3 μmol l^{-1}) (solid columns). Data are presented as the change in perfusion pressure (mmHg) produced as a result of electrical stimulation within any one artery. Columns represent mean values of ten experiments; bars show s.e.mean. Significant difference from pretreatment values, for paired t test: $*P < 0.05$. In control tissues (stimulation repeated in the absence of drugs) there were no significant differences between the corresponding responses within each tissue.

The ileocolic artery ring preparation: the effect of increasing concentrations of nifedipine

The effect of nifedipine (0.3–30 μmol l^{-1}) on vasoconstrictions produced by electrical field stimulation (10 Hz, 40 V, 0.3 ms for 20 s) under conditions of α_1-adrenoceptor blockade (prazosin, 0.3 μmol l^{-1}) were studied. Prazosin (0.3 μmol l^{-1}) on its own attenuated the second component of the response to a greater degree (Figure 2). The subsequent administration of nifedipine (0.3 μmol l^{-1}) signficantly attenuated only the first component of the response. Subsequent increasing concentrations of nifedipine (1–10 μmol l^{-1}) had no further effect. The subsequent administration of nifedipine (30 μmol l^{-1}) significantly attenuated the first, but not the second, component of the vasoconstrictor response further (Figure 2).

The ileocolic artery ring preparation: the effect of nifedipine on its own and after α_1-adrenoceptor blockade or P_{2x}-purinoceptor desensitization

For this series of experiments, the highest concentration of nifedipine was used (30 μmol l^{-1}) and consequently a higher concentration of ethanol (from the nifedipine solution) was present in the bathing medium. The effect of ethanol was therefore taken into consideration.

The effect of nifedipine on vasoconstrictions produced by electrical field stimulation (4–32 Hz, 40 V, 0.3 ms for 1 s) were studied. On its own, nifedipine (30 μmol l^{-1}) significantly attenuated the nerve-mediated responses at 8, 16 and 32 Hz frequencies (Figure 3a). With longer trains of pulses (5 Hz and 10 Hz for 20 s), biphasic responses were produced. With these longer durations of stimulation only the first phase of the response was reduced by nifedipine (30 μmol l^{-1}), whilst the second phase was not significantly affected (Figure 3b). The subsequent addition of prazosin (0.3 μmol l^{-1}) and α,β-MeATP (3 μmol l^{-1}) completely abolished the responses (Figure 3a and b).

In the presence of prazosin (0.3 μmol l^{-1}) the attenuation of the electrically evoked vasoconstrictor responses by nifedipine (30 μmol l^{-1}) was more marked (Figure 4a and b). The attenuation was signficant at all parameters of stimulation studied. The subsequent administration α,β-MeATP (3 μmol l^{-1}) completely abolished the responses (Figure 4a and b).

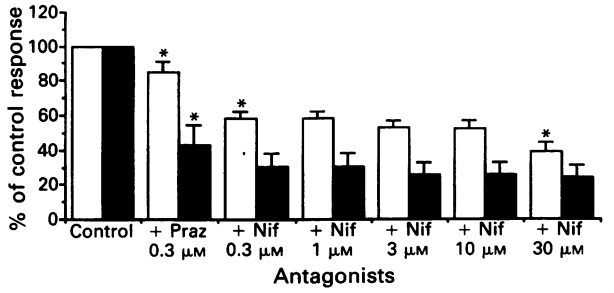


Figure 2 The effect of increasing concentrations of nifedipine in conditions of α-adrenoceptor blockade on biphasic vasoconstrictor responses of the ileocolic artery. Arteries were stimulated electrically at 10 Hz for 20 s repeatedly to produce biphasic vasoconstrictions. The interval between trains of pulses was 5 min. Ring preparations of artery were electrically stimulated, first before the addition of antagonist, then after prazosin (Praz, 0.3 μmol l^{-1}), then after subsequent increasing concentrations of nifedipine (Nif, 0.3–30 μmol l^{-1}). Data are presented as a percentage of the maximum control response at each phase produced as a result of electrical stimulation within any one artery. The first phase (open columns) at 10 Hz 20 s was taken as the peak constrictor height which occurred 5–9 s after the onset of stimulation, and the second phase (solid columns) as the peak height between 18–23 s. Columns represent mean values of five experiments; bars show s.e.mean. Significant difference from pretreatment values, for paired t test: * $P < 0.05$. In control tissues (stimulation repeated in the absence of drugs) there were no significant differences between the corresponding responses within each tissue.

In the presence of a P_{2x}-purinoceptor desensitizing concentration of α,β-MeATP (3 μmol l^{-1}) (see McGrath *et al.*, 1990) the addition of nifedipine (30 μmol l^{-1}) in ethanol produced no further attenuation of the responses and indeed enhanced them significantly at all parameters studied (Figure 5a and b). After the addition of α,β-MeATP (3 μmol l^{-1}), the same concentration of ethanol (0.66%) as used in the nifedipine solution, produced potentiations of the nerve-mediated responses especially at higher frequencies and longer pulse durations of stimulation (Figure 6a and b). On its own, ethanol potentiated the second component of the vasoconstrictor response at 10 Hz 20 s and responses at 16 Hz and 32 Hz for 1 s. In the presence of prazosin (0.3 μmol l^{-1}), ethanol had no effect (Bulloch & McGrath, unpublished observations). The further addition of prazosin (0.3 μmol l^{-1}) after nifedipine abolished the residual responses (Figure 5a and b).

Proximal saphenous artery

Contractile responses of the rabbit isolated saphenous artery to electrical stimulation (4–64 Hz, 25–30 V, 0.1 ms pulse width for 1 s) were reduced but not abolished by 1 μmol l^{-1} prazosin (Figure 7a). The remaining prazosin-resistant component was significantly attenuated and almost completely abolished at lower frequencies by desensitization with 3 μmol l^{-1} α,β-MeATP (results not shown).

The relatively low dose of nifedipine (1 μmol l^{-1}) produced a significant reduction of the responses that remained after the addition of prazosin (1 μmol l^{-1}) by around 50% (Figure 7a). The remaining nifedipine resistant component was almost completely abolished by α,β-MeATP (not shown) confirming that the nifedipine-resistant component that remained after prazosin treatment, was purinergic.

Nifedipine (1 μmol l^{-1}) had no effect on responses after α,β-MeATP addition (Figure 7b). The further addition of prazosin after α,β-MeATP and nifedipine, abolished the responses (not shown), confirming that the nifedipine resistant component after α,β-MeATP treatment was adrenergic.

Nifedipine (1 μmol l^{-1}) was dissolved in ethanol to give a final bath concentration of 0.02%. This concentration of ethanol on its own has no significant effect on nerve-mediated responses (Bulloch & McGrath, unpublished observations).

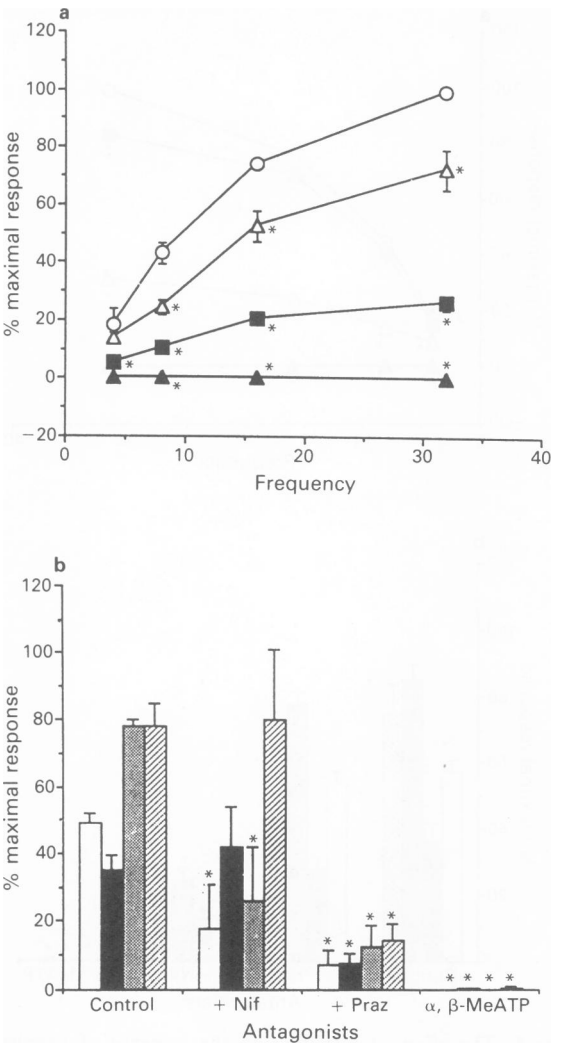


Figure 3 The effect of nifedipine on responses at different frequencies in the rabbit ileocolic artery is illustrated in (a). Arteries were stimulated electrically at various frequencies for 1 s duration (35–40 V, at frequencies of 4, 8, 16 and 32 Hz, pulse width 0.1–0.3 ms) to produce isometric contractions. Additional stimuli of 5 Hz and 10 Hz for 20 s, were performed before each frequency response curve as examples of a low frequency/long duration stimuli. The interval between trains of pulses, during frequency response curves (FRC), was 5 min. Arterial rings were electrically stimulated, (a) first before the addition of nifedipine (○), then after nifedipine (30 μmol l^{-1}) (△), then after prazosin (0.3 μmol l^{-1}) (■) and finally after desensitization with α,β-methylene ATP (α,β-MeATP) (3 μmol l^{-1}) (▲). Data are presented as a percentage of the maximum response produced as a result of electrical stimulation within any one artery. The effect of nifedipine on the biphasic responses in the ileocolic artery is illustrated in (b). The first phase at 5 Hz (open columns) and 10 Hz (stippled columns) was taken as the peak constrictor height which occurred 5–9 s after the onset of stimulation, and the second phase at 5 Hz (solid columns) and 10 Hz (hatched columns) as the peak height between 18–23 s. Columns represent mean values of five experiments; bars show s.e.mean. Significant difference from pretreatment values, for paired t test: * $P < 0.05$. In control tissues (stimulation repeated in the absence of drugs) there were no significant differences between the corresponding responses within each tissue.

Discussion

The ileocolic artery and the saphenous artery of the rabbit are blood vessels in which noradrenaline (NA)-ATP co-transmission have been demonstrated (von Kügelgen & Starke, 1985; Burnstock & Warland, 1987; Bulloch & Starke, 1988; 1990). The degree of involvement of either the adrenergic or purinergic components of the response to sympathetic nerve stimulation in these blood vessels depends on the

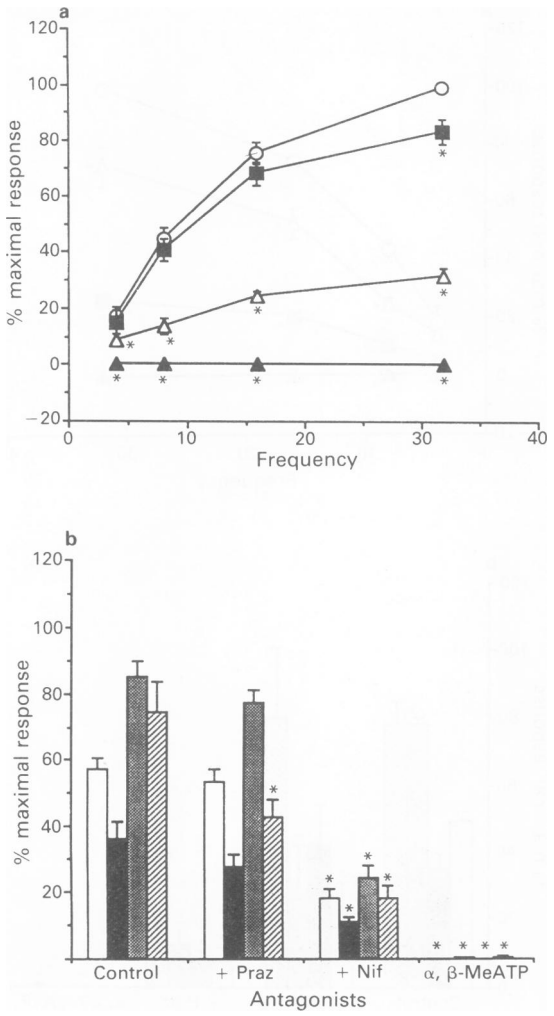


Figure 4 The effect of nifedipine in the presence of prazosin on responses of the ileocolic artery at different frequencies, as detailed in Figure 3, is illustrated. (a) Arterial rings were electrically stimulated, first before the addition of antagonists (○), then after prazosin ($0.3\,\mu mol\,l^{-1}$) (■), then after nifedipine ($30\,\mu mol\,l^{-1}$) (△) and finally after desensitization with α,β-methylene ATP ($3\,\mu mol\,l^{-1}$) (▲). Data are presented as a percentage of the maximum response produced as a result of electrical stimulation within any one artery. The effect of nifedipine on the biphasic responses in the ileocolic artery is illustrated in (b). The first phase at 5 Hz (open columns) and 10 Hz (stippled columns) was taken as the peak constrictor height which occurred 5–9 s after the onset of stimulation, and the second phase at 5 Hz (solid columns) and 10 Hz (hatched columns) as the peak height between 18–23 s. Columns represent mean values of five experiments; bars show s.e.mean. Praz, prazosin; Nif, nifedipine; α,β-MeATP, α,β-methylene ATP. Significant difference from pretreatment values, for paired *t* test: $*P < 0.05$. In control tissues (stimulation repeated in the absence of drugs) there were no significant differences between the corresponding responses within each tissue.

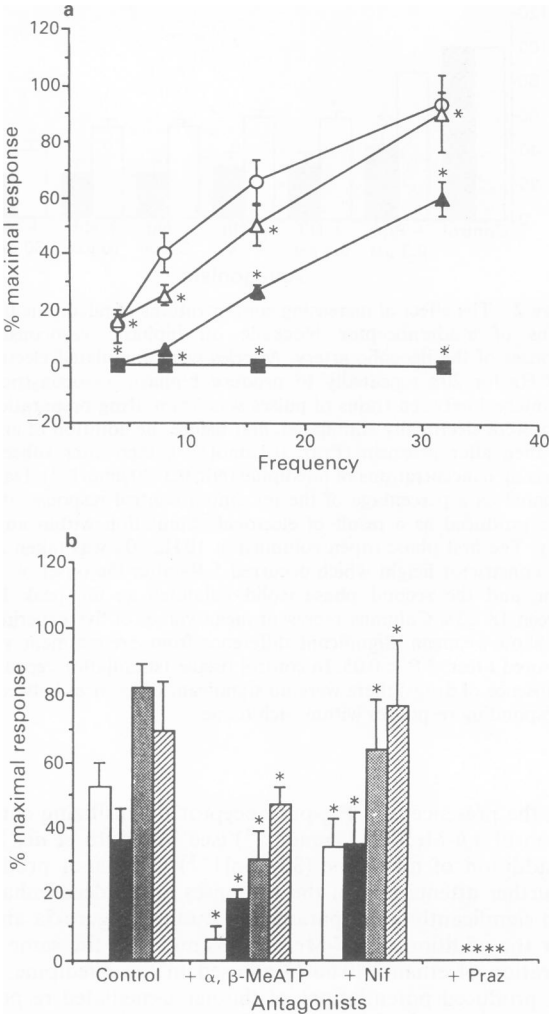


Figure 5 The effect of nifedipine in the presence of α,β-methylene ATP (α,β-MeATP) on responses of the ileocolic artery at different frequencies, as detailed in Figure 3, is illustrated in (a). Arterial rings were electrically stimulated, first before the addition of drugs (○), then after desensitization with α,β-MeATP ($3\,\mu mol\,l^{-1}$) (▲), then after nifedipine ($30\,\mu mol\,l^{-1}$) (△) and finally after prazosin ($0.3\,\mu mol\,l^{-1}$) (■). Data are presented as a percentage of the maximum response produced as a result of electrical stimulation within any one artery. The effect of nifedipine on the biphasic responses in the ileocolic artery is illustrated in (b). The first phase at 5 Hz (open columns) and 10 Hz (stippled columns) was taken as the peak constrictor height which occurred 5–9 s after the onset of stimulation, and the second phase at 5 Hz (solid columns) and 10 Hz (hatched columns) as the peak height between 18–23 s. Columns represent mean values of five experiments; bars show s.e.mean. Nif, nifedipine; Praz, prazosin. Significant difference from pretreatment values, for paired *t* test: $*P < 0.05$. In control tissues (stimulation repeated in the absence of drugs) there were no significant differences between the corresponding responses within each tissue.

parameters of stimulation employed (Bulloch & Starke, 1988; 1990; McGrath *et al.*, 1990). At lower frequencies (and a stimulation period of 1 s) the purinergic component dominates the response, with the noradrenergic component playing an increasing role at higher frequencies (32 Hz) (Figures 3a, 4a and 5a and see Bulloch & Starke, 1990). For longer trains of pulses (train lengths of 20 s) two distinct phases of the contraction can be differentiated, the first one was greatly reduced by α,β-MeATP and hence was mediated by ATP, whilst the second one was partly sensitive to prazosin and hence was, to a considerable degree, noradrenergic (Figures 3b, 4b and 5b).

Where P_{2x}-purinoceptors had already been desensitized with α,β-MeATP (Figure 3), the subsequent addition of nifedipine (dissolved in ethanol and distilled water giving a final bath concentration of 0.66%) appeared to potentiate the responses. However, this effect can be attributed solely to ethanol, which selectively potentiates the adrenergic component of the sympathetic nerve-mediated responses in this tissue (Bulloch & McGrath, unpublished observations; and see Figure 6). The inhibitory action of nifedipine is best seen where the adrenergic component has been antagonized by prazosin (Figure 4) but it is also evident in the absence of prazosin (Figure 3), since in this tissue the purinergic component dominates the response.

The purinergic component of the response to stimulation of the sympathetic nerves was reduced by about 50% by nifedipine, whereas the adrenergic component was relatively resistant. This is similar to the situation found in the rat iso-

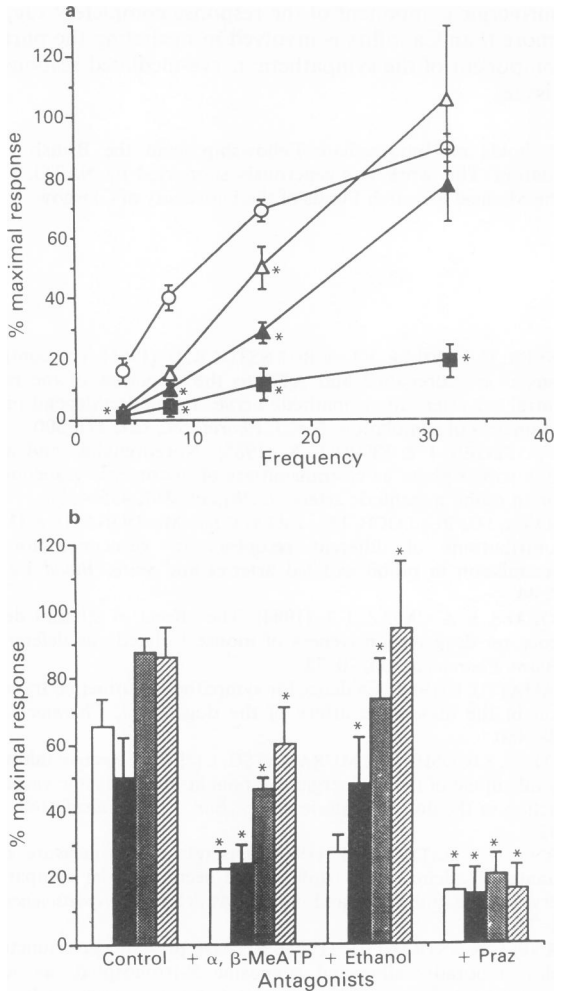


Figure 6 The effect of ethanol in the presence of α,β-methylene ATP (α,β-MeATP) on responses of the ileocolic artery at different frequencies, as detailed in Figure 3, is illustrated in (a). Arterial rings were electrically stimulated, first before the addition of drugs (○), then after desensitization with α,β-MeATP (3 μmol l^{-1}) (▲), then after ethanol (0.66%) (△) and finally after prazosin (0.3 μmol l^{-1}) (■). Data are presented as a percentage of the maximum response produced as a result of electrical stimulation within any one artery. The effect of ethanol on the biphasic responses in the ileocolic artery is illustrated in (b). The first phase at 5 Hz (open columns) and 10 Hz (stippled columns) was taken as the peak constrictor height which occurred 5–9 s after the onset of stimulation, and the second phase at 5 Hz (solid columns) and 10 Hz (hatched columns) as the peak height between 18–23 s. Columns represent mean values of five experiments; bars show s.e.mean. Praz, prazosin. Significant difference from pretreatment values, for paired t test: * $P < 0.05$. In control tissues (stimulation repeated in the absence of drugs) there were no significant differences between the corresponding responses within each tissue.

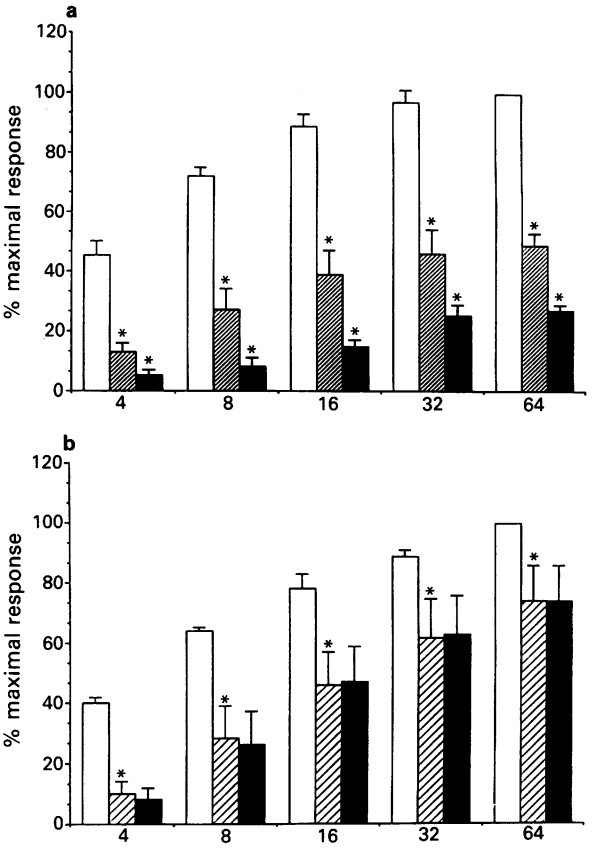


Figure 7 The effect of nifedipine in the presence of (a) prazosin and (b) α,β-methylene ATP (α,β-MeATP) is illustrated on responses of the proximal saphenous artery. Arteries were stimulated electrically at varying frequencies for one second duration (35–40 V, at frequencies of 4, 8, 16, 32 and 64 Hz, pulse width 0.1–0.3 ms) to produce isometric contractions. The interval between trains of pulses, during frequency-response curves (FRC), was 5 min. Arterial rings were electrically stimulated (a) before the addition of drugs (open columns), then after prazosin (0.3 μmol l^{-1}) (hatched columns), then after nifedipine (1 μmol l^{-1}) (solid columns) and (b) before the addition of drugs (open columns), then after desensitization with α,β-MeATP (3 μmol l^{-1}) (hatched columns), then after nifedipine (1 μmol l^{-1}) (solid columns). Data are presented as a percentage of the maximum response produced as a result of electrical stimulation within any one artery. Columns represent mean values of five experiments; bars show s.e.mean. Significant difference from pretreatment values, for paired t test: * $P < 0.05$. In control tissues (stimulation repeated in the absence of drugs) there were no significant differences between the corresponding responses within each tissue.

lated vas deferens, where nifedipine showed selectivity against the purinergic component of transmission (Blakeley *et al.*, 1981; Brown *et al.*, 1983).

It should be noted however that both in the pithed rat (Bulloch & McGrath, 1988b, Figures 1, 3 and 4) and the isolated vas deferens of the rat (Brown *et al.*, 1983, Figure 6) there was a component of the non-adrenergic response which was resistant to nifedipine, although in both cases it was a relatively smaller component of the overall response than in the present study. This may indicate that in the isolated blood vessels used in this present study a relatively smaller part of the purinergic response is propagated via the action potential than in small resistance vessels (as found in the pithed rat) or the tightly coupled smooth muscle cells of the vas deferens.

Studies on small mesenteric arteries from the rat show a marked sensitivity to lowered calcium, of responses at low frequency nerve stimulation and much less sensitivity at higher frequencies (Sjöblom-Widfeldt & Nilsson, 1989). The latter authors concluded that this effect could not simply be attributed to a reduction in transmitter output as a result of a decreased availability of calcium since this effect was best seen at low frequencies and suggested that the transmitter responsible for the low-frequency response (possibly ATP) may differ with respect to calcium sensitivity. The results from this present study note a greater effect of nifedipine on the purinergic component of the electrically mediated vasoconstrictor responses.

It is also unlikely that attenuation of the nerve-mediated response by nifedipine is a result of its interference with presynaptic feedback mechanisms as found in the rat brain (Ilu *et al.*, 1987) since the attenuation of the nerve-mediated response is also evident at very short pulse trains (train lengths of 1 s) where conditions for autoinhibition may not be present (Bulloch & Starke, 1990). It is also unlikely that nifedipine is acting presynaptically by directly inhibiting transmitter release, since this inhibition would have to be selective against the release of ATP so leaving the release of its co-transmitter

unaffected as the postjunctional adrenergic response is unaffected (Figures 4 and 5). Studies measuring [^{3}H]-NA efflux during nerve stimulation in dog mesenteric arteries found no interaction of nifedipine (0.01–1 μmol l^{-1}) with [^{3}H]-NA efflux (Omote *et al.*, 1989).

In conclusion, nifedipine shows selectivity for the purinergic component of the electrically evoked nerve mediated response in the rabbit ileocolic artery. However, its inability to block the purinergic component of the response completely suggests that more than Ca influx is involved in mediating the purinergic component of the sympathetic nerve-mediated response in this tissue.

J.M.B. holds an Intermediate Fellowship from the British Heart Foundation. This work was generously supported by NATO, SERC and the Medical Research Funds of the University of Glasgow.

References

BLAKELEY, A.G.H., BROWN, D.A., CUNNANE, T.C., FRENCH, A.M., McGRATH, J.C. & SCOTT, N.C. (1981). Effects of nifedipine on electrical and mechanical responses of rat and guinea pig vas deferens. *Nature*, **294**, 759–761.

BROWN, D.A., DOCHERTY, J.R., FRENCH, A.M., MacDONALD, A., McGRATH, J.C. & SCOTT, N.C. (1983). Separation of adrenergic and nonadrenergic contractions to field stimulation in the rat vas deferens. *Br. J. Pharmacol.*, **79**, 379–393.

BULLOCH, J.M., DALY, C.J., MacDONALD, A., McGRATH, J.C. & WILSON, V.G. (1988). The effect of nifedipine on nerve-mediated responses of blood vessels *in vivo* and *in vitro*. *Br. J. Pharmacol.*, **95**, 563P.

BULLOCH, J.M. & McGRATH, J.C. (1986). Blockade of vasopressor and vas deferens responses by alpha, beta-methylene ATP in the pithed rat. *Br. J. Pharmacol.*, **89**, 577P.

BULLOCH, J.M. & McGRATH, J.C. (1988a). An investigation of purinergic co-transmission in sympathetic vascular control and in the vas deferens motor response. *Br. J. Pharmacol.*, **94**, 103–108.

BULLOCH, J.M. & McGRATH, J.C. (1988b). The effect of nifedipine on nerve-mediated pressor responses of blood vessels *in vivo* and *in vitro*. *Br. J. Pharmacol.*, **95**, 695–700.

BULLOCH, J.M. & STARKE, K. (1988). Presynaptic alpha$_2$-autoinhibition in the rabbit ileocolic artery: a blood vessel where ATP and noradrenaline act as co-transmitters. In *Proceedings of the International Symposium on Biosignalling in Cardiac and Vascular Systems* ed. Fujiwara, M., Narumiya, S. & Miwa, S. pp. 122–128. Oxford: Pergamon Press.

BULLOCH, J.M. & STARKE, K. (1990). Presynaptic alpha$_2$-autoinhibition in the rabbit ileocolic artery: a blood vessel where ATP and noradrenaline act as co-transmitters. *Br. J. Pharmacol.*, **99**, 279–284.

BURNSTOCK, G. & WARLAND, J.J.I. (1987). A pharmacological study of the rabbit saphenous artery *in vitro*: a vessel with a large purinergic contractile response to sympathetic nerve stimulation. *Br. J. Pharmacol.*, **90**, 111–190.

CAMBRIDGE, D., DAVEY, M.J. & MASSINGHAM, R. (1977). Prazosin, a selective antagonist of post-synaptic α-adrenoceptors. *Br. J. Pharmacol.*, **54**, 514–515.

ILU, P.S., LINDGREN, E., JACOBSON, K. & FREDHOLM, B.B. (1987). Interaction of dihydropyridine calcium channel agonists and antagonists with adenosine receptors. *Pharmacol. Toxicol.*, **61**, 121–125.

ISHIKAWA, S. (1985). Actions of ATP and α,β-methylene ATP on neuromuscular transmission and smooth muscle membrane of the rabbit and guinea pig mesenteric arteries. *Br. J. Pharmacol.*, **86**, 777–787.

KENNEDY, C., SAVILLE, V.L. & BURNSTOCK, G. (1986). The contributions of noradrenaline and ATP to the responses of the rabbit central ear artery to sympathetic nerve stimulation depend on the parameters of stimulation. *Eur. J. Pharmacol.*, **122**, 291–300.

von KÜGELGEN, I. & STARKE, K. (1985). Noradrenaline and adenosine triphosphate as co-transmitters of neurogenic vasoconstriction in rabbit mesenteric artery. *J. Physiol.*, **367**, 435–455.

McGRATH, J.C., BULLOCH, J.M., DALY, C.J. & MacDONALD, A. (1990). Contributions of different receptors to vasoconstrictor co-transmission in rabbit isolated arteries and veins. *Blood Vessels*, **27**, 44.

de MORAES, S. & CAPAZ, F.R. (1984). The effects of ethanol dependence on drug responsiveness of mouse isolated vas deferens. *J. Pharm. Pharmacol.*, **36**, 70–72.

MURAMATSU, I. (1986). Evidence for sympathetic purinergic transmission in the mesenteric artery of the dog. *Br. J. Pharmacol.*, **87**, 478–480.

OMOTE, S., KIGOSHI, S. & MURAMATSU, I. (1989). Selective inhibition by nifedipine of the purinergic component of neurogenic vasoconstriction in the dog mesenteric artery. *Eur. J. Pharmacol.*, **160**, 239–245.

STJÄRNE, L. & ASTRAND, P. (1984). Discrete events measure single quanta of adenosine 5'-triphosphate secreted from sympathetic nerves of the guinea pig and mouse vas deferens. *Neuroscience*, **13**, 21–28.

STJÄRNE, L. & ASTRAND, P. (1985). Relative pre- and post-junctional roles of noradrenaline and adenosine 5'-triphosphate as neurotransmitters of sympathetic nerves of the guinea pig and mouse vas deferens. *Neuroscience*, **14**, 929–946.

SJÖBLOM-WIDFELDT, N. & NILSSON, H. (1989). Sympathetic transmission in small mesenteric arteries from the rat: highly calcium dependent at low stimulation rates. *Acta Physiol. Scand.*, **135**, 505–511.

SNEDDON, P. & BURNSTOCK, G. (1984a). Inhibition of excitatory junction potentials in guinea pig vas deferens by α,β-methylene ATP: further evidence for ATP and noradrenaline as cotransmitters. *Eur. J. Pharmacol.*, **100**, 85–90.

SNEDDON, P. & BURNSTOCK, G. (1984b). ATP as co-transmitter in rat tail artery. *Eur. J. Pharmacol.*, **106**, 149–152.

SNEDDON, P., WESTFALL, D.P. & FEDAN, J.S. (1983). Cotransmitters in the motor nerves of the guinea pig vas deferens: electrophysiological evidence. *Science*, **218**, 693–695.

WEITZELL, R., TANAKA, T. & STARKE, K. (1979). Pre- and post-synaptic effects of yohimbine stereoisomers on noradrenergic transmission in the pulmonary artery of the rabbit. *Naunyn Schmiedebergs Arch. Pharmacol.*, **308**, 127–136.

(Received November 21, 1990
Revised March 7, 1991
Accepted March 11, 1991)

Br. J. Pharmacol. (1991), **103**, 1691–1696 © Macmillan Press Ltd, 1991

Comparison of the haemodynamic effects of adenosine monophosphate with sodium nitroprusside in a canine model of acute global left ventricular dysfunction

†B.A. Finegan & *,[1]A.S. Clanachan

Departments of †Anaesthesia and *Pharmacology, University of Alberta, Edmonton, Alberta, Canada T6G 2H7

1 The haemodynamic effects of adenosine 5'-monophosphate (AMP) and sodium nitroprusside (SNP) were compared in anaesthetized dogs following the induction of acute left ventricular (LV) dysfunction.

2 LV dysfunction was induced by the intracoronary administration of glass microbeads until left ventricular end diastolic pressure (LVEDP) was increased from 5 to 15 mmHg. This was associated with a decrease in LV *dP/dt* and cardiac index (CI) of 30% and 27%, respectively, and an increase in systemic vascular resistance index (SVRI) of 37%.

3 Graded doses of AMP (100 to 1000 $\mu g\,kg^{-1}\,min^{-1}$) or SNP (1 to 10 $\mu g\,kg^{-1}\,min^{-1}$) reduced SVRI and increased CI in a dose-related manner. Heart rate was not altered by either agent. At doses that caused similar reductions in SVRI, CI was increased more by AMP than by SNP.

4 The mechanisms responsible for the greater elevation of CI by AMP relative to SNP may be related to its more selective arterial vasodilator activity. SNP reduced cardiac preload that limited the expected increase in CI.

5 The haemodynamic profile of AMP suggests that it may be useful in the pharmacological management of acute cardiac failure, either when used alone or in combination with positive inotropic agents and/or selective venodilators.

Keywords: Adenosine 5'-monophosphate; sodium nitroprusside; cardiac output; left ventricular dysfunction; afterload reduction; vasodilators

Introduction

Adenosine is an endogenous nucleoside that participates in a multitude of biochemical and physiological processes throughout the body. In the cardiovascular system, adenosine affects both cardiac function (see review by Belardinelli *et al.*, 1989) and vascular resistance (see review by Collis, 1989). It is used clinically in the diagnosis and management of some forms of cardiac dysrhythmias (Di Marco *et al.*, 1983) and for the induction of deliberate hypotension during anaesthesia (Owall *et al.*, 1987). It has not been tested clinically or experimentally in left ventricular (LV) dysfunction, yet the pharmacological profile of adenosine and its nucleotides suggests that they may possess beneficial effects in this situation.

Pharmacological management of acute LV dysfunction normally involves the intravenous administration of catecholamines, such as dopamine, with or without vasodilators. As systemic vascular resistance (SVR) is a major determinant of impedance to left ventricular ejection (afterload), vasodilators, by reducing afterload, can prevent significant increases in myocardial O_2 consumption that may otherwise lead to a further deterioration of myocardial performance (Ford, 1980). Glyceryl trinitrate (GTN) and sodium nitroprusside (SNP) are the vasodilators usually employed. Potential advantages of adenosine in this role include inhibition of atrial and ventricular automaticity (Szentmiklosi, 1980; Wainright & Parratt, 1988), protection of cardiac muscle from ischaemic damage (Babbit *et al.*, 1989; Gruber *et al.*, 1989; Ledingham *et al.*, 1990) and anti-renin activity (Lagerkranser *et al.*, 1985) in addition to its potent vascular smooth muscle relaxant properties (see Collis, 1989). We have shown previously, in normal anaesthetized dogs, that AMP-induced afterload reduction increases cardiac output more than equi-effective afterload reducing doses of SNP (Finegan *et al.*, 1990).

The objective of this study was to assess the effects of adenosine 5'-monophosphate (AMP) in a canine model of acute LV dysfunction and to compare its haemodynamic effects with the clinically used vasodilator, SNP. Preliminary data from part of this study have been published (Finegan & Clanachan, 1990).

[1] Author for correspondence.

Methods

This study was approved by the Animal Care Committee of the University of Alberta. Healthy mongrel dogs ($n = 14$) of either sex weighing between (19 to 30 kg; mean 25.8 kg) were studied.

Animal preparation

The animals were anaesthetized with pentobarbitone (30 $mg\,kg^{-1}$, i.v.), intubated by a cuffed endotracheal tube and ventilated mechanically with an O_2/air mixture to maintain $PaCO_2$ between 35 to 40 mmHg and PaO_2 greater than 120 mmHg. Several blood-gas determinations were made throughout each experiment and end-tidal CO_2 levels were monitored continuously by a Beckman monitor (Beckman LB2). Anaesthesia was maintained by a constant infusion (4 $ml\,kg^{-1}\,h^{-1}$) of pentobarbitone (3 $mg\,kg^{-1}\,h^{-1}$). ECG was monitored continuously using standard leads; heart rate was derived from R–R intervals by a cardiotachometer. Arterial pressure (left femoral artery) and pulmonary and central venous pressures (Swan-Ganz catheter inserted via the left jugular vein) were measured with fluid filled catheters connected to pressure transducers. Cardiac output was determined periodically by thermodilution, each value being an average of four individual determinations. Stroke index (SI), cardiac index (CI), systemic vascular resistance index (SVRI) and right (RVSWI) and left (LVSWI) ventricular stroke work indices were calculated by use of standard formulae (Keefer & Barash, 1985). A triple lumen catheter was placed in the right femoral vein for infusion of the test drugs, administration rates being controlled by Harvard infusion pumps. A left coronary artery catheter (8F; 3.5 cm) was advanced via the left femoral artery and guided by fluoroscopy so that the tip was positioned in the left coronary ostium. This was confirmed by

the injection of contrast medium. The heart was exposed via a medial thoracotomy and suspended in a pericardial cradle. A purse-string suture was placed in the apex of the left ventricle and a Konigsberg pressure transducer was inserted via a stab-wound incision to measure left ventricular (LV) pressure. This signal was differentiated to yield LV *dP/dt*. Following instrumentation of the animal, a 60 min period was allowed for optimization of fluid status, serum K^+, blood gases and pH. Preload was standardized to a pulmonary capillary wedge pressure (PCWP) of 7 to 10 mmHg by infusion of dextran 70 in 0.9% NaCl. Corrections were made at this stage and stability attained before cardiac failure was initiated.

Induction of left ventricular dysfunction

Initial baseline values were recorded 60 min after instrumentation and repeated every 10 min for 30 min to evaluate the stability of the experimental preparations. The last two sets of baseline values were designated C_1 and C_2, respectively. Acute LV dysfunction was then induced over the following 50 to 60 min. Glass microspheres with a diameter of 47 to 53 μm, were diluted in dextran 70 to make a final concentration of 6.6 mg ml^{-1} (about 24,000 beads ml^{-1}) and were injected into the left coronary artery. Beads were administered every 5 min, the first three doses in 10 ml volumes followed by 5 ml boluses. After the first 20 to 30 ml, each injection was accompanied by a decrease in LV *dP/dt* and an increase in left ventricular end diastolic pressure (LVEDP). The level of functional impairment was controlled by incremental bead administration that continued until LV *dP/dt* was decreased by 25% or LVEDP was increased to approximately 15 mmHg. Haemodynamic values were again measured every 10 min for 30 min (F_1 to F_4) to determine the stability of the failure state. On satisfying our criteria for stability (see below), graded doses of AMP (100 to 2000 μg kg^{-1} min^{-1}) or SNP (0.5 to 10 μg kg^{-1} min^{-1}) were infused for periods of 10 min. Each animal received both AMP and SNP in a crossover design, and the order of drug administration was randomized. To avoid the compounding effect of hypotension, drug infusions were terminated if MAP decreased below 80 mmHg.

Following completion of the infusion of the first vasodilator, a period of 30 min was allowed to ensure the continued stability of the preparation. Further control values were taken during this period (F_5 to F_6) and only animals with haemodynamic parameters that were within 10% of the F_4 values received the second vasodilator.

Following completion of the infusion of the second vasodilator, a final set of haemodynamic values was obtained (F_7) and the animal excluded if these values differed by more than 20% from corresponding F_4 values.

Statistical analysis

Data are presented as mean ± s.e.mean. The significance of the differences between haemodynamic variables after the induction of LV dysfunction and those in the presence of graded doses of each vasodilator were determined by multivariate analysis of variance (MANOVA). If statistical significance was established, the effects of individual concentrations of each vasodilator were further analysed by Wilcoxan signed-rank tests for paired data. Potential crossover effects resulting from the order of vasodilator administration were also analysed by MANOVA. Differences were judged to be statistically significant when $P < 0.05$.

Chemicals and drugs

Adenosine 5'-monophosphate (sodium salt, isolated from yeast) was dissolved in 0.9% NaCl to a final concentration of 15 mg ml^{-1} for infusion. Sodium nitroprusside was dissolved in 5% dextrose in water to a final concentration of 200 μg ml^{-1} and was protected from light with aluminium foil. Both drugs were purchased from Sigma Chemical Co.

Results

Two animals were excluded from the study. One developed significant ventricular dysrhythmias and instability following the induction of acute LV dysfunction. Subsequent analysis of serum K^+ in this animal revealed a hypokalaemic state ($K^+ < 3$ mM). All other animals received KCl intravenously in order to maintain serum K^+ levels > 4 mM. This appeared to contribute to normal cardiac rhythms following the induction of LV dysfunction. A second animal died in ventricular fibrillation during placement of the left coronary artery catheter, possibly due to coronary artery occlusion. Initial baseline measurements in the remainder ($n = 12$) indicated that the animals were in a stable haemodynamic state before the induction of LV dysfunction.

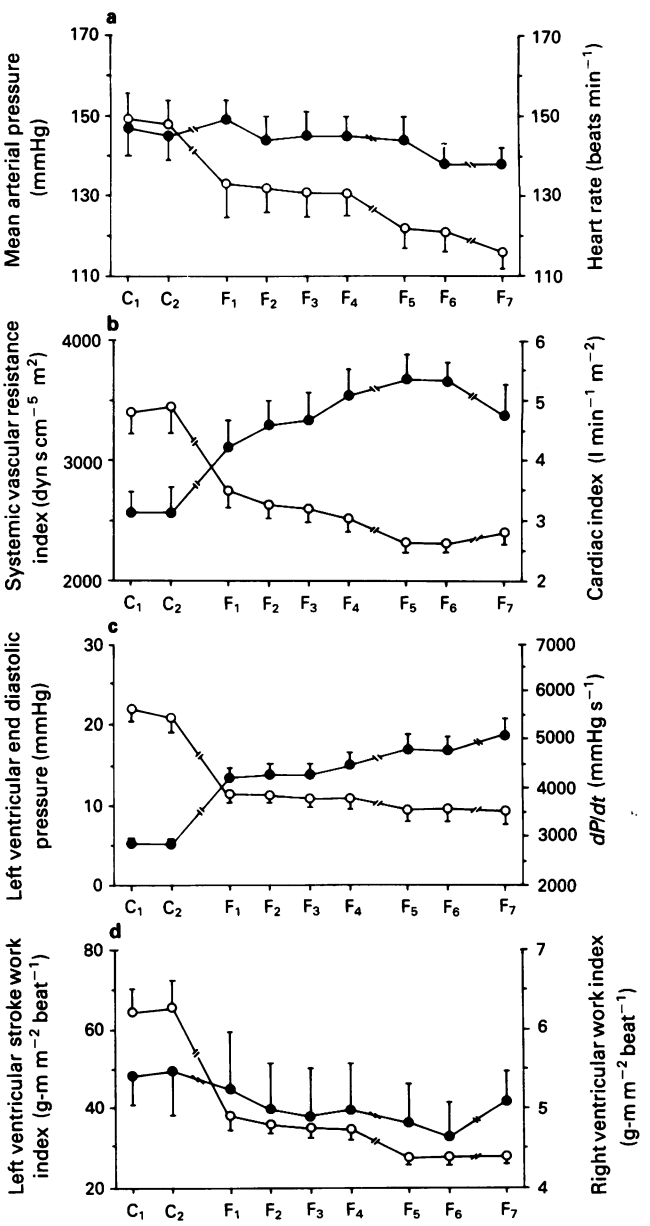


Figure 1 Haemodynamic values (a) mean arterial pressure (MAP, ○) and heart rate (HR, ●); (b) systemic vascular resistance index (SVRI, ●) and cardiac index (CI, ○); (c) left ventricular end diastolic pressure (LVEDP, ●) and LV *dP/dt* (○); (d) right (RVSWI, ●) and left (LVSWI, ○) ventricular stroke work indices before (C_1, C_2) and after (F_1 to F_7) induction of left ventricular (LV) dysfunction in pentobarbitone anaesthetized dogs. Graded doses of the vasodilators were infused in a randomized crossover design between F_4 and F_5 and between F_6 and F_7.

Table 1 Haemodynamic parameters before (C_2) and after (F_4) the induction of failure and at the end of the experimental protocol (F_7)

	Baseline	*LV dysfunction*	
	(C_2)	(F_4)	(F_7)
HR	145 ± 6	144 ± 5	137 ± 4
MAP	148 ± 6	131 ± 6**	116 ± 4***
LVSP	174 ± 7	153 ± 6**	142 ± 7**
LVEDP	5.0 ± 0.4	14.9 ± 1.5***	18.4 ± 2.2***
CI	4.9 ± 0.4	3.1 ± 0.3***	2.8 ± 0.2***
SVRI	2570 ± 210	3530 ± 240***	3370 ± 260***
LV *dP/dt*	5420 ± 300	3780 ± 700***	3520 ± 260***
LVSWI	66 ± 7	34 ± 3***	28 ± 2***
RVSWI	5.5 ± 0.6	5.0 ± 0.6	5.1 ± 0.4

Values are means ± s.e.mean, $n = 12$. HR, heart rate (beats min^{-1}); MAP, mean arterial pressure (mmHg); LVSP, left ventricular systolic pressure (mmHg); LVEDP, left ventricular end diastolic pressure (mmHg); CI, cardiac index ($l\,min^{-1}\,m^{-2}$); SVRI, systemic vascular resistance index (dyn $s\,cm^{-5}\,m^2$); LVSWI, left ventricular stroke work index ($g\text{-}m\,m^{-2}$ $beat^{-1}$); RVSWI, right ventricular stroke work index ($g\text{-}m\,m^{-2}$ $beat^{-1}$). Asterisks indicate P values for differences from baseline (C_2): ** $0.01 > P > 0.001$; *** $P < 0.001$. No significant differences were found between haemodynamic parameters at F_4 and F_7.

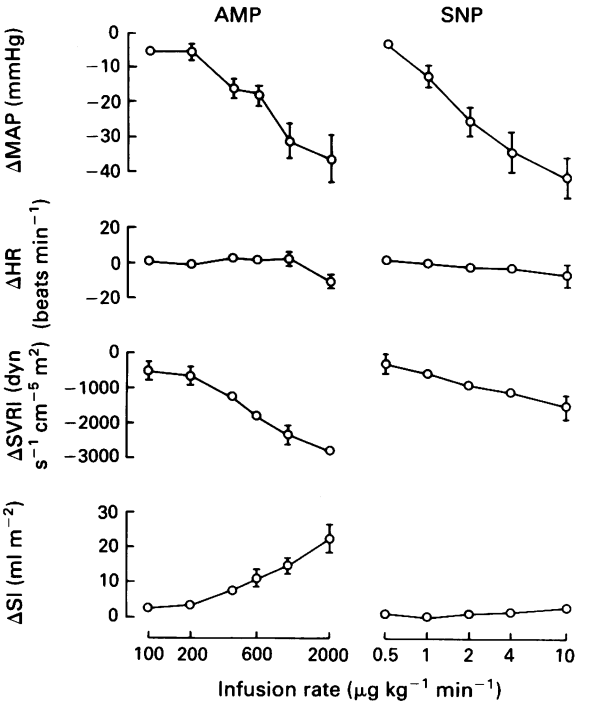


Figure 2 Changes in mean arterial pressure (Δ MAP), heart rate (Δ HR), systemic vascular resistance index (Δ SVRI) and stroke index (Δ SI) produced by graded infusions of adenosine 5'-monophosphate (AMP, 100 to 2000 $\mu g\,kg^{-1}\,min^{-1}$) and sodium nitroprusside (SNP, 0.5 to 10 $\mu g\,kg^{-1}\,min^{-1}$) in dogs with acute left ventricular (LV) dysfunction.

Microbead administration into the left coronary artery produced step-wise increases in LVEDP from 5 to 15 mmHg ($P < 0.001$) and decreases in LV *dP/dt* and CI to 63% ($P < 0.001$) and 58% ($P < 0.001$) of baseline, respectively (Figure 1). Mean arterial pressure (MAP) fell by 11% ($P < 0.01$) while SVRI increased by 37% ($P < 0.001$). Ventricular dysfunction was limited, as expected, to the left side; RVSWI remained close to baseline values ($P > 0.05$) while LVSWI fell by 48% ($P < 0.001$). Heart rate did not change ($P > 0.05$). The haemodynamic state in these animals was relatively stable (Figure 1, Table 1). Following completion of the vasodilator dose-response studies, approximately 180 min after the induction of LV dysfunction (F_7), further small decreases in LV *dP/dt* and CI had occurred (to 60% and 55% of baseline, respectively). Haemodynamic parameters at F_7 were not significantly different from those at F_4. Crossover analysis indicated that the order of vasodilator administration has no significant effect on final haemodynamic parameters.

AMP (100 to 2000 $\mu g\,kg^{-1}\,min^{-1}$) and SNP (0.5 to 10 $\mu g\,kg^{-1}\,min^{-1}$) decreased systemic mean arterial pressure ($0.01 > P > 0.001$ and $P < 0.001$, respectively) by a similar extent and in a dose-dependent manner (Figure 2). In some animals, the higher infusion rates of each vasodilator reduced MAP to below 80 mmHg at which point drug infusions were terminated. Data were only included in the analysis if the infusion was completed in five or more animals. Heart rate was not significantly altered by either vasodilator. SVRI decreased by up to 72% ($P < 0.001$) and 38% ($0.01 > P > 0.001$) in response to AMP and SNP, respectively. Stroke index was unchanged during SNP administration ($P > 0.1$) whereas significant ($P < 0.001$) increases were induced by AMP (Figure 2). At infusion rates that caused approximately equivalent decreases in MAP (Table 2), CI was significantly increased by AMP (400 $\mu g\,kg^{-1}\,min^{-1}$) by 42% ($0.01 > P > 0.001$) whereas during SNP administration (4 $\mu g\,kg^{-1}\,min^{-1}$) CI changed by 17% ($P > 0.1$). When compared at equieffective vasodilator doses over a range of infusion rates (Figure 3), AMP-induced increases in CI were greater ($P < 0.01$) than those during SNP

Table 2 Comparison of the effects of approximately equi-effective hypotensive doses of adenosine monophosphate (AMP) and sodium nitroprusside (SNP) during acute left ventricular (LV) dysfunction in anaesthetized dogs

	AMP (400 $\mu g\,kg^{-1}\,min^{-1}$) ($n = 10$)			*SNP* (4 $\mu g\,kg^{-1}\,min^{-1}$) ($n = 7$)		
	Pre-	Post-	*P*	Pre-	Post-	*P*
HR	139 ± 5	142 ± 6	NS	155 ± 5	153 ± 4	NS
MAP	125 ± 5	109 ± 7	0.004	142 ± 7	108 ± 7	0.016
LVSP	143 ± 6	135 ± 8	NS	165 ± 7	129 ± 9	0.016
LVEDP	16.0 ± 1.4	16.1 ± 1.8	NS	18.6 ± 1.8	10.2 ± 1.9	0.03
CI	2.8 ± 0.2	4.0 ± 0.4	0.006	3.29 ± 0.3	3.4 ± 0.2	NS
SI	20.1 ± 3.1	27.7 ± 8.0	0.010	21.1 ± 1.9	22.1 ± 1.5	NS
SVRI	3600 ± 250	2380 ± 310	0.002	3550 ± 310	2540 ± 200	0.016
LV*dP/dt*	3730 ± 270	3950 ± 440	NS	4210 ± 130	3690 ± 400	NS
LVSWI	30 ± 2	35 ± 3	NS	37 ± 4	30 ± 3	NS
RVSWI	5.0 ± 0.5	6.8 ± 0.8	0.004	5.8 ± 0.9	3.8 ± 0.6	0.016

Values are means ± s.e.mean for n observations. HR, heart rate (beats min^{-1}); MAP, mean arterial pressure (mmHg); LVSP, left ventricular systolic pressure (mmHg); LVEDP, left ventricular end diastolic pressure (mmHg); CI, cardiac index ($l\,min^{-1}\,m^{-2}$); SI, stroke index ($ml\,m^{-2}$); SVRI, systemic vascular resistance index (dyn $s\,cm^{-5}\,m^2$); LVSWI, left ventricular stroke work index ($g\text{-}m\,m^{-2}\,beat^{-1}$); RVSWI, right ventricular stroke work index ($g\text{-}m\,m^{-2}\,beat^{-1}$). *P* values for differences between pre- and post-drug parameters were estimated by two tailed Wilcoxan signed rank tests for paired data; NS, not significant.

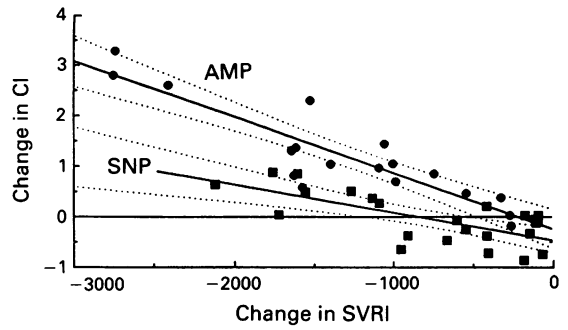


Figure 3 Comparison of the effect of sodium nitroprusside (SNP, ■) with that of adenosine monophosphate (AMP, ●) on the cardiac index (CI) of anaesthetized dogs with acute left ventricular (LV) dysfunction. Changes in CI are plotted against associated changes in systemic vascular resistance index (SVRI). At infusion rates that induced equivalent reduction in SVRI, CI was increased more by AMP than by SNP. Points represent individual values obtained with three doses of each vasodilator in each of 12 dogs. The hatched lines show 95% confidence intervals.

administration. AMP was significantly less effective in reducing preload. PCWP and LVEDP were unaltered by AMP ($P > 0.01$) whereas SNP significantly ($0.05 > P > 0.01$) reduced both of these parameters (Figure 4). Although adenosine receptor stimulation has been associated with negative inotropic effects, no cardiac depression, as evidenced by alterations in LV *dP/dt*, was demonstrable ($P > 0.05$). RVSWI was increased by AMP ($P < 0.001$) and SNP ($0.01 > P > 0.001$), whereas LVSWI (Figure 4) was unaltered by either vasodilator ($P > 0.1$).

Discussion

In the presence of acute LV dysfunction, AMP infusion produced significantly greater increases in cardiac and stroke indices than SNP when compared at equivalent afterload

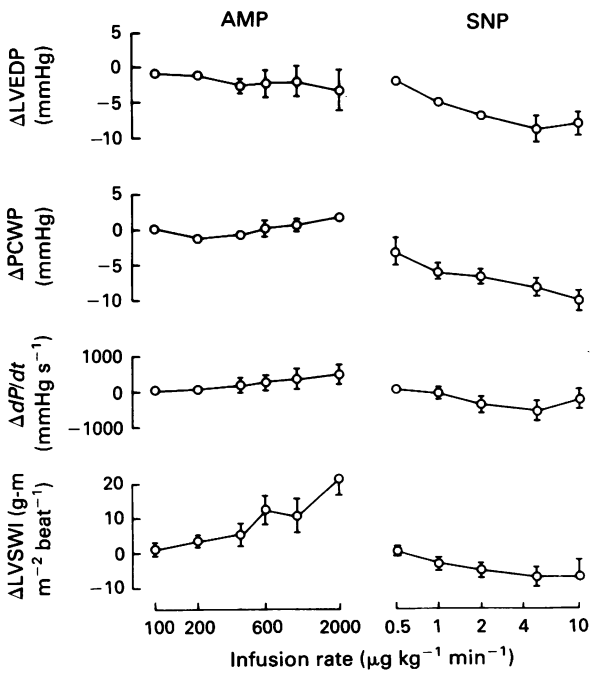


Figure 4 Changes in left ventricular end diastolic pressure (Δ LVEDP), pulmonary capillary wedge pressure (Δ PCWP), LV *dP/dt* (Δ *dP/dt*) and left ventricular stroke work index (Δ LVSWI) produced by graded infusions of adenosine monophosphate (AMP, 100 to 2000 $\mu g\,kg^{-1}\,min^{-1}$) and sodium nitroprusside (SNP, 0.5 to 10 $\mu g\,kg^{-1}\,min^{-1}$) in dogs with acute left ventricular dysfunction.

reducing doses. This significant haemodynamic benefit of AMP-induced afterload reduction in this model suggests that AMP may have advantages over SNP in the pharmacological management of acute, low output cardiac failure.

The model of acute LV dysfunction used in this study was based on that described by Smiseth & Mjos (1982) and used extensively by others (e.g. Vik-Mo *et al.*, 1985; Reikeras & Gunnes, 1986). Acute LV dysfunction was produced by a relatively simple and reproducible method that involved the administration of glass microbeads into the left coronary artery. This embolization procedure produces numerous small infarcts throughout the LV as the spheres lodge within small arteries and arterioles. The severity of global ischaemia was controlled by the step-wise administration of microbeads until LVEDP rose to 12 to 16 mmHg or LV *dP/dt* decreased by 20 to 25%. The resulting haemodynamic state was relatively stable and was similar to acute, low output cardiac failure characterized by depressed cardiac output and LV *dP/dt* and elevated SVRI and LVEDP. In preliminary experiments, the embolization procedure induced significant abnormalities in cardiac rhythm, particularly multiple ventricular ectopic beats. Careful attention to serum K^+ levels and administration of K^+ supplements to maintain serum K^+ within the range of 4 to 5 mM prevented cardiac instability. Lignocaine, which has been used by others to maintain ventricular stability in this model (Reikeras & Gunnes, 1986), was not required in these experiments, thus avoiding any adenosine-lignocaine interactions (Homeister *et al.*, 1990). Following the induction of failure, a window of at least 180 min was available for assessing drug interventions; no significant deterioration was noted in haemodynamic parameters following recovery from the second vasodilator (F_7) relative to those following the induction of failure (F_4). The vasodilators were administered in a randomized, crossover design, and no influences of the order of vasodilator administration were detectable. This would not be unexpected considering the rapid elimination of these drugs.

Most of the effects of AMP were likely to have been mediated by adenosine receptor stimulation because AMP is rapidly dephosphorylated to adenosine by 5'-nucleotidase located on the plasma membrane of many cells, including vascular endothelial cells (Pelleg *et al.*, 1987; Coade & Pearson, 1989). AMP was, therefore, acting mainly as a soluble adenosine pro-drug.

Both vasodilators reduced MAP and increased CI, but at infusion rates that caused equivalent decreases in SVRI, AMP was more effective than SNP in elevating CI. These data are consistent with our previous study in normal anaesthetized dogs (Finegan *et al.*, 1990). Differences in the arterial and venous selectivity of AMP and SNP, as revealed by their effects on LVEDP and PCWP, most likely contributed to their differing effects on CI. SNP causes both arterial and venous smooth relaxation (Tinker *et al.*, 1976), so SNP-induced reductions in preload and end-diastolic volume may have limited the expected increase in CI. AMP, like adenosine (Solevi, 1986), acted as a selective arterial vasodilator and did not decrease either LVEDP or PCWP. While the absence of significant reductions in preload would be a disadvantage in the management of heart failure, a combination of a selective venodilator, e.g., GTN and AMP would allow preload and afterload to be adjusted independently thus offering advantages over SNP.

Thus, AMP affects the systemic circulation in a manner similar to hydralazine (Verma *et al.*, 1987). In patients with acute cardiac failure secondary to myocardial infarction, hydralazine-induced afterload reduction resulted in a greater and more pronounced increase in cardiac output than that induced by the venodilator, isosorbide dinitrate (Nelson *et al.*, 1983). However, the long duration of action of hydralazine with the attendant difficulty in controlling the plasma concentration and obtaining the desired response severely curtails its use in the treatment of acute cardiac failure. AMP and adenosine have pharmacokinetic profiles similar to SNP and GTN,

thereby facilitating both administration by infusion and afterload control.

Adenosine A_1 receptor stimulation depresses cardiac contractility *in vitro* (Evans *et al.*, 1982) but no evidence of myocardial depression, as assessed by LV *dP/dt* measurements, was observed at the dose levels used in this study. This is supported by a recent detailed assessment of the effects of adenosine on systolic and diastolic LV performance in normal conscious dogs (Freeman *et al.*, 1990). More detailed analysis of the actions of AMP on ischaemic myocardium will require assessment by afterload-independent indices of myocardial contractility. Nevertheless, AMP, but not SNP, increased CI and SI in the present study. This apparent reversal of myocardial depression by AMP may have resulted from either adenosine-induced coronary hyperaemia and/or the catabolism of AMP to inosine. This nucleoside increases the contractility of normal and ischaemic myocardium (Czarnecki & Noble, 1983) and has resulted in haemodynamic improvement in patients with cardiogenic shock (Czarnecki & Czarnecki, 1989).

Cardiac metabolism may also be favourably affected by AMP. Afterload reduction for the failing heart redirects energy into increasing the volume of blood pumped by the heart rather than into developing pressure (Chatterjee *et al.*, 1976). AMP lowered afterload and increased cardiac output, but the energy cost of this enhanced output was not measured. Interestingly, adenosine increases the efficiency of myocardial O_2 consumption in perfused hearts *in vitro* (Headrick & Willis, 1989) and exogenous inosine, in an ischaemic LV failure model similar to that used in the present study, enhanced cardiac contractility without altering cardiac levels of high energy phosphates (Smiseth, 1983).

Heart rate considerations also indicate that AMP may have advantages over SNP or hydralazine. Adenosine (and presumably AMP) decrease SA nodal depolarization (Szentmiklosi, 1980) and so should attenuate any reflex tachycardia in response to decreases in arterial pressure. However, in the present study heart rate was not changed by AMP or SNP. The profound sympathoadrenal stimulation in response to cardiac failure and the lack of attenuation of baroreceptor reflexes in the presence of pentobarbitone anaesthesia seems to have masked any direct negative chronotropic effects of AMP. In our previous study in normal dogs anaesthetized with a combination of pentobarbitone and fentanyl (Finegan *et al.*, 1990), baseline heart rates were lower (approximately 90 beats min^{-1}) and reflex tachycardia in response to graded reductions in MAP were less during the administration of AMP than SNP. Also, adenosine-induced hypotension is associated with less tachycardia than that induced by SNP (Fukunaya *et al.*, 1982) or GTN (Hintze *et al.*, 1985).

Malignant ectopic pacemaker activity, that frequently coexists with acute cardiac failure, was not observed in this model so the antidysrythmic activity of AMP and SNP could not be compared. Other studies have shown that adenosine reduces reperfusion dysrythmias following ischaemia in dogs (Wainright & Parratt, 1988) and so adenosine agonists may possess beneficial antidysrythmic properties in acute heart failure.

Extensive clinical data are available on the cardiovascular effects resulting from adenosine receptor stimulation (see reviews by Sollevi, 1986; Belardinelli, 1989). Dose-dependent decreases in SVR and increases in cardiac output have been observed in conscious subjects (Bush *et al.*, 1989), but reflexly-mediated increases in heart rate occur, and at higher doses, subjective symptoms such as nausea and pain, may limit the clinical utility of adenosine (Edlund *et al.*, 1989). Clinical evaluations of AMP have not been reported.

This study has shown that, in a canine model of acute LV dysfunction, AMP reduces afterload and increases cardiac output in an easily controllable manner. Studies are underway to examine potential advantages of more selective adenosine A_1 and A_2 agonists either when used alone or in combination with positive inotropic agents and/or selective venodilators such as GTN when both afterload and preload can be altered independently to suit clinical circumstances.

We thank Dr C. Coulson for her assistance with the statistical analysis of the data. Supported by grant (MA-11037) from MRC (Canada).

References

BABBIT, D.G., VIRMANI, R. & FORMAN, M.B. (1989). Intracoronary adenosine administered after reperfusion limits vascular injury after prolonged ischemia in the canine model. *Circulation*, **80**, 1388–1399.

BELARDINELLI, L., LINDEN, J. & BERNE, R.M. (1989). The cardiac effects of adenosine. *Prog. Cardiovasc. Dis.*, **32**, 73–97.

BUSH, A., BUSST, C.M., CLARKE, B. & BARNES, P.J. (1989). Effect of infused adenosine on cardiac output and systemic vascular resistance in normal subjects. *Br. J. Clin. Pharmacol.*, **27**, 165–171.

CHATTERJEE, K., SWAN, H.J., KAUSHIK, V.S., JOBIN, G., MAGNUSSON, P. & FORRESTER, J.S. (1976). Effects of vasodilator therapy for severe pump failure in acute myocardial infarction on short-term and late prognosis. *Circulation*, **53**, 797–802.

COADE, S.B. & PEARSON, S.D. (1989). Metabolism of adenine nucleotides in human blood. *Circ. Res.*, **65**, 531–537.

COLLIS, M.G. (1989). The vasodilator role of adenosine. *Pharmacol. Ther.*, **41**, 143–162.

CZARNECKI, W. & CZARNECKI, A. (1989). Haemodynamic effects of inosine. A new drug for the failing human heart? *Pharmacol. Res.*, **21**, 587–594.

CZARNECKI, W. & NOBLE, M.I.M. (1983). Mechanisms of the inotropic action of inosine on canine myocardium. *Cardiovasc. Res.*, **12**, 735–739.

DI MARCO, J.P., SELLERS, T.D., WEST, G.A. & BELARDINELLI, L. (1983). Adenosine: electrophysiologic effects and therapeutic use for terminating paroxysmal supraventricular tachycardia. *Circulation*, **68**, 1254–1258.

EDLUND, A., STRAAT, E. & HENRIKSSON, P. (1989). Infusion of adenosine provokes myocardial ischaemia in patients with ischaemic heart disease. *Clin. Physiol.*, **9**, 307–311.

EVANS, D.B., SCHENDEN, J.A. & BRISTOL, J.A. (1982). Adenosine receptors mediating cardiac depression. *Life Sci.*, **31**, 2425–2432.

FINEGAN, B.A., CHEN, H-J., SINGH, Y.N. & CLANACHAN, A.S. (1990). Comparison of hemodynamic changes induced by adenosine monophosphate and sodium nitroprusside alone and during dopamine infusion in the anesthetized dog. *Anesth. Analg.*, **70**, 44–52.

FINEGAN, B.A. & CLANACHAN, A.S. (1990). Comparison of the haemodynamic effects of SNP and AMP following acute microsphere-induced ischaemic ventricular dysfunction. *Can. J. Anaesth.*, **37**, S149.

FORD, L.E. (1980). Effect of afterload reduction on myocardial energetics. *Circ. Res.*, **46**, 161–166.

FREEMAN, G.L., COLSTON, J.T. & HULTMAN, J. (1990). Influence of adenosine on left ventricular performance in conscious dogs. *Am. J. Physiol.*, **258**, H424–H430.

FUKUNAYA, A.G., FLACKE, W.E. & BLOOR, B.C. (1982). Hypotensive effects of adenosine and adenosine triphosphate compared with sodium nitroprusside. *Anesth. Analg.*, **61**, 273–278.

GRUBER, H.E., HOFFER, M.E., MCALLISTER, D.R., LAIKIND, P.K., LANE, T.A., SCHMID-SCHOENBEIN, G.W. & ENGLER, R.L. (1989). Increased adenosine concentration in blood from ischemic myocardium by AICA riboside. Effects on flow, granulocytes and injury. *Circulation*, **80**, 1400–1411.

HEADRICK, J. & WILLIS, R.J. (1989). Endogenous adenosine improves work rate to oxygen consumption ratio in catecholamine stimulated isovolumic rat heart. *Pflügers Arch.*, **413**, 354–358.

HINTZE, T.H., BELLONI, F.L., HARRISON, J.E. & SHAPIRO, G.C. (1985). Apparent reduction in baroreflex sensitivity to adenosine in conscious dogs. *Am. J. Physiol.*, **249**, 4554–4559.

HOMEISTER, J.W., HOFF, P.T., FLETCHER, D.D. & LUCCHESI, B.R. (1990). Combined adenosine and lidocaine administration limits myocardial reperfusion injury. *Circulation*, **82**, 595–608.

KEEFER, J.R. & BARASH, P.G. (1985). Pulmonary artery catheterization. In *Monitoring in Anesthesia and Critical Care Medicine*. ed. Blitt, C.D. pp. 177–228. New York: Churchill Livingstone.

LAGERKRANSER, M., SOLLEVI, A., IRESTAST, L., TIDGREN, B. &

ANDREEN, M. (1985). Renin release during controlled hypotension with sodium nitroprusside, nitroglycerin and adenosine: a comparative study in the dog. *Acta Anesthesiol. Scand.*, **29**, 45–59.

LEDINGHAM, S., KATAYAMA, O., LACHNO, D., PATEL, N. & YACOUB, M. (1990). Beneficial effect of adenosine during reperfusion following prolonged cardioplegic arrest. *Cardiovasc. Res.*, **24**, 247–253.

NELSON, G.I.C., AHUJA, R.C., SILKE, B., HUSSAIN, M. & TAYLOR, S.H. (1983). Arteriolar or venous dilation in left ventricular failure following acute myocardial infarction: A haemodynamic trial of hydralazine and isosorbide dinitrate. *J. Cardiovasc. Pharmacol.*, **5**, 574–579.

OWALL, A., GORDON, E., LAGERKRANSER, M., LINDQUIST, C., RUDEHILL, A. & SOLLEVI, A. (1987). Clinical experience with adenosine for controlled hypotension during cerebral aneurysm surgery. *Anesth. Analg.*, **66**, 229–234.

PELLEG, A., MITSUOKA, T. & MICHELSON, E.L. (1987). Adenosine mediates the negative chronotropic action of adenosine 5'-triphosphate in the canine sinus node. *J. Pharmacol. Exp. Ther.*, **242**, 791–795.

REIKERAS, O. & GUNNES, P. (1986). Renal blood flow during acute ischaemic heart failure in dogs: effects of dopamine and high doses of insulin. *Scand. J. Clin. Lab. Invest.*, **46**, 671–675.

SMISETH, O.A. (1983). Inosine infusion in dogs with acute ischaemic left ventricular failure: favourable effects on myocardial performance and metabolism. *Cardiovasc. Res.*, **17**, 192–199.

SMISETH, O.A. & MJOS, O.D. (1982). A reproducible and stable model of acute ischemic left ventricular failure in dogs. *Clin. Physiol.*, **2**, 225–239.

SOLLEVI, A. (1986). Cardiovascular effects of adenosine in man: possible clinical implications. *Prog. Neurobiol.*, **27**, 319–349.

SZENTMIKLOSI, A.J. (1980). Effect of adenosine on sinoatrial and ventricular automaticity of the guinea pig. *Naunyn Schmiedebergs Arch. Pharmacol.*, **311**, 147–149.

TINKER, J.H. & MICHENFELDER, J.D. (1976). Sodium nitroprusside: pharmacology, toxicology and therapeutics. *Anesthesiology*, **45**, 340–354.

VERMA, S.P., SILKE, B., HUSSAIN, M., NELSON, G.I., REYNOLDS, G.W., RICHMOND, A. & TAYLOR, S.H. (1987). First-line treatment of left ventricular failure complicating acute myocardial infarction: a randomized evaluation of immediate effects of diuretic, venodilator, arteriodilator and positive inotropic drugs on left ventricular function. *J. Cardiovasc. Pharmacol.*, **10**, 38–46.

VIK-MO, H., YASAY, G., MAROKO, P.R. & RIBEIRO, L.G.T. (1985). Comparative effects of dobutamine and corwin, a β_1-adrenergic partial agonist, in experimental left ventricular failure. *J. Cardiovasc. Pharmacol.*, **7**, 784–790.

WAINWRIGHT, C.L. & PARRATT, J.R. (1988). An antiarrhythmic effect of adenosine during myocardial ischaemia and reperfusion. *Eur. J. Pharmacol.*, **145**, 183–194.

(Received January 2, 1991
Revised February 25, 1991
Accepted March 11, 1991)

Br. J. Pharmacol. (1991), **103**, 1697–1702 © Macmillan Press Ltd, 1991

Effects of pinacidil on contractile proteins in high K^+-treated intact, and in β-escin-treated skinned smooth muscle of the rabbit mesenteric artery

[1]Takeo Itoh, Satoshi Suzuki & Hirosi Kuriyama

Department of Pharmacology, Faculty of Medicine, Kyushu University, Fukuoka 812, Japan

1 The effects of pinacidil were investigated on changes in cellular Ca^{2+} concentration ($[Ca^{2+}]_i$) and tension in intact and chemically skinned smooth muscle strips of the rabbit mesenteric artery.

2 High K^+ (128 mM) produced a large phasic followed by a tonic increase in $[Ca^{2+}]_i$ and tension in intact muscle strips. Pinacidil at 10 μM but not 1 μM, inhibited the phasic and tonic contractions induced by 128 mM K^+ without a corresponding change in $[Ca^{2+}]_i$.

3 In β-escin-treated skinned smooth muscle, the minimum Ca^{2+} concentration that produced contraction was 0.1 μM and the maximum contraction was obtained at 10 μM. Pinacidil at 10 μM but not 1 μM, shifted the pCa-tension relation curve to the right and also inhibited the maximum contraction induced by Ca^{2+}. The concentrations of Ca^{2+} required for half maximal tension were 0.9 μM in control and 1.5 μM in the presence of 10 μM pinacidil. Calmodulin (2 μM) increased the contraction induced by 0.3 μM Ca^{2+} (but not by 10 μM Ca^{2+}) in the skinned strips. Pinacidil (10 μM) inhibited the contraction induced by 0.3 μM or 10 μM Ca^{2+} in the presence of 2 μM calmodulin.

4 Noradrenaline (NA, 10 μM) with guanosine triphosphate (GTP, 3 μM), guanosine 5'-O-(3-thiotriphosphate) (GTPγS, 3 μM) or 12-O-tetradecanoylphorbol-13-acetate (TPA, 0.1 μM) all enhanced the contraction induced by 0.3 μM Ca^{2+}. Pinacidil (10 μM) inhibited the contraction induced by 0.3 μM Ca^{2+} more strongly in the presence of the above agents than in their absence.

5 Following application of 2 mM adenosine-5'-O-(3-thiotriphosphate) (ATPγS) with 0.3 μM Ca^{2+}, 4 mM MgATP produced contraction in skinned strips in Ca^{2+}-free solution containing 4 mM EGTA ('Ca^{2+}-independent contraction'). The amplitude of the Ca^{2+}-independent contraction was almost the same as that obtained with 10 μM Ca^{2+}. Pinacidil (10 μM) had no effect on the amplitude of the Ca^{2+}-independent contraction nor did it have any effect on the contraction induced by a solution containing no MgATP ('rigor contraction').

6 It is concluded that pinacidil (10 μM) acts directly on the contractile apparatus to inhibit Ca^{2+}-induced contraction in smooth muscle of the rabbit mesenteric artery. The site of action of pinacidil may be between Ca^{2+}-calmodulin complex formation and phosphorylation of the myosin light chain.

Keywords: Pinacidil; skinned smooth muscle; cellular Ca^{2+} concentration; rabbit mesenteric artery; contractile proteins; high K^+

Introduction

Pinacidil ((±)-N-cyano-4-pyridyl-N-1,2,2-trimethyl-propyl-guanodine monohydrate) is a novel vascular relaxant which hyperpolarizes the membrane of vascular smooth muscle cells at concentrations between 0.1 μM and 10 μM, in a concentration-dependent manner (Southerton *et al.*, 1988; Videbaek *et al.*, 1988; Quast & Cook, 1989; Standen *et al.*, 1989; Nakashima *et al.*, 1991). These authors suggested that the membrane hyperpolarization inhibits the vasospasmogenic agent-induced contraction by increasing the threshold for activation of the voltage-dependent Ca^{2+} channel. In our preliminary experiments, however, we found that pinacidil, in concentrations over 10 μM, inhibited the contractions induced by 128 mM K^+ in smooth muscle strips of the rabbit mesenteric artery. Glibenclamide, an inhibitor of the ATP-sensitive K^+ channel, did not modify this action of pinacidil. Since under these conditions pinacidil cannot produce membrane hyperpolarization in smooth muscle cells (Nakashima *et al.*, 1991), this suggested that an effect of pinacidil other than its membrane hyperpolarizing action may underlie its inhibition of high K^+-induced contraction.

To clarify the action of pinacidil, we studied the effects of this agent on the increases in $[Ca^{2+}]_i$ and tension induced by 128 mM K^+ in intact smooth muscle and on Ca^{2+}-induced contraction in chemically skinned muscle.

[1] Author for correspondence.

Methods

Male albino rabbits (1.9–2.5 kg) were anaesthetized by injection of pentobarbitone sodium (40 mg kg^{-1}, i.v.), and were then exsanguinated. The third branch of the mesenteric artery was excised immediately and cleaned by removal of the connective tissue in Krebs solution at room temperature. To prevent NA outflow from sympathetic nerve terminals, 3 μM guanethidine was added to the Krebs solution for over 2 h.

Ca^{2+} and tension measurement

To enable recording of isometric tension, fine circularly-cut strips (0.3–0.5 mm long, 0.04–0.05 mm wide, 0.02–0.03 mm thick) were prepared as described previously (Itoh *et al.*, 1983). Endothelial cells were removed by gentle rubbing of the internal surface of the vessels with small knives. The absence of function of the endothelial cells was confirmed by the inability of acetylcholine (1 μM) or A23187 (0.1 μM) to cause relaxation during contractions induced by NA. The strip was transferred to a chamber of 0.3 ml volume and mounted horizontally on an invert-microscope (Diaphoto TMD with special optics for epifluorescence, Nikon).

To enable loading of Fura-2 into smooth muscle cells of the strip, 1 μM acetoxy methyl ester of Fura-2 (Fura-2AM) was applied for 1 h in Krebs solution at room temperature (20–23°C). After this period, the solution containing Fura-2AM

was washed out with Krebs solution for 1 h to ensure sufficient esterification of Fura-2AM in the cells. The position of the strip was adjusted to the centre of the field with a mask placed in an intermediate image plane to reduce background fluorescence (0.04 mm square). The Fura-2 fluorescence emission at 510 nm using an interference filter (centred at 510 nm and full width at half transmission, 20 nm) was collected through the lens (20 times CF Fluor objective lens, Nikon) and collected in a photomultiplier tube (R928, side-on type, Hamamatsu Photonics, Japan) via a dichroic mirror (DM-400, Nikon) which was substituted for the photochanger in a Nikon Diaphoto-TMD microscope. Two alternative excitation wavelengths, 340 nm and 380 nm (each slit 5 nm) were applied by a spectro-fluorimeter (Spex, NJ, U.S.A.) and the data were analyzed with customized software provided by Spex (DM-3000CM).

The ratio of Fura-2 fluorescence intensities excited by 340 or 380 nm was calculated after subtraction of the background fluorescence. Background fluorescence (including the autofluorescence of the strip) as excited by 340 and 380 nm u.v.-light was obtained by application of a solution containing 50 μM ionomycin, 20 mM $MnCl_2$, 110 mM KCl and 10 mM MOPS (pH 4.8) after the experiment. Under these conditions, the background fluorescence intensity was 10–15% of the Fura-2 signals in smooth muscle strips at either excitation wave length. Cytosolic Ca^{2+} concentrations were calculated by the formula of Grynkiewicz *et al.* (1985) and using *in vitro* calibration (Poenie *et al.*, 1986; Becker *et al.*, 1989). The ratio of the maximum (F_{max}) to the minimum fluorescence (F_{min}) was determined in the calibration solution after subtraction of background excited by either 340 or 380 nm. The signals excited by 380 nm u.v.-light were assumed to decrease by 15% in the cell due to the possible intracellular viscosity effects on the dye (Becker *et al.*, 1989). The K_d value for Fura-2 was estimated to be 200 nM (Becker *et al.*, 1989). This method of calculating Ca^{2+} may not be accurate if Fura-2 binds to some proteins in the cell (Konishi *et al.*, 1988).

Experiments on chemically skinned smooth muscle

Chemically skinned smooth muscle strips were made by use of β-escin (Kobayashi *et al.*, 1989). The methods used to prepare skinned muscle and the composition of the solutions have been described elsewhere (Itoh *et al.*, 1986a; Kobayashi *et al.*, 1989). Ionomycin (1 μM) was present throughout the experiment to deplete the intracellularly stored Ca^{2+}.

Solutions

The ionic composition of the Krebs solution was as follows (mM): Na^+ 137.4, K^+ 5.9, Mg^{2+} 1.2, Ca^{2+} 2.6, HCO_3^- 15.5, $H_2PO_4^-$ 1.2, Cl^- 134 and glucose 11.5. The concentration of K^+ was modified as required by replacing NaCl with KCl, isosmotically. The calibration solution for Ca^{2+}-measurement in intact strips contained ethyleneglycol-*bis*-(β-aminoethyl)-N,N,N'N'-tetraacetic acid (EGTA) 11 mM, KCl 110 mM, $MgCl_2$ 1 mM, Fura-2 2 μM and N-2-hydroxyethylpiperazine-N'-2-ethanesulphonic acid (HEPES) (pH 7.1) 20 mM with or without $CaCl_2$ 11 mM.

For experiments on skinned muscle, the composition of the relaxing solution was (mM): potassium methanesulphonate (KMs) 87, piperazine-N-N'-bis-(2-ethanesulphonic acid) (PIPES) 20, $Mg(Ms)_2$ 5.1, ATP 5.2, phosphocreatine 10, EGTA 4 and ionomycin 1 μM. Various Ca^{2+} concentrations were prepared by adding appropriate amounts of $Ca(Ms)_2$ to 4 mM EGTA, based on the calculation given previously (Itoh *et al.*, 1986a). The pH of the solution was adjusted to 7.1 at 25°C with KOH and the ionic strength was standardized at 0.2 by changing the amount of KMs added.

To obtain a Ca^{2+}-independent contraction in the skinned strips, a solution containing ATPγS and 0.3 μM Ca^{2+} or a rigor-producing solution was used. The ATPγS solution was composed of (mM): HEPES 20, $Mg(Ms)_2$ 2.6, ATPγS 2 and EGTA 4. The ionic strength of the solution was adjusted to 0.2 M by adding KMs. The free Ca^{2+} concentration was calculated to be 0.3 μM. The composition of the rigor-producing solution was (mM): KMs 130, $Mg(Ms)_2$ 1, EGTA 4 and HEPES 2 and the pH was adjusted to 7.1 using KOH.

Drugs

Drugs used were Fura-2, Fura-2AM, EGTA, PIPES, HEPES and MOPS (Dojin), NA, guanosine triphosphate (GTP), β-escin, 12-O-tetradecanoylphorbol-13-acetate (TPA), guanosine 5'-O-(3-thiotriphosphate) (GTPγS) and glibenclamide (Sigma), guanethidine (Tokyo Kasei), ATP (Na salt, Kojin), ionomycin (Calbiochem), ATPγS (Boehringer Mannheim-Yamanouchi) and pinacidil (Shionogi).

Statistics

The values recorded were expressed as mean ± s.d., and statistical significance was determined by Student's *t* test. Probabilities less than 5% ($P < 0.05$) were considered significant.

Results

Effects of pinacidil (10 μM) on changes in cytosolic Ca^{2+} concentration ($[Ca^{2+}]_i$) and tension induced by 128 mM K^+ were observed in smooth muscle strips of the rabbit mesenteric artery. Resting $[Ca^{2+}]_i$ was 135 ± 25 nM ($n = 5$) and no spontaneous fluctuations were observed. When 128 mM K^+ was applied to the strip, $[Ca^{2+}]_i$ immediately increased to a peak within 4–5 s (phasic phase) and then decayed to a steady level (tonic phase). Following the increase in $[Ca^{2+}]_i$, tension developed with a phasic and a subsequent tonic phase (Figure 1). The levels of $[Ca^{2+}]_i$ at the peak and in the tonic phase in the presence of 128 mM K^+ were 1055 ± 134 nM and 347 ± 79 nM, respectively ($n = 4$). Pinacidil (1 or 10 μM) did not significantly modify these $[Ca^{2+}]_i$ increases induced by 128 mM K^+, although the rate of the decay of $[Ca^{2+}]_i$ following the phasic contraction was slightly accelerated (the levels of $[Ca^{2+}]_i$ at the peak and in the tonic phase in the presence of 128 mM K^+ were 1028 ± 128 nM and 360 ± 81 nM in the presence of 1 μM pinacidil and 991 ± 126 nM and 311 ± 70 nM in the presence of 10 μM pinacidil, respectively, $P > 0.05$, $n = 4$). However, pinacidil at 10 μM but not at 1 μM, significantly reduced both the phasic and tonic contractions induced

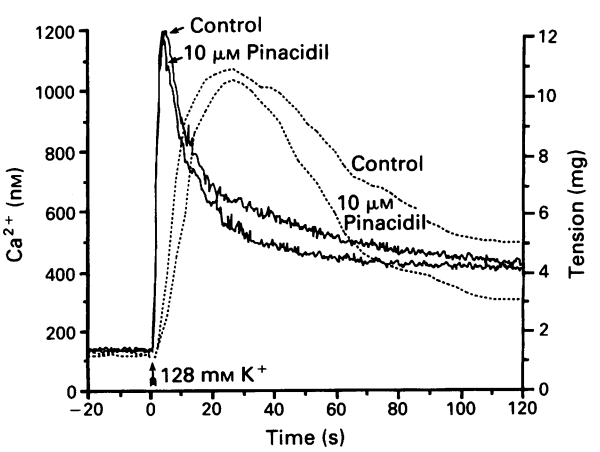


Figure 1 Effects of 10 μM pinacidil on changes in $[Ca^{2+}]_i$ and tension induced by 128 mM K^+ in smooth muscle strip of rabbit mesenteric artery. High K^+ was applied at the arrow. $[Ca^{2+}]_i$ is indicated by the continuous lines and tension by the dotted lines. Pinacidil was applied 10 min before the application of 128 mM K^+ and was present throughout the experiment. The same effect was observed in 3 other sets of experiments.

by 128 mM K^+ (the values of absolute tension at the peak and in the tonic phase in the presence of 128 mM K^+ were 11.2 ± 0.6 mg and 6.4 ± 1.1 mg in control, respectively and these were 10.9 ± 0.5 mg and 6.0 ± 2.7 mg in the presence of 1 μM pinacidil, $P > 0.05$, $n = 4$ and 9.4 ± 0.7 mg and 2.4 ± 0.4 mg in the presence of 10 μM pinacidil, respectively, $P < 0.01$, $n = 4$). The pinacidil-induced inhibition of the contraction induced by 128 mM K^+ recovered slowly after washout of this drug (42 ± 15 min was required for 80% recovery of the tonic contraction induced by 128 mM K^+, $n = 3$). Glibenclamide (1 or 10 μM) did not modify this action of pinacidil. These results suggest that pinacidil (10 μM) may inhibit the tonic contraction induced by 128 mM K^+ via its direct inhibitory action on the contractile apparatus in smooth muscle.

To investigate the direct action of pinacidil on the contractile proteins, its effect was observed on Ca^{2+}-induced contraction in the presence of 1 μM ionomycin in β-escin-treated, skinned smooth muscle strips. In the skinned strip, the minimum concentration of Ca^{2+} that produced contraction was 0.1 μM and the maximum contraction was obtained at 10 μM, as previously observed in saponin-skinned smooth muscle (Itoh *et al.*, 1983). Figure 2 shows the effects of pinacidil on contraction induced by various concentrations of Ca^{2+} (0.1–10 μM) in the skinned strips. Pinacidil (1 μM) produced no detectable effects on the pCa-tension relationship but, at 10 μM it shifted the curve to the right and reduced the maximum contraction induced by 10 μM Ca^{2+}. The concentrations of Ca^{2+} required for half maximal tension were 0.94 ± 0.4 μM in control and 1.49 ± 0.38 μM in the presence of 10 μM pinacidil ($n = 7$) and these were significantly different ($P < 0.05$). Glibenclamide (10 μM) did not affect the inhibitory action of pinacidil on the contraction induced by 0.3 μM Ca^{2+} (Figure 4a). Neomycin (0.5 mM), an inhibitor of phospholipase C, did not modify the pCa-tension relationship observed under control conditions or in the presence of 10 μM pinacidil (Figure 3).

Calmodulin shifts the pCa-tension relationship to the left

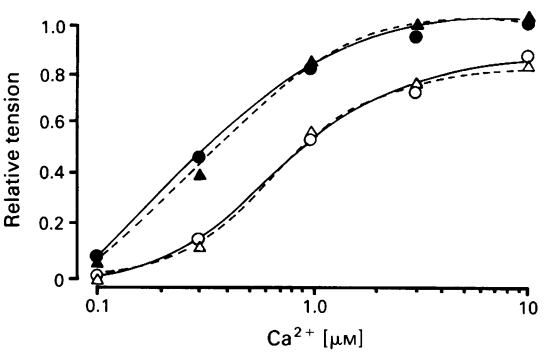


Figure 3 Effects of 0.5 mM neomycin on pCa-tension relationship in the presence or absence of 10 μM pinacidil: (●) control; (▲) in the presence of 0.5 mM neomycin; (○) in the presence of 10 μM pinacidil; (△) in the presence of 10 μM pinacidil and 0.5 mM neomycin. Continuous lines and dotted lines indicate results obtained in the absence or presence of 0.5 mM neomycin, respectively. This experiment was done using a single strip. The amplitude of contraction induced by 10 μM Ca^{2+} in the control experiment was normalized as 1.0. Similar results were obtained in another 2 strips.

(Itoh *et al.*, 1986a). To investigate the effects of calmodulin on the pinacidil-induced inhibition of the contraction induced by Ca^{2+}, the effects of 10 μM pinacidil on the contraction induced by 0.3 μM or 10 μM Ca^{2+} were observed in the presence of 2 μM calmodulin. Calmodulin (2 μM) increased the contraction induced by 0.3 μM Ca^{2+} (1.5 times control, see Figure 4a) but had no effect on the contraction induced by 10 μM Ca^{2+} (1.06 ± 0.04 times the control, $n = 4$). Pinacidil (10 μM) inhibited the contraction induced by either 0.3 μM or 10 μM Ca^{2+} in the presence of 2 μM calmodulin (Figure 4). The extent of the pinacidil-induced inhibition of the contraction induced by 10 μM Ca^{2+} was identical whether or not 2 μM calmodulin was present although the same concentration of calmodulin did slightly inhibit the action of pinacidil on the contraction

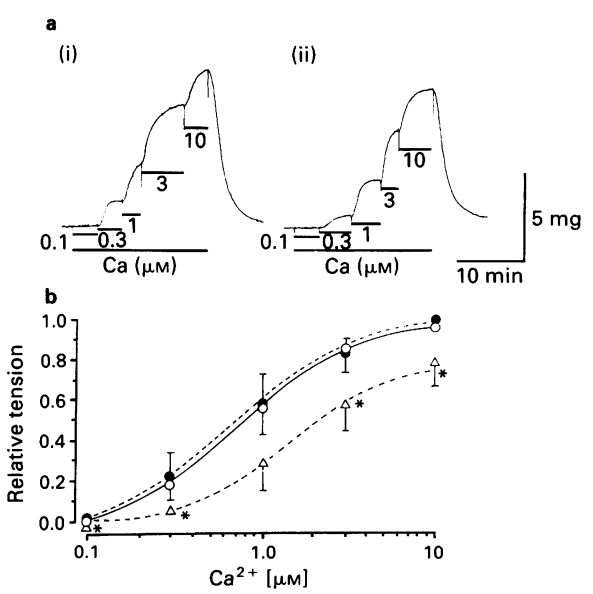


Figure 2 Effects of 10 μM pinacidi on pCa-tension relationship in β-escin treated skinned smooth muscle strips of rabbit mesenteric artery. (a) Actual records under control conditions (i) and in the presence of 10 μM pinacidil (ii); (i) and (ii) were contiguous records. Ca^{2+} was cumulatively applied in a step-wise manner. Pinacidil was applied 10 min before the application of Ca^{2+} and was present throughout the experiment. (b) Effects of pinacidil on pCa-tension relationship: (●) control; (○) in the presence of 1 μM pinacidil; (△) in the presence of 10 μM pinacidil. The amplitude of contraction induced by 10 μM Ca^{2+} was normalized as 1.0. Results shown are means of 4–6 observations with s.d. shown by vertical bars. * indicates significant difference from the corresponding results in the absence of 10 μM pinacidil ($P < 0.05$).

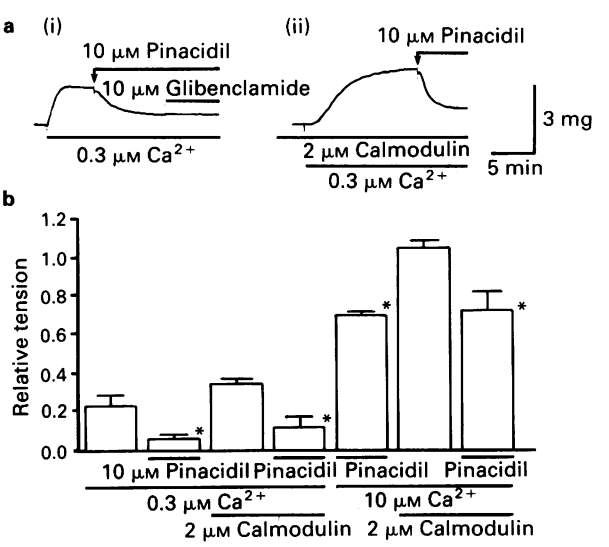


Figure 4 (a) Effects of 2 μM calmodulin on Ca^{2+}-induced contraction in the presence or absence of 10 μM pinacidil: (i) effects of 10 μM pinacidil and 10 μM glibenclamide on contraction induced by 0.3 μM Ca^{2+}; (ii) effect of 10 μM pinacidil on contraction induced by 2 μM calmodulin in the presence of 0.3 μM Ca^{2+}; (i) and (ii) were contiguous records. (b) Effects of 10 μM pinacidil on contraction induced by 0.3 μM or 10 μM Ca^{2+} in the presence or absence of 2 μM calmodulin. Pinacidil (10 μM) was applied on the steady level of the Ca^{2+}-induced contraction. Calmodulin (2 μM) was applied 10 min before application of the Ca^{2+} and was present throughout the experiment. The amplitude of contraction induced by 10 μM Ca^{2+} was normalized as 1.0. Results represented are means of 3–4 observations with s.d. shown by vertical bars. * indicates significant difference from the results obtained in the absence of 10 μM pinacidil ($P < 0.05$).

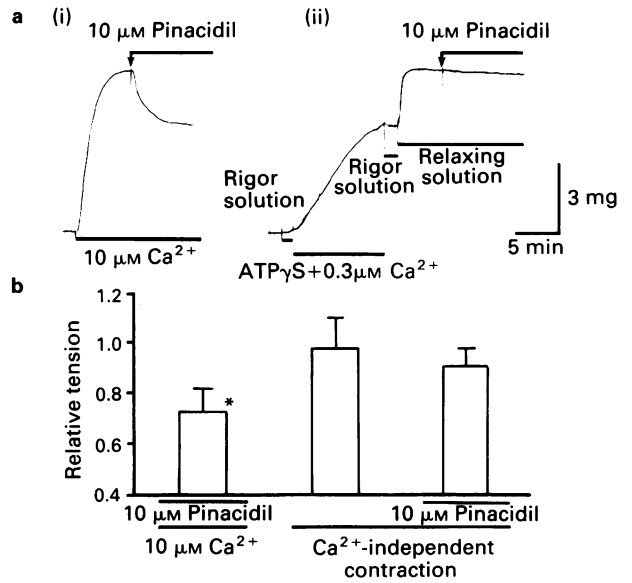


Figure 5 (a) Effects of 10 μM pinacidil on Ca^{2+}-independent contraction: (i) effects of 10 μM pinacidil on contraction induced by 10 μM Ca^{2+}. In (ii), rigor solution (Ca^{2+}-free, no ATP containing solution) was applied for 1.5 min. After application of 2 mM adenosine-5'-O-(3-thiotriphosphate) (ATPγS) with 0.3 μM Ca^{2+} for 10 min in rigor solution, the strip was rinsed with rigor solution for 1.5 min and the relaxing solution (containing 4 mM MgATP and no Ca^{2+} with 4 mM EGTA) was applied. When the tension reached a steady level 10 μM pinacidil was applied. (b) Effects of 10 μM pinacidil on the contraction induced by 10 μM Ca^{2+} and on the Ca^{2+}-independent contraction. The amplitude of contraction was normalized relative to the contraction induced by 10 μM Ca^{2+} in the absence of 10 μM pinacidil. Results shown are means of 3–4 observations with s.d. shown by vertical bars. * indicates significant difference from the results obtained in the absence of 10 μM pinacidil ($P < 0.05$).

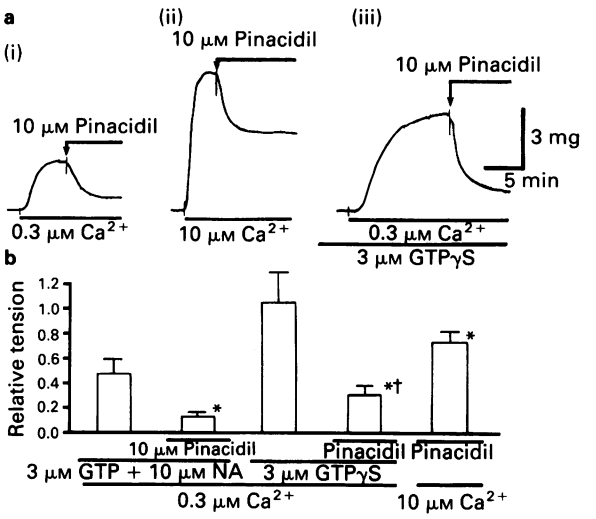


Figure 6 (a) Effects of 10 μM pinacidil on the contraction induced by 0.3 or 10 μM Ca^{2+} in the presence of 10 μM noradrenaline (NA) with 3 μM guanosine triphosphate (GTP) (i, ii) or 3 μM guanosine 5'-O-(3-thiotriphosphate) (GTPγS) (iii). Typical examples are shown of the effect of 10 μM pinacidil on the contraction induced by 0.3 μM Ca^{2+} (i), 10 μM Ca^{2+} (ii) and 0.3 μM Ca^{2+} with 3 μM GTPγS (iii); (i–iii) were contiguous records. NA (10 μM) with GTP (3 μM) or GTPγS (3 μM) were applied for 5 min before and during the application of Ca^{2+}. (b) Effects of 10 μM pinacidil on the contraction induced by 0.3 μM or 10 μM Ca^{2+} in the presence or absence of 10 μM NA with 3 μM GTP or 3 μM GTPγS. The amplitude of contraction was normalized relative to the contraction induced by 10 μM Ca^{2+}. Results shown are means of 3–4 observations with s.d. shown by vertical bars. * indicates significant difference from the results obtained in the absence of 10 μM pinacidil ($P < 0.05$). † indicates significant difference from the results obtained in the presence of 10 μM Ca^{2+} with 10 μM pinacidil.

induced by 0.3 μM Ca^{2+} (Figure 4b). These results suggest that pinacidil inhibited the Ca^{2+}-induced contraction through a mechanism not dependent upon calmodulin.

To investigate further the mechanism of action of pinacidil on the contractile proteins, the effect of this drug on Ca^{2+}-independent contraction was observed. The experimental procedure is indicated in Figure 5. After the maximum contraction had been induced by 10 μM Ca^{2+}, the strip was rinsed with the relaxing solution until it was completely relaxed. Following application of the rigor solution (Ca^{2+}-free solution containing no ATP) for 1.5 min, only a small contraction was evoked ('rigor contraction'). When 2 mM ATPγS with 0.3 μM Ca^{2+} was applied for 10 min, tension developed slowly. Subsequent application of the Ca^{2}-free solution containing no ATP halted the contraction at the level reached at the termination of the application of ATPγS with Ca^{2+}. Then, when the relaxing solution (a Ca^{2+}-free solution containing 4 mM EGTA, 4 mM MgATP and 10 mM phosphocreatine) was applied to the strip, additional tension rapidly developed and the contraction was sustained at the same amplitude for over 30 min ('Ca^{2+}-independent contraction'). The amplitude of this Ca^{2+}-independent contraction was almost the same as that induced by 10 μM Ca^{2+}. Pinacidil (10 μM) did not modify the Ca^{2+}-independent contraction (Figure 5).

The effect of pinacidil on the rigor contraction was also observed. Following application of 10 μM Ca^{2+} to the strips, the solution was rinsed off with Ca^{2+}-free solution containing 4 mM EGTA and no ATP and thus a rigor contraction was produced, as described previously (Itoh *et al.*, 1986a). Pinacidil (10 μM) had no effect on this rigor contraction (not shown) suggesting that pinacidil did not inhibit actin-myosin interactions directly.

NA with GTP enhances the Ca^{2+}-induced contraction in α-toxin treated, chemically skinned smooth muscle strips (Nishimura & van Breemen, 1988; Kitazawa *et al.*, 1989; Kobayashi *et al.*, 1989). To investigate the mechanism of action of pinacidil on the Ca^{2+}-induced contraction further, its effect on the Ca^{2+}-induced contraction was observed in the presence of NA with GTP. NA (10 μM) with GTP (3 μM) enhanced the contraction induced by 0.3 μM Ca^{2+} (Figure 6). Pinacidil (10 μM) inhibited the contraction induced by 0.3 μM Ca^{2+} more strongly in the presence of 10 μM NA with 3 μM GTP than in its absence. Thus, the pinacidil-inhibited contractions were 0.40 ± 0.13 times and 0.27 ± 0.33 times control in the absence or presence of NA with GTP, respectively ($n = 4$). GTPγS (3 μM) also enhanced the contraction induced by 0.3 μM Ca^{2+}, as found previously for saponin-treated skinned muscle (Fujiwara *et al.*, 1989). Pinacidil (10 μM) inhibited the contraction induced by 0.3 μM Ca^{2+} with 3 μM GTPγS more strongly than it did the control (Figure 6b).

A phorbol ester, 12-O-tetradecanoylphorbol-13-acetate (TPA), activates protein kinase C and enhances the Ca^{2+}-induced contraction in skinned smooth muscle strips (Itoh *et al.*, 1986b; Fujiwara *et al.*, 1988). As shown in Figure 7, TPA (0.1 μM) enhanced the contraction induced by 0.3 μM Ca^{2+} by a factor of 3.74, the enhanced contraction being 0.83 ± 0.02 times the contraction induced by 10 μM Ca^{2+} ($n = 4$). Pinacidil (10 μM) inhibited the contraction induced by 0.3 μM Ca^{2+} with 0.1 μM TPA more strongly than that induced by 10 μM Ca^{2+}. Thus, pinacidil reduced the former to 0.46 ± 0.10 times control and the latter to 0.73 ± 0.09 times control ($n = 3$, $P < 0.05$. Figure 7b).

Discussion

Pinacidil hyperpolarizes the smooth muscle membrane through activation of the K^+ channel and then causes vascular relaxation (Southerton *et al.*, 1988: Standen *et al.*, 1989). Glibenclamide is a selective inhibitor of this channel in vascular smooth muscles (Standen *et al.*, 1989). In the present experiments, however, we observed that pinacidil (10 μM)

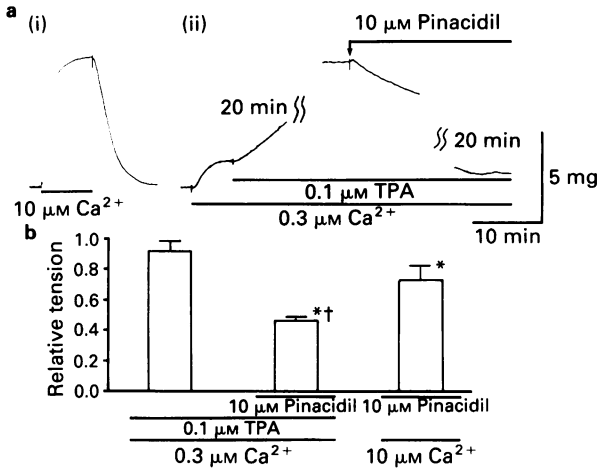


Figure 7 (a) Effect of pinacidil on the contraction induced by 0.3 μM Ca^{2+} in the presence of 0.1 μM 12-O-tetradecanoylphorbol-13-acetate (TPA): (i) contraction induced by 10 μM Ca^{2+}; (ii) effects of 10 μM pinacidil on the contraction induced by 0.3 μM Ca^{2+} with 0.1 μM TPA; (i) and (ii) were contiguous records. Pinacidil (10 μM) was applied during the steady level of the Ca^{2+}-induced contraction in the presence of 0.1 μM TPA. (b) Effects of pinacidil on the contraction induced by 0.3 μM Ca^{2+} with TPA or 10 μM Ca^{2+}. The amplitude of contraction was normalized relative to the contraction induced by 10 μM Ca^{2+} in the absence of 10 μM pinacidil. Results shown are means of 3–4 observations with s.d. shown by vertical bars. * indicates significant difference from the results obtained in the absence of 10 μM pinacidil ($P < 0.05$). † indicates significant difference from the results obtained in the presence of 10 μM Ca^{2+} with 10 μM pinacidil.

inhibited the contraction induced by 128 mM K^+ without any change in $[Ca^{2+}]_i$. Under these conditions, the membrane hyperpolarizing effect of pinacidil may be negligible because the experiments were done with high concentrations of extracellular K^+ (Nakashima *et al.*, 1990) and glibenclamide did not affect the inhibitory action of pinacidil. The extent of the contraction induced by high K^+ is thought to be closely related to the $[Ca^{2+}]_i$ (Morgan & Morgan, 1984), yet 10 μM pinacidil inhibited the contraction without any decrease in $[Ca^{2+}]_i$. These results suggest that pinacidil, at higher concentrations, may have a direct inhibitory action on the contractile apparatus in smooth muscle.

In smooth muscle of the rabbit mesenteric artery, myosin phosphorylation has a crucial role in the Ca^{2+}-induced contraction (Kamm & Stull, 1985; Satoh *et al.*, 1987: Fujiwara *et al.*, 1988). In our experiments, pinacidil shifted the pCa-tension relation curve to the right and inhibited the maximum Ca^{2+}-induced contraction in β-escin-treated, skinned smooth muscle. Neomycin, an inhibitor of phospholipase C in skinned smooth muscle (Kitazawa *et al.*, 1989), did not modify this inhibitory action of pinacidil on the pCa-tension relationship. Pinacidil (10 μM) inhibited the contraction induced by 10 μM Ca^{2+} in the presence or absence of 2 μM calmodulin and the extent of the inhibition was similar in the two conditions. However, pinacidil had no effect on the contraction induced by the Ca^{2+}-free, 4 mM MgATP-containing solution following application of ATPγS with Ca^{2+} ('Ca^{2+}-independent contraction'). This Ca^{2+}-independent contraction is due to the irreversible thio-phosphorylation of myosin light chain by myosin light chain kinase in the presence of ATPγS with Ca^{2+}, because the thio-phosphorylated myosin light chain is resistant to phosphatase (Cassidy *et al.*, 1979). Furthermore, pinacidil (10 μM) also had no effect on the rigor contraction induced by application of the solution containing no ATP. These results suggest that in concentrations over 10 μM, pinacidil probably acts on the process between Ca^{2+}-calmodulin complex formation and myosin light chain phosphorylation and thus inhibits the contraction of the smooth muscle.

NA with GTP or GTPγS enhanced the contraction induced by 0.3 μM Ca^{2+} and this was inhibited by guanosine 5'-O-(β-thiodiphosphate) ($GDP_\beta S$) in α-toxin-treated, skinned smooth muscle (Fujiwara *et al.*, 1989; Kitazawa *et al.*, 1989). These workers suggested that an action of NA with GTP on the contractile proteins of smooth muscle may underly the agonist-induced tonic contraction at low $[Ca^{2+}]_i$ levels. Recently, Nishimura & van Breemen (1988) reported that 1-(5-isoquinolinesulphonyl)-2-methylpiperazine (H-7), an inhibitor of protein kinase C, inhibits the enhancement of the Ca^{2+}-induced contraction induced by NA with GTP in skinned muscle. These results suggest that GTP-binding protein activated by NA may be implicated in the increase in the Ca^{2+}-induced contraction via activation of protein kinase C. In the present experiment, pinacidil (10 μM) inhibited the Ca^{2+}-induced contraction more strongly in the presence of NA with GTP or TPA than under control conditions. These results suggest that pinacidil inhibits the action of protein kinase C, though the mechanism is unknown.

In the present experiments, 10 μM pinacidil inhibited the tonic contraction induced by 128 mM K^+ more than the phasic ones. Raising $[Ca^{2+}]_i$ induced by 128 mM K^+ may provoke the hydrolysis of phosphatidylinositol-4,5-bisphosphate and lead to the production of inositol-1,4,5-trisphosphate and diacylglycerol (DG), as reported in non-muscle cells (Cockcroft & Stutchfield, 1988). DG or its analogue slowly enhances Ca^{2+}-induced contraction in skinned smooth muscles through an activation of protein kinase C (Nishizuka, 1984; Itoh *et al.*, 1986b). The inhibition of protein kinase C (described above) by pinacidil may relate to the much stronger inhibition of the tonic contraction induced by 128 mM K^+ than the phasic ones.

We conclude that at high concentrations (> 10 μM), pinacidil acts directly on the contractile proteins in smooth muscle of the rabbit mesenteric artery and inhibits the Ca^{2+}-induced contraction in high K^+ conditions in intact as well as in skinned muscle strips. The sites of action of pinacidil have not been identified, but a modification of myosin phosphorylation after Ca^{2+}-calmodulin complex formation is postulated.

We thank Dr R.J. Timms for the language editing. This work was partly supported by a Grant-In-Aid from the Ministry of Education of Japan (02807010).

References

BECKER, P.L., SINGER, J.J., WALSH, J.V. & FAY, F.S. (1989). Regulation of calcium concentration in voltage-clamped smooth muscle cells. *Science*, **244**, 211–214.

CASSIDY, P.S., HOAR, P.E. & KERRICK, W.G.L. (1979). Irreversible thiophosphorylation and activation of tension in functionally skinned rabbit ileum strips by (^{35}S)ATPγS. *J. Biol. Chem.*, **254**, 11148–11153.

COCKCROFT, S. & STUTCHFIELD, J. (1988). G-proteins, the inositol lipid signalling pathway, and secretion. *Phil. Trans. R. Soc.*, **B320**, 247–265.

FUJIWARA, T., ITOH, T., KUBOTA, Y. & KURIYAMA, H. (1988). Actions of a phorbol ester on factors regulating contraction in rabbit mesenteric artery. *Circ. Res.*, **63**, 893–902.

FUJIWARA, T., ITOH, T., KUBOTA, Y. & KURIYAMA, H. (1989). Effects of guanosine nucleotides on skinned smooth muscle tissue of the rabbit mesenteric artery. *J. Physiol.*, **408**, 535–547.

GRYNKIEWICZ, G., POENIE, M. & TSIEN, R.Y. (1985). A new generation of Ca^{2+} indicators with greatly improved fluorescence properties. *J. Biol. Chem.*, **260**, 3440–3450.

ITOH, T., KANMURA, Y. & KURIYAMA, H. (1986a). Inorganic phosphate regulates the contraction-relaxation cycle in skinned muscles of the rabbit mesenteric artery. *J. Physiol.*, **376**, 231–252.

ITOH, T., KANMURA, Y., KURIYAMA, H. & SUMIMOTO, K. (1986b). A phorbol ester has dual actions on the mechanical response in the rabbit mesenteric and porcine coronary arteries. *J. Physiol.*, **375**, 515–534.

ITOH, T., KURIYAMA, H. & SUZUKI, H. (1983). Differences and similarities in noradrenaline- and caffeine-induced mechanical responses in the rabbit mesenteric artery. *J. Physiol.*, **337**, 609–629.

KAMM, K.E. & STULL, J.T. (1985). The function of myosin and myosin light chain kinase phosphorylation in smooth muscle. *Annu. Rev. Pharmacol. Toxicol.*, **25**, 593–620.

KITAZAWA, T., KOBAYASHI, S., HORIUTI, K., SOMLYO, A.V. & SOMLYO, A.P. (1989). Receptor-coupled, permeabilized smooth muscle. *J. Biol. Chem.*, **264**, 5339–5342.

KOBAYASHI, S., KITAZAWA, T., SOMLYO, A.V. & SOMLYO, A.P. (1989). Cytosolic heparin inhibits muscarinic and α-adrenergic Ca^{2+} release in smooth muscle. *J. Biol. Chem.*, **264**, 17997–18004.

KONISHI, M., OLSON, A., HOLLINGWORTH, S. & BAYLOR, S.M. (1988). Myoplasmic binding of fura-2 investigated by steady state fluorescence and absorbance measurements. *Biophys. J.*, **54**, 1089–1104.

MORGAN, J.P. & MORGAN, K.G. (1984). Stimulus-specific patterns of intracellular calcium levels in smooth muscle of ferret portal vein. *J. Physiol.*, **351**, 155–167.

NAKASHIMA, M., LI, Y., SEKI, N. & KURIYAMA, H. (1990). Pinacidil inhibits neuromuscular transmission indirectly in the guinea-pig and rabbit mesenteric arteries. *Br. J. Pharmacol.*, **101**, 581–586.

NISHIZUKA, Y. (1984). The role of protein kinase C in cell surface signal transduction and tumour promotion. *Nature*, **308**, 693–698.

NISHIMURA, J. & VAN BREEMEN, C. (1989). Direct regulation of smooth muscle contractile elements. *Biochem. Biophys. Res. Commun.*, **163**, 929–935.

POENIE, M., ALDERTON, J., STEINHART, R.A. & TSIEN, R.Y. (1986). Calcium rises abruptly and briefly throughout the cell at the onset of anaphase. *Science*, **233**, 886–889.

QUAST, U. & COOK, N.S. (1989). Moving together: K^+ channel openers and ATP-sensitive K^+ channels. *Trends Pharmacol. Sci.*, **10**, 431–435.

SATOH, S., KUBOTA, Y., ITOH, T. & KURIYAMA, H. (1987). Mechanisms of the Ba^{2+}-induced contraction in smooth muscle cells of the rabbit mesenteric artery. *J. Gen. Physiol.*, **89**, 215–237.

SOUTHERTON, J.S., WESTON, A.H., BRAY, K.M., NEWGREEN, D.T. & TAYLOR, S.G. (1988). The potassium channel opening action of pinacidil; studies using biochemical, ion flux and microelectrode techniques. *Naunyn-Schmiedebergs Arch. Pharmacol.*, **338**, 310–318.

STANDEN, N.B., QUAYLE, J.M., DAVIES, N.W., BRAYDEN, J.E., HUANG, Y. & NELSON, M.T. (1989). Hyperpolarizing vasodilators activate ATP-sensitive K^+ channels in arterial smooth muscle. *Science*, **245**, 177–180.

VIDEBAEK, L.M., AALKJAERM, C. & MULVANY, M.J. (1988). Pinacidil opens K^+-selective channels causing hyperpolarization and relaxation of noradrenaline contractions in rat mesenteric resistance vessels. *Br. J. Pharmacol.*, **95**, 103–108.

(Received November 23, 1990
Revised March 13, 1991
Accepted March 18, 1991)

Br. J. Pharmacol. (1991), **103**, 1703–1708 © Macmillan Press Ltd, 1991

(+)-S-12967 and (−)-S-12968: 1,4-dihydropyridine stereoisomers with calcium channel agonistic and antagonistic properties in rat resistance arteries

Dolores Prieto, Michael J. Mulvany & [1]Niels C.B. Nyborg

Department of Pharmacology, University of Aarhus, DK-8000 Aarhus C, Denmark

1 The actions of (+)-S-12967 and (−)-S-12968 two isomers of a new 1,4-dihydropyridine (DHP) derivative, were studied on 125 mM K^+-, Ca^{2+}- and noradrenaline-induced contractions in rat isolated mesenteric resistance arteries and compared to those of nifedipine.

2 The action of (+)-S-12967 and (−)-S-12968 was slow in onset in contrast to nifedipine. Both isomers had a dual contractile and relaxant action in arteries contracted with 125 mM K^+; however, the (−)-isomer was about 300 times more potent than the (+)-isomer. The response to 125 mM K^+, being depressed by 70%, recovered within 20 to 30 min for all DHP derivatives. All vessels were treated with 1×10^{-6} M phenoxybenzamine thus excluding the possibility that the contraction is mediated by activation of amine-receptors.

3 Both (+)-S-12967 and (−)-S-12968 at low concentrations potentiated responses induced by Ca^{2+} in arteries activated by 125 mM K^+ and inhibited the responses at higher concentrations. (+)-S-12967 and (−)-S-12968 had no contractile action in arteries kept in normal buffer. Nifedipine had only an inhibitory action on vessel responses to 125 mM K^+ and Ca^{2+}.

4 Both isomers and nifedipine depressed the maximal vessel response to noradrenaline by about 20% and 44%, respectively.

5 The results confirm that DHP calcium antagonists selectively inhibit vascular smooth muscle responses induced by high potassium and that the potency of 1,4-DHP isomers may vary considerably. Furthermore, since the agonistic/antagonistic properties on the calcium channel were shared by both stereoisomers of the 1,4-DHP molecule and apparently dependent on their concentration and the vascular smooth muscle membrane potential, it suggests that the agonistic action of 1,4-DHPs may be ascribed to functional characteristics of their binding site regulating the Ca^{2+}-channel.

Keywords: 1,4-dihydropyridine; isomers; calcium channel; noradrenaline; potassium; calcium; rat mesenteric resistance artery

Introduction

Transmembrane calcium influx via specific calcium channels plays a crucial role in the excitation-contraction coupling of cardiac and smooth muscle (Bolton, 1979). One of the most common criteria used to classify the different types of calcium channels has been their sensitivity to the blocking action of 1,4-dihydropyridines (DHPs), the most potent and selective calcium entry blockers (Fleckenstein, 1977), which seem to inhibit preferentially opening of the membrane potential-sensitive calcium-channels in the cell membrane (Cauvin *et al.*, 1983; Godfraind *et al.*, 1986; Janis *et al.*, 1987). Moreover, DHPs have become important pharmacological tools for studying voltage-sensitive calcium channels, especially since the discovery that some derivatives of this group, for example Bay K 8644 (Schram *et al.*, 1983) and CGP 28392 (Loutzenhiser *et al.*, 1984), can act directly as voltage-sensitive calcium channel activators. With these drugs it was further demonstrated that the calcium agonistic action of Bay K 8644 was associated with only one of its stereoisomers, suggesting that DHP derivatives may behave as calcium entry blockers or calcium entry activators depending on the stereochemistry (Franckowiak *et al.*, 1985; Hof *et al.*, 1985).

The present study evaluates the action of the two isomers (+)-S-12967 and (−)-S-12968 of a new 1,4-DHP derivative [2-(7 amino 2,5-dioxaheptyl)3-ethoxycarbonyl 4-(2,3-dichlorophenyl) 5-methoxycarbonyl 6-methyl 1,4-dihydropyridine] (Figure 1) on mechanical responses of vascular smooth muscle of rat mesenteric resistance arteries to potassium, calcium and noradrenaline and compares it with that of nifedipine, a symmetrical DHP molecule.

[1] Author for correspondence.

Methods

Dissection and mounting

Male Wistar rats (body wt 300–350 g) were killed by cervical dislocation and bled. The superior mesenteric artery in the proximal part of the jejunum was removed and placed in cold oxygenated (5% CO_2 in O_2) physiological salt solution (PSS, see below). Two ring segments (1–2 mm long) were dissected out from the second or third branch of the superior mesenteric artery, threaded on two stainless steel wires (40 μm diameter) and mounted on a double myograph which allowed direct determination of the isometric wall tension while the internal circumference was controlled (Mulvany & Halpern, 1977; Mulvany & Nyborg, 1980). After an equilibration period of 30 min in PSS at 37°C the vessels were normalized, that is, the internal circumference, L_1, was set to 90% of L_{100} where L_{100} is the internal circumference the vessels would have *in situ* under a transmural pressure of 13.3 kPa (100 mmHg)

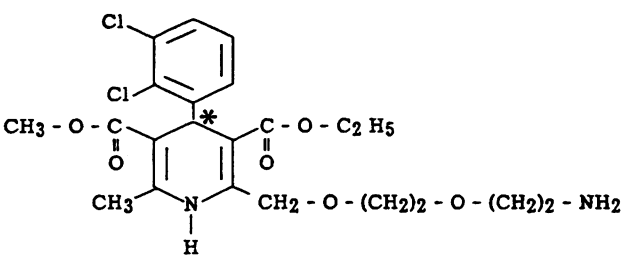


Figure 1 Chemical structure of (+)-S-12967 and (−)-S-12968, [2-(7 amino 2,5-dioxaheptyl) 3-ethoxycarbonyl 4-(2,3-dichlorophenyl) 5-methoxycarbonyl 6-methyl 1,4-dihydropyridine]. *indicates asymmetric C-atom in the dihydropyridine ring.

(Mulvany & Halpern, 1977). The vessels were finally activated three times with K-PSS (see below).

Protocol

In the first set of experiments the time-course of the effects of (+)-S-12967 and (−)-S-12968 was determined and compared with those of nifedipine. The vessels were contracted with 125 mM K-PSS and once the response had stabilized after 30 min a single concentration of either of the two isomers or nifedipine was added to the bath. The action of the compounds was studied for 120 min, the maximum time the vessels could maintain a constant contraction to 125 mM K^+ (K-PSS). The recovery of the K-PSS-induced responses was studied over the next 2 h after the vessels were washed thoroughly in drug-free PSS by activating the vessels with K-PSS (5 min) every 15 min.

The effects of (+)-S-12967, (−)-S-12968 and nifedipine were further studied on potassium-activated calcium concentration-response characteristics. The vessels were incubated in Ca^{2+}-free PSS (see below) for 5 min. The vessels were then washed twice with Ca^{2+}-free K-PSS (see below) for 10 min before Ca^{2+} was added to the tissue bath again. The vessels were then incubated with different concentrations of the isomers for 2 h and nifedipine for 30 min, respectively, in Ca^{2+}-free K-PSS before they were exposed to increasing concentrations of $CaCl_2$ again.

The vessels were initially incubated with 1 μM phenoxybenzamine for 10 min and then washed for 30 min, in order to block α-adrenoceptors and avoid the effects of the neuronally released noradrenaline (NA) by K-PSS depolarization in the experiments with vessels exposed to K-PSS.

Finally, the effects of (+)-S-12967, (−)-S-12968 and nifedipine on NA-induced contractions were studied. Two NA concentration-response curves were obtained, the first serving as control. The vessels were incubated either 2 h (isomers) or 30 min (nifedipine), respectively, before the NA concentration-response curve was repeated in the presence of the calcium antagonist. Because of the difficulty in washing out the isomers from the tissue bath, the vessels were exposed only to a single concentration of the drugs.

Solutions and drugs

The vessels were dissected and kept relaxed in PSS with the following composition (mM): NaCl 119, $NaHCO_3$ 25, KCl 4.7, KH_2PO_4 1.18, $MgSO_4$ 1.17, $CaCl_2$ 1.5, EDTA 0.026 and glucose 11.

K-PSS was similar to PSS except that NaCl was exchanged with KCl on an equimolar basis.

Ca^{2+}-free PSS and Ca^{2+}-free K-PSS were similar to PSS and K-PSS, respectively, except that $CaCl_2$ was omitted and replaced with 1×10^{-4} M EGTA. EGTA was omitted when $CaCl_2$ was readministered.

Drugs used were phenoxybenzamine (Smith Kline & French), (−)-noradrenaline HCl (Sigma); nifedipine (Bayer AG); (+)-S-12967 and (−)-S-12968 tartrate (Servier). Stock solutions of nifedipine and phenoxybenzamine were made in ethanol and then diluted in distilled water. Nifedipine solution was protected from light and experiments were carried out in darkness. (+)-S-12967 and (−)-S-12968 were water-soluble and light-insensitive.

Statistics

Vessel responses are expressed as either active wall tension, $N\,m^{-1}$ (force per vessel wall length) or as a percentage of the maximum contraction in the control concentration-response curves. In the time course experiments the effects of the drugs are expressed as a percentage of the K-PSS response at time 0, i.e., just prior to the addition of the drugs. The inhibitory potency of the drugs was estimated by determining the EC_{50}[M]-concentration, i.e. the concentration of the antagonist causing a 50% inhibition of the 125 mM K^+-induced response after 2 h of incubation with the isomers. EC_{50}[M] for nifedipine was determined in separate experiments where the vessels were exposed to increasing concentrations of nifedipine. EC_{50}[M]s were estimated by fitting plots of responses, R, vs. concentration, A[M], on a log-scale to the equation $R = R_{max} \times A[M]^n/(A[M]^n + EC_{50}[M]^n)$, where R_{max} is maximal tissue response to drug, using the commercially available GraphPAD programme. In each concentration-response experiment, sensitivities to the agonists are expressed in terms of pD_2 values where $pD_2 = -\log([EC_{50}[M])$. Differences between means were compared by Student's t test for paired observations. Significance level was for both tests set at $P < 0.05$. Values are given as mean ± s.e.mean.

Results

Both (+)-S-12967 and (−)-S-12968 had a contractile and a relaxant effect on the mesenteric resistance vessels depolarized with 125 mM K-PSS (Figure 2) in a narrow concentration range between 3×10^{-10} M and 3×10^{-9} M for (−)-S-12968 and between 1×10^{-7} M and 6×10^{-7} M for (+)-S-12967. The (−)-isomer was about 300 times more potent than the (+)-isomer. At the lowest concentrations used, (+)-S-12968 (3×10^{-10} M) and (−)-S-12967 (1×10^{-7} M) elicited contractions, of 70 ± 13% ($n = 5$) and 80 ± 11% ($n = 4$), respectively, above the K-PSS-induced response. Nifedipine, 1×10^{-6} M, totally abolished the contraction induced by both isomers ($n = 4$). The effect of the isomers became relaxations at slightly higher concentrations. The inhibitions caused by (−)-S-12968

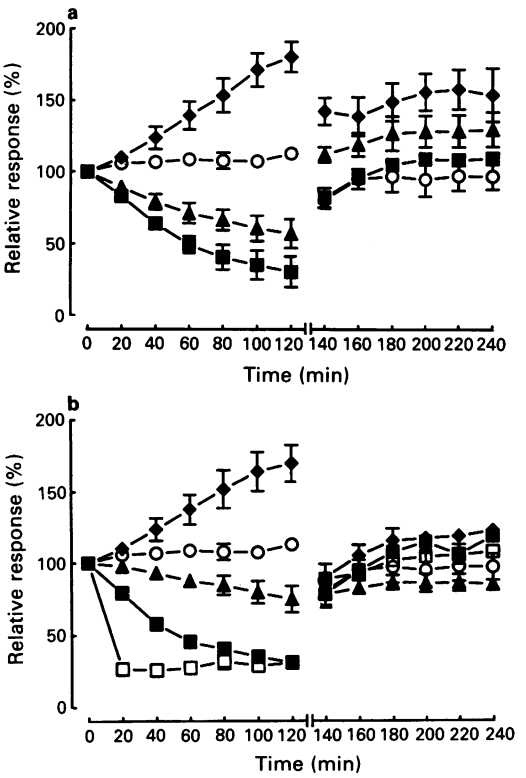


Figure 2 Time-course of the action of (+)-S-12967 (a), (−)-S-12968 (b) and nifedipine (lowest curve) on rat isolated mesenteric resistance arteries contracted with 125 mM K^+ (○, represent control) and recovery of vessel responses to 125 mM K^+ after wash out of the drugs. Wash out is indicated by a gap in the X-axes. Concentrations of antagonists: in (a): (◆) 1×10^{-7} M; (▲) 3×10^{-7} M and (■) 6×10^{-7} M; in (b) (◆) 3×10^{-10} M; (▲) 1×10^{-9} M; (■) 3×10^{-9} M and (□) nifedipine, 1×10^{-9} M. Each point represents mean of 4–8 vessels and vertical bars show ± s.e.mean. Responses are given as percentage of initial vessel tone to 125 mM K^+ just prior to addition of drug at time zero.

(3×10^{-9} M) and (+)-S-12967 (6×10^{-7} M) were $69 \pm 4\%$ ($n = 4$) and $70 \pm 11\%$ ($n = 4$), respectively, of the K^+-induced responses. No change was observed with the two isomers in normal PSS at the range of concentrations mentioned above. On the contrary, nifedipine did not elicit any contractile effect in the vessels depolarized with 125 mM K^+ when tested at low concentrations (1×10^{-15} M–1×10^{-12} M) (results not shown), but relaxed them at higher concentrations (10^{-11} M–10^{-7} M). The relative inhibitory potencies of the three drugs were in the order: nifedipine >(−)-S-12968 >(+)-S-12967, the IC_{50} values being 3.8×10^{-11} M for nifedipine, 1.9×10^{-9} M for (−)-S-12968 and 1.4×10^{-7} M for (+)-S-12967.

Both the potentiation and the inhibition induced by the isomers were characterized by a slow onset, reaching its maximal effects in about 2 h, whereas the maximal inhibition elicited by a single dose of nifedipine (1 nM) was reached in the first 20 min and remained constant thereafter throughout the 2 h drug-contact time. Recovery of the 125 mM K-induced responses was obtained within 20–30 min after the drug washout for both nifedipine and both isomers; however, the K^+-induced contractions which developed in the arteries treated with (−)-S-12968 and (+)-S-12967, especially those with the (+)-isomer, were significantly increased compared with the controls during the 2 h washout period.

Figure 3 shows the effects of (−)-S-12968 and (+)-S-12967 and nifedipine on the calcium concentration-response characteristics of mesenteric resistance arteries activated with 125 mM K-PSS. (−)-S-12968 (3×10^{-10} M) and (+)-S-12967 (1×10^{-7} M) induced a significant leftward shift of the concentration-response curves but no change in the maximal responses (Table 1). Higher concentrations of the two isomers reduced in a non-competitive concentration-dependent manner both the sensitivity and maximal contraction (Figure 3, Table 1). Nifedipine, tested in a wider range of concentrations (1×10^{-10} M–1×10^{-7} M), did not potentiate the calcium-induced contractions but decreased both sensitivity and maximal tension gradually.

Table 1 Effect of (+)-S-12967, (−)-S-12968 and nifedipine on sensitivity and maximal response to Ca^{2+} in 125 mM K^+ activated rat mesenteric resistance arteries

	(+)-S-12967	
Concentration, (M)	pD_2	ΔT_{max}
Control	3.08 ± 0.04	2.91 ± 0.08 (12)
0.1 μM	3.55 ± 0.08[b]	3.10 ± 0.21[NS] (4)
0.3 μM	2.10 ± 0.29[b]	1.93 ± 0.38[b] (4)
0.6 μM	0.42 ± 0.11[a]	0.36 ± 0.08[a] (4)
	(−)-S-12968	
Concentration, (M)	pD_2	ΔT_{max}
Control	2.93 ± 0.08	2.70 ± 0.16 (13)
0.3 nM	3.70 ± 0.09[b]	2.85 ± 0.32[NS] (5)
1 nM	2.18 ± 0.13[c]	2.00 ± 0.26[c] (4)
3 nM	0.93 ± 0.11[a]	0.79 ± 0.12[b] (4)
	Nifedipine	
Concentration, (M)	pD_2	ΔT_{max}
Control	3.22 ± 0.05	2.14 ± 0.16 (19)
1 nM	2.71 ± 0.09[b]	1.92 ± 0.22[c] (7)
10 nM	1.78 ± 0.11[a]	1.22 ± 0.25[b] (8)
100 nM	1.07 ± 0.12[a]	0.38 ± 0.08[b] (4)

Values given as mean ± s.e.mean (number of vessels). Sensitivities are expressed as pD_2-values and ΔT_{max} is maximal tension developed by vessels to Ca^{2+}. Control values represent mean for all vessels used. [a] $P < 0.05$; [b] $P < 0.01$; and [c] $P < 0.001$ different from control value tested by Student's t test for paired data. NS is not significant.

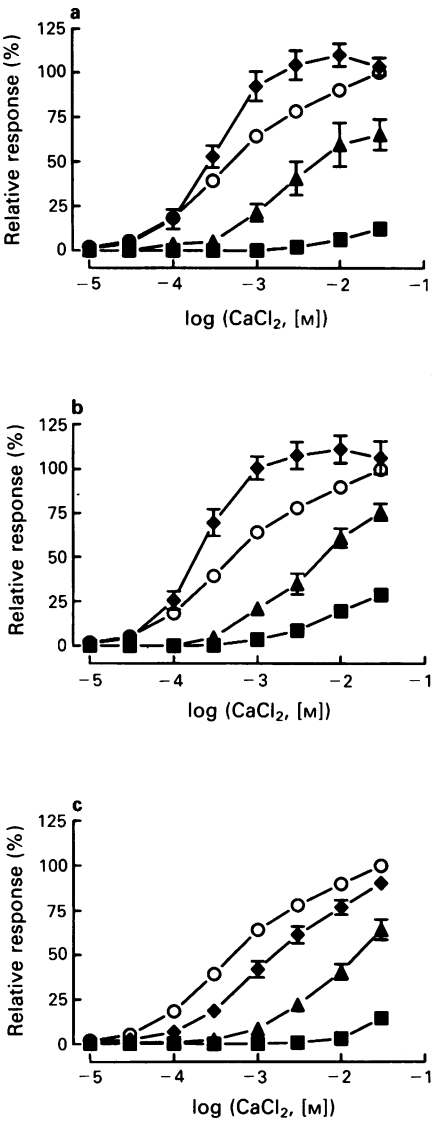


Figure 3 Effect of (a) (+)-S-12967, (b) (−)-S-12968 and (c) nifedipine on Ca^{2+} concentration-response characteristics of isolated mesenteric resistance arteries activated with 125 mM K^+ in Ca^{2+}-free PSS. Responses are calculated with reference to maximal response of the control concentration-response curve (○). Points represent means of 4–19 vessels and vertical bars show ± s.e.mean. Concentration of antagonists are: in (a) (◆) 1×10^{-7} M; (▲) 3×10^{-7} M and (■) 6×10^{-7} M; in (b): (◆) 3×10^{-10} M; (▲) 1×10^{-9} M and (■) 3×10^{-9} M; and in (c): (◆) 1×10^{-9} M; (▲) 1×10^{-8} M and (■) 1×10^{-7} M.

The effects of (−)-S-12968, (+)-S-12967 and nifedipine on NA contraction-response characteristics of the mesenteric resistance arteries are illustrated in Figure 4. Sensitivity and maximal contractions to NA of the arteries are given in Table 2. Responses to NA were much less affected by the isomers than those induced by calcium. The maximal responses still present at the highest concentrations of (−)-S-12968 (1×10^{-8} M) and (+)-S-12967 (1×10^{-6} M) were $80 \pm 1\%$ ($n = 4$) and $80 \pm 1\%$ ($n = 4$) of the controls, respectively. There was a small decrease in sensitivity to NA at these concentrations and also a slight but signficant increase in NA sensitivity in arteries treated with 3×10^{-7} M (+)-S-12967. Nifedipine affected the contractile responses to NA more than (−)-S-12968 and (+)-S-12967. When used in the same range of concentrations as that for the calcium curves (1×10^{-9} M–1×10^{-7} M), nifedipine caused a gradual decrease in both sensitivity and maximal tension development to NA. The maximal response to NA at the highest concentration of

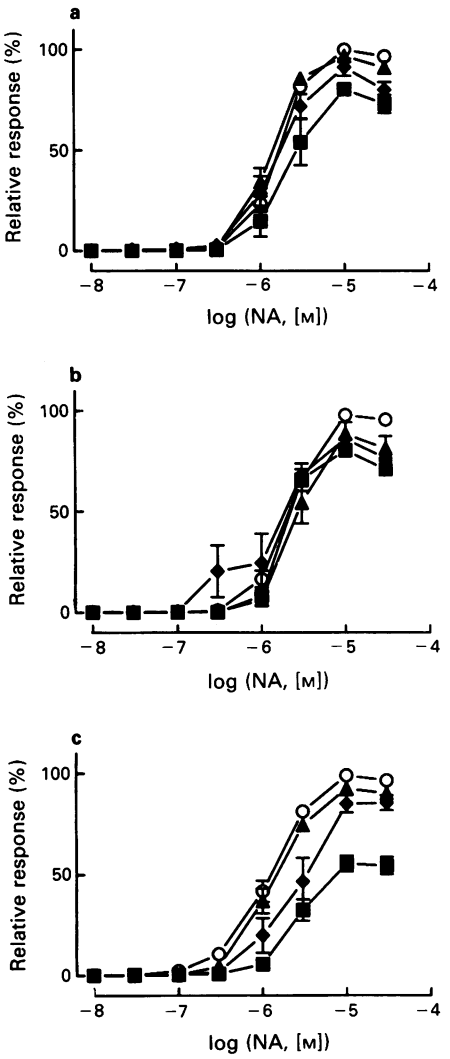


Figure 4 Effect of (a) (+)-S-12967, (b) (−)-S-12968 and (c) nifedipine on noradrenaline (NA) concentration-response characteristics of isolated mesenteric resistance arteries. Responses are calculated with reference to maximal response of the control concentration-response curve (○). Points represent means of 4–20 vessels and vertical bars show ± s.e.mean. Concentration of antagonists are: in (a): (◆) 1×10^{-7} M; (▲) 3×10^{-7} M and (■) 1×10^{-6} M; in (b): (◆) 3×10^{-10} M; (▲) 1×10^{-9} M and (■) 1×10^{-8} M; in (c): (◆) 1×10^{-9} M; (▲) 1×10^{-8} M and (■) 1×10^{-7} M.

nifedipine was 56 ± 4% ($n = 6$) of the control response and the pD_2 was 14 fold reduced.

Discussion

We have examined in the present study the effects of the two isomers of a new 1,4-DHP derivative on rat mesenteric resistance vessels, and the following observations can be made from these investigations. First, significant stereoselectivity of action has been detected, the (−)-isomer being about 300 times as potent as the (+)-isomer; there is no stereoselectivity, however, concerning opposing biological activities, since both isomers shared dual agonistic/antagonistic properties depending on only the concentration of drug used. Second, the isomers may be included in the new group of 1,4-DHPs with slow onset and long-lasting action, such as amlodipine (Burges *et al.*, 1985), lacidipine (Carpi *et al.*, 1986) and OPC-13340 (Nakayama *et al.*, 1990). Third, both isomers were much more effective on potassium and calcium-induced contractions than on those elicited by NA, thus indicating a selective action on the voltage-dependent as opposed to the receptor-operated calcium channels.

Table 2 Effect of (+)-S-12967, (−)-S-12968 and nifedipine on sensitivity and maximal response to noradrenaline (NA) in rat mesenteric resistance arteries

	(+)-S-12967	
Concentration, (M)	pD_2	ΔT_{max}
Control	5.77 ± 0.04	3.44 ± 0.27 (14)
0.1 μM	5.72 ± 0.08^{NS}	2.80 ± 0.47^{NS} (6)
0.3 μM	5.86 ± 0.05^{c}	3.35 ± 0.27^{b} (4)
1 μM	5.46 ± 0.09^{b}	3.22 ± 0.43^{b} (4)
	(−)-S-12968	
Concentration, (M)	pD_2	ΔT_{max}
Control	5.65 ± 0.05	3.45 ± 0.20 (20)
0.3 nM	5.92 ± 0.22^{NS}	2.67 ± 0.21^{a} (6)
1 nM	5.54 ± 0.02^{NS}	3.39 ± 0.51^{NS} (6)
10 nM	5.53 ± 0.03^{c}	3.41 ± 0.09^{a} (4)
	Nifedipine	
Concentration, (M)	pD_2	ΔT_{max}
Control	5.93 ± 0.01	2.76 ± 0.20 (18)
1 nM	5.54 ± 0.14^{c}	2.80 ± 0.34^{c} (8)
10 nM	5.83 ± 0.07^{b}	2.42 ± 0.54^{c} (4)
100 nM	4.87 ± 0.11^{b}	1.22 ± 0.24^{a} (6)

Values given as mean ± s.e.mean (number of vessels). Sensitivities are expressed as pD_2-values and ΔT_{max} is maximal tension developed by vessels to NA. Control values represent mean for all vessels used. $^{a}P < 0.05$; $^{b}P < 0.01$; and $^{c}P < 0.001$ different from control value tested by Student's t test for paired data. NS is not significant.

Dual calcium channel activator/inhibitor properties have previously been reported for some 1,4-DHP derivatives. Thus, nifedipine, nicardipine, nimodipine and nitrendipine have been shown to display an agonistic activity at low concentrations (Schram *et al.*, 1983; Hess *et al.*, 1984; Thomas *et al.*, 1984; Schwartz *et al.*, 1984; Dubé *et al.*, 1985; Frank, 1990). On the other hand, the antagonistic activity of Bay K 8644 at high concentrations (Thomas *et al.*, 1984; Schwartz *et al.*, 1984; Dubé *et al.*, 1985) has been attributed, in part, to the racemic mixture of Bay K 8644 in which one of the isomers exhibits agonist activity and the other has the opposite effect on the membrane potential-operated calcium channel (Hof *et al.*, 1985). However, this explanation does not seem to be sufficient to explain the mechanism of action of all 1,4-DHP calcium channels activators and inhibitors, since the action of these drugs can be changed from antagonistic to agonistic and *vice versa* not only by modifications in the molecular conformation, but also by changes in the concentration (Thomas *et al.*, 1984; Franckowiak *et al.*, 1985; McDonald *et al.*, 1987) and membrane potential (Hess *et al.*, 1984; Kokubun *et al.*, 1986). Thus, in the study by Franckowiak *et al.* (1985), the agonistic isomer (−)-Bay K 8644 had a partial antagonistic effect at high concentrations on guinea-pig aortic rings and isolated perfused heart; in addition, the calcium channel-activating effect of the (+)-(S)-enantiomer of 202-791 became a blocking effect at holding membrane potentials postive to −20 mV (Kokubun *et al.*, 1986).

Our experiments with the new 1,4-DHP isomers in rat mesenteric vascular smooth muscle demonstrate that the ability to act as an agonist or an antagonist on the calcium channel resides in the same molecule and is determined by the concentration of the drug rather than by its molecular conformation or isomeric properties at least when the vessels are kept in K-PSS. Similar results have been recently reported for another 1,4-DHP derivative, DHMP (Kaplita *et al.*, 1990), which behaves as a weak mixed calcium agonist/antagonist on guinea-pig ileum at low and high concentrations, respectively. However, the authors attribute these properties to the sym-

metry of DHMP molecule. In addition, the action of both (−)-S-12968 and (+)-S-12967 seems to be voltage-dependent, since they exhibited their agonistic effect only in arteries depolarized with 125 mM K-PSS, but not in the basal resting state. This agrees, in part, with that reported for the two isomers of another 1,4-dihydropyridine derivative, isradipine (PN 200 110, Morel & Godfraind, 1987). In this case, membrane depolarization increased both the blocking effect on KCl contractions and the binding affinity of the two isomers. The authors explain this according to the 'modulated receptor theory' (Godfraind, 1986) in which the binding of a drug to a site within the calcium channel is modulated by the state of activation of the channel which again is regulated by the membrane potential. We must note that a definitive proof of regulation of membrane potential-operated calcium-channels by the isomers studied here can only be derived from patch- or whole cell clamp experiments but the complete relaxation of vessels contracted with low agonistic concentrations of both isomers on top of the K-PSS-induced response with a high concentration of nifedipine supports the view that both isomers activate these calcium-channels in the mesenteric vascular smooth muscle. Furthermore the very high concentration of phenoxybenzamine used would eliminate all amine receptor and cholinoceptor systems in the vessels.

Our results strongly confirm the stereoselectivity reported for several pairs of isomers of 1,4-DHPs, the (−)-enantiomer being 2–3 orders of magnitude more potent than the (+)-enantiomer, as has been demonstrated for Bay K 8644 (Franckowiak *et al.*, 1985), S-202 791 (Hof *et al.*, 1985) and amlodipine (Rigby *et al.*, 1988). The potency and the difference between the isomers studied here is however greater than that published by Randle *et al.* (1990) using the same isomers in binding studies on heart and vascular smooth muscle. An agonistic activity of the isomers was not observed on the inward Ca^{2+} current in guinea-pig isolated myocytes (Randle *et al.*, 1990).

One of the main differences found in the present study between the two isomers and nifedipine, the prototype of the 1,4-DHP family, is their slow onset in action. This property has also been described for amlodipine in rat aorta and portal vein (Burges *et al.*, 1987) and pig and human coronary arteries (Matlib *et al.*, 1988), and for lacidipine in rabbit ear artery (Michelli *et al.*, 1990). This pharmacological feature of amlodipine has been attributed to its low lipid solubility due to the presence of the side chain in the 2-position of the DHP ring carrying a basic amino group which gives the molecule a pKa of 8.6, thus rendering the molecule more than 90% ionized at physiological pH (Burges *et al.*, 1989). This is also the case for (+)-S-12967 and (−)-S-12968 (pKa 8.6), and it seems that this chemical feature is responsible for marked differences in physicochemical, pharmacological and pharmacokinetic properties of this new group of slow-acting DHPs, since binding experiments demonstrate that amlodipine displays slow association and dissociation rates with the calcium channel receptor. Furthermore, the haemodynamic responses of amlodipine in animals are also characterized by a gradual onset of action and by long plasma half-life (Burges *et al.*, 1989).

It has also been reported that the effect of this new type of 1,4-DHPs was reversed very slowly after wash-out *in vitro* (Carpi *et al.*, 1986; Burges *et al.*, 1987; Michelli *et al.*, 1990). In our experiments, 125 mM K^+-induced contractions reached pre-drug levels 20–30 min after wash-out of the two isomers as well as nifedipine. This was expected for nifedipine according to its kinetics of action. However, the quick recovery of the vessel responses after the long-lasting action of the isomers could be explained by the contractile effect of these drugs at low concentrations, assuming that some drug is still present in the cell membrane.

There is now considerable evidence suggesting that there are at least two types of calcium channels in the smooth muscle cells (Bolton, 1979; Cauvin *et al.*, 1983; Janis *et al.*, 1987): potential-operated channels (POCs) and receptor-operated channels (ROCs) which are activated by membrane depolarization and receptor occupation by agonists, respectively. One of the most common criteria used to establish this distinction has been that POCs are selectively blocked by organic calcium antagonists, whereas ROCs are much more resistant to this blocking effect. In addition, the extracellular calcium-dependence and release of calcium from intracellular pools induced by several agonists, has also to be taken in account when determining the presence of ROCs in vascular smooth muscle.

The results of the present study clearly demonstrate that (+)-S-12967 and (−)-S-12968 are much more effective in blocking contractions of vessels activated by potassium than by NA. This selectivity of calcium antagonists has been reported in several vascular beds (Schuman *et al.*, 1975; Kondo *et al.*, 1980; Godfraind *et al.*, 1986), and specifically for some new 1,4-DHP derivatives such as felodipine in rat resistance mesenteric vessels (Nyborg & Mulvany, 1984) and amlodipine in rat aorta (Matlib *et al.*, 1988). In addition, the electrophysiological study by Mulvany *et al.* (1982) demonstrates that NA (10 μM) induces a significant depolarization in rat mesenteric arteries; therefore, the possibility cannot be excluded that at least a part of the noradrenaline contraction in these arteries is due to the influx of calcium through POCs, since it is known that NA responses in rat resistance mesenteric arteries are mostly dependent on the influx of extracellular calcium (Mulvany & Nyborg, 1980; Högestätt, 1984; Nyborg & Mulvany, 1984). However, the action of (+)-S-12967 and (−)-S-12967 seems to be rather selective on POCs, since NA contractions are very little affected even by higher concentrations than those which almost totally block calcium contractions in potassium-activated vessels. The effect of nifedipine compared with that of (+)-S-12967 and (−)-S-12968, appears to be less selective since both sensitivity and maximal responses to NA are greatly reduced at the same concentration range as that used to depress the calcium-induced responses.

In summary, the present study demonstrates that (+)-S-12967 and (−)-S-12968 behave as slow-acting calcium channel modulators in rat resistance mesenteric arteries in contrast to nifedipine; the action of the isomers is stereoselective, but they both share agonistic/antagonistic properties on the calcium channel. Nifedipine had only an inhibitory action on the mesenteric resistance arteries. In addition, the two isomers selectively act on contractions induced by potassium as opposed to those induced by NA.

The authors thank Mrs Lotte Påby for valuable technical assistance. This work was generously supported by Servier, Paris, France, and the Danish Health Science Research Council, Grant No. 12-8717.

References

BOLTON, T.B. (1979). Mechanisms of action of transmitters and other substances on smooth muscle. *Physiol. Rev.*, **59**, 606–718.

BURGES, R.A., CARTER, A.J., GARDINER, D.G. & HIGGINS, A.J. (1985). Amlodipine, a new dihydropyridine calcium channel blocker with slow onset and long duration of action. *Br. J. Pharmacol.*, **85**, 281P.

BURGES, R.A., DODD, M.G. & GARDINER, D.G. (1989). Pharmacological profile of amlodipine. *Am. J. Cardiol.*, **64**, I10–I20.

BURGES, R.A., GARDINER, D.G., GWILT, M., HIGGINS, A.J., BLACKBURN, K.J., CAMPBELL, S.F., CROSS, P.E. & STUBBS, J.K. (1987). Calcium channel blocking properties of amlodipine in vascular and cardiac smooth muscle: evidence for voltage modulation of vascular dihydropyridine receptors. *J. Cardiovasc. Pharmacol.*, **9**, 110–119.

CARPI, C., GAVIRAGHI, G. & SENERARO, C. (1986). GX 1048 (GR 43659X), a new dihydropyridine calcium antagonist with potent

and long-lasting anti-hypertensive action. *Br. J. Pharmacol.*, **89**, 758P.

CAUVIN, C., LOUTZENHISER, R. & VAN BREEMEN, C. (1983). Mechanisms of calcium-induced vasodilatation. *Annu. Rev. Pharmacol. Toxicol.*, **23**, 273–296.

DUBE, G.P., BAIK, Y.H., VAGHY, P.L. & SCHWARTZ, A. (1985). Nitrendipine potentiates BAY K 8644-induced contraction of isolated porcine coronary artery: evidence for functionally distinct dihydropyridine receptors. *Biochem. Biophys. Res. Commun.*, **128**, 1295–1302.

FLECKENSTEIN, A. (1977). Specific pharmacology of calcium in myocardium, cardiac pacemakers and vascular smooth muscle. *Annu. Rev. Pharmacol. Toxicol.*, **17**, 149–166.

FRANK, B.G. (1990). Dihydropyridine calcium channel antagonists block and agonists potentiate high potassium contractures but not twitches in frog skeletal muscle. *Jpn. J. Physiol.*, **40**, 205–224.

FRANCKOWIAK, G., BECHEM, M., SCHRAMM, M. & THOMAS, G. (1985). The optical isomers of the 1,4-dihydropyridine Bay K 8644 show opposite effects on Ca channels. *Eur. J. Pharmacol.*, **114**, 223–226.

GODFRAIND, T. (1986). Calcium entry blockade and excitation contraction coupling in the cardiovascular system (with an attempt of pharmacological classification). *Acta Pharmacol. Toxicol.*, **58**, suppl. II, 5–30.

GODFRAIND, T., MILLER, R. & WIBO, M. (1986). Calcium antagonists and calcium entry blockade. *Pharmacol. Rev.*, **38**, 321–416.

HESS, P., LANSMAN, J.B. & TSIEN, R. (1984). Different modes of Ca channel gating behaviour favoured by dihydropyridines Ca agonists and antagonists. *Nature*, **311**, 538–544.

HOF, R.P., RÜEGG, A., HOF, A. & VOGEL, A. (1985). Stereoselectivity at the calcium channel: opposite action of the enantiomers of a 1,4-dihydropyridine. *J. Cardiovasc. Pharmacol.*, **7**, 689–696.

HÖGESTÄTT, E.D. (1984). Characterization of two different calcium entry pathways in small mesenteric arteries from rat. *Acta Physiol. Scand.*, **122**, 483–495.

JANIS, R.A., SILVER, P.J. & TRIGGLE, D.J. (1987). Drug action and cellular calcium regulation. *Adv. Drug Res.*, **16**, 309–391.

KAPLITA, P.V., WILKINS, D.E., ADAMS, T.C. & HANSON, R.C. (1990). A symmetrical 1,4-dihydropyridine with opposite actions on K^+-induced contractions in guinea-pig ileum. *Arch. Int. Pharmacodyn.*, **305**, 25–31.

KONDO, K., SUZUKI, H., OKUNO, T., SUDA, M. & SARUTA, T. (1980). Effects of nifedipine, diltiazem, and verapamil on the vasoconstrictor responses to norepinephrine and potassium ions in the rat mesenteric artery. *Arch. Int. Pharmacodyn. Ther.*, **245**, 211–217.

KOKUBUN, S., PROD'HOM, B., BECKER, C., PORZIG, H. & REUTER, H. (1986). Studies on Ca channels in intact cardiac cells: Voltage-dependent effects and cooperative interactions of dihydropyridine enantiomers. *J. Pharmacol. Exp. Ther.*, **30**, 571–584.

LOUTZENHISER, R., RÜEGG, U.T., HOF, A. & HOF, R.P. (1984). Studies on the mechanism of action of the vasoconstrictive dihydropyridine, CGP 23 392. *Eur. J. Pharmacol.*, **105**, 229–237.

MATLIB, M.A., FRENCH, J.F., GRUPP, P.L., VAGHY, P.L., GRUPP, G. & SCHWARTZ, A. (1988). Vascular action of amlodipine on rat aorta, pig coronary artery, human coronary artery, and on isolated Langendorff perfused rat heart preparations. *J. Cardiovasc. Pharmacol.*, **12**, suppl. 7, S50–S54.

McDONALD, J.F., MILJKOVIC, Z. & HEISLER, S. (1987). Opposing actions of the enantiomers of BAY K 8644 on calcium currents and ACTH secretion in clonal corticotrophs. *Can. J. Physiol. Pharmacol.*, **65**, 2409–2414.

MICHELLI, D., COLLODEL, A., SEMERARO, C., GAVIRAGHI, G. & CARPI, C. (1990). Lacidipine: A calcium antagonist with potent and long-lasting antihypertensive effects in animal studies. *J. Cardiovasc. Pharmacol.*, **15**, 666–675.

MOREL, N. & GODFRAIND, T. (1987). Prolonged depolarization increases the pharmacological effect of dihydropyridines and their binding affinity for calcium channels of vascular smooth muscle. *J. Pharmacol. Exp. Ther.*, **243**, 711–715.

MULVANY, M.J. & HALPERN, W. (1977). Contractile properties of small arterial resistance vessels in spontaneously hypertensive and normotensive rats. *Circ. Res.*, **42**, 19–26.

MULVANY, M.J. & NYBORG, N. (1980). An increased calcium sensitivity of mesenteric resistance vessels in young and adult spontaneously hypertensive rats. *Br. J. Pharmacol.*, **71**, 585–596.

MULVANY, M.J., NILSSON, H. & FLATMAN, J.A. (1982). Role of membrane potential in the response of rat small mesenteric resistance arteries to exogenous noradrenaline stimulation. *J. Physiol.*, **332**, 363–373.

NAKAYAMA, N., IKEZONE, K., MORI, T., YAMASHITA, S., NAKAYAMA, S., TANAKA, Y., HOSAKAWA, T., MINAMI, Y., MASUTANI, K., YANAMURA, Y. & YABUUCHI, Y. (1990). Antihypertensive activity of OPC-13340, a new potent and long-acting dihydropyridine calcium antagonist. *J. Cardiovasc. Pharmacol.*, **15**, 836–844.

NYBORG, N.C.B. & MULVANY, M.J. (1984). Effect of felodipine, a new dihydropyridine vasodilator, on the contractile responses to potassium, noradrenaline, and calcium in mesenteric resistance vessels of the rat. *J. Cardiovasc. Pharmacol.*, **6**, 499–505.

RANDLE, J.C.R., LOMBET, A., NAGEL, N., ABRAHAM, C., APTEL, H., PEGLION, J.-L. & RENAUD, J.-F. (1990). Ca^{2+} channel inhibition by a new dihydropyridine derivative, S11568, and its enantiomers S12967 and S12968. *Eur. J. Pharmacol.*, **190**, 85–96.

RIGBY, J.B., GARDINER, D.G., GREENGRASS, P.M. & BURGES, R.A. (1988). Amlodipine: interaction with the calcium channel binding sites. *J. Cardiovasc. Pharmacol.*, **12**, suppl. 6, S144.

SCHUMAN, H.J., GORLITZ, B.D. & WAGNER, J. (1985). Influence of papaverine, D600, and nifedipine on the effects of noradrenaline and calcium on the isolated aorta and mesenteric artery of the rat. *Naunyn Schmiedebergs Arch. Pharmacol.*, **289**, 409–418.

SCHRAM, M., THOMAS, G., TOWART, R. & FRANCKOWIAK, G. (1983). Novel dihydropyridines with positive inotropic action through activation of Ca^{2+} channels. *Nature*, **303**, 535–537.

SCHWARTZ, A., GRUPP, I.L., GRUPP, G., WILLIAMS, J.S. & VAGHY, P.L. (1984). Effects of dihydropyridine calcium channel modulators in the heart: Pharmacological and radioligand binding correlations. *Biochem. Biophys. Res. Commun.*, **125**, 387–394.

THOMAS, G., GROB, R. & SCHRAM, M. (1984). Calcium channel modulation: ability to inhibit or promote calcium influx resides in the same dihydropyridine molecule. *J. Cardiovasc. Pharmacol.*, **6**, 1170–1176.

(Received January 2, 1991
Revised March 2, 1991
Accepted March 18, 1991)

Br. J. Pharmacol. (1991), **103**, 1709–1712 © Macmillan Press Ltd, 1991

The cyclosporin-erythromycin interaction: impaired first pass metabolism in the pig

[1]D.J. Freeman, *D.R. Grant & †S.G. Carruthers

Robarts Research Institute, *University Hospital, the University of Western Ontario, London, Ontario, and †Victoria General Hospital, Dalhousie University, Halifax, Nova Scotia, Canada

1 The pharmacokinetic interaction between cyclosporin (CsA) and erythromycin has been studied in the weanling pig model.

2 Blood CsA and metabolite-1 (M1) concentrations were monitored by high performance liquid chromatography in portal, hepatic and jugular venus blood before and after treatment with erythromycin stearate for 7 days.

3 Erythromycin significantly increased maximum concentration (C_{max}) and area under the concentration-time curve from 0 to 24 h (AUC) of CsA in the peripheral circulation. This was accompanied by a significant reduction in the hepatic extraction ratio calculated from portal and hepatic C_{max} and AUC data.

4 The extraction ratio appears to be concentration-dependent in that values derived from C_{max} (high concentrations) were greater than those from AUC (average concentrations).

5 Time to C_{max} (t_{max}) and $t_{1/2}$ of CsA were essentially unchanged and no significant changes were observed in peripheral M1 kinetics apart from a small increase in t_{max}.

6 The pharmacokinetic changes observed in the pig suggest that the CsA-erythromycin interaction is caused by inhibition of hepatic metabolism and the impact of inhibition is greatest during first-pass when CsA concentrations are at their highest.

Keywords: Cyclosporin; erythromycin; interaction; hepatic metabolism

Introduction

Cyclosporin (CsA) is a cyclic undecapeptide which is used as an immunosuppressant in transplantation procedures and in experimental treatment of various autoimmune diseases. The major problem with its use in man is nephrotoxicity associated with a narrow therapeutic range. Clinical judgments made on the basis of CsA concentrations measured in blood or serum are difficult in some cases due to drug interactions with coadministered medications. One such drug is erythromycin. We (Freeman *et al.*, 1987a) and others (Ptachcinski *et al.*, 1985; Hourmant *et al.*, 1986; Martell *et al.*, 1986; Gonwa *et al.*, 1986; Wadhwa *et al.*, 1987) have previously observed that coadministration of oral CsA and erythromycin in man causes CsA concentrations to increase dramatically. Whether this effect is due to decreased hepatic metabolism or increased absorption is not clear (Freeman *et al.*, 1987a; Gupta *et al.*, 1988). Studies were conducted in our laboratory on the weanling pig as an experimental model to investigate the mechanism of this interaction. CsA pharmacokinetics in the pig have been assessed previously (Freeman *et al.*, 1990).

Methods

We studied 7 female Duroc-Hampshire weanling pigs (15–20 kg) following a protocol approved by our institution's Animal Research Committee. Laparotomy was conducted under halothane anaesthesia and a gastric-tube inserted into the lumen of the stomach. The tube was externalized through the side of the body cavity and extended to the animal's back. Portal, hepatic and jugular catheters were also installed at the same time. These were tunnelled beneath the skin and exposed on the animal's back in the same location as the gastric-tube. Both tube and catheters were taped into place for dosing and blood sampling in conscious animals. Catheters were flushed twice a day with heparinized saline. Each animal was allowed to recover from surgery for a minimum of 4 days before experiments were started.

Control CsA concentration-time profiles were generated in fasting (12 h) pigs following administration of CsA (10 mg kg^{-1}) in 20 ml milk through the gastric-tube. Milk solution remaining in the tube was flushed into the stomach with 20 ml water. Blood samples (1.5 ml) were drawn from each catheter with a syringe and placed in 5 ml EDTA vaccutainer tubes immediately before dosing and at 0.25, 0.5, 0.75, 1, 1.5, 2, 2.5, 3, 4, 6, 8, 12 and 24 h. Samples at 0.25, 0.75, 1.5, and 2.5 h were collected only from the last 3 pigs.

CsA and a major metabolite in the pig, M1, were measured in whole blood by high performance liquid chromatography (h.p.l.c.) (Carruthers *et al.*, 1983; Freeman *et al.*, 1987b). After the 24 h sample was drawn each pig was dosed twice daily for 7 days with 10 ml erythromycin stearate suspension (Abbott, 250 mg ml^{-1}). On day 8 the kinetics of CsA were again studied after a 10 mg kg^{-1} dose.

The following pharmacokinetic parameters were measured by standard techniques; maximum concentration (C_{max}), time to C_{max} (t_{max}) area under the concentration-time curve from 0 to 24 h (AUC), terminal half-life ($t_{1/2}$) and oral clearance (CL_0). The hepatic extraction ratios (ER) of CsA and M1 were derived from the following relationship:

$$ER = [C(P) - C(H)]/C(P)$$

where C(P) and C(H) are the concentrations of CsA or M1 in the portal and hepatic blood, respectively. Calculations were made using C_{max} data to give ER at high concentrations and from AUC data which gives an average value of hepatic ER across the whole sampling period (24 h). Results are expressed as means ± s.e. Statistical evaluation was performed with the t test for paired data, $P < 0.05$ being considered statistically significant.

Results

The effect of erythromycin on concentrations of CsA and M1, the major porcine metabolite, in portal, hepatic and jugular

[1] Author for correspondence at: Clinical Pharmacology, Robarts Research Institute, 100 Perth Drive, London, Ontario, Canada, N6A 5K8.

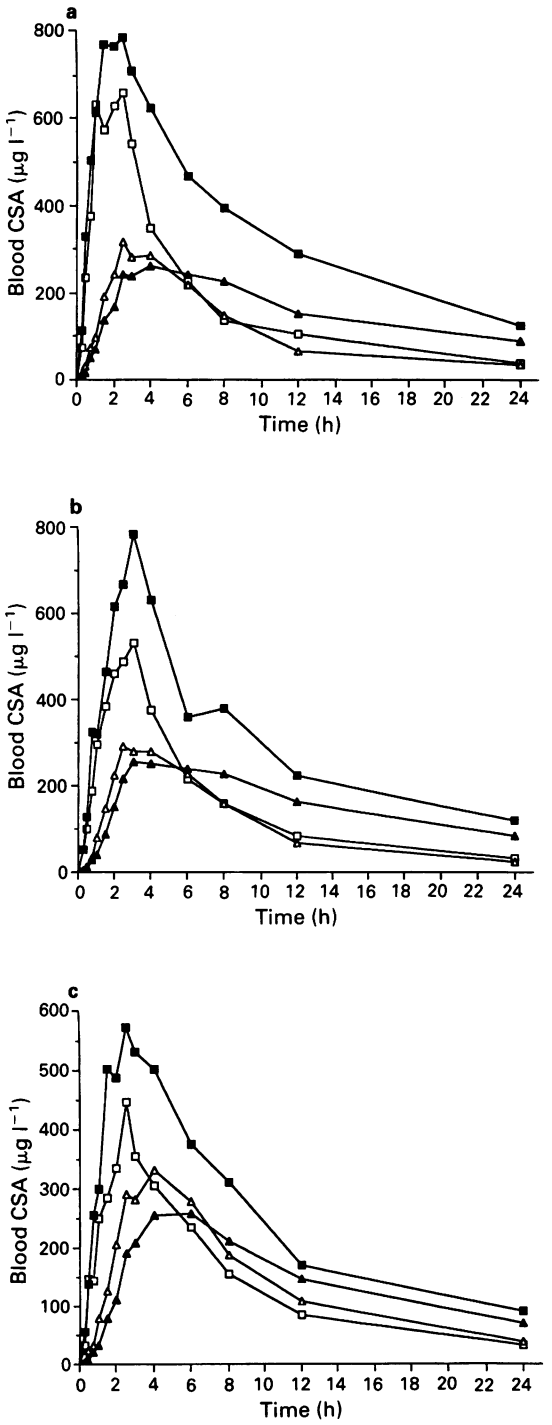


Figure 1 Cyclosporin (CsA, □, ■) and metabolite-1 (M1, △, ▲) concentrations in (a) portal, (b) hepatic and (c) jugular blood of the pig following single doses of CsA before (□, △) and after (■, ▲) erythromycin administered for 7 days. Standard error bars are omitted for clarity.

blood is shown in Figure 1. The error bars have been omitted for clarity. Tables 1 and 2 display CsA and M1 pharmacokinetic data before and after erythromycin administration. The control CsA concentration-time profiles obtained from all sampling sites were parallel and graded with portal AUC (and C_{max}) being the largest; hepatic, intermediate and jugular, the smallest. After erythromycin treatment C_{max} and AUC increased proportionally at each sampling site with corresponding declines in CL_0. C_{max} and AUC in peripheral (jugular) blood increased by 150% and 180% respectively, compared to control but there was no change in t_{max}. An increase (28%) in $t_{1/2}$ was observed but this did not reach statistical significance. As in man (Freeman *et al.*, 1987a), the response of peripheral CsA concentrations to erythromycin administration was variable with C_{max} increasing from 106% to as much as 279%.

Unlike parent CsA, the C_{max} of M1 did not change significantly at any sampling site after erythromycin treatment. However, AUC increased significantly in the portal (35%) and hepatic blood (50%) but was attenuated to an insignificant level in the peripheral circulation (15%). The increased AUC in portal and hepatic venous blood in t_{max} for M1 was generally unaltered but $t_{1/2}$ tended to be longer.

Comparison of hepatic ERs (Tables 1 and 2) indicated that extraction of CsA but not M1, was significantly reduced following erythromycin treatment. (C_{max}: pre 0.31, post 0.13 vs AUC: pre 0.18, post 0.08).

Discussion

The results of this study demonstrate that the effect of erythromycin on the kinetics of oral CsA in the pig model is similar to that observed in healthy male volunteers (Freeman *et al.*, 1987a). In the latter study it was not clear whether the interaction was due to reduced hepatic metabolism or increased absorption. Several *in vitro* studies have shown that erythromycin is a substrate for hepatic P-450 enzyme systems and therefore could potentially alter CsA metabolism (Kronbach *et al.*, 1988; Henricsson *et al.*, 1988; Fabre *et al.*, 1988; Larrey *et al.*, 1983). However, it is not fully appreciated that *in vitro*, CsA is unbound whereas *in vivo* it is bound almost entirely to circulating lipoproteins and red cells. There is little doubt such binding would affect distribution and access of CsA to intact cells (Brunner *et al.*, 1988). The alternative explanation, that erythromycin increases intestinal CsA absorption, was proposed by Gupta *et al.* (1988) based on pharmacokinetic studies which appeared to show that the erythromycin interaction occurs with oral but not intravenous CsA. Changes in the amount of CsA absorbed could potentially explain this interaction because the gastointestinal absorption of CsA is incomplete and variable in man (Grevel, 1988). We previously showed that CsA bioavailability in the pig is similar to that in man (Freeman *et al.*, 1990) and in the present study, bioavailability assessed on paired oral and intravenous AUC data in two pigs was 25% and 30%. Since the ER in the pig is about 0.3 (Table 1), similar to man, the low bioavailability is due mainly to poor absorption.

The results of the present study show little evidence of an increase in the rate or amount of CsA absorbed. t_{max} was not altered by erythromycin and the increases in portal C_{max} and AUC after treatment are most probably due to elevated CsA concentrations in blood returning from the peripheral circulation. On the other hand, viewed from the peripheral circulation, the reduction in CsA hepatic ER, the significant elevations in C_{max} and AUC and the absence of parallel changes for M1, strongly suggest that erythromycin inhibits hepatic CsA metabolism. The relatively small effect of this interaction on $t_{1/2}$ may be explained by the apparent time- and/or concentration-dependence of the hepatic extraction ratio. The almost two fold difference in the ratio, depending on whether it is calculated with C_{max} (high CsA concentrations) or AUC (average concentrations), suggests that the hepatic clearance of CsA increases as concentrations rise. This favours a first-pass effect and explains why $t_{1/2}$, which is normally calculated from relatively low post-distribution data in the terminal phase of the concentration-time profile is affected only to a small extent by erythromycin. Comparison of concentration-time profiles for M1 (Figure 1) reveal a tendency for both the formation and elimination of M1 to be slowed after erythromycin treatment in accord with reduced CsA metabolism. Comparison of C_{max} AUC and $t_{1/2}$ data for M1 (Table 2) also reflect these changes but statistical significance could not be demonstrated. The reason for the

Table 1 Effect of erythromycin on cyclosporin kinetics in the pig

	*Vein**	n	*Control*	*Erythromycin*	P
C_{max} ($mg l^{-1}$)	PV	5	717.3 (56.3)	832.8 (52.5)	0.250
	HV	6	553.6 (69.1)	815.6 (103)	0.030
	JV	7	429.4 (56.3)	631.5 (77.6)	0.036
t_{max} (h)	PV	5	2.0 (0.45)	2.6 (0.43)	0.284
	HV	6	3.0 (0.43)	2.7 (0.21)	0.444
	JV	7	2.6 (0.50)	2.6 (0.34)	0.736
$t_{1/2}$ (h)	PV	5	6.7 (0.48)	8.8 (1.46)	0.310
	HV	6	6.6 (0.67)	8.7 (0.90)	0.195
	JV	7	6.8 (0.65)	8.7 (1.00)	0.248
AUC ($\mu g l^{-1} h^{-1}$)	PV	5	4510 (561)	7718 (1523)	0.084
	HV	6	3714 (373)	7227 (1506)	0.052
	JV	7	3358 (439)	6006 (1316)	0.042
CL_0 ($l h^{-1} kg^{-1}$)	PV	5	2.14 (0.18)	1.39 (0.25)	0.023
	HV	6	2.50 (0.23)	1.50 (0.29)	0.006
	JV	7	2.73 (0.32)	1.82 (0.39)	0.004
ER [C_{max}]**		5	0.31 (0.04)	0.13 (0.06)	0.019
ER [AUC]		5	0.18 (0.01)	0.08 (0.05)	0.043

* PV = portal vein, HV = hepatic vein, JV = jugular vein.
** ER = Hepatic extraction ratio.
Values are expressed as mean (±s.e.).

Table 2 Effect of erythromycin on cyclosporin-M1 in the pig

	*Vein**	n	*Control*	*Erythromycin*	P
C_{max} ($mg l^{-1}$)	PV	5	304.6 (40.4)	279.8 (57.2)	0.553
	HV	6	297.4 (32.4)	290.5 (43.3)	0.837
	JV	7	344.1 (30.7)	279.8 (57.2)	0.125
t_{max}	PV	5	3.5 (0.45)	5.4 (1.08)	0.146
	HV	6	3.5 (0.43)	4.8 (0.91)	0.102
	JV	7	3.8 (0.49)	5.1 (0.74)	0.047
$t_{1/2}$ (h)	PV	5	7.4 (1.00)	13.9 (4.95)	0.241
	HV	6	5.4 (0.73)	12.5 (4.43)	0.165
	JV	7	6.1 (1.00)	13.4 (4.85)	0.193
AUC ($\mu g l^{-1} h^{-1}$)	PV	5	2798 (488)	3790 (741)	0.030
	HV	6	2519 (407)	3791 (588)	0.003
	JV	7	2700 (443)	3101 (599)	0.689
ER [C_{max}]**		5	0.05 (0.020)	0.00 (0.004)	0.086
ER [AUC]		5	0.09 (0.044)	−0.04 (0.020)	0.058

* PV = portal vein, HV = hepatic vein, JV = jugular vein.
** ER = Hepatic extraction ratio.
Values are expressed as mean (±s.e.).

increased AUC in hepatic and portal blood is not clear but may be due to decreased clearance of M1 resulting from inhibition of subsequent oxidation steps (i.e. dihydroxylation to M10 or M16). Nevertheless, based on AUC data, the ratio of M1 to CsA is reduced by 21% (PV) and 23% (HV) as a result of erythromycin treatment.

In conclusion, the erythromycin-CsA interaction frequently observed in man has been reproduced in the pig model. Our results suggest that erythromycin reduces CsA clearance by inhibiting hepatic metabolism and that greatest inhibitory activity is most likely to occur during the early post-absorptive first-pass period when portal CsA concentrations are high.

This work was supported by a grant from the Medical Research Council of Canada.

References

BRUNNER, L.J., VADIEI, K. & LUKE, D.R. (1988). Cyclosporine disposition in the hyperlipidemic rat model. *Res. Commun. Chem. Path. Pharmacol.*, **59**, 339–347.

CARRUTHERS, S.G., FREEMAN, D.J., KOEGLER, J., HOWSON, W., KEOWN, P.A., LAUPACIS, P.A. & STILLER, C.R. (1983). Simplified liquid-chromatographic analysis of cyclosporine A and comparison with radioimmunoassay. *Clin. Chem.*, **29**, 180–183.

FABRE, I., FABRE, G., MAUREL, P., BERTAULT-PERES, P. & CANO, J.-P. (1988). Metabolism of cyclosporin A: III. Interaction of the macrolide antibiotic, erythromycin, using rabbit hepatocytes and microsomal fractions. *Drug Metab. Dispos.*, **16**, 296–301.

FREEMAN, D.J., GRANT, D.R., LIPOHAR, C. & KREEFT, J. (1990). Pharmacokinetics of cyclosporine in the weanling pig. *Transplantation*, **50**, 892–893.

FREEMAN, D.J., KOEGLER, J. & CARRUTHERS, S.G. (1987b). Improved extraction and chromatography of cyclosporins. *Clin. Chem.*, **33**, 477.

FREEMAN, D.J., MARTELL, R., CARRUTHERS, S.G., HEINRICHS, D., KEOWN, P.A. & STILLER, C.R. (1987a). Cyclosporin-erythromycin interaction in normal subjects. *Br. J. Clin. Pharmacol.*, **23**, 776–777.

GONWA, T.A., NGHIEM, J.A., SCHULAK, J.A. & CORRY, R.J. (1986). Erythromycin and cyclosporine. *Transplantation*, **41**, 797–799.

GREVEL, J. (1988). Significance of cyclosporine pharmacokinetics. *Transpl. Proc.*, **20**, (2 suppl 2), 428–434.

GUPTA, S.K., BAKRAN, A., JOHNSON, R.W. & ROWLAND, M. (1988). Erythromycin enhances the absorption of cyclosporine. *Br. J. Clin. Pharmacol.*, **25**, 401–402.

HENRICSSON, S. & LINDHOLM, A. (1988). Inhibition of cyclosporine metabolism by other drugs *in vitro*. *Transpl. Proc.*, **20** (2 suppl 2), 569–571.

HOURMANT, M., LEBIGOT, J.F., VERNILLET, L., SAGNIEZ, G., REMI, J.P. & SOULILLOU, J.P. (1986). Coadministration of erythromycin results in an increase of blood cyclosporine to toxic levels. *Transpl. Proc.*, **17**, 2723–2727.

KRONBACH, T., FISCHER, V. & MEYER, U.A. (1988). Cyclosporine

metabolism in human liver: identification of a cytochrome P-450 III gene family as the major cyclosporine metabolizing enzyme explains interactions of cyclosporine with other drugs. *Clin. Pharmacol. Ther.*, **43**, 630–635.

LARREY, D., FUNCK-BRENTANO, C., BREIL, P., VITAUX, J., THEODORE, C., BABANY, G. & PESSAYRE, D. (1983). Effects of erythromycin on hepatic drug-metabolizing enzymes in humans. *Biochem. Pharmacol.*, **32**, 1063–1068.

MARTELL, R., HEINRICHS, D., STILLER, C.R., JENNER, M.R., KEOWN, P.A. & DUPRE, J. (1986). Erythromycin in cyclosporin treated patients. *Ann. Intern. Med.*, **104**, 660–661.

PTACHCINSKI, R.J., CARPENTER, J., BURKART, G.J., VENKATARAMANAN, R. & ROSENTHAL, J.T. (1985). Effect of erythromycin on cyclosporine levels. *N. Engl. J. Med.*, **313**, 1416–1417.

WADHWA, N.K., SCHROEDER, T.J., O'FLAHERTY, E., PESCE, A.J., MYER, S.A., MUNDA, R. & FIRST, M.R. (1987). Interaction between erythromycin and cyclosporine in a kidney and pancreas allograft recipient. *Ther. Drug. Monit.*, **9**, 123–125.

(Received September 25, 1990
Revised March 13, 1991
Accepted March 18, 1991)

Br. J. Pharmacol. (1991), **103**, 1713–1718 © Macmillan Press Ltd, 1991

Comparison of the effects of the novel vasodilator FK409 with those of nitroglycerin in isolated coronary artery of the dog

Hiroaki Yamada, Fumiya Yoneyama, Keisuke Satoh & Norio Taira

Department of Pharmacology, Tohoku University School of Medicine, Sendai 980, Japan

1 The vasorelaxant effects of FK409, a new nitrovasodilator synthesized from a microbial product, were compared with those of nitroglycerin in isolated coronary artery rings of the dog contracted with U46619 (10^{-7} M).

2 FK409 (10^{-11}–10^{-5} M) and nitroglycerin (10^{-9}–10^{-4} M) each produced a concentration-dependent relaxation. Comparison of EC_{50} values showed that FK409 was about 25 times more potent than nitroglycerin.

3 Submaximum concentrations of nitroglycerin (10^{-6} M) and FK409 (3×10^{-8} M) elevated guanosine 3':5'-cyclic monophosphate (cyclic GMP) levels, effects associated with vasorelaxation. Adenosine 3':5'-cyclic monophosphate (cyclic AMP) levels were unaffected.

4 The concentration-relaxation curves for nitroglycerin and FK409 were shifted to the right by methylene blue (3×10^{-6}–3×10^{-5} M), an inhibitor of soluble guanylate cyclase, and to the left by M&B22,948 (3×10^{-6}–3×10^{-5} M), an inhibitor of cyclic GMP phosphodiesterase.

5 After exposure of coronary arteries to the maximally-effective concentration of nitroglycerin (10^{-4} M), the mean EC_{50} value of FK409 did not change significantly, although that of nitroglycerin increased about 60 fold. After exposure to the maximally-effective concentration of FK409 (10^{-5} M), the mean EC_{50} value of FK409 increased about 6 fold and that of nitroglycerin about 11 fold.

6 These results suggest that the vasorelaxant effect of FK409, like that of nitroglycerin, is due to activation of soluble guanylate cyclase and a resultant increase in intracellular cyclic GMP. However, compared with nitroglycerin, there was less self-tolerance to the relaxant effects of FK409 and relatively little cross-tolerance between the two agents.

Keywords: FK409; nitroglycerin; dog coronary artery; self-tolerance; cross-tolerance; cyclic GMP

Introduction

(±)-(E)-4-ethyl-2-[(E)-hydroxyimino]-5-nitro-3 - hexenamide (FK409; FR900409) (Figure 1) is a structurally unique vasodilator discovered in the search for compounds with vasodilator and antiplatelet activities in fermentation products of *Streptomyces griseosporeus* (Hino *et al.*, 1989). FK409 showed a potent relaxant activity on rat isolated aortae contracted with noradrenaline (Hino *et al.*, 1989). The drug also exerted a relaxant effect on dog isolated arterial strips contracted with KCl, and its relaxant potency was greater in coronary than in basilar, renal, mesenteric and saphenous arteries (Sato *et al.*, 1990). In anaesthetized dogs whose hearts underwent ischaemia by partial coronary occlusion, FK409 decreased left ventricular end-diastolic pressure and arterial blood pressure, and increased endomyocardial blood flow and increased the flow ratio of endomyocardium/epimyocardium (Sato *et al.*, 1990). These effects of FK409 are very similar to those observed with nitroglycerin in patients with ischaemic heart disease and in animal models of cardiac ischaemia (Becker & Pitt, 1971). In addition, FK409 inhibits platelet aggregation (Hino *et al.*, 1989), and nitrates also exert similar effects (Schafer *et al.*, 1980; Mellion *et al.*, 1981). Despite the close similarity between FK409 and nitroglycerin in vasodilator and anti-platelet aggregation activities, FK409 is not a nitrate. However, in view of its chemical structure it may produce nitric oxide by biotransformation, although this has not yet been elucidated.

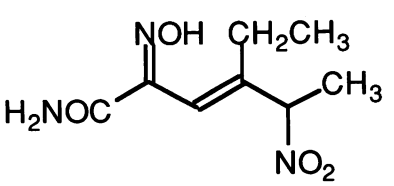


Figure 1 Chemical structure of FK409.

Tolerance to nitroglycerin is a significant clinical problem (Horowitz & Henry, 1987; Packer *et al.*, 1987; Katz, 1990). Unlike nitroglycerin, however, FK409 has been reported to develop neither self-tolerance nor cross-tolerance to nitroglycerin (Sato *et al.*, 1990). Thus, in the present study we initially compared the vasorelaxant effect of FK409 with that of nitroglycerin in dog isolated coronary arteries. Secondly, we investigated changes in cyclic nucleotide levels produced by the two vasodilators simultaneously with their relaxant effect. Thirdly, we determined whether the effects of FK409 were modified by methylene blue, an inhibitor of soluble guanylate cyclase (Ignarro *et al.*, 1981), or by M&B22,948, an inhibitor of cyclic GMP phosphodiesterase (Souness *et al.*, 1989). Finally, we studied the extent to which self-tolerance and cross-tolerance developed to the effects of FK409 and nitroglycerin.

Methods

Isolated coronary ring preparation

Mongrel dogs of either sex, weighing 7 to 12 kg were anaesthetized with pentobarbitone sodium (30 mg kg^{-1}, i.v.) and their hearts were removed. The proximal portion of the circumflex branch of the left coronary artery was dissected out from surrounding myocardial tissue and isolated coronary arterial rings (about 2 mm in length) were prepared by cutting with scissors. After the endothelium had been removed by rubbing, each ring was suspended in a 25 ml, thermostatically-controlled (37°C) organ bath containing Krebs-Henseleit solution bubbled with a mixture of 95% O_2 and 5% CO_2. The composition of this solution was as follows (mM): NaCl 118, $NaHCO_3$ 24.9, KCl 4.7, KH_2PO_4 1.2, $CaCl_2$ 2.5, $MgSO_4$ 1.2

and glucose 11.1. A resting tension of 2 g was applied throughout the 60 min equilibration period. Isometric changes in muscle tension were recorded on pen recorders (TOA, FBR252A) by means of isometric force transducers (NEC San-ei, 45196A).

Experimental protocol

Cumulative concentration-effects of FK409 and nitroglycerin were evaluated on preparations contracted with 10^{-7} M U46619 (an EC_{80}). Successive concentrations were applied when the vasorelaxant effect of the previous concentration had reached a nadir. Methylene blue (3×10^{-6}–3×10^{-5} M) and M&B22,948 (3×10^{-6}–3×10^{-5} M) were added to the Krebs-Henseleit solution 30 min before introduction of U46619. Tolerance was induced by means of the method of Henry *et al.* (1989). In brief, preparations were exposed for 60 min to the maximally-effective concentration of either nitroglycerin (10^{-4} M) or FK409 (10^{-5} M), and washed every 10 min for an additional 60 min before introduction of U46619.

Cyclic nucleotide assay

In experiments in which guanosine 3′:5′-cyclic monophosphate (cyclic GMP) and adenosine 3′:5′-cyclic monophosphate (cyclic AMP) contents were measured simultaneously with tension, coronary artery rings were removed from the baths at predetermined times after introduction of nitroglycerin or FK409, and immediately frozen in liquid nitrogen. The cyclic GMP and cyclic AMP contents of these frozen samples were measured with sensitive radioimmunoassay methods described elsewhere (Endoh & Taira, 1983).

Drugs

Nitroglycerin (0.05% aqueous solution in ampoule; Nippon Kayaku) FK409 (Fujisawa) and M&B22,948 (2-*o*-propoxyphenyl-8-azapurine-6-one; May & Baker) were generous gifts from each company. U46619 (9,11-dideoxy-11α,9α-epoxymethano-prostaglandin $F_{2\alpha}$, Sigma), methylene blue (Wako Pure Chemical), and cyclic GMP-[^{125}I] and cyclic AMP-[^{125}I] assay kits (Amersham) were purchased. FK409 was dissolved in distilled water at a concentration of 10^{-2} M and methylene blue at a concentration of 10^{-1} M. M&B22,948 was dissolved in 10% triethanolamine at a concentration of 10^{-1} M. U46619 was dissolved in 99.5% ethanol at a concentration of 10^{-3} M. These stock solutions and nitroglycerin solution were diluted with distilled water to the desired concentrations when necessary.

Analysis of concentration-relaxation curves and statistics

In concentration-relaxation curves for nitroglycerin and FK409, relaxant effects were expressed as % inhibition of 10^{-7} M U46619-induced contraction, which we defined as 100%, and computer fitted to a logistic equation:

$$Y = M \times D^p/(K^p + D^p)$$

where M is the maximum effect of each drug, D is drug concentration, K is EC_{50} value of each drug and p is the slope parameter (Parker & Waud, 1971).

Experimental values are expressed in terms of mean ± s.e.mean. Comparisons of concentration-relaxation curves were made by analysis of variance. Statistical significance of differences between mean values was estimated by *t* test. A *t* test for the paired comparison was used when it was applicable. A *P* value smaller than 0.05 was considered to be significant.

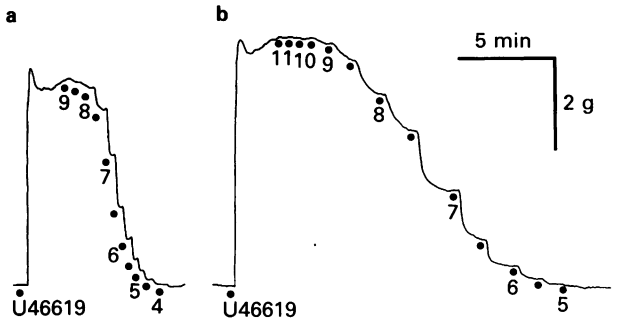


Figure 2 Representative traces showing the relaxant effects of (a) nitroglycerin and (b) FK409 on dog coronary artery rings contracted with U46619 (10^{-7} M). The drugs were added at the points shown. Concentrations of the drugs are shown as −log [M].

Results

Vasorelaxant effects of FK409 and nitroglycerin

In isolated coronary artery rings contracted with U46619, cumulative administration of FK409 (10^{-11}–10^{-5} M) or nitroglycerin (10^{-9}–10^{-4} M) induced a concentration-dependent relaxation, and the maximum relaxation produced by each was a little more than 100%. Typical experiments are reproduced in Figure 2, and concentration-relaxation curves for both drugs are presented in Figure 3. The vasorelaxant effect of FK409 developed more slowly than that of nitroglycerin (Figure 2). The mean EC_{50} values of FK409 and nitroglycerin derived from 24 preparations for each were 4.2×10^{-9} M and 1.0×10^{-7} M, respectively. Thus, the vasorelaxant potency of FK409 was 24.4 times that of nitroglycerin. Slope parameters and maxima were not significantly different between nitroglycerin and FK409 (Figure 3).

Time course of relaxation and that of changes in cyclic nucleotide levels produced by nitroglycerin and FK409

The basal contents of cyclic GMP and cyclic AMP in isolated coronary rings contracted with U46619 were 29.1 ± 4.3 fmol mg^{-1} wet wt and 405.7 ± 90.3 fmol mg^{-1} wet wt, respectively. U46619 had no significant effect on either the cyclic GMP or the cyclic AMP content of the tissues. The time course of the relaxation and that of the changes in cyclic GMP and cyclic AMP levels in response to submaximum concentrations of nitroglycerin (10^{-6} M) and FK409 (3×10^{-8} M) are shown in Figures 4 and 5. After administration of nitroglycerin cyclic GMP levels increased rapidly

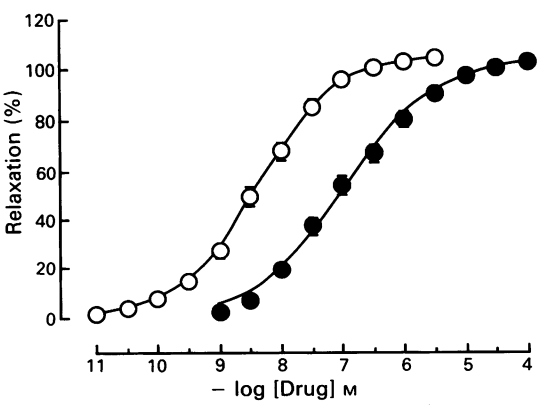


Figure 3 Mean concentration-relaxation curves for FK409 (○) and nitroglycerin (●) in U46619-contracted dog coronary artery rings. Each point represents the mean of 24 experiments; s.e.mean shown by vertical bars if larger than the point.

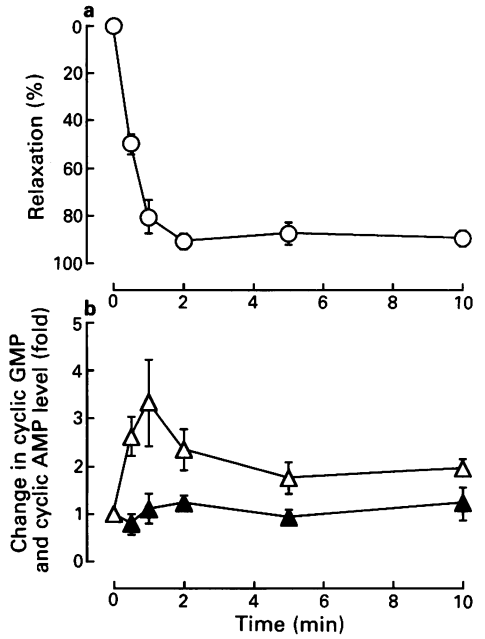


Figure 4 Time course of (a) the relaxation (○) and (b) of the changes in cyclic GMP (△) and cyclic AMP (▲) levels in response to nitroglycerin (10^{-6} M) in U46619-contracted dog coronary artery rings. Each point represents the mean of 6 experiments; s.e.mean shown by vertical bars.

and reached a peak in 1 min, and then decreased, although the cyclic GMP content remained higher than basal values. At their peak, cyclic GMP levels increased 3.3 ± 0.9 fold ($n = 6$). However, the mechanical relaxation reached a nadir 2 min after the introduction of nitroglycerin with a maximum inhibition of 90.7 ± 3.5% ($n = 6$) (Figure 4). On exposure to FK409, cyclic GMP levels increased gradually and reached a maximum value after 5 min at which time cyclic GMP levels had increased 2.8 ± 0.5 fold ($n = 6$). The relaxation produced by FK409 reached a nadir after 10 min at which time the relaxation was 91.5 ± 3.5% ($n = 6$) (Figure 5). Both drugs, however, had no significant effects on cyclic AMP levels.

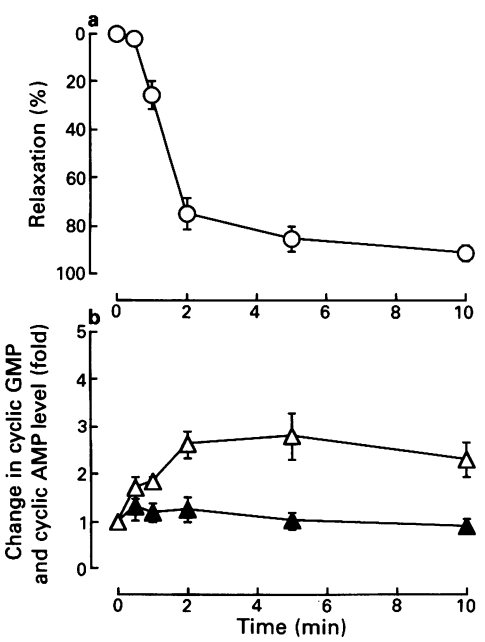


Figure 5 Time course of (a) the relaxation (○) and (b) of the changes in cyclic GMP (△) and cyclic AMP (▲) levels in response to FK409 (3×10^{-8} M) in U46619-contracted dog coronary artery rings. Each point represents the mean of 6 experiments; s.e.mean shown by vertical bars.

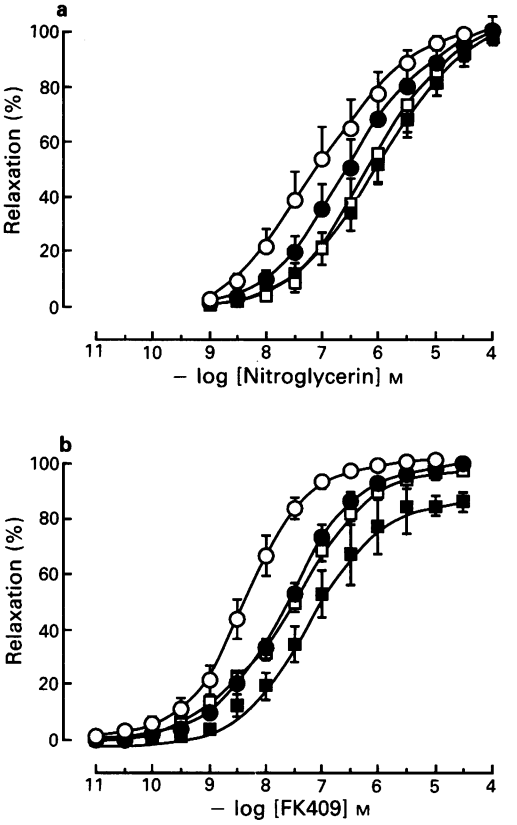


Figure 6 Mean concentration-relaxation curves for (a) nitroglycerin and (b) FK409 in U46619-contracted dog coronary artery rings in the presence of methylene blue added 30 min before introduction of U46619: (○) control; (●) 3×10^{-6} M; (□) 1×10^{-5} M and (■) 3×10^{-5} M. Each point represents the mean of 6 experiments; s.e.mean shown by vertical bars.

Modifications by methylene blue and M&B22,948 of the vasorelaxant effects of nitroglycerin and FK409

In the presence of methylene blue (3×10^{-6}–3×10^{-5} M) the concentration relaxation curves for nitroglycerin and FK409 were shifted to the right (Figure 6). The mean EC_{50} values for nitroglycerin were significantly increased by 10^{-5} and 3×10^{-5} M methylene blue, and those of FK409 were also significantly increased by 3×10^{-6}, 10^{-5} and 3×10^{-5} M methylene blue ($n = 6$) (Table 1). The magnitudes of changes in the mean EC_{50} values produced by each concentration of methylene blue were similar for both nitroglycerin and FK409 (Table 1).

The concentration-relaxation curves for nitroglycerin and FK409 were shifted to the left in the presence of M&B22,948

Table 1 pEC_{50} values (negative logarithm of EC_{50} values) of nitroglycerin and FK409 in the absence (control) and presence of methylene blue and M&B22,948

	pEC_{50} value	
	Nitroglycerin	*FK409*
Methylene blue		
Control	7.01 ± 0.33	8.35 ± 0.14
3×10^{-6} M	6.45 ± 0.32	7.74 ± 0.08*
1×10^{-5} M	6.05 ± 0.25*	7.42 ± 0.09*
3×10^{-5} M	6.01 ± 0.21*	7.01 ± 0.33*
M&B22,948		
Control	6.93 ± 0.21	8.62 ± 0.10
3×10^{-6} M	7.30 ± 0.19	9.23 ± 0.12*
1×10^{-5} M	7.59 ± 0.17*	9.47 ± 0.24*
3×10^{-5} M	7.68 ± 0.19*	9.89 ± 0.26*

Values are means ± s.e.mean of six experiments. * $P < 0.05$ compared with control values.

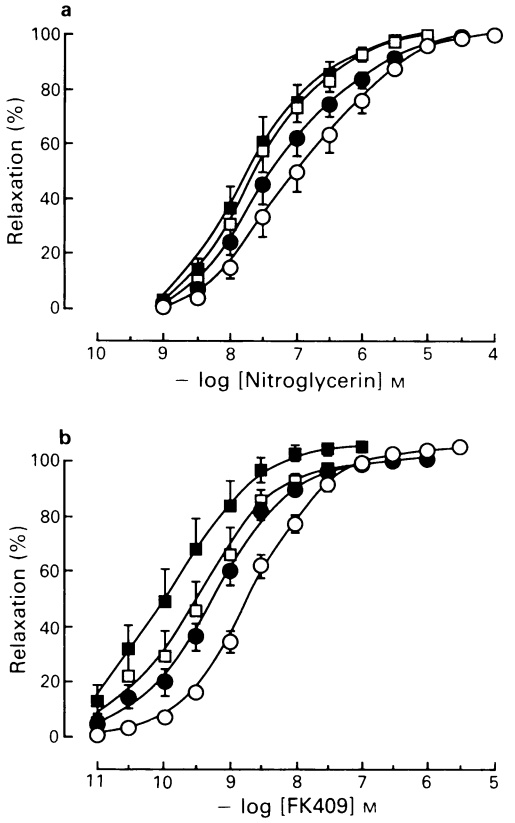


Figure 7 Mean concentration-relaxation curves for (a) nitroglycerin and (b) FK409 in U46619-contracted dog coronary artery rings in the presence of M&B22,948 added 30 min before addition of U46619: (○) control; (●) 3×10^{-6} M; (□) 1×10^{-5} M and (■) 3×10^{-5} M. Each point represents the mean of 6 experiments; s.e.mean shown by vertical bars.

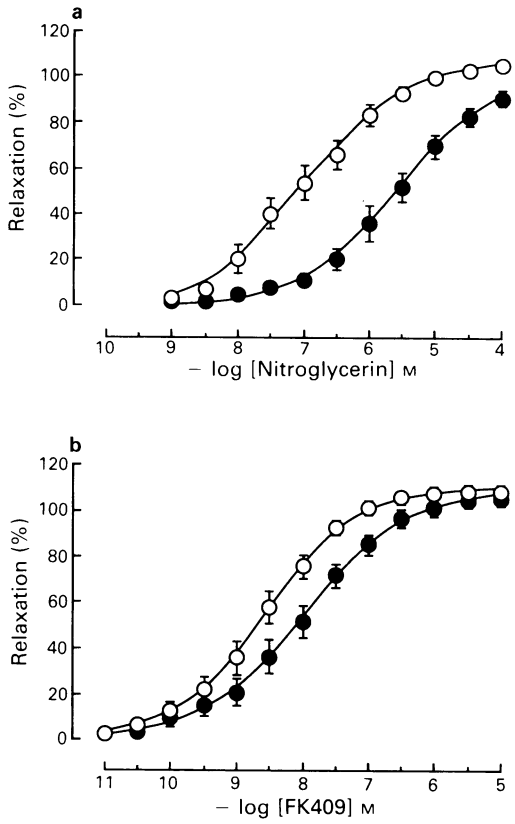


Figure 8 Mean concentration-relaxation curves for (a) nitroglycerin and (b) FK409 in U46619-contracted dog coronary artery rings in the tolerance study: (○) control; (●) after exposure to the maximum concentration of nitroglycerin (a, 1×10^{-4} M) or FK409 (b, 1×10^{-5} M). Each point represents the mean of 6 experiments; s.e.mean shown by vertical bars.

(3×10^{-6}–3×10^{-5} M) (Figure 7). The mean EC_{50} values for nitroglycerin were significantly decreased by 10^{-5} and 3×10^{-5} M M&B22,948, and those of FK409 by 3×10^{-6}, 10^{-5} and 3×10^{-5} M M&B22,948 ($n = 6$) (Table 1). The magnitudes of changes in the mean EC_{50} values produced by each concentration of M&B22,948 were similar for both nitroglycerin and FK409 (Table 1).

Contractions induced by U46619 were unaffected by methylene blue but were reduced by about 43% in the presence of the highest concentration (3×10^{-5} M) of M&B22,948 ($n = 6$).

Self-tolerance and cross-tolerance to the vasorelaxant effects of nitroglycerin and FK409

Isolated coronary artery rings of the dog pre-exposed for 60 min to either nitroglycerin (10^{-4} M) or FK409 (10^{-5} M) became significantly less responsive to the vasorelaxant actions of each drug than time-matched control rings (Figure 8). The mean EC_{50} value of nitroglycerin increased 61.5 fold ($n = 6$), but the increase in the mean EC_{50} value of FK409 was only 5.7 fold ($n = 6$) (Table 2).

Table 2 pEC_{50} values of nitroglycerin and FK409 in control and after exposure to nitroglycerin or FK409

	pEC_{50} value	
	Nitroglycerin	*FK409*
Control	7.29 ± 0.40	8.25 ± 0.10
Nitroglycerin (10^{-4} M)	5.50 ± 0.21*	8.10 ± 0.20
Control	7.07 ± 0.11	8.56 ± 0.15
FK409 (10^{-5} M)	6.03 ± 0.07*	8.00 ± 0.15*

Values are means ± s.e.mean of six experiments. * $P < 0.05$ compared with control values.

Rings pre-exposed to 10^{-5} M FK409 also became less responsive to the vasorelaxant action of nitroglycerin than time-matched control rings, with a 10.9 fold increase in the mean EC_{50} value of nitroglycerin ($n = 6$) (Figure 9). The concentration-relaxation curve for FK409 tended to shift to the right following pre-exposure to 10^{-4} M nitroglycerin, but the resulting mean EC_{50} value of FK409 was not significantly different from that of the time-matched control group ($n = 6$) (Table 2).

Pre-exposure to either nitroglycerin (10^{-4} M) or FK409 (10^{-5} M) for 60 min had no effect on contraction induced by U46619 (10^{-7} M).

Discussion

In the present experiments on dog isolated coronary artery rings, FK409 was a very potent vasorelaxant; comparing EC_{50} values, FK409 was about 25 times more potent than nitroglycerin, while the vasorelaxant effect of FK409 developed more slowly than that of nitroglycerin. There was, however, no significant difference between the slopes and maxima of concentration-relaxation curves to FK409 and nitroglycerin.

The vasorelaxant mechanism of nitroglycerin is currently understood to involve an increase in intracellular cyclic GMP levels (Kukovetz *et al.*, 1979). In the present experiments, nitroglycerin increased cyclic GMP levels and the peak increase coincided with its relaxant effects. FK409 at a submaximal concentration (3×10^{-8} M) also elevated cyclic GMP levels. This increase occurred more slowly than with nitroglycerin and remained elevated in the presence of FK409. Thus, as is the case with nitroglycerin, FK409 seems to produce vasorelaxation via an increase in intracellular cyclic

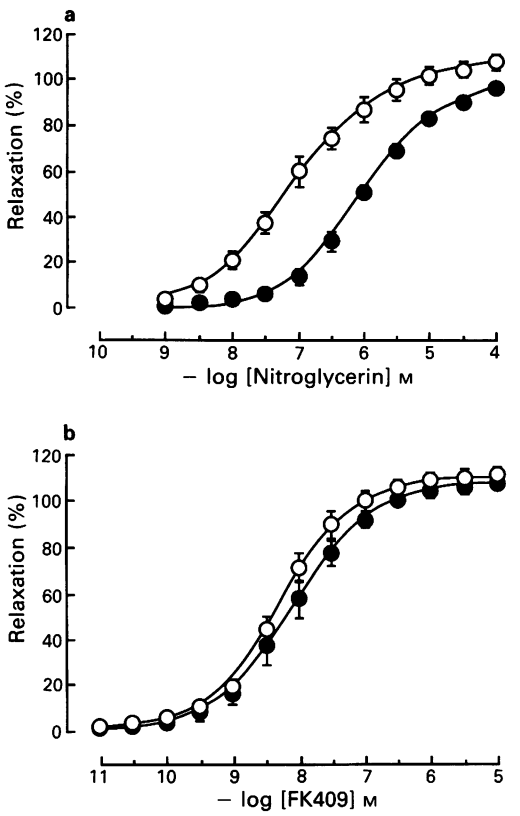


Figure 9 Mean concentration-relaxation curves for (a) nitroglycerin and (b) FK409 in U46619-contracted dog coronary artery rings in the cross-tolerance study: (○) control; (●) after exposure to the maximum concentration of FK409 (a, 1×10^{-5} M) or nitroglycerin (b, 1×10^{-4} M). Each point represents the mean of 6 experiments; s.e.mean shown by vertical bars.

GMP. It is known that this effect of nitroglycerin is the result of activation of soluble guanylate cyclase (Ignarro *et al.*, 1981). Consequently, the vasorelaxant effect of nitroglycerin is inhibited by methylene blue, an inhibitor of soluble guanylate cyclase (Ignarro *et al.*, 1981; Martin *et al.*, 1984; Shibata *et al.*, 1986; Ohba *et al.*, 1987). In the present experiments, the vasorelaxant effect of FK409 was also inhibited by methylene blue as was that of nitroglycerin. M&B22,948 is a selective inhibitor of cyclic GMP phosphodiesterase (Souness *et al.*, 1989). If an increase in intracellular cyclic GMP plays a key role in the vasorelaxant effect of FK409, its effect should be potentiated by M&B22,948. Indeed, the present study showed that the vasorelaxant effect of FK409 was potentiated by M&B22,948 essentially to the same extent as that of nitroglycerin. Thus, it is highly likely that FK409, although not a nitrate, activates soluble guanylate cyclase and produces vasorelaxation through accumulation of cyclic GMP as does nitroglycerin. The greater potency of FK409 than nitroglycerin may indicate that FK409 activates soluble guanylate cyclase more efficiently than nitroglycerin.

Recently nitroglycerin tolerance has become a significant clinical problem, because it limits the usefulness of nitroglycerin (Horowitz & Henry, 1987; Packer *et al.*, 1987). In the present experiments, after exposure to the maximally-effective concentration of nitroglycerin (10^{-4} M) the vasorelaxant potency of this agent was reduced to about 1/60. In contrast the potency of FK409 after exposure to its maximally-effective concentration (10^{-5} M) was reduced to only about 1/6. Thus, the degree of FK409 tolerance was about 1/10 that of nitroglycerin tolerance. Furthermore, after exposure to nitroglycerin there was no significant change in the vasorelaxant potency of FK409, although the potency of nitroglycerin was reduced to about 1/10 after exposure to FK409. The mechanism of tolerance to nitrovasodilators is probably closely associated with their metabolism within the tissue (Horowitz *et al.*, 1987; Fung *et al.*, 1989; Katz, 1990). Organic nitrates must first undergo reduction by organic nitrate reductase to form nitrite ions and consequently nitric oxide or S-nitrosothiols, and in these processes thiol donors are required (Ignarro *et al.*, 1981). Thus, the depletion of such donors results in the failure to form nitric oxide or S-nitrosothiol and thus eventually a reduced vasorelaxation. Nitric oxide and/or S-nitrosothiol are thought to be intermediates capable of activating soluble guanylate cyclase (Ignarro *et al.*, 1981). Based on this conceptual framework, the lower liability of FK409 for developing self-tolerance or cross-tolerance to nitroglycerin could be explained if the initial steps required for the metabolism of other organic nitrates are somehow bypassed by FK409 to allow the formation of nitric oxide or S-nitrosothiols more readily. Similar explanations have been put forward for other non-nitrate drugs such as molsidomine or its active metabolite SIN-1 (Fung *et al.*, 1989; Katz, 1990). Alternatively it is possible that FK409 directly stimulates guanylate cyclase. Whatever mechanism may be involved in the lower liability of FK409 to produce self-tolerance and cross-tolerance to nitroglycerin, this property should make this drug advantageous over tolerance-producing nitrates currently in clinical use.

This study was supported by a Grant-in-Aid for Scientific Research (No. 01571247) from the Ministry of Education, Science and Culture, Japan. We are grateful to Fujisawa Pharmaceutical Co., Ltd., Osaka, Japan for the supply of FK409, Nippon Kayaku Co., Ltd., Tokyo, Japan for nitroglycerin and Rhône-Poulenc-Rorer Ltd., Dagenham, Essex, U.K. for M&B22,948.

References

BECKER, L. & PITT, B. (1971). Regional mycoardial blood flow, ischemia, and antianginal drugs. *Ann. Clin. Res.*, **3**, 353–361.

ENDOH, M. & TAIRA, N. (1983). Relationship between relaxation and cyclic GMP formation caused by nicorandil in canine mesenteric artery. *Naunyn-Schmiedebergs Arch. Pharmacol.*, **322**, 319–321.

FUNG, H.-L., CHONG, S. & KOWALUK, E. (1989). Mechanisms of nitrate action and vascular tolerance. *Eur. Heart J.*, **10**, Suppl. A, 2–6.

HENRY, P.J., HOROWITZ, J.D. & LOUIS, W.J. (1989). Determinants of *in vitro* nitroglycerin tolerance induction and reversal: influence of dose regimen, nitrate-free period, and sulfhydryl supplementation. *J. Cardiovasc. Pharmacol.*, **14**, 31–37.

HINO, M., IWAMI, M., OKAMOTO, M., YOSHIDA, K., HARUTA, H., OKUHARA, M., HOSODA, J., KOHSAKA, M., AOKI, H. & IMANAKA, H. (1989). FK409, a novel vasodilator isolated from the acid-treated fermentation broth of *Streptomyces griseosporeus*. I. Taxonomy, fermentation, isolation, and physico-chemical and biological characteristics. *J. Antibiotics*, **42**, 1578–1583.

HOROWITZ, J.D. & HENRY, P.J. (1987). Recent developments in nitrate therapy of ischaemic heart disease. *Med. J. Aust.*, **146**, 93–96.

IGNARRO, L.J., LIPPTON, H., EDWARDS, J.C., BARICOS, W.H., HYMAN, A.L., KADOWITZ, P.J. & GRUETTER, C.A. (1981). Mechanism of vascular smooth muscle relaxation by organic nitrates, nitrites, nitroprusside and nitric oxide: evidence for the involvement of S-nitrosothiols as active intermediates. *J. Pharmacol. Exp. Ther.*, **218**, 739–749.

KATZ, R.J. (1990). Mechanisms of nitrate tolerance: a review. *Cardiovasc. Drugs Ther.*, **4**, 247–252.

KUKOVETZ, W.R., HOLZMANN, S., WURM, A. & PÖCH, G. (1979). Evidence for cyclic GMP-mediated relaxant effects of nitro-compounds in coronary smooth muscle. *Naunyn-Schmiedebergs Arch. Pharmacol.*, **310**, 129–138.

MARTIN, W., VILLANI, G.M., JOTHIANANDAN, D. & FURCHGOTT, R.F. (1984). Selective blockade of endothelium-dependent and glyceryl trinitrate-induced relaxation by hemoglobin and by methylene blue in the rabbit aorta. *J. Pharmacol. Exp. Ther.*, **232**, 708–716.

MELLION, B.T., IGNARRO, L.J., OHLSTEIN, E.H., PONTECORVO, E.G., HYMAN, A.L. & KADOWITZ, P.J. (1981). Evidence for the inhibitory role of guanosine 3',5'-monophosphate in ADP-induced human platelet aggregation in the presence of nitric oxide and

related vasodilators. *Blood*, **57**, 946–955.

OHBA, Y., SHIRAKI, Y. & SAKAI, K. (1987). Comparative vasorelaxing profiles of nicorandil, isosorbide dinitrate and nitroglycerin in isolated coronary arteries of the dog. *Jpn. J. Pharmacol.*, **45**, 397–404.

PACKER, M., LEE, W.H., KESSLER, P.D., GOTTLIEB, S.S., MEDINA, N. & YUSHAK, M. (1987). Prevention and reversal of nitrate tolerance in patients with congestive heart failure. *N. Engl. J. Med.*, **317**, 799–804.

PARKER, R.B. & WAUD, D.R. (1971). Pharmacological estimation of drug-receptor dissociation constants. Statistical evaluation. I. Agonists. *J. Pharmacol. Exp. Ther.*, **177**, 1–12.

SATO, N., OHTSUKA, M., KOIBUCHI, Y., SAKAI, S., ISONO, T., SUDO, Y., ONO, T., MORI, J. & SHIBAYAMA, F. (1990). Cardiovascular profile of FR900409, a newly synthesized vasodilator, in isolated dog vascular preparations and in anesthetized dogs and rats. *Jpn. J. Pharmacol.*, **52**, Suppl. 1, 218P.

SCHAFER, A.I., ALEXANDER, R.W. & HANDIN, R.I. (1980). Inhibition of platelet function by organic nitrate vasodilators. *Blood*, **55**, 649–654.

SHIBATA, T., OGAWA, K., ITO, T., HASHIMOTO, H., NAKAGAWA, H. & SATAKE, T. (1986). Role of cyclic GMP of canine vascular smooth muscle in relaxation by organic nitrates. *Jpn. Circ. J.*, **50**, 1091–1099.

SOUNESS, J.E., BRAZDIL, R., DIOCEE, B.K. & JORDAN, R. (1989). Role of selective cyclic GMP phosphodiesterase inhibition in the myorelaxant actions of M&B22,948, MY-5445, vinpocetine and 1-methyl-3-isobutyl-8-(methylamino)xanthine. *Br. J. Pharmacol.*, **98**, 725–734.

(Received January 23, 1991
Revised March 13, 1991
Accepted March 18, 1991)

Br. J. Pharmacol. (1991), **108**, 1719–1724 © Macmillan Press Ltd, 1991

Prehispanolone, a novel platelet activating factor receptor antagonist from *Leonurus heterophyllus*

[1]Chi-Ming Lee, Li-Ming Jiang, *,[2]Hong-Sheng Shang, *Po-Ming Hon, *Yun He & †Henry N.C. Wong

Department of Biochemistry, *Chinese Medicinal Material Research Centre and †Department of Chemistry, The Chinese University of Hong Kong, Shatin, N.T., Hong Kong

1 Using an *in vitro* radioligand binding assay for the platelet activating factor (PAF) receptor, we have identified a novel, specific PAF antagonist, prehispanolone, from a Chinese medicinal herb *Leonurus heterophyllus*.

2 The presence of sodium ions inhibited specific [^{3}H]-PAF binding to rabbit platelet membrane with an IC_{50} of 5.2 mM, decreased the inhibitory potency of PAF but increased the inhibitory potency of prehispanolone.

3 Prehispanolone and several of its derivatives inhibited the binding of [^{3}H]-PAF to rabbit platelets with potencies closely resembling that of inhibition of PAF-induced aggregation.

4 The integrity of the tetrahydrofuran ring of prehispanolone is critical for its interaction with the PAF receptor.

5 By hydrogenating the dihydrofuran ring and replacing the keto group of prehispanolone with a hydroxyl group, we obtained a compound, LC5507, that is more stable and more active than prehispanolone as a PAF receptor antagonist.

Keywords: PAF receptor; rabbit platelet; BN52021; platelet aggregation; tetrahydrofuran; guanyl nucleotides; prehispanolone; *Leonurus heterophyllus*

Introduction

Platelet activating factor (PAF), also known as acetyl glyceryl ether phosphorylcholine (AGEPC), antihypertensive polar renal medullary lipid (APRL) or PAF-acether, was first identified as a potent mediator for aggregation and degranulation of platelets and neutrophils (Benveniste *et al.*, 1972). Its structure was determined in 1979 as 1-O-alkyl-2-acetyl-sn-glyceryl-3-phosphorylcholine (Benveniste *et al.*, 1979; Blank *et al.*, 1979; Demopoulos *et al.*, 1979) and is now known to produce a wide spectrum of biological responses in addition to platelet activation (Snyder, 1987; Winslow & Lee, 1987). There is considerable evidence suggesting its involvement in the pathogenesis of shock, ischaemia, glomerulonephritis, gastric ulcer formation, asthma and systemic anaphylaxis (Braquet *et al.*, 1987; Feuerstein & Hallenbeck, 1987; Grandel, 1987; Vargaftig & Braquet, 1987). Thus, specific antagonists of PAF may be useful therapeutic agents in a variety of inflammatory, respiratory, immunological and cardiovascular disorders (Saunders & Handley, 1987). Several PAF antagonists (including kadsurenone, BN52021 and WEB 2086) have indeed been reported to provide protection against the damage induced by ischaemia/reperfusion in the heart, kidney and brain in animal studies and to inhibit antigen-induced responses in asthmatic patients (Braquet *et al.*, 1987; 1989).

The presence of pharmacologically specific PAF receptors has been reported in cells that respond to PAF including human, dog and rabbit platelets (Valone *et al.*, 1982; Hwang *et al.*, 1983; Tahraoui *et al.*, 1988), human neutrophils (Valone & Goetzl, 1983), human lung tissues (Hwang *et al.*, 1985) and murine macrophages (Valone, 1988). The properties of PAF receptors and their interaction with drugs can be studied conveniently by radioligand binding assays using [^{3}H]-PAF with high specific activity (Inarrea *et al.*, 1984; Hwang *et al.*, 1986a; Tahraoui *et al.*, 1988).

We have recently isolated a novel labdane diterpene, prehispanolone (9α, 13R; 15,16-diepoxy-labdane-14-en-7-one, LC5504), from a Chinese medicinal herb *Leonurus heterophyllus* (Figure 1, Hon *et al.*, 1990a). The aqueous extract of this herb can reduce blood viscosity and inhibit platelet aggregation (Zou *et al.*, 1989) and it has been used to treat myocardial ischaemia and oedema in chronic and acute nephritis (Wang *et al.*, 1985; Chang & But, 1987). In the present study, we provide radioligand binding and functional data to characterize prehispanolone as a specific PAF receptor antagonist. We have also performed a structure activity relationship study

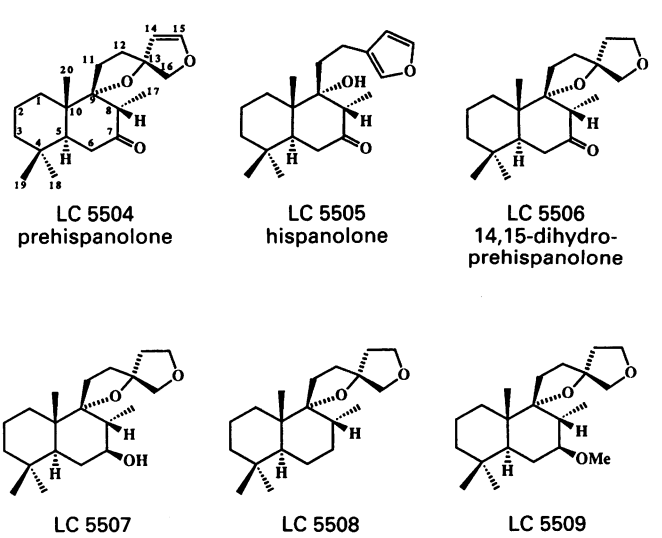


Figure 1 Chemical structure of prehispanolone and of its related analogues.

[1] Author for correspondence.

[2] Present address: Department of Immunology, Beijing Medical University, Beijing 100083, China.

in the hope of improving its stability and identifying the key structural elements involved in its interaction with the PAF receptor.

Methods

Preparation of platelets

Adult New Zealand rabbits were anaesthetized with pentobarbitone (25 mg kg^{-1}, i.v.). Nine volumes (45 ml) of blood from the heart was drawn directly into 1 volume (5 ml) of ACD solution (0.8% citric acid, 2.2% sodium citrate and 2.45% glucose). The mixture was centrifuged at 270 *g* for 10 min at room temperature. The top platelet-rich plasma (PRP) was removed carefully and used in aggregation experiments.

For binding experiments, the PRP was centrifuged at 1100 *g* for 15 min at room temperature to obtain the platelet pellet and the supernatant was centrifuged again at 1800 *g* for 20 min to obtain the platelet-poor plasma (PPP). The platelet pellet was gently resuspended in buffer A (composition, mM: NaCl 100, $MgCl_2$ 15, EDTA 5 and Tris-HCl 50, pH 7.4) and centrifuged at 1100 *g* for 15 min. This washing procedure was repeated twice, first with buffer A followed by buffer B (Tris-HCl 50 mM, bovine serum albumin (BSA) 2.5 mg ml^{-1} and sucrose 0.3 M). The final pellet was resuspended in buffer B to give a concentration of 1–2 × 10^8 platelets ml^{-1} and used in binding experiments immediately. Platelets were counted with a haemocytometer (Neubauer improved) under a microscope.

Preparation of platelet membranes

PRP was prepared as described above except 3.8% sodium citrate was used in place of ACD solution since there was no need to provide glucose as an energy source. The PRP was centrifuged at 1100 *g* for 20 min to obtain the platelet pellet. The pellet was homogenized in 10 ml of ice cold buffer C (Tris-HCl 50 mM, BSA 2.5 mg ml^{-1}, pH 7.2) with a polytron (setting 6, 20–30 s). The homogenate was centrifuged at 39200 *g* for 10 min at 4°C. The supernatant was decanted and the pellet resuspended in 10 ml of ice cold buffer C by polytron (setting 6, 10 s) and centrifuged again. This washing procedure was repeated twice and the final pellet was stored at −70°C or resuspended in buffer C for receptor assay.

[^{3}H]-*PAF and other radioligand binding experiments*

Unless otherwise mentioned, the binding of [^{3}H]-PAF was routinely measured in duplicate in the absence of sodium. For intact platelet binding, about 2 × 10^7 platelets were incubated at 20°C for 60 min with 2 nM [^{3}H]-PAF in a final volume of 500 μl containing Tris-HCl 50 mM, pH 7.4, sucrose 0.3 M, BSA 2.5 mg ml^{-1} and various test drugs or the appropriate vehicle (0.36% dimethyl sulphoxide in buffer C). For platelet membrane binding, membrane aliquots (about 50 μg protein) were incubated at 0°C for 30 min with [^{3}H]-PAF 2 nM in a final volume of 200 μl containing Tris-HCl 50 mM, pH 7.2, BSA 0.31–5 mg ml^{-1} and various test drugs.

At the end of the incubation period, the reaction was stopped by rapid filtration under reduced pressure through Whatman GF/C glass fibre filters (presoaked in buffer C for 2 h before use) using a Brandel or a Skatron cell harvester. Filters were washed 3 times with 5 ml of ice cold buffer each. They were dried and radioactivity was measured by liquid scintillation spectrometry. Nonspecific binding was defined in the presence of 2.5 μM non-radioactive PAF. Specific binding was calculated by subtracting nonspecific binding from total binding.

Other radioligand binding assays were performed as described previously (Wong *et al.*, 1983; Shi *et al.*, 1984; Hon *et al.*, 1990b). The binding of [^{3}H]-nitrendipine to dihydropyridine-sensitive calcium channel was determined with rat cerebral cortex membranes. The binding of [^{3}H]-flunitrazepam and [^{3}H]-phenylisopropyl adenosine to central benzodiazepine and adenosine A_1 receptors respectively, was determined with bovine cerebral cortex membranes. The binding of [^{3}H]-Ro5-4864 and [^{3}H]-N-ethylcarboxamidoadenosine to peripheral benzodiazepine and adenosine A_2 receptors was determined with rat liver and striatum membranes respectively, whereas [^{3}H]-nitrobenzylthioinosine binding to nucleoside transporters was determined with guinea-pig lung membranes.

Rabbit platelet aggregation assay

Freshly prepared platelets were counted with a haemocytometer (Neubauer improved) under a microscope and adjusted with PPP to give a concentration of 1–2 × 10^8 platelet ml^{-1}. PRP was stored in a polypropylene tube with stopper at room temperature. Aggregation experiments were performed 30 min after PRP preparation and finished within 3 h.

Aggregation of platelets was monitored by measuring the changes in turbidity with a Chronolog platelet aggregometer, model 669 (Havertown, PA) at 37°C. Aliquots of PRP (200 μl) were incubated at 37°C for 5 min and then 25 μl of various test drugs or the appropriate vehicle (0.18% dimethyl sulphoxide in buffer C) were added and incubated for another min. Aggregation was induced by the addition of 25 μl of PAF (final concentration 2 nM in the aggregation cuvette) in BSA 2.5 mg ml^{-1}. The percentage of platelet aggregation was calculated from the change in light transmission by assigning the transmittance of unstimulated PRP to be 0% and that of PPP to be 100%. Typically, 2 nM PAF induced a 65% aggregation at the beginning of experiment. To control for time-dependent changes in platelet sensitivity to PAF, vehicle controls were included before and after every two drug tests and data were expressed as percentage of the mean of the controls.

Drug sources

[^{3}H]-PAF (1-O-[^{3}H]-hexadecyl-2-acetyl-sn-glyceryl-3-phosphorylcholine) was purchased from New England Nuclear, Boston, MA, U.S.A. with a specific activity of 56.7 Ci mmol^{-1}. [^{3}H]-nitrendipine and [^{3}H]-Ro 5-4864 were also from New England Nuclear. [^{3}H]-N-ethylcarboxamidoadenosine, [^{3}H]-phenylisopropyladenosine and [^{3}H]-flunitrazepam were from Amersham, Buckinghamshire, England. [^{3}H]-nitrobenzylthioinosine was purchased from Moravek Biochemicals, Brea, CA, U.S.A. Unlabelled PAF was obtained from Calbiochem Corporation, San Diego, CA, U.S.A. and RIA grade BSA, thrombin, collagen, Gpp NHp, ADP and ATP were from Sigma Chemical Co., St. Louis, MO, U.S.A. BN52021 (Ginkgolide B) was a generous gift from Dr P. Braquet (Institut Henri Beaufour, Le Plessis, France). Prehispanolone and its derivatives were prepared in our laboratory (Hon *et al.*, 1990a). Details of the chemistry involved in their preparation will be published elsewhere. Prehispanolone and its derivatives were dissolved in dimethyl sulphoxide to give 15 mM stock solutions. They were diluted with buffer C to give the appropriate working solutions for binding and aggregation experiments. Stock solutions of [^{3}H]-PAF and PAF in ethanol were also diluted with buffer C to give the appropriate working solutions of 10 nM [^{3}H]-PAF (0.41% ethanol) and 10 μM PAF (0.10% ethanol).

Statistical analysis

The results, unless otherwise stated, are expressed as the mean ± s.d.. Data, where appropriate, were compared by

Student's paired t test and were considered to be significantly different when $P < 0.05$. Statistical analysis of correlation was done with SPSS/PS+ statistical package.

Results

General properties of [^{3}H]-PAF binding

Initial experiments showed little difference between total and nonspecific binding of [^{3}H]-PAF to rabbit platelet membranes in the absence of BSA. However, reproducible specific binding could be detected in the presence of BSA. As illustrated in Figure 2, there was a marked reduction of nonspecific binding accompanied by a graduate increase in specific binding when the BSA concentration was increased from 0.31 to 5 mg ml^{-1}. This was not a result of [^{3}H]-PAF binding to BSA since no specific binding was observed when platelet membranes were omitted.

Initial experiments also indicated that [^{3}H]-PAF binding to rabbit platelet membranes and intact platelets reached equilibrium after 20 min at 0°C and after 45 min at 20°C respectively. Thus, incubation periods of 30 min at 0°C and 60 min at 20°C were adopted for all subsequent experiments.

Typically, with washed rabbit platelet membranes incubated with 2 nM [^{3}H]-PAF at 0°C in the presence of 2.5 mg ml^{-1} BSA, total binding was about 8450 c.p.m. whereas nonspecific binding assayed in the presence of 2.5 μM PAF was about 2850 c.p.m. Thus under standard binding conditions, two-thirds of the total binding of [^{3}H]-PAF was specific.

The presence of sodium chloride was found to inhibit the specific binding of [^{3}H]-PAF to rabbit platelet membranes in a concentration-dependent manner with an IC_{50} (concentration which inhibited 50% of specific [^{3}H]-PAF binding) of 5.2 mM (Figure 3). This effect seemed to be specific for sodium because potassium chloride tested between 1.5 and 150 mM did not significantly affect [^{3}H]-PAF binding (Figure 3). Both NaCl and KCl had no significant effect on nonspecific binding of [^{3}H]-PAF at the concentration range examined.

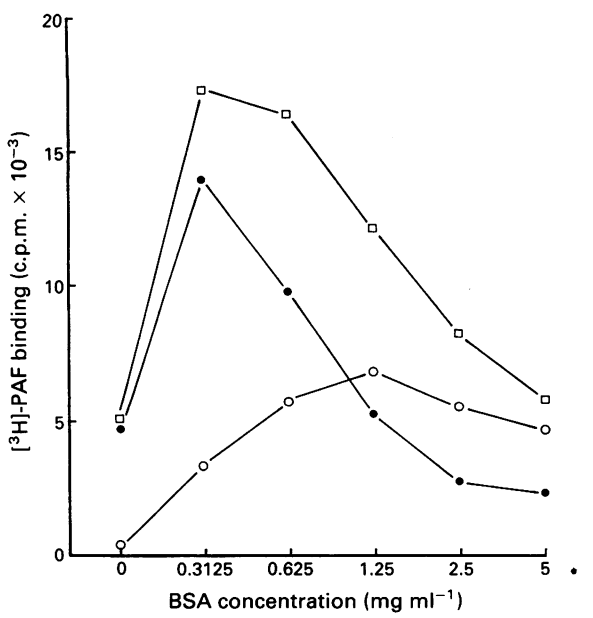


Figure 2 Effects of different concentrations of bovine serum albumin (BSA) on the total (□), nonspecific (●) and specific (○) binding of [^{3}H]-PAF (2 nM, 30 min, 0°C) to rabbit platelet membranes. Data shown are those of a typical experiment. Similar results were obtained in 3 separate experiments performed in duplicate.

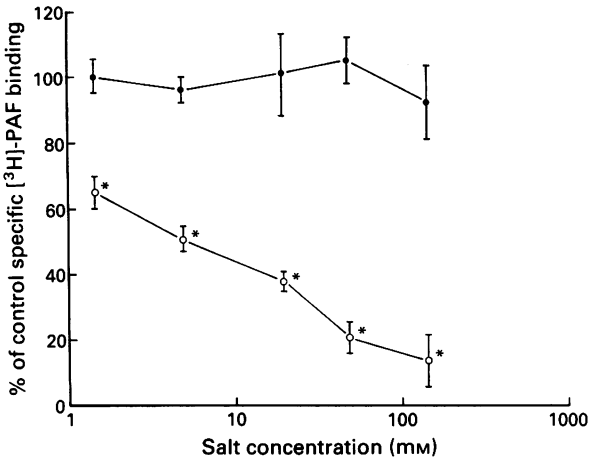


Figure 3 Effects of different concentrations of NaCl (○) and KCl (●) on the specific binding of [^{3}H]-PAF to rabbit platelet membranes. Results are the mean (with s.d. indicated by vertical bars) of 3 separate experiments performed in duplicate. * $P < 0.05$.

Similar to results obtained with other G-protein (guanine nucleotide dependent protein)-coupled receptors (Snyder, 1979), the specific binding of [^{3}H]-PAF to platelet membranes at 0°C was inhibited by GppNHp (guanylyl-5'-imidophosphate), a metabolically stable analogue of GTP (guanosine-5'-triphosphate). The inhibition was concentration-dependent and up to 58% inhibition was obtained at 1000 μM (Figure 4). Other nucleotides such as ATP (adenosine triphosphate) and ADP (adenosine diphosphate) were inactive at similar concentrations (Figure 4).

Effect of sodium on the inhibition of [^{3}H]-PAF binding to platelet membranes by prehispanolone and PAF

Prehispanolone (LC5504) inhibited specific [^{3}H]-PAF binding to rabbit platelet membranes with an IC_{50} of 9 μM in the absence of NaCl (Figure 5). The presence of 5 and 10 mM NaCl in the incubation mixture increased the inhibitory potency of prehispanolone to 3.6 and 3.3 μM respectively. On

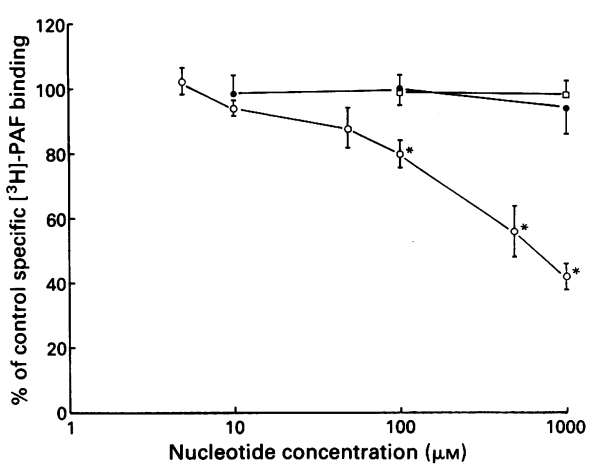


Figure 4 Effects of Gpp NHp (○), ADP (□) and ATP (●) on specific [^{3}H]-PAF (2 nM) binding to rabbit platelet membranes at 0°C. Data represent the mean (s.d. indicated by vertical bars) of 3 separate experiments performed in duplicate. * $P < 0.05$.

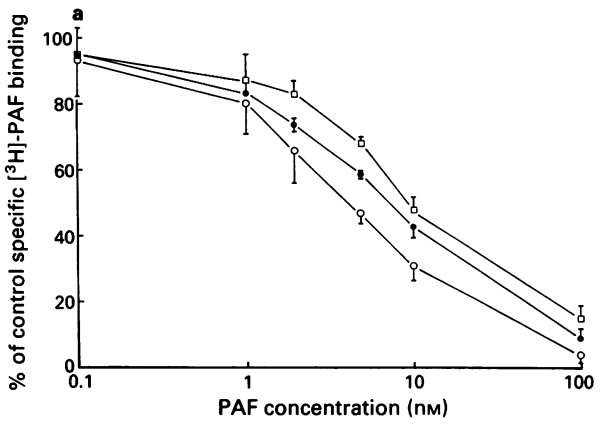


Figure 5 Effects of 5 mM (●) and 10 mM (□) NaCl on the inhibition of specific [^{3}H]-PAF binding to rabbit platelet membranes by PAF (a) and prehispanolone (b); (○), control. Results are the mean (s.d. indicated by vertical bars) of (n) separate experiments performed in duplicate. In (a), control, $n = 8$; 5 mM NaCl, $n = 4$; 10 mM NaCl, $n = 3$. In (b), control, $n = 4$; 5 mM NaCl, $n = 3$; 10 mM NaCl, $n = 3$.

the other hand, the presence of 5 and 10 mM NaCl decreased the inhibitory potency of PAF from 4.1 nM (no NaCl) to 7.3 and 9.2 nM respectively (Figure 5).

Inhibition of [^{3}H]-PAF binding and PAF-induced aggregation of intact platelets by prehispanolone and its analogues

Prehispanolone (LC5504) inhibited specific [^{3}H]-PAF (2 nM) binding to intact rabbit platelets with an IC_{50} of 14.1 ± 7.9 μM (mean ± s.d., $n = 4$, Table 1). It also inhibited aggregation induced by 2 nM PAF in a concentration-dependent manner, with an IC_{50} of 28.4 ± 7.3 μM (mean ± s.d., $n = 3$, Table 1, Figure 6). As shown in Figure 7, prehispanolone concentration-dependently inhibited both the shape change and platelet aggregation induced by 2 nM PAF. These effects were specific since prehispanolone and 14,15-dihydroprehispanolone (50 μM) did not inhibit the aggregation induced by thrombin (0.1 i u ml^{-1}), ADP (1 μM) and collagen (12.5 μg ml^{-1}) (Table 2). Prehispanolone (50 μM) also had little or no effect on [^{3}H]-nitrendipine binding to rat cerebral cortex calcium channels, [^{3}H]-flunitrazepam binding to bovine cerebral cortex central benzodiazepine receptors, [^{3}H]-NECA binding to rat striatum A_2 adenosine receptors, [^{3}H]-Ro5-4864 binding to rat liver peripheral benzodiazepine receptors, [^{3}H]-phenylisopropyladenosine binding to bovine cerebral cortex A_1 adenosine receptors and [^{3}H]-nitrobenzylthioinosine binding to guinea-pig lung nucleoside transporter (Table 3).

Table 1 Inhibition of specific [^{3}H]-PAF binding to intact rabbit platelets and PAF-induced aggregation by prehispanolone (LC5504) and its derivatives

	IC_{50} (μM)	
Inhibitors	*[^{3}H]-PAF binding*	*Aggregation*
BN52021	4.8 ± 1.6 ($n = 4$)	3.3 ± 1.2 ($n = 3$)
LC5504	14.1 ± 7.9 ($n = 4$)	28.4 ± 7.3 ($n = 3$)
LC5505	Inactive*	Inactive*
LC5506	13.4 ± 7.4 ($n = 4$)	19.0 ± 7.9 ($n = 3$)
LC5507	1.2 ± 0.7 ($n = 4$)	4.6 ± 1.9 ($n = 3$)
LC5508	14.2 ± 7.7 ($n = 4$)	59.7 ± 1.2 ($n = 3$)
LC5509	5.7 ± 2.7 ($n = 4$)	11.4 ± 2.1 ($n = 3$)

IC_{50} is the concentration of drug required to give 50% inhibition of specific [^{3}H]-PAF binding or platelet aggregation induced by 2 nM PAF. Results are the mean ± s.d. of (n) separate determinations performed in duplicate. * Inactive when tested at 20–100 μM.

In order to understand the key structural elements involved in the interaction of prehispanolone with the PAF receptor,

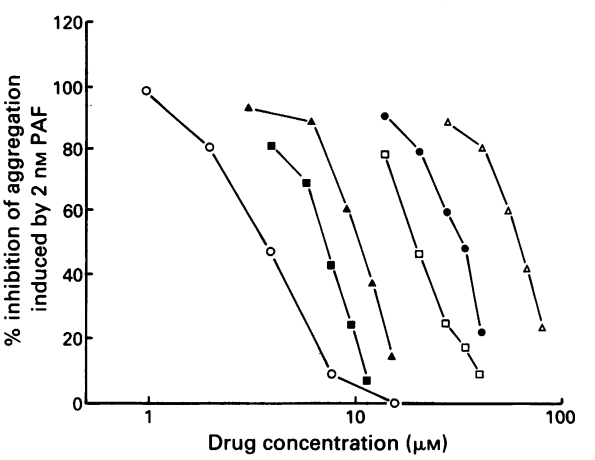


Figure 6 Inhibition of rabbit platelet aggregation induced by 2 nM PAF by BN52021 (○), prehispanolone (●), LC5506 (□), LC5507 (■), LC5508 (△) and LC5509 (▲). Data are those of a typical experiment. Similar results were obtained in 3 separate experiments.

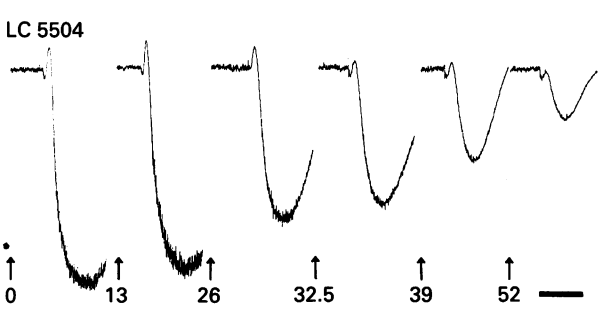


Figure 7 A typical tracing to illustrate the inhibitory effect of prehispanolone (LC5504) on rabbit platelet aggregation induced by 2 nM PAF. LC5504 was added at the arrows. Numerals indicate the concentrations of prehispanolone in μM. Bar indicates 1 min.

Table 2 Comparison of the effects of prehispanolone (LC5504) and 14,15-dihydroprehispanolone (LC5506) on rabbit platelet aggregation induced by thrombin, collagen, ADP and PAF

	Platelet aggregation (%)		
Aggregating agents	*Control*	*LC5504*	*LC5506*
Thrombin (0.1 i u ml^{-1})	57.7 ± 1.2	58.0 ± 2.6	57.7 ± 0.58
Collagen (12.5 μg ml^{-1})	86.8 ± 0.23	87.0 ± 2.6	87.0 ± 3.6
ADP (1 μM)	62.7 ± 1.2	63.0 ± 1.0	62.7 ± 0.58
PAF (2 nM)	64.3 ± 2.7	30.3 ± 12.5*	21.0 ± 11.5*

Results are the mean ± s.d. of 3 separate experiments. LC5504 and LC5506 were tested at 50 μM for thrombin, collagen and ADP but at 30 μM for PAF. * $P < 0.05$ when compared with control by Student's paired t test.

we have prepared several derivatives from it and studied their structure activity relationship. The chemical structures of these compounds are shown in Figure 1. The ability of these compounds and BN 52021, a classical PAF receptor antagonist, to inhibit [^{3}H]-PAF binding and PAF-induced aggregation in intact rabbit platelets are shown in Table 1. Opening up the tetrahydrofuran ring in LC5504 by acid treatment resulted in LC5505 which is inactive in these assays even when tested at 100 μM. Hydrogenation of the dihydrofuran ring of LC5504, on the other hand, did not alter its bioactivity (compare LC5504 and LC5506). The replacement of the keto group in LC5504 by a hydrogen was similarly without significant effect (compare LC5504 and LC5508). Activity of LC5504 was actually improved when its keto group was replaced with a methoxy (LC5509) or a hydroxyl (LC5507) group. The hydroxy analogue (LC5507) was the most potent compound in this series and its activity was comparable to that of BN52021 (Table 1). The rank order of potencies of BN52021, prehispanolone and its analogues in inhibiting specific [^{3}H]-PAF binding to rabbit platelets was LC5507 > BN52021 > LC5509 > LC5506 ⩾ LC5504 ⩾ LC5508 ⩾ LC5505. This correlated significantly with their rank order of potencies in inhibiting PAF-induced platelet aggregation, BN52021 ⩾ LC5507 > LC5509 > LC5506 > LC5504 > LC5508 ⩾ LC5505 ($r = 0.77$, $P < 0.01$). The positive correlation of the ability of these drugs in inhibiting [^{3}H]-PAF binding and PAF-induced aggregation supports the notion that they may block PAF-induced aggregation by inhibiting PAF binding to its receptors.

Discussion

Sodium ions and guanyl nucleotides have been shown to regulate differentially the receptor binding of agonists and antagonists at G-protein coupled receptors including the opiate receptor, α-adrenoceptor, bradykinin, histamine H_1 and adenosine A_1 receptors (Snyder, 1979; 1983). Typically, the presence of sodium ions or guanyl nucleotides decreases the affinity of agonists while having little or no effect on the affinity of antagonists. Similar observations have been made for the PAF receptor where the presence of sodium ions lowered agonist affinity but increased or had no effect on antagonist affinity (Hwang *et al.*, 1986a,b). In the present study, we have confirmed the inhibitory effect of sodium ions and guanyl nucleotide on specific binding of [^{3}H]-PAF to rabbit platelet membranes. Moreover, the inhibitory potency of PAF was lower in the presence of sodium ions indicating a decrease in its affinity for the PAF receptor. On the other hand, the inhibitory potency of prehispanolone was actually higher in the presence of sodium ions. This behaviour of prehispanolone resembles that of several PAF antagonists including CV3988, Ono-6240, BN52021, L-651,142, alprazolam, kadsurenone and dihydrokadsurenone but differs from RP48740 and RP52770 which are insensitive to the presence of sodium ions (Hwang *et al.*, 1986a,b). Indeed, prehispanolone as predicted by its positive sodium shift in the radioligand binding assay, behaved as a PAF receptor antagonist and inhibited platelet aggregation induced by PAF. This effect was specific as it did not inhibit the aggregation of platelets induced by thrombin, ADP and collagen. Prehispanolone, up to 50 μM, displayed no interaction at the dihydropyridine-sensitive calcium channel and central benzodiazepine receptor. This distinguished it from several other PAF receptor antagonists which are calcium channel blockers (e.g. gallopamil and diltiazem) and benzodiazepine receptor ligands (e.g. alprazolam and triazolam) (Braquet *et al.*, 1987).

All of the natural PAF receptor antagonists which have been identified from plants to date are furanoid compounds. For instance, the ginkgolides (e.g. BN52021) from *Ginkgo biloba* contain a tetrahydrofuran cycle; kadsurenone, kadsurin A and B and piperenone from *Piper futokadsurae* as well as mirandine, burchellein and chrysophyllin from Brazilian Lauraceas are benzofuranoid compounds; veraguensin and calopiptin from *Magnolia acuminata*, galbelgin and galgravin from *Himantandra belgravena*, grandisin from *Litsea grandis* and nectandrin A and B from *Nectandra rigida* are 2,3,4,5-tetrasubstituted furanoid lignans; burseran from *Bursera microphylla* as well as presteganes A and B and other butanolides

Table 3 Effects of 50 μM prehispanolone in various radioligand binding assays

Receptor type	*^{3}H-ligand*	*Radioligand concentration* (nM)	*Binding* (% of control)
Dihydropyridine-sensitive calcium channel	[^{3}H]-nitrendipine	0.3	89 ± 8 (3)
Central benzodiazepine	[^{3}H]-flunitrazepam	1	102 ± 5 (4)
Peripheral benzodiazepine	[^{3}H]-Ro 5-4864	1	98 ± 4 (4)
Adenosine A_1	[^{3}H]-phenylisopropyladenosine	1	92 ± 7 (3)
Adenosine A_2	[^{3}H]-N-ethylcarboxamidoadenosine	20	100 ± 4 (3)
Nucleoside transporter	[^{3}H]-nitrobenzylthioinosine	0.5	90 ± 7 (3)

Values presented are the mean ± s.d. of (n) separate experiments performed in duplicate. Nonspecific binding was defined as follows: [^{3}H]-nitrendipine, 1 μM nifedipine; [^{3}H]-flunitrazepam, 2 μM diazepam; [^{3}H]-Ro 5-4864, 1 μM Ro 5-4864; [^{3}H]-phenylisopropyladenosine, 10 μM cyclohexyladenosine; [^{3}H]-ethylcarboxamido-adenosine, 100 μM N-ethylcarboxamidoadenosine; [^{3}H]-nitrobenzyl-thioinosine, 20 μM nitrobenzylthioguanosine.

from *Steganotaenia araliacea* are 3,4-disubstituted furanoid lignans; liroresinol-B dimethyl ether, magnolin, pinoresinol dimethyl ether, fargesin, demethoxyaschantin and aschantin from *Magnolia biondi* are substituted furofurans (Braquet *et al.*, 1987; Cordeiro *et al.*, 1989). Prehispanolone from *Leonurus heterophyllus* is no exception as it also contains a tetrahydrofuran ring. In the present study, we have also demonstrated the importance of the structural integrity of the natural tetrahydrofuran framework in its interaction with the PAF receptor. Opening up the tetrahydrofuran ring of prehispanolone by mild acid treatment resulted in a loss of PAF receptor antagonist activity as determined by radioligand binding and functional assays.

Prehispanolone (LC5504) was not stable in acidic conditions and can be converted into the inactive hispanolone (LC5505) readily by dilute hydrochloric acid treatment (Hon *et al.*, 1990a). In an attempt to stabilize prehispanolone, we converted it into 14,15-dihydroprehispanolone (LC5506) by hydrogenation. Indeed, 14,15-dihydroprehispanolone was stable and did not undergo the same rearrangement reaction as prehispanolone in acidic conditions. Moreover it displayed more or less the same antagonistic activity at the PAF receptor as prehispanolone.

The keto group appears to be non-essential since its replacement by a hydrogen (LC5508) or a methoxy group (LC5509) had a minimal effect on the activity of 14,15-dihydroprehispanolone. On the other hand, the replacement of the keto group by a hydroxyl group (LC5507) actually increased its potency as a PAF receptor antagonist.

In conclusion, we have provided radioligand binding and biological data to support the role of prehispanolone as a specific PAF receptor antagonist. Moreover, by hydrogenating the dihydrofuran ring and replacing the keto group of prehispanolone with a hydroxyl group we obtained a compound LC5507 which is more stable and more active than prehispanolone as a PAF receptor antagonist.

The generous supply of BN52021 by Dr P. Braquet (I.H.B., Le Plessis, France) is gratefully acknowledged. This work was supported in part by a grant from the Hong Kong Jockey Club (Charities) Ltd.

References

BENVENISTE, J., HENSON, P.M. & COCHRANE, C.G. (1972). Leukocyte-dependent histamine release from rabbit platelets: the role of IgE, basophils and a platelet activating factor. *J. Exp. Med.*, **136**, 1356–1377.

BENVENISTE, J., TENCE, M., VARENNE, P., BIDAULT, J., BOULLET, C. & POLONSKY, J. (1979). Semi-synthesis and proposed structure of platelet-activating factor (PAF): PAF-acether, an alkyl ether analog of lysophosphatidylcholine. *C.R. Acad. Sci.*, **289D**, 1037–1040.

BLANK, M.L., SNYDER, F., BYERS, L.W., BROOKS, B. & MUIRHEAD, E.E. (1979). Antihypertensive activity of an alkyl ether analog of phosphatidylcholine. *Biochem. Biophys. Res. Commun.*, **90**, 1194–1200.

BRAQUET, P., PAUBERT-BRAQUET, M., KOLTAI, M., BOURGAIN, R., BUSSOLINO, F. & HOSFORD, D. (1989). Is there a case for PAF antagonists in the treatment of ischemic states? *Trends Pharmacol. Sci.*, **10**, 23–30.

BRAQUET, P., TOUQUI, L., SHEN, T.Y. & VARGAFTIG, B.B. (1987). Perspectives in platelet-activating factor research. *Pharmacol. Rev.*, **39**, 97–145.

CHANG, H.M. & BUT, P.P.H. (1987). *Pharmacology and Applications of Chinese Materia Medica*, **2**, 989–993.

CORDEIRO, R.S.B., AMORIM, C.Z., MARTINS, M.A., RODRIGUES E SILVA, P.M. & HENRIQUES, M.G.M.O. (1989). PAF antagonists from plants. *Drug News & Perspect.*, **2**, 287–291.

DEMOPOULOS, C.A., PINCKARD, R.N. & HANAHAN, D.J. (1979). Platelet activating factor: evidence for 1-O-alkyl-2-acetyl-sn-glyceryl-3-phosphorylcholine as the active compound (a new class of lipid chemical mediators). *J. Biol. Chem.*, **254**, 9355–9358.

FEUERSTEIN, G. & HALLENBECK, J.M. (1987). Prostaglandins, leukotrienes and platelet activating factor in shock. *Annu. Rev. Pharmacol. Toxicol.*, **27**, 301–313.

GRANDEL, K.E. (1987). Platelet activating factor. *Drugs Today*, **23**, 257–268.

HON, P.M., LEE, C.M., SHANG, H.S., CUI, Y.X., WONG, H.N.C. & CHANG, H.M. (1990a). Prehispanolone, a new labdane diterpene from *Leonurus heterophyllus*. *Phytochemistry*, (in press).

HON, P.M., LEE, C.M., CHOANG, T.F., CHUI, K.Y. & WONG, H.N.C. (1990b). Structure of a new ligustilide dimer from *Angelica sinensis*. *Phytochemistry*, **29**, 1189–1191.

HWANG, S.B., LEE, C.S.C., CHEAH. M.J. & SHEN, T.Y. (1983). Specific receptor sites for 1-O-alkyl-2-acetyl-sn-glycero-3-phosphocholine (platelet activating factor) on rabbit platelet and guinea pig smooth muscle membranes. *Biochemistry*, **22**, 4756–4763.

HWANG, S.B., LAM, M.H. & SHEN, T.Y. (1985). Specific binding sites for platelet activating factor in human lung tissues. *Biochem. Biophys. Res. Commun.*, **128**, 972–979.

HWANG, S.B., LAM, M.Y. & PONG, S.S. (1986a). Ionic and GTP regulation of binding of platelet activating factor to receptors and platelet activating factor induced activation of GTPase in rabbit platelet membranes. *J. Biol. Chem.*, **261**, 532–537.

HWANG, S.B., LAM, M.H. & CHANG, M.N. (1986b). Specific binding of [^{3}H]Dihydrokadsurenone to rabbit platelet membranes and its inhibition by the receptor agonists and antagonists of platelet activating factor. *J. Biol. Chem.*, **261**, 13720–13726.

INARREA, P., GOMEZ-CAMBRONERO, J., NIETO, M. & SANCHEZ CRESPO, M. (1984). Characteristics of the binding of platelet activating factor to platelets of different animal species. *Eur. J. Pharmacol.*, **105**, 309–315.

SAUNDERS, R.N. & HANDLEY, D.A. (1987). Platelet activating factor antagonists. *Annu. Rev. Pharmacol. Toxicol.*, **27**, 237–255.

SHI, M.M., WU, J.S., LEE, C.M. & YOUNG, J.D. (1984). Nucleoside transport. Photoaffinity labelling of high affinity nitrobenzylthioinosine binding sites in rat and guinea pig lung. *Biochem. Biophys. Res. Commun.*, **119**, 594–600.

SNYDER, F. (1987). *Platelet Activating Factor and Related Lipid Mediators*. New York: Plenum Press.

SNYDER, S.H. (1979). Peptide and neurotransmitter receptors in the brain: regulation by ions and guanyl nucleotides. In *Central Regulation of the Endocrine System*. ed. Fuxe, K., Hokfelt, T. & Luft, R., pp. 109–117. New York: Plenum Press.

SNYDER, S.H. (1983). Molecular aspects of neurotransmitter receptors: an overview. In *Handbook of Psychopharmacology*, Vol. 17, ed. Iversen, L., Iversen, S.D. & Snyder, S.H. pp. 1–12. New York: Plenum Press.

TAHRAOUI, L., FLOCH, A., MONDOT, S. & CAVERO, I. (1988). High affinity specific binding sites for tritiated platelet factor in canine platelet membranes: counterparts of platelet activating factor receptors mediating platelet aggregation. *Mol. Pharmacol.*, **34**, 145–151.

VALONE, F.H. (1988). Identification of platelet-activating factor receptors in P388D1 murine macrophages. *J. Immunol.*, **140**, 2389–2394.

VALONE, F.H., COLES, E., REINHOLD, V.R. & GOETZL, E.J. (1982). Specific binding of phospholipid platelet activating factor by human platelets. *J. Immunol.*, **129**, 1637–1641.

VALONE, F.H. & GOETZL, E.J. (1983). Specific binding by human polymorphonuclear leukocytes of the immunological mediator 1-O-hexadexyl/octadecyl-2-acetyl-sn-glycero-3-phosphorylcholine (AGEPC). *Immunology*, **48**, 141–149.

VARGAFTIG, B.B. & BRAQUET, P.G. (1987). PAF-acether today – relevence for acute experimental anaphylaxis. *Br. Med. Bull.*, **43**, 312–335.

WANG, Z.S., LI, D.W., XIA, W.J., YIN, H.Q., ZHU, L.Y., YE, J.H. & YU, Y. (1985). Observations of 100 cases of myocardial ischaemia treated with *Leonurus heterophyllus*. *J. Tradit. Chin. Med.*, **3**, 29–30.

WINSLOW, C.M. & LEE, M.L. (1987). *New Horizons in Platelet Activating Factor Research*. London: John Wiley & Sons Ltd.

WONG, D.T., BYMASTER, F.P., REID, L.R. & THRELKELD, P.G. (1983). Fluoxetine and two other serotonin uptake inhibitors without affinity for normal receptors. *Biochem. Pharmacol.*, **32**, 1287–1293.

ZOU, Q.Z., BI, R.G., LI, J.M., FENG, J.B., YU, A.M., CHAN, H.P. & ZHEN, M.X. (1989). Effect of Motherwort on blood hyperviscosity. *Am. J. Chin. Med.*, **17**, 65–70.

(Received January 15, 1991
Revised February 22, 1991
Accepted March 18, 1991)

Br. J. Pharmacol. (1991), **103**, 1725–1732 © Macmillan Press Ltd, 1991

Effects of N^G-nitro-L-arginine methyl ester on vasodilator responses to acetylcholine, 5′-N-ethylcarboxamidoadenosine or salbutamol in conscious rats

[1]Sheila M. Gardiner, Philip A. Kemp & Terence Bennett

Department of Physiology and Pharmacology, Queen's Medical Centre, Nottingham NG7 2UH

1 Conscious, Long Evans rats ($n = 16$), chronically instrumented for the measurement of regional haemodynamics were given 3 min, randomized infusions of two doses of sodium nitroprusside (1.5 and 15 $\mu g\,min^{-1}$), acetylcholine (0.4 and 4 $\mu g\,min^{-1}$), 5′-N-ethylcarboxamidoadenosine (NECA; 45 and 450 $ng\,min^{-1}$), and salbutamol (24 and 240 $ng\,min^{-1}$) in the absence and in the presence of N^G-nitro-L-arginine methyl ester (L-NAME; 1 $mg\,kg^{-1}\,h^{-1}$), a potent inhibitor of nitric oxide biosynthesis.

2 Sodium nitroprusside caused hyperaemic vasodilatation in the mesenteric, and common carotid vascular beds. These effects were enhanced in the presence of L-NAME, as was the hypotension.

3 Acetylcholine caused hyperaemic vasodilatation in the renal, internal carotid and common carotid vascular beds. These effects were attenuated in the presence of L-NAME, but the hypotension was unaffected.

4 NECA caused hyperaemic vasodilatation in the renal, mesenteric, hindquarters, internal carotid and common carotid vascular beds. However, only the hindquarters and internal carotid responses were diminished in the presence of L-NAME and the hypotension was unchanged.

5 Salbutamol caused hyperaemic vasodilatation in the hindquarters vascular bed only. This effect was reduced in the presence of L-NAME, but the hypotension was unchanged.

6 The results indicate marked regional variations in the sensitivity of vasodilator responses to L-NAME that can depend on the vasodilator agent chosen and the dose employed. It is clear from these findings also that measurement of mean arterial blood pressure alone cannot provide adequate information on which to judge the involvement of L-NAME-sensitive mechanisms in vasodilator responses *in vivo*.

Keywords: N^G-nitro-L-arginine methyl ester; acetylcholine; 5′-N-ethylcarboxamidoadenosine; salbutamol; regional blood flow

Introduction

On the basis of many *in vitro* experiments, there is now persuasive evidence that the major endothelium-derived relaxing factor is nitric oxide (see Moncada *et al.*, 1989; Moncada & Higgs, 1990). Considering the ability of inhibitors of nitric oxide synthesis to abolish endothelium-dependent vasorelaxation *in vitro*, it is notable that, although these substances cause cardiovascular changes consistent with inhibition of an important vasodilator tone *in vivo* (Rees *et al.*, 1989; Aisaka *et al.*, 1989a; Gardiner *et al.*, 1990c,d,e), their ability to antagonize regional haemodynamic responses to classical 'endothelium-dependent' vasodilators in this setting is less impressive (see Gardiner *et al.*, 1990e). These observations led us (Gardiner *et al.*, 1990e) to suggest that, *in vivo*, different vasodilator agonists might depend, to varying extents, on nitric oxide for their effects. In addition, we proposed that nitric oxide-dependent and nitric oxide-independent responses to any given vasodilator agonist might be involved to different degrees in different vascular beds (Gardiner *et al.*, 1990e). If this is the case it means that susceptibility of any particular regional vasodilator response to antagonism by, for example, N^G-nitro-L-arginine methyl ester (L-NAME, Moore *et al.*, 1990; Rees *et al.*, 1990) is a good indication that nitric oxide is involved in that response. However, resistance of the response to inhibition by L-NAME does not necessarily mean nitric oxide is not involved (Giles *et al.*, 1990), or that the response is endothelium-independent. Despite this caveat, it would be of interest to know whether or not one could clearly demonstrate regional selectivity in the inhibitory effects of L-NAME on vasodilator responses to a range of agonists, and, particularly, if this selective antagonism differed depending on the agonist.

In our previous studies (Gardiner *et al.*, 1990e) the vasodilator challenges used were single bolus doses of glyceryl trinitrate, acetylcholine, bradykinin and endothelin-1, given before and after a bolus dose of L-NAME (10 $mg\,kg^{-1}$), which we had previously shown to provide a stable haemodynamic profile for up to 60 min (Gardiner *et al.*, 1990d). However, it could be argued that apparent resistance to L-NAME of the responses to bolus injections of vasodilators was due to their dependence only on release of nitric oxide from a pre-formed pool that was not influenced by inhibition of nitric oxide synthesis (Aisaka *et al.*, 1989b). Therefore, we adopted a different strategy in the present study and examined vasodilator responses to infusions of depressor agents at two different dose levels, since infusion of a vasodilator to cause sustained effects ought to be more dependent on *de novo* synthesis of nitric oxide, if nitric oxide were involved in the response (see Mustafa *et al.*, 1990; Tolins *et al.*, 1990; Walder *et al.*, 1991).

In order to assess fully the haemodynamic responses to infusions of vasodilator agents in the presence of L-NAME, the haemodynamic effects of the latter needed to be established and relatively stable for longer than 60 min. Therefore, we administered L-NAME by continuous infusion. Furthermore, it was necessary to use vasodilator agents other than endothelin-1, glyceryl trinitrate and bradykinin since, in conscious rats, infusion of endothelin-1 does not cause vasodilatation (Gardiner *et al.*, 1989; 1990a), glyceryl trinitrate does not cause sustained hypotension, and bradykinin does not produce reproducible responses (unpublished observations). However, because our objective was to determine whether or not L-NAME could be shown to inhibit, selectively, different regional vasodilator responses to different agonists, it was

[1] Author for correspondence.

necessary only to use agents that had clear-cut and wide-ranging effects on regional blood flow. In considering possible candidates we asked ourselves, why choose only vasodiltor agents that are said to be 'endothelium-dependent' (see Furchgott & Vanhoutte, 1989) from the findings of *in vitro* studies? On the basis of this heresy, and some pilot experiments, we therefore proceeded to investigate the regional haemodynamic effects of infusions of two doses of sodium nitroprusside, acetylcholine, 5'-N-ethylcarboxamidoadenosine (NECA; Rose'Meyer & Hope, 1990) and salbutamol, in the absence and in the presence of L-NAME.

Methods

Male, Long Evans rats (350–450 g) were used in all experiments. Under sodium methohexitone anaesthesia (60 mg kg^{-1}, i.p., supplemented as required) pulsed Doppler probes (Haywood *et al.*, 1981) were sutured around the left renal and superior mesenteric arteries and the distal abdominal aorta, below the level of the ileocaecal artery (to measure hindquarters blood flow) (Gardiner *et al.*, 1990c,d,e). In other animals probes were sutured around both common carotid arteries after the external carotid artery had been ligated on the left side. This arrangement permitted measurement of changes in common and internal carotid blood flow simultaneously (Gardiner *et al.*, 1990f). At least 7 days after probe implantation, animals were briefly re-anaesthetized (sodium methohexitone 40 mg kg^{-1}, i.p.) for the placement of intravascular catheters in the abdominal aorta (via the caudal artery) for monitoring systemic arterial blood pressure and in the right jugular vein for drug administration. Animals were left to recover for at least 24 h before experiments were begun, and the protocols ran over the following 1–2 days. There were 8 animals with renal, mesenteric and hindquarters probes and 8 with internal and common carotid probes.

In random order, 3 min infusions (at 0.15 ml min^{-1}) of sodium nitroprusside (1.5 and 15 μg min^{-1}), acetylcholine (0.4 and 4 μg min^{-1}), NECA (45 and 450 ng min^{-1}) and salbutamol (24 and 240 ng min^{-1}) were given separated by at least 20 min; in all cases the low doses were given before the high doses. The lower dose of each agent was selected on the basis of it causing clear haemodynamic effects with minimum change in mean arterial blood pressure, whereas the higher dose was selected because it caused clear hypotension. On the second experimental day L-NAME was infused (0.3 ml h^{-1}, 1 mg kg^{-1} h^{-1}) continuously starting 60 min before infusion of the vasodilators. Throughout the experiments continuous recordings were made of mean arterial blood pressure and regional Doppler shift signals, both phasic and mean (using a modified Crystal Biotech VF-1 system; Gardiner *et al.*, 1990b). Since all comparisons of the effects of vasodilator agents in the absence and presence of L-NAME were made in the same animals, absolute Doppler shift values were taken as indices of flow and regional vascular conductances were calculated by dividing mean Doppler shift by mean blood pressure (Gardiner *et al.*, 1990c,d,e).

Data analysis

Within any experimental run, changes relative to baseline were analysed by Friedman's test (Theodorsson-Norheim, 1987). Comparisons of resting cardiovascular status in the absence and presence of L-NAME were made by Wilcoxon's ranks sums test, and the same test was used when responses to any given vasodilator agent were considered in the absence and presence of L-NAME. In that case, areas under or over curves, derived by computer analysis (Gardiner *et al.*, 1990d,e), were compared. A P value <0.05 was taken as significant.

Drugs

Sodium nitroprusside (Sigma), acetylcholine chloride (Sigma), NECA (Sigma), salbutamol (Sigma) and L-NAME hydrochloride (Sigma) were all dissolved in isotonic saline. Administration of isotonic saline alone at the volumes employed in the present study had no systemic effects.

Results

Effects of sodium nitroprusside in the absence and in the presence of L-NAME

Mean arterial blood pressure Sodium nitroprusside caused dose-dependent hypotension in the absence of L-NAME (Figures 1 and 2). In the presence of L-NAME, mean arterial blood pressure was increased, but under these conditions only the overall hypotensive effect of the higher dose of sodium nitroprusside was enhanced (Figures 1 and 2).

Renal haemodynamics In the absence of L-NAME, the lower dose of sodium nitroprusside caused a small fall in renal blood flow but no significant change in vascular conductance, whereas the higher dose caused renal vasodilatation unaccompanied by a significant change in renal blood flow (Figure 1). L-NAME did not affect renal blood flow or vascular conductance significantly and under those conditions the haemo-

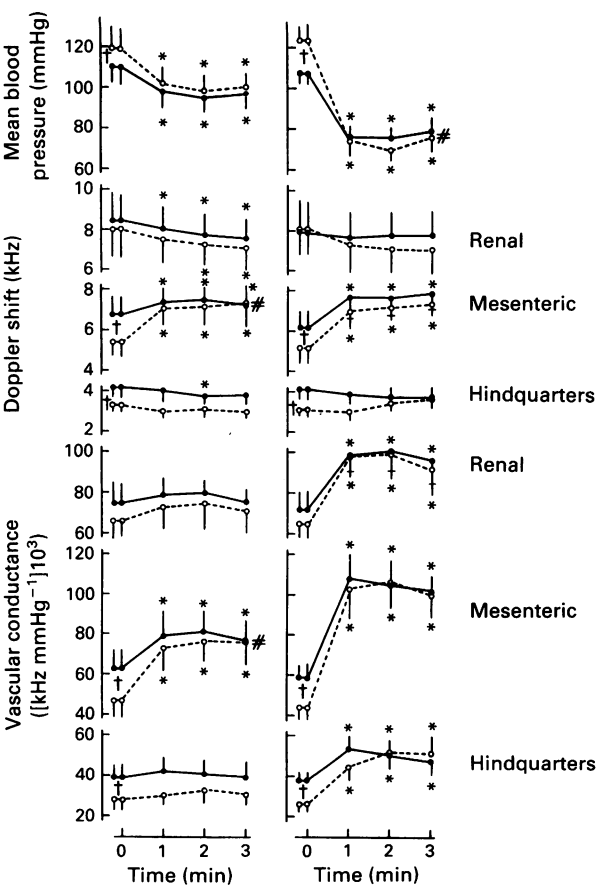


Figure 1 Changes in cardiovascular variables during 3 min infusions of sodium nitroprusside (left-hand panels, responses to sodium nitroprusside at 1.5 μg min^{-1}; right-hand panels, sodium nitroprusside at 15 μg min^{-1}) in the same conscious, Long Evans rats ($n = 8$) in the absence (●) and in the presence (○) of N^G-nitro-L-arginine methyl ester (L-NAME) (infused at 1 mg kg^{-1} h^{-1}). Values are mean and bars show s.e.mean. *$P < 0.05$ vs. baseline; †$P < 0.05$ for resting values in the absence and presence of L-NAME; #$P < 0.05$ for areas under or over curves in the absence and in the presence of L-NAME.

dynamic response to sodium nitropursside in the renal vascular bed was unchanged (Figure 1).

Mesenteric haemodynamics Sodium nitroprusside, in the absence of L-NAME, caused dose-dependent increases in mesenteric blood flow and vascular conductance (Figure 1). L-NAME caused a reduction in mesenteric blood flow and vascular conductance (Figure 1), but under those conditions only the haemodynamic response to the lower dose of sodium nitroprusside in the mesenteric vascular bed was enhanced (Figure 1).

Hindquarters haemodynamics In the absence of L-NAME, the lower dose of sodium nitroprusside caused a small fall in hindquarters blood flow but no change in vascular conductance, whereas the higher dose caused vasodilatation unaccompanied by a change in blood flow (Figure 1). In the presence of L-NAME, there was a reduction in hindquarters blood flow and a vasoconstriction, but under those conditions the haemodynamic effect of sodium nitroprusside in the hindquarters was unchanged (Figure 1).

Internal carotid haemodynamics Neither dose of sodium nitroprusside affected internal carotid blood flow, in the absence of L-NAME, but there were dose-dependent increases in vascular conductance (Figure 2). L-NAME caused a fall in blood flow and vascular conductance and under those conditions both doses of sodium nitroprusside increased internal carotid blood flow and these effects were greater than in the absence of L-NAME (Figure 2). However, only the rise in vascular conductance with the higher dose of sodium nitroprusside was enhanced (Figure 2).

Common carotid haemodynamics Common carotid blood flow was increased only by the higher dose of sodium nitroprusside, in the absence of L-NAME, but there was a dose-dependent vasodilatation (Figure 2). L-NAME reduced common carotid blood flow and vascular conductance, and under these conditions there was a dose-dependent increase in common carotid blood flow in response to sodium nitroprusside. The increases in blood flow were greater than those seen in the absence of L-NAME (Figure 2). However, only the rise in vascular conductance with the higher dose of sodium nitroprusside was enhanced (Figure 2).

Effects of acetylcholine in the absence and in the presence of L-NAME

Mean arterial blood pressure In the absence of L-NAME, the lower dose of acetylcholine had no significant effect on mean arterial blood pressure, whereas the higher dose caused modest hypotension (Figures 3 and 4). L-NAME increased mean arterial blood pressure but did not affect the responses to acetylcholine (Figures 3 and 4).

Renal haemodynamics Acetylcholine caused dose-dependent increases in both renal blood flow and vascular conductance, in the absence of L-NAME (Figure 3). Although L-NAME did not cause a significant reduction in renal blood flow, there was a significant renal vasoconstriction (Figure 3). Under those conditions, the renal haemodynamic response to the lower dose of acetylcholine was unchanged, but the renal

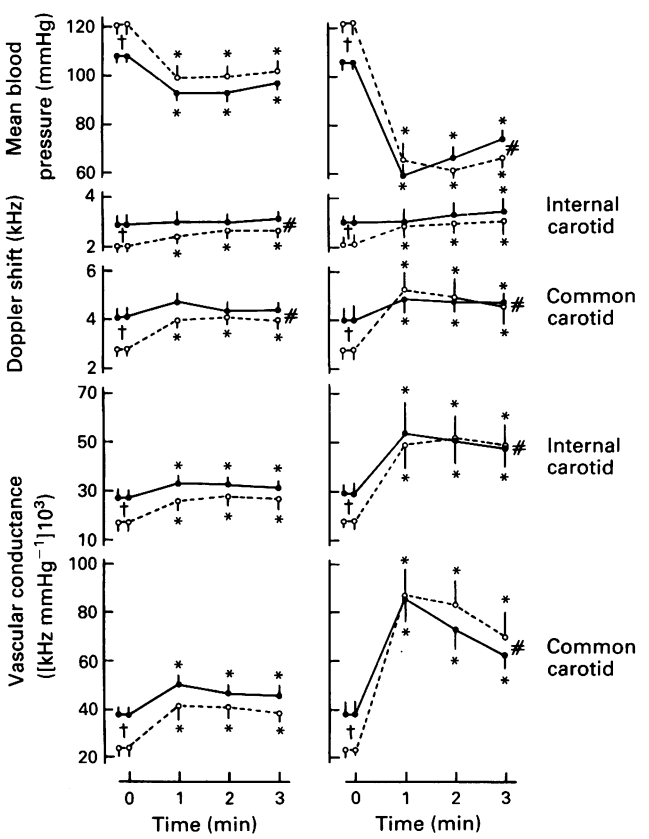


Figure 2 Changes in cardiovascular variables during 3 min infusions of sodium nitroprusside (left-hand panels, responses to sodium nitroprusside at 1.5 $\mu g\,min^{-1}$; right-hand panels, sodium nitroprusside at 15 $\mu g\,min^{-1}$) in the same conscious, Long Evans rats ($n = 8$) in the absence (●) and in the presence (○) of N^G-nitro-L-arginine methyl ester (L-NAME) (infused at 1 $mg\,kg^{-1}\,h^{-1}$). Values are mean and bars show s.e.mean. *$P < 0.05$ vs. baseline; †$P < 0.05$ for resting values in the absence and presence of L-NAME; #$P < 0.05$ for areas under or over curves in the absence and in the presence of L-NAME.

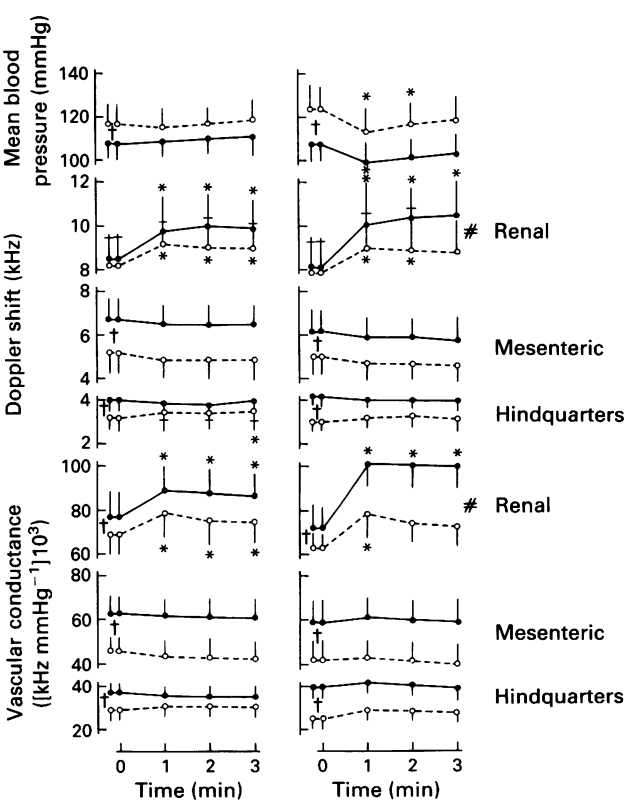


Figure 3 Changes in cardiovascular variables during 3 min infusions of acetylcholine (left-hand panels, responses to acetylcholine at 0.4 $\mu g\,min^{-1}$; right-hand panels, acetylcholine at 4 $\mu g\,min^{-1}$) in the same conscious, Long Evans rats ($n = 8$) in the absence (●) and in the presence (○) of N^G-nitro-L-arginine methyl ester (L-NAME) (infused at 1 $mg\,kg^{-1}\,h^{-1}$). Values are mean and bars show s.e.mean. *$P < 0.05$ vs. baseline; †$P < 0.05$ for resting values in the absence and presence of L-NAME; #$P < 0.05$ for areas under curves in the absence and in the presence of L-NAME.

hyperaemic and vasodilator responses to the higher dose of acetylcholine were reduced (Figure 3).

Mesenteric haemodynamics In the absence and in the presence of L-NAME, acetylcholine had no effect on mesenteric blood flow or vascular conductance (Figure 3).

Hindquarters haemodynamics There were no responses to either dose of acetylcholine in the absence or in the presence of L-NAME (Figure 3).

Internal carotid haemodynamics In the absence of L-NAME there were increases in both blood flow and dose-dependent rises in vascular conductance in response to acetylcholine (Figure 3). In the presence of L-NAME the responses to the lower dose of acetylcholine were attenuated, whereas those to the higher dose were not (Figure 4).

Common carotid haemodynamics There was a dose-dependent increase in both blood flow and vascular conductance in response to acetylcholine in the absence of L-NAME (Figure 4). In the presence of L-NAME the rise in blood flow in response to the lower dose of acetylcholine was attenuated, whereas that to the higher dose was not (Figure 4). However, the increase in vascular conductance with both doses of acetylcholine was reduced (Figure 4).

Effects of NECA in the absence and in the presence of L-NAME

Mean arterial blood pressure In the absence of L-NAME, there was a fall in mean arterial blood pressure only in response to the higher dose of NECA (Figures 5 and 6). The overall pattern of change in mean arterial blood pressure in response to NECA was unaffected in the presence of L-NAME, although the slight hypotension, following administration of the lower dose of NECA in the animals with carotid probes was significant under these conditions (Figure 6).

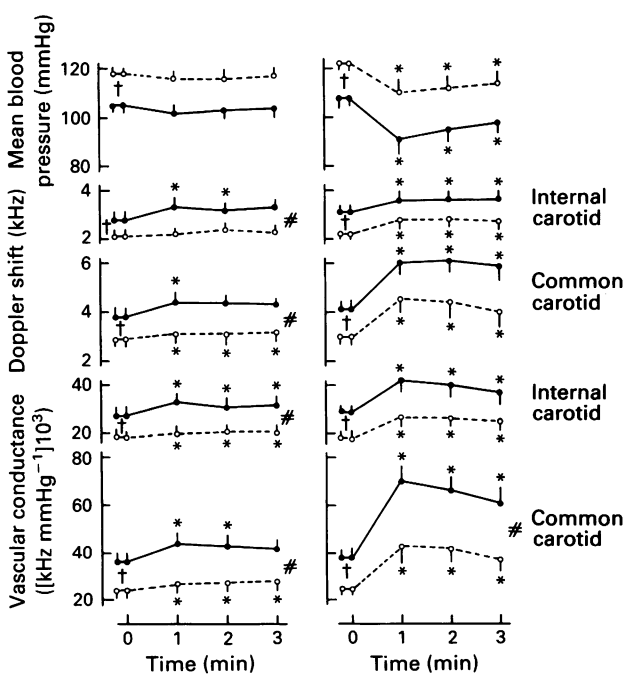


Figure 4 Changes in cardiovascular variables during 3 min infusions of acetylcholine (left-hand panels, responses to acetylcholine at $0.4\,\mu g\,min^{-1}$; right-hand panels, acetylcholine at $4\,\mu g\,min^{-1}$) in the same conscious, Long Evans rats ($n = 8$) in the absence (●) and in the presence (○) of N^G-nitro-L-arginine methyl ester (L-NAME) (infused at $1\,mg\,kg^{-1}\,h^{-1}$). Values are mean and bars show s.e.mean. $*P < 0.05$ vs. baseline; $\dagger P < 0.05$ for resting values in the absence and presence of L-NAME; $\#P < 0.05$ for areas under curves in the absence and in the presence of L-NAME.

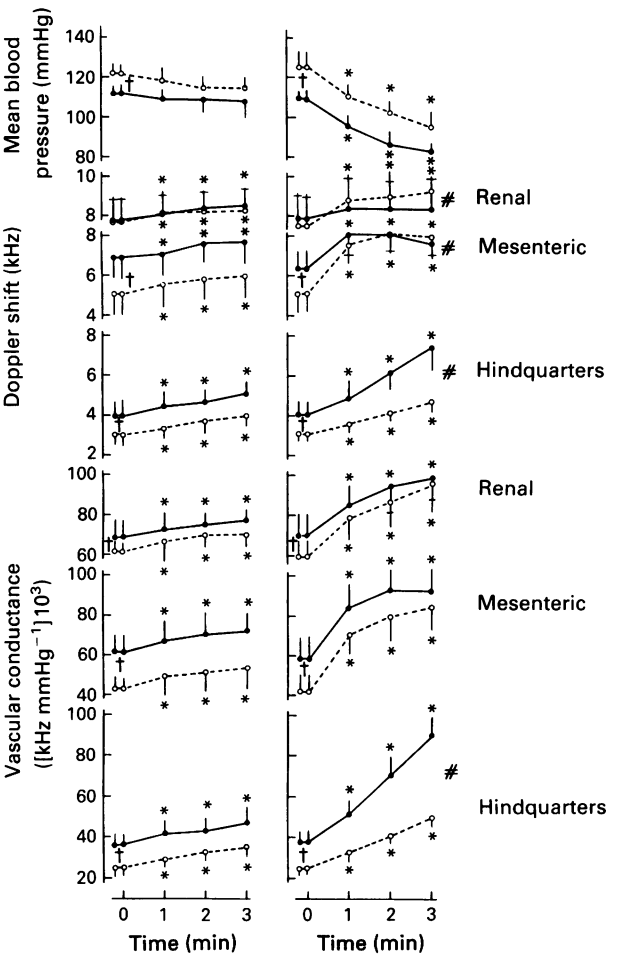


Figure 5 Changes in cardiovascular variables during 3 min infusions of 5'-N-ethylcarboxamidoadenosine (NECA) (left-hand panels, responses to NECA at $45\,\mu g\,min^{-1}$; right-hand panels, NECA at $450\,\mu g\,min^{-1}$) in the same conscious, Long Evans rats ($n = 8$) in the absence (●) and in the presence (○) of N^G-nitro-L-arginine methyl ester (L-NAME) (infused at $1\,mg\,kg^{-1}\,h^{-1}$). Values are mean and bars show s.e.mean. $*P < 0.05$ vs. baseline; $\dagger P < 0.05$ for resting values in the absence and presence of L-NAME; $\#P < 0.05$ for areas under curves in the absence and in the presence of L-NAME.

Renal haemodynamics The lower dose of NECA caused a slight increase in renal blood flow, whereas the higher dose had no significant effect in the absence of L-NAME (Figure 5); however, there was a dose-dependent vasodilatation in the renal vascular bed (Figure 5). In the presence of L-NAME, there was a significant enhancement of the renal hyperaemic response to the higher dose of NECA (Figure 5), but there were no other significant changes in the responses to NECA (Figure 5).

Mesenteric haemodynamics In the absence of L-NAME, NECA caused a dose-dependent increase in both mesenteric blood flow and vascular conductance (Figure 5). In the presence of L-NAME, there was a significant augmentation of the hyperaemic response to the higher dose of NECA, but no other significant changes in the responses to NECA (Figure 5).

Hindquarters haemodynamics There was a slowly-developing, dose-dependent increase in both blood flow and vascular conductance in response to NECA in the absence of L-NAME. In the presence of L-NAME, there were significant attenuations of the responses to the higher dose, but not to the lower dose, of NECA (Figure 5).

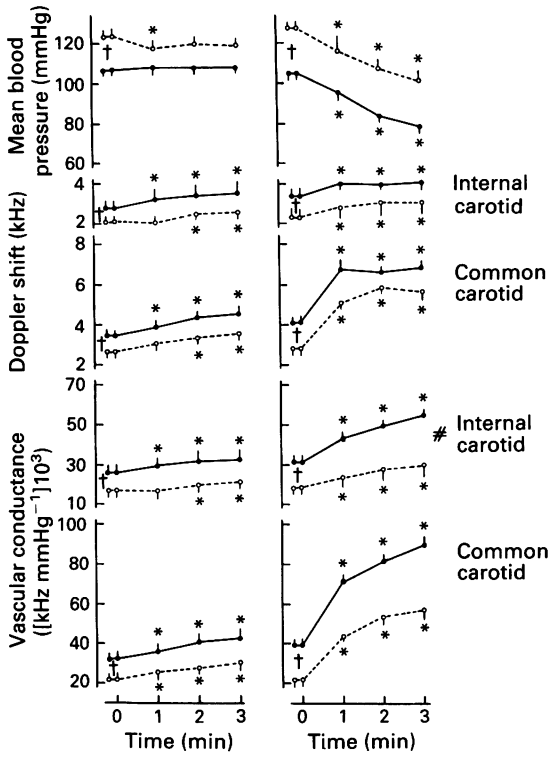


Figure 6 Changes in cardiovascular variables during 3 min infusions of 5'-N-ethylcarboxamidoadenosine (NECA) (left-hand panels, responses to NECA at 45 μg min^{-1}; right-hand panels, NECA at 450 μg min^{-1}) in the same conscious, Long Evans rats ($n = 8$) in the absence (●) and in the presence (○) of N^G-nitro-L-arginine methyl ester (L-NAME) (infused at 1 mg kg^{-1} h^{-1}). Values are mean and bars show s.e.mean. *$P < 0.05$ vs. baseline; †$P < 0.05$ for resting values in the absence and presence of L-NAME; #$P < 0.05$ for areas under curves in the absence and in the presence of L-NAME.

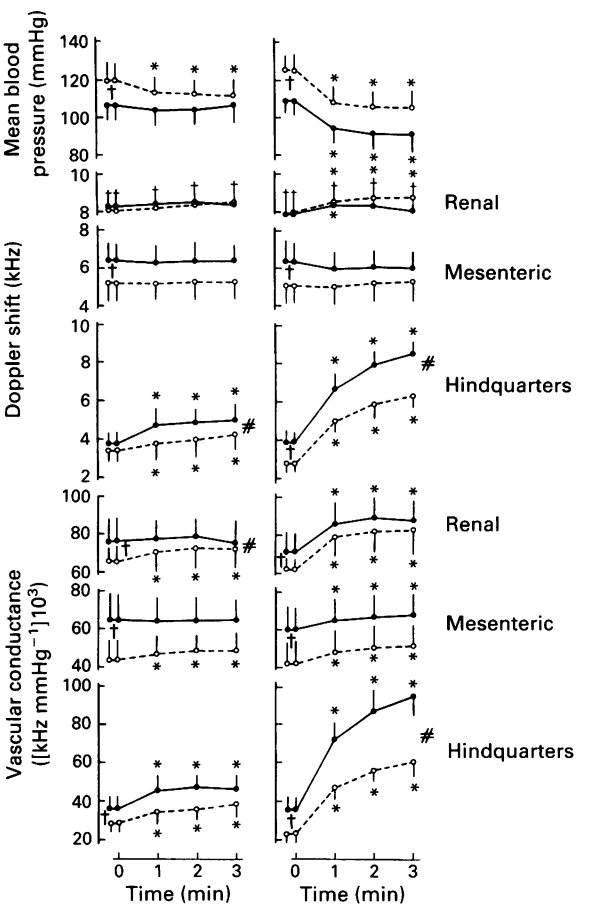


Figure 7 Changes in cardiovascular variables during 3 min infusions of salbutamol (left-hand panels, responses to salbutamol at 24 μg min^{-1}; right-hand panels, salbutamol at 240 μg min^{-1}) in the same conscious, Long Evans rats ($n = 8$) in the absence (●) and in the presence (○) of N^G-nitro-L-arginine methyl ester (L-NAME) (infused at 1 mg kg^{-1} h^{-1}). Values are mean and bars show s.e.mean. *$P < 0.05$ vs. baseline; †$P < 0.05$ for resting values in the absence and presence of L-NAME; #$P < 0.05$ for areas under curves in the absence and in the presence of L-NAME.

Internal carotid haemodynamics In the absence of L-NAME, NECA caused a dose-dependent rise in both internal carotid blood flow and vascular conductance (Figure 6). L-NAME attenuated the rise in vascular conductance in response to the higher dose of NECA, but had no other significant effect on the responses to NECA (Figure 6).

Common carotid haemodynamics There was a dose-dependent increase in both common carotid blood flow and vascular conductance in response to NECA and these were unaffected by L-NAME (Figure 6).

Effects of salbutamol in the absence and presence of L-NAME

Mean arterial blood pressure In the absence of L-NAME, only the higher dose of salbutamol caused a reduction in mean arterial blood pressure (Figures 7 and 8). However, in the presence of L-NAME, both doses of salbutamol induced hypotension, although the responses were not different from those seen in the absence of L-NAME (Figures 7 and 8).

Renal haemodynamics Only the higher dose of salbutamol caused a small increase in renal blood flow together with a vasodilatation in the absence of L-NAME (Figure 7). In the presence of L-NAME, these responses were unchanged, but there was also a rise in renal vascular conductance in response to the lower dose of salbutamol that was significantly greater than in the absence of L-NAME (Figure 7).

Mesenteric haemodynamics In the absence of L-NAME, salbutamol had no effect on mesenteric blood flow, although the higher dose caused vasodilatation (Figure 7). In the presence of L-NAME, there were no significant changes in mesenteric blood flow in response to salbutamol but there were vasodilatations with both doses (Figure 7).

Hindquarters haemodynamics There was a dose-dependent increase in both blood flow and vascular conductance in response to salbutamol in the absence of L-NAME (Figure 7). In the presence of L-NAME, the hyperaemias were attenuated, but only the rise in vascular conductance in response to the higher dose of salbutamol was reduced (Figure 7).

Internal carotid haemodynamics In the absence of L-NAME, the lower dose of salbutamol had no effect on internal carotid blood flow, and the higher dose caused a fall, although there was a slight rise in vascular conductance after administration of both doses (Figure 8). In the presence of L-NAME, there was no change in blood flow in response to either dose of salbutamol, and hence there was a significant difference between the effects of the higher dose of salbutamol in the presence and in the absence of L-NAME (Figure 8). However, L-NAME did not change the slight vasodilator effect of salbutamol (Figure 8).

Common carotid haemodynamics In the absence of L-NAME, there was a slight increase in both common carotid blood flow

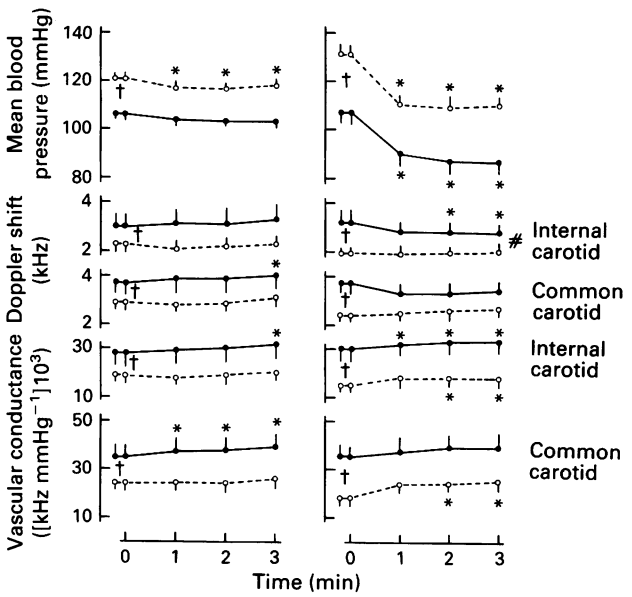


Figure 8 Changes in cardiovascular variables during 3 min infusions of salbutamol (left-hand panels, responses to salbutamol at 24 μg min^{-1}; right-hand panels, salbutamol at 240 μg min^{-1}) in the same conscious, Long Evans rats (n = 8) in the absence (●) and in the presence (○) of N^G-nitro-L-arginine methyl ester (L-NAME) (infused at 1 mg kg^{-1} h^{-1}). Values are mean and bars show s.e.mean. *P < 0.05 vs. baseline; †P < 0.05 for resting values in the absence and presence of L-NAME; #P < 0.05 for areas under curves in the absence and in the presence of L-NAME.

and vascular conductance in response to the lower dose of salbutamol, but no significant effects of the higher dose (Figure 8). In the presence of L-NAME, there was no significant change in the blood flow response to salbutamol, although the higher dose caused a slight vasodilatation (Figure 8).

Discussion

In the present work, we compared a range of vasodilators with differing regional haemodynamic profiles in the absence and in the presence of L-NAME, a potent inhibitor of nitric oxide synthesis (Moore *et al.*, 1990; Rees *et al.*, 1990). Our primary objective was to identify and quantify any differential regional haemodynamic effects that were selectively inhibited by L-NAME.

Administration of L-NAME caused hypertension associated with reductions in mesenteric, hindquarters and internal and common carotid blood flows and decreases in renal, mesenteric, hindquarters and internal and common carotid vascular conductances (Gardiner *et al.*, 1990d,e). These changes, themselves, might have been expected to influence subsequent responses to vasodilator agents. In other studies, the hypotensive response to a vasodilator has been expressed as a percentage of the immediately preceding baseline level, in order to allow for any augmentation of the response due to the hypertension caused by inhibition of nitric oxide production (e.g. Walder *et al.*, 1991). However, this approach presents a problem in the case of vascular conductance since inhibition of nitric oxide production causes a reduction in conductance and expressing any rise in conductance in response to a vasodilator agent as a percentage of the reduced baseline level could give the impression that the response was unaffected when, in absolute terms, it was reduced. Furthermore, we know of no evidence that elevation of mean arterial blood pressure would, necessarily, enhance the effect of all depressor agents. For these reasons, in the present work, we analysed all data in their raw forms and compared responses in different conditions by considering areas under or over curves (expressed as absolute units).

Responses to sodium nitroprusside

Although sodium nitroprusside is well-known as a vasodilator agent, the lower dose caused an increase only in mesenteric blood flow, while the higher dose caused mesenteric and common carotid hyperaemia. Hence, the renal, internal carotid and hindquarters vasodilatation seen under the latter circumstance could have been entirely autoregulatory. Those vascular beds (mesenteric and common carotid) that had shown hyperaemic vasodilatation in response to sodium nitroprusside alone exhibited enhanced responses in the presence of L-NAME, to either the low or the high dose of sodium nitroprusside.

Several questions arise from these observations. Firstly, why are some vascular beds more susceptible than others to the vasodilator effects of sodium nitroprusside? It is interesting to note that a similar regional haemodynamic profile is seen with glyceryl trinitrate (Gardiner *et al.*, 1990e and unpublished observations) and yet the two compounds release nitric oxide by different mechanisms (Feng & Hedner, 1990). Indeed, sodium nitroprusside releases nitric oxide spontaneously (Feng & Hedner, 1990), so it is unlikely that regional differences in its pharmacokinetics could account for the differences seen in its regional vasodilator effects. One possibility is that the vascular beds that were apparently insensitive to sodium nitroprusside simply had more effective counterregulatory mechanisms (but see below for acetylcholine).

The second question arising from our findings is why did the vascular beds that were the most sensitive to the vasodilator effect of sodium nitroprusside show enhanced responses in the presence of L-NAME? It seems that the vasoconstriction induced by L-NAME could not, itself, account for this because the hindquarters vascular bed was constricted by L-NAME but its vasodilator response to sodium nitroprusside was not changed significantly (although there was a trend towards potentiation). There is some evidence from *in vitro* experiments which indicates that in the absence of a functional endothelium, or in the presence of the L-arginine analogue, N^G-monomethyl-L-arginine (to inhibit endogeneous nitric oxide production), vasorelaxant responses to sodium nitroprusside (Shirasaki & Su, 1985), SIN-1 (Lüscher *et al.*, 1989; Busse *et al.*, 1989; Flavahan & Vanhoutte, 1989) and glyceryl trinitrate (Forster *et al.*, 1990) are enhanced. It is feasible that the present findings are an *in vivo* corollary of those *in vitro* observations, and possibly due to increased sensitivity of guanylate cyclase to exogenous nitric oxide when production of endogenous nitric oxide is reduced. If, in the presence of L-NAME, there is enhancement of the effects of sodium nitroprusside, use of this compound as an internal control, as advocated for glyceryl trinitrate (Gardiner *et al.*, 1990e), could be misleading. However, in the case of glyceryl trinitrate we could detect no evidence of sensitization in the presence of L-NAME if neurohumoral mechanisms were also blocked (Gardiner *et al.*, 1990e).

Responses to acetylcholine

At the doses used it was possible to demonstrate regionally-selective hyperaemic vasodilatation (renal, internal carotid and common carotid) in response to acetylcholine that was attenuated in the presence of L-NAME. This suggests that at least a component of the vasodilatation was due to acetylcholine-induced release of endothelium-derived nitric oxide, consistent with *in vitro* observations (Moore *et al.*, 1990; Rees *et al.*, 1990). Previously, it was not possible for us straightforwardly to demonstrate inhibition by L-NAME of

any regional haemodynamic effects of acetylcholine (Gardiner *et al.*, 1990e). However, a major difference between our two studies is that in this one we used an infusion of acetylcholine, whereas previously we gave rapid bolus injections. Thus, it is feasible that the responses elicited by infusion of acetylcholine depend, to some extent, on newly-formed nitric oxide, the production of which is inhibited by L-NAME. However, other factors must be involved because in the present work L-NAME attenuated the internal carotid vasodilator response to infusion of the lower, but not of the higher dose, of acetylcholine. Hence, in different vascular beds there may be subtle differences in the interactions between L-NAME and the L-arginine/nitric oxide pathway, and these may be more or less obvious, depending on the dose of vasodilator agonist used.

Even in those cases where vasodilator responses to acetylcholine were attenuated by L-NAME, there were still significant increases in blood flow in response to acetylcholine in the presence of L-NAME (but see Tolins *et al.*, 1990). Possible explanations for the inability of L-NAME to obliterate totally the effects of acetylcholine are: (1) insufficient L-NAME was given: (2) the residual responses were mediated by a source of nitric oxide not blocked by L-NAME; (3) nitric oxide was not the mediator of the vasodilatation (Long & Berkowitz, 1990), and (4) the hyperaemia that was resistant to L-NAME was not endothelium-dependent, but was due to acetylcholine exerting a pre-junctional inhibitory action on noradrenergic vasoconstrictor tone (Vanhoutte & Levy, 1980). This latter proposition is consistent with the finding that, in the presence of ganglion blockade the renal vasodilator responses to bolus doses of acetylcholine showed increased sensitivity to L-NAME (Gardiner *et al.*, 1990e). However, this is not likely to be a complete explanation since in the present experiments acetylcholine infusions did not cause hyperaemia in the hindquarters in spite of the fact that this vascular bed has a high degree of noradrenergic tone *in vivo* (Gardiner & Bennett, 1988).

It is particularly noteworthy that the vascular beds that dilated most to acetylcholine (renal, internal and common carotid) were not identical to those which responded most markedly to sodium nitroprusside (mesenteric and common carotid). Thus, neither regional differences in sensitivity to nitric oxide nor differential effectiveness of counterregulatory mechanisms can be the sole explanation of these findings. It is feasible that for acetylcholine there are regional differences in pre- and post-junctional muscarinic receptor distribution (Thomas *et al.*, 1988), and/or post-receptor coupling mechanisms.

Responses to NECA

The regional haemodynamic profile of NECA was interesting inasmuch as all vascular beds showed hyperaemic vasodilatation, but the time-course and extent of the changes varied between regions. In the mesenteric and, to a lesser extent, the common carotid vascular beds, the vasodilatation was relatively prompt in onset, whereas the vasodilatation in the internal carotid and particularly the hindquarters vascular bed, developed more slowly; the latter but not the former was attenuated by L-NAME. Differential involvement of L-NAME-susceptible vasodilator responses to NECA in different vascular beds is consistent with *in vitro* data showing that vasorelaxant effects of NECA may involve at least two different mechanisms (Rose'Meyer & Hope, 1990). From the present work it appears that the hindquarters and internal carotid vascular beds show vasodilator responses to NECA that are particularly sensitive to L-NAME.

The fact that the higher dose of NECA caused substantial hyperaemic vasodilatation in all vascular beds, in spite of marked hypotension is consistent with the proposition that the failure of all vascular beds to dilate in response to sodium nitroprusside or acetylcholine was not due to recruitment of baroreflex-mediated mechanisms (see above). Indeed, in the presence of L-NAME there were significant increases in the hyperaemic responses to the higher dose of NECA in the renal and mesenteric vascular beds, indicating sensitization to this agonist under those conditions. This effect, at least in the renal vascular bed, was not associated with a reduction in blood flow by L-NAME; the mechanism involved remains to be elucidated.

Responses to salbutamol

Under all conditions salbutamol caused hindquarters hyperaemia, consistent with the presence of β_2-adrenoceptor-mediated vasodilator mechanisms in that vascular bed (Gardiner & Bennett, 1988). However, although it is generally considered that β_2-adrenoceptor-mediated vasodilatation is endothelium-independent (Furchgott & Vanhoutte, 1989), in the present work the hindquarters hyperaemic vasodilator effect of salbutamol was reduced significantly in the presence of L-NAME. These results are in agreement with some *in vitro* data showing that β-adrenoceptor-mediated vasorelaxant effects may involve the endothelium (Rubanyi & Vanhoutte, 1985; Kamata *et al.*, 1989; Gray & Marshall, 1991). Nonetheless, the substantial residual hindquarters vasodilator response to salbutamol in the presence of L-NAME is consistent with additional involvement of nitric oxide-independent mechanisms.

Conclusions

Depending on the vasodilator agent used and the doses employed it is possible to demonstrate L-NAME-sensitive increases in blood flow and vascular conductance in most peripheral vascular beds *in vivo*. However, it seems such effects are not necessarily more apparent with a higher dose of the vasodilator agent. Furthermore, although sodium nitroprusside and NECA can cause potent mesenteric hyperaemic vasodilatations we have yet clearly to demonstrate L-NAME-sensitive vasodilatation to any agent in this vascular bed *in vivo*. Finally, it is apparent that proper assessment of the involvement of L-NAME-sensitive mechanisms in the responses to agents such as acetylcholine, NECA and salbutamol must involve measurement of regional haemodynamics, since monitoring mean arterial blood pressure alone would give misleading results.

References

AISAKA, K., GROSS, S.S., GRIFFITH, O.W. & LEVI, R. (1989a). N^G-methylarginine, an inhibitor of endothelium-derived nitric oxide synthesis, is a potent pressor agent in the guinea-pig: does nitric oxide regulate blood pressure *in vivo*? *Biochem. Biophys. Res. Commun.*, **160**, 881–886.

AISAKA, K., GROSS, S.S., GRIFFITH, O.W. & LEVI, R. (1989b). L-arginine availability determines the duration of acetylcholine-induced systemic vasodilatation *in vivo*. *Biochem. Biophys. Res. Commun.*, **163**, 710–717.

BUSSE, R., POHL, U., MÜLSCH, A. & BASSENGE, E. (1989). Modulation of the vasodilator action of SIN-1 by the endothelium. *J. Cardiovasc. Pharmacol.*, **14**, Suppl. 11, S81–S85.

FENG, Q. & HEDNER, T. (1990). Endothelium-derived relaxing factor (EDRF) and nitric oxide (NO). *Clin. Physiol.*, **10**, 503–526.

FLAVAHAN, N.A. & VANHOUTTE, P.M. (1989). Mechanisms underlying the inhibitory interaction between the nitrovasodilator SIN-1 and the endothelium. *J. Cardiovasc. Pharmacol.*, **14**, Suppl. 11, S86–S90.

FORSTER, C., MAIN, J.S. & ARMSTRONG, P.W. (1990). Endothelium modulation of the effects of nitroglycerin on blood vessels from dogs with pacing-induced heart failure. *Br. J. Pharmacol.*, **101**, 109–114.

FURCHGOTT, R.F. & VANHOUTTE, P.M. (1989). Endothelium-derived relaxing and contracting factors. *FASEB J.*, **3**, 2007–2018.

GARDINER, S.M. & BENNETT, T. (1988). Regional haemodynamic responses to adrenoceptor antagonism in conscious rats. *Am. J. Physiol.*, **255**, H813–H824.

GARDINER, S.M., COMPTON, A.M. & BENNETT, T. (1989). Regional hemodynamic effects of endothelin-1 in conscious, unrestrained, Wistar rats. *J. Cardiovasc. Pharmacol.*, **12**, Suppl. 5, S202–S204.

GARDINER, S.M., COMPTON, A.M. & BENNETT, T. (1990a). Regional haemodynamic effects of endothelin-1 and endothelin-3 in conscious Long Evans and Brattleboro rats. *Br. J. Pharmacol.*, **99**, 107–112.

GARDINER, S.M., COMPTON, A.M., BENNETT, T. & HARTLEY, C.J. (1990b). Can pulsed Doppler technique measure changes in aortic flow in conscious rats? *Am. J. Physiol.*, **259**, H448–H456.

GARDINER, S.M., COMPTON, A.M., BENNETT, T., PALMER, R.M.J. & MONCADA, S. (1990c). Control of regional blood flow by endothelium-derived nitric oxide. *Hypertension*, **15**, 486–492.

GARDINER, S.M., COMPTON, A.M., KEMP, P.A. & BENNETT, T. (1990d). Regional and cardiac haemodynamic effects of N^G-nitro-L-arginine methyl ester in conscious, Long Evans rats. *Br. J. Pharmacol.*, **101**, 625–631.

GARDINER, S.M., COMPTON, A.M., KEMP, P.A. & BENNETT, T. (1990e). Regional and cardiac haemodynamic responses to glyceryl trinitrate, acetylcholine, bradykinin and endothelin-1 in conscious rats: effects of N^G-nitro-L-arginine methyl ester. *Br. J. Pharmacol.*, **101**, 632–649.

GARDINER, S.M., COMPTON, A.M., BENNETT, T., KEMP, P.A. & NEY, U. (1990f). Synergistic internal carotid vasodilator effects of human α-calcitonin gene-related peptide and nimodipine in conscious rats. *Br. J. Pharmacol.*, **99**, 830–834.

GILES, H., BOLOFO, M.L. & MARTIN, G.R. (1990). Agonist- and tissue-dependence of susceptibility of endothelium-dependent relaxations to L-NAME. *Br. J. Pharmacol.*, **100**, 452P.

GRAY, D.W. & MARSHALL, I. (1991). Isoprenaline relaxation of rat thoracic aorta is endothelium-dependent, releases nitric oxide and raises cyclic GMP and cyclic AMP. *Br. J. Pharmacol.*, Proc. Suppl. **102**, 125P.

HAYWOOD, J.R., SHAFFER, R., FASTENOW, C., FINK, G.D. & BRODY, M.J. (1981). Regional blood flow measurement with pulsed Doppler flowmeter in conscious rat. *Am. J. Physiol.*, **241**, H273–H278.

KAMATA, K., MIYATA, N. & KASUYA, Y. (1989). Involvement of endothelial cells in relaxation and contraction responses of the aorta to isoproterenol in naive and streptozotocin-induced diabetic rats. *J. Pharmacol. Exp. Ther.*, **249**, 890–894.

LONG, C.J. & BERKOWITZ, B.A. (1989). What is the relationship between the endothelium derived relaxant factor and nitric oxide? *Life Sci.*, **45**, 1–14.

LÜSCHER, T.F., RICHARD, V. & YANG, Z. (1989). Interaction between endothelium-derived nitric oxide and SIN-1 in human and porcine blood vessels. *J. Cardiovasc. Pharmacol.*, **14**, Suppl. 11, S76–S80.

MONCADA, S. & HIGGS, E.A. (1990). *Nitric Oxide from L-Arginine: A Bioregulatory System.* Amsterdam: Excerpta Medica.

MONCADA, S., PALMER, R.M.J. & HIGGS, E.A. (1989). The discovery of nitric oxide as the endogenous nitrovasodilator. *Hypertension*, **12**, 365–372.

MOORE, P.K., AL-SWAYEH, O.A., CHONG, N.W.S., EVANS, R.A. & GIBSON, A. (1990). L-N^G-nitro arginine (L-NOARG), a novel, L-arginine-reversible inhibitor of endothelium-dependent vasodilatation *in vitro*. *Br. J. Pharmacol.*, **99**, 408–412.

MUSTAFA, M., MESTER, P.A., THIEMERMANN, C., HECKER, M. & VANE, J.R. (1990). N^{ω}-nitro-L-arginine (NO_2Arg) and NO_2Arg-L-phenylalanine inhibit endothelium-dependent vasodilatations *in vitro* in rabbits and *in vivo* in the anaesthetized rat. *J. Physiol.*, **429**, 72P.

REES, D.D., PALMER, R.M.J. & MONCADA, S. (1989). Role of endothelium-derived nitric oxide in the regulation of blood pressure. *Proc. Natl. Acad. Sci., U.S.A.*, **86**, 3375–3378.

REES, D.D., PALMER, R.M.J., SCHULZ, R., HODSON, H.F. & MONCADA, S. (1990). Characterization of three inhibitors of endothelial nitric oxide synthase *in vitro* and *in vivo*. *Br. J. Pharmacol.*, **101**, 746–752.

ROSE'MEYER, R.B. & HOPE, W. (1990). Evidence that A_2 purinoceptors are involved in endothelium-dependent relaxation of the rat thoracic aorta. *Br. J. Pharmacol.*, **100**, 576–580.

RUBANYI, G.M. & VANHOUTTE, P.M. (1985). Endothelium removal decreases relaxations of canine coronary arteries caused by beta-adrenergic agonists and adenosine. *J. Cardiovasc. Pharmacol.*, **7**, 139–144.

SHIRASAKI, Y. & SU, C. (1985). Endothelium removal augments vasodilation by sodium nitroprusside and sodium nitrite. *Eur. J. Pharmacol.*, **114**, 93–96.

THEODORSSON-NORHEIM, E. (1987). Friedman and Quade tests: BASIC computer program to perform non-parametric two-way analysis of variance and multiple comparisons on ranks of several related samples. *Comput. Biol. Med.*, **17**, 85–99.

THOMAS, G.R., THIEMERMANN, C., WALDER, C. & VANE, J.R. (1988). The effects of endothelium-dependent vasodilators on cardiac output and their distribution in the anaesthetized rat: a comparison with sodium nitroprusside. *Br. J. Pharmacol.*, **95**, 986–992.

TOLINS, J.P., PALMER, R.M.J., MONCADA, S. & RAIJ, L. (1990). Role of endothelium-derived relaxing factor in regulation of renal hemodynamic responses. *Am. J. Physiol.*, **258**, H655–H662.

VANHOUTTE, P.M. & LEVY, M.N. (1980). Prejunctional cholinergic modulation of adrenergic neurotransmission in the cardiovascular system. *Am. J. Physiol.*, **238**, H275–H281.

WALDER, C., THIEMERMANN, C. & VANE, J.R. (1991). The involvement of endothelium-derived relaxing factor in the regulation of renal cortical blood flow in the rat. *Br. J. Pharmacol.*, **102**, 967–973.

(Received January 4, 1991
Revised February 28, 1991
Accepted March 20, 1991)

Br. J. Pharmacol. (1991), **103**, 1733–1739 © Macmillan Press Ltd, 1991

The effect of ω-conotoxin GVIA on synaptic transmission within the nucleus accumbens and hippocampus of the rat *in vitro*

A.L. Horne & [1]J.A. Kemp

Merck, Sharp and Dohme Research Laboratories, Neuroscience Research Centre, Terlings Park, Eastwick Road, Harlow, Essex CM20 2QR

1 The actions of two calcium channel antagonists, the N-channel blocker ω-conotoxin GVIA (ω-CgTx) and the L-channel antagonist nisoldipine, on synaptic transmission were investigated in the hippocampus and nucleus accumbens of the rat *in vitro*.

2 ω-CgTx (100 nM for 10 min) produced a marked and irreversible reduction of focally evoked population spikes and intracellularly recorded excitatory postsynaptic potentials (e.p.s.ps) in the nucleus accumbens, which could not be overcome by increasing the stimulus strength.

3 Nisoldipine (10 μM for 10 min) had no effect on population spikes in the nucleus accumbens or the CA1 of the hippocampus.

4 In the hippocampus, population spikes were not irreversibly reduced by ω-CgTx (100 nM for 10 min) but rather, multiple population spikes were produced along with spontaneous synchronous discharges. This indicated that inhibitory synaptic transmission was being preferentially reduced.

5 Intracellular recordings demonstrated that ω-CgTx powerfully reduced inhibitory synaptic transmission in an irreversible manner and that excitatory transmission was also reduced but to a lesser extent. Unlike excitatory transmission in the nucleus accumbens and inhibitory transmission in the hippocampus, increasing the stimulus strength overcame the reduction of hippocampal excitatory transmission.

6 It is concluded that ω-CgTx-sensitive calcium channels are involved in the calcium entry that precedes the synaptic transmission in all these synapses. The apparent lower sensitivity of the hippocampal excitatory fibres to ω-CgTx may indicate that calcium entry that promotes transmitter release at central synapses may be mediated by pharmacologically distinct calcium channels.

Keywords: Calcium channel; calcium channel antagonist; amino acid neurotransmitter; central synapse; nucleus accumbens; hippocampus

Introduction

The involvement of calcium ions in the mediation of neurotransmitter release was first elucidated from the pioneering work of Harvey & Macintosh (1940) and del Castillo & Katz (1954). These workers observed that lowering the concentration of extracellular calcium led to a reduction in neurotransmission in the superior cervical ganglion and neuromuscular junction respectively. These original observations have been extended to many other mammalian peripheral and central synapses with the result that it has now become generally accepted that calcium entry into the presynaptic terminal is an absolute requirement for subsequent neurotransmitter release (Smith & Augustine, 1988).

Calcium ions are believed to enter the nerve terminal through voltage-sensitive channels that become permeable to the ion following depolarization of the plasma membrane. Such voltage-dependent calcium channels in vertebrate neurones have been classified into three sub-types (Fox *et al.*, 1987). These have been termed L-, N- and T-, with each differing in its voltage and current activation and inactivation properties. Specific probes have been proposed for the L- (Fox *et al.*, 1987) and T-channels (Tang *et al.*, 1988; Coulter *et al.*, 1989), whilst the N-channel is blocked by the marine snail venom ω-conotoxin GVIA (ω-CgTx; Fox *et al.*, 1987). However, this toxin may also block neuronal L-channels (Fox *et al.*, 1987).

ω-CgTx has been shown to inhibit neurotransmitter release from a number of preparations (Kerr & Yoshikami, 1984; Dooley *et al.*, 1987; 1988; Hirning *et al.*, 1988; Mohy El-din & Malik, 1988). As these actions are generally not produced by specific L-channel blockers (Middlemiss & Spedding, 1985; Hirning *et al.*, 1988; Mohy El-din & Malik, 1988) it has been proposed that N-channels may mediate the calcium entry that initiates calcium-dependent neurotransmitter release. Therefore, we have examined the actions of ω-CgTx on synaptic transmission at a number of excitatory and inhibitory synapses in the central nervous system of the rat, *in vitro*. A preliminary account of some of these results has been published (Horne & Kemp, 1989).

Methods

Experiments were performed on two brain areas, the hippocampus and the nucleus accumbens. Male Sprague Dawley rats (60–80 g) were killed by decapitation and the whole brain was removed. Parasaggital slices 350 μm thick of hippocampus or nucleus accumbens were cut, with a Vibratome. Slices were then allowed a preincubation period of about 30 min after which they were transferred to a perfusion chamber. Such slices were submerged in the perfusion medium which was heated to 33°C and delivered at a rate of ~2 ml min^{-1}. Stimulation of the tissue was performed by passing square wave pulses down bipolar tungsten stimulating electrodes. Pulses up to 1 ms width and 15 V amplitude were generally used to obtain control synaptic responses.

In the hippocampus the stimulating electrodes were placed in the stratum radiatum and recordings were made either in

[1] Author for correspondence.

the radiatum or the CA1 cell body region. Alternatively, stimulating electrodes were placed in the dentate hilus for recordings made in the CA3 cell body layer. Slices of nucleus accumbens, taken from the level where the anterior commissure forms a boundary along most of the length of the accumbens-striatum border, were stimulated just ventral to the anterior commissure. Recording electrodes were placed rostral with respect to the stimulating electrodes. Extracellular recordings were made with glass microelectrodes (~5 MΩ) filled with 3 M NaCl. The signal was amplified and filtered (low pass below 1 kHz) by a Neurolog system (Digitimer). For intracellular 'current clamp' experiments, electrodes (60–200 MΩ) were usually filled with 3 M KAc. Intracellular current pulses were delivered, and responses amplified and monitored with either an Axoclamp-2A (Axon Instruments) in bridge mode (filtered above 3 kHz) or, in some early experiments, a Neurolog NL102 d.c. intracellular amplifier (Digitimer). In voltage clamp studies, electrodes (50–100 MΩ) were filled with CsAc and connected to an Axoclamp-2A in single electrode voltage clamp mode. The headstage was continuously monitored to ensure that adequate settling occurred. Sampling frequencies of 4–6 kHz were generally used. In voltage clamp mode, the evoked postsynaptic currents that give rise to the subsequent potentials (Araki & Terzuolo, 1962) were examined. These experiments were performed at holding potentials of −20 to −30 mV for excitatory synapses, and −15 to −30 mV for inhibitory synapses. Holding potentials were selected for individual experiments according to the level where spontaneous inward sodium and calcium conductances were inactivated and where synaptic signals of sufficient magnitude to be measured reliably and adequately clamped were obtained.

Postsynaptic responses in the hippocampus consisted of a fast monosynaptic excitatory input, and a fast and slow inhibitory input (Newberry & Nicoll, 1985). These responses were examined either unmodified or following attempts to separate the excitatory and inhibitory components. Excitatory synaptic inputs were dissected free of the fast inhibitory input by the addition of 30 μM bicuculline in combination with 30 μM picrotoxin to antagonize the postsynaptic actions of the inhibitory transmitter. Inhibitory potentials can be studied in isolation of excitatory potentials by adding 6,7-dinitroquinoxaline-2,3-dione to the superfusate. Such quinoxalinediones are antagonists of non-NMDA excitatory amino acid receptors (Drejer & Honoré, 1988) and therefore inhibit excitatory synaptic inputs onto the pyramidal cells and also the interneutrones (Collingridge *et al.*, 1988). However, if the stimulating electrodes are placed in close proximity to the recording electrode an apparently pure inhibitory input can be evoked (Collingridge *et al.*, 1988) that presumably results from the direct electrical activation of the interneurone(s).

Slices were cut and all experiments were performed in a medium of the following composition (mM): NaCl 124, KCl 2, KH_2PO_4 1.25, $MgSO_4$ 2, $CaCl_2$ 2, $NaHCO_3$ 25 and glucose 11, apart from field potential experiments where the perfusion medium was supplemented with a further 3 mM KCl. All solutions were gassed with a 95% O_2/5% CO_2 mixture. Bulk chemicals were purchased from either BDH or FSA laboratory supplies. (+)-Bicuculline and picrotoxin were purchased from Sigma: N-methyl-D-aspartate (NMDA), D-(−)-2-amino-5-phosphonovalerate (D-AP5) and 6,7-dinitroquinoxaline-2,3-dione (DNQX) from Tocris Neuramin; ω-conotoxin GVIA (ω-CgTx) from Peninsula Laboratories; nisoldipine was obtained from Miles Pharmaceuticals and dizocilpine (MK801) and 7-chlorokynurenate (7-Cl KYNA) were synthesized in-house.

All drugs were added to the tissue bathing media and bath applied. (+)-Bicuculline was initially dissolved in 0.013 M HCl to a concentration of 10 mM and diluted into other solutions as required. DNQX and 7-Cl KYNA were initially dissolved into the minimum required quantity of NaOH. Nisoldipine was initially dissolved in ethanol to a concentration of 10 mM. Nisoldipine experiments were performed in a darkened laboratory and all solutions containing nisoldipine were used in reservoirs protected from the light. All other compounds were sufficiently soluble in water to be directly added to the media. Results are expressed as mean values ± s.e.mean.

Results

Nucleus accumbens

Extracellular studies Focal stimulation of the accumbens tissue evoked an apparent population spike (Figure 1a) which has previously been shown to be sensitive to antagonists of excitatory amino acid receptors (Horne *et al.*, 1990; Pennartz *et al.*, 1990). The addition of 100 nM ω-CgTx for 10 min led to a reduction in the population spike amplitude. In 5 slices the mean reduction of a submaximal spike was 75.6 ± 5.5%. When attempted, this effect could not be overcome ($n = 3$) by increasing the stimulus strength and was essentially irreversible over 2 h. The L-channel blocker nisoldipine (10 μM) had no effect on the population spike ($n = 3$). This is a concentration greatly in excess of those that have been shown to block L-channels (Morel & Godraind 1991).

Intracellular studies The effect of focal stimulation within the nucleus accumbens is shown in Figure 1b. Following the stimulus artefact there was a delay of 1–2 ms before an excit-

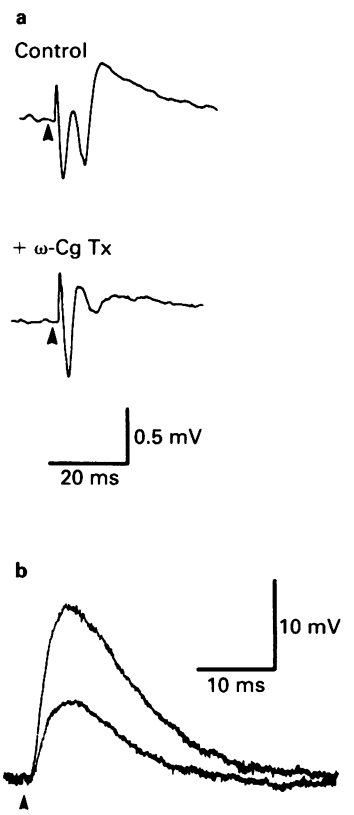


Figure 1 Synaptic potentials in the nucleus accumbens: (a) illustrates the form of the extracellularly recorded field potential. The first large negative (downward) deflection probably reflects electrically evoked action potentials in the presynaptic elements. Following this a second negative wave, a presumed population spike, was produced. This probably reflects action potentials in postsynaptic cells and rises from a positively going field excitatory postsynaptic potential (e.p.s.p.) (cf. hippocampal population spikes; Andersen *et al.*, 1971a). ω-Conotoxin GVIA (ω-CgTx) had little effect on the presynaptic spike but markedly reduced the population spike and field e.p.s.p. On this and all subsequent figures where the stimulus artefacts are blanked out for clarity, they occurred at the position indicated by the arrow. (b) Intracellularly recorded e.p.s.ps. The larger control e.p.s.p. was reduced in both amplitude and duration following 10 min exposure to 100 nM ω-CgTx (smaller trace). Resting membrane potential = −80 mV.

atory postynaptic potential (e.p.s.p.) developed. Little evidence of any concomitant inhibitory postsynaptic potentials (i.p.s.ps) was obtained. Following exposure to ω-CgTx (100 nM, 10 min) the evoked e.p.s.ps were reduced in amplitude and duration (Figure 1b). The percentage reduction of the amplitude of these e.p.s.ps (sub-threshold for action potential initiation) was 63.9 ± 4.8% ($n = 5$). The application of ω-CgTx did not affect the apparent membrane resistance in any cell tested.

Hippocampus

Extracellular studies Stimulation of the stratum radiatum activated Schaffer collateral and commissural fibres that form synapses mediated by an excitatory amino acid neurotransmitter onto CA1 pyramidal cells (Collingridge *et al.*, 1983). At the end of a 10 min application of ω-CgTx (100 nM), the population spike evoked from this region (Figure 2) was transiently reduced by 31.2 ± 4.2% ($n = 7$). In each case the population spike steadily recovered over the following 20–60 min. An additional effect that appeared during the application of ω-CgTx in all 7 slices, was the production of multiple population spikes following the synaptic stimulus (Figure 2). In 4 slices, spontaneous synchronized burst discharges also occurred upon application of ω-CgTx (Figure 2). Little recovery from these effects was obtained after up to 3 h washout. Nisoldipine (10 μM for 10 min) had no effect on the CA1 population spikes either when added alone ($n = 4$) or following exposure of the slice to ω-CgTx ($n = 4$).

Field e.p.s.ps recorded in the radiatum were of the classical form (Andersen *et al.*, 1971b). ω-CgTx (100 nM for 10 min) reduced the rate of rise of the postsynaptic component by 44.2 ± 13.3% ($n = 4$); as with cell body fields, a slow but generally incomplete recovery occurred. Full recovery was achieved by increasing the stimulus strength by up to 3× control.

Intracellular studies Stimulation of the stratum radiatum evoked synaptic responses in CA1 pyramidal cells (Figure 3). These have been shown to comprise an excitatory amino acid mediated e.p.s.p. (Collingridge *et al.*, 1983), a fast $GABA_A$-mediated i.p.s.p. and a slow $GABA_B$-mediated i.p.s.p. (Newberry & Nicoll, 1985; Dutar & Nicoll, 1988). Similar responses were obtained upon activation of mossy fibre inputs onto CA3 pyramidal cells although the i.p.s.p. was often the more predominant response. ω-CgTx (100 nM, 10 min) strongly attenuated the i.p.s.ps in both CA1 ($n = 5$) and CA3 ($n = 4$), whilst the e.p.s.ps often showed an increase in both amplitude and duration.

The i.p.s.ps of the CA1 were sensitive to concentrations of ω-CgTx as low as 10 nM when applied for longer periods (30 min). This concentration also reduced the rate of rise of the e.p.s.p. by 20.3 ± 15.5% ($n = 3$) after this time. Perfusion of 30 nM ω-CgTx for 30 min reduced the rate of rise of e.p.s.ps by 51.4 ± 3.3% ($n = 4$). Similar experiments using 1 μM ω-CgTx (30 min) produced greater variation. The reduction in the rate of rise of the e.p.s.p. was 45.9 ± 18.7% ($n = 5$). This highest concentration of the toxin reduced the amplitudes of 4 of these e.p.s.ps, completely inhibiting 2. In every case these effects of ω-CgTx on the e.p.s.ps could be reversed by increasing the stimulus strength. Only on 2 occasions did the i.p.s.p. show a partial recovery on increasing the stimulus strength. The application of ω-CgTx, at these concentrations, did not affect resting membrane resistance ($n = 5$ CA1 : $n = 3$ CA3).

Isolated hippocampal excitatory postsynaptic potentials

The monosynaptically evoked e.p.s.p. is usually rapidly curtailed by a fast i.p.s.p. which results from concurrent activation of feedforward inhibitory interneurones in the CA1. It is possible that if ω-CgTx were having an effect on both inhibitory and excitatory synapses, then the effect of the e.p.s.p. may have been masked by the reduction in the curtailment produced by the i.p.s.p. Thus, it was necessary to examine the effects of ω-CgTx on these potentials in isolation and thus unmodified by concurrent synaptic activity.

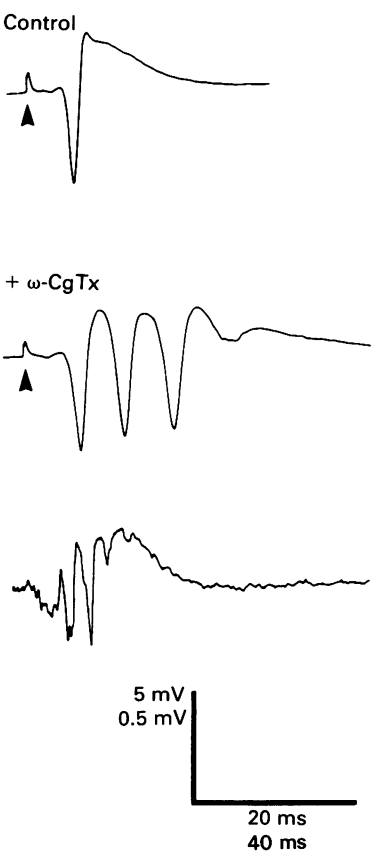


Figure 2 Effect of ω-conotoxin GVIA (ω-CgTx) on field potentials in the CA1. Recordings of the evoked field potentials in the cell body layer. Large negative (downward) population spikes were produced superimposed on a positive excitatory postsynaptic potential (e.p.s.p.). Following exposure to 100 nM ω-CgTx for 10 min, multiple population spikes were evoked and often, spontaneous discharges (lower record) appeared.

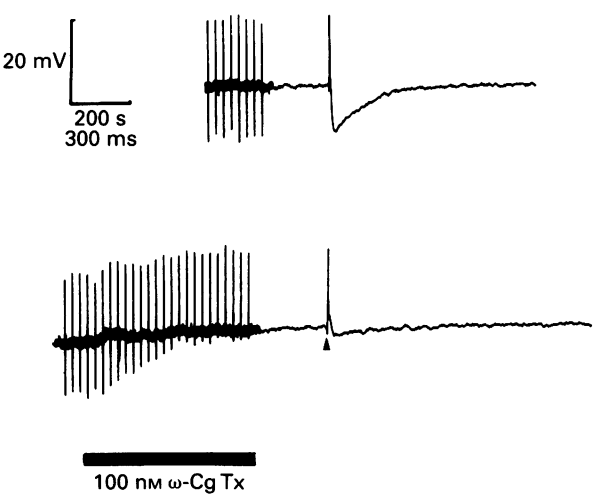


Figure 3 Effect of ω-conotoxin GVIA (ω-CgTx) on intracellularly recorded synaptic potentials in the hippocampus. Each synaptic response comprised an excitatory postsynaptic potential (e.p.s.p.), upon which an action potential was produced, and a fast and a slow inhibitory postsynaptic potential (i.p.s.p). These responses are shown at two sweep speeds (top record). During application of ω-CgTx the i.p.s.ps were selectively reduced. The amplitude of the action potentials was truncated by the chart recorder. Resting membrane potential = −60 mV.

Perfusion of slices with a combination of 30 μM bicuculline and 30 μM picrotoxin antagonized the fast i.p.s.p. Therefore the evoked e.p.s.p. was not so rapidly attenuated and was augmented. This led to the production of paroxysmal depolarizing shifts (p.d.s's) (Matsumoto & Ajmone-Marsan, 1964; Dichter & Spencer, 1969) which, at low stimulus intensities and hyperpolarized membrane potentials, could often be visualized as a secondary hump in the e.p.s.p. (Figure 4a). In p.d.s's that reached threshold for action potential activation, multiple action potentials were produced (Figure 4b), and the p.d.s. tended to merge with the initial e.p.s.p.

In the presence of $GABA_A$-receptor antagonists, p.d.s's occurred upon synaptic stimulation but not upon direct intracellular current injection, and whether the CA3 was intact ($n = 7$) or surgically removed ($n = 4$). They were not abolished in the presence of the NMDA antagonist D(−)-AP5 (30 μM; $n = 4$), when applied in combination with either MK801 (500 nM) or 7-Cl KYNA (50 μM). A combination of a competitive antagonist, such as AP5 (Evans *et al.*, 1982), and a non-competitive antagonist such as MK-801 (Wong *et al.*, 1986) or 7-Cl KYNA (Kemp *et al.*, 1988) should provide a large antagonism of NMDA receptors whilst reducing the possible risk of non-NMDA effects if the equivalent concentration of a single agent has been added. Both the initial e.p.s.p. and the p.d.s. were reversibly abolished by 3 μM DNQX ($n = 3$), demonstrating that they were synaptic in origin.

Eight CA1 cells displaying subthreshold e.p.s.ps and p.d.s's were exposed to 100 nM ω-CgTx for 10 min. In all cases both excitatory components were sensitive to the toxin. The peak of the e.p.s.p./p.d.s. was reduced by a mean value of 86.2 ± 3.8%. By increasing the amplitude of the stimulus to the stratum radiatum by between 0.3 and 1.5 V the reduction in the e.p.s.p./p.d.s. could be reversed in every case ($n = 4$; Figure 4c). In some cases suprathreshold CA1 e.p.s.p./p.d.s's also showed a slight sensitivity to ω-CgTx. These events were either unchanged ($n = 2$) or showed delayed onset/rise times ($n = 4$) following exposure to 100 nM ω-CgTx (10 min). Later action potentials in 3 of these 4 latter e.p.s.ps were also lost or delayed (data not shown). To quantify this action of ω-CgTx, cells were voltage-clamped so that the excitatory postsynaptic current (e.p.s.c.) underlying each e.p.s.p. could be examined (Figure 5a). At holding potentials of −20 to −30 mV the peak amplitude of supramaximal e.p.s.cs was reduced by 11.7 ± 4.3% ($n = 4$) following exposure to ω-CgTx (100 nM, 10 min).

In the CA3, the p.d.s. produced in the presence of $GABA_A$ antagonists was also examined (Figure 5b). ω-CgTx (100 nM, 10 min) had little effect on these e.p.s.ps ($n = 3$). In this respect the CA3 e.p.s.ps/p.d.s's appeared less susceptible to the toxin than those in the CA1.

Isolated CA1 inhibitory postsynaptic potentials

'Pure' i.p.s.ps were evoked by stimulating in close proximity to the recorded cell in the presence of 10 μM DNQX, as described in the methods (Figure 6a). These i.p.s.ps were very sensitive to inhibition by ω-CgTx (100 nM, 10 min, $n = 7$). This antagonism could not be overcome in any of the cells tested ($n = 5$). On increasing the stimulus strength beyond a certain intensity, action potentials, arising from the stimulus artefact were evoked in the pyramidal cell, presumably as a result of direct electrical activation. In voltage-clamp mode the outward current underlying the i.p.s.p., the inhibitory postsynaptic current (i.p.s.c.) was examined (Figure 6b). This was performed at Vhold of −15 to −30 mV. ω-CgTx (100 nM, 10 min) reduced the peak amplitude to the i.p.s.c. by 70.3 ± 11.9% ($n = 4$).

Exogenously applied GABA-mimetics

To determine whether the effect of the ω-CgTx involved an action on postsynaptic $GABA_A$-receptor-mediated responses, its effect on the actions of the $GABA_A$-receptor agonist, isoguvacine, was examined. Isoguvacine (10 μM) evoked a hyperpolarization associated with a conductance increase (Figure 7). The mean peak amplitude of the hyperpolarization evoked was 4.3 ± 0.4 mV ($n = 5$) whilst the mean conductance increase in these cells was 9.9 ± 1.3 nS. No significant reduction of either action was produced following exposure to 100 nM ω-CgTx for 10 min (Student's paired t test: $P > 0.05$ in both cases). ω-CgTx had no effect on the actions of isoguvacine on cells where the toxin produced the reduction in

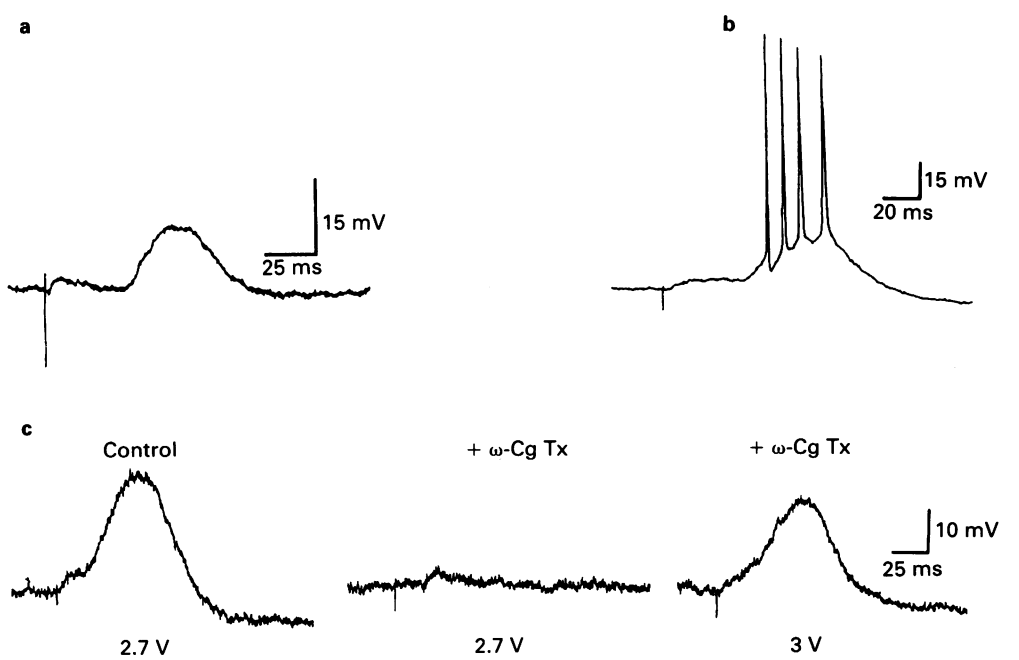


Figure 4 Paroxysmal depolarization shifts (p.d.s's) in CA1. In the presence of $GABA_A$ antagonists, p.d.s's appeared as secondary humps following the evoked excitatory postsynaptic potential (e.p.s.p.)(a). This allowed cells with otherwise subthreshold e.p.s.ps to produce action potentials (b). ω-Conotoxin GVIA (ω-CgTx) produced marked inhibitions of sub-threshold e.p.s.ps and p.d.s's that could, nonetheless, be reversed upon increasing the stimulus strength (c). Records (a) and (c) were taken from the same cell (resting membrane potential = −61 mV). Record (b) was taken from a different cell that was hyperpolarized to −80 mV by constant current injection.

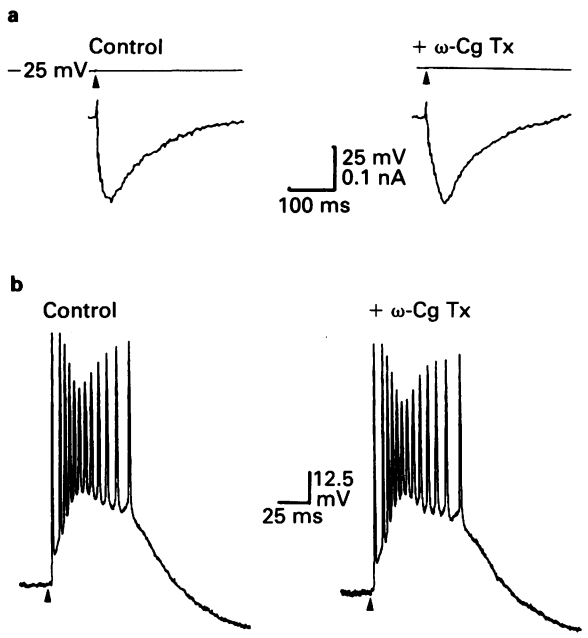


Figure 5 Paroxysmal depolarization shifts recorded under voltage- and current-clamp. (a) The current underlying supramaximal paroxysmal depolarization shifts (p.d.s's) recorded in the CA1. Cells where voltage clamped at depolarizing membrane potentials to avoid spontaneous sodium and calcium currents, ω-conotoxin GVIA (ω-CgTx) had only a limited effect on these synaptic responses. (b) Paroxysmal depolarization shifts in CA3. Recorded in current-clamp, the excitatory postsynaptic potential (e.p.s.p.) and p.d.s. merged to form large excitatory potentials giving rise to many action potentials. These responses were unaffected by exposure to ω-CgTx. In this example the p.d.s. was slightly accentuated and produced an additional action potential during ω-CgTx application. Resting membrane potential = −66 mV.

the evoked i.p.s.p. that was documented above. ω-CgTx had no effect on the action of the $GABA_B$ agonist, baclofen (Figure 7).

Discussion and conclusions

The involvement of calcium in neurotransmission has been established over many years and, in most cases, the entry of calcium into the presynaptic terminal is the causative action

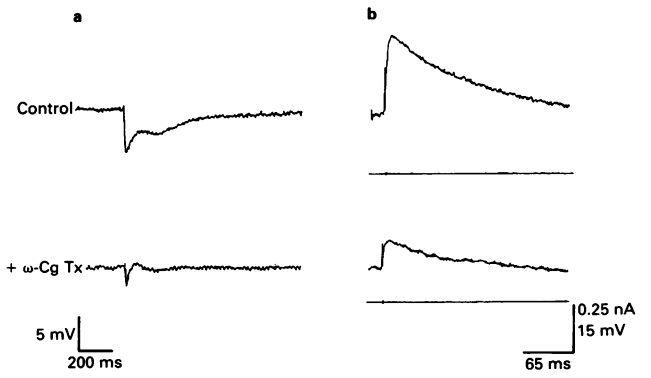


Figure 6 Monosynaptically evoked inhibitory synapses in CA1. Inhibitory postsynaptic potentials (i.p.s.ps) (a) and the current underlying them, the inhibitory postsynaptic currents (i.p.s.cs) (b), were evoked by direct electrical stimulation of the interneurones in the presence of the excitatory amino acid antagonist 6,7-dinitroquinoxaline-2,3-dione (DNQX) (see text). In both current- and voltage-clamp these inhibitory synapses were strongly attenuated by ω-conotoxin GVIA (ω-CgTx). Record (a) was taken from a cell of resting membrane potential −59 mV whereas record (b) was taken from a different cell voltage-clamped at −30 mV.

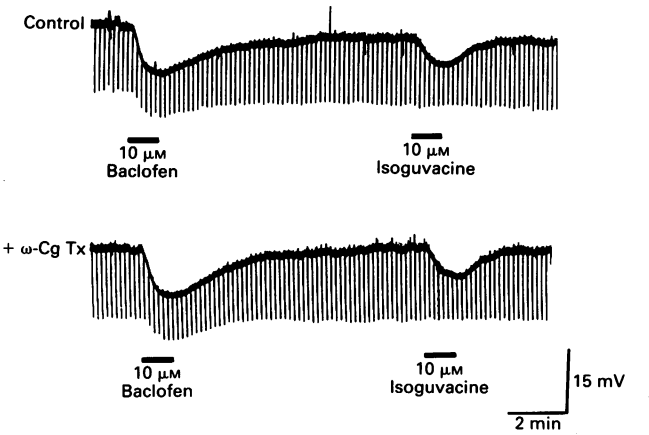


Figure 7 Lack of effect of ω-conotoxin GVIA (ω-CgTx) on GABA-receptor activation in CA1. Responses to 1 min applications of 10 μM baclofen and 10 μM isoguvacine before and after application of ω-CgTx. Regular downward deflections were produced by direct intracellular hyperpolarizing current pulses of 0.2 nA magnitude. Resting membrane potential = −62 mV.

for transmitter release (Smith & Augustine, 1988). The mode of calcium entry has attracted much interest, with the description of multiple calcium channels in vertebrate neurones allowing investigations into the channel sub-type(s) that may be involved. In this study we have examined the effects of two calcium channel blockers, nisoldipine and ω-CgTx, on synaptic responses in the nucleus accumbens and hippocampus. Any dependence of this transmission on L-channels would be expected to be demonstrated by a sensitivity of the synaptic transmission to both nisoldipine and perhaps ω-CgTx whereas a reliance on N-channels should be demonstrated by a sensitivity to ω-CgTx alone (Fox *et al.*, 1987).

The lack of effect of nisoldipine on the field potentials in both the nucleus accumbens and the CA1 suggests that dihydropyridine-sensitive L-channels are not significantly involved in the release of neurotransmitter from the presynaptic terminals that were activated in our *in vitro* conditions. However, such a conclusion may be compromised by the reported voltage-dependence of the block of L-channels by dihydropyridines and their low efficacy of action on hippocampal neurones (Docherty & Brown, 1986; Ozawa *et al.*, 1989; Meyers & Barker, 1989). By contrast, ω-CgTx had pronounced effects on these synaptic potentials. In the nucleus accumbens, ω-CgTx strongly inhibited the population spike and intracellularly recorded e.p.s.p. The toxin had no effect on the resting membrane conductance, suggesting that its effects were mediated presynaptically. The inhibition of the excitatory potentials in the nucleus accumbens is consistent with a role of N-channels in the release of the excitatory amino acid neurotransmitter (Horne *et al.*, 1990) in this region.

In the CA1 region of the hippocampus, a 10 min application of 100 nM ω-CgTx produced a transient reduction in the population spike amplitude and an inhibition of the radiatum dendritic field potential. This suggests therefore, that the e.p.s.ps in the hippocampus are sensitive to the toxin. Intracellular studies indicated that the i.p.s.ps within the CA1 and CA3 were also markedly reduced by the toxin. The lack of effect of ω-CgTx on either resting membrane conductance or the action of GABA-mimetics, along with the voltage-clamp data suggests that these actions of ω-CgTx were exerted at a presynaptic locus and not at postsynaptic GABA receptors or calcium channels such as have been described in hippocampal neurones (Docherty & Brown, 1986; Meyers & Barker, 1989). This suggests that ω-CgTx sensitive channels are involved also in these synaptic processes (Kamiya *et al.*, 1988; Krishtal *et al.*, 1989; Dutar *et al.*, 1989).

It was a common finding, however, that in the CA1 or CA3 the i.p.s.p. appeared to be more sensitive to ω-CgTx than was

the e.p.s.p. This was indicated directly in the intracellular studies, and indirectly by the production of multiple population spikes in the extracellular experiments. The appearance of the spontaneous discharges also suggests that the balance of excitatory and inhibitory inputs was altered in favour of the excitation. The lack of these discharges in the intracellular studies may reflect the lower potassium concentrations used. This phenomenon was not reported in the extracellular studies of Krishtal *et al.* (1989) although it was noted, to a small extent, in the intracellular work of Dutar *et al.* (1989). Further evidence for a distinction between the sensitivity of the e.p.s.p. and the i.p.s.p. to ω-CgTx was provided by the present study in that the effects of ω-CgTx on the e.p.s.p. could be overcome by increasing the stimulus magnitude. This procedure was patently less successful in overcoming the effects on hippocampal i.p.s.ps or e.p.s.ps in the nucleus accumbens. This apparent differential sensitivity could have arisen from the synaptic arrangement within the CA1. E.p.s.ps were normally rapidly curtailed by the powerful inhibitory effects of the i.p.s.p. Therefore, it is possible that small decreases in the output of excitatory transmitter may not have produced a smaller e.p.s.p. if release of inhibitory transmitter, and therefore the effectiveness of the i.p.s.p., was also decreased. For this reason the potentials were dissected free of each other and their sensitivity to ω-CgTx re-examined.

By perfusing with antagonists of $GABA_A$ receptors, the fast component of the i.p.s.p. was inhibited. The e.p.s.p. was, therefore, relatively isolated from the i.p.s.p. which allowed the production of a secondary component to the e.p.s.p., known as the paroxysmal depolarizing shift (p.d.s.; Matsumoto & Ajmone-Marsan, 1964; Dichter & Spencer, 1969). Previous studies have indicated that the p.d.s. appears to be synaptic in origin (Johnston & Brown, 1984; Neuman *et al.*, 1989). This is supported by the present observation that they were blocked by antagonists of excitatory amino acid receptors, and that p.d.s's were only present following a synaptic stimulus and not following direct intracellular current injection. These events could be recorded in the CA1 even following removal of the CA3 region of the slice. Therefore, they presumably result from circuitry within the CA1, similar to that proposed for such events within the CA3 (Schwartzkroin & Prince, 1978; Wong & Traub, 1983). That they were not abolished by selective NMDA antagonists suggests that these events were not dependent on NMDA receptors.

The e.p.s.p./p.d.s. complex appeared to be relatively insensitive to 100 nM ω-CgTx applied for 10 min. Although these potentials could be shown to be sensitive to the toxin, this was usually only the case when small potentials evoked by very submaximal stimuli were studied. Only small and inconsistent effects were produced on potentials large enough to give rise to action potentials and only a small reduction in the synaptic current was observed in voltage-clamp. As before, any effect of ω-CgTx was reversible by increasing the stimulus strength. It did not appear, therefore, that these synaptic inputs onto the hippocampal pyramidal cells showed any increased sensitivity to ω-CgTx after removal of the concurrent inhibition. This suggests that the e.p.s.ps may indeed be less sensitive to the toxin and that the removal of the shunt normally provided by the inhibitory transmitter does not mask an effect of ω-CgTx on the excitatory potential.

As the i.p.s.p. in the CA1 is normally activated via di/polysynaptic pathways following stratum radiatum stimulation, whilst the e.p.s.p. results from monosynaptic activation, it may be that the di/polysynaptic pathways would appear to be the more susceptible even if all synapses were being equally affected. However, when the i.p.s.ps were activated monosynaptically, in isolation from e.p.s.ps, they continued to show strong sensitivity to ω-CgTx.

That the effects of ω-CgTx on the hippocampal e.p.s.p. were overcome by increasing the stimulus strength suggests that in these synapses, unlike the inhibitory synapses in this region or the excitatory synapses in the nucleus accumbens, transmission is not dependent upon the channels that were blocked during the application of the toxin. This may be the result if the extent of calcium entry into the excitatory terminal was far in excess of that required for neurotransmitter release. A prediction of this explanation is that hippocampal e.p.s.ps should be more resistant to failure in low calcium media compared to the i.p.s.ps. Such an effect has been reported by Rausche *et al.* (1990), who found that on lowering the calcium concentration, an initial period of transient epileptiform bursting was produced prior to synaptic failure.

An alternative explanation is that a distinct sub-class of N-channels may mediate the calcium entry into the excitatory terminals of the hippocampus. That N-channels may not form a homogeneous population is implicit in a number of experimental observations. Reynolds *et al.* (1986) observed that ω-CgTx at low concentrations inhibited only ~30% of depolarization-induced calcium uptake into synaptosomes and that a second inhibitory component occurred at higher concentrations, and Hans *et al.* (1990) have reported a <50% block of calcium currents, that were dependent on hyperpolarized membrane potentials, by the toxin. The studies of Plummer *et al.* (1989) suggest that the block of N-channels by ω-CgTx may involve both an irreversible and a reversible component. These latter authors suggest that their results can be explained by the existence of sub-classes of N-channels with different sensitivities to the toxin. The effects we observed on the hippocampal e.p.s.p. are not inconsistent with a role for the reversibly blocked N-channels in these synapses. Variation in the sensitivity of synaptic transmission to ω-CgTx has been suggested previously. The release of substance P can be shown to be dependent on dihydropyridine-sensitive L-type channels (Rane *et al.*, 1987) rather than ω-CgTx-sensitive N-type channels (Maggi *et al.*, 1988). Inhibitory synaptic inputs onto anococcygeus muscle are also resistant to ω-CgTx (McKnight *et al.*, 1989). Differential sensitivities of autonomic neuroeffector transmission in various tissues to ω-CgTx have recently been reported (De Luca *et al.*, 1990). The nerve terminals of the neurohypophysis have been shown to possess both L- and N-type calcium channels (Lemos & Nowycky 1989) and thus it has been suggested that both channel types could, conceivably, be involved in transmitter release under the appropriate physiological conditions. Furthermore, the N-type channels from this area appeared to differ from N-channels recorded from other neurones.

In conclusion, our results suggest that ω-CgTx-sensitive (presumably N-type) calcium channels mediate calcium entry into presynaptic elements and thereby initiate excitatory amino acid neurotransmitter release in the nucleus accumbens of the rat. Excitatory and inhibitory transmission in the CA1 and CA3 also seem to involve similar channels. The inhibitory synapses within the hippocampus appear to be the more sensitive to ω-CgTx suggesting that slight differences may exist in the physiological mechanism(s) that underly the concurrent excitatory and inhibitory synaptic processes in this region.

We are grateful to Eleanor Brawn and Sue Burton for their typing skills and to Roy Hammans, Andy Butler and Richard Stockwell for photographic work.

References

ANDERSEN, P., BLISS, T.V.P. & SKREDE, K.K. (1971a). Unit analysis of hippocampal population spikes. *Exp. Brain Res.*, **13**, 208–221.

ANDERSEN, P., BLISS, T.V.P. & SKREDE, K.K. (1971b). Lamellar organization of hippocampal excitatory pathways. *Exp. Brain Res.*, **13**, 222–238.

ARAKI, T. & TERZUOLO, C.A. (1962). Membrane currents in spinal motoneurons associated with the action potential and synaptic activity. *J. Neurophysiol.*, **25**, 772–789.

DEL CASTILLO, J. & KATZ, B. (1954). Quantal components of the end-plate potential. *J. Physiol.*, **124**, 560–573.

COLLINGRIDGE, G.L., DAVIES, C. & DAVIES, S.N. (1988). Actions of APV + CNQX on synaptic responses in rat hippocampal slices. In *Frontiers in Excitatory Amino Acid Research.* ed. Lehmann, J., Turski, L. & Cavalheiro, E. A. pp. 171–178. New York: Liss.

COLLINGRIDGE, G.L., KEHL, S.J. & McLENNAN, H. (1983). Excitatory amino acids in synaptic transmission in the Schaffer collateral-commissural pathway of the rat hippocampus. *J. Physiol.*, **334**, 33–46.

COULTER, D.A., HUGUENARD, J.R. & PRINCE, D.A. (1989). Specific petit mal anticonvulsants reduce calcium currents in thalamic neurones. *Neurosci. Lett.*, **98**, 74–78.

DE LUCA, A., LI, C.G., RAND, M.J., REID, J.J., THAINA, P. & WANG-DUSTING, H.K. (1990). Effects of ω-conotoxin GVIA on autonomic neuroeffector transmission in various tissues. *Br. J. Pharmacol.*, **101**, 437–447.

DICHTER, M. & SPENCER, W.A. (1969). Penicillin induced interictal discharges from the cat hippocampus 1. Characteristics and topographical features. *J. Neurophysiol.*, **32**, 649–662.

DOCHERTY, R.J. & BROWN, D.A. (1986). Interaction of 1,4-dihydropyridines with somatic Ca currents in hippocampal CA1 neurones of the guinea-pig *in vitro*. *Neurosci. Lett.*, **70**, 110–115.

DOOLEY, D.J., LUPP, A. & HERTTING, G. (1987). Inhibition of central neurotransmitter release by ω-conotoxin GVIA, a peptide modulator of the N-type voltage-sensitive calcium channel. *Naunyn-Schmiedebergs Arch. Pharmacol.*, **336**, 467–470.

DOOLEY, D.J., LUPP, A., HERTTING, G. & OSSWALD, H. (1988). ω-Conotoxin GVIA and pharmacological modulation of hippocampal noradrenaline release. *Eur. J. Pharmacol.*, **148**, 261–267.

DREJER, J. & HONORÉ, T. (1988). New quinoxalinediones show potent antagonism of quisqualate responses in cultured mouse cortical neurons. *Neurosci. Lett.*, **87**, 104–108.

DUTAR, P. & NICOLL, R.A. (1988). A physiological role for $GABA_B$ receptors in the central nervous system. *Nature*, **332**, 156–158.

DUTAR, P., RASCOL, O. & LAMOUR, Y. (1989). ω-Conotoxin GVIA blocks synaptic transmission in the CA1 field of the hippocampus. *Eur. J. Pharmacol.*, **174**, 261–266.

EVANS, R.H., FRANCIS, A.A., JONES, A.W., SMITH, D.A.S. & WATKINS, J.C. (1982). The effects of a series of ω-phosphonic α-carboxylic amino acids on electrically evoked and excitant amino acid induced responses in isolated spinal cord preparations. *Br. J. Pharmacol.*, **75**, 65–75.

FOX, A.P., NOWYCKY, M. C. & TSIEN, R.W. (1987). Kinetic and pharmacological properties distinguishing three types of calcium currents in chick sensory neurones. *J. Physiol.*, **394**, 149–172.

HANS, M., ILLES, P. & TAKEDA, K. (1990). The blocking effects of ω-conotoxin on Ca current in bovine chromaffin cells. *Neurosci. Lett.*, **114**, 63–68.

HARVEY, A.M. & MACINTOSH, F.C. (1940). Calcium and synaptic transmission in a sympathetic ganglion. *J. Physiol.*, **97**, 408–416.

HIRNING, L.D., FOX, A.P., McCLESKEY, E.W., OLIVERA, B.M., THAYER, S.A., MILLER, R.J. & TSIEN, R.W. (1988). Dominant role of N-type Ca^{2+} channels in evoked release of norepinephrine from sympathetic neurones. *Science*, **239**, 57–61.

HORNE, A.L. & KEMP, J.A. (1989). Action of ω-conotoxin GVIA on rat hippocampal synaptic transmission *in vitro*. *J. Physiol.*, **410**, 14P.

HORNE, A.L., WOODRUFF, G.N. & KEMP, J.A. (1990). Synaptic potentials mediated by excitatory amino acid receptors in the nucleus accumbens of the rat, in-vitro. *Neuropharmacology*, **29**, 917–921.

JOHNSTON, D. & BROWN, T.H. (1984). Mechanisms of neuronal burst generation. In *Electrophysiology of Epilepsy.* ed. Schwartzkroin, P.A. & Wheal, H.V. pp. 277–302. New York: Academic Press.

KAMIYA, H., SAWADA, S. & YAMAMOTO, C. (1988). Synthetic ω-conotoxin blocks synaptic transmission in the hippocampus *in vitro*. *Neurosci. Lett.*, **91**, 84–88.

KEMP, J.A., FOSTER, A.C., LEESON, P.D., PRIESTLEY, T., TRIDGETT, R., IVERSEN, L.L. & WOODRUFF, G.N. (1988). 7-Chlorokynurenic acid is a selective antagonist at the glycine modulatory site of the N-methyl-D-aspartate receptor complex. *Proc. Natl. Acad. Sci., U.S.A.*, **85**, 6547–6550.

KERR, L.M. & YOSHIKAMI, D. (1984). A venom peptide with a novel presynaptic blocking action. *Nature*, **308**, 282–284.

KRISHTAL, O.A., PETROV, A.V., SMIRNOV, S.V. & NOWYCKY, M.C. (1989). Hippocampal synaptic plasticity induced by excitatory amino acids includes changes in sensitivity to the calcium channel blocker ω-conotoxin. *Neurosci. Lett.*, **102**, 197–204.

LEMOS, J.R. & NOWYCKY, M.C. (1989). Two types of calcium channels coexist in peptide-releasing vertebrate nerve terminals. *Neuron*, **2**, 1419–1426.

MAGGI, C.A., PATACCHINI, R., SANTICIOLI, P., LIPPE, I.T., GIULIANI, S., GEPPETTI, P., DEL BIANCO, E., SELLERI, S. & MELI, A. (1988). The effect of omega conotoxin GVIA, a peptide modulator of the N-type voltage sensitive calcium channels, on motor responses produced by activation of efferent and sensory nerves in mammalian smooth muscle. *Naunyn-Schmeidebergs Arch. Pharmacol.*, **338**, 107–113.

MATSUMOTO, H. & AJMONE-MARSAN, C. (1964). Cortical and cellular phenomena in experimental epilepsy: interictal manifestations. *Exp. Neurol.*, **9**, 286–304.

McKNIGHT, A.T., MAGUIRE, J.J. & WOODRUFF, G.N. (1989). Selective block by ω-conotoxin GVIA of motor adrenergic nerves in rat anococcygeus, *in vitro*. *J. Physiol.*, **409**, 50P.

MEYERS, D.E.R. & BARKER, J.L. (1989). Whole-cell patch-clamp analysis of voltage-dependent calcium conductances in cultured embryonic rat hippocampal neurones. *J. Neurophysiol.*, **61**, 467–477.

MIDDLEMISS, D.N. & SPEDDING, M. (1985). A functional correlate for the dihydropyridine binding site in rat brain. *Nature*, **314**, 94–96.

MOHY EL-DIN, M.M. & MALIK, K.U. (1988). Differential effect of ω-conotoxin on release of the adrenergic transmitter and the vasoconstrictor response to noradrenaline in the rat isolated kidney. *Br. J. Pharmacol.*, **94**, 355–362.

MOREL, N. & GODFRAIND, T. (1991). Characterization in rat aorta of the binding sites responsible for blockade of noradrenaline-evoked calcium entry by nisoldipine. *Br. J. Pharmacol.*, **102**, 467–477.

NEUMAN, R.S., CHERUBINI, E. & BEN-ARI, Y. (1989). Endogenous and network bursts induced by N-methyl-D-aspartate and Mg free medium in the CA3 region of the hippocampal slice. *Neurosci.*, **28**, 393–399.

NEWBERRY, N.R. & NICOLL, R.A. (1985). Comparison of the action of baclofen with γ-aminobutyric acid on rat hippocampal pyramidal cells *in vitro*. *J. Physiol.*, **360**, 161–185.

OZAWA, S., TSUZUKI, K., IINO, M., OGURA, A. & KUDO, Y. (1989). Three types of voltage-dependent calcium current in cultured rat hippocampal neurones. *Brain Res.*, **495**, 329–336.

PENNARTZ, C.M.A., BOEIJINGA, P.H. & LOPES DA SILVA, F.H. (1990). Locally evoked potentials in slices of rat nucleus accumbens: NMDA and non-NMDA receptor mediated components and modulation by GABA. *Brain Res.*, **529**, 30–41.

PLUMMER, M.R., LOGOTHETIS, D.E. & HESS, P. (1989). Elementary properties and pharmacological sensitivities of calcium channels in mammalian peripheral neurons. *Neuron*, **2**, 1453–1463.

RANE, S.G., HOLZ, G.G. & DUNLAP, K. (1987). Dihydropyridine inhibition of neuronal calcium current and substance P release. *Pflügers Arch.*, **409**, 361–366.

RAUSCHE, G., IGELMUND, P. & HEINEMANN, U. (1990). Effects of changes in extracellular potassium, magnesium and calcium concentration on synaptic transmission in area CA1 and the dentate gyrus of rat hippocampal slices. *Pflügers Arch.*, **415**, 588–593.

REYNOLDS, I.J., WAGNER, J.A., SNYDER, S.H., THAYER, S.A., OLIVERA, B.M. & MILLER, R.J. (1986). Brain voltage-sensitive calcium channel subtypes differentiated by ω-conotoxin fraction GVIA. *Proc. Natl. Acad. Sci., U.S.A.*, **83**, 8804–8807.

SCHWARTZKROIN, P.A. & PRINCE, D.A. (1978). Cellular and field potential properties of epileptogenic hippocampal slices. *Brain Res.*, **147**, 117–130.

SMITH, S.J. & AUGUSTINE, G.J. (1988). Calcium ions, active zones and synaptic transmitter release. *Trends Neurosci.*, **11**, 458–464.

TANG, C.M., PRESSER, F. & MORAD, M. (1988). Amiloride selectively blocks the low threshold (T) calcium channel. *Science*, **240**, 213–215.

WONG, E.H.F., KEMP, J.A., PRIESTLEY, T., KNIGHT, A.R., WOODRUFF, G.N. & IVERSEN, L.L. (1986). The anticonvulsant MK-801 is a potent N-methyl-D-aspartate antagonist. *Proc. Natl. Acad. Sci., U.S.A.*, **83**, 7104–7108.

WONG, R.K.S. & TRAUB, R.D. (1983). Synchronised burst discharge in disinhibited hippocampal slice 1. Initiation in CA2-CA3 region. *J. Neurophysiol.*, **49**, 442–458.

(Received January 9, 1991
Revised March 19, 1991
Accepted March 26, 1991)

Br. J. Pharmacol. (1991), **103**, 1740–1744 © Macmillan Press Ltd, 1991

Mechanisms of platelet activating factor-induced changes in sheep tracheal blood flow

[1]D.R. Corfield, S.E. Webber & J.G. Widdicombe

Department of Physiology, St George's Hospital Medical School, Cranmer Terrace, London SW17 0RE

1 The effects of platelet activating factor (PAF) have been studied on the cervical tracheal vasculature and smooth muscle of anaesthetized sheep.

2 The predominant action of PAF (2 pmol–2 nmol) was a dose-dependent fall in tracheal vascular resistance. The maximum fall in resistance was −41.6% (−38.5 to −44.7%, 95% confidence interval) and the ED_{50} was 17 pmol (12–28 pmol). Lyso-PAF (200 pmol) did not change vascular resistance.

3 PAF had no effect on tracheal smooth muscle tone assessed by measuring changes in the external diameter of the trachea.

4 The fall in vascular resistance produced with PAF was unaffected by the anti-asthma drug nedocromil sodium (1 mg, i.a.), the cyclo-oxygenase inhibitor indomethacin (5 mg kg^{-1}, i.v.), the leukotriene receptor antagonist FPL55712 (2 mg kg^{-1}, i.v.), or a combination of the histamine H_1- and H_2-antagonists mepyramine (2 mg kg^{-1}, i.v.) with cimetidine (5 mg kg^{-1}, i.v.). The PAF antagonist WEB 2086 (300 μg kg^{-1}, i.v.) significantly reduced the vasodilatation produced by PAF (before, −40.8 ± 4.2%; after −16.5 ± 5.9%, $P < 0.05$).

5 Thus in this model, PAF is a potent vasodilator of the tracheal circulation but has no action on tracheal smooth muscle. The vasodilatation is mediated by specific PAF receptors and is not due to the release of prostanoids, leukotrienes or histamine.

Keywords: Platelet activating factor (PAF); airways blood flow; trachea

Introduction

Platelet activating factor (PAF) is released from a number of inflammatory cells and is likely to play an important role in the pathology of asthma (Barnes *et al.*, 1988; Spina *et al.*, 1989). *In vivo* it produces bronchoconstriction both in animals and man (Morley *et al.*, 1984; Cuss *et al.*, 1986) and it weakly stimulates tracheal submucosal gland secretions (Lang *et al.*, 1987). The most important action of PAF is to produce a non-specific hyperresponsiveness in the airways (Spina *et al.*, 1989). Many of the actions of PAF, including the development of hyperresponsiveness, may be indirect through its chemotactic action on inflammatory cells and its ability to produce secondary release of other inflammatory mediators such as 5-hydroxytryptamine (5-HT), prostaglandins, leukotrienes, bradykinin and oxygen radicals from these cells (Barnes *et al.*, 1988). More recently PAF has been shown to release weakly histamine from mast cells (Misawa & Huang, 1990). In man PAF-induced skin weal and erythema can be reduced by pretreatment with an H_1-histamine antagonist (Fadel *et al.*, 1990).

Airway mucosal wall thickness produced by inflammation and oedema can have substantial effects on airway function (Moreno *et al.*, 1986; Hogg *et al.*, 1987). The tracheobronchial circulation will have an important role in modulating these actions. However, the actions of PAF on airways blood flow has been little studied (Laitinen *et al.*, 1987) and its mode of action is unknown. PAF induces microvascular leakage in the airways which may be due to a direct rather than indirect action on the vasculature since in guinea-pigs it is independent of cyclo-oxygenase or lipoxygenase products (Evans *et al.*, 1987).

In sheep the blood supply to the cervical trachea can be isolated and perfused *in vivo* (Webber *et al.*, 1988; 1989; 1990). Here this preparation has been used to study the actions of PAF on the circulation and on tracheal smooth muscle. The role of the secondary release of other mediators by PAF was tested with the cyclo-oxygenase inhibitor, indomethacin, the leukotriene receptor antagonist, FPL55712 and the H_1- and H_2-antihistamines, mepyramine and cimetidine. The effects of the anti-asthma drug, nedocromil sodium, were also tested. The role of specific PAF receptors was examined by use of the PAF antagonist WEB 2086.

[1] Author for correspondence.

Methods

Experiments were performed on 12 female sheep (all approximately 1 year old and weighing 27–32 kg). All sheep were anaesthetized with sodium pentobarbitone (initially 20 mg kg^{-1}, i.v.). Additional anaesthetic was given as required to maintain surgical anaesthesia. One femoral artery was catheterized and connected to a pressure transducer (P23, Gould) for the measurement of systemic arterial pressure. An external jugular vein was also catheterized for administration of heparin, gallamine and supplemental doses of anaesthetic.

A low cervical tracheostomy was performed and a tracheal cannula inserted. All animals were paralysed with gallamine triethiodide (1 mg kg^{-1}) and ventilated with a tidal volume of 12–16 ml kg^{-1} at a constant rate of 28 breaths per min. Inspired air was supplemented with 100% oxygen (2–5 l min^{-1}). Anaesthetic was maintained during paralysis as previously described (Webber *et al.*, 1988).

Measurements of tracheal perfusion flow

The preparation of the tracheal arteries in sheep has been described previously (Webber *et al.*, 1988). The common carotid arteries were exposed on both sides of the trachea. In all the sheep, vessels supplying the trachea were predominantly from the left side. One or two arteries were isolated coming from the left common carotid artery in the middle of the neck. These generally divided into several branches going to trachea, skeletal muscle, oesophagus and glandular tissue. As far as possible, all branches which did not supply the trachea were tied off. The left carotid artery cranial to the isolated tracheal arteries was ligated so that blood perfused only the trachea. A square-wave electromagnetic flowmeter (1.6 mm internal diameter; Carolina Medical Electronics) was placed between two catheters inserted into the carotid artery

below the tracheal arteries which allowed perfusion to this segment to be measured. The occluded left carotid artery was by-passed from the right carotid artery with a plastic Y-tube connection to ensure an intact blood supply to the brain and a normal pressure in the carotid sinuses. Thus, perfusion of the cranial trachea was via an isolated segment of the left common carotid artery. Heparin (50,000 units i.v.) was administered before the perfusion was connected. Distribution of the perfusion was assessed by injecting Evans blue dye in 0.15 M NaCl (saline) into the catheter inserted below the tracheal arteries. The arteries perfused the trachea on both sides over a length of between eight and twelve cartilagenous rings; a small amount of dye was occasionally seen in adjacent tissues such as the oesophagus.

Measurement of tracheal smooth muscle tone

In six of the sheep, changes in tracheal smooth muscle tone were measured by recording changes in the external diameter of the cranial trachea (Webber *et al.*, 1988). A fixed bar was placed on one side of the trachea and a thin lever connected to a force-displacement transducer (FT03C, Grass) was gently placed on the other side with a micromanipulator. Changes in force were calibrated to represent displacement of the lever tip (range ± 1.6 mm) indicating a change in external tracheal diameter.

Administration of agonists

Injections of PAF, lyso-PAF and methacholine were given directly into the arterial input of the perfusion circuit supplying the vascular bed, in 0.1 or 0.2 ml of saline. Drugs were injected at intervals of at least 10 min, allowing for complete recovery from the previous injection. Doses of PAF (2–2000 pmol) were given to 7 sheep to establish a dose-response relationship; each sheep received between 3–7 different doses of agonist. PAF and lyso-PAF, the inactive precursor, were given separately to a further 5 sheep to establish if there were any non-specific effects of the drugs on the circulation.

Control injections of 0.1 and 0.2 ml saline were given into the perfusion circuit. These produced brief falls in perfusion flow followed by small increases; these effects have previously been shown to be artefactual due to injection pressure and transient reduction in the viscosity of the blood respectively (Salonen *et al.*, 1988). All these effects were transient and were taken into account in assessing the responses to the drugs, where peak changes usually occurred and were measured after the artefactual effects of the injection had passed.

Administration of inhibitors

The concentrations of inhibitors used were: indomethacin ($5\,mg\,kg^{-1}$, i.v., $n = 5$), FPL55712 ($2\,mg\,kg^{-1}$, i.v., $n = 5$), mepyramine maleate ($2\,mg\,kg^{-1}$, i.v., $n = 5$) combined with cimetidine ($5\,mg\,kg^{-1}$, i.v., $n = 5$), nedocromil sodium (1 mg, i.a., $n = 5$) and WEB 2086 ($200\,\mu g\,kg^{-1}$, i.v., $n = 4$).

In seven animals a single dose of PAF (between 100 and 1000 pmol) was chosen which produced approximately 70% of the maximum PAF-induced vasodilatation in each particular sheep. This dose was administered before and after each inhibitor. All the inhibitors except nedocromil sodium were administered intravenously 10–15 min before the test dose of PAF. Nedocromil sodium was administered intra-arterially in a 0.1 ml bolus 1 min before PAF. An average of 3–4 different inhibitors was tested in each sheep. The order of administration was random except for WEB 2086 which was always given as the final inhibitor.

Evaluation of results

The maximum change in each variable was measured for each intervention. In most sheep, PAF produced a simple increase in blood flow which returned to baseline within a few minutes. In three animals the response was more complex. Blood flow rose to a peak, fell towards baseline and then peaked a second time before finally returning to baseline. The magnitude of the fall was not consistent and in some interventions the fall was transiently below the initial baseline. For these results the larger of the two peaks was measured; this was generally the earlier of the two.

All results are given as the mean $\pm$ standard error of the mean (mean $\pm$ s.e.mean). For the vascular responses, results were expressed as changes in vascular resistance where vascular resistance was calculated by dividing mean systemic arterial blood pressure (MAP) by tracheal blood flow, measured at the same instant. The log dose-response curve was obtained by pooling the results from all experiments. The ED_{50} value (the estimated dose producing 50% of the maximum response of the agonist), the maximum responses and the associated 95% confidence interval were estimated by a computerized non-linear least squares estimate.

Other statistical comparisons were made by the Wilcoxon signed rank non-parametric test for paired data.

Drugs

PAF, methacholine chloride, indomethacin, mepyramine maleate and cimetidine were obtained from Sigma Chemicals; lyso-PAF from Bachem; sodium pentobarbitone (Sagatal) and gallamine triethiodide from May and Baker; heparin sodium from CP Pharmaceuticals; and Evans blue dye from Aldrich Chemical Corporation. FPL55712 (7-[3-(4-acetyl-3-hydroxy-2-propylphenoxy)-2-hydroxypropoxy]-4-oxo-8-propyl-4H-1-benzopyran-2-carboxylic acid) and nedocromil sodium were kindly donated by Fisons and WEB 2086 (3-(4-(2-chlorophenyl)-9-methyl-6H-thieno-(3,2-f) (1,2,4)-triazolo-(4,3-a)-(1,4)-diazepine-2-yl)-1-(4-morpholinyl)-1-propanone) by Pfizer.

Results

Vascular responses to PAF and lyso-PAF

The baseline values in the 12 sheep prior to any interventions were $5.3 \pm 0.6\,ml\,min^{-1}$ for tracheal blood flow, $27.0 \pm 2.3\,mmHg\,ml^{-1}\,min^{-1}$ for tracheal vascular resistance and 130 ± 5 mmHg for mean arterial blood pressure (MAP).

In 3 sheep, following injection of PAF, tracheal blood flow rose initially indicating a fall in vascular resistance. Blood flow then fell towards baseline, rose again to a second peak and returned to baseline; on occasion the intermediate fall was to below baseline indicating a vasoconstriction. In the remaining sheep, PAF produced a simple increase in blood flow that reached a maximum and fell towards baseline; an example of one such response is shown in Figure 1. The falls in vascular resistance produced with PAF (2–2000 pmol) were dose-dependent (Figure 2). The calculated ED_{50} value was 17 pmol (12–28 pmol, 95% confidence limits) and the maximum fall in vascular resistance was -41.6% (-38.5 to -44.7%). The maximum changes in vascular resistance occurred between 20

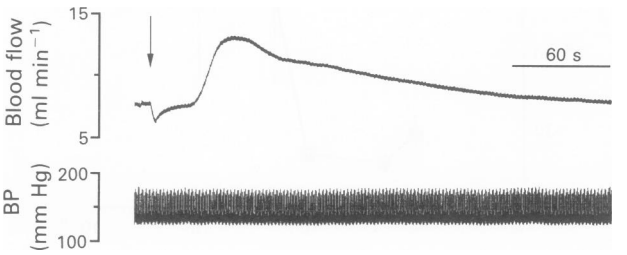


Figure 1 The effects of platelet activating factor (200 pmol at arrow) on tracheal blood flow and systemic arterial blood pressure (BP) in one sheep. Following a brief injection artefact the drug produced a marked increase in blood flow with no effect on BP.

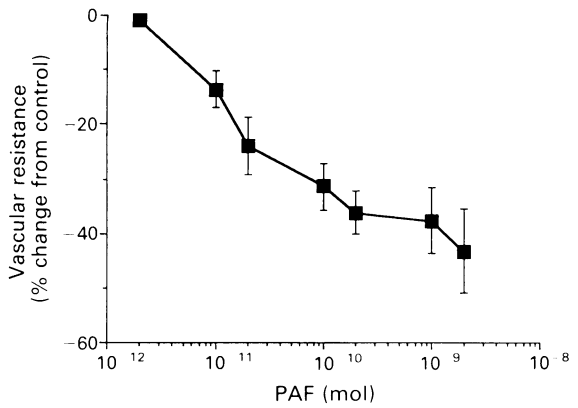


Figure 2 Dose-response curves showing the effects of platelet activating factor (PAF) on tracheal vascular resistance. Points are the means of 3–8 determinations in 7 sheep; the vertical lines represent s.e.mean.

and 84 s following injection. At the doses studied PAF had no systemic actions except at higher doses when on three occasions it produced a small (5–8%) and transient fall in MAP. The duration of each response was assessed by the time taken for the blood flow to return from the maximum to a value half way to the initial baseline value ($t_{0.5}$). The $t_{0.5}$ was weakly dose-related and ranged from 15 to 90 s (Figure 3).

In five separate sheep, PAF (200 pmol) produced a fall in vascular resistance of $-27.1 \pm 16.7\%$ while lyso-PAF (200 pmol) produced no significant change in vascular resistance ($-0.6 \pm 0.8\%$).

Actions on tracheal smooth muscle

PAF had no measurable effects on tracheal diameter at any dose in the six sheep where this was measured. In contrast methacholine (5 nmol) decreased tracheal diameter on 4 out of 5 occasions by -0.29 ± 0.19 mm ($n = 5$) indicating contraction of tracheal smooth muscle.

Effects of the inhibitors

Indomethacin was the only inhibitor to alter the baseline conditions; it produced a sustained increase in MAP ($36.8 \pm 5.2\%$) and in tracheal vascular resistance ($47.9 \pm 3.5\%$, Figure 4).

The fall in vascular resistance produced with a single dose of PAF was unchanged by nedocromil sodium, mepyramine and cimetidine, indomethacin and FPL55712 (Figure 5). The response was however substantially attenuated by WEB 2086 (before, $-40.8 \pm 4.2\%$; after, $-16.5 \pm 5.9\%$; Figure 5). The $t_{0.5}$ was not significantly altered by any of the inhibitors

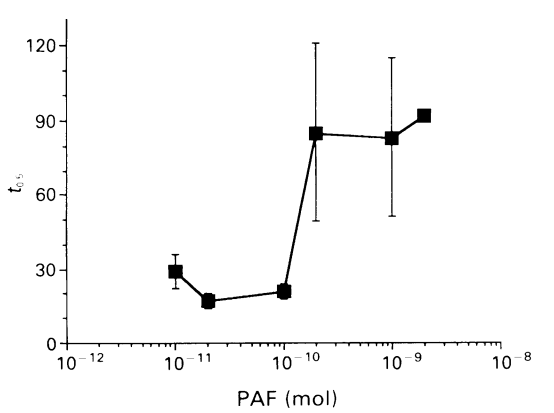


Figure 3 Curve showing the duration of the response ($t_{0.5}$) in tracheal vasculature produced by platelet activating factor (PAF); s.e.mean shown by vertical lines.

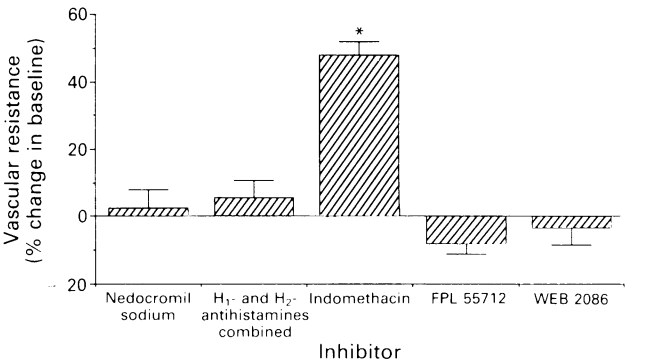


Figure 4 The effects of the inhibitors on baseline vascular resistance. Indomethacin was the only inhibitor that significantly changed the baseline vascular resistance (* $P > 0.05$).

(Figure 6). Analysis of the 'area under the curve' of the change in blood flow produced by PAF was also performed. WEB 2086 was the only inhibitor that significantly reduced the response assessed in this way ($P < 0.05$).

Discussion

The effects of a number of vasoactive agents have now been studied on the tracheal circulation of dogs and sheep. These include histamine, methacholine, 5-HT, peptides and prostaglandins (Laitinen *et al.*, 1987; Salonen *et al.*, 1988; Webber *et al.*, 1988; 1989; 1990; Corfield *et al.*, 1991). Here PAF has been shown to be one of the most potent vasodilators yet

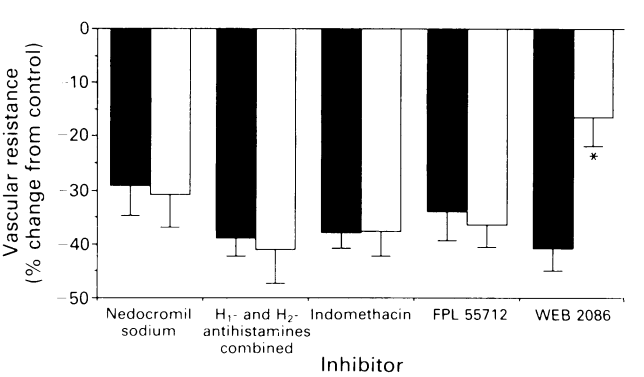


Figure 5 The change in tracheal vascular resistance produced by a dose of PAF before (solid columns) and after (open columns) five inhibitors. WEB 2086 was the only inhibitor that significantly reduced the response (* $P < 0.05$).

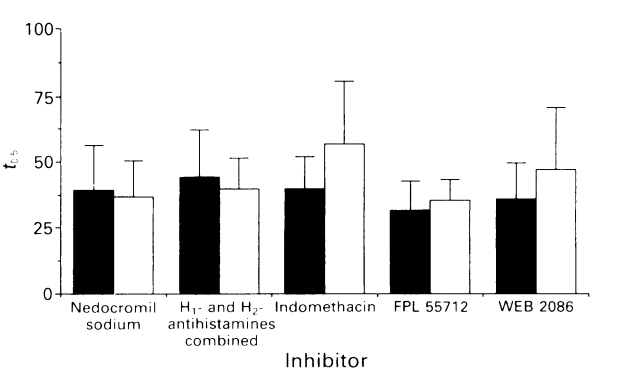


Figure 6 The duration of the PAF-induced vasodilatation ($t_{0.5}$) before (solid column) and after (open column) five inhibitors; vertical lines show s.e.mean.

studied in this system, second only to the other inflammatory mediator bradykinin which is also notable for its extremely long duration of action (Corfield *et al.*, 1991). Both drugs produce similar maximum falls in vascular resistance.

The other target tissue studied here was the tracheal smooth muscle; PAF had no action on this. However, in other preparations PAF contracts airways smooth muscle (Barnes *et al.*, 1988). In sheep, PAF increases airways resistance when instilled directly into the airway lumen, this effect being blocked both by a specific PAF antagonist and by nedocromil sodium (Soler *et al.*, 1990). PAF may have different effects on tracheal and bronchial smooth muscle or the intraluminal action may be outside the dose-range studied here. Further, the specific effects may depend on the route of administration.

The actions of PAF on the tracheal circulation may be produced by direct effects on the vascular endothelium and smooth muscle or indirectly through the release of further mediators from other target cells. PAF releases a variety of mediators including prostaglandins, leukotrienes (Barnes *et al.*, 1988; Spina *et al.*, 1989) and possibly histamine (Fadel *et al.*, 1990; Misawa & Huang, 1990). If PAF were to release these mediators in the airways they could produce a subsequent vasodilatation at the tracheal circulation. In the present study, the mechanism of the PAF-induced vasodilatation was tested by the administration of a number of potential inhibitors. The change in vascular resistance produced with PAF was not affected by a combination of H_1- and H_2-antihistamines, cyclo-oxygenase inhibition, lipoxygenase receptor blockade or the anti-asthma agent, nedocromil sodium. Of these, indomethacin, the cyclo-oxygenase inhibitor, was the only agent to alter baseline conditions and this action is therefore, perhaps, harder to interpret. However, the percentage fall in vascular resistance produced with methacholine is the same before and after indomethacin when there are similar changes in baseline conditions (Corfield *et al.*, 1991). Therefore it appears that indomethacin does not affect the PAF-induced vasodilatation. The doses of inhibitors administered here have been used successfully in the same preparation; mepyramine alone will inhibit the responses to exogenous histamine (Webber *et al.*, 1988); cimetidine is without effect indicating this action to be exclusively through H_1-histamine receptors. The vasodilatation produced with *Ascaris suum* antigen is largely attenuated by a combination of indomethacin and FPL55712 (Webber *et al.*, 1989) and is reduced slightly by intra-arterial nedocromil sodium (Corfield *et al.*, 1990b). Therefore it is unlikely that the PAF-induced vasodilatation here is mediated by these other mediators or, by implication, that the vasodilatation produced by *Ascaris suum* (Webber *et al.*, 1989) is mediated by PAF. Although nedocromil sodium was without effect, it reduces PAF-induced airway hyperresponsiveness (Soler *et al.*, 1990).

The vasodilatation was substantially attenuated by WEB 2086, a specific PAF antagonist. Lyso-PAF, the inactive precursor of PAF with the same detergent properties, was inactive. It is clear therefore that the vasodilatation is receptor mediated and not due to a nonspecific detergent action. PAF can dilate other vascular beds without the release of further mediators such as prostaglandins (Braquet *et al.*, 1987) and may act directly through the release of endothelium-derived relaxing factor (Kamata *et al.*, 1989).

In a few of the sheep, PAF both constricted and dilated the vascular bed. Unfortunately the vasoconstrictor action was inconsistent and possibly masked by the vasodilatation and could not be studied further. This dual action of a single mediator on the sheep tracheal circulation has also been seen for histamine (Webber *et al.*, 1988) and 5-HT (Webber *et al.*, 1990) although the mechanisms are not always clear. The vasoconstrictions seen here could be produced by the release of 5-HT from platelets by PAF.

In airways inflammation, hyperaemia will result from the actions of a number of mediators. This will affect airways function by increasing mucosal thickness, directly increasing the size of the blood volume compartment (Laitinen *et al.*, 1986; Corfield *et al.*, 1990a) and indirectly influencing the magnitude of oedema formation in the tissue. Tissue oedema and plasma exudation into the airway lumen will depend on the degree of vascular leakage and on blood flow to the tissue. A mediator that both increases blood flow and enhances leakage will have greater effects than an agent producing only one; PAF as well as being a potent vasodilator, produces vascular leakage in the airways (Evans *et al.*, 1987). In guinea-pigs, PAF-induced leakage, like the vasodilatation seen here, is not mediated by prostaglandins (Evans *et al.*, 1987). Interestingly, plasma leakage produced by bradykinin is, at least in part, mediated by PAF (Rogers *et al.*, 1990) while the plasma leakage produced with ovalbumin in sensitized guinea-pigs is not mediated by PAF (Evans *et al.*, 1988). The vascular actions of PAF may contribute to the nonspecific hyperresponsiveness produced by the mediator. Increasing blood flow to target tissues may enhance inflammatory cell infiltration; increasing blood volume and tissue oedema in the airway mucosa will enlarge the changes in airways resistance produced with smooth muscle contraction (Moreno *et al.*, 1986; Hogg *et al.*, 1987).

In conclusion, PAF in this model has potent actions on the tracheal circulation but no action on tracheal smooth muscle. The vascular action is predominantly a vasodilatation; this is mediated via specific PAF receptors and does not involve the secondary release of histamine, prostaglandins or leukotrienes. The response is not attenuated by nedocromil sodium. The actions of PAF on the vasculature are of particular interest because of the interaction between blood flow and plasma leakage which influences oedema formation in the airways.

D.R.C. is supported by the National Asthma Campaign. We wish to thank Amanda Skasick for technical assistance.

References

BARNES, P.J., CHUNG, K.F. & PAGE, C.P. (1988). Inflammatory mediators and asthma. *Pharmacol. Rev.*, **40**, 49–84.

BRAQUET, P., TOUQUI, L., SHEN, T.Y. & VARGAFTIG., B.B. (1987). Perspectives in platelet-activating factor research. *Pharmacol. Rev.*, **39**, 97–145.

CORFIELD, D.R., HANAFI, Z., WEBBER, S.E. & WIDDICOMBE, J.G. (1990a). Changing blood flow alters tracheal mucosal thickness in anaesthetized sheep. *J. Physiol.*, **430**, 96P.

CORFIELD, D.R., WEBBER, S.E. & WIDDICOMBE, J.G. (1990b). The effects of nedocromil sodium on the actions of *Ascaris Suum* and PAF on the tracheal circulation. *Eur. Respir. J.*, **3**, suppl 10, 327.

CORFIELD, D.R., WEBBER, S.E., HANAFI, Z. & WIDDICOMBE, J.G. (1991). The actions of bradykinin and lys-bradykinin on tracheal blood flow and smooth muscle in anaesthetized sheep. *Pulmonary Pharmacol.*, **4**, 85–90.

CUSS, F.M., DIXON, C.M.S. & BARNES, P. (1986). Effects of inhaled platelet activation factor on pulmonary function and bronchial responsiveness in man. *Lancet*, **ii**, 189–192.

EVANS, T.W., CHUNG, K.F., ROGERS, D.F. & BARNES, P.J. (1987). Effect of platelet-activating factor on airway vascular permeability: possible mechanisms. *J. Appl. Physiol.*, **63**, 479–484.

EVANS, T.W., DENT, G., ROGERS, D.F., AURSUDKIJ, B., CHUNG, K.F. & BARNES, P.J. (1988). Effect of a Paf antagonist, WEB 2086, on airway microvascular leakage in the guinea-pig and platelet aggregation in man. *Br. J. Pharmacol.*, **94**, 164–168.

FADEL, R., DAVID, B., HERPIN-RICHARD, N., BORGNON, A., RASSEMONT, R. & RIHOUX, J.P. (1990). *In vivo* effects of cetirizine on cutaneous reactivity and eosinophil migration induced by platelet-activation factor (PAF-acether) in man. *J. Allergy Clin. Immunol.*, **86**, 314–320.

HOGG, J.C., PARÉ, P.D. & MORENO, R. (1987). The effects of submucosal edema on airways resistance. *Am. Rev. Respir. Dis.*, **135**, S54–S56.

KAMATA, K., MORI, T., SHIGENOBU, K. & KASUYA, Y. (1989). Endothelium-dependent vasodilator effects of platelet activating factor on rat resistance vessels. *Br. J. Pharmacol.*, **98**, 1360–1364.

LAITINEN, L.A., ROBINSON, N.P., LAITINEN, A. & WIDDICOMBE, J.G. (1986). Relationship between tracheal mucosal thickness and vascular resistance in dogs. *J. Appl. Physiol.*, **61**, 2186–2193.

LAITINEN, L.A., LAITINEN, M.A. & WIDDICOMBE, J.G. (1987). Dose-related effects of pharmacological mediators on tracheal vascular resistance in dogs. *Br. J. Pharmacol.*, **92**, 703–709.

LANG, M., HANSEN, D. & HAHN, H.L. (1987). The effects of the PAF-antagonist CV-3988 on PAF induced changes in mucus secretion and in respiratory and circulatory variables in ferrets. *Agents Actions*, Suppl. 21, 245–252.

MISAWA, M. & HUANG, S.C. (1990). The effects of platelet-activating factor on histamine release from rat peritoneal mast cells. *Jpn. J. Pharmacol.*, **53**, 75–80.

MORENO, R.H., HOGG, J.C. & PARÉ, P.D. (1986). Mechanics of airway narrowing. *Am. Rev. Respir. Dis.*, **133**, 1171–1180.

MORLEY, J., SANJAR, S. & PAGE, C.P. (1984). The platelet in asthma. *Lancet*, **ii**, 1142–1144.

ROGERS, D.F., DIJK, S. & BARNES, P.J. (1990). Bradykinin-induced plasma exudation in guinea-pig airways: involvement of platelet activating factor. *Br. J. Pharmacol.*, **101**, 739–745.

SALONEN, R.O., WEBBER, S.E. & WIDDICOMBE, J.G. (1988). Effects of neuropeptides and capsaicin on the canine tracheal vasculature *in vivo*. *Br. J. Pharmacol.*, **95**, 1262–1270.

SOLER, M., MANSOUR, E., FERNANDEZ, A., D'BROT, J., AHMED, T. & ABRAHAM, W.M. (1990). PAF-induced airway responses in sheep: effects of a PAF antagonist and nedocromil sodium. *J. Allergy Clin. Immunol.*, **85**, 661–668.

SPINA, D., COYLE, A.J. & PAGE, C.P. (1989). The role of platelet activating factor in allergic inflammation. *Pulmonary Pharmacol.*, **2**, 13–19.

WEBBER, S.E., SALONEN, R.O., DEFFEBACH, M.E. & WIDDICOMBE, J.G. (1989). Effects of antigen on tracheal circulation and smooth muscle in sheep of different ages. *J. Appl. Physiol.*, **67**, 1256–1264.

WEBBER, S.E., SALONEN, R.O. & WIDDICOMBE, J.G. (1988). H_1- and H_2-receptor characterization in the tracheal circulation of sheep. *Br. J. Pharmacol.*, **95**, 551–561.

WEBBER, S.E., SALONEN, R.O. & WIDDICOMBE, J.G. (1990). Receptors mediating the effects of 5-hydroxytryptamine on the tracheal vasculature and smooth muscle of sheep. *Br. J. Pharmacol.*, **99**, 21–26.

(Received November 27, 1990
Revised February 11, 1991
Accepted February 19, 1991)

Br. J. Pharmacol. (1991), **103**, 1745–1751 © Macmillan Press Ltd, 1991

Inhibition by cations of antagonist binding to histamine H_1-receptors: differential effect of sodium ions on the binding of two radioligands

[1]J.M. Treherne, J.S. Stern, W.J. Flack & [2]J.M. Young

Department of Pharmacology, University of Cambridge, Tennis Court Road, Cambridge CB2 1QJ

1 Measurements have been made of the inhibition by mono- and divalent cations of the binding of [^{3}H]-(+)-N-methyl-4-methyldiphenhydramine ([^{3}H]-QMDP) to histamine H_1-receptors in homogenates of guinea-pig cerebellum.

2 The binding of [^{3}H]-QMDP was inhibited by monovalent cations with an order of potency $Li^+ = Na^+ > K^+ > Cs^+ = Rb^+$. The IC_{50} for Li^+ was 39 mM, but that for K^+ was 132 mM. Hill coefficients for inhibition curves for Li^+ and Na^+ were < 1.

3 Divalent cations also inhibited the binding of [^{3}H]-QMDP. The most potent cations examined were Hg^{2+}, Cd^{2+} and Zn^{2+}, with IC_{50} values of 5, 17 and 41 μM, respectively. Ca^{2+} and Mg^{2+} were relatively weak inhibitors (IC_{50} 12 and 34 mM, respectively). The potency of Ni^{2+}, Co^{2+} and Mn^{2+} was intermediate between these groups. Hill coefficients for inhibition curves for Hg^{2+}, Cd^{2+} and Zn^{2+} were > 1, but Hill coefficients for the other cations were < 1.

4 Both mono- and divalent cations also inhibited the binding of [^{3}H]-mepyramine. The divalent cations were approximately equipotent in inhibiting the binding of [^{3}H]-QMDP and [^{3}H]-mepyramine. The same was true for Li^+. However, Na^+ was markedly more effective against [^{3}H]-QMDP binding than against the binding of [^{3}H]-mepyramine.

5 The effect of 40 mM Li^+ on the parameters of binding of [^{3}H]-mepyramine was to increase the best-fit value of the concentration giving half-maximal binding EC_{50}, by approximately 2 fold without having any significant effect on the maximum amount of binding. Cd^{2+} (15 μM) caused both an increase in EC_{50} and a decrease in B_{max} (32 ± 4% inhibition). Na^+, 100 mM, had no significant effect on either EC_{50} or B_{max} for [^{3}H]-mepyramine binding.

Keywords: Histamine H_1-receptors; [^{3}H]-(+)-N-methyl-4-methyldiphenhydramine; [^{3}H]-mepyramine; mercury; cadmium; zinc; nickel; cobalt; sodium; lithium

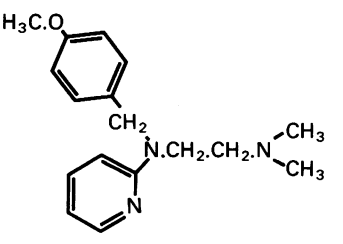
Introduction

The binding of histamine and other agonists to histamine H_1-receptors is inhibited by Li^+ and Na^+, and potentiated by Mn^{2+} and Mg^{2+} (Chang & Snyder, 1980; Toll & Snyder, 1982). In contrast, the binding of [^{3}H]-mepyramine, an antagonist, is reported to be relatively unaffected by these cations (Chang & Snyder, 1980). However, this does not appear to be a general rule for H_1-antagonists, since in the course of an investigation of the binding properties of a new quaternary radioligand for the H_1-receptor, [^{3}H]-(+)-N-methyl-4-methyldiphenhydramine ([^{3}H]-QMDP), we observed that the receptor binding of [^{3}H]-QMDP was reduced by 100 mM NaCl (Treherne & Young, 1988a). We describe here the results of a more extensive study of the effect of cations on the binding of [^{3}H]-QMDP and [^{3}H]-mepyramine. Both of these compounds have the 'classical' antihistamine structure (Figure 1), are a similar size and have a similar affinity for the H_1-receptor, K_d *circa* 1 nM (Treherne & Young, 1988a). We show that the binding of both [^{3}H]-QMDP and [^{3}H]-mepyramine is inhibited by a range of mono- and divalent cations, but that Na^+ distinguishes between the binding of the two radioligands. Some of these results have been presented in preliminary form to the British Pharmacological Society (Treherne *et al.*, 1989).

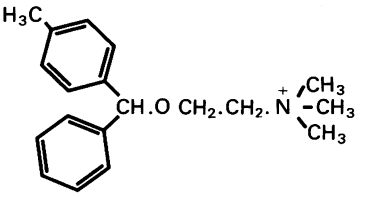
Methods

Preparation of cerebellar membranes

Cerebella from Dunkin-Hartley strain guinea-pigs (males, 250–600 g; Tucks, Battlebridge, Essex) were washed in 50 mM 2-amino-2-hydroxymethylpropan-1,3-diol hydrochloride (Tris-HCl) buffer, pH 7.5, containing 1 mM ethylenediaminetetracetic acid (EDTA), and then homogenized in 10 volumes of the same buffer in a Teflon-glass homogenizer with a motor-driven pestle (3,000 r.p.m., 5 or 6 up and down strokes). The homogenate was centrifuged at 17,000 *g* for 30 min and the pellet then resuspended in Tris buffer, but without EDTA, and centrifuged again at 17,000 *g* for 30 min. The resulting pellet was suspended in 50 mM Tris buffer, pH 7.5, to give a final protein concentration of 6–10 mg ml^{-1} and



Mepyramine



QMDP

Figure 1 Structures of mepyramine and (+)-N-methyl-4-methyldiphenhydramine (QMDP).

[1] Present address: Abteilung Pharmakologie, Biozentrum der Universität Basel, Klingelbergstrasse 70, CH-4056 Basel, Switzerland.
[2] Author for correspondence.

was stored at −20°C until required for use. Protein was determined essentially as described by Lowry et al. (1951) with bovine serum albumin used as a standard.

Measurement of the binding of [^{3}H]-mepyramine and [^{3}H]-QMDP

Incubations in 50 mM Tris-HCl buffer, pH 7.5, contained [^{3}H]-mepyramine or [^{3}H]-QMDP (both usually in the concentration range 0.4–0.7 nM for inhibition curves), metal salt (where appropriate) and homogenate (0.19–0.27 mg protein) in a total volume of 1.00–1.11 ml (4–5 replicates at each inhibitor concentration, 8–16 replicates in the absence of metal ions, spread through the experiment). A set of incubations with 100 mM NaCl was included occasionally in experiments with other metal salts in order to check the consistency of the effects of ions. Non-H_1-receptor binding (non-specific binding) was determined as the binding insensitive to inhibition by 1 μM temelastine, which has a low affinity for secondary, non-H_1-receptor, binding sites for [^{3}H]-QMDP (Treherne & Young, 1988a). The dissociation constant for temelastine binding to the H_1-receptor in 50 mM Tris-buffer, determined in one experiment from inhibition of [^{3}H]-mepyramine binding, was 0.70 ± 0.16 nM, similar to the values 0.63 ± 0.04 and 0.83 ± 0.07 nM determined in 50 mM Na-K phosphate buffer from inhibition of the binding of [^{3}H]-mepyramine and [^{3}H]-QMDP, respectively (Treherne & Young, 1988a). The extent of the non-specific binding at 0.4–0.6 nM ^{3}H-ligand in 50 mM Tris-HCl buffer was usually 25–30% of total binding with [^{3}H]-QMDP and 9–16% with [^{3}H]-mepyramine. The temelastine-insensitive binding was always measured at each metal ion concentration. Equilibration was for 60 min at 30°C and was terminated by filtration through Whatman GF/B glass fibre paper, pre-soaked in 0.3% (w/v) polyethylenimine for 3–5 h, using a Brandel (Gaithersburg, Md, U.S.A.) cell harvester. The filters were washed with ice-cold buffer and then transferred to scintillation insert vials containing 4.8 ml scintillator and allowed to stand overnight before determination of tritium by liquid scintillation counting. The scintillator was Quickszint 212 (Zinnser)/water, 95:5 (v/v) or Emulsifier-Safe (Packard).

Analysis of data

To obtain unbiased estimates ± estimated s.e. of IC_{50}, the concentration of cation producing 50% inhibition of the temelastine-sensitive binding of [^{3}H]-QMDP, and n, the Hill coefficient, the temelastine-sensitive binding of the radioligand was assumed to follow a Hill equation (logistic equation), and the inhibition data were fitted to the equation: Percentage of uninhibited binding = $100/((M/IC_{50})^n + 1)$, where M is the concentration of cation. The fitting was carried out using the Harwell Library non-linear regression routine VB01A. All points were weighted according to the reciprocal of the variance associated with them.

In experiments in which the effect of metal cations on the parameters of [^{3}H]-mepyramine binding were measured, curves of the specific binding both in the presence and in the absence of a fixed concentration of the ion were always determined in the same experiment. The curves were first fitted to a Hill equation: $B = B_{max} \cdot C^n/(C^n + EC_{50}^n)$, where B is the amount of specific binding of [^{3}H]-mepyramine, B_{max} the maximum binding capacity, C the concentration of [^{3}H]-mepyramine, EC_{50}, the concentration of [^{3}H]-mepyramine giving half-maximal binding and n the Hill coefficient, in order to check that the Hill coefficients did not differ significantly from unity. The curves in the presence and absence of the metal ion were then fitted simultaneously to the Hill equation without any constraints and with n constrained to be the same for both curves (see Crawford & Young, 1990, for details), in order to test for any significant difference between the values of n in the presence and absence of the metal cation. One experiment in which there was a significant difference in the Hill coefficient was discarded (1 out of 17 experiments). Two further experiments in which n was closely similar for the two curves, but significantly less than unity, were also discarded, although the ratios of EC_{50} and B_{max} (both for $CdCl_2$) were in the range of the values given in Table 2. Best-fit values of EC_{50} and B_{max} for the remaining curves were then obtained by fitting each curve to an hyperbola: $B = B_{max} \cdot C/(C + EC_{50})$. In the absence of inhibitors, EC_{50} is equivalent to the dissociation constant, K_d.

Drugs

[^{3}H]-mepyramine (26 Ci mmol^{-1}) was obtained from Amersham International. [^{3}H]-QMDP was synthesized and purified as described previously (Treherne & Young, 1988a). Metal ion salts were all analar grade and all were chloride salts, except for zinc, which was the sulphate. Magnesium chloride was dried *in vacuo* before use. Temelastine was a kind gift from Smith, Kline & French Research Ltd.

Results

Inhibition of [^{3}H]-QMDP binding by monovalent cations

NaCl inhibited both the temelastine-insensitive (non-specific) and total binding of [^{3}H]-QMDP to cerebellar membranes, measured in 50 mM Tris-HCl buffer, but with a greater effect on the total binding (Figure 2), in accord with earlier observations of the effect on the binding of [^{3}H]-QMDP in Na-K phosphate buffer of the addition of further NaCl (Treherne & Young, 1988a). The greater effect of NaCl on the total binding indicates that the temelastine-sensitive component (H_1-receptor binding), the difference between the two curves, is also inhibited. A curve of the inhibition by NaCl of the H_1-receptor binding component, constructed from the combined data from 8 experiments, is shown in Figure 3.

The temelastine-sensitive binding of [^{3}H]-QMDP was also inhibited by other monovalent ions (Figure 3). LiCl was practically equipotent with NaCl, but KCl was much less effective, as was CsCl and (not shown) RbCl. Unbiased estimates of the values of IC_{50} and the Hill coefficient, obtained by fitting the curves assuming that the binding follows a Hill equation, are set out in Table 1. For both LiCl and NaCl the Hill coefficients were significantly less than unity. The difference in potency of the metal chlorides indicates that the inhibition is not just due to an increase in the ionic strength of the medium

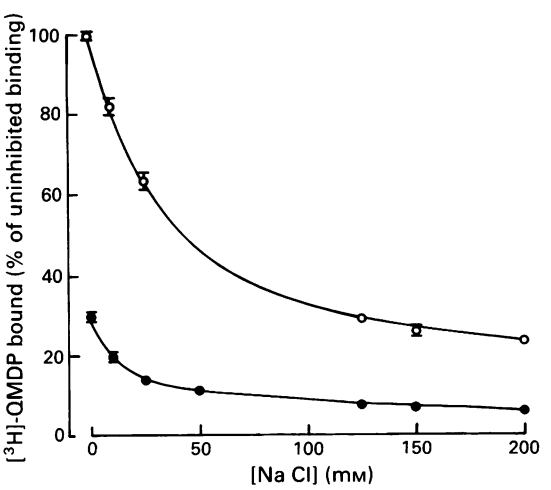


Figure 2 Inhibition by NaCl of the total and non-specific binding of 0.52 nM [^{3}H]-(+)-N-methyl-4-methyldiphenhydramine ([^{3}H]-QMDP). Each point is the mean of 5 replicate determinations from a single experiment; vertical bars show s.e.mean. The experiment was repeated 8 times with similar results. The lines through the points have been drawn by inspection. (○) Total binding of [^{3}H]-QMDP; (●) binding in the presence of 1 μM temelastine.

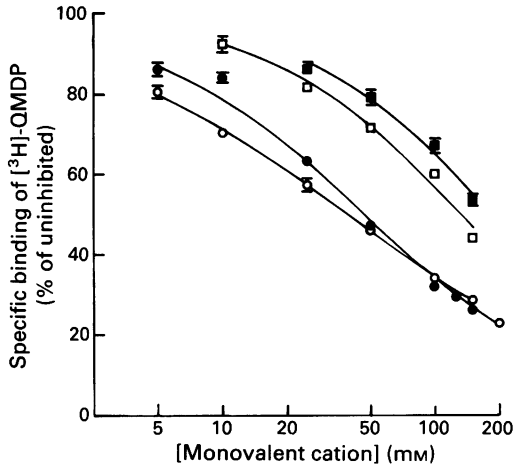


Figure 3 Inhibition of [^{3}H]-(+)-N-methyl-4-methyldiphenhydramine ([^{3}H]-QMDP) binding to the histamine H_1-receptor by monovalent cations. Points are the difference between the binding of 0.39–0.71 nM [^{3}H]-QMDP in the absence and presence of 1 μM temelastine and are the combined values (weighted means with s.e.mean shown by vertical bars) from 2 (CsCl), 4 (LiCl), 5 (KCl) or 8 (NaCl) experiments. The position of the inhibition curve for RbCl was similar to that for CsCl. The lines drawn were obtained by fitting the data to a Hill equation (see Methods). Best-fit values of IC_{50} are given in Table 1. (○) LiCl; (●) NaCl; (□) KCl; (■) CsCl.

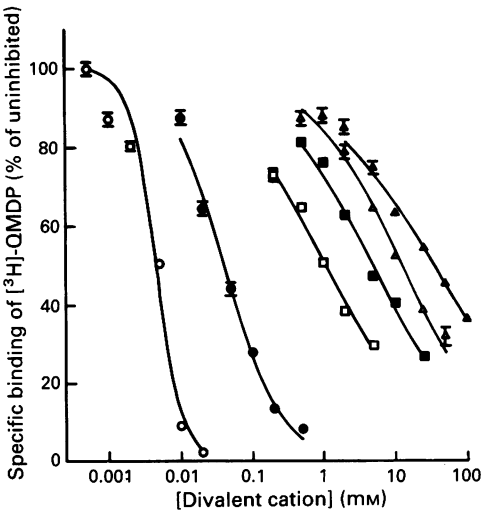


Figure 4 Inhibition of [^{3}H]-(+)-N-methyl-4-methyldiphenhydramine ([^{3}H]-QMDP) binding to the histamine H_1-receptor by divalent cations. Points are the difference between the binding of 0.37–0.70 nM [^{3}H]-QMDP in the absence and presence of 1 μM temelastine and are the combined values (weighted means with s.e.mean shown by vertical bars) from 4 ($MgCl_2$), 5 ($CaCl_2$) or 6 ($HgCl_2$, $MnCl_2$ $NiCl_2$, $ZnSO_4$) experiments. The lines drawn were obtained by fitting the data to a Hill equation (see Methods). Best-fit values of IC_{50} are given in Table 1. Curves for $CdCl_2$ and $CoCl_2$ have been omitted for clarity. The curve for $CdCl_2$ is shown in Figure 5. (○) $HgCl_2$; (●) $ZnSO_4$; (□) $NiCl_2$; (■) $MnCl_2$; (△) $CaCl_2$; (▲) $MgCl_2$.

and makes it probable that it is largely or wholly a property of the cation. Direct comparison in 3 experiments of the inhibitory effects of NaCl, Na_2SO_4 and $NaNO_3$, equimolar with respect to Na^+, failed to show any consistent difference between the different salts.

The temelastine-insensitive binding of [^{3}H]-QMDP was inhibited by Li^+, K^+, Cs^+ and Rb^+ in the same way as by Na^+ (cf. Figure 2) and with a similar potency. The initial drop in the non-specific binding may represent inhibition by the monovalent cations (IC_{50} 15–30 mM) of a medium-affinity, temelastine-insensitive binding site for [^{3}H]-QMDP (Treherne & Young, 1988a), since this component was not apparent in experiments with [^{3}H]-mepyramine.

Table 1 IC_{50} values and Hill coefficients for inhibition of [^{3}H]-(+)-N-methyl-4-methyldiphenhydramine ([^{3}H]-QMDP) binding by mono- and divalent cations

Inhibitor	IC_{50} (μM)	n_H
$HgCl_2$	5 ± 1	2.38 ± 0.43
$CdCl_2$	14 ± 3	0.96 ± 0.05
$ZnSO_4$	41 ± 3	1.09 ± 0.13
$NiCl_2$	1,100 ± 90	0.61 ± 0.05
$CoCl_2$	1,900 ± 200	0.54 ± 0.04
$MnCl_2$	5,000 ± 200	0.63 ± 0.04
$CaCl_2$	12,400 ± 600	0.67 ± 0.03
$MgCl_2$	33,800 ± 2,400	0.52 ± 0.04
LiCl	39,000 ± 800	0.68 ± 0.01
NaCl	46,900 ± 2,100	0.86 ± 0.02
KCl	132,000 ± 11,000	0.97 ± 0.10
CsCl	>150,000	
RbCl	>150,000	

Values of IC_{50}, the concentration of metal salt producing 50% inhibition of the binding of [^{3}H]-QMDP sensitive to 1 μM temelastine, and n_H, the Hill coefficient, ± estimated s.e., were obtained by fitting inhibition curves derived from the combined data from 3–6 experiments with each inhibitor (cf. Figures 3, 4 and 5) to a Hill equation (see Methods). The concentration of [^{3}H]-QMDP present was normally 0.4–0.6 nM.

Inhibition of [^{3}H]-QMDP binding by divalent cations

The conclusion that the inhibition of [^{3}H]-QMDP binding is largely due to the cation was strengthened by the wide variation in potency of a series of divalent ions (Figure 4). $HgCl_2$ was a highly potent inhibitor of the temelastine-sensitive binding of [^{3}H]-QMDP, with an IC_{50} of 5 μM, whereas $CaCl_2$ and $MgCl_2$ were much less potent, with IC_{50} values of 13 and 37 mM, respectively (Table 1). The order of potency was $Hg^{2+} > Cd^{2+} > Zn^{2+} > Ni^{2+} > Co^{2+} > Mn^{2+} > Ca^{2+} > Mg^{2+}$. All of the divalent cation salts examined were chlorides, except for Zn^{2+}, which was the sulphate. The difference in the slopes of the inhibition curves for the potent and weaker divalent cations, evident in Figure 4, is reflected in the best-fit values of the Hill coefficients (Table 2).

The temelastine-insensitive, non-specific, binding of [^{3}H]-QMDP was also inhibited by the divalent cations. As with the monovalent ions, there appeared to be an initial more rapid decline in the temelastine-insensitive binding, but the IC_{50} for this component, where the concentrations of the ions were high enough for it to be defined, varied from approximately 0.1 mM (Zn^{2+}) to approximately 3 mM (Mg^{2+}).

Comparison of the effects of ions on the binding of [^{3}H]-QMDP and [^{3}H]-mepyramine

The divalent ions were effective inhibitors of the binding of [^{3}H]-mepyramine as well as that of [^{3}H]-QMDP. The effect of Cd^{2+} and Ca^{2+} on the temelastine-sensitive binding of [^{3}H]-QMDP and [^{3}H]-mepyramine is shown in Figure 5. The other divalent ions (except Co^{2+}, which was not tested) were similarly practically equipotent against the two ^{3}H-ligands, the biggest difference being with Ni^{2+}, which was 2 fold more potent in inhibiting the binding of [^{3}H]-QMDP than that of [^{3}H]-mepyramine.

Of the monovalent cations, Li^+ was virtually equipotent in inhibiting the binding of [^{3}H]-QMDP and [^{3}H]-mepyramine (Figure 6a). However, Na^+, which was practically equipotent with Li^+ in inhibiting the binding of [^{3}H]-QMDP (Figure 3), was strikingly more effective in inhibiting the binding of [^{3}H]-QMDP than that of [^{3}H]-mepyramine (Figure 6b). The mean

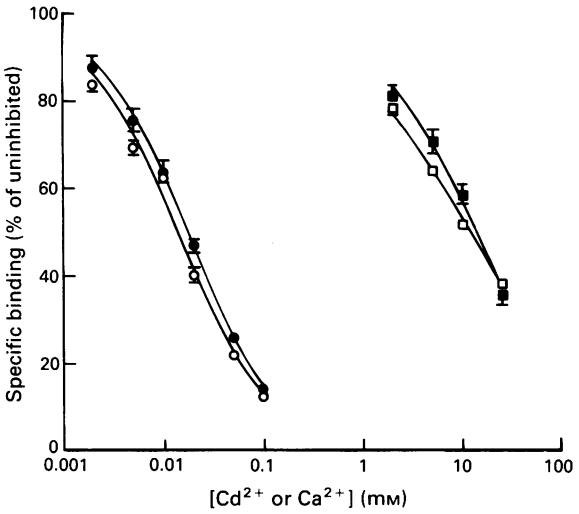


Figure 5 Comparison of the effect of Cd^{2+} and Ca^{2+} on the binding of [^{3}H]-(+)-N-methyl-4-methyldiphenhydramine ([^{3}H]-QMDP) and [^{3}H]-mepyramine to the histamine H_1-receptor. Points are the difference in the binding of 0.53–0.72 nM [^{3}H]-QMDP or 0.36–0.80 nM [^{3}H]-mepyramine in the absence and presence of 1 μM temelastine and are the combined values (weighted means with s.e.mean shown by vertical bars) from 4–5 experiments with [^{3}H]-QMDP (○, □) and 2–3 experiments with [^{3}H]-mepyramine (●, ■). The lines drawn were obtained by fitting the data to a Hill equation (see Methods). (○, ●) $CdCl_2$; (□, ■) $CaCl_2$.

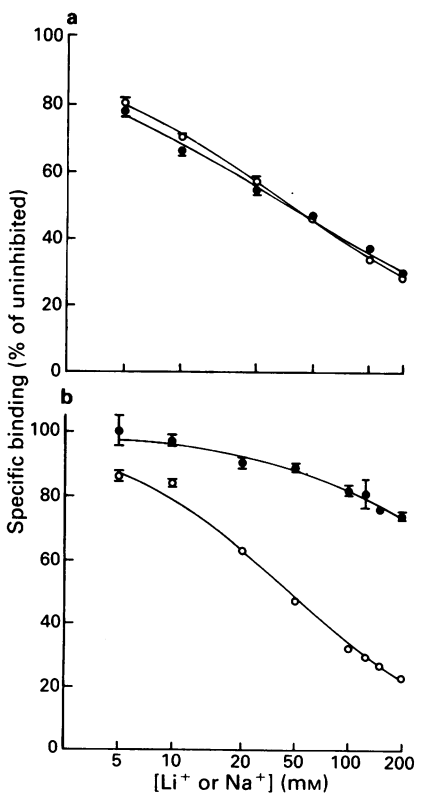


Figure 6 Comparison of the effect of LiCl (a) and NaCl (b) on the binding of [^{3}H]-(+)-N-methyl-4-methyldiphenhydramine ([^{3}H]-QMDP) and [^{3}H]-mepyramine to the histamine H_1-receptor. Points are the difference in the binding of the ^{3}H-ligand in the absence and presence of 1 μM temelastine. The lines drawn were obtained by fitting the data to a Hill equation (see Methods). (a) LiCl: combined data (weighted means with s.e.mean shown by vertical bars) from 4 experiments with 0.57–0.71 nM [^{3}H]-QMDP (○) and 3 experiments with 0.42–0.69 nM [^{3}H]-mepyramine (●). (b) NaCl: combined data (weighted mean with s.e.mean shown by vertical bars) from 8 experiments with 0.39–0.67 nM [^{3}H]-QMDP (○) and 4 experiments with 0.34–0.69 nM [^{3}H]-mepyramine (●).

effect of 100 mM Na^+ was 69 ± 1% inhibition of the binding of [^{3}H]-QMDP (25 measurements) and 13 ± 2% inhibition of the binding of [^{3}H]-mepyramine (13). K^+, a weak inhibitor of [^{3}H]-QMDP binding (Figure 3), was slightly less effective against [^{3}H]-mepyramine, but the difference was comparatively small (28 ± 1 (5 measurements) and 19 ± 1% (3) inhibition by 50 mM K^+ of [^{3}H]-QMDP and [^{3}H]-mepyramine binding, respectively, and 40 ± 1 (4) and 35 ± 3% (3) inhibition by 100 mM K^+).

The selective action of Na^+ appears to be related to changes in [^{3}H]-QMDP or [^{3}H]-mepyramine binding, rather than to an effect on the binding of 1 μM temelastine, which was used to define H_1-receptor binding. In two experiments a direct comparison was made of the effect of 100 mM Li^+ and 100 mM Na^+ on the level of the temelastine-insensitive binding of both [^{3}H]-QMDP and [^{3}H]-mepyramine. In both experiments the levels of binding were similar for a given radioligand, consistent with the lack of any selective effect of Na^+ on temelastine binding. This is in accord with the similar dissociation constants determined for temelastine in 50 mM Tris and 50 mM Na-K phosphate buffers (see Methods).

Effect of Cd^{2+}, Li^+ and Na^+ on the parameters of [^{3}H]-mepyramine binding

As a first step towards investigating the mechanism of the inhibitory action of the cations, measurements were made of the effect on the parameters of [^{3}H]-mepyramine binding of Cd^{2+}, as a representative potent divalent cation, Li^+, which does not distinguish [^{3}H]-QMDP and [^{3}H]-mepyramine, and Na^+, which gives only a very modest inhibition of the binding of [^{3}H]-mepyramine. The concentrations of Cd^{2+} and Li^+ chosen, 15 μM and 40 mM, were those which gave approximately 50% inhibition in the inhibition experiments (Figures 5 and 6a). The effect of Cd^{2+} was to cause an approximately two fold increase in the EC_{50} for [^{3}H]-mepyramine binding, together with a statistically significant decrease in B_{max}, the maximum binding (Table 2). In 4 out of 5 experiments with Li^+ there was a small numerical decrease in B_{max}, but overall the reduction was not statistically significant, whereas the EC_{50} was increased by a factor of 2.3. Na^+, 100 mM, had no significant effect on either EC_{50} or B_{max} for [^{3}H]-mepyramine binding (Table 2), in agreement with the observation of Chang & Snyder (1980).

The EC_{50} for [^{3}H]-mepyramine binding in the absence of added ions, equivalent to the dissociation constant, K_d, was 0.72 ± 0.09 nM (Table 2). A similar value, 0.59 ± 0.02 nM was obtained in a single experiment in which the inhibition of the binding of 0.55 nM [^{3}H]-mepyramine by mepyramine was

Table 2 Effect of $CdCl_2$, LiCl and NaCl on the parameters of [^{3}H]-mepyramine binding

	Change in parameter (% of value in the absence of metal ion)	
Metal salt	EC_{50}	B_{max}
$CdCl_2$ 15 μM	189 ± 23 (5)*	68 ± 4 (5)*
LiCl 40 mM	230 ± 25 (5)*	91 ± 4 (5)
NaCl 100 mM	145 ± 29 (4)	108 ± 6 (4)

The binding of [^{3}H]-mepyramine sensitive to 1 μM temelastine was measured in the presence and in the absence of the metal ion in each experiment. The best-fit values of EC_{50} and B_{max} for each curve were obtained as described under Methods. Values are the mean ± s.e.mean of the percentages from the number of individual experiments shown in parentheses. The mean value of EC_{50} for [^{3}H]-mepyramine in the absence of metal salt, equivalent to the dissociation constant, K_d, was 0.72 ± 0.09 nM (14).

* Significantly different from 100 ($P < 0.05$), assuming that the means of the ratios from different experiments are normally distributed.

measured. Both of these values are similar to the mean value for K_d, 0.63 nM, obtained from several studies in which measurements were made in 50 mM Na-K phosphate buffer (37.8 mM Na_2HPO_4, 12.2 mM KH_2PO_4) (Aceves *et al.*, 1985), consistent with the lack of any marked effect of Na^+ on [^{3}H]-mepyramine binding. The mean value for K_d for [^{3}H]-QMDP determined from binding curves in 50 mM Tris-HCl buffer (in the absence of metal ions) was 0.55 ± 0.11 nM (6 measurements). This is less than the value, 0.88 ± 0.02 nM, measured in 50 mM Na-K phosphate buffer (Treherne & Young, 1988a), although it should be noted that the cerebellar homogenate in those experiments had not been washed in EDTA.

Discussion

The two main findings of this study are (i) that the binding of antagonists to the histamine H_1-receptor is inhibited by cations and (ii) that sodium ions distinguish between the binding of [^{3}H]-QMDP and [^{3}H]-mepyramine. The relatively weak effect of Na^+ on [^{3}H]-mepyramine binding and the use of a single, 1 mM, concentration of Ca^{2+} and Mg^{2+} are probably the main reasons why the effect of cations was missed in the earlier study (Chang & Snyder, 1980), although the small inhibitory effect reported with 5 and 10 mM Mn^{2+} contrasts with our observation (Table 1) that the IC_{50} for Mn^{2+} is *circa* 5 mM and is similar for [^{3}H]-QMDP and [^{3}H]-mepyramine. However, there were some methodological differences, in that the earlier study used membrane preparations from guinea-pig whole brain, rather than from cerebellum, and there was no wash with EDTA. No measurements were made in the earlier paper of the most striking group of inhibitors namely the divalent cations from group IIB; Zn^{2+}, Cd^{2+} and Hg^{2+}.

The high potency of the divalent cations from group IIB raises the question of whether the mechanism of action is the same as for the much weaker divalent cations of group IIA, Mg^{2+} and Ca^{2+}. It is notable that the slope of the inhibition curves for the group IIB cations and those from the other divalent cations appear to fall into two distinct groups, with the Hill coefficients for Zn^{2+}, Cd^{2+} and Hg^{2+} being $\geqslant 1$ and the Hill coefficients for the others being < 1. The notable chemical property of the group IIB cations, especially Hg^{2+}, is the ready formation of complexes with nitrogen and sulphur electron donors. Thiol groups are one obvious target, but the thiol group reagent N-ethylmaleimide, which shifts the IC_{50} for curves of histamine inhibition of [^{3}H]-mepyramine binding to lower values and changes the Hill coefficient, has been reported not to have an effect on the binding of [^{3}H]-mepyramine itself (Yeramian *et al.*, 1985). Interestingly, two organic mercurials, *p*-chloromercuriphenylsulphonic acid (1 mM) and mersalyl (0.1 mM), examined in that study did cause a marked inhibition of [^{3}H]-mepyramine binding (Yeramian *et al.*, 1985). We have not yet investigated whether thiol group reagents alter the inhibitory action of the group IIB cations, but in an early experiment, carried out with a membrane preparation which had not been washed with EDTA, pretreatment with 1 mM N-ethylmaleimide had no significant effect on either the EC_{50} or B_{max} for [^{3}H]-QMDP binding to cerebellar membranes, measured in 50 mM Tris buffer. Similarly, 1,4-dithiothreitol, the disulphide bond reducing agent, which changes curves of histamine inhibition of [^{3}H]-mepyramine binding to homogenates of guinea-pig cerebellum in the same way as N-ethylmaleimide, but which again has no effect on the parameters of [^{3}H]-mepyramine binding (Donaldson & Hill, 1986) caused only a 10% inhibition of [^{3}H]-QMDP binding at a concentration of 1 mM and did not distinguish between the binding of [^{3}H]-QMDP and [^{3}H]-mepyramine (Treherne & Young, unpublished observations).

The inhibitory action of less potent cations, such as Ca^{2+}, Mg^{2+} or Li^+, seems much less likely to involve complex formation with thiol or amino functions, but any proposed mechanism has to encompass both this inhibition, which is not radioligand-selective, with the selective action of Na^+ in distinguishing between the binding of [^{3}H]-QMDP and [^{3}H]-mepyramine. Modulation of antagonist binding by Na^+ has not been reported previously for the H_1-receptor, but it is well established for other receptors. Selective actions of Na^+ on both agonist and antagonist binding, with different antagonists being affected to differing extents, was reported in the original study on opiate binding by Pert & Snyder (1974) and have been confirmed in more recent investigations (Paterson *et al.*, 1986; Kosterlitz *et al.*, 1987; Nijssen & Childers, 1987). Similarly Na^+ affects the binding of different antagonists to the dopamine D_2 receptor to differing degrees (Jarvie *et al.*, 1987; Urwyler, 1987) and there is an interesting analogy with the present results in that certain permanently uncharged analogues of dopamine, which have no D_2-agonist action, inhibit the binding of [^{3}H]-spiperone to D_2-receptors, but this inhibition is much reduced in the presence of 125 mM NaCl (Wallace *et al.*, 1988).

The usual explanation for the effect of Na^+ is that it induces a conformational change in the receptor such that the proportion in a state which has a high affinity for agonists is reduced. However, the connection, if any, between ion effects on agonist and on antagonist binding at the H_1-receptor remains to be established. Both Na^+ and Li^+ reduce H_1-agonist inhibition of [^{3}H]-mepyramine binding (Chang & Snyder, 1980; Toll & Snyder, 1982), but only Na^+ distinguishes between the binding of [^{3}H]-QMDP and [^{3}H]-mepyramine. However, a Na^+-induced conformational change is most likely to be the basis of the differential effect on the binding of [^{3}H]-QMDP and [^{3}H]-mepyramine. If Na^+ were acting directly at the antagonist binding site to inhibit [^{3}H]-QMDP binding, then it would be difficult to understand why it should be relatively ineffective in inhibiting the binding of [^{3}H]-mepyramine. There is also some indirect evidence that the site at which Na^+ acts is not accessible from the extracellular medium. The K_d for QMDP inhibition of histamine-induced contraction of longitudinal muscle strips from guinea-pig small intestine suspended in Krebs-Henseleit medium (containing 143 mM Na^+) is 0.56 nM (Treherne & Young, 1988a) and is closely similar to the value, 0.55 nM, determined from the binding of [^{3}H]-QMDP in 50 mM Tris buffer (see Results).

Considerations of the site of action of Na^+ and the other cations are complicated by the fact that the histamine H_1-receptor belongs to the family of G-protein-coupled receptors (Claro *et al.*, 1989; Hill, 1990), consistent with the effect of GTP on histamine inhibition of [^{3}H]-mepyramine binding (Chang & Snyder, 1980). Ions are known to influence receptor-G-protein interactions and the complex effects of Mg^{2+} in particular are well documented (Gilman, 1987). Na^+ can also modulate receptor-G-protein interaction, since the reduction of GTPase activity in NG108-15 cell membranes by an opiate antagonist (but not all antagonists) can be regulated by Na^+ (Costa *et al.*, 1990). However, Na^+ modulation of [^{3}H]-SCH 23390 binding to dopamine D_1-receptors in rat striatal membranes does not require a functional coupled G-protein (Urwyler, 1989), implying a direct action on the receptor macromolecule. The same could well be true for the H_1-receptor, since the effects of Na^+, Mn^{2+} and Mg^{2+} on the parameters of H_1-agonist inhibition of [^{3}H]-doxepin binding in guinea-pig brain membranes are retained in digitonin-solubilized preparations, whereas the effect of GTP on histamine binding is lost (Toll & Snyder, 1982).

Whether Li^+ or Ca^{2+} or Mg^{2+} act at the same site as Na^+ is not clear, although if they did it would mean that they caused a change to a different conformation which bound neither [^{3}H]-QMDP nor [^{3}H]-mepyramine. The evidence available does not support any simple mechanism of action. The difference in potency among mono- or divalent cation chlorides argues against any effect due to an increase in the ionic strength of the medium or to a change in membrane surface charge, which appears to be the basis of the effects of ions on binding to muscarinic receptors (Birdsall *et al.*, 1979)

and κ-opioid receptors (Sargent et al., 1988). A simple competitive action of Li^+ at the antagonist binding site is consistent with the decrease in the EC_{50} for [^{3}H]-mepyramine binding in the presence of Li^+ (Table 2), and the lack of a significant effect on B_{max} (Table 2). However, it is not consistent with a Hill coefficient significantly less than unity (Table 1). Conversely, the Hill coefficient for the Cd^{2+} inhibition curve is near unity, but the decrease in B_{max} is inconsistent with a competitive mechanism of action. This difference in the effects of two cations gives some support to the proposition that the sites or mechanisms of action may differ. The decrease in B_{max} caused by Cd^{2+} is also inconsistent with a simple allosteric action to stabilize a changed conformation of the receptor, unless the conformational change is very slow. We have not investigated the kinetics of the action of the cations at the H_1 receptor, but it may be noted that the Na^+ induced increase in [^{3}H]-naloxone binding to rat brain membranes at 25°C requires 30–40 min to reach maximum effect (Nijssen & Childers, 1987). In earlier studies we failed to detect any slow conformational changes induced by the binding of either [^{3}H]-mepyramine (Wallace & Young, 1983) or [^{3}H]-QMDP (Treherne & Young, 1988b).

The accessibility or otherwise from the extracellular medium of the site for the cations other than Na^+ is also uncertain. The IC_{50} for Li^+ inhibition of histamine-induced contraction of guinea-pig intestinal muscle strips, measured in the presence of approximately 140 mM Na^+, is 44 mM (Hori et al., 1989), which is close to the IC_{50} for inhibition of [^{3}H]-QMDP binding, 39 mM (Table 1). However, the IC_{50} values for Li^+ against carbachol- and K^+-induced contraction of the muscle strips were also in the range of 40–45 mM and the degree of inhibition correlated well with the concentration of intracellularly accumulated Li^+, which appeared to have direct effects on the contractile proteins (Hori et al., 1989). Clearly, evaluation of the inhibitory effects of ions on tissue responses remote from receptor activation presents difficulties, particularly with the divalent cations such as Ni^{2+} which are also channel blockers.

In assessing the data on ion effects presented above it must be borne in mind that all of our measurements have been made in 50 mM Tris-HCl buffer. We have used this buffer in order to be able to relate our results to those from the earlier studies on the action of cations at the H_1-receptor, but the Tris cation can itself have effects on antagonist binding. This is illustrated by a study of the effect of cations on the binding of [^{3}H]-nitrendipine, a dihydropyridine L-type calcium channel antagonist, in which 50 mM Tris was shown to obscure the effect of 100 mM Na^+ (Bolger & Skolnick, 1986). This example is given some relevance by the observation that the IC_{50} values for inhibition of the binding of another dihydropyridine derivative, [^{3}H]-(+)-PN 200-110, to portal vein membranes by Cd^{2+}, Ni^{2+} and Co^{2+} (Dacquet et al., 1989) are similar to those for inhibition of [^{3}H]-QMDP binding. However, although there are some interesting analogies between binding to L-type Ca^{2+} channels and to H_1-receptors, the two seem to be clearly distinguished by La^{3+}, which is a potent inhibitor of [^{3}H]-(+)-PN 200-110 binding (IC_{50} 10 μM), but which in preliminary measurements we have found to be much less effective against [^{3}H]-QMDP binding (IC_{50} *circa* 1 mM). Dihydropyridines themselves are weak inhibitors of [^{3}H]-QMDP binding (Treherne & Young, 1988a).

The structural features which are important in distinguishing the binding of [^{3}H]-QMDP and [^{3}H]-mepyramine in the presence of Na^+ remain undefined . However, the most notable difference between the two molecules is that [^{3}H]-QMDP is a quaternary amine and therefore permanently positively charged, whereas mepyramine is a tertiary amine, although largely charged at physiological pH. The quaternary derivative of histamine, N^α,N^α,N^α-trimethylhistamine, is a very weak agonist, but N^α,N^α-dimethylhistamine is an effective H_1-receptor agonist and the suggestion has been made that the important difference is that at physiological pH the tertiary amine possesses a transferable proton (Ganellin, 1982). How relevant this analogy is to apparent differences in antagonist binding will be more apparent when a range of H_1-antagonist structures have been screened.

This work was supported in part by the Wellcome Trust. We are grateful to Merck, Sharp & Dohme for the research studentship held by J.M.T.

References

ACEVES, J., MARISCAL, S., MORRISON, K.E. & YOUNG, J.M. (1985). The binding of doxepin to histamine H_1-receptors in guinea-pig and rat brain. *Br. J. Pharmacol.*, **84**, 417–424.

BIRDSALL, N.J.M., BURGEN, A.S.V., HULME, E.C. & WELLS, J.W. (1979). The effects of ions on the binding of agonists and antagonists to muscarinic receptors. *Br. J. Pharmacol.*, **67**, 371–377.

BOLGER, G.T. & SKOLNICK, P. (1986). Novel interactions of cations with dihydropyridine calcium antagonist binding sites in brain. *Br. J. Pharmacol.*, **88**, 857–866.

CHANG, R.S.L. & SNYDER, S.H. (1980). Histamine H_1-receptor binding sites in guinea pig brain membranes: regulation of agonist interactions by guanine nucleotides and cations. *J. Neurochem.*, **34**, 916–922.

CLARO, E., GARCIA, A. & PICATOSTE, F. (1989). Carbachol and histamine stimulation of guanine-nucleotide-dependent phosphoinositide hydrolysis in rat brain cortical membranes. *Biochem. J.*, **261**, 29–35.

COSTA, T., LANG, J., GLESS, C. & HERZ, A. (1990). Spontaneous association between opioid receptors and GTP-binding regulatory proteins in native membranes: specific regulation by antagonists and sodium ions. *Mol. Pharmacol.*, **37**, 383–394.

CRAWFORD, M.L.A. & YOUNG, J.M. (1990). Potentiation by GABA of α_1-agonist-induced accumulation of inositol phosphates in slices of rat cerebral cortex. *J. Neurochem.*, **54**, 2100–2109.

DACQUET, C., LOIRAND, G., RAKOTOARISOA, J., MIRONNEAU, C. & MIRONNEAU, J. (1989). (+)-[^{3}H]-PN 200-110 binding to cell membranes and intact strips of portal vein smooth muscle: characterization and modulation by membrane potential and divalent ions. *Br. J. Pharmacol.*, **97**, 256–262.

DONALDSON, J. & HILL, S.J. (1986). 1,4-Dithiothreitol-induced alteration in histamine H_1-agonist binding in guinea-pig cerebellum and cerebral cortex. *Eur. J. Pharmacol.*, **129**, 25–31.

GANELLIN, C.R. (1982). Chemistry of drugs acting at histamine receptors. In *Pharmacology of Histamine Receptors*. ed. Ganellin, C.R. & Parsons, M.E. pp. 10–102. Bristol: Wright PSG.

GILMAN, A.G. (1987). G proteins: transducers of receptor-generated signals. *Annu. Rev. Biochem.*, **56**, 615–649.

HILL, S.J. (1990). Distribution, properties and functional characteristics of three classes of histamine receptor. *Pharmacol. Rev.*, **42**, 45–83.

HORI, M., SHIMIZU, K., NAKAJYO, S. & URAKAWA, N. (1989). Inhibitory effects of lithium on muscle contractions caused by various stimulants in guinea-pig ileum. *Eur. J. Pharmacol.*, **165**, 63–70.

JARVIE, K.R., NIZNIK, H.B. & SEEMAN, P. (1987). Dopamine D-2 receptors in canine brain: ionic effects on [^{3}H]-neuroleptic binding. *Eur. J. Pharmacol.*, **144**, 163–171.

KOSTERLITZ, H.W., PATERSON, S.J., ROBSON, L.E. & TRAYNOR, J.R. (1987). Effects of cations on binding, in membrane suspensions, of various opioids at μ-sites of rabbit cerebellum and κ-sites of guinea-pig cerebellum. *Br. J. Pharmacol.*, **91**, 431–437.

LOWRY, O.H., ROSEBROUGH, N.J., FARR, A.L. & RANDALL, R.J. (1951). Protein measurements with the Folin phenol reagent. *J. Biol. Chem.*, **193**, 265–275.

NIJSSEN, P.C.G. & CHILDERS, S.R. (1987). Characteristics of sodium-induced increase in opiate antagonist binding sites in rat brain membranes. *Eur. J. Pharmacol.*, **135**, 355–364.

PATERSON, S.J., ROBSON, L.E. & KOSTERLITZ, H.W. (1986). Control by cations of opioid binding in guinea-pig brain membranes. *Proc. Natl. Acad. Sci. U.S.A.*, **83**, 6216–6220.

PERT, C.B. & SNYDER, S.H. (1974). Opiate receptor binding of agonists and antagonists affected differentially by sodium. *Mol. Pharmacol.*, **10**, 868–879.

SARGENT, D.F., BEAN, J.W., KOSTERLITZ, H.W. & SCHWYZER, R. (1988). Cation dependence of opioid receptor binding supports

theory on membrane-mediated receptor selectivity. *Biochemistry*, **27**, 4974–4977.

TOLL, L. & SNYDER, S.H. (1982). Solubilization and characterization of histamine H_1 receptors in brain. *J. Biol. Chem.*, **257**, 13593–13601.

TREHERNE, J.M., STERN, J.S., FLACK, W.J. & YOUNG, J.M. (1989). Na^+ ions distinguish between the binding of a tertiary and a quaternary [^{3}H]-antagonist to the histamine H_1 receptor. *Br. J. Pharmacol.*, **98**, 612P.

TREHERNE, J.M. & YOUNG, J.M. (1988a). [^{3}H]-(+)-N-methyl-4-methyldiphenhydramine, a quaternary radioligand for the histamine H_1-receptor. *Br. J. Pharmacol.*, **94**, 797–810.

TREHERNE, J.M. & YOUNG, J.M. (1988b). Temperature-dependence of the kinetics of the binding of [^{3}H]-(+)-N-methyl-4-methyl-diphenhydramine to the histamine H_1-receptor: comparison with the kinetics of [^{3}H]-mepyramine. *Br. J. Pharmacol.*, **94**, 811–822.

URWYLER, S. (1987). Affinity shifts by cations do not reliably predict the agonistic or antagonistic nature of ligands at brain dopamine receptors. *J. Neurochem.*, **49**, 1415–1420.

URWYLER, S. (1989). Mono- and divalent cations modulate the affinities of brain D1 and D2 receptors for dopamine by a mechanism independent of receptor coupling to guanyl nucleotide binding proteins. *Naunyn Schmiedebergs Arch. Pharmacol.*, **339**, 374–382.

WALLACE, R.A., FAROOQUI, T., WALLACE, L., ARES, J., CHANG, Y.A., MILLER, D.D. & URETSKY, N.J. (1988). Interaction of permanently uncharged dopamine analogs with the D-2 dopaminergic receptor. *Biochem. Pharmacol.*, **37**, 2077–2084.

WALLACE, R.M. & YOUNG, J.M. (1983). Temperature dependence of the binding of [^{3}H]mepyramine and related compounds to the histamine H_1-receptor. *Mol. Pharmacol.*, **23**, 60–66.

YERAMIAN, E., GARBARG, M. & SCHWARTZ, J.-C. (1985). N-Ethylmaleimide-induced changes in agonist affinity for histamine H_1-receptors in the guinea pig brain. *Mol. Pharmacol.*, **28**, 155–162.

(Received September 27, 1990
Revised February 10, 1991
Accepted February 22, 1991)

Br. J. Pharmacol. (1991), **103**, 1752–1756 © Macmillan Press Ltd, 1991

On the histamine-induced depolarization of the isolated superior cervical ganglion of the rat

Julie L. Field & [1]Nigel R. Newberry

Merck, Sharp and Dohme Research Laboratories, Neuroscience Research Centre, Terlings Park, Eastwick Road, Harlow, Essex CM20 2QR

1 Using a grease-gap technique, we studied the action of histamine on the d.c. potential recorded between the internal carotid nerve and the main body of the isolated superior cervical ganglion of the rat.

2 A small, slow depolarization was evoked by 10–300 μM histamine. This response was not reduced by lowering the calcium concentration in the superfusing medium (from 2.5 to 0.1 mM), or by superfusing tetrodotoxin, N-methylatropine, or propranolol (all at 1 μM).

3 Mepyramine (10 nM) antagonized this depolarization, but cimetidine (10 μM), metiamide (30 μM), burimamide (10 μM) and impromidine (1 μM) did not. Two other agonists also evoked a mepyramine-sensitive slow depolarization. The rank order of potencies was histamine > N^{α}-methyl-histamine > 2-methyl-histamine.

4 At concentrations greater than 1 mM, histamine also evoked a larger, faster depolarization. This response was undiminished by reducing the calcium concentration of the medium to 0.1 mM or by adding 1 μM tetrodotoxin. The rank order of potency for the agonists was N^{α}-methyl-histamine > histamine $\approx$ 2-methyl-histamine. The histamine-induced fast response was not antagonized by any of the above-mentioned antagonists. It was slightly reduced by (+)-tubocurarine (100 μM) and N-methylbicuculline (100 μM) but such effects were not consistent with the blockade of nicotinic or $GABA_A$ receptor-mediated responses.

5 It was concluded that histamine depolarized the isolated superior cervical ganglion of the rat by activating H_1 receptors. Relatively high concentrations of histamine also evoked a fast depolarization of this preparation, but this did not appear to be mediated by H_1, H_2 or H_3 receptors.

Keywords: Histamine; sympathetic ganglion; rat superior cervical ganglion; depolarization

Introduction

It is now well established that there is more than one type of receptor for histamine. In 1966, Ash & Schild defined the H_1 receptor as being sensitive to low concentrations of anti-histamine drugs (the pA_2 for mepyramine was >9). In 1972, Black *et al.* characterized the H_2 receptor using a novel selective antagonist, burimamide ($K_b = 7 \times 10^{-6}$ M). Subsequently H_1 receptors were shown to be linked to inositol phospholipid turnover (Subraminian *et al.*, 1980; Daum *et al.*, 1983) and H_2 receptors were reported to mediate an inhibition of adenylyl cyclase (Hegstrand *et al.*, 1976). The finding that histamine could inhibit its own release from brain slices (Arrang *et al.*, 1983) prompted the suggestion of another receptor. This H_3 receptor was clearly demonstrated by use of the selective agonist (**R**)-α-methyl-histamine and the selective antagonist thioperamide (Arrang *et al.*, 1987). At the same time, the H_3 receptor was demonstrated to mediate the histamine-induced inhibition of transmitter release in the guinea-pig mesenteric artery (Ishikawa & Sperelakis, 1987). In this preparation the H_2 antagonists cimetidine and metiamide were weak antagonists (K_b > 30 μM), whereas impromidine and burimamide had relatively high antagonist affinities (K_bs of 48 and 330 nM, respectively). The antagonist action of impromidine was intriguing since it was initially reported to be a potent H_2 receptor partial agonist (Ganellin, 1982).

The first neuronal actions of histamine to be described were a direct stimulant action on the feline superior cervical ganglion *in situ* and a facilitation of transmission across its synapse (Trendelenburg, 1954; 1957). The former action was shown to be sensitive to mepyramine before the H_1 receptor was defined (Trendelenburg, 1954). A facilitation of transmission through the rabbit superior cervical ganglion was shown to be mediated by H_1 receptors but a depression of transmission in the same preparation was blocked by an H_2 antagonist (Brimble & Wallis, 1973). The activation of H_1 receptors on sympathetic neurones, and the subsequent release of noradrenaline, is thought to mediate the pressor action of intravenous histamine in the guinea-pig (Krstic, 1988). Recent intracellular studies in the guinea-pig superior cervical ganglion have revealed that the H_1 receptor mediates a depolarization associated with an increase in the neuronal input resistance (Christian *et al.*, 1989). On the rat superior cervical ganglion, however, histamine-induced depolarizations have been reported to be small or absent (Watson, 1970), but, as seen on the rabbit ganglion, an H_1-mediated facilitation and an H_2-mediated depression of transmission have been observed (Snow & Weinreich, 1987).

We observed that histamine does induce a small, slow depolarization of rat superior cervical ganglion cells *in vitro*. This paper describes our investigation of the pharmacology of this slow response which was compared with that of a fast depolarization induced by relatively high concentrations of histamine.

Methods

Male Sprague-Dawley rats (150–200 g) were killed by stunning followed by exsanguination. Two superior cervical ganglia were excised from each animal. Each ganglion was desheathed and set up in a three compartment bath as previously described (Newberry & Priestley, 1987). The d.c. potential between the ganglion body and the internal carotid nerve was recorded across a grease-gap with Ag/AgCl electrodes. The central compartment in which ganglion body was immersed (volume ca. 0.5 ml) was perfused with an aqueous medium (25°C) at ca. 2 ml min^{-1}. This medium contained (in mM):

[1] Author for correspondence at present address: Oxford University SmithKline Beecham Centre for Applied Neuropsychobiology, Radcliffe Infirmary, Woodstock Road, Oxford, OX2 6HE.

NaCl 125, $NaHCO_3$ 25, D-glucose 10, $CaCl_2$ 2.5, KCl 2, KH_2PO_4 1 and $MgSO_4$ 1, and was equilibrated with 5% CO_2 in O_2.

Histamine (100 μM) was applied to the ganglion body via the perfusion system for 1 min every 45 min until two equal responses were obtained. After the recovery of the last of these responses, the ganglion was superfused with an antagonist for one hour or, as a control, the ganglion was superfused with unadulterated medium for the same length of time. The concentration-response relationship of an agonist was then determined by 1 min superfusions at intervals of 45–60 min, in an ascending order of concentration. The peak responses of the agonists were expressed as ratios. They were related to the depolarization evoked by the last application of histamine prior to the 1 h incubation. This protocol was rigidly adhered to for the reasons given in the Results. The relative response of a given concentration of agonist on a number of ganglia was cumulated as the geometric mean (± s.e.mean).

To confirm the antagonist properties of a given compound on $GABA_A$ and nicotinic responses, we determined its IC_{50} against 10 μM GABA and 30 μM 1,1-dimethyl-4-phenylpiperazinium (DMPP), respectively. The IC_{50} was the concentration necessary to reduce the approximately half-maximal agonist response by 50%.

Burimamide, metiamide, impromidine trihydrochloride, N^{α}-methyl-histamine dihydrochloride and 2-methyl-histamine dihydrochloride were kind gifts from Smith, Kline and French. Histamine dihydrochloride, mepyramine (pyrilamine) maleate, cimetidine, (+)-tubocurarine chloride, N-methylatropine nitrate, propranolol, γ-aminobutyric acid, 1,1-dimethyl-4-phenylpiperazinium iodide and N-methyl-bicuculline chloride were obtained from Sigma Chemical Company. The last was also supplied by Research Biochemicals Inc., as was mecamylamine. Tetrodotoxin was purchased from Sankyo.

An *n* number refers to the number of ganglia, each from a different rat, which were tested under a particular condition.

Results

Histamine (10–300 μM) routinely induced a small, slow depolarization of the rat superior cervical ganglion. To obtain the largest response to a given concentration of histamine, it was necessary to superfuse it for 2 min. However, the response to histamine was prone to long-lasting tachyphylaxis (see Figure 1a). To try to avoid this, it was necessary to apply histamine for 1 min periods every 45 to 60 min. The 1 min application produced about 90% of the response to that of the 2 min superfusion. Although tachyphylaxis was not evident with this protocol, the response to a given concentration of histamine increased gradually throughout the day. Consequently, the effect of an antagonist on the histamine dose-response curve could only be realistically determined if the same protocol was performed during every experiment. The ganglia incubated with an antagonist could then be compared with untreated ganglia (see Methods). Without this methodology, it was only possible to assess whether an antagonist affected the response to one or two concentrations of histamine.

The slow depolarizing response to 300 μM histamine (1 min) was not depressed by 1 μM tetrodotoxin ($n = 2$) or by lowering the calcium chloride concentration in the medium to 0.1 mM ($n = 4$). This response was unaffected by a 30 min superfusion of the ganglion with propranolol or N-methylatropine (1 μM, $n = 4$ each). It was also undiminished by the H_2 antagonists, cimetidine (10 μM, $n = 2$) and metiamide (30 μM, $n = 4$) and the H_2/H_3 receptor compounds impromidine (1 μM, $n = 4$) and burimamide (10 μM, $n = 4$). None of these compounds had a direct action by itself. In particular, the H_2 agonist impromidine did not evoke a direct response when superfused at 10 μM for 1 min ($n = 2$). In contrast the H_1 antagonist mepyramine (1 μM, 30 min) largely abolished the slow depolarization to 300 μM histamine (see Figure 1b). The histamine receptor

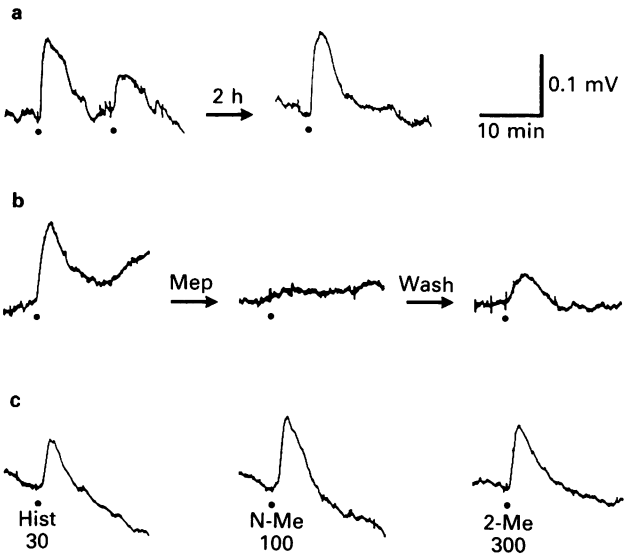


Figure 1 The pharmacology of the depolarization induced by histamine (Hist), N^{α}-methyl-histamine (N-Me), and 2-methyl-histamine (2-Me) on the rat superior cervical ganglion. Depolarization is upward in this and all subsequent figures. The agonist superfusions, indicated by the dots, were for 1 min. Histamine was superfused at 300 μM unless otherwise indicated. Each line (a, b, c) depicts an experiment from a different ganglion: (a) shows that repeating the application of histamine at short intervals results in a smaller response, but after 2 h the response recovered. Line (b) shows that the response to 300 μM histamine was abolished by mepyramine (Mep, 1 μM, 30 min), and partial recovery was obtained after washing the ganglion for 3 h in mepyramine-free medium. Line (c) shows the relative potencies for evoking the slow depolarization of the three compounds: the superfused concentrations (in μM) are shown.

agonists N^{α}-methyl-histamine and 2-methyl-histamine also evoked the slow depolarization (see Figure 1c).

The dose-response curve to histamine is illustrated in Figure 2. It appeared to begin to level off at about 100–300 μM, but clearly started to rise again at greater than 1 mM. Mepyramine (0.01, 0.1 and 1 μM) antagonized the response to concentrations less than 300 μM, but the responses to greater than 1 mM were less affected. The dose-response curves to 2-methyl-histamine and, in particular, N^{α}-methyl-histamine were also biphasic (Figure 3). At concentrations less than 300 μM

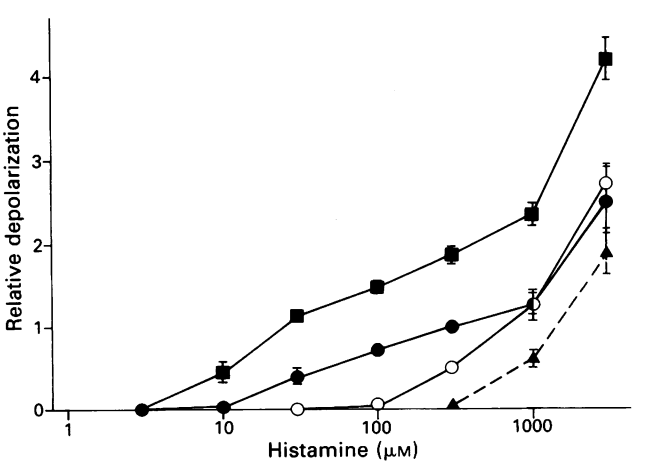


Figure 2 The concentration-response curve of the depolarization of the rat superior cervical ganglion to histamine (■). The effect of a 1 h incubation with different concentrations of mepyramine is also shown: 0.01 μM (●); 0.1 μM (○); 1 μM (▲). Values are the geometric means (± s.e.mean, shown by vertical bars) from 5 ganglia. Each response was expressed as a ratio of the response to 300 μM histamine before the incubation period (see Methods).

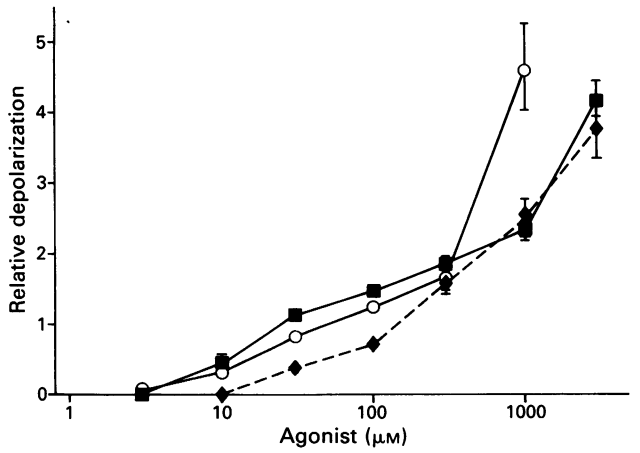


Figure 3 Concentration-response curves of the depolarizations to histamine (■), N^{α}-methyl-histamine (○) and 2-methyl-histamine (◆) on the rat superior cervical ganglion. Accumulated data of the agonists were from 5, 7 and 6 different ganglia, respectively.

the rank order of potency of the three agonists was histamine > N^{α}-methyl-histamine > 2-methyl-histamine (see also Figure 1c), but with concentrations of over 1 mM the ranking was N^{α}-methyl-histamine > histamine ≈ 2-methyl- histamine. Mepyramine (10 nM) antagonized the responses to <300 μM of both N^{α}-methyl-histamine and 2-methyl-histamine to a similar extent to that seen with <300 μM histamine (not shown, $n = 4$ for each). An examination of the responses (Figure 4) revealed that a fast depolarization was evoked by high concentrations of histamine, and particularly by N^{α}-methyl-histamine.

Appropriate controls were sought when it was discovered that 3 mM histamine dihydrochloride reduced the pH of the superfusing medium from ca. 7.4 to ca. 7.0. (A similar drop in pH was noted with 3 mM N^{α}-methyl-histamine dihydrochloride). Control solutions were prepared by adding sufficient hydrochloric or sulphuric acid to similarly reduce the pH. When superfused for 1 min periods, these solutions evoked apparent fast depolarizations, but the responses were only 22–56% (median = 26, $n = 5$) of the response to 3 mM histamine recorded in the presence of 1 μM mepyramine. Furthermore, in experiments where the pH of the solutions containing either histamine or N^{α}-methyl-histamine (3 mM) was kept at 7.4 (by adding sufficient 0.5 M NaOH) the fast depolarizing response was still present, although it was 33–40% smaller than that recorded without adjusting the pH ($n = 3$).

Given that the agonist pharmacology of the fast response appeared to be different from that of the smaller slow response, we determined the sensitivity of the response to 3 or 10 mM histamine to a range of antagonists. Using such high

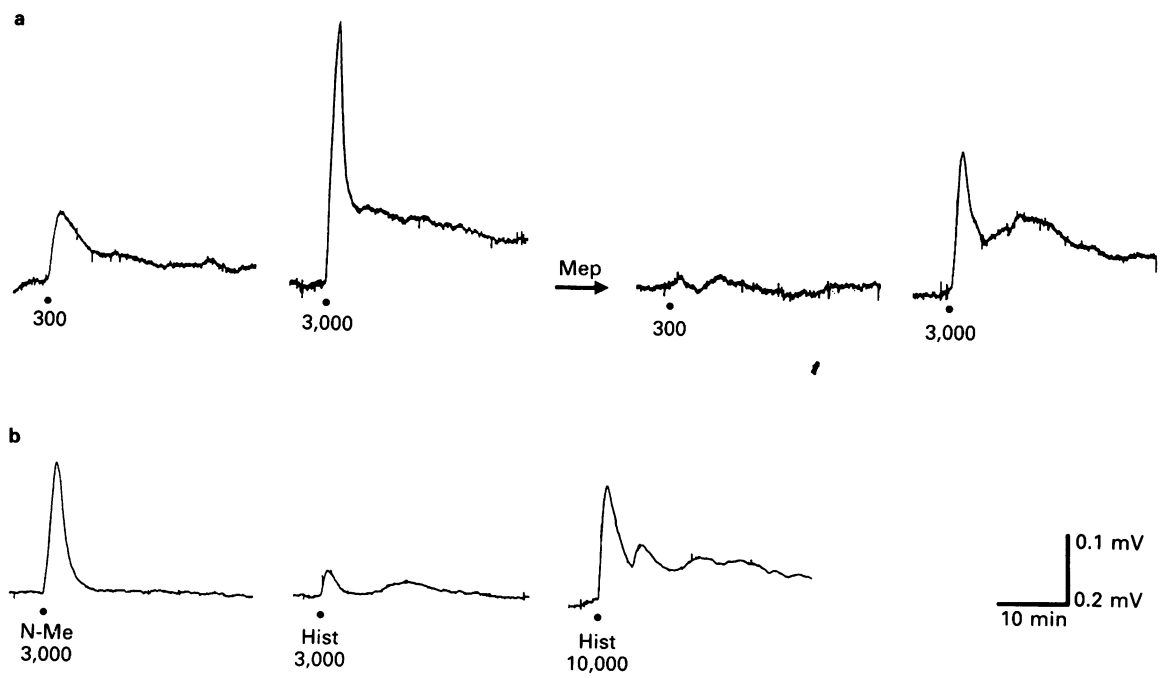


Figure 4 The pharmacology of the fast depolarization evoked by histamine (Hist) and N^{α}-methyl-histamine (N-Me) on the rat superior cervical ganglion. In (a) is shown the action of mepyramine (1 μM) on the responses to two different concentrations of histamine; (b) shows the relative potency of N^{α}-methyl-histamine and histamine in evoking the fast response in the presence of 1 μM mepyramine. The gains of the traces on the bottom line were half of those on the top line. The micromolar concentration of the agonists are indicated.

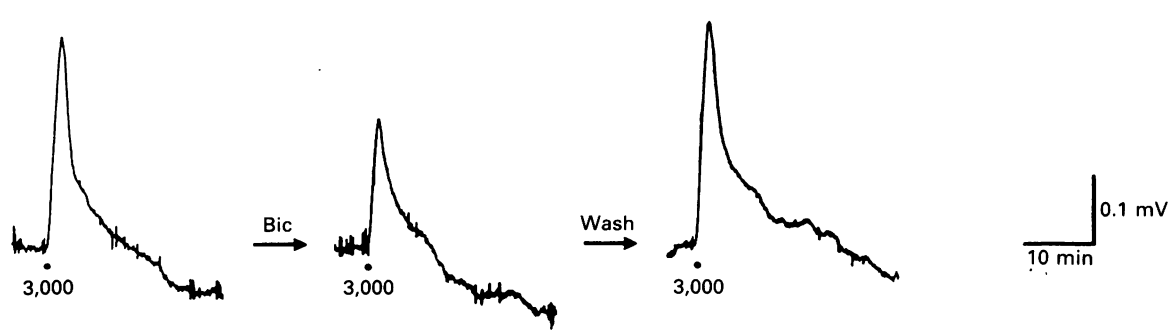


Figure 5 The action of N-methylbicuculline (Bic, 100 μM, 40 min) on the fast ganglionic depolarization to histamine recorded in the presence of 1 μM mepyramine. The micromolar concentration of histamine is shown.

concentrations of histamine, we repeated the responses at intervals of 1 h or greater and superfused each antagonist for 30–45 min. The fast response was not reduced by the histamine antagonists cimetidine (10 μM, $n = 4$), impromidine (1 μM, $n = 4$) and burimamide (10 μM, $n = 4$). It was also unaffected by N-methylatropine (1 μM, $n = 8$), propranolol (1 μM, $n = 4$) or mecamylamine (10 μM, $n = 6$). At the present time, the only antagonists of this response are (+)-tubocurarine (100 μM, $n = 6$, 0–25%) and N-methylbicuculline (100 μM, $n = 7$, 30–45%, see Figure 5). At this concentration, the latter did not reduce the slow depolarization to 300 μM histamine ($n = 4$). The reduction of the fast response by N-methylbicuculline was observed in the presence or absence of mepyramine (1 μM).

By contrast with their action on the fast histamine response, the geometric mean IC_{50} values for mecamylamine and (+)-tubocurarine against DMPP were 0.7 and 30 μM, respectively ($n = 4$ for each). N-methylbicuculline and (+)-tubocurarine antagonized the GABA-induced depolarization ($n = 4$) with IC_{50}s of 2 and 17 μM, respectively. Finally, in contrast to the lack of action on the histamine-induced fast response, lowering the calcium in the medium (from 2.5 to 0.1 μM) reduced the nicotinic depolarization to DMPP by 50–75% ($n = 4$).

Discussion

The principal finding of this study was that histamine (10–300 μM) evoked a small, slow depolarization of the rat superior cervical ganglion that was sensitive to mepyramine. At concentrations greater than 1 mM it also induced a larger, faster depolarization which did not appear to be mediated by H_1, H_2 or H_3 receptors. The rank order of potency of agonists to evoke the slow depolarization was different from that necessary to induce the fast depolarizing response.

The slow depolarization to histamine appeared to be a direct action on the ganglion cells since it was not reduced by tetrodotoxin or by reducing the calcium concentration in the medium, either of which would reduce synaptic transmission. Slow ganglionic depolarizations can also be evoked by muscarinic receptors and β-adrenoceptors, but this histamine action was unlikely to be mediated by these receptors because of its resistance to N-methylatropine and propranolol. Thus, this response was probably mediated by a direct action of histamine on histamine receptors.

The sensitivity of the slow depolarization to mepyramine (estimated pA_2 of 9) and the lack of effect of H_2 and H_3 antagonists indicated that it was mediated by H_1 receptors. Two other histamine analogues N^{α}-methyl-histamine and 2-methyl-histamine also evoked a slow mepyramine-sensitive ganglionic depolarization. They were about 3 and about 10 times less potent than histamine, respectively.

Relatively high concentrations of histamine also evoked a fast depolarization. This was initially considered to be a non-specific action since such concentrations of histamine dihydrochloride reduced the pH of the superfusing medium. Comparable pH controls did evoke similar fast depolarizations, but these responses could only account for ca. 25% of the response to histamine. In addition, the fast response was still present when the pH was kept at 7.4. This complication, however, should be borne in mind when considering the pharmacology of the histamine-induced fast depolarization, since the pH of the medium was not routinely restored to 7.4.

The peak of the dose-response curve for the fast depolarization was not determined, but it was clearly much larger than that of the slow depolarization. The rank order of potency of the agonists in producing this response was different from that for the slow depolarization. N^{α}-methyl-histamine was about 3 times more potent than the other 2 agonists which were approximately equipotent. This potential change was not only insensitive to muscarinic and β-adrenoceptor antagonists, but it was also unaffected by the H_1, H_2 and H_3 antagonists tested. Mepyramine did reduce the peak of the fast response to these concentrations of histamine, but its IC_{50} (0.1–1.0 μM) was clearly greater than that against the slow response evoked by lower concentrations of histamine (IC_{50} ca. 10 nM, see Figure 2). Indeed, the antagonism of the fast response could be explained partly by a reduction of the underlying slow response.

A fast depolarization of this preparation can be evoked by the activation of nicotinic, $GABA_A$ and 5-HT_3 receptors, so we first considered whether histamine could be activating one of these receptors. It is known that histamine interacts with the nicotinic receptor at the neuromuscular junction, albeit in an apparently competitive antagonist manner (Ariyoshi *et al.*, 1985), but we tested for the possibility that it could activate a nicotinic response on this preparation. The resistance of this response to mecamylamine and the small effect of (+)-tubocurarine indicated that the opening of nicotinic receptor-linked ion channels was improbable. Furthermore, unlike the depolarization to the nicotinic agonist DMPP, the fast histamine response was not reduced by superfusing low calcium containing medium. The relative resistance of the fast histamine response to (+)-tubocurarine was very informative. In addition to its antinicotinic properties, it also antagonizes 5-HT_3 (Yakel & Jackson, 1988) and $GABA_A$ (Simmonds, 1986) receptor-mediated responses, so the fast histamine response was unlikely to be mediated by such receptors. It was therefore surprising when another $GABA_A$ antagonist, N-methylbicuculline, reduced this response; however, the concentration used (100 μM) was well above its affinity for $GABA_A$ receptors (pA_2 5.9, Simmonds, 1986) and its IC_{50} value against the GABA response on this preparation (2 μM).

The pharmacology of the histamine-induced fast depolarization was distinct from that of H_1, H_2 and H_3 receptors, but considering the problems of interpretation arising from the pH changes and the absence of a potent and selective antagonist, it would be premature to conclude that this response was mediated by 'H_4' receptors. N-methylbicuculline did reduce the fast response without blocking the underlying slow depolarization, but its apparent affinity was low. We know of no other fast response to histamine on mammalian tissues which has this agonist and antagonist pharmacology, but histamine has been shown to evoke fast chloride-mediated responses on fly photoreceptors (Hardie, 1989) and lobster olfactory receptor neurones (McClintock & Ache, 1989). It is possible that the fast histamine-induced response of the rat superior cervical ganglion is mediated by a similar mechanism, since the opening of chloride channels (e.g. by GABA, Adams & Brown, 1975) will depolarize these cells. Quite clearly, however, further experiments are necessary before any conclusions can be drawn.

It has been shown that H_2 receptors mediate a depression of transmission across the rabbit (Brimble & Wallis, 1973) and rat (Snow & Weinreich, 1987) superior cervical ganglion. We found no evidence for an H_2-mediated change in the membrane potential of these cells: H_2 antagonists had no effect on the potential changes evoked by histamine and the H_2 receptor agonist, impromidine, evoked no response by itself. Consequently, our evidence would support the conclusion of Snow & Weinreich (1987) that the depression of transmission is likely to be mediated presynaptically.

In conclusion, a small slow depolarization to histamine was recorded from the rat superior cervical ganglion. This response was probably mediated via H_1 receptors. It could contribute to the facilitation of transmission previously observed on this preparation (Snow & Weinreich, 1987). High concentrations of histamine also evoked a large, fast depolarization, but the pharmacology of this response was unlike that of H_1, H_2 or H_3 receptors.

We thank Dr Jan Skidmore at Smith, Kline and French for the kind supply of compounds. We are also grateful to Juliet Davis for her help.

References

ADAMS, P.R. & BROWN, D.A. (1975). Actions of gamma-aminobutyric acid on sympathetic ganglion cells. *J. Physiol.*, **250**, 85–120.

ARIYOSHI, M., HASUO, H., KOKETSU, K., OHTA, Y. & TOKIMASA, T. (1985). Histamine is an antagonist of the acetylcholine receptor at the frog endplate. *Br. J. Pharmacol.*, **85**, 65–73.

ARRANG, J.-M., GARBARG, M. & SCHWARTZ, J.-C. (1983). Auto-inhibition of brain histamine release mediated by a novel class (H_3) of histamine receptor. *Nature*, **302**, 832–837.

ARRANG, J.-M., GARBARG, M., LANCELOT, J.-C., LECOMTE, J.-M., POLLARD, H., ROBBA, M., SCHUNACK, W. & SCHWARTZ, J.-C. (1987). Highly potent and selective ligands for histamine H_3-receptors. *Nature*, **327**, 117–123.

ASH, A.S.F. & SCHILD, H.O. (1966). Receptors mediating some actions of histamine. *Br. J. Pharmacol. Chemother.*, **27**, 427–439.

BLACK, J.W., DUNCAN, W.A.M., DURANT, C.J., GANELLIN, C.R. & PARSONS, E.M. (1972). Definition and antagonism of histamine H_2-receptors. *Nature*, **236**, 385–390.

BRIMBLE, M.J. & WALLIS, D.I. (1973). Histamine H_1- and H_2-receptors at a ganglionic synapse. *Nature*, **246**, 156–158.

CHRISTIAN, E.P., UNDEM, B.J. & WEINREICH, D. (1989). Endogenous histamine excites neurones in the guinea-pig superior cervical ganglion *in vitro*. *J. Physiol.*, **409**, 297–312.

DAUM, P.R., DOWNES, C.P. & YOUNG, J.M. (1983). Histamine-induced inositol phospholipid breakdown mirrors H_1-receptor density in brain. *Eur. J. Pharmacol.*, **87**, 497–498.

GANELLIN, C.R. (1982). Chemistry and structure-activity relationship of drugs acting at histamine receptors. In *Pharmacology of Histamine Receptors* ed. Ganellin, C.R. & Parsons, M.E. pp. 10–102. Bristol: Wright.

HARDIE, R.C. (1989). A histamine-activated chloride channel involved in neurotransmission at a photoreceptor synapse. *Nature*, **339**, 704–706.

HEGSTRAND, L.R., KANOF, P.D. & GREENGARD, P. (1976). Histamine-sensitive adenylate cyclase in mammalian brain. *Nature*, **260**, 163–165.

ISHIKAWA, S. & SPERELAKIS, N. (1987). A novel class (H_3) of histamine receptors on perivascular nerve terminals. *Nature*, **327**, 158–160.

KRSTIC, M.K. (1988). Pressor response mediated via histamine H_1-receptors of the guinea-pig sympathetic ganglia. *Neuropharmacology*, **27**, 1215–1219.

McCLINTOCK, T.S. & ACHE, B.W. (1989). Histamine directly gates a chloride channel in lobster olfactory receptor neurons. *Proc. Natl. Acad. Sci. U.S.A.*, **86**, 8137–8141.

NEWBERRY, N.R. & PRIESTLEY, T. (1987). Pharmacological differences between two muscarinic responses of the rat superior cervical ganglion *in vitro*. *Br. J. Pharmacol.*, **92**, 817–826.

SUBRAMANIAN, N., WHITMORE, W.L., SEIDLER, F.J. & SLOTKIN, T.A. (1980). Histamine stimulates brain phospholipid turnover through direct H_1 receptor-mediated mechanism. *Life Sci.*, **27**, 1315–1320.

SIMMONDS, M.A. (1986). Classification of inhibitory amino acid receptors in the mammalian nervous system. *Med. Biol.*, **64**, 301–311.

SNOW, R.W. & WEINREICH, D. (1987). Presynaptic and postsynaptic effects of histamine and histamine agonists in the superior cervical ganglion of the rat. *Neuropharmacology*, **26**, 743–752.

TRENDELENBURG, U. (1954). The action of histamine and pilocarpine on the superior cervical ganglion and the adrenal gland of the cat. *Br. J. Pharmacol. Chemother.*, **9**, 481–487.

TRENDELENBURG, U. (1957). The action of histamine, pilocarpine and 5-hydroxytryptamine on transmission through the superior cervical ganglion. *J. Physiol.*, **135**, 66–72.

WATSON, P.J. (1970). Drug receptor sites in the isolated superior cervical ganglion of the rat. *Eur. J. Pharmacol.*, **12**, 183–193.

YAKEL, J.L. & JACKSON, M.B. (1988). 5-HT_3 receptors mediate rapid responses in cultured hippocampus and a clonal cell line. *Neuron*, **1**, 615–621.

(Received February 8, 1991
Accepted February 26, 1991)

Br. J. Pharmacol. (1991), **103**, 1757–1763 © Macmillan Press Ltd, 1991

Characterization of prejunctional muscarinic autoreceptors in the guinea-pig trachea

[1]H. Kilbinger, R. Schneider, H. Siefken, D. Wolf & *G. D'Agostino

Pharmakologisches Institut, Universität Mainz, Obere Zahlbacher Str. 67, D-6500 Mainz, F.R.G. and *Istituto di Farmacologia, Università di Pavia, Viale Taramelli 14, I-27100 Pavia, Italy

1 The effects of ten muscarinic antagonists on electrically evoked [^{3}H]-acetylcholine release and muscle contraction were compared in an epithelium-free preparation of the guinea-pig trachea that had been preincubated with [^{3}H]-choline.

2 The M_3-selective antagonists UH-AH 37, 4-diphenyl-acetoxy-*N*-piperidine methobromide and *para*-fluorohexahydrosiladiphenidol were more potent in reducing the contractile response than in facilitating the evoked [^{3}H]-acetylcholine release. Hexahydrosiladiphenidol did not discriminate between pre- and postjunctional effects. The rank order of the postjunctional potencies of the ten antagonists as well as the postjunctional pA_2 values obtained for hexahydrosiladiphenidol (7.95) and AQ-RA 741 (7.08) identified the muscular receptor as an M_3 subtype.

3 The M_2-selective antagonists methoctramine, AF-DX 116 and AQ-RA 741 were more potent in facilitating the evoked [^{3}H]-acetylcholine release than in inhibiting the contractile response. The increase in release by low concentrations of methoctramine, AF-DX 116 and AQ-RA 741 was paralleled by an enhancement of the stimulation-evoked contractions.

4 Comparison of the pre- and postjunctional potencies of the M_1-, M_2- and M_3-selective antagonists suggests that autoinhibition of acetylcholine release is mediated via an 'M_2-like' receptor which differs from the cardiac type M_2 receptor in its relatively high affinity for hexahydrosiladiphenidol.

Keywords: Trachea; acetylcholine release; muscarinic autoreceptors; M_2 receptors; M_3 receptors

Introduction

The release of acetylcholine from guinea-pig airways can be inhibited by prejunctional muscarinic autoreceptors. This has been demonstrated in functional studies (Maclagan & Barnes, 1989; Starke *et al.*, 1989) and more recently in release experiments (D'Agostino *et al.*, 1990). Muscarinic receptors can be subdivided pharmacologically into at least three subtypes (M_1, M_2, M_3; for review see Hulme *et al.*, 1990). It has been suggested that the prejunctional autoreceptor in guinea-pig airways is an M_2 receptor since gallamine and methoctramine enhanced the electrically evoked contractions of the trachea *in vivo* (Fryer & Maclagan, 1984) and *in vitro* (Minette & Barnes, 1988; Watson *et al.*, 1989). To our knowledge, further studies to classify these autoreceptors with other antagonists are lacking.

The objective of the present study was to characterize in release experiments the muscarinic autoreceptor in the isolated trachea of the guinea-pig. For this purpose the pre- and postjunctional potencies of ten antagonists were compared on a novel preparation which allows the simultaneous determination of acetylcholine release and smooth muscle contraction (D'Agostino *et al.*, 1990). The antagonists tested are compiled in Table 1 and comprise those which are partially selective at M_1, M_2 or M_3 receptors. Complete concentration-response curves were performed for prejunctional (facilitation of electrically evoked acetylcholine release) and postjunctional (inhibition of evoked muscle contraction) effects, and the potencies of the antagonists were compared at the levels of the EC_{50} values.

The smooth muscle receptor has been classified in the past as M_3 receptor according to its relatively high affinity for the antagonists 4-diphenyl-acetoxy-N-piperidine methobromide (4-DAMP), *para*-fluorohexahydrosiladiphenidol (pFHHSiD) and UH-AH 37, and its relatively low affinity to the antagonists pirenzepine, methoctramine, and AF-DX 116 (see Table 1). In the present study we have extended this classification by the determination of the postjunctional pA_2 values for the M_3-selective antagonist hexahydrosiladiphenidol (HHSiD) (Mutschler & Lambrecht, 1984) and the M_2-selective antagonist AQ-RA 741 (Doods & Ziegler, 1989; Eberlein *et al.*, 1989).

A preliminary report of parts of this work has been given (Kilbinger *et al.*, 1990).

Table 1 Postjunctional pA_2 values of antagonists used in this study as determined in the guinea-pig trachea

Antagonist	pA_2	*Reference*
M_1-selective:		
Pirenzepine	6.9	Eglen & Whiting (1988)
M_2-selective:		
AQ-RA 741	7.0	This study
Methoctramine	6.1	Eglen & Whiting (1988)
AF-DX 116	6.3	Micheletti *et al.* (1987)
M_3-selective:		
4-DAMP	9.1	Eglen & Whiting (1988)
UH-AH 37	7.9	Eberlein *et al.* (1989)
HHSiD	8.0	This study
pFHHSiD	7.1	Eglen *et al.* (1990)
Non-selective:		
Ipratropium	9.6	Roffel (1990)

The table is based on studies in which pA_2 values were determined from Schild plots with slopes not different from unity. For abbreviations, see text.

Methods

Tissue preparation

Guinea-pigs were killed by a blow to the head and exsanguinated. The trachea was rapidly removed, placed in a prewarmed (37°C) and oxygenated (95% O_2 plus 5% CO_2) medium (composition in mmol l^{-1}: NaCl 137, KCl 2.7, $CaCl_2$ 1.8, $MgCl_2$ 1.05, $NaHCO_3$ 11.9, NaH_2PO_4 0.42, D-glucose 5.6 and choline chloride 0.001) and gently cleaned from adhering

[1] Author for correspondence.

connective tissue. Unless stated otherwise, the epithelium was removed by rubbing the luminal surface with a moistened stem-pipe cleaner. This method was found consistently to cause complete removal of epithelium without damaging other tissue structures. A clip-connected strip was then prepared from one trachea as described in detail by D'Agostino et al. (1990).

Outflow of ^3H activity

The strip was suspended isometrically under a tension of 1 g in a 2 ml organ bath and superfused at a rate of 2 ml min^{-1} during a 30 min equilibration period. Superfusion was then stopped and the preparation incubated for 60 min with [^{3}H]-choline (2.5 μCi ml^{-1}; final concentration 1 μmol l^{-1}) under electrical stimulation. Square wave pulses of 1 ms duration were applied by two platinum electrodes positioned parallel to the trachea strip. The voltage drop between the electrodes was 10 V cm^{-1} and the stimulation frequency 20 Hz (trains of 100 impulses applied at intervals of 30 s). At the end of the incubation the strip was superfused with medium that contained in addition 10 μmol l^{-1} hemicholinium-3. After 90 min of washout the superfusate was collected continuously in 3 min fractions. In most experiments five stimulation periods were carried out on each preparation (S_1–S_5; generally in 27 min intervals). Each stimulation period consisted of 600 impulses applied in trains of 100 impulses at a frequency of 20 Hz in intervals of 30 s. The first stimulation started 9 min after the end of the washout period. Tritium content of the samples was measured by liquid scintillation spectrometry and corrected for the counting efficiency by the external standardisation method. The stimulation-evoked outflow of ^{3}H activity was calculated from the difference between the total outflow during the stimulation plus the following 9 min, and the basal outflow. The basal outflow was assumed to decline linearly from the two samples immediately preceding the stimulation to the two samples 15–21 min after the onset of stimulation.

Testing of antagonists

Muscarinic antagonists were added after S_1 to the perfusion medium in cumulatively increasing concentrations so that complete concentration-response curves for both pre- and postjunctional effects were obtained in each experiment (cf. Figures 3 and 4). Depending on the concentrations tested, the antagonists were added to the medium either 24 min (<10 nmol l^{-1}), 18 min (0.01–1 μmol l^{-1}) or 15 min (>1 μmol l^{-1}) before the onset of the respective stimulation. The prejunctional effects of the drugs were expressed as ratios S_x/S_1 (S_x: $S_2 - S_5$).

Contractions of the smooth muscle were recorded simultaneously with a force displacement transducer and displayed on a Hellige recorder. The peak tension developed by all twitches during S_1 were added up, and this total was compared to that obtained by adding up the individual responses in S_2, S_3, S_4 and S_5.

Concentration-response curves for pre- and postjunctional effects were constructed by expressing the ratio S_x/S_1 in the presence of an antagonist as a percentage of the equivalent ratio obtained in control experiments in the absence of antagonists. The concentrations which produced half-maximal responses (EC_{50}) were determined graphically from individual concentration-response curves on a semilogarithmic plot.

Separation of labelled choline and acetylcholine

In some experiments the nature of radioactivity released by electrical stimulation was determined. In these studies the amount of [^{3}H]-choline used for labelling was increased to 5 μCi ml^{-1}, and superfusion rate was reduced to 1 ml min^{-1}. Neostigmine (10 μmol l^{-1}) and hyoscine (0.1 mol l^{-1}) were present in the superfusion medium from 30 min before the stimulation onwards. [^{14}C]-choline (2 nCi) and [^{14}C]-acetylcholine (2–4 nCi) were added to each superfusate sample as internal standards. Labelled acetylcholine and choline were extracted from the medium by ion-pair extraction with tetraphenylborate/allylcyanid and separated by thin-layer chromatography as described earlier (Kilbinger & Nafziger, 1985). The ion-pair extraction is selective for acetylcholine and choline, and phosphorylcholine in particular is not extracted from the aqueous into the organic phase (Barker et al., 1972; Lindmar et al., 1982). Recoveries were determined in separate experiments by adding authentic [methyl-^{3}H]-choline and [acetyl-^{3}H]-choline (each 10 nCi) to 5 ml of the physiological salt solution. The samples were carried through the above mentioned procedure of ion-pair extraction and thin layer chromatography and the recoveries were 97 $\pm$ 3% for acetylcholine and 88 $\pm$ 5% for choline (each $n = 3$).

Determination of postjunctional pA_2 values

The epithelium-free trachea was cut spirally, divided into sections 1–2 cm long and suspended isometrically under a tension of 1 g in a physiological salt solution (composition see above) at 37°C. Following an equilibrium period of 1 h the tissue was exposed, on 3 occasions, to 10 μmol l^{-1} of acetylcholine. Only when consistent responses were obtained to this concentration of acetylcholine were experiments performed. Cumulative concentration-response curves to oxotremorine were then constructed using successive concentrations incrementally spaced at 0.5 log intervals. After construction of the first concentration-response curve, the preparation was washed at 10 min intervals for 30 min, during which time the tension returned to baseline levels. The preparation was then exposed for 30 min to the antagonist, and a second curve to oxotremorine was constructed. All contraction heights were expressed as a percentage of the maximal effect of oxotremorine in the first curve. Parallel control experiments without antagonist were performed under identical conditions. These control experiments allowed for any correction to be made for changes in sensitivity to oxotremorine. The pA_2 values were determined from Schild plots by regression analysis (Arunlakshana & Schild, 1959).

Statistics

Results are given as means $\pm$ s.e.mean. EC_{50} values were converted to logarithmic form before the values from individual experiments were averaged and the s.e. were calculated. Statistical testing (two-tailed t test) was performed with the negative logarithms of the EC_{50} values. If one control group was compared with more than one group of treatments a one way analysis of variance was performed followed by Dunnett's test (Dunnett, 1964).

Drugs

[Methyl-^{3}H]-choline (NEN, Dreieich, F.R.G.); AF-DX 116; AQ-RA 741 (11-[[4-[4-(diethylamino)butyl]-1-piperidinyl]-acetyl]-5,11-dihydro-6H-pyrido[2,3-b][1,4]benzodiazepine-6-one hydrochloride); pirenzepine dihydrochloride monohydrate; UH-AH 37 (6-chloro-5,10-dihydro-5-[(1-methyl-4-piperidinyl)-acetyl]-11H-dibenzo-[b,e][1,4]diazepine-11-one hydrochloride) (all gifts from Thomae, Biberach, F.R.G.); 4-DAMP (4-diphenyl-acetoxy-N-piperidine methobromide; gift from Dr Barlow, Bristol, U.K.); hexahydrosiladiphenidol hydrochloride (HHSiD); *para*-fluorohexahydrosiladiphenidol hydrochloride (pFHHSiD) (gifts from Profs. Lambrecht and Mutschler, Frankfurt, F.R.G.); hyoscine hydrobromide; oxotremorine sesquifumarate (Sigma, St. Louis, MO, U.S.A.); ipratropium bromide (Boehringer, Ingelheim, F.R.G.); methoctramine hydrochloride (RBI, Natick, MA, U.S.A.).

Results

Outflow of ^3H activity from strips preincubated with [^3H]-choline

In a first series of experiments the outflow of ^3H activity was characterized. Intermittent stimulation at 20 Hz caused an increase in outflow which was similar from epithelium-free strips (S_1: 1284 ± 276 d.p.m. mg^{-1}; $n = 5$) and from epithelium-containing preparations (S_1: 1058 ± 253 d.p.m. mg^{-1}; $n = 6$). Omission of calcium from the medium accelerated the basal outflow from both preparations (Figure 1). The stimulation-evoked outflow from epithelium-free strips was abolished, whereas the outflow from strips with the epithelium present was not reduced but slightly enhanced in the absence of extracellular calcium. Contractions of the trachealis muscle in response to electrical stimulation were abolished in both types of preparations.

The outflow of ^3H activity from epithelium-free strips was further analyzed after separation of [^3H]-acetylcholine and [^3H]-choline in the superfusate which contained neostigmine plus hyoscine. Electrical stimulation caused an increase in outflow of ^3H activity which consisted of 104 ± 11% ($n = 4$) of [^3H]-acetylcholine (Figure 2). The outflow of [^3H]-choline remained unchanged. The sum of labelled choline and acetylcholine in the samples of spontaneous outflow before and after stimulation accounted for 98 ± 6% (0–5 min) and 97 ± 9% (25–30 min), respectively, of the total ^3H radioactivity.

In some experiments the effects of oxotremorine on the evoked outflow of ^3H activity were studied. Strips were stimulated twice (S_1, S_2; 20 Hz, 600 pulses) and 1 μmol l^{-1} oxotremorine was added 18 min before S_2. In the presence of oxotremorine the electrically-evoked outflow of ^3H activity from epithelium-free trachea strips was only 27 ± 5% ($n = 7$) of that elicited during S_1. The calcium-independent outflow from strips with the epithelium present was not significantly affected by oxotremorine and was 96 ± 17% ($n = 4$) of that caused by S_1.

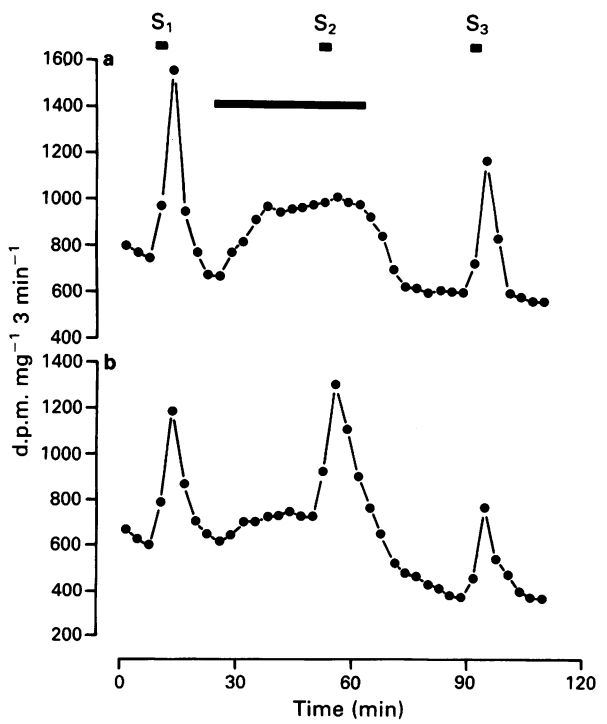


Figure 1 The effect of calcium withdrawal on the outflow of ^3H activity from epithelium-free (a; $n = 5$) and epithelium-containing (b; $n = 6$) tracheal preparations preincubated with [^3H]-choline (5 μCi). Time '0 min' (abscissa scale) corresponds to the end of the 90 min washout period. Each stimulation period (S_1, S_2, S_3) consisted of 6 trains of 100 pulses delivered at intervals of 30 s at a frequency of 20 Hz. Calcium was omitted from the superfusion medium as indicated by the horizontal bar. Given are mean values; standard errors were 4–18% of corresponding means.

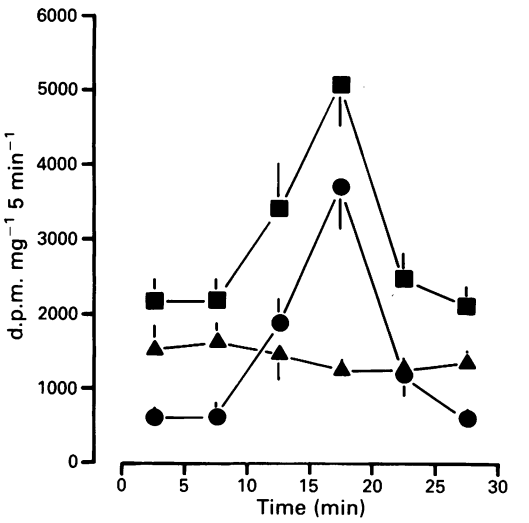


Figure 2 Outflow of total ^3H radioactivity (■), [^3H]-acetylcholine (●) and [^3H]-choline (▲) from epithelium-free tracheal strips that had been preincubated with [^3H]-choline (10 μCi). The tissue was stimulated electrically from 10–13 min (trains of 100 pulses delivered every 30 s at 20 Hz). Each point represents the mean of 4 experiments; vertical lines show s.e.mean.

Effects of muscarinic antagonists on outflow and contractions in epithelium-free strips

Strips were stimulated five times (S_1–S_5) and the antagonists were added cumulatively. Figures 3 and 4 show representative time courses of the experiments. In the control experiments the outflow evoked by S_2, S_3, S_4 and S_5 was 81 ± 3, 68 ± 3,

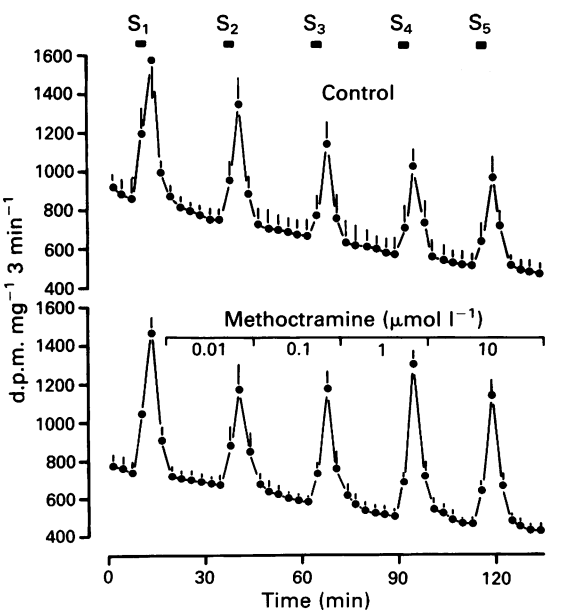


Figure 3 Effects of methoctramine on the field stimulation-evoked outflow of ^3H radioactivity from tracheal strips that had been preincubated with [^3H]-choline. Stimulation periods are indicated at the top of the figure (S_1–S_5; 20 Hz, 600 pulses applied in trains of 100 pulses every 30 s). Horizontal bar indicates superfusion with increasing concentrations of methoctramine ($n = 6$). Upper curve, control experiments ($n = 7$). Values are mean with s.e.mean indicated by the vertical lines.

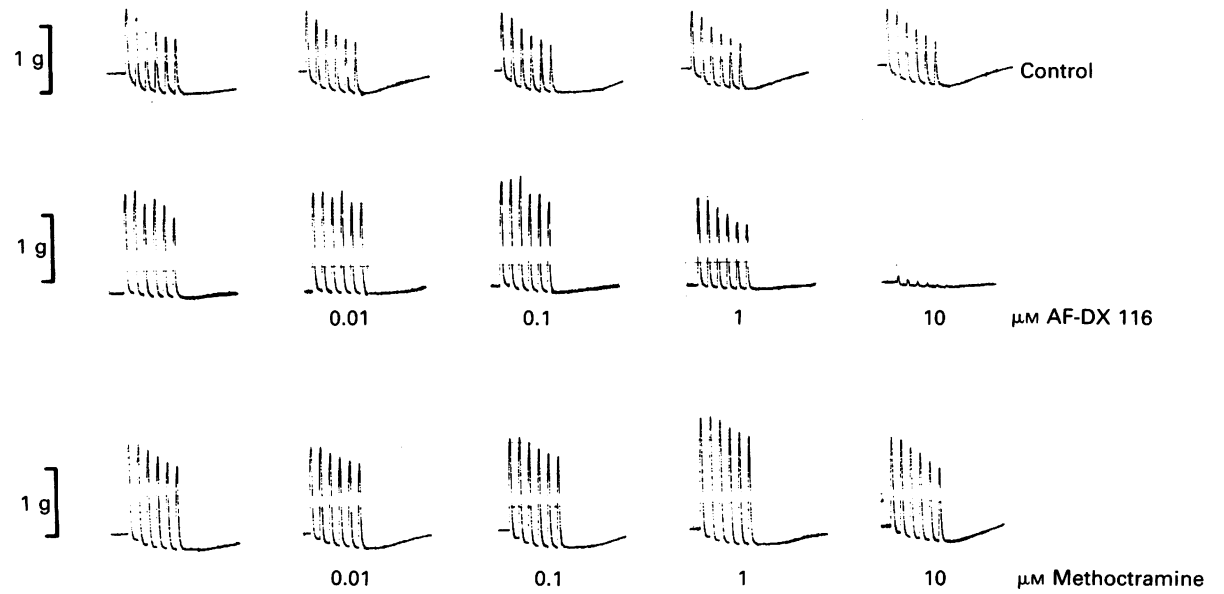


Figure 4 Typical responses of the trachealis muscle to electrical field stimulation (S_1–S_5) in the presence of increasing concentrations of AF-DX 116 and methoctramine. Upper panel, control experiment. Each stimulation period consisted of 6 trains of 100 pulses delivered at 20 Hz in 30 s intervals. Horizontal line, 1 g.

67 ± 3 and 56 ± 3% (n = 19), respectively, of that caused by S_1. All antagonists produced concentration-dependent increases in the evoked outflow (Figure 5). Some antagonists showed bell-shaped prejunctional concentration-response curves which may be due to an unspecific inhibitory effect of the large concentrations on the evoked outflow. None of the compounds affected the basal outflow of tritium. The increase in outflow by low concentrations of the M_2-selective antagonists methoctramine, AF-DX 116 and AQ-RA 741 was paralleled by a significant enhancement of the stimulation-evoked contractile response and only higher concentrations of these drugs inhibited the contractions. It should be noted that methoctramine up to 10 μmol l^{-1} failed to reduce significantly the postjunctional response. In separate experiments in which the effect of 50 μmol l^{-1} methoctramine was tested, a significant inhibition (by 71 ± 7%, n = 4) of the electrically-evoked contraction was found. The M_3-selective antagonists UK-AH 37, 4-DAMP and pFHHSiD displayed another pattern: stimulation-evoked contractions were already largely inhibited at concentrations that did not yet significantly increase the evoked outflow.

The negative logarithms of the pre- and postjunctional EC_{50} values are given in Table 2. M_2-selective antagonists (methoctramine, AF-DX 116, AQ-RA 741) were more potent contraction was found. The M_3-selective antagonists UH-AH 37, 4-DAMP and pFHHSiD at the postjunctional receptors. Surprisingly, HHSiD did not discriminate between pre- and postjunctional muscarinic receptors. Likewise, hyoscine, ipratropium and pirenzepine had similar potencies at pre- and postjunctional receptors.

Since the relaxation response elicited by field stimulation (cf. Figure 4) might have been mediated by the release of noradrenaline, we have studied the effects of propranolol. The tracheal strips were stimulated twice (20 Hz, 600 pulses) and 1 μmol l^{-1} propranolol was added 18 min before the second stimulation. In the presence of propranolol the relaxation remained unchanged and the electrically evoked ^3H outflow was not affected (111 ± 6% of the control value, n = 4). The pre- and postjunctional effects of the M_2- and M_3-selective compounds AF-DX 116 and 4-DAMP were also studied in the presence of 1 μmol l^{-1} propranolol. The −log of the pre- and postjunctional EC_{50} values for AF-DX 116 (7.58 ± 0.53 and 5.53 ± 0.06; n = 3) and for 4-DAMP (7.61 ± 0.12 and 8.85 ± 0.26; n = 3) were not different from the respective values in Table 2. All this shows that under the present experimental conditions a possible effect of endogenously released noradrenaline could not be detected, and that the relaxation of the smooth muscle is probably due to the release of a non-adrenergic non-cholinergic inhibitory transmitter.

Postjunctional pA_2 values

To our knowledge pA_2 values for the effects of HHSiD and AQ-RA 741 on guinea-pig trachealis smooth muscle have not

Table 2 Comparison of pre- and postjunctional potencies of muscarinic antagonists in the guinea-pig isolated trachea

Antagonist	$-log\ EC_{50}\ pre$	$-log\ EC_{50}\ post$	$\frac{EC_{50}\ pre}{EC_{50}\ post}$
Pirenzepine	7.08 ± 0.18	6.83 ± 0.10	0.56
Methoctramine	6.84 ± 0.16	4.55 ± 0.06**	0.005
AF-DX 116	7.48 ± 0.25	5.55 ± 0.05**	0.011
AQ-RA 741	7.53 ± 0.24	6.24 ± 0.09**	0.05
HHSiD	7.40 ± 0.10	7.26 ± 0.15	0.72
pFHHSiD	6.02 ± 0.16	6.82 ± 0.06**	6.3
UH-AH 37	6.70 ± 0.13	7.58 ± 0.03**	7.6
4-DAMP	7.78 ± 0.18	8.89 ± 0.11*	12.9
Hyoscine	8.85 ± 0.38	8.89 ± 0.21	1.1
Ipratropium	8.95 ± 0.23	8.53 ± 0.03	0.38

The $-log\ EC_{50}$ values are mean ± s.e.mean of 4–8 experiments. Significance of difference between pre- and postjunctional $-log\ EC_{50}$ values: * $P < 0.05$; ** $P < 0.01$ (paired t test). Values for methoctramine were compared by unpaired t test since prejunctional (n = 6) and postjunctional (n = 4) EC_{50} values were determined in separate experiments.

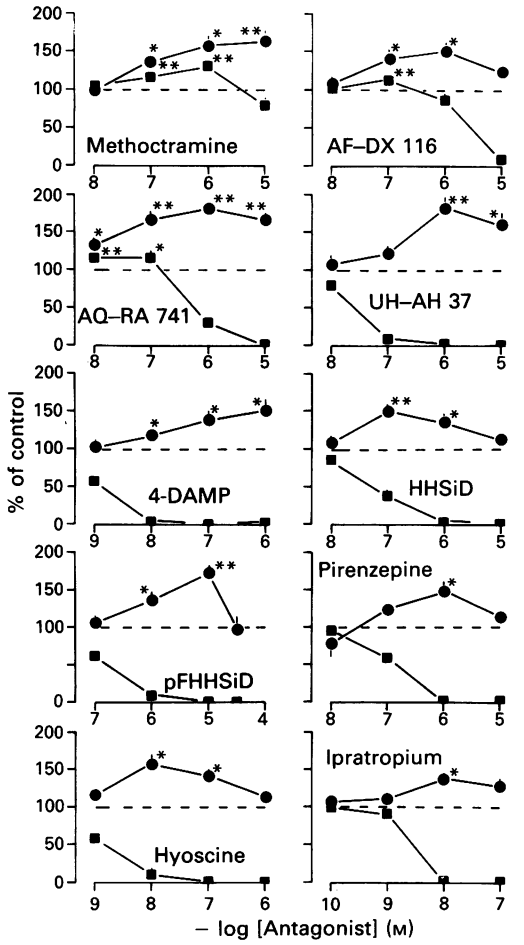


Figure 5 Effects of muscarinic receptor antagonists on outflow of ^3H activity (●) and smooth muscle contraction (■) evoked by electrical stimulation of epithelium-free tracheal preparations. Tracheal strips were stimulated 5 times and the antagonists added in cumulatively increasing concentrations before each stimulation period. Control experiments were run in parallel, and the effects of the antagonists are given as a percentage of the corresponding control value. Each point is the mean (s.e.mean shown by vertical lines) of 4–8 experiments. Significance of increases in ^3H outflow and muscle contractions: $^*P < 0.05$; $^{**}P < 0.01$ (ANOVA followed by Dunnett's test).

been reported before. HHSiD (0.01, 0.1, 1.0 and 10 μmol l^{-1}; each $n = 4$) and AQ-RA 741 (0.1, 0.3, 1.0 and 3.0 μmol l^{-1}; each $n = 4$) caused parallel shifts to the right of the concentration-response curves for oxotremorine without affecting the maximal contraction. When the log (concentration ratio − 1) was plotted against log antagonist concentration, straight regression lines were obtained with slopes of 0.99 ± 0.08 (HHSiD; mean ± s.d.) and 0.97 ± 0.07 (AQ-RA 741). The pA_2 values (with confidence limits) were 7.95 (7.69–8.28) for HHSiD, and 7.08 (6.93–7.27) for AQ-RA 741.

Discussion

Release of [^3H]-acetylcholine from guinea-pig trachea

Intermittent field stimulation of the epithelium-free trachea strip that had been preincubated with [^3H]-choline causes an outflow of ^3H activity which for the following reasons is thought to be a reliable indicator for release of [^3H]-acetylcholine: the evoked outflow is calcium-dependent, and as shown recently (D'Agostino *et al.*, 1990), is abolished by tetrodotoxin. Furthermore, the electrically evoked outflow of ^3H activity consists of 100% [^3H]-acetylcholine, and the sum of labelled choline and acetylcholine during rest and field stimulation is about 100% of the outflow of the total ^3H radioactivity (Figure 2). This suggests that a release of other [^3H]-choline metabolites does not contribute to the outflow of ^3H activity from the present epithelium-free preparation. On the other hand, most of the ^3H outflow evoked by field stimulation of an epithelium-containing trachea was [^3H]-phosphorylcholine in addition to [^3H]-acetylcholine, whereas field stimulation of an epithelium-free trachea preparation did not elicit a significant release of [^3H]-phosphorylcholine (Wessler *et al.*, 1990). The release of ^3H activity from the epithelium-containing trachea is not blocked by tetrodotoxin (Wessler *et al.*, 1990) and presumably arises from non-neural cells. In the present experiments the evoked outflow of this non-neuronal ^3H activity was neither reduced by the agonist oxotremorine nor by omission of calcium from the medium. On the other hand, oxotremorine strongly inhibited the evoked outflow of neuronal [^3H]-acetylcholine from the epithelium-free tracheal strip stimulated intermittently at 20 Hz.

Characterization of the prejunctional muscarinic receptor

Comparison of pre- and postjunctional potencies of the antagonists shows that the muscarinic receptors located at both sites of the cholinergic neuroeffector junction are pharmacologically different. The postjunctional receptor has been classified in the past as an M_3 receptor, and this has been corroborated in the present study (Table 1). Our pA_2 value obtained with the M_3-selective antagonist HHSiD (7.95) agrees with the value found at the M_3 receptor of the ileal smooth muscle (8.22; Fuder *et al.*, 1985). Further, the present value for the cardioselective antagonist AQ-RA 741 (7.08) is close to the pA_2 value obtained at ileal M_3 receptors (6.55) and distinctly different from that at cardiac M_2 receptors (8.49; Doods & Ziegler, 1989). Finally, the rank order of the postjunctional $-\log EC_{50}$ values (Table 2) is similar to the rank order of the pA_2 values for these antagonists at the trachealis muscle (Table 1) and also identifies the muscular receptor as an M_3 receptor.

Pirenzepine did not discriminate between pre- and postjunctional effects, which suggests that the autoreceptor is not an M_1 receptor. Several lines of evidence indicate that the prejunctional receptor is similar to the M_2 subtype. Firstly, low concentrations of the M_2-selective antagonists methoctramine, AF-DX 116 and AQ-RA 741 increased the contractile response to electrical stimulation, presumably due to selective facilitation of acetylcholine release. A similar enhancement of cholinergic neurotransmission through selective blockade of prejunctional muscarinic receptors by methoctramine has also been observed on the sphincter muscle of guinea-pig iris (Bognar *et al.*, 1990). Secondly, AQ-RA 741, AF-DX 116 and methoctramine were 20–200 times more potent at pre- than at postjunctional receptors. It should be noted that for methodological reasons the postjunctional $-\log EC_{50}$ value for methoctramine is somewhat too low (and hence the ratio EC_{50} pre/EC_{50} post too low) since a possible inhibitory effect of low concentrations of methoctramine on muscle contraction is masked by the enhanced acetylcholine release. Nevertheless, the differences in pre- and postjunctional potencies are close to the differences between the pA_2 values at M_2 receptors in guinea-pig atria (methoctramine: 7.7–8.1, Melchiorre, 1988; AF-DX 116: 7.3, Micheletti *et al.*, 1987; AQ-RA 741: 8.5, Doods & Ziegler, 1989) and postjunctional M_3 receptors of the trachea (cf. Table 1). Thirdly, the M_3-selective antagonists pFHHSiD, UH-AH 37 and 4-DAMP were 6–13 times more potent at the postjunctional than at the prejunctional receptor. Again, these differences in potencies correspond to the differences in pA_2 values determined on M_3 receptors (Table 1) and on cardiac M_2 receptors (4-DAMP: 7.6, Barlow *et al.*, 1976; UH-AH 37: 7.1, Doods & Ziegler, 1989; pFHHSiD: 6.0, Lambrecht *et al.*, 1988).

The pre- and postjunctional potencies of the non-selective antagonists hyoscine and ipratropium were similar. Ipratropium was included since this antagonist increased *in vivo* the

vagally induced bronchoconstriction even at very low doses which had no effect on postjunctional muscarinic receptors (Fryer & Maclagan, 1987). In our experiments ipratropium was the most potent of the ten antagonists at the autoreceptor, but ipratropium displayed no preferential effect at the prejunctional receptor. This was to be expected because the affinity of ipratropium for M_2 receptors (pA_2 8.8; Van Charldorp *et al.*, 1989) is not higher than that for M_3 receptors (pA_2 9.6; Roffel, 1990).

So far, the data of our study suggest that the prejunctional muscarinic receptor belongs to the M_2 subtype. However, HHSiD did not discriminate between pre- and postjunctional effects, although HHSiD is known to be about 50 times more potent on M_3 than on M_2 receptors (Mutschler & Lambrecht, 1984; Fuder *et al.*, 1985). Moreover, the difference in potency between hyoscine and HHSiD at the prejunctional muscarinic receptor (28 fold, Table 2) is much smaller than the difference in the affinities at cardiac M_2 receptors (630 fold) where pA_2 values of 9.1 (hyoscine, Fuder *et al.*, 1981) and 6.3 (HHSiD, Fuder *et al.*, 1985) were determined. The findings with HHSiD cannot be explained by the occurrence of a mixture of M_2 and M_3 receptors since the other selective antagonists clearly discriminated between both subtypes. Differences in the diffusion of HHSiD to pre- and postjunctional muscarinic receptors can also not account for the atypical behaviour of HHSiD because pre- and postjunctional effects were measured in the same experiment. The classification of muscarinic receptor subtypes has recently been extended by the cloning of 5 distinct subtypes (ml-m5; Bonner, 1989). The m4 gene encodes a muscarinic receptor with the greatest homology to the cardiac m2 receptor. Binding studies showed that the m4 gene product displayed a relatively high affinity not only for the M_2-selective antagonists AF-DX 116 and methoctramine but also for HHSiD (Buckley *et al.*, 1989). However, classification of the autoreceptor in the guinea-pig trachea as an M_4 subtype appears premature until selective antagonists for the M_4 receptor become available.

In conclusion, the depolarization-evoked release of acetylcholine from the guinea-pig trachea is inhibited by an 'M_2-like' autoreceptor. The autoreceptor differs from the cardiac M_2 receptor in its relatively high affinity for HHSiD. The selective blockade of the prejunctional receptor by methoctramine, AF-DX 116 and AQ-RA 741 has postjunctional consequences and leads to enhanced muscle contraction. If the vagus nerve in human airways were also endowed with similar autoreceptors, such drugs could enhance vagally induced bronchoconstriction.

This work was supported by the Deutsche Forschungsgemeinschaft (Ki 210/6-4). We are grateful to Drs Barlow, Lambrecht and Mutschler for gifts of 4-DAMP, HHSiD and pFHHSiD and the pharmaceutical companies for donation of AF-DX 116, AQ-RA 741, ipratropium, pirenzepine and UH-AH 37. The paper contains parts of the Dr. med. Theses of R.S. and H.S.

References

ARUNLAKSHANA, O. & SCHILD, H.O. (1959). Some quantitative uses of drug antagonists. *Br. J. Pharmacol. Chemother.*, **14**, 48–58.

BARKER, L.A., DOWDALL, M.J. & WHITTAKER, V.P. (1972). Choline metabolism in the cerebral cortex of guinea pigs. *Biochem. J.*, **130**, 1063–1080.

BARLOW, R.B., BERRY, K.J., GLENTON, P.A.M., NIKOLAOU, N.M. & SOH, K.S. (1976). A comparison of affinity constants for muscarine-sensitive acetylcholine receptors in guinea-pig atrial pacemaker cells at 29°C and in ileum at 29°C and 37°C. *Br. J. Pharmacol.*, **58**, 613–620.

BOGNAR, I., WESNER, M.T. & FUDER, H. (1990). Muscarine receptor types mediating autoinhibition of acetylcholine release and sphincter contraction in the guinea-pig iris. *Naunyn-Schmiedebergs Arch. Pharmacol.*, **341**, 22–29.

BONNER, T.I. (1989). The molecular basis of muscarinic receptor diversity. *Trends Neurosci.*, **12**, 148–151.

BUCKLEY, N.J., BONNER, T.I., BUCKLEY, C.M. & BRANN, M.R. (1989). Antagonist binding properties of five cloned muscarinic receptors expressed in CHO-K1 cells. *Mol. Pharmacol.*, **35**, 469–476.

D'AGOSTINO, G., CHIARI, M.C., GRANA, E., SUBISSI, A. & KILBINGER, H. (1990). Muscarinic inhibition of acetylcholine release from a novel *in vitro* preparation of the guinea-pig trachea. *Naunyn-Schmiedebergs Arch. Pharmacol.*, **342**, 141–145.

DOODS, H.N. & ZIEGLER, H.W. (1989). AQ-RA 741 and UH-AH 37—two pirenzepine analogues with an opposite selectivity for atrial and ileal muscarinic receptors. *Trends Pharmacol. Sci.*, **10** (Suppl.), 113.

DUNNETT, C.W. (1964). New tables for multiple comparisons with a control. *Biometrics*, **20**, 482–491.

EBERLEIN, W.G., ENGEL, W., MIHM, G., RUDOLF, K., WETZEL, B., ENTZEROTH, M., MAYER, N. & DOODS, H.N. (1989). Structure-activity relationships and pharmacological profile of selective tricyclic antimuscarinics. *Trends Pharmacol. Sci.*, **10** (Suppl.), 50–54.

EGLEN, R.M. & WHITING, R.L. (1988). Comparison of the muscarinic receptors of the guinea-pig oesophageal muscularis mucosae and trachea *in vitro*. *J. Auton. Pharmacol.*, **8**, 181–189.

EGLEN, R.M., MICHEL, A.D., MONTGOMERY, W.W., KUNYSZ, E.A., MACHADO, C.A. & WHITING, R.L. (1990). The interaction of *para*-fluorohexahydrosiladiphenidol at muscarinic receptors *in vitro*. *Br. J. Pharmacol.*, **99**, 637–642.

FRYER, A.D. & MACLAGAN, J. (1984). Muscarinic inhibitory receptors in pulmonary parasympathetic nerves in the guinea-pig. *Br. J. Pharmacol.*, **83**, 973–978.

FRYER, A.D. & MACLAGAN, J. (1987). Ipratropium bromide potentiates bronchoconstriction induced by vagal nerve stimulation in the guinea-pig. *Eur. J. Pharmacol.*, **139**, 187–191.

FUDER, H., MEISER, C., WORMSTALL, H. & MUSCHOLL, E. (1981). The effects of several muscarinic antagonists on pre- and postsynaptic receptors in the isolated rabbit heart. *Naunyn-Schmiedebergs Arch. Pharmacol.*, **316**, 31–37.

FUDER, H., KILBINGER, H. & MÜLLER, H. (1985). Organ selectivity of hexahydrosiladifenidol in blocking pre- and postjunctional muscarinic receptors studied in guinea-pig ileum and rat heart. *Eur. J. Pharmacol.*, **113**, 125–127.

HULME, E.C., BIRDSALL, N.J.M. & BUCKLEY, N.J. (1990). Muscarinic receptor subtypes. *Annu. Rev. Pharmacol. Toxicol.*, **30**, 633–673.

KILBINGER, H. & NAFZIGER, M. (1985). Two types of neuronal muscarine receptors modulating acetylcholine release from guinea-pig myenteric plexus. *Naunyn-Schmiedebergs Arch. Pharmacol.*, **328**, 304–309.

KILBINGER, H., WOLF, D. & D'AGOSTINO, G. (1990). Pre- and postjunctional effects of muscarine receptor antagonists in the isolated guinea pig trachea. *Naunyn-Schmiedebergs Arch. Pharmacol.*, **341**, R 79.

LAMBRECHT, G., FEIFEL, R., FORTH, B., STROHMANN, C., TACKE, R. & MUTSCHLER, E. (1988). *p*-Fluoro-hexahydrosiladifenidol: the first M2β-selective muscarinic antagonist. *Eur. J. Pharmacol.*, **152**, 193–194.

LINDMAR, R., LÖFFELHOLZ, K. & WEIDE, W. (1982). Interstitial washout and hydrolysis of acetylcholine in the perfused heart. *Naunyn-Schmiedebergs Arch. Pharmacol.*, **318**, 295–300.

MACLAGAN, J. & BARNES, P.J. (1989). Muscarinic pharmacology of the airways. *Trends Pharmacol. Sci.*, **10** (Suppl.), 88–92.

MELCHIORRE, C. (1988). Polymethylene tetramines: a new generation of selective muscarinic antagonists. *Trends Pharmacol. Sci.*, **9**, 216–220.

MICHELETTI, R., MONTAGNA, E. & GIACHETTI, A. (1987). AF-DX 116, a cardioselective muscarinic antagonist. *J. Pharmacol. Exp. Ther.*, **241**, 628–634.

MINETTE, P.A. & BARNES, P.J. (1988). Prejunctional inhibitory muscarinic receptors on cholinergic nerves in human and guinea pig airways. *J. Appl. Physiol.*, **64**, 2532–2537.

MUTSCHLER, E. & LAMBRECHT, G. (1984). Selective muscarinic agonists and antagonists in functional tests. *Trends Pharmacol. Sci.*, **5** (Suppl.), 39–44.

ROFFEL, A.F. (1990). Muscarinic receptor subtypes in airway smooth muscle. *PhD. Thesis, Groningen*, pp. 1–235.

STARKE, K., GÖTHERT, M. & KILBINGER, H. (1989). Modulation of neurotransmitter release by presynaptic autoreceptors. *Physiol. Rev.*, **69**, 864–989.

VAN CHARLDORP, K.J. & VAN ZWIETEN, P.A. (1989). Comparison of the muscarinic receptors in the coronary artery, cerebral artery

and atrium of the pig. *Naunyn-Schmiedebergs Arch. Pharmacol.*, **339**, 403–408.

WATSON, N., BARNES, P.J. & MACLAGAN, J. (1989). Evidence for an effect of methoctramine on ganglionic nicotinic cholinoceptors in the guinea-pig trachea *in vitro*. *Br. J. Pharmacol.*, **98**, 719P.

WESSLER, I., HELLWIG, H. & RACKE, K. (1990). Epithelium-derived inhibition of [^{3}H]acetylcholine release from the isolated guinea-pig trachea. *Naunyn-Schmiedebergs Arch. Pharmacol.*, **342**, 387–393.

(Received September 12, 1990
Revised February 4, 1991
Accepted February 22, 1991)

Br. J. Pharmacol. (1991), **103**, 1764–1768 © Macmillan Press Ltd, 1991

Heterogeneous involvement of endothelium in calcitonin gene-related peptide-induced relaxation in coronary arteries from rat

[1]Dolores Prieto, [1]Sara Benedito & [2]Niels C. Berg Nyborg

Department of Pharmacology, University of Aarhus, DK-8000 Aarhus C, Denmark

1 The effects of rat- and human-CGRP and capsaicin were studied in isolated rings of rat proximal epicardial (PC) and distal intramyocardial (DC) coronary arteries.

2 The relaxing effect of rat-CGRP was dependent on the level of vessel tone induced by prostaglandin $F_{2\alpha}$ ($PGF_{2\alpha}$) in PC but not in DC arteries. Submaximally contracted DC and PC arteries were more sensitive to rat- than human-CGRP. There was no difference in sensitivity to rat- and human-CGRP between PC and DC arteries.

3 Substance P elicited a small relaxation only in 4 of the 6 PC arteries tested. PC and DC arteries were concentration-dependently relaxed by capsaicin. The relaxation was partly inhibited by ruthenium red, thus suggesting that capsaicin causes specific release of CGRP from sensory nerve endings in rat coronary arteries.

4 The relaxant effect of rat-CGRP was antagonized by endothelium removal and indomethacin but not methylene blue in endothelium-intact PC arteries. The relaxation in DC arteries was not affected by any of these treatments, indicating a heterogeneous involvement of the endothelium in CGRP-mediated coronary vasodilatation and the release of a cyclo-oxygenase product in PC arteries in rats.

5 Glibenclamide had no inhibitory effect on the CGRP-induced relaxation of PC and DC arteries, thus excluding the involvement of glibenclamide-sensitive K^+-channels in the mechanism of action of CGRP in rat coronary arteries.

Keywords: Calcitonin gene-related peptide; endothelium; indomethacin; methylene blue; capsaicin; glibenclamide; coronary artery of rat

Introduction

The vasodilator effect of calcitonin gene-related peptide (CGRP) (Amara *et al.*, 1982) has been extensively studied in the coronary circulation of several mammals (Holman *et al.*, 1986; Franco-Cereceda *et al.*, 1987; Greenberg *et al.*, 1987; Shoji *et al.*, 1987; Franco-Cereceda, 1988; Bény *et al.*, 1989) including man (McEwan *et al.*, 1986; Franco-Cereceda & Lundberg, 1987; Thom *et al.*, 1987). CGRP-immunoreactivity is present in high concentration in cardiac tissue and in nerve fibres associated with coronary blood vessels (Mulderry *et al.*, 1985). CGRP may be released upon activation of cardiac sensory nerves by capsaicin and during ischaemia (Franco-Cereceda *et al.*, 1989).

The relaxation induced by CGRP has been reported to be endothelium-dependent in rat aorta (Brain *et al.*, 1985; Grace *et al.*, 1987) and some human vessels (Thom *et al.*, 1987) and also endothelium-independent in cat cerebral arteries (Edvinsson *et al.*, 1985), human skeletal muscle and pig splenic arteries (Pernow, 1989), rabbit mesenteric resistance arteries (Nelson *et al.*, 1990) and bovine (Greenberg *et al.*, 1987) and porcine coronary arteries (Franco-Cereceda *et al.*, 1987; Shoji *et al.*, 1987). The CGRP-induced relaxation of rabbit mesenteric resistance arteries may possibly be mediated through opening of K^+-channels which are blocked by glibenclamide (Nelson *et al.*, 1990).

The present study examines the relaxant effects of rat- and human-CGRP in rat proximal epicardial (PC) and distal intramyocardial (DC) coronary arteries in relation to the level of vascular tone, the presence of endothelium and involvement of secondary mediators.

Methods

Segments (1–2 mm long) of the proximal (PC) and distal (DC) part of the left anterior descending coronary artery in hearts obtained from 3 month old male Wistar rats were dissected as previously described (Nyborg, 1990) and mounted as ring preparations on two 40 μm diameter stainless steel wires on a double myograph (Mulvany & Nyborg, 1980) which allowed direct determination of the isometric wall tension while the internal circumference of the vessels was controlled.

After mounting, the arteries were equilibrated in physiological saline solution (PSS) at 37°C, pH 7.4 for 30 min. The vessels were then stretched to their optimal lumen diameter $l_0 = 0.9 \times l_{100}$, where l_{100} is an estimate of the diameter the vessels would have if subjected a passive transmural pressure of 13.3 kPa (100 mmHg), for active tension development (Nyborg *et al.*, 1987). The arteries were then repetitively stimulated with K-PSS (equivalent to PSS except that NaCl is exchanged with KCl on an equimolar basis) until reproducible responses were recorded. The maximal contractile capacity of the vessels (E_{max}) was estimated by activating the vessels with K-PSS to which prostaglandin $F_{2\alpha}$ ($PGF_{2\alpha}$) and 5-hydroxytryptamine, both 10^{-5} M, were added.

In the first series of experiments, cumulative concentration-response curves for rat-CGRP and human-CGRP, were constructed by using vessels submaximally (50–60% of E_{max}) or maximally (>70% of E_{max}) contracted with $PGF_{2\alpha}$ obtained by a final concentration of $PGF_{2\alpha}$ in the tissue bath between 10^{-7} M and 10^{-5} M. Because of the development of tachyphylaxis to rat- and human-CGRP, arterial segments were used only once when challenged with these agonists.

In a second series of experiments the role of the endothelium was determined by using two consecutive arterial segments; one was used as a control and the other segment had its endothelium removed as previously described (Nyborg, 1990). Successful removal of the endothelium was tested by the absence of relaxation to acetylcholine (10^{-5} M).

[1] Present address: Department of Physiology, Faculty of Veterinary Sciences, Universidad Complutense, 28040-Madrid, Spain.
[2] Author for correspondence.

Finally, the effect of rat-CGRP was tested after incubating the arteries with either indomethacin or methylene blue, both at 3×10^{-6} M, or 10^{-6} M glibenclamide, a blocker of the ATP-sensitive K^+-channels in arterial smooth muscle (Standen *et al.*, 1989). In this series of experiments, and also in those where the endothelium was removed, proximal coronary arteries were submaximally contracted with $PGF_{2\alpha}$ (10^{-7}–10^{-6} M).

PSS had the following composition (in mM): NaCl 119, NaH_2CO_3 25, KCl 4.7, $CaCl_2$ 1.5, KH_2PO_4 1.18, $MgSO_4$ 1.17, ethylene diamine tetraacetic acid (EDTA) 0.026 and glucose 11. K-PSS was similar to PSS escept that NaCl was exchanged for KCl on an equimolar basis.

Drugs used were rat- and human calcitonin gene-related peptide (CGRP), capsaicin, ruthenium red, 5-hydroxytryptamine creatinine sulphate complex, acetylcholine HCl (all Sigma, U.S.A.), prostaglandin $F_{2\alpha}$ (Dinoprost, UpJohn, Belgium), methylene blue (DAK, Denmark) and indomethacin (Merck, F.R.G.). Capsaicin was dissolved in 96% ethanol while other drugs were dissolved in distilled water. Stock solutions were stored at −20°C and dilutions were made just before experimentation.

Vessel responses are expressed as either active tension (Newton per meter of vessel wall, $N\,m^{-1}$) or as a percentage of the response induced by $PGF_{2\alpha}$. Sensitivities to the agonists are expressed as pD_2-values, where $pD_2 = -\log(EC_{50}[M])$, and $EC_{50}[M]$ is the agonist-concentration required to produce half-maximal relaxation. $EC_{50}[M]$s were estimated by fitting plots of responses (R) vs. concentration (A[M]) on a log-scale to the equation $R = R_{max} \times A[M]^n/(A[M]^n + EC_{50}[M]^n)$, where R_{max} is the maximal tissue response to agonist, using the commercial available GraphPAD programme. Results are given as mean ± s.e.mean, (number of vessels).

Differences between mean values were analyzed by Student's *t* test for paired or unpaired observation where appropriate. The level of significance was for both tests set at *P* values less than 0.05.

Results

Effect of initial vessel contraction on relaxation of PC and DC arteries

Concentration-response relations for rat- and human-CGRP in sub- and maximally $PGF_{2\alpha}$-contracted segments of PC and DC arteries with intact endothelium are shown in Figure 1. The maximal relaxation induced by rat-CGRP (3×10^{-8} M) was significantly ($P < 0.001$) greater in PC arteries contracted submaximally (50–60% of E_{max}) than in arteries contracted to a higher level (>70% of E_{max}) by $PGF_{2\alpha}$. Submaximally contracted PC arteries were more sensitive ($P < 0.05$) to rat- than human-CGRP, pD_2 values being 8.48 ± 0.03 ($n = 7$) and 8.12 ± 0.08 ($n = 9$).

The relaxation induced by rat-CGRP in DC arteries was in contrast to PC arteries independent of the magnitude of the preconstricting tone. Maximal relaxations were 85 ± 6% ($n = 4$) and 83 ± 4% ($n = 7$) and pD_2 values were 8.49 ± 0.09 ($n = 4$) and 8.53 ± 0.11 ($n = 7$) in DC arteries contracted with $PGF_{2\alpha}$ to 51 ± 5% ($n = 4$) and 81 ± 2% ($n = 7$) of E_{max}, respectively. DC arteries were also more sensitive ($P < 0.05$) to rat- than human-CGRP, pD_2 values being 8.52 ± 0.07 ($n = 11$) and 8.19 ± 0.10 ($n = 8$), respectively. PD_2 values in PC and DC arteries were not significantly different.

Effect of substance P and capsaicin

Substance P (SP) (10^{-10}–10^{-7} M) did not elicit a significant relaxation in rings of DC arteries with intact endothelium. However, SP induced a small relaxation, 10 ± 3% ($n = 4$) in 4 of 6 PC arteries contracted with 10^{-6} M $PGF_{2\alpha}$.

Capsaicin (10^{-6}–3×10^{-5} M) induced a concentration-dependent relaxation of PC and DC arteries (Figure 2). The maximal responses to capsiacin, 3×10^{-5} M, were 63 ± 7% ($n = 6$) and 66 ± 7% ($n = 6$) in PC and DC arteries, respectively. The capsaicin-induced relaxations were antagonized by 10^{-5} M ruthenium red (Figure 2). Higher concentration than 10^{-5} M of ruthenium red was not tested systematically because it caused a decrease in the $PGF_{2\alpha}$-induced contraction.

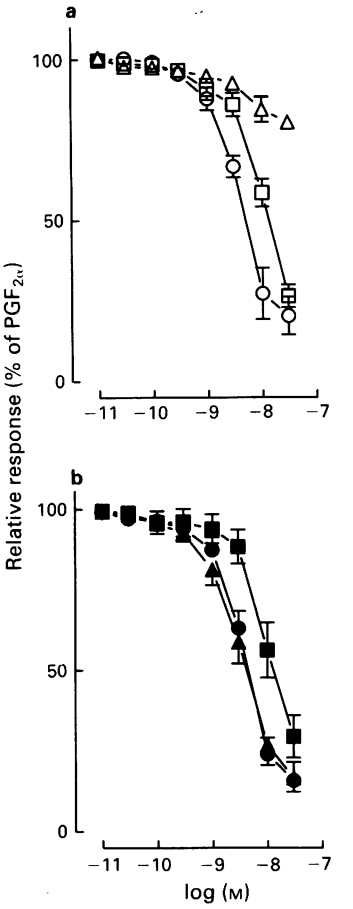


Figure 1 Relaxant effects of human-calcitonin gene-related peptide (CGRP) (squares) and rat-CGRP in proximal epicardial (a) and distal intra myocardial, (b) arteries submaximally (50–60% of E_{max}) (circles) and maximally (>70% of E_{max}) (triangles) contracted with prostaglandin $F_{2\alpha}$. Points represent mean values of 4–11 vessels. Vertical bars indicate s.e.mean where this value exceeds the size of symbol.

Effect of endothelium-denudation

Acetylcholine (ACh) (10^{-5} M) relaxed endothelium-intact and -denuded PC arteries 82 ± 5% ($n = 7$) and 8 ± 4% ($n = 6$) respectively. Removal of endothelium was accompanied by an increase in the spontaneous myogenic tone but the total active tension (spontaneous tone plus that induced by $PGF_{2\alpha}$) was always kept in a range between 50–60% of E_{max}, mean active tension being 52 ± 3% ($n = 6$) of E_{max}, in order to avoid bias comparing the relaxing effect of rat-CGRP in endothelium-intact and denuded arteries. The maximal relaxation elicited by rat-CGRP was significantly ($P < 0.001$) reduced in endothelium-denuded PC arteries compared to control vessels: 18 ± 5% ($n = 6$) vs. 80 ± 6% ($n = 7$), respectively (Figure 3a).

The 10^{-5} M ACh-induced relaxation of endothelium-intact and -denuded DC arteries was 83 ± 7% ($n = 6$) and 5 ± 3% ($n = 6$), respectively. The concentration-response relations for rat-CGRP were unaffected by the absence of endothelium in DC arteries (Figure 3b), pD_2 values being 8.42 ± 0.12 ($n = 6$) and 8.47 ± 0.09 ($n = 6$) and maximal relaxations 77 ± 4% ($n = 6$) and 74 ± 9% ($n = 6$) in endothelium-intact and -denuded arteries, respectively.

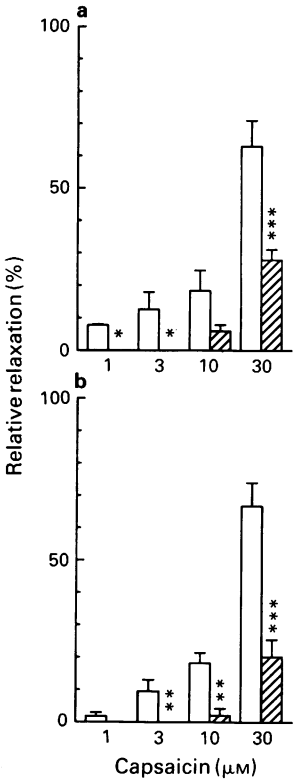


Figure 2 Columns showing the inhibitory action of 10^{-5} M ruthenium red (hatched columns) on the relaxant effect of capsaicin (open columns) in six rat proximal epicardial (a) and distal intramyocardial (b) arteries. Responses are expressed as relative relaxation of arteries contracted with 10^{-6} M prostaglandin $F_{2\alpha}$. Vertical lines show s.e.mean. $*P < 0.05$; $**P < 0.01$; $***P < 0.001$.

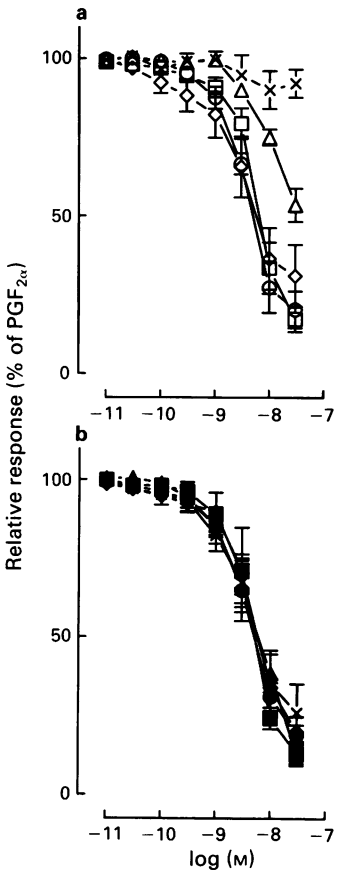


Figure 3 Rat-calcitonin gene-related peptide (CGRP) concentration-response relations of proximal epicardial (a) and distal intramyocardial (b) arteries in control condition (circles), and in presence of 3×10^{-6} M indomethacin (triangles), 3×10^{-6} M methylene blue (squares), 10^{-6} M glibenclamide (diamonds) and after removal of endothelium (crosses). Points show mean values of 3–15 observations. Vertical bars indicate s.e.mean where this value exceeds the size of symbol.

Effect of indomethacin, methylene blue and glibenclamide

Incubation of endothelium-intact PC arteries with 3×10^{-6} M indomethacin partially blocked the relaxation induced by rat-CGRP; maximal relaxations were $80 \pm 6\%$ ($n = 7$) and $52 \pm 3\%$ ($n = 7$) ($P < 0.001$) in the absence and presence of indomethacin, respectively (Figure 3a). However, the concentration-response curve for rat-CGRP in DC arteries was not affected by indomethacin (Figure 3b).

Methylene blue (3×10^{-6} M) and glibenclamide (10^{-6} M) had no effect on the relaxation induced by rat-CGRP in either PC or DC arteries (Figure 3).

Discussion

The present study demonstrates that CGRP induces potent relaxation of rat coronary arteries via endothelium-dependent and -independent mechanisms in the proximal and distal part of the left coronary artery, respectively, in rats. The present results are thus in agreement with earlier studies reporting that both rat- and human-CGRP evoke dose-dependent decreases in perfusion pressure in rat hearts (Al-Kazwini *et al.*, 1985; Holman *et al.*, 1986) and in agreement with *in vitro* studies on bovine (Greenberg *et al.*, 1987), porcine (Franco-Cereceda *et al.*, 1987; Shoji *et al.*, 1987; Bény *et al.*, 1989) and human (Franco-Cereceda & Lundberg, 1987) coronary arteries.

The magnitude of the CGRP-induced relaxation in PC arteries was, in contrast to DC arteries, highly dependent on the level of tone induced by $PGF_{2\alpha}$. Previous studies on mesenteric (Al-Kazwini *et al.*, 1986) and coronary (Shoji *et al.*, 1987) vascular smooth muscle have shown that the extent of relaxation elicited by CGRP is dependent on the type of vasoconstrictor used; thus CGRP was less effective when the arteries were contracted by high K^+-concentrations than by $PGF_{2\alpha}$. This suggests that the smooth muscle membrane potential may play an important role in determining the magnitude of relaxation induced by CGRP. However, the relaxation induced by CGRP was independent of the level of contraction in DC arteries suggesting either that the membrane potential is independent of the level of $PGF_{2\alpha}$-induced vessel tone or that the mechanism involved in the CGRP-mediated relaxation is independent of smooth muscle membrane potential as in pig distal coronary arteries (Bény *et al.*, 1989).

CGRP may be released from sensory nerve endings by myocardial ischaemia as well as by capsaicin (Franco-Cereceda *et al.*, 1989). Capsaicin may also induce release of other neuropeptides (Buck & Burks, 1986). Substance P had no effect in DC arteries at all and induced only a small and sporadic relaxation in PC arteries. Neuropeptide Y has only a constrictor effect in rat coronary arteries (Prieto *et al.*, 1990) and bradykinin is without effect (results not shown). Ruthenium red, which probably inhibits capsaicin-induced release of CGRP by a calcium-antagonistic action on sensory nerve endings (Maggi *et al.*, 1988), antagonized the relaxant effect of capsaicin in PC and DC arteries suggesting that at least a large part of the relaxation of these arteries is mediated primarily by release of CGRP. The density of CGRP-containing nerves or at least the amount of CGRP released in PC and DC arteries appears to be equal since the concentration-response relations to exogenous CGRP and capsaicin, respectively, were similar in these arteries. The concentration of capsaicin used to elicit mechanical responses in rat coronary

arteries is rather high compared to those necessary for responses in guinea-pig urinary bladder (Maggi *et al.*, 1989), bronchus and left atria (Maggi *et al.*, 1988).

Although the CGRP-receptor discriminated between human- and rat-CGRP there was no difference in effect of CGRP between PC (submaximally contracted) and DC arteries, as previously shown in the proximal and distal part of the guinea-pig mesenteric (Edvinsson *et al.*, 1989) arteries. However, there are important differences concerning the mechanisms underlying the CGRP-induced relaxation between large and small arteries in the rat coronary vascular bed. CGRP induced an endothelium-independent direct relaxation of DC vascular smooth muscle, which is consistent with that reported for pig (Franco-Cereda *et al.*, 1987; Shoji *et al.*, 1987) and bovine coronary arteries (Greenberg et al., 1987), and also for cerebral (Edvinsson *et al.*, 1985), splenic and skeletal muscle arteries (Pernow, 1989). In contrast, the relaxation induced by CGRP in PC arteries was almost totally dependent on the endothelium, which is partly consistent with that reported for rat aorta (Brain *et al.*, 1985; Kubota *et al.*, 1985; Grace *et al.*, 1987), where the response to CGRP was completely abolished after removal of the endothelium. It seems, therefore, that the action of CGRP in rat PC arteries may be a transition between that in aorta and small intramyocardial arteries. The transition may be attributed to the differential morphogenesis of the proximal and distal part of the coronary circulation which is derived from aortic and myocardial mesenchyme, respectively (Conte & Pellegrini, 1984).

The endothelial factor released by CGRP in PC arteries appears to be a cyclo-oxygenase product since indomethacin but not methylene blue had an inhibitory effect on the relaxation. The concentration of indomethacin used (3×10^{-6} M) did not antagonize the CGRP-induced relaxation to the same extent as did endothelium-denudation. This is probably due to a partial inhibition of the cyclo-oxygenase by indomethacin. We could not test this since unspecific relaxation of PC arteries occurs at higher concentrations of indomethacin (Nyborg & Mikkelsen, 1990).

There is much evidence in the literature that CGRP mediates its action through adenosine 3',5'-cyclic monophosphate (cyclic AMP) generation in endothelial and vascular smooth muscle cells (Edvinsson *et al.*, 1985; Kubota *et al.*, 1985; Grace *et al.*, 1987; Hirta *et al.*, 1988; Crossmann *et al.*, 1990). In addition, some of these studies demonstrated also that CGRP has no effect on cyclic GMP generation, which in part supports the lack of effect of methylene blue on the CGRP-induced relaxation of PC and DC arteries in the present study. However, Nelson *et al.* (1990) recently demonstrated that CGRP hyperpolarizes rabbit mesenteric resistance artery smooth muscle by opening K^+-channels, and that the hyperpolarization as well as the CGRP-induced relaxation of these arteries was reversed by glibenclamide, a blocker of ATP-sensitive K^+-channels (Standen, 1989). The present experiments do not confirm the involvement of glibenclamide-sensitive K^+-channels in the CGRP-induced relaxation of rat coronary arteries. However, this does not exclude the involvement of other types of K^+-channels in the direct CGRP-mediated smooth muscle relaxation in rat coronary arteries; this requires further studies on second messengers and on the effect of other K^+-channel inhibitors.

D.P. and S.B. were supported by the Spanish Ministry of Education and Science. This study was supported by the Danish Medical Research Council, Grant No. 12-7744 and 12-8717.

References

AL-KAZWINI, S.J., CRAIG, R.K., HOLMAN, J.J. & MARSHALL, I. (1985). Human and rat calcitonin gene related peptides (CGRP) are vasodilators in coronary and mesenteric vasculature. *Br. J. Pharmacol.*, **86**, 544P.

AL-KAZWINI, S.J., CRAIG, R.K., HOLMAN, J.J. & MARSHALL, I. (1986). Different potencies of calcitonin gene-related peptides (CGRP) on mesenteric vasculature constricted by noradrenaline or potassium. *Br. J. Pharmacol.*, **88**, 439P.

AMARA, S.G., JONAS, V., ROSENFELD, M.G., ONG, E.S. & EVANS, R.M. (1982). Alternative RNA processing in calcitonin gene expression generates mRNAs encoding different polypeptide products. *Nature*, **298**, 240–244.

BÉNY, J.L., BRUNET, P.C. & HUGGEL, H. (1989). Effects of substance P, calcitonin gene-related peptide and capsaicin on tension and membrane potential of pig coronary artery *in vitro*. *Regul. Pept.*, **25**, 25–36.

BUCK, S.H. & BURKS, T.F. (1986). The neuropharmacology of capsaicin: Review of some recent observations. *Pharmacol. Rev.*, **38**, 179–226.

BRAIN, S.D., WILLIAMS, T.J., TIPPINS, J.R., MORRIS, H.R. & MACINTYRE, I. (1985). Calcitonin gene-related peptide is a potent vasodilator. *Nature*, **313**, 54–56.

CONTE, G. & PELEGRINI, A. (1984). On the development of the coronary arteries in human embryos, stage 14–19. *Anat. Embryol.*, **169**, 209–218.

CROSSMAN, D.C., DASHWOOD, M.R., BRAIN, S.D., McEWAN, J. & PEARSON, J.D. (1990). Action of calcitonin gene-related peptide upon bovine vascular endothelial and smooth muscle cells grown in isolation and co-culture. *Br. J. Pharmacol.*, **99**, 71–76.

EDVINSSON, L., FREDHOLM, B.B., HAMEL, E., JANSEN, I. & VERRECCHIA, C. (1985). Perivascular peptides relax arteries concomitant with stimulation of cyclic AMP accumulation or release of an endothelium derived relaxing factor. *Neurosci. Lett.*, **58**, 213–220.

EDVINSSON, L., GULBENKIAN, S., JANSEN, I., WHARTON, J., CERVANTES, C. & POLAK, J.M. (1989). Comparison of peptidergic mechanisms in different parts of the guinea-pig superior mesenteric artery: immunocytochemistry at the light and ultrastructural levels and responses *in vitro* of large and small arteries. *J. Auton. Nerv. Syst.*, **28**, 141–154.

FRANCO-CERECEDA, A. (1988). Calcitonin gene-related peptide and tachykinins in relation to local sensory control of cardiac contractility and coronary vascular tone. *Acta Physiol. Scand.*, Suppl. **569**, 1–63.

FRANCO-CERECEDA, A. & LUNDBERG, J.M. (1987). Potent effects of neuropeptide Y and calcitonin gene-related peptide on human coronary vascular tone "*in vitro*". *Acta Physiol. Scand.*, **131**, 159–160.

FRANCO-CERECEDA, A., RUDEHILL, A. & LUNDBERG, J.M. (1987). Calcitonin gene-related peptide but not substance P mimics capsaicin induced coronary vasodilation in the pig. *Eur. J. Pharmacol.*, **142**, 235–243.

FRANCO-CERECEDA, A., SARIA, A. & LUNDBERG, J.M. (1989). Differential release of calcitonin gene-related peptide and neuropeptide Y from the isolated heart by capsaicin, ischemia, nicotine, bradykinin and ouabain. *Acta Physiol. Scand.*, **135**, 173–187.

GRACE, G.C., DUSTING, G.J., KEMP, B.E. & MARTIN, T.J. (1987). Endothelium and the vasodilator action of rat calcitonin gene-related peptide. *Br. J. Pharmacol.*, **91**, 729–733.

GREENBERG, B., RHODEN, K. & BARNES, P. (1987). Calcitonin gene-related peptide (CGRP) is a potent non-endothelium-dependent inhibitor of coronary vasomotor tone. *Br. J. Pharmacol.*, **92**, 789–794.

HIRATA, Y., TAKAGI, Y., TAKATA, S., FUKUDA, Y., YOSHIMI, H. & FUJITA, T. (1988). Calcitonin gene-related peptide receptor in cultured vascular smooth muscle and endothelial cells. *Biochem. Biophys. Res. Commun.*, **151**, 1113–1121.

HOLMAN, J.J., CRAIG, R.G. & MARSHALL, I. (1986). Human α- and β-CGRP and rat α-CGRP are coronary vasodilators in the rat. *Peptides*, **7**, 231–235.

KUBOTA, M., MOSELEY, J.M., BUTERA, L., MACDONALD, P.S. & MARTIN, T.J. (1985). Calcitonin gene-related peptide stimulates cyclic AMP formation in rat aortic smooth muscle cells. *Biochem. Biophys. Res. Commun.*, **132**, 88–94.

MAGGI, C.A., SANTOCIOLI, P., GEPPETTI, P., PARLANI, M., ASTOLFI, M., PRA DELLES, P., PATACCHINI, R. & MELI, A. (1988). The antagonism induced by Ruthenium Red of the actions of capsaicin on the peripheral terminals of sensory neurons: further studies. *Eur. J. Pharmacol.*, **154**, 1–10.

MAGGI, C.A., PATACCHINI, R., SANTOCIOLI, P., GIULIANI, S., BIANCO, E.D., GEPPETTI, P. & MELI, A. (1989). The 'efferent' function of capsiacin-sensitive nerves: Ruthenium Red discriminates between different mechanisms of activation. *Eur. J. Pharmacol.*, **170**, 167–177.

McEWAN, J., LARKIN, S., DAVIES, G., CHIERCHIA, S., BROWN, M., STEVENSON, J., MCINTYRE, I. & MASERI, A. (1986). Calcitonin gene-related peptide: a potent dilator of epicardial coronary arteries. *Circulation*, **74**, 1243–1247.

MULDERRY, P.K., GHATEI, M.A., RODRIGO, J., ALLEN, J.M., ROSENDFELD, POLAK, J.M. & BLOOM, S.R. (1985). Calcitonin gene-related peptide in cardiovascular tisues of the rat. *Neurosci.*, **14**, 947–954.

MULVANY, M.J. & NYBORG, N. (1980). An increased calcium sensitivity of mesenteric resistance vessels in young and adult spontaneously hypertensive rats. *Br. J. Pharmacol.*, **71**, 585–596.

NELSON, M.T., HUANG, Y., BRAYDEN, J.E., HESCHELER, J. & STANDEN, N.B. (1990). Arteriolar dilations in response to calcitonin gene-related peptide involve citivation of K^+-channels. *Nature*, **344**, 770–773.

NYBORG, N.C.B. (1990). Action of noradrenaline on isolated rat proximal and distal coronary arteries: Selective release of endothelium-derived relaxing factor in proximal arteries. *Br. J. Pharmacol.*, **100**, 552–556.

NYBORG, N.C.B., BAANDRUP, U., MIKKELSEN, E.O. & MULVANY, M.J. (1987). Active, passive and myogenic characteristics of isolated rat intramural coronary resistance arteries. *Pflügers Arch./Eur. J. Physiol.*, **410**, 664–670.

NYBORG, N.C.B. & MIKKELSEN, E.O. (1990). 5-Hydroxytryptamine does not induce release of endothelium-derived relaxing factor in rat coronary arteries. *Eur. J. Pharmacol.*, **186**, 295–300.

PERNOW, J. (1989). Actions of constrictor (NPY and endothelin) and dilator (substance P, CGRP and VIP) peptides on pig splenic and human skeletal muscle arteries: involvement of the endothelium. *Br. J. Pharmacol.*, **97**, 983–989.

PRIETO, D., BENEDITO, S., SIMONSEN, U. & NYBORG, N.C.B. (1990). Neuropeptide Y contracts and potentiates noradrenaline and 5-hydroxytryptamine induced vasoconstriction of rat isolated coronary arteries. *Eur. J. Pharmacol.* **183**, 2219–2220.

SHOJI, T., ISHIHARA, H., ISHIKAWA, T., SAITO, A. & GOTO, K. (1987). Vasodilating effects of human and rat calcitonin gene-related peptides in isolated porcine coronary arteries. *Naunyn-Schmiedebergs Arch. Pharmacol.*, **336**, 438–444.

STANDEN, N.B., QUALE, J.M., DAVIES, N.W., BRAYDEN, J.E., HUANG, Y. & NELSON, M.T. (1989). Hyperpolarizing vasodilators activate ATP-sensitive K^+ channels in arterial smooth muscle. *Science*, **245**, 177–180.

THOM, S.M.J., HUGHES, A.D., GOLDBERG, P., MARTIN, G., SCHACHTER, M. & SEVER, P.S. (1987). The actions of calcitonin gene-related peptide and vasoactive intestinal polypeptide as vasodilators in man *in vivo* and *in vitro*. *Br. J. Clin. Pharmacol.*, **24**, 129–134.

(Received October 30, 1990
Revised February 4, 1991
Accepted February 27, 1991)

Br. J. Pharmacol. (1991), **103**, 1769–1775 © Macmillan Press Ltd, 1991

Inhibition of reflex responses of neonate rat lumbar spinal cord by 5-hydroxytryptamine

H. Crick & D.I. Wallis

Department of Physiology, University of Wales College of Cardiff, Cardiff CF1 1SS

1 Monosynaptic (MSR) and polysynaptic (PSR) segmental reflex responses were recorded from a ventral root of the neonate rat hemisected spinal cord. Amplitudes of the two components were monitored with a peak height detector.

2 5-Hydroxytryptamine (5-HT) depressed the MSR and PSR in a concentration-dependent manner. The IC_{50} for MSR depression was 9.5 ± 3.2 μM and for PSR depression was 9.0 ± 4.8 μM.

3 Blockade of neuronal uptake of 5-HT by citalopram (0.1 μM) greatly increased sensitivity to 5-HT. In the presence of citalopram, the IC_{50} for MSR depression was 30 ± 18 nM and for PSR depression was 89 ± 23 nM.

4 5-HT did not depress the MSR or the PSR by releasing glycine since strychnine (1 μM) did not prevent these actions of 5-HT.

5 5-Carboxamidotryptamine (5-CT), 8-hydroxy-2-(di-n-propylamino)tetralin (8-OH-DPAT), RU 24969, 1-[3-(trifluoromethyl)phenyl]-piperazine (TFMPP) and methysergide were full agonists for depression of the MSR. The IC_{50} for 5-CT was 3.6 ± 0.5 nM, for 8-OH-DPAT was 0.4 ± 0.04 μM, for TFMPP was 0.93 ± 0.3 μM and for methysergide was 21.8 ± 3.0 nM. The order of potency was 5-CT > methysergide > 5-HT > 8-OH-DPAT > TFMPP.

6 8-OH-DPAT, RU 24969, TFMPP and methysergide had either no or only a minor action in reducing the PSR. 5-CT caused a 50% depression at the highest concentration tested (30 nM).

7 Neither ketanserin (1 μM) nor spiperone (1 μM) caused appreciable blockade of 5-HT depression of the MSR or 5-HT depression of the PSR.

8 Blockers of neuronal 5-HT uptake (citalopram 0.1 or 1 μM, fluvoxamine 1 μM) usually reduced the MSR and, to a lesser extent, the PSR. Reflex depressions were reversed by ketanserin (1 μM).

9 It was concluded that 5-HT has a potent depressant action on segmental reflexes; depression of the MSR is unrelated to depolarization of motoneurones. Although depression of the MSR was mimicked by 5-HT_{1A} receptor ligands, the action of endogenous 5-HT may be mediated through 5-HT_2 receptors. Exogenous 5-HT may act at a mixture of 5-HT receptor subtypes to depress the MSR.

Keywords: 5-HT; monosynaptic reflex; polysynaptic reflex; spinal cord; 5-HT_1-like receptors; 5-HT_2 receptors

Introduction

Descending pathways releasing 5-hydroxytryptamine (5-HT) are present in the ventral horn of the spinal cord and 5-HT has been localized in the terminal plexuses near the cell bodies and dendrites of large motoneurones in the rat (Steinbusch *et al.*, 1978; Holstege & Kuypers, 1987). Although 5-HT has a direct depolarizing action on spinal motoneurones (Wang & Dun, 1990; Elliott & Wallis, 1990a) and increases their excitability (Ahlman *et al.*, 1971; Barasi & Roberts, 1974; Roberts *et al.*, 1988), 5-HT and 5-HT agonists, such as 5-methoxy-dimethyltryptamine and 8-hydroxy-2-(di-n-propylamino)tetralin (8-OH-DPAT), are reported to depress reflex responses evoked by dorsal root stimulation (Saito *et al.*, 1982; Nagano *et al.*, 1988). On the other hand, facilitation of reflex responses can occur on stimulation of the nucleus raphe medianus and this effect is blocked by 5-HT antagonists (Barasi & Roberts, 1974). It is clear that the role of 5-HT in regulating motoneurone activity remains to be clarified. Whether 5-HT exerts its effects via different subtypes of 5-HT receptor is also unclear.

In the isolated spinal cord of the neonate rat, stimulation of the ipsilateral dorsal root elicits a short latency discharge in the segmental ventral root, which is assumed to be the equivalent of the monosynaptic reflex (MSR) in the adult (Otsuka & Konishi, 1974). This is followed by a longer latency polysynaptic reflex response (PSR). 5-HT has been shown to inhibit reflex responses in neonate rat isolated spinal cord, although the type of 5-HT receptor involved is unresolved (Saito *et al.*, 1982; Ohno & Warnick, 1989). Further, methysergide was reported to act selectively as an agonist to depress the MSR (Saito *et al.*, 1982), an observation not always confirmed in other laboratories (Ault, 1981; Evans, 1989). The depressant effect of 5-HT on the PSR was not mimicked by methysergide nor blocked by methysergide (Saito *et al.*, 1982). 5-HT also depresses the mechanism responsible for generating the dorsal root potential on stimulation of an adjacent dorsal root (Lansdown *et al.*, 1980).

These experiments seek to clarify the action of 5-HT on reflex responses in the isolated spinal cord of the neonate rat and identify the subtype of 5-HT receptor involved. A preliminary account of this work has been presented to the British Pharmacological Society (Crick & Wallis, 1990).

Methods

Preparation

Female rats, 3–8 days old, were anaesthetized with ether. Following decapitation, the vertebral column was removed and placed in a dish containing oxygenated modified Krebs solution at room temperature (23°C). A laminectomy was performed from the ventral surface. The exposed spinal roots could now be cut as they entered and left the column, thus allowing the cord to be floated free. The cord was then pinned to a dissecting dish, the dura removed and the cord hemisected sagitally. The preparation was allowed to rest for an hour in oxygenated Krebs solution at room temperature (20–23°C) before experimentation began.

Recording and stimulation

Suction electrodes were used both for stimulation and recording. The hemisected cord was placed in a Sylgard-filled trough (volume 1 ml) cut into a Perspex block. The cord was superfused at 2–3 ml min^{-1} via a stainless steel inlet tube of 1 mm diameter and the overflow removed by suction from a drainage area connected to the preparation chamber by a piece of nappy-liner. The temperature of the superfusion fluid was maintained at 25°C. At higher temperatures, it was found that the cord was subject to large spontaneous depolarizations which left it unresponsive to stimulation. Identification of the spinal roots proved relatively simple. Dorsal roots are generally more vascularized than the ventral roots and also tend to be thicker. The ventral roots leave the cord in a fan-like manner. The root pairs used were L3 to L5 and were identified as they entered and left the cord at the lumbar enlargement.

The suction electrodes were constructed from Microcap tubes the tips of which were melted in a Bunsen flame to the correct size for the spinal roots used, i.e. so that the roots did not slip out but were not damaged by compression. A chlorided silver wire made contact with the Krebs solution in the suction tip into which the ventral root was drawn. The stimulating electrode, into which the dorsal root was drawn, was of similar design except that the silver wire was not chlorided and there was an insulated copper wire, with the copper tip exposed, wound around the outside of the glass Microcap tube. A silver chloride pellet entering the side of the bath formed the reference electrode.

Supramaximal square wave pulses 0.1 ms in duration were used. The stimulus voltage was adjusted to be 50% above that required for maximal stimulation. The dorsal root was stimulated once every 15 s (0.067 Hz). Reflex responses were studied only when the monosynaptic reflex (MSR) was constant in amplitude and more than 1 mV.

The reflex response was amplified and fed into a peak height detector (Courtice, 1977), modified to provide twin windows able to sample voltages occurring during different periods after the triggering stimulus (Figure 1). The windows or gates used sample and hold circuits to detect the peak voltages occurring during the MSR and the polysynaptic reflex (PSR). Signals proportional to the peak voltages were displayed on a chart recorder. A further chart recorder was used to monitor the d.c. level. The reflex was also displayed on an oscilloscope linked to an X-Y plotter to provide a hard copy.

It could be established that depression of the reflex by 5-HT was not due to greater temporal dispersion of the compound

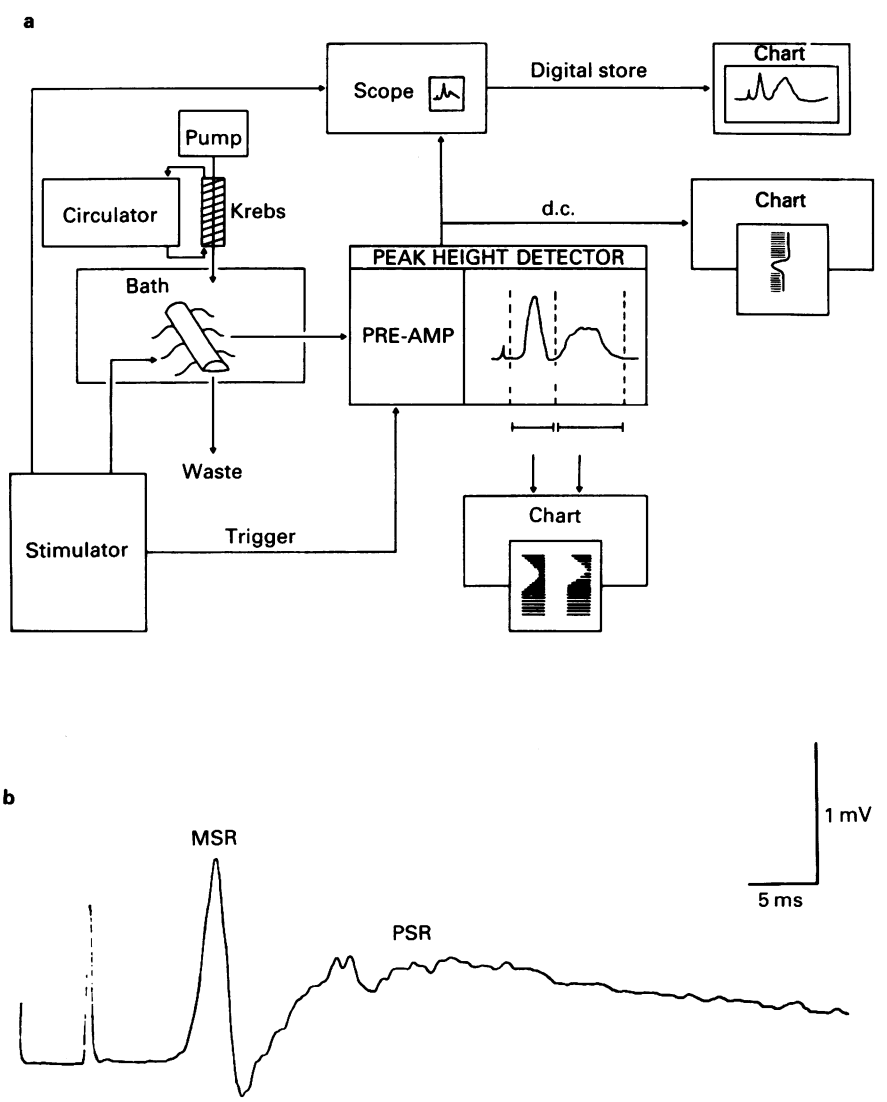


Figure 1 Arrangement for recording the segmental monosynaptic reflex (MSR) and polysynaptic reflex (PSR) from neonate rat hemisected spinal cord. (a) Block diagram of equipment showing amplification and relay of signal from ventral root to peak height detector, oscilloscope and chart recorders. (b) Chart record from oscilloscope digital store of reflex response recorded by a suction electrode from a ventral root on stimulation (10 V, 0.1 ms) of the segmental dorsal root. The initial component is the MSR and the slower component the PSR.

action potential, nor was there a change in its latency (see Figure 4). Thus, signals derived from the peak height detector were taken to be an accurate reflection of reflex depression.

Solutions and drugs

A modified Krebs solution of the following composition (mM) was used: NaCl 118, KCl 3, KH_2PO_4 1.2, $CaCl_2$ 1.2, $MgSO_4 \cdot H_2O$ 0.6, $NaHCO_3$ 25 and glucose 11; it was gassed with 5% CO_2 and 95% O_2 (Preston & Wallis, 1980).

The drugs used were: baclofen (BAC) (Sigma); 5-carboxamidotryptamine maleate (5-CT) (Glaxo); citalopram hydrobromide (Lundbeck Ltd); fluvoxamine maleate (Duphar); 8-hydroxy-2-(di-n-propylamino)tetralin hydroxybromide (8-OH-DPAT) (RBI/Semat); 5-hydroxytryptamine creatinine sulphate (5-HT) (Sigma); ketanserin tartrate (Janssen); methysergide bimaleate (Sandoz); ritanserin (Janssen); RU24969 (5-methoxy-3-[1,2,3,6-tetrahydro-4-pyridinyl]- 1-H-indole succinate, Roussel Uclaf), spiperone (Janssen), strychnine (Sigma) and TFMPP (1-[3-(trifluoromethyl)phenyl]-piperazine hydrobromide, RBI/Semat).

5-CT, 5-HT and methysergide were dissolved in modified Krebs solution, while baclofen, citalopram, fluvoxamine, 8-OH-DPAT, RU 24969, ketanserin, spiperone, strychnine and TFMPP were dissolved in distilled water; a solution of ritanserin was made in 0.01% HCl before dilution in Krebs solution.

Statistical analysis

Change in MSR or PSR amplitude was measured as the % reduction in amplitude of the responses preceding application of the agonist. IC_{50} values were estimated from individual concentration-response curves. All measures of variation quoted are standard errors. Student's t test was used to assess the significance of differences between mean values.

Results

Effect of 5-hydroxytryptamine on reflex responses

Superfusion of the cord with concentrations of 5-HT ranging from 1–100 μM caused a concentration-related depression of both the monosynaptic and the polysynaptic reflex (Figure 2). In preliminary experiments in which the superfusion period was varied, it was established that superfusion for 3–4 min was required for blockade to reach a maximum. To allow responses to plateau and also to minimize subsequent tachyphylaxis, a standard application time of 4 min was routinely adopted for 5-HT at all concentrations except for 100 μM which was applied for 2 min. Applications were repeated after a wash period of 20–30 min, depending on the concentration of agonist applied. Other agonists were applied for 4 min except for methysergide which was applied for 3 min, following Saito *et al.* (1982). Using the standard application time, mean latency to peak depression and mean recovery times for the MSR and the PSR are given in Table 1. Latency to peak depression appeared unaffected by concentration, while recovery time increased with increasing concentration. The IC_{50} for depression of the MSR was 9.5 ± 3.2 μM (n = 7), while the IC_{50} for depression of the PSR was 9.0 ± 4.8 μM (n = 7). As can be seen from Figure 2, the depressant action of 5-HT on the MSR at various concentrations closely paralleled its blocking action on the PSR. Times to peak depression and recovery for MSR and PSR were closely comparable (Table 1).

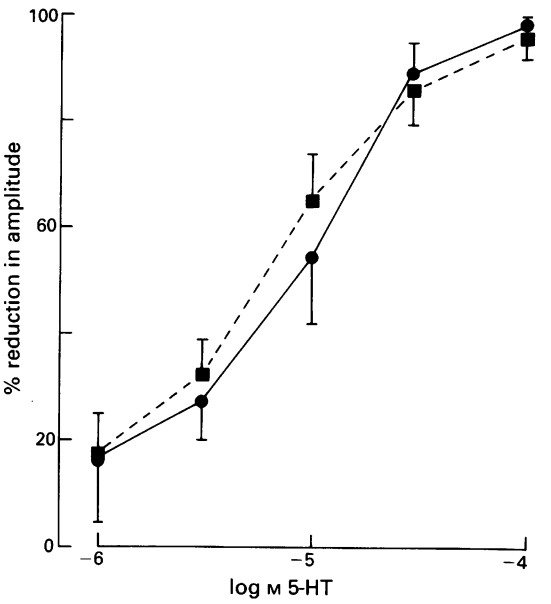


Figure 2 Effect of 5-hydroxytryptamine (5-HT) on relative amplitudes of monosynaptic (●) and polysynaptic (■) ventral root reflex. Complete abolition of the response was taken as 100%. Pooled data from 7 experiments, points show means with s.e.means indicated by vertical bars.

The close parallel between the two depressant actions of 5-HT was less apparent, however, after blockade of neuronal uptake of 5-HT with citalopram (0.1 μM). Under these circumstances concentration-response curves for depression of both the MSR and the PSR were shifted to the left (Figure 3). Whereas the curve for the PSR was shifted approximately 100 fold to the left, the curve for the MSR was shifted approximately 300 fold. Because citalopram itself caused a reduction of the MSR in a proportion of experiments (see below), determination of the IC_{50} after citalopram was possible in only a small number of preparations. In the presence of citalopram, the IC_{50} for depression of the MSR was 30 ± 18 nM (n = 4) and the IC_{50} for depression of the PSR was 89 ± 23 nM (n = 4).

A depolarization by 5-HT was also observed with the higher concentrations employed. However, this was not seen with other agonists active at this site (see below). Depolarizations were not studied systematically because in our hands the suction electrode technique often failed to give a satisfactory record of depolarization. Nevertheless, the depolarization was observed to have a time course different from depression of the reflex response. It was considered possible that the depressant action of 5-HT was an indirect one via release of inhibitory amino acid transmitters. In an attempt to rule out an action through release of glycine, cords were incubated with strychnine (1 μM). The results of one such experiment are

Table 1 Time course of depression by 5-hydroxytryptamine (5-HT) of monosynaptic reflex (MSR) and polysynaptic reflex (PSR): cords were superfused with 5-HT for 4 min

	MSR				*PSR*			
Conc of 5-HT (M)	3×10^{-6}	10^{-5}	3×10^{-5}	10^{-4}	3×10^{-6}	10^{-5}	3×10^{-5}	10^{-4}
Time to peak depression (min)	3.7 ± 0.4 (n = 7)	4.0 ± 0.3 (n = 7)	4.4 ± 0.6 (n = 7)	3.3 ± 0.6 (n = 5)	3.1 ± 0.4 (n = 6)	3.0 ± 0.4 (n = 7)	3.1 ± 0.6 (n = 7)	2.9 ± 0.9 (n = 5)
Time to recovery to control value (min)	7.5 ± 0.9 (n = 7)	9.1 ± 0.7 (n = 7)	17.2 ± 2.2 (n = 7)	26.9 ± 3.1 (n = 5)	8.2 ± 0.8 (n = 6)	9.4 ± 0.6 (n = 7)	16.7 ± 2.5 (n = 7)	22.5 ± 2.6 (n = 5)

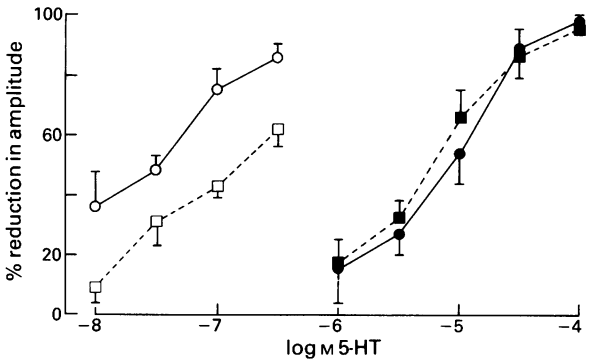


Figure 3 Effect of 0.1 μM citalopram on 5-hydroxytryptamine-induced depression of monosynaptic (MSR) and polysynaptic (PSR) ventral root reflex. Filled symbols are results from 4 cords in the absence of citalopram: (●) MSR; (■) PSR. Open symbols results from the same 4 cords after incubation with 0.1 μM citalopram for at lease 1 h; (○) MSR; (□) PSR.

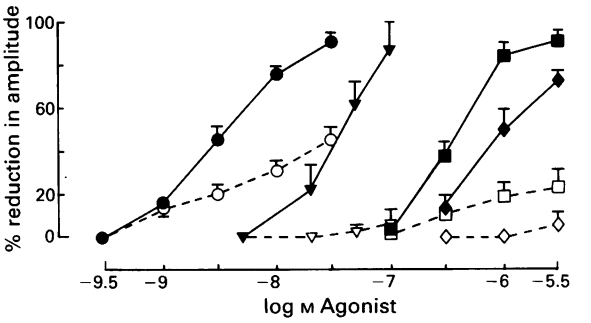


Figure 5 Concentration-response curves showing effects of 5-carboxamidotryptamine (5-CT), methysergide, 8-hydroxy-2-(di-n-propylamino)tetralin (8-OH-DPAT) and 1-[3-(trifluoromethyl) phenyl]-piperazine (TFMPP) on monsynaptic (MSR) and polysynaptic ventral root reflex (PSR). Solid lines and symbols show MSR and broken lines and open symbols show PSR. (○) 5-CT, $n = 5$; (▽) methysergide, $n = 3$; (□) 8-OH-DPAT, $n = 4$; (◇) TFMPP, $n = 3$.

shown in Figure 4. It can be seen that strychnine itself facilitated later components in the PSR but did not prevent a depressant action by 5-HT. A similar result was obtained in 2 other experiments.

Agonist action of 5-hydroxytryptamine receptor ligands

A number of 5-HT receptor ligands were able to depress reflex responses. 5-CT was very potent in depressing the MSR (IC_{50} 3.6 ± 0.5 nM, $n = 5$), but caused only a 50% depression of the PSR at a concentration of 30 nM (Figure 5). The effects of higher concentrations of 5-CT were not tested because of the very long-lasting depressant action on the MSR produced by this agent. Unlike 5-HT, 5-CT did not cause any detectable depolarization of motoneurones in concentrations up to 30 nM. 8-OH-DPAT was also capable of producing nearly complete inhibition of the MSR (IC_{50} 0.4 ± 0.04 μM, $n = 4$), but reduced the PSR by a maximum of only 20% (Figure 5). Similarly, TFMPP depressed the MSR (IC_{50} 0.93 ± 0.3 μM, $n = 3$, Figure 5), but had very little effect on the PSR. In confirmation of Saito *et al.* (1982), methysergide was an effective agonist for MSR depression (IC_{50} 21.8 ± 3.0 nM, $n = 3$, Figure 5). Methysergide had very little effect on the PSR. RU 24969 (0.05–10 μM) also caused depression of the MSR, which was of very slow onset and which could not be reversed on washing. RU 24969 had no effect on the PSR. No attempt was made to estimate an IC_{50} for RU 24969.

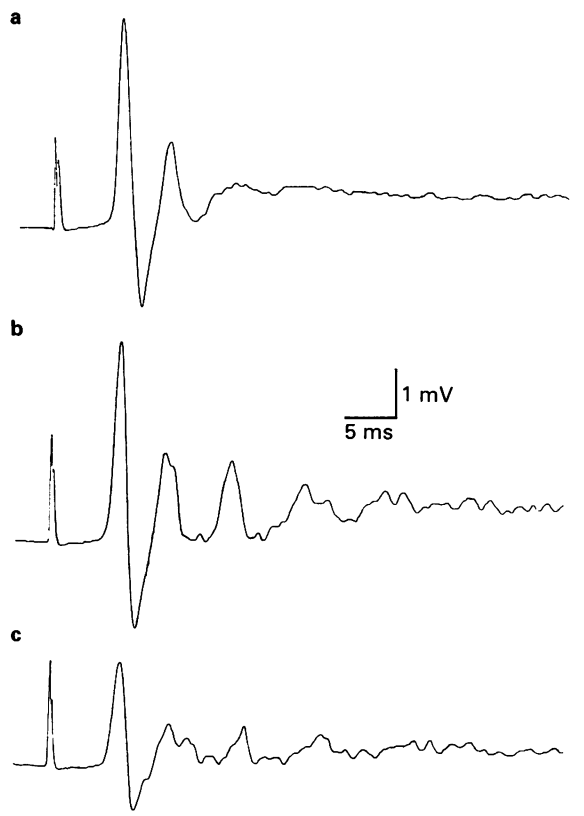


Figure 4 Effect of strychnine and 5-hydroxytryptamine (5-HT) in the presence of strychnine on reflex responses of neonate rat spinal cord: (a) control; (b) response in the presence of 1 μM strychnine and (c) depression of the response by 3 μM 5-HT in the continued presence of 1 μM strychnine.

Failure of ketanserin and spiperone to antagonize responses to 5-hydroxytryptamine

In control experiments, it was established that a second concentration-response curve could be constructed from the preparation following a wash period of 1 h after the last response determined for the first curve. The IC_{50} values for the depressant action of 5-HT on the MSR and PSR, determined for the second concentration-response curve for a preparation, were 10.0 ± 3.2 μM ($n = 5$) and 3.6 ± 0.9 μM ($n = 5$), respectively, and not significantly different from the IC_{50} values determined for the initial concentration-response curve.

The agonist action of 5-CT, 8-OH-DPAT and RU 24969 suggested that a 5-HT_1-like receptor may mediate the depression of reflex responses. In confirmation of this, the 5-HT_2 receptor antagonist ketanserin (1 μM), caused no appreciable blockade of responses to 5-HT (Figure 6). In the same experiments, baclofen (0.3 μM) was used as a control agonist mediating reflex depression. In 3 series of experiments 0.3 μM baclofen depressed the MSR by 12–36% and the PSR, on average, by 10%. Ketanserin (1 μM) did not reduce the depressant action exerted by baclofen.

Spiperone (1 μM) also failed to cause any significant blockade of these depressant actions of 5-HT (Figure 6). Neither the action of 5-HT in depressing the MSR nor its action in depressing the PSR were affected by spiperone.

Depression of reflex responses by blockers of neuronal 5-hydroxytryptamine uptake

Superfusion of the cord with a 5-HT uptake blocker such as citalopram sometimes caused a depression of reflex responses. This was seen consistently at a concentration of 1 μM citalopram and, usually, with a concentration of 0.1 μM citalopram. As can be seen from Table 2, 0.1 μM citalopram caused a reduction of the MSR by about 45% and a non-signficant reduction of the PSR. That the depressant effect was due to an

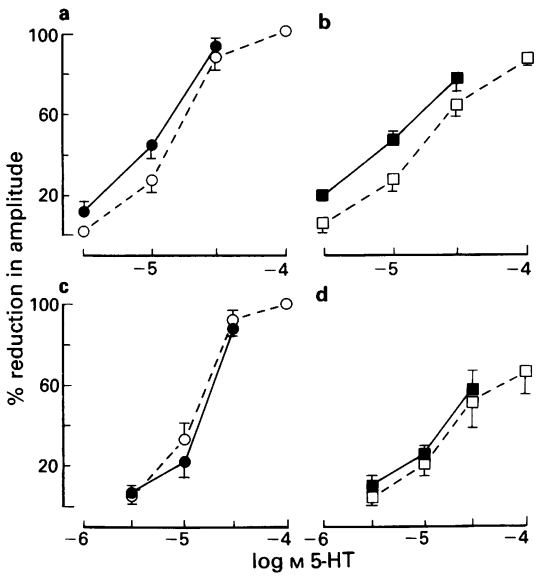


Figure 6 Effects of ketanserin (a,b) and spiperone (c,d) on depression of monsynaptic (MSR) and polysynaptic ventral root reflex (PSR) by 5-hydroxytryptamine (5-HT). Pooled data from 4 experiments with ketanserin and 4 experiments with spiperone. (a) Effect of 1 μM ketanserin on MSR, filled symbols and open symbols after incubation with ketanserin for at least 1 h. (b) Effect of 1 μM ketanserin on PSR in same cords; filled symbols controls and open symbols after ketanserin. (c) Effect of 1 μM spiperone on MSR; filled symbols controls and open symbols after incubation with spiperone for at least 1 h. (d) Effect of 1 μM spiperone on PSR in same cords; filled symbols controls and open symbols after spiperone.

action of citalopram itself was unlikely because a similar effect was observed with the uptake blocker, fluvoxamine (1 μM) (Table 2). Paradoxically, the 5-HT_2 receptor blocker, ketanserin at a concentration of 1 μM which did not block the depressant action of exogenous 5-HT (see above), was capable of reversing the depressant action of citalopram and fluvoxamine (Table 2). Ritanserin (1 μM) had a similar action.

In the presence of citalopram (0.1 μM) and ketanserin (1 μM), the concentration-response curve to 5-HT showed a small rightward shift such that the IC_{50} for depression of the MSR was 64.4 $\pm$ 0.9 nM ($n = 4$) and the IC_{50} for depression of the PSR was 298 $\pm$ 96 nM ($n = 4$).

Discussion

These experiments confirm that 5-HT has a potent depressant action on reflex responses generated in motoneurones by stimulation of a dorsal root. A depression of segmental transmission to neonatal rat motoneurones by 5-HT has been identified in intracellular studies on the hemisected cord (Elliott & Wallis, 1990a,b) and spinal cord slice (Wang *et al.*, 1990). The use of motoneurone population responses has the advantages of averaging fluctuations in PSR amplitude seen in records from individual motoneurones (Elliott & Wallis, unpublished) and of permitting studies with agonists and antagonists of many hours duration.

Since 5-HT has a direct depolarizing action on motoneurones (Takahashi & Berger, 1990; Wang & Dun, 1990), the depolarization itself might occlude or shunt the excitatory postsynaptic potential (e.p.s.p.) and so reduce reflex responses. This seems unlikely as a principal mode of action because (a) the time courses of depolarization and reflex depression were different, (b) 5-CT caused reflex depression at concentrations that did not elicit depolarization, (c) agents such as 8-OH-DPAT and RU 24969 depressed the reflex but did not depolarize motoneurones (Elliott & Wallis, 1990b), (d) the EC_{50} for depolarization by 5-HT (1.5 μM, Elliott & Wallis, 1990b) is different from the IC_{50} for reflex depression of MSR when both are determined after blockade of neuronal 5-HT uptake (30 nM) and (e) depolarization itself which is accompanied by an increase in input resistance (Larkman *et al.*, 1989; Wang & Dun, 1990) would be expected to increase MSR amplitude (Barasi & Roberts, 1974).

5-HT can cause an increase in the frequency of inhibitory postsynaptic potentials (i.p.s.ps) arising in motoneurones (Wang & Dun, 1990; Elliott & Wallis, unpublished), due presumably to excitation of inhibitory interneurones. However, the depressant action of 5-HT on reflex responses was not due to release of glycine from interneurones because the depressant action was undiminished in the presence of strychnine. Strychnine was applied in an effective concentration since it facilitated the PSR, presumably by reducing reciprocal inhibition. This suggests but does not prove that the depressant action of 5-HT is via presynaptic receptors on the segmental pathway to motoneurones, as proposed by Wang *et al.* (1990). Assuming such presynaptic receptors are located on primary afferent terminals they will cause a consequent reduction in the monosynaptic e.p.s.p. However, the e.p.s.p. generated by polysynaptic pathways might be modulated in a more complex fashion because of interaction of 5-HT with interneurones in the pathway. This is borne out by the differences in the pharmacology of the 5-HT action on the MSR compared to its action on the PSR (see below).

Blocking neuronal uptake of 5-HT greatly affected the sensitivity of the reflexes to 5-HT. It follows that uptake of 5-HT into neurones must be particularly effective in the cord or at least in the vicinity of the 5-HT receptors responsible for the actions described here. After blockade, the IC_{50} for MSR depression was 30 nM while the IC_{50} for PSR depression was 89 nM. Blocking neuronal 5-HT uptake may possibly reveal a significant difference in sensitivity to 5-HT between MSR and PSR in a larger series of experiments. In these studies, the IC_{50} could only be determined in experiments where citalopram itself did not depress the MSR.

The agonist profile and the order of agonist potency for the depression of the MSR and depression of the PSR are shown in Table 3. 5-HT, 5-CT, methysergide, 8-OH-DPAT, RU

Table 2 Depressant effect of blockers of neuronal 5-hydroxytryptamine (5-HT) uptake on monosynaptic reflex (MSR) and polysynaptic reflex (PSR) amplitude

	MSR			*PSR*		
	Control	*Cit*	*Cit + Ket*	*Control*	*Cit*	*Cit + Ket*
Amplitude (mV)	2.00 $\pm$ 0.17	1.11 $\pm$ 0.20*	2.14 $\pm$ 0.19	0.74 $\pm$ 0.07	0.61 $\pm$ 0.06	0.72 $\pm$ 0.14
n	11	11	5	11	11	5
	Control	*Flu*	*Flu + Ket*	*Control*	*Flu*	*Flu + Ket*
Amplitude (mV)	2.11 $\pm$ 0.19	1.14 $\pm$ 0.15*	2.48 $\pm$ 0.36	0.69 $\pm$ 0.08	0.63 $\pm$ 0.09	0.73 $\pm$ 0.10
n	6	6	6	6	6	6

Cit: 0.1 μM citalopram; Flu: 1 μM fluvoxamine; Ket: 1 μM ketanserin.
* $P < 0.01$

Table 3 Pharmacology of 5-hydroxytryptamine (5-HT) responses of neonate rat spinal motoneurones

	Order of agonist potency	*Inactive*
Depression of monosynaptic reflex	5-CT > methysergide > 5-HT > 8-OH-DPAT > TFMPP	
Depression of polysynaptic reflex	5-HT > 5-CT	[8-OH-DPAT] RU 24969 TFMPP
Depolarization of motoneurone	5-HT > α-Me-5-HT > 5-CT > 5-MOT ⩾ T*	8-OH-DPAT RU 24969

5-MOT: 5-methoxytryptamine; T: tryptamine; 5-CT: 5-carboxamidotryptamine; 8-OH-DPAT: 8-hydroxy-2-(di-n-propylamino)tetralin; TFMPP: 1-[3-(trifluoromethyl)phenyl]-piperazine
* Connell & Wallis (1989)

24969 and TFMPP caused near maximal reduction of the MSR. On the other hand, only 5-HT caused complete inhibition of the PSR, while 5-CT caused partial inhibition over the range of concentrations tested. 8-OH-DPAT, RU 24969, TFMPP and methysergide had either no or only a minor action in reducing the PSR (Table 3).

For reduction of the MSR, the IC_{50} for 5-HT (after blockade of neuronal uptake) was in the nmolar range, as was that for 5-CT and methysergide. IC_{50} values for 8-OH-DPAT and TFMPP were in the μmolar range. The order of potency was: 5-CT > methysergide > 5-HT > 8-OH-DPAT > TFMPP (Table 3). The agonist profiles for reflex depression can be contrasted with the profile for the receptor mediating motoneurone depolarization (Table 3), using data from Connell & Wallis (1989).

The results on depression of the MSR by 5-HT and 5-HT analogues may suggest mediation by a 5-HT_{1A} receptor, as suggested by Wang *et al.* (1990). A 5-HT_3 receptor is not involved because MDL 72222 is without effect on 5-HT depression of the MSR (Wang *et al.*, 1990) nor does the agonist profile suggest a 5-HT_4 receptor. However, our findings with antagonists and uptake blockers are not consistent with mediation by a 5-HT_{1A} receptor. Firstly, spiperone, which has a high affinity for 5-HT_{1A} receptors (Hoyer, 1989), did not block the effect of 5-HT and, secondly, the depression of the MSR by citalopram and fluvoxamine, presumably as a result of accumulation of endogenous 5-HT within the cord, was reversed by ketanserin. The latter observation indicates an involvement of 5-HT_2 receptors. Both spiperone and ketanserin should have blocked an action by exogenous 5-HT on 5-HT_2 receptors. Since they did not significantly reduce the actions of exogenous 5-HT before uptake blockade and ketanserin caused only a small rightward shift of the 5-HT concentration-response curve after uptake blockade, it may be concluded that exogenous 5-HT acts principally via a 5-HT_1-like receptor to depress the MSR. Perhaps the very avid uptake system or diffusional barriers limit access of exogenous 5-HT to the 5-HT_2 sites activated by endogenous 5-HT to reduce the MSR. Clearly, further experiments are required to resolve this paradox. It is possible that the complex pharmacology of these 5-HT actions might be the result of activation of a mixture of 5-HT receptor subtypes. Preliminary experiments indicate that the action of 8-OH-DPAT in depressing the MSR is antagonized by spiperone (Crick & Wallis, unpublished), which adds weight to this idea. Presynaptic inhibition of the synaptic input to rat locus coeruleus neurones is reported to be mediated by a mixed population of 5-HT_{1A} and 5-HT_{1B} receptors (Bobker & Williams, 1989).

It may be significant that in the spinalized cat a depression of the MSR can be induced by stimulation of the caudal raphe nuclei, perhaps by release of 5-HT (Clineschmidt & Anderson, 1970); the effect was mimicked by methysergide. In the neonate rat isolated spinal cord, the 5-HT-releaser, *p*-chloroamphetamine has also been shown to depress the MSR (Ohno & Warnick, 1989). Thus, the physiological pathway may involve a receptor at which methysergide is an agonist, a feature of 5-HT_1-like receptors (Bradley *et al.*, 1986).

At present, it is not possible to attribute depression of the PSR by 5-HT to a particular receptor subtype. Although neither 5-HT_{1A} nor 5-HT_2 receptors seem to be involved, the pharmacological profile is incomplete.

In conclusion, 5-HT has been shown to exert a potent depressant action on segmental reflexes; depression of the MSR is unrelated to the action of 5-HT in depolarizing motoneurones. Although depression of the MSR is mimicked by 5-HT_{1A} receptor ligands, the action of endogenous 5-HT may be mediated through 5-HT_2 receptors. Exogenous 5-HT may act at a mixture of 5-HT receptor subtypes to depress the MSR.

This work was supported by the Wellcome Trust. We would like to thank Sandoz Ltd. for the gift of methysergide, Glaxo Ltd for 5-CT, Roussel Uclaf Ltd for RU 24969, Janssen Ltd. for ketanserin and spiperone, Lundbeck Ltd. for citalopram and Duphar for fluvoxamine.

References

AHLMAN, A., GRILLNER, S. & UDO, M. (1971). The effect of 5-HTP on the static fusimotor activity and the tonic stretch reflex of an extensor muscle. *Brain Res.*, **27**, 393–396.

AULT, B. (1981). Effects of monoamines and structurally related compounds on the isolated rat spinal cord preparation. Ph.D. Thesis, University of Bristol.

BARASI, S. & ROBERTS, M.H.T. (1974). The modification of lumbar motoneurone excitability by stimulation of a putative 5-hydroxytryptamine pathway. *Br. J. Pharmacol.*, **52**, 339–348.

BOBKER, D.H. & WILLIAMS, J.T. (1989). Serotonin agonists inhibit synaptic potentials in the rat locus ceruleus *in vitro* via 5-hydroxytryptamine$_{1A}$ and 5-hydroxytryptamine$_{1B}$ receptors. *J. Pharmacol. Exp. Ther.*, **250**, 37–43.

BRADLEY, P.B., ENGEL, G., FENIUK, W., FOZARD, J.R., HUMPHREY, P.P.A., MIDDLEMISS, D.W., MYLECHARANE, E.J., RICHARDSON, B.P. & SAXENA, P.R. (1986). Proposals for the classification and nomenclature of functional receptors for 5-hydroxytryptamine. *Neuropharmacology*, **25**, 563–576.

CRICK, H. & WALLIS, D.I. (1990). Effect of 5-hydroxytryptamine on reflex responses of neonate rat spinal motoneurones. *Br. J. Pharmacol.*, **100**, 308P.

COURTICE, C.J. (1977). A circuit for recording evoked action potential amplitudes. *J. Physiol.*, **268**, 1P.

CLINESCHMIDT, B.V. & ANDERSON, E.G. (1970). The blockade of bulbospinal inhibition by 5-hydroxytryptamine antagonists. *Exp. Brain Res.*, **11**, 175–186.

CONNELL, L.A. & WALLIS, D.I. (1989). 5-hydroxytryptamine depolarizes neonatal rat motoneurones through a receptor unrelated to an identified binding site. *Neuropharmacology*, **28**, 625–634.

ELLIOTT, P. & WALLIS, D.I. (1990a). The action of 5-hydroxytryptamine on lumbar motoneurones in neonatal rat spinal cord *in vitro*. *J. Physiol.*, **426**, 54P.

ELLIOTT, P. & WALLIS, D.I. (1990b). Preliminary studies of the action of 5-hydroxytryptamine on single lumbar motoneurones in the spinal cord of the neonate rat. *Br. J. Pharmacol.*, **100**, 394P.

EVANS, R.H. (1989). The pharmacology of segmental transmission in the spinal cord. *Progr. Neurobiol.*, **33**, 255–279.

HOLSTEGE, J.C. & KUYPERS, H.G.J.M. (1987). Brainstem projections to spinal motoneurones: an update. *Neuroscience*, **23**, 809–821.

HOYER, D. (1989). 5-Hydroxytryptamine receptors and effector coupling mechanisms in peripheral tissues. In *Peripheral Actions of 5-Hydroxytryptamine*. ed. Fozard, J.R. pp. 72–909. Oxford: University Press.

LANSDOWN, M.J.R., NASH, H.L., PRESTON, P.R., WALLIS, D.I. & WILLIAMS, R.G. (1980). Antagonism of 5-hydroxytryptamine receptors by quipazine. *Br. J. Pharmacol.*, **68**, 525–532.

LARKMAN, P.M., PENINGTON, N.J. & KELLY, J.S. (1989). Electrophysiology of adult rat facial motoneurones: the effects of serotonin (5-HT) in a novel *in vitro* brainstem slice. *J. Neurosci. Methods*, **28**, 133–146.

NAGANO, N., ONO, H. & FUKUDA, H. (1988). Functional significance of subtypes of 5-HT receptors in the rat spinal reflex pathway. *Gen. Pharmacol.*, **19**, 789–793.

OHNO, Y. & WARNICK, J.E. (1989). Presynaptic activation of the spinal serotonergic system in the rat by phencyclidine *in vitro*. *J. Pharmacol. Exp. Ther.*, **250**, 177–183.

OTSUKA, M. & KONISHI, S. (1974). Electrophysiology of mammalian spinal cord *in vitro*. *Nature*, **252**, 733–734.

PRESTON, P.R. & WALLIS, D.I. (1980). Characteristics of dorsal root potentials recorded from the isolated spinal cord of the neonate rat. *J. Neural Transm.*, **48**, 271–287.

ROBERTS, M.H.T., DAVIES, M., GIRDLESTONE, D. & FOSTER, G.A. (1988). Effects of 5-hydroxytryptamine agonists and antagonists on the responses of rat spinal motoneurones to raphe obscurus stimulation. *Br. J. Pharmacol.*, **95**, 437–448.

SAITO, K., ITO, S., KITAZAWA, T. & OHGA, A. (1982). Selective inhibition by methysergide of the monosynaptic reflex discharge in the isolated spinal cord of the newborn rat. *Brain Res.*, **251**, 117–125.

STEINBUSCH, H.W.M., VERHOFSTAD, A.A. & JOOSTER, H.W.J. (1978). Localization of serotonin in the central nervous system by immunohistochemistry: description of a specific and sensitive technique and some applications. *Neuroscience*, **3**, 811–819.

TAKAHASHI, T. & BERGER, A.J. (1990). Direct excitation of rat spinal motoneurones by serotonin. *J. Physiol.*, **423**, 63–76.

WANG, M.Y. & DUN, N.J. (1990). 5-hydroxytryptamine responses in neonate rat motoneurones *in vitro*. *J. Physiol.*, **430**, 87–103.

WANG, M.Y., WU, S.Y., DUN, N.J. & KARCZMAR, A.G. (1990). Characterization of 5-HT responses in rat motoneurones. *Soc. Neurosci. Abstr.* (in press).

(Received November 27, 1990
Revised February 7, 1991
Accepted March 7, 1991)

Br. J. Pharmacol. (1991), **103**, 1776–1780 © Macmillan Press Ltd, 1991

The effects of naloxone on the cardiovascular and respiratory effects of centrally administered corticotrophin releasing factor in conscious rabbits

[1]C.N. May, C.J. Whitehead & C.J. Mathias

Department of Medicine, St. Mary's Hospital Medical School, London W2

1 The effects of intracerebroventricular (i.c.v.) and intracisternal (i.c.) administration of corticotrophin releasing factor (CRF) (0.5 nmol kg^{-1}) were examined in conscious rabbits. The effect of opioid receptor antagonism was examined to determine whether the responses to CRF were mediated by endogenous opioid peptides.

2 After i.c.v. CRF there was a rise in mean arterial pressure (MAP), heart rate (HR), plasma noradrenaline and adrenaline, and increased behavioural activity. Respiration rate increased, $Paco_2$ fell, but Pao_2 was unchanged.

3 The pressor and behavioural effects of i.c.v. CRF were unaltered by high doses of intravenous naloxone (9 μmol kg^{-1} bolus followed by 9 μmol kg^{-1} min^{-1} infusion); these effects of CRF were also not prevented by double this dose of naloxone. Naloxone attenuated the CRF-induced tachycardia, blocked the increase in respiration rate and increased the fall in $Paco_2$.

4 After i.c. CRF (0.5 nmol kg^{-1}) there were similar changes in MAP, HR, plasma catecholamines, respiration and behaviour.

5 These results indicate that in conscious rabbits the pressor effects of i.c.v. CRF are not mediated by endogenous opioid peptides. The finding that the effects of CRF were similar after i.c.v. and i.c. administration suggests that these responses may result from actions on brainstem rather than periventricular sites.

Keywords: Blood pressure; catecholamines; central administration; corticotrophin releasing factor; naloxone; conscious rabbits; respiration.

Introduction

Corticotrophin releasing factor (CRF) is a 41 amino acid peptide that was isolated from ovine hypothalami and causes secretion of corticotrophin (ACTH) and β-endorphin (Vale *et al.*, 1981). Intracerebroventricular (i.c.v.) administration of CRF increases blood pressure and heart rate (HR); effects which are thought to result from an increase in sympathetic nervous activity and an inhibition of vagal outflow to the heart (Fisher & Brown, 1984). In conscious rats the CRF-induced cardiovascular effects and the increased behavioural activity and grooming following i.c.v. injection were blocked by the opiate antagonist, naloxone, suggesting that they were mediated by endogenous opioid peptides (Saunders & Thornhill, 1986). In conscious rabbits i.c.v. and intracisternal (i.c.) administration of the selective δ-opioid agonist [D-Pen 2,5] enkephalin (DPDPE) raised blood pressure and heart rate (HR) and increased behavioural activity (May *et al.*, 1989a). This finding raised the possibility that the effects of CRF may be mediated by release of endogenous opioid peptides that act on δ-opioid receptors.

In the present experiments the cardiovascular and respiratory responses to i.c.v. CRF were studied in conscious rabbits and the effect of pretreatment with naloxone was examined. CRF was also given intracisternally (i.c.) to establish whether its effects result from an action on periventricular or brainstem sites.

Methods

Experiments were carried out on male Sandy Half-Lop rabbits (National Institute for Medical Research, Mill Hill, London), weighing between 2.2 and 3.6 kg, allowed free access to food and water.

Surgical procedures

For injection into the right lateral ventricle, cannulae (Harvard apparatus) were implanted aseptically under general anaesthesia (Saffan, Glaxovet) (May *et al.*, 1989c). Coordinates were 1.0 mm caudal to bregma, 3.0 mm lateral to midline and 8.5 mm below the dura. Injections were given in a volume of 25 μl over 30 s from a sterilized Hamilton syringe with a 25G needle that protruded 1.0 mm from the cannula tip. The injection was flushed in with 25 μl of sterile, non-pyrogenic, isotonic saline (saline) through a needle that reached half way down the cannula shaft. For injection into the cisterna magna the catheter was inserted as previously described under Saffan general anaesthesia (May *et al.*, 1989b). Injections were given in 25 μl of saline from a sterilized Hamilton syringe with a 30G needle. This was flushed in with 20 μl of saline; the dead volume of the catheter was 10 μl. In previous studies we have demonstrated that in concious rabbits i.c.v. and i.c. administration of saline has no cardiovascular or respiratory actions and does not alter plasma catecholamine levels or have any behavioural effects (May *et al.*, 1989b).

The injection site was confirmed at the end of a series of experiments by injection of 25 μl of bromophenol blue (1%) either i.c.v. or i.c. followed by the appropriate volume of saline. The animal was killed with an overdose of pentobarbitone, the brain removed and the distribution of dye examined.

Experimental protocol

Animals were not used for at least 7 days post operation. Before each experiment cannulae were inserted into the central artery and marginal vein of the ear under 1% lignocaine local anaesthesia. The arterial cannula was connected to a pressure transducer (Bell and Howell) and blood pressure

[1] Author for correspondence at present address: Dr C.N. May, Howard Florey Institute, University of Melbourne, Parkville 3052, Victoria, Australia.

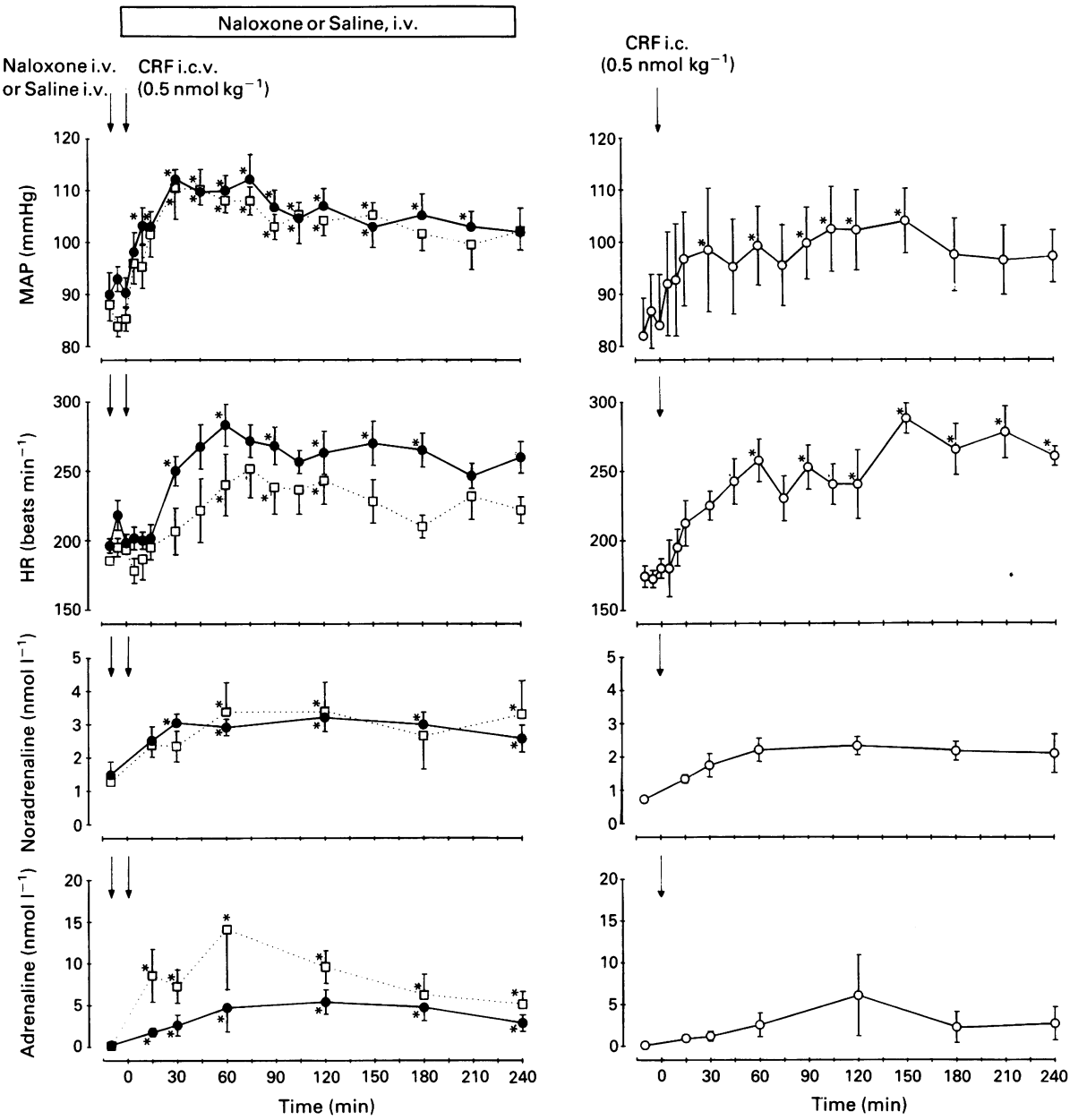


Figure 1 Effect of centrally administered corticotrophin releasing factor (CRF) on mean arterial pressure (MAP), heart rate (HR) and plasma catecholamines in conscious rabbits. Left panels: after a 30 min control period an i.v. bolus, followed by an i.v. infusion of saline (●) or naloxone (□) was given 10 min before i.c.v. CRF. The following doses were used: saline (300 μl kg^{-1} followed by 6 ml h^{-1}, $n = 6$); naloxone (9 μmol kg^{-1} followed by 9 μmol kg^{-1} min^{-1}, $n = 4$; 18 μmol kg^{-1} followed by 18 μmol kg^{-1} min^{-1} $n = 2$) and CRF (0.5 nmol kg^{-1}). Right panels: after a 30 min control period i.c. CRF (0.5 nmol kg^{-1}, $n = 4$) was given at 0 min (○). Each point represents the mean with s.e.mean shown by vertical lines. * $P < 0.05$ for comparisons with control.

and heart rate (HR) were recorded on a Devices polygraph. Before the start of the experiment the patency of the i.c.v. or i.c. cannula was assessed by checking that saline flowed freely into the cannula under gravity. The animal was used only if the cannula was patent and there were no cardiovascular or behavioural effects. Intervals of at least 7 days were allowed between studies.

CRF (1 mg) (rat/human, Bachem) was dissolved in 175 μl 0.1 M HCl in saline to which 700 μl of saline was added. This was filtered through a 0.2 μm filter and frozen at −20°C in 50 μl aliquots. On each experimental day an aliquot was thawed and diluted in saline immediately before use.

In pilot experiments the effect of a range of doses of i.c.v. CRF (0.1 to 4.0 nmol kg^{-1}) was examined. A dose of 0.5 nmol kg^{-1} was chosen for subsequent experiments as this increased MAP without causing excessive behavioural activation. After a 30 min control period six conscious rabbits were given i.v. saline (300 μl kg^{-1} bolus followed by 6 ml h^{-1} infusion for 4 h) or i.v. naloxone (9 μmol kg^{-1} bolus followed by 9 μmol kg^{-1} h^{-1} for 4 h) in four rabbits and double these doses of naloxone in an additional two rabbits. At 10 min after the bolus dose of saline or naloxone, i.c.v. CRF (0.5 nmol kg^{-1}) was given. The effects of naloxone (9 μmol kg^{-1} bolus followed by 9 μmol kg^{-1} h^{-1} for 4 h) given alone were also examined. In addition, the effects of i.c. CRF (0.5 nmol kg^{-1}) were examined in four conscious rabbits.

Blood collection and analysis

Arterial blood samples were collected at the end of the control period and then at 15, 30, 60, 120, 180, and 240 min after administration of CRF. Blood removed was replaced with an equal volume of saline. Catecholamines were measured in plasma from blood (2.5 ml) collected into cooled tubes containing 50 μl of EGTA (0.095%)/glutathione (0.06%) and kept on ice until centrifugation at 4°C and then storage at −70°C.

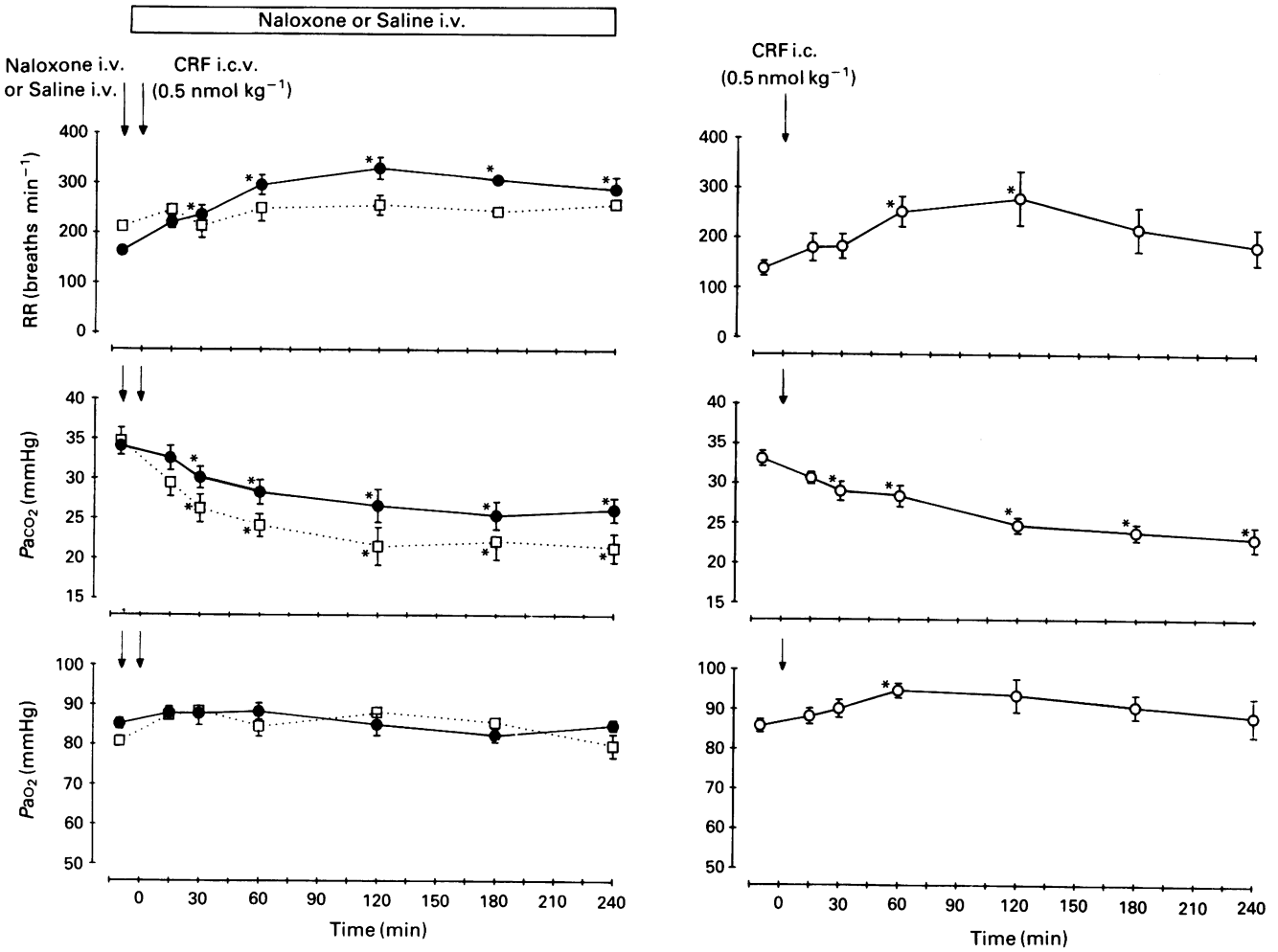


Figure 2 Changes in respiration rate (RR), $Paco_2$ and Pao_2 following central administration of corticotrophin releasing factor (CRF) in conscious rabbits. Left panels: after a 30 min control period an i.v. bolus, followed by an i.v. infusion of saline (●) or naloxone (□) was given 10 min before i.c.v. CRF. The same doses were used as in Figure 1. Right panels: after a 30 min control period i.c. CRF (0.5 nmol kg^{-1}, $n = 4$) was given at 0 min (○). Each point represents the mean with s.e.mean shown by vertical lines. * $P < 0.05$ for comparisons with control.

Catecholamines were separated by high performance liquid chromatography and detected by electrochemical detection (May *et al.*, 1988). Blood gases were measured immediately after collection of arterial blood in a heparinised capillary tube (100 μl) (Instrument Laboratory 230 blood gas analyser).

Data analysis

Data are presented as means ± s.e.mean. Analysis was performed on the differences from the control values by use of the SAS statistical programme. The control values for mean arterial pressure (MAP) and HR consisted of the mean of six readings taken during the control period. A logarithmic transformation was performed on the values for plasma noradrenaline and adrenaline before analysis. The data were subjected to analysis of variance and where the null hypothesis was rejected Bonferroni's comparisons were performed on the means; $P < 0.05$ was considered significant.

Results

Cardiovascular effects

In six conscious rabbits i.c.v. CRF (0.5 nmol kg^{-1}) had an immediate and sustained pressor action; MAP was significantly elevated from 10 until 210 min after CRF ($P < 0.05$) (Figure 1). In contrast, the effect on HR was delayed, there was no change for the first 15 min but by 30 min HR was significantly increased and remained elevated for 240 min ($P < 0.05$) (Figure 1). Naloxone was given i.v. (9 μmol kg^{-1} bolus followed by 9 μmol kg^{-1} h^{-1} infusion) to four rabbits and double these doses were given to two further rabbits. The results from the two groups were indistinguishable and the findings have been combined and are presented together (Figure 1). Naloxone had no effect on the CRF-induced pressor rise, but reduced the tachycardia, this being significant at 180 min ($P < 0.05$). Administration of naloxone alone had no effects on MAP or HR, in agreement with previous work showing that high doses of naloxone have no cardiovascular effects in conscious, normovolaemic rabbits (Rutter *et al.*, 1987).

CRF (0.5 nmol kg^{-1}) given i.c. to four conscious rabbits caused similar increases in MAP and HR to those seen after i.c.v. administration (Figure 1). At 60 min after i.c. CRF there was an increase in MAP of 17 ± 5 mmHg and in HR of 83 ± 13 beats min^{-1}, compared with increases after i.c.v. CRF of 20 ± 4 mmHg and 87 ± 14 beats min^{-1} respectively.

Studies of the distribution of dye injected i.c.v. showed strong staining throughout the ventricular system and along the spinal canal, and weak staining on the ventral surface of the brainstem. In contrast, after i.c. injection of dye there was staining on the dorsal and ventral surfaces of the brainstem but in none of the animals was staining observed in the ventricular system. This distribution following i.c.v. and i.c. administration was originally demonstrated in cats by Feldberg (1976), and the present studies indicate that the same is true in rabbits.

Effects on plasma catecholamines

Following i.c.v. CRF (0.5 nmol kg^{-1}) plasma noradrenaline increased by 1.56 ± 0.19 nmol l^{-1} ($P < 0.05$) after 30 min and remained significantly elevated at this level for 240 min (Figure 1). Plasma adrenaline was significantly increased at all times after CRF reaching a peak of 5.19 ± 1.50 nmol l^{-1} above control after 120 min (Figure 1). Naloxone had no effect on the CRF-induced increase in plasma noradrenaline, but the increase in plasma adrenaline tended to be greater after naloxone, and was significant at 30 and 240 min after CRF. This resulted from higher adrenaline levels (49.2 and 13.55 nmol l^{-1}) in two of the four rabbits treated with the lower dose of naloxone and a level of 10.4 nmol l^{-1} in one of the two rabbits treated with the higher dose. In the other three animals the responses were slightly greater after naloxone.

After i.c. CRF (0.5 nmol kg^{-1}) the increases in plasma noradrenaline and adrenaline were similar to those after i.c.v. CRF (Figure 1).

Respiratory effects

There was a significant increase in respiration rate and fall in Pa_{CO_2} which lasted from 15 to 240 min after i.c.v. CRF (0.5 nmol kg^{-1}) ($P < 0.05$), but there was no effect on Pa_{O_2} (Figure 2). After 60 min, respiration rate had increased from 164 ± 4 to 297 ± 20 breaths min^{-1} and Pa_{CO_2} had fallen from 34.1 ± 1.2 to 28.3 ± 1.6 mmHg and they remained at these levels for the 240 min measurements were made after CRF. Naloxone significantly reduced the CRF-induced rise in respiration rate at all times from 30 to 240 min ($P < 0.05$), but increased the fall in Pa_{CO_2} at 30 and 60 min ($P < 0.05$) (Figure 2). The changes in respiration after i.c. administration of CRF were similar to those that occurred after i.c.v. administration. After 60 min respiration rate had increased by 114 ± 17 breaths min^{-1} ($P < 0.05$), Pa_{CO_2} had fallen by 4.7 ± 1.5 mmHg ($P < 0.05$) and Pa_{O_2} had increased by 8.9 ± 0.6 mmHg ($P < 0.05$) (Figure 2).

Behavioural effects

Following i.c.v. CRF (0.5 nmol kg^{-1}) there was an increase in locomotor activity and the rabbits were hyperresponsive to external stimuli. These changes began 10–15 min after injection and lasted for 30–60 min. By 90 min after CRF the rabbits sat quietly but remained sensitive to external stimuli and this lasted for 3–4 h. Defaecation occurred in the majority of rabbits. No grooming occurred after i.c.v. administration of CRF. None of the behavioural effects of i.c.v. CRF were prevented by i.v. naloxone. These behavioural effects of i.c.v. CRF were dose-related with no observable changes after 0.1 nmol kg^{-1} but greater effects after 1–3 nmol kg^{-1}. Following the higher doses, some animals became so active they had to be returned to their cages. Two rabbits died, 120 and 210 min after i.c.v. CRF (1.0 and 3.0 nmol kg^{-1} respectively) and another rabbit died during the night after 1.0 nmol kg^{-1}.

After i.c. CRF there were similar behavioural changes to those after i.c.v. CRF; increased locomotor activity and hyperresponsiveness to external stimuli. The severity and duration of these effects was similar with either route of administration.

Discussion

The present findings demonstrate that in conscious rabbits i.c.v. CRF causes an immediate and strikingly prolonged increase in MAP, HR and plasma catecholamines. The rise in both noradrenaline and adrenaline indicates that CRF increases outflow to both sympathetic nerves and to the adrenal as noradrenaline is not found in, or secreted from, the adrenal medulla in the rabbit (Hökfelt, 1952; West, 1950). The tachycardia probably results from a combination of a reduction in cardiac vagal tone and an increase in cardiac sympathetic activity. Similar increases in MAP and HR have been reported in conscious rats and sheep, and the rise in pressure has been shown to result from an increase in cardiac output rather than in peripheral resistance (Fisher *et al.*, 1982; Scoggins *et al.*, 1984). The importance of neural mechanisms has been further demonstrated by the finding that the pressor effect is prevented by ganglionic blockade (Fisher & Brown, 1984), but ACTH, angiotensin II and vasopressin do not appear to be involved as the rise in MAP was not blocked by hypophysectomy, captopril or a vasopressin antagonist respectively (Fisher *et al.*, 1983).

These previous studies have not resolved the site of action of CRF. Our findings, demonstrating similar changes in MAP, HR, sympatho-adrenal outflow, respiration and behaviour in rabbits after i.c.v. and i.c. CRF, indicate that the effects of i.c.v. CRF could result from an action on brainstem sites which will be reached after administration via either route. Anatomical studies have demonstrated the presence of CRF receptor sites and high concentrations of mRNA for CRF in rat brainstem (Wynn *et al.*, 1984; Thompson, *et al.*, 1987). CRF immunoreactivity has been demonstrated in the dorsal vagal complex and the A1 and A5 catecholamine containing cell groups in the brainstem, as well as in hypothalamic nuclei, of the rat (Sawchenko & Swanson, 1985). However, in the rabbit the levels of immunoreactive CRF were considerably lower than those in the rat (Fischman & Moldow, 1982) and autoradiographic studies found only low densities of CRF binding at sites in pons and medulla, and around the 3rd ventricle (Chai *et al.*, 1990). These autoradiographic studies, therefore, give no clear indication of possible sites of action for CRF in the rabbit following i.c.v. or i.c. administration. CRF may act on areas with low densities of receptors or, alternatively, it may have actions in the spinal cord where, in the rat, large numbers of CRF immunoreactive fibres and terminals have been found (Merchenthaler *et al.*, 1983). Further studies using more discrete injections are required to localise the sites of action of CRF.

CRF also caused respiratory stimulation after both i.c.v. and i.c. administration. There was an increase in respiration rate and a fall in Pa_{CO_2}, and the lack of an increase in Pa_{O_2} may reflect the increase in oxygen consumption reported after i.c.v. CRF (Brown *et al.*, 1982). These respiratory effects probably result from an action on brainstem sites as they occurred after both i.c. and i.c.v. administration. The respiratory effects of centrally administered CRF have only previously been studied in anaesthetized, paralysed, vagotomized, artificially ventilated rabbits in which fourth ventricular administration of CRF increased the peak amplitude of integrated phrenic nerve activity (Bohmer *et al.*, 1985). The increase in locomotor activity and hyperresponsiveness to external stimuli following CRF in this study were similar to the findings in wild rabbits (Tarjan *et al.*, 1987), but unlike rats there was no grooming.

A role for endogenous opioids as mediators of the effects of CRF was suggested by the finding that naloxone prevented the cardiovascular and behavioural excitatory effects of i.c.v. CRF in conscious rats (Saunders & Thornhill, 1986). Opiate receptor blockade has also been shown to block the hypertensive response to different stressors (Florentino *et al.*, 1987). These findings suggest that in the rat, stress-induced cardiovascular effects may result from an increase in CRF and be mediated by opioid peptides. However, in the present study high doses of naloxone did not prevent the pressor or behavioural effects of i.c.v. CRF in rabbits. The tachycardia was reduced by naloxone suggesting that this response to CRF may be mediated partly be opioid peptides, but these studies give no indication of the mechanism involved. An action on baroreflexes is unlikely as naloxone does not alter sensitivity in normovolaemic rabbits (Burke & Dorwood, 1988), although further studies are required to exclude an effect in the presence of CRF.

The doses of naloxone used in these studies would be expected to block central δ-opioid receptors as they were similar to those which caused a pressor effect when given to

rabbits after haemorrhage (Rutter et al., 1986), an effect which is mediated by central δ-opioid receptors (Evans et al., 1989). The doses of naloxone were also higher than those which reversed the effects of centrally administered μ- and δ-opioid agonists in conscious rabbits (May et al., 1989a). Thus, the present findings suggest that in the rabbit, in contrast to the rat, the rise in blood pressure and increase in behavioural activity following i.c.v. CRF do not appear to be mediated by opioid peptides.

These studies have demonstrated that in conscious rabbits centrally administered CRF causes a prolonged increase in MAP, HR and respiratory activity and an increase in behavioural activity. All these actions support the putative role for CRF as a mediator of the responses to stress. The finding that similar responses occurred after i.c.v. and i.c. CRF, and the low level of CRF binding sites reported in the rabbit hypothalamus and brainstem (areas reached following i.c.v. and i.c. administration) raises questions as to the site of action which await further investigation. Opioid receptor blockade with naloxone did not prevent the pressor and behavioural effects of CRF, suggesting that in the rabbit these responses are not mediated by endogenous opioid peptides.

The authors are grateful for support from the Wellcome Trust.

References

BOHMER, G., SCHMID, D., OPPERMANN, D. & RAMSBOTT, M. (1985). Effects of human corticotrophin-releasing factor on central respiratory activity in the rabbit. *Pflügers Arch.*, **405**, R48.

BROWN, M.R., FISHER, L.A., RIVIER, J., SPIESS, J., RIVIER, C. & VALE, W. (1982). Corticotrophin-releasing factor: Effects on the sympathetic nervous system and oxygen consumption. *Life Sci.*, **30**, 207–210.

BURKE, S.L. & DORWOOD, P.K. (1988). Influence of endogenous opiates and cardiac afferents on renal nerve activity during haemorrhage in conscious rabbits. *J. Physiol.*, **402**, 9–27.

CHAI, S.Y., TARJAN, E., McKINLEY, M.J., PAXINOS, G. & MENDELSON, F.A.O. (1990). Corticotrophin-releasing factor receptors in the rabbit brain visualised by in vitro autoradiography. *Brain Res.*, **512**, 60–69.

EVANS, R.G., LUDBROOK, J. & VAN LEEUWEN, A.F. (1989). Role of central opiate receptor subtypes in the circulatory responses of awake rabbit to graded caval occlusions. *J. Physiol.*, **419**, 15–31.

FELDBERG, W. (1976). The ventral surface of the brainstem: a scarcely explored region of pharmacological sensitivity. *Neuroscience*, **1**, 427–441.

FISCHMAN, A.J. & MOLDOW, R.L. (1982). Distribution of CRF-like immunoreactivity in the rabbit. *Peptides*, **3**, 841–843.

FISHER, L.A. & BROWN, M.R. (1984). Corticotrophin-releasing factor and angiotensin II: comparison of CNS actions to influence neuroendocrine and cardiovascular function. *Brain Res.*, **296**, 41–47.

FISHER, L.A., JESSEN, G. & BROWN, M.R. (1983). Corticotrophin-releasing factor (CRF): mechanism to elevate mean arterial pressure and heart rate. *Regul. Pept.*, **5**, 153–161.

FISHER, L.A., RIVIER, J., RIVIER, C., SPEISS, J., VALE, W. & BROWN, M.R. (1982). Corticotrophin-releasing factor: central effects on mean arterial pressure and heart rate in rats. *Endocrinology*, **110**, 2222–2224.

FLORENTINO, A., JIMENEZ, I., NARANJO, J.R., URDIN, M.C. & FUENTES, J.A. (1987). Hypotensive effect of naloxone on high blood pressure induced by stress in the rat. *Life Sci.*, **41**, 2445–2453.

HOKFELT, B. (1952). Noradrenaline and adrenaline in mammalian tissues. *Acta Physiol. Scand.*, **25**, (suppl. 92), 39–58.

MAY, C.N., HAM, I.W., HESLOP, K.E., STONE, F.A. & MATHIAS, C.J. (1988). Intravenous morphine causes hypertension, hyperglycaemia and increases sympatho-adrenal outflow in conscious rabbits. *Clin. Sci.*, **75**, 71–77.

MAY, C.N., DASHWOOD, M.R., WHITEHEAD, C.J. & MATHIAS, C.J. (1989a). Differential cardiovascular responses to central administration of selective opioid agonists in conscious rabbits: correlation with receptor distribution. *Br. J. Pharmacol.*, **98**, 903–913.

MAY, C.N., WHITEHEAD, C.J., DASHWOOD, M.R. & MATHIAS, C.J. (1989b). Investigation of the central sites at which morphine acts to cause hypertension in conscious rabbits. *Br. J. Pharmacol.*, **97**, 833–881.

MAY, C.N., WHITEHEAD, C.J., HESLOP, K.E. & MATHIAS, C.J. (1989c). Evidence that intravenous morphine stimulates central opiate receptors to increase sympatho-adrenal outflow and cause hypertension in conscious rabbits. *Clin. Sci.*, **76**, 431–437.

MERCHENTHALER, I., HYNES, M.A., VIGH, S., SCHALLY, A.V. & PETRUSZ, P. (1983). Immunocytochemical localisation of corticotrophin-releasing factor in the rat spinal cord. *Brain Res.*, **275**, 373–377.

RUTTER, P.C., POTOCNIK, S.J. & LUDBROOK, J. (1986). Factors influencing the effects of intravenous naloxone on arterial pressure and heart rate after haemorrhage in conscious rabbits. *Clin. Exp. Pharmacol. Physiol.*, **13**, 383–398.

SAUNDERS, W.S. & THORNHILL, J.A. (1986). Pressor, tachycardic and behavioural excitatory responses in conscious rats following i.c.v. administration of ACTH and CRF are blocked by naloxone pretreatment. *Peptides*, **7**, 597–601.

SAWCHENKO, P.E. & SWANSON, L.W. (1985). Localisation, colocalisation and plasticity of corticotrophin-releasing factor immunoreactivity in rat brain. *Fed. Proc.*, **44**, 221–227.

SCOGGINS, B.A., COGHLAN, J.P., DENTON, D.A., NELSON, M.A., LAMBERT, P.F., PARKES, D.G., TREGEAR, G.W., TRESHAM, J.J. & WANG, X.M. (1984). The effect of intracerebroventricular infusions of CRF, sauvagine, ACTH (1–24) and ACTH (4-10) on blood pressure in sheep. *Hypertension*, **2**, (suppl. 3), 67–68.

TARJAN, E., DENTON, D.A., ONG, F., TREGEAR, G. & WADE, J. (1987). Effect of i.c.v. administration of CRF and POMC peptides on the sodium and water metabolism of wild rabbits. *Proceedings of the Second World Congress of Neuroscience*, 425.

THOMPSON, R.C., SEASHOLTZ, A.F. & HERBERT, E. (1987). Rat corticotrophin-releasing gene; sequence and tissue-specific expression. *Mol. Endocrinol.*, **1**, 363–370.

VALE, W., SPIESS, J., RIVIER, C. & RIVIER, J. (1981). Characterisation of a 41-residue ovine hypothalamic peptide that stimulates secretion of corticotrophin and β-endorphin. *Science*, **213**, 1394–1397.

WEST, G.B. (1950). Liberation of adrenaline from the suprarenal gland of the rabbit. *Br. J. Pharmacol. Chemother.*, **5**, 542–548.

WYNN, P.C., HAUGER, R.L., HOMES, M.C., MILLAN, M.A., CATT, K.J. & ANGUILERA, G. (1984). Brain and pituitary receptors for corticotrophin-releasing factor: localisation and differential localisation after adrenalectomy. *Peptides*, **5**, 1077–1084.

(Received June 8, 1990
Revised January 22, 1991
Accepted March 5, 1991)

Br. J. Pharmacol. (1991), **103**, 1781–1789 © Macmillan Press Ltd, 1991

Neuropeptide Y inhibits Ca^{2+} influx into cultured dorsal root ganglion neurones of the rat via a Y_2 receptor

[1]D. Bleakman, *W.F. Colmers, †A. Fournier & R.J. Miller

Department of Pharmacological and Physiological Sciences, University of Chicago, Chicago, 947 E58th Street, Chicago, Illinois, U.S.A.; *Department of Pharmacology, University of Alberta, Edmonton, Alberta, Canada and †INRS Santé, Pointe-Claire, Québec, Canada

1 The identity of the neuropeptide Y (NPY) receptor associated with the observed inhibition of neuronal Ca^{2+} currents (I_{Ca}) in rat dorsal root ganglion (DRG) cells has been established on the basis of agonist responses to analogues and carboxy terminal (C-terminal) fragments of the NPY molecule.

2 Whole cell barium currents (I_{Ba}) in DRG cells were reversibly inhibited by 100 nM NPY, 100 nM PYY and C-terminal fragments of NPY in a manner that correlated with the length of the NPY fragments (for inhibition of the I_{Ba} NPY = PYY > NPY2–36 > NPY13–36 > NPY16–36 > NPY18–36 ≫ NPY25–36).

3 C-terminal fragments of NPY were also effective in reversibly reducing the I_{Ca}, the associated increase in the intracellular Ca^{2+} concentration ($[Ca^{2+}]_i$) and the increased $[Ca^{2+}]_i$ produced by evoked action potentials in the DRG cells. In addition, a Ca^{2+}-activated Cl^- conductance was also reversibly reduced by NPY fragments only when accompanied by a reduction in Ca^{2+} entry.

4 We conclude that the Y_2 receptor for neuropeptide Y is coupled to inhibition of Ca^{2+} influx via voltage-sensitive calcium channels in DRG cells.

Keywords: neuropeptide Y; neuropeptide Y fragments; calcium currents; intracellular calcium; fura-2; voltage clamp; sensory neurones; Y_2 receptor; current clamp

Introduction

Neuropeptide Y (NPY) is one of the most abundant and widely distributed putative neuromodulators in the mammalian nervous system. The actions of NPY include the inhibition of neurotransmitter release at sympathetic neuroeffector junctions (Wahlestedt, 1987) and at glutamatergic synapses in hippocampus (Colmers *et al.*, 1988). Physiological evidence from several neuronal preparations indicate that NPY can inhibit Ca^{2+} influx through voltage-dependent Ca^{2+} channels into neurones such as rat dorsal root ganglion (DRG) neurones in culture (Walker *et al.*, 1988; Ewald *et al.*, 1988). The action of the NPY receptor is mediated through G-proteins, some, but possibly not all, of which are sensitive to the action of pertussis toxin (Ewald *et al.*, 1989; Colmers & Pittman, 1989).

Recent evidence indicates the existence of at least two types of NPY receptors which have been differentiated on the basis of agonist responses to analogues and carboxyl terminal (C-terminal) fragments of the NPY molecule. The Y_1 receptor requires the intact NPY molecule or its natural analogue, PYY, for its activation, whereas the Y_2 receptor was defined on the basis of its sensitivity to C-terminal fragments as short as NPY13–36. The Y_2 receptor has been implicated in the inhibition of transmitter release at both the sympathetic neuroeffector junction (Wahlestedt *et al.*, 1986) and at the stratum radiatum-CA1 glutamatergic synapse in rat hippocampus (Colmers *et al.*, 1991). In the present study, we have examined the action of NPY fragments and analogues on rat DRG cells in culture in order to determine the nature of the NPY receptor mediating the inhibition of Ca^{2+} influx in these cells, using several complementary methodological approaches. The results indicate that the NPY receptor in cultured DRG cells of the rat is identical with the Y_2 receptor which inhibits release of neurotransmitters at sympathetic neuroeffector junctions and hippocampal glutamatergic synapses.

[1] Author for correspondence.

Methods

Cell culture

Neurones were cultured from the dorsal root ganglia (DRG) of neonatal rats essentially as described previously (Thayer *et al.*, 1988). Briefly DRG neurones were dissected from the thoracic and lumbar segments of 1–3 day old Sprague-Dawley rats, incubated for 15 min at 37°C in collagenase/dispase (0.8 and 0.4 u ml^{-1}) and then dissociated into single cells by trituration through a Pasteur pipette. The cells were then plated on laminim-fibronectin-coated coverglasses (25 mm diameter) and incubated in Ham's medium mixture F-12, supplemented (GIBCO, Grand Island, NY, U.S.A.) with 5% heat inactivated rat serum, 4% 17-day embryonic extract, 50 ng ml^{-1} nerve growth factor, 44 mM glucose, 2 mM L-glutamine, 1% MEM 100 × vitamins and penicillin/streptomycin (100 u ml^{-1} and 100 mg ml^{-1} respectively) which was replaced every 2–3 days. Cultures were maintained at 37°C in a water-saturated atmosphere with 5% CO_2. Cells in culture between 4 and 15 days were used for the present experiments.

Whole cell patch clamp

The tight seal whole-cell configuration of the patch-clamp technique (Hamill *et al.*, 1981) was used to record the transmembrane I_{Ca} from single cells while simultaneously measuring changes in $[Ca^{2+}]_i$. Cells were mounted in a perfusion chamber and thoroughly rinsed with a buffer solution composed of (in mM), NaCl 138, $CaCl_2$ 2, $MgCl_2$ 1, KCl 5, HEPES 10 and glucose 10, adjusted to pH 7.4 with NaOH. Voltage clamp experiments were performed in a solution containing (in mM); tetraethylammonium chloride (TEACl) 143, $CaCl_2$ 2, $MgCl_2$ 1, HEPES 10 and glucose 10, pH adjusted to 7.4 with TEAOH. A cell was then approached with a fire-polished pipette containing a solution composed of (in mM): fura-2 pentapotassium salt 0.1, CsCl 135, $MgCl_2$ 1, HEPES 10, diTris phosphocreatinine 14; MgATP 3.6 and creatinine phosphokinase 50 u ml^{-1}; adjusted to pH 7.1 with CsOH. Current clamp experiments on cells were performed

with a pipette solution composed of (in mM): fura-2 pentapotassium salt 0.1, KCl 135, $MgCl_2$ 1, HEPES 10, diTris phosphocreatinine 14, MgATP 3.6 and creatine phosphokinase 50 u ml^{-1}, pH adjusted to 7.1 with KOH. For the current clamp experiments, cells were exposed to (in mM): NaCl 138, $CaCl_2$ 2, $MgCl_2$ 1, KCl 5, HEPES 10 and glucose 10, adjusted to pH 7.4 with NaOH. Action potentials were evoked by brief current pulses. The membrane potential aquisition rate was 1 ms^{-1} in order to obtain combined fura-2/electrophysiological records over 4 s periods. Consequently certain action potential traces display variable peak action potential heights due to this slow sampling rate. Background fluorescence was recorded after formation of a gigaseal but before breaking into the cell, thus accounting for fluorescence contributed by the fura-2 in the pipette. Since the pipette approached the cell from above, the objective was focused below the pipette near the middle of the cell, to minimize the pipette fluorescence. Fluorescent recordings were made from the cell soma alone. Full diffusion of the fura-2 into the cell occurs over a period of 1–3 min. Currents were recorded by a List EPC-7 amplifier, filtered by an 8-pole low pass Bessel filter with a cut off frequency of 200 Hz and stored on a computer used for the fluorescence data acquisition. Linear leak corrections were performed by averaging 16, 10 mV hyperpolarizing pulses from the holding potential. The d.c. component of the averaged leak current was then modelled so as to increase the signal to noise ratio. Digital summation of this leak template after appropriate scaling with the current obtained during depolarizing test pulses provided the leak correction. Series resistance compensation of approximately 40% was possible with the uncompensated portion of the series resistance ranged between 1.8 and 3MΩ. Peak I_{Ca} and I_{Ba} values rarely exceeded 1.5 nA or 2.0 nA respectively giving approximate maximum voltage errors of 4.5 mV and 6.0 mV. Cells were discarded when the steady leakage current at the holding potential was greater than 5% of the peak inward current. All experiments were performed at room temperature.

Fura-2 fluorescence techniques

The methods used for this study have been described previously in detail (Thayer *et al.*, 1988). Briefly, for excitation of the fluorescent calcium probe fura-2 (pentapotassium salt), the collimated beam of light from a 200 W Hg arc lamp was passed through a dual spectrophotometer (Phoenix Instruments, Philadelphia, PA, U.S.A.) which alternated wavelengths from 340 to 380 nm by means of a spinning chopper (60 Hz). The light source was placed outside a darkened Faraday cage which enclosed the vibration isolation table supporting a microscope. A fused silica lens was positioned to focus light upon a liquid light guide (3 mm × 1 mm, Oriel, Stratford, CT, U.S.A.) and a similar lens, placed at the terminating end of the guide, was positioned to direct light through the epifluorescent illuminator of the microscope. The light guide eliminated problems associated with vibration from the chopper and electrical noise from the arc lamp. The light was reflected off a dichroic mirror (Nikon, DM 400) and focused through a 70 × oil immersion objective (E. Leitz Inc., Rockleigh, NJ, U.S.A., numerical aperture 1.15). The emission fluorescence was selected for wavelengths with a 480 nm barrier filter and recordings were spatially defined with an adjustable rectangular diaphragm. The fluorescence emission was analyzed with a photomultiplier tube (bialkali) and discriminator (APED II; Thorn EMI Gencom Inc., Plainview, NY, U.S.A.). The discriminator output was converted to pulses which were then integrated by passing the signal through an 8 pole Bessel filter at 500 Hz. The gain on this detection system could be adjusted from 1 to 100 fold by increasing the pulse length. The conversion of light intensity to voltage by this process was confirmed to be linear over the range of the light levels used in these experiments. The signal from the filter was fed into one channel of an analog to digital convertor (PDP-11/73) computer system (Indec Systems, Sunnyvale, CA, U.S.A.). The signals from two photodiodes, each placed in a small portion of the light beam directed toward the monochromators, were connected to two additional channels of the analogue to digital converter.

Sorting the fluorescence output into signals corresponding to excitation at these two wavelengths was performed entirely by software written in BASIC-23 (Cheshire Data, Indec Systems). The photomultiplier output was sorted into signals from 340 and 380 nm excitation by using the photodiode outputs as timing signals and the output observed on-line throughout the experiment.

Cover slips (25 mm diameter), plated with cells, were mounted in the perfusion chamber which was positioned on the opening of the microscope stage. The solution change in the cell superfusion system approximated a step occurring over 10 s. The tubing between the large media reservoirs and the inlet to the chambers delayed the onset of the solution change by an additional 10 s. Figures have been corrected for the perfusion delay.

Calibration and analysis

Records were corrected for experimentally determined background values and the ratio of 340/380 nm fluorescence calculated off-line. Ratios were converted to free Ca^{2+} by the equation, $Ca^{2+} = K(R - R_{min})/(R_{max} - R)$ in which R is the 340/380 nm fluorescent ratio (Grynkiewicz *et al.*, 1985). The maximum ratio (R_{max}), the minimum ratio (R_{min}) and the constant K, the product of the dissociation product for fura-2 and the ratio of the free and bound forms of the dye at 380 nm, were determined from a fit to a standard curve using the above equation with a non-linear least squares analysis computer programme (Fabatio & Fabatio, 1979). The standard curve was determined for the fura-2 salt in calibration buffer (in mM: 4-(2-hydroxyethyl)-1-piperazineethanesulphonic acid (HEPES) 20, KCl 120, NaCl 5, $MgCl_2$ 1, pH 7.1) containing 10 mM ethylene gylcol *bis* (B-aminoethyl)-N,N,N',N'-tetraacetic acid (EGTA), $K_s = 3.696 \times 10^6\ M^{-1}$ with calculated amounts of Ca^{2+} added to give free calcium concentrations ranging between approximately 0 to 2000 nM. Identical calibration curves were obtained if CsCl was used to replace KCl. Experiments performed over long periods of time (>30 s) were digitally filtered with an algorithm which added 1/2 the value of each datum point to 1/4 of the value of each neighbouring point. The data were cycled through this routine 5 times. The $[Ca^{2+}]_i$ traces in patchclamp experiments were digitally filtered by a single cycle through an 11 point moving average algorithm.

Peptide synthesis

Fragments of NPY were synthesized by the solid phase method using a manual home-made multireactor synthesizer. The syntheses were carried out with a benzhydrylamine resin (Pietta *et al.*, 1974) since the peptides bear an amide C-terminal function. All amino acids were coupled via the BOP/DMF method (Fournier *et al.*, 1988), according to a recently-described protocol (Forest & Fournier, 1990). The Boc amino acids with appropriate side-chain protection were obtained from commercial sources. Completed peptides were cleaved from the resin support and deprotected by a 90 min treatment at 0°C with liquid hydrofluoric acid containing m-cresol and dimethyl sulphide as scavengers (10 : 1 : 1 v/v).

After extraction from the resin and lyophilization, the peptides were purified by reverse-phase chromatography on a Waters Deltapak column, using an eluent of (A) H_2O (0.06% trifluoracetic acid, TFA) and (B) acetronitrile-H_2O (0.06% TFA). Peptides were eluted with successive linear gradients of solvent B. Analytical high performance liquid chromatography (h.p.l.c.) of the individual fractions were carried out and the fractions corresponding to the purified peptide were lyophilized. The purified material was

characterized by analytical h.p.l.c., capillary electrophoresis and amino acid analysis.

Results

Electrophysiological recordings

Experiments in this series were performed on a total of 42 cells. Of these, 19 were studied in voltage clamp mode alone using Ba^{2+} as the charge carrier and in 7 cells Ca^{2+} influx was examined by fura-2 based microfluorimetry under voltage clamp conditions. Of these 26 cells, 21 cells responded to NPY with an inhibition of peak I_{Ca} or I_{Ba}. A response was defined as a reduction in I_{Ca} or I_{Ba} by 20% or more produced by 100 nM NPY. A robust effect in magnitude enabled us to compare reliably the effects of NPY fragments with the native molecule (see below). In 16 cells, Ca^{2+} influx was examined by fura-2 based microfluorimetry under current clamp conditions.

Peptide actions on barium currents

Neuropeptide Y and PYY Tight seal, whole cell recordings of Ba^{2+} currents (I_{Ba}) were made from DRG neurones at a holding potential of −80 mV. Peak whole-cell currents were observed during steps to 0 mV (Figure 1). The initial peak I_{Ba} ranged between 0.3 and 2.0 nA and declined gradually with time. In agreement with earlier observations for I_{Ca}, bath application of 100 nM NPY caused an inhibition of between 20 and 60% of control I_{Ba} amplitudes (Ewald *et al.*, 1988). Mean inhibition of the I_{Ba} by 100 nM NPY was 33.8 ± 2.0% (n = 13). The inhibition was also often accompanied by a slowing of the kinetics of activation of the I_{Ba}, as has been reported for other neurotransmitters (Bean, 1989) although the magnitude of this effect varied and was not always apparent (e.g. compare Figure 1a and b). The inhibition reversed readily upon washout of the peptide (Figure 1a). Higher concentrations (1 μM) of NPY were only slightly more effective than 100 nM NPY, indicating that this concentration produced almost a maximal response (Figure 1, 35.9 ± 6.1% for 100 nM and vs 42.7 ± 5.9% for 1 μM, n = 3). A concentration of 100 nM was

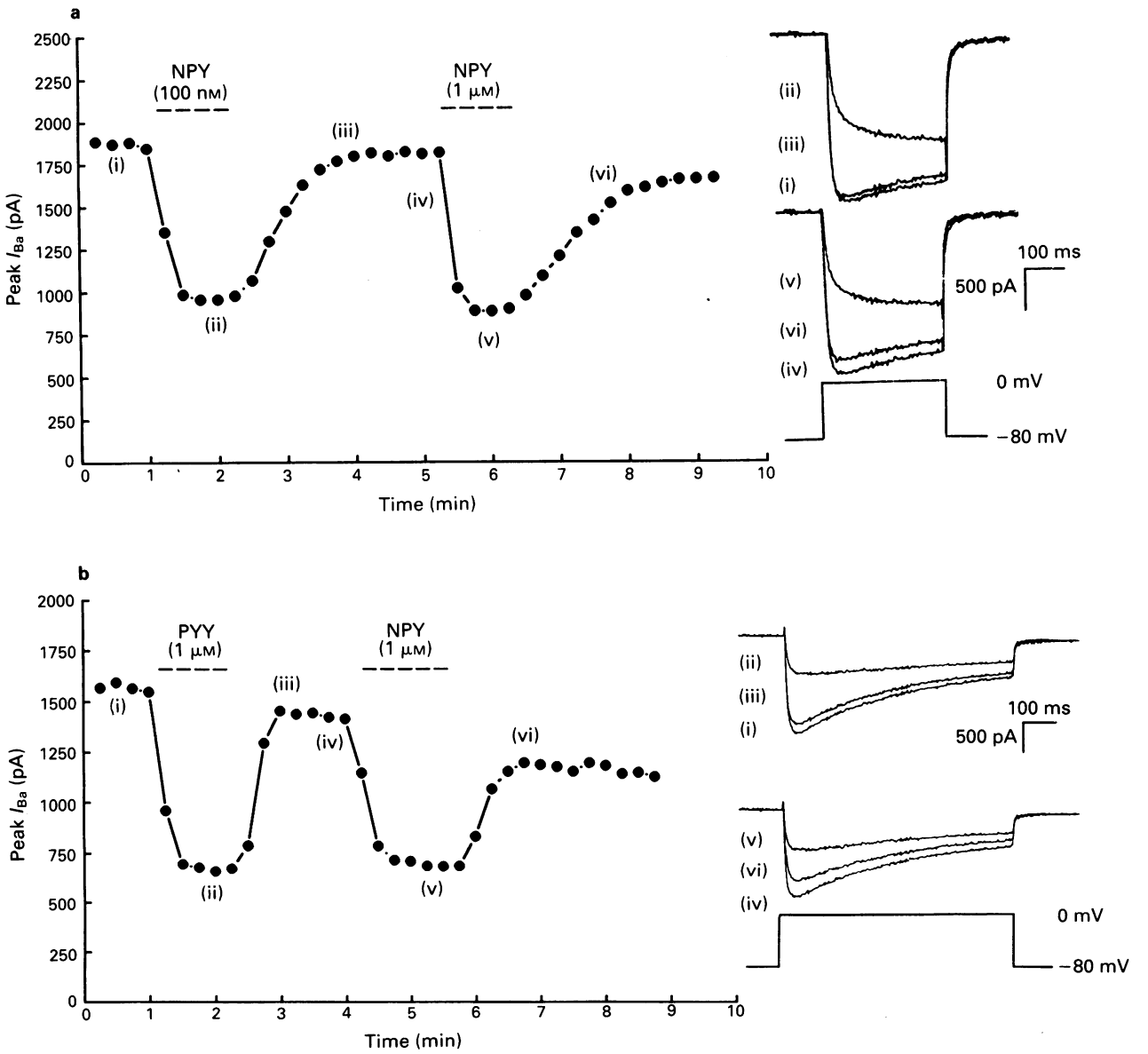


Figure 1 Neuropeptide Y (NPY)- and PYY-mediated inhibition of I_{Ba} in single DRG neurones. (a) The timecourse of inhibition of I_{Ba} by two concentrations of NPY is shown with 20 mM BAPTA in the patch pipette. The insets show superimposed individual current traces evoked from Vh = −80 mV to Vt = 0 mV at the timepoints indicated. The figure is representative of 3 similar experiments. (b) Timecourse of inhibition of I_{Ba} by PYY and NPY with 20 mM BAPTA in the patch pipette. Insets as in (a). The figure is representative of 3 similar experiments.

used for comparison of the actions of NPY analogues and NPY fragments. Application of the full-sequence naturally occurring analogue, PYY (1 μM), also elicited an inhibition of the I_{Ba} which was not significantly different from that observed with NPY (1 μM) (Figure 1b).

Neuropeptide and NPY fragments Application of C-terminal fragments of NPY also elicited reversible inhibitions of the I_{Ba} in DRG neurones (Figure 2). The degree of inhibition of the I_{Ba} was correlated with the length of the fragment, with NPY2–36 being 85% as effective as NPY and PYY (Figure 2a). As observed with NPY, the NPY fragments also appeared to alter the kinetics of the I_{Ba} (Figure 2b). Current-voltage relationships were obtained for NPY and NPY13–36 (Figure 2c and d). A comparison of the relative effects of NPY fragments on the inhibition of the peak I_{Ba} to NPY alone is shown in Figure 3. It may be seen that a significant reduction of the peak I_{Ba} was observed for C-terminal fragments NPY18–36 and longer.

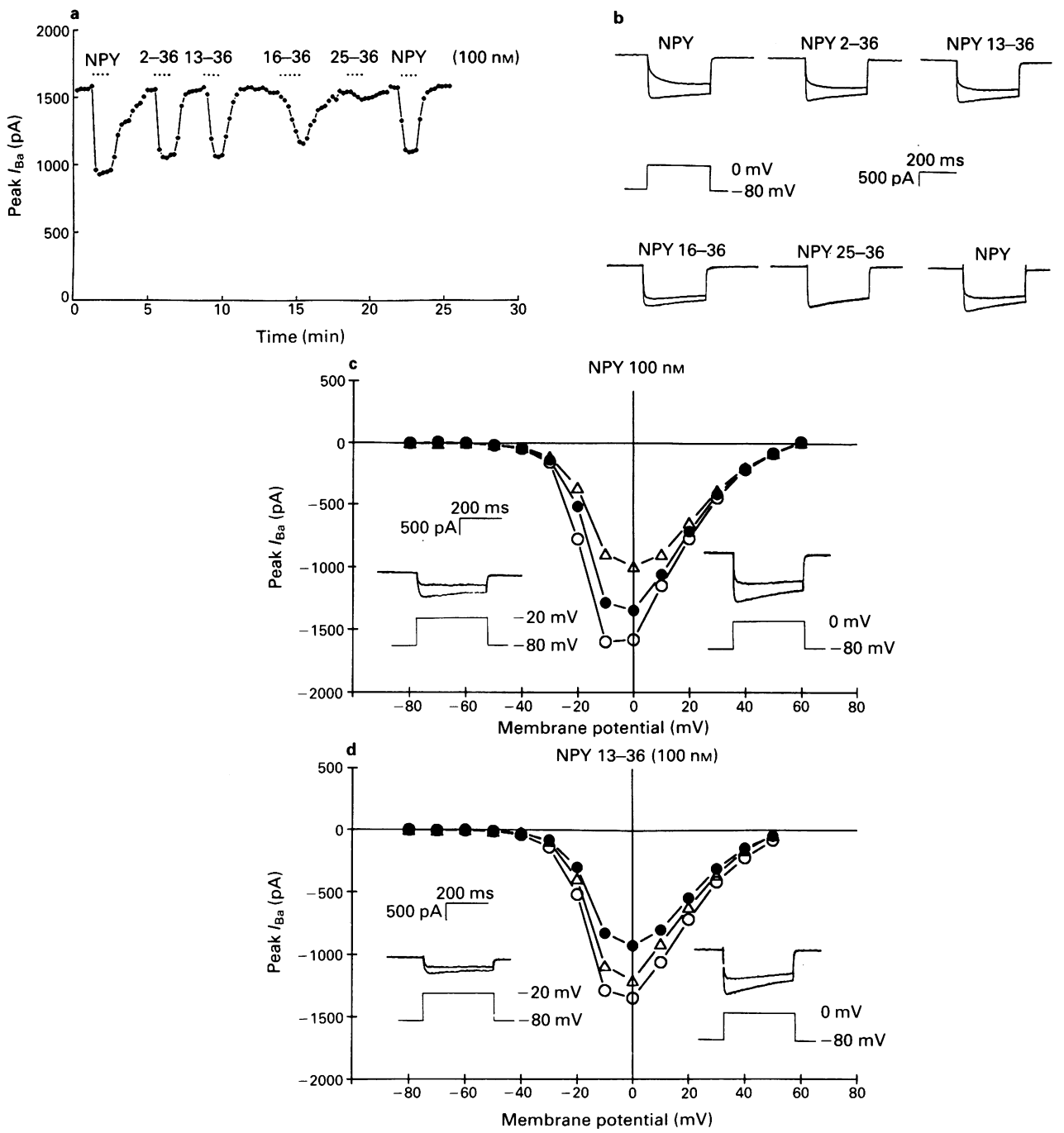


Figure 2 Effect of 100 nM neuropeptide Y (NPY) and 100 nM concentrations of different C-terminal fragments on the I_{Ba} in a DRG neurone. (a) Timecourse of inhibition of peak I_{Ba} by NPY and fragments with 20 mM BAPTA in the patch pipette from Vh = −80 mV to Vt = 0 mV. Fragments were presented in order of decreasing length, while NPY itself was applied both before and after the series of fragments. (b) Effects of NPY and fragments on individual I_{Ba}s in the presence and absence of the peptides as indicated. (c) Current voltage relationship for the effect of 100 nM NPY on the peak I_{Ba} measured in the presence of 20 mM BAPTA in the pipette. The traces show the current-voltage relationship from a Vh of −80 mV to various test potentials in the absence (○) and presence (△) of NPY and following washout of the peptide (●). Insets show individual current traces in the absence and presence of NPY for two different test potentials. (d) Current-voltage relationship for the effect of 100 nM NPY13–36 on the peak I_{Ba} measured in the presence of 20 mM BAPTA in the pipette from the same neurone as shown in (c). The traces show the current-voltage relationship from a Vh of −80 mV to various test potentials in the absence (○) presence (●) of 100 nM NPY13–36 and following washout of the peptide (△). Insets as in (c).

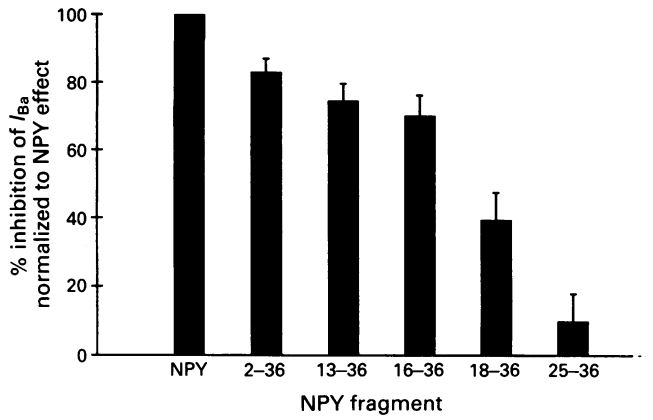


Figure 3 Comparative inhibition of the peak I_{Ba} by neuropeptide Y (NPY) and C-terminal fragments of NPY (all at 100 nM) in DRG neurones. Inhibition of the peak I_{Ba} by C-terminal fragments is normalized to the inhibition produced by 100 nM NPY itself in the same cell. The results are the mean with standard error of the mean for 5 cells in which comparisons were made with full sequence NPY.

Combined voltage clamp/$[Ca^{2+}]_i$ measurements

We further investigated the effects of NPY and C-terminal fragments on I_{Ca} and $[Ca^{2+}]_i$ by simultaneously monitoring the I_{Ca} and $[Ca^{2+}]_i$ in single DRG cells under voltage clamp conditions in which the pipette solution contained 100 μM fura-2 (Figure 4). Brief (80 ms) voltage steps from a holding potential of −80 mV to a test potential of 0 mV were applied every 30 s and the increase in $[Ca^{2+}]_i$ measured. The peak I_{Ca}s in this series of experiments ranged between 0.3 and 1.3 nA. The rate of decay of the inward current carried by Ca^{2+} was significantly more rapid than when Ba^{2+} was the charge carrier in agreement with earlier observations (Bleakman *et al.*, 1990). $[Ca^{2+}]_i$ levels increased in response to the voltage clamp step (Figure 4a). Neither 100 nM NPY nor 100 nM NPY13–36 caused changes in the basal $[Ca^{2+}]_i$, but they did produce a reversible inhibition of the I_{Ca} (28.5 ± 3.5% and 17.7 ± 3.0%, $n = 4$ respectively). The simultaneously recorded increase in $[Ca^{2+}]_i$ was also reduced in the presence of NPY13–36 (100 nM) in parallel with the I_{Ca} and also recovered upon washout (Figure 4b). As with the other experiments, NPY also reversibly reduced the I_{Ca} and

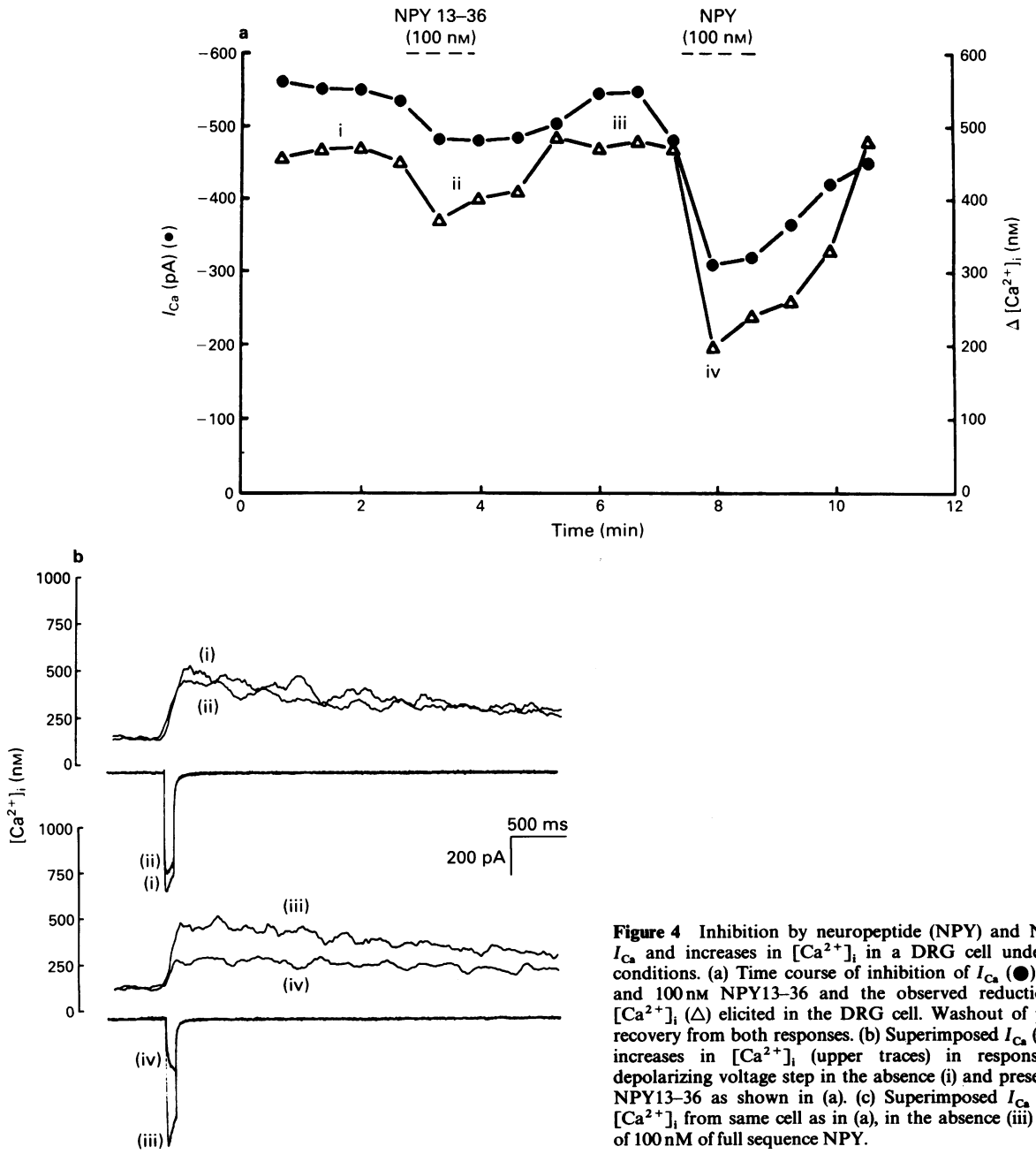


Figure 4 Inhibition by neuropeptide (NPY) and NPY13–36 of the I_{Ca} and increases in $[Ca^{2+}]_i$ in a DRG cell under voltage clamp conditions. (a) Time course of inhibition of I_{Ca} (●) by 100 nM NPY and 100 nM NPY13–36 and the observed reductions in the peak $[Ca^{2+}]_i$ (△) elicited in the DRG cell. Washout of peptides led to a recovery from both responses. (b) Superimposed I_{Ca} (lower traces) and increases in $[Ca^{2+}]_i$ (upper traces) in response to an 80 ms depolarizing voltage step in the absence (i) and presence (ii) of 100 nM NPY13–36 as shown in (a). (c) Superimposed I_{Ca} and increases in $[Ca^{2+}]_i$ from same cell as in (a), in the absence (iii) and presence (iv) of 100 nM of full sequence NPY.

the $[Ca^{2+}]_i$ in DRG cells (Figure 4c). The mean inhibition of the increase in peak $[Ca^{2+}]_i$ in response to an 80 ms voltage clamp step was $32.0 \pm 8.1\%$ and $27.8 \pm 7.0\%$ ($n = 4$) for 100 nM NPY and 100 nM NPY13–36 respectively.

Combined current clamp/$[Ca^{2+}]_i$ measurements

Experiments were also performed on DRG cells under current clamp conditions in which trains of action potentials were elicited by trains of brief depolarizing current pulses (4 ms). The membrane potential was maintained during the course of the experiment to a value of approximately −60 mV. Once stable $[Ca^{2+}]_i$ responses to identical trains of action potentials had been obtained, 100 nM NPY was applied via the bath. As observed with the above experiments under voltage clamp, NPY application itself had no effect on the baseline levels of $[Ca^{2+}]_i$. However, NPY caused a reversible reduction in the rise in $[Ca^{2+}]_i$ which resulted from the evoked action potential train (Figure 5a). In 12 of 16 neurones examined, NPY caused a mean reduction in the peak increase in the $[Ca^{2+}]_i$ of $46 \pm 6\%$. This inhibition reversed upon washout of NPY. In the same 12 neurones, NPY13–36 also caused a reversible inhibition of Ca^{2+} influx in response to a train of action potentials (Figure 5b). At 100 nM, NPY13–36 was only $68.6 \pm 6.7\%$ ($n = 12$ cells) as effective as NPY in inhibiting Ca^{2+} influx elicited in this manner.

Effect of neuropeptide Y and C terminal fragments on $[Ca^{2+}]_i$-dependent membrane events

It has previously been shown that for a subpopulation of DRG cells that were loaded with Cl^-, the action potential was

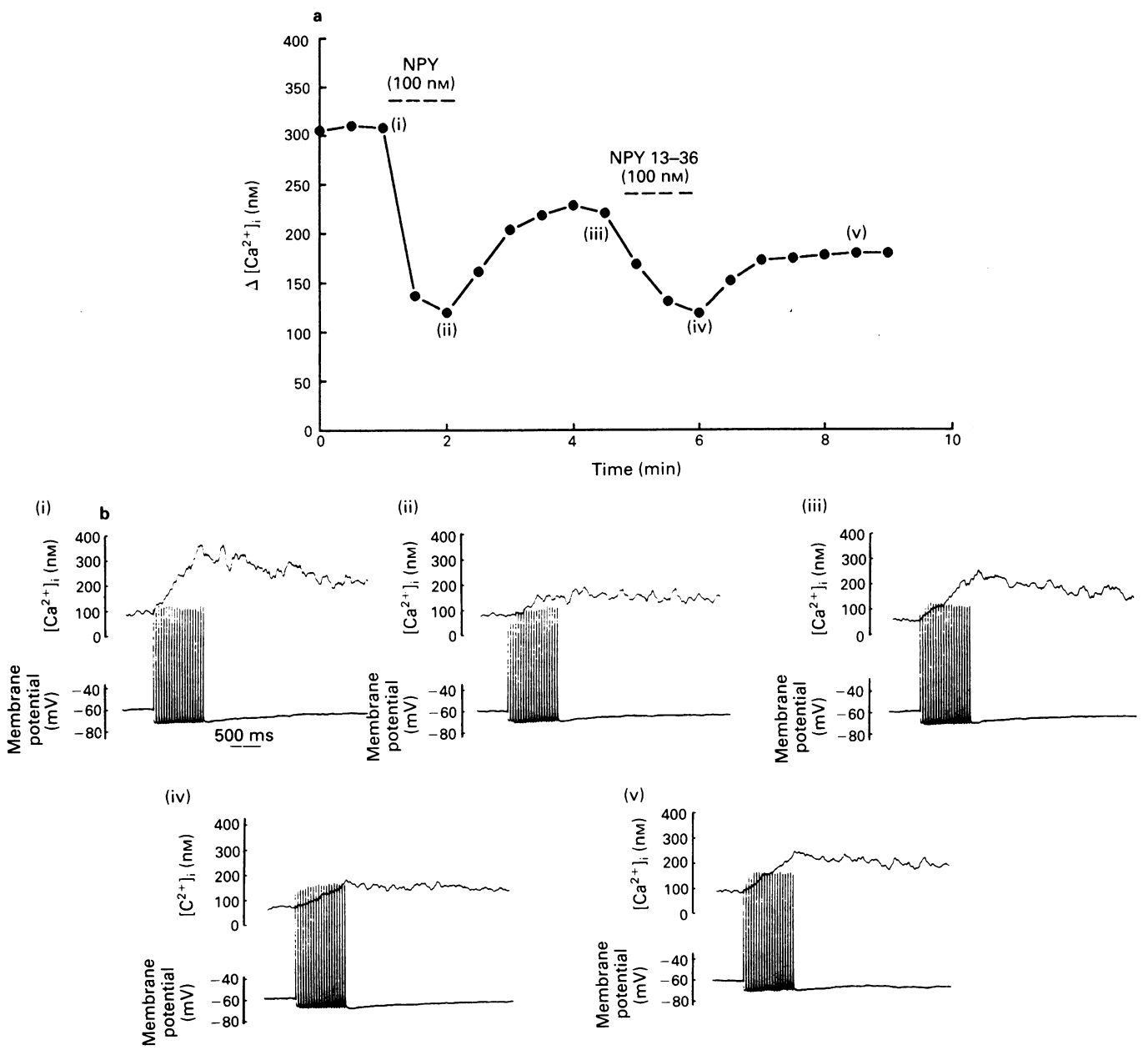


Figure 5 Inhibition by neuropeptide Y (NPY) and NPY13–36 of action potential-evoked increases in $[Ca^{2+}]_i$ in a single DRG cell under current clamp. (a) Time course of inhibition of action potential train-mediated increases (peak-basal) in $[Ca^{2+}]_i$ by 100 nM NPY and 100 nM NPY13–36. Each time point represents the $\Delta[Ca^{2+}]_i$ which results from the firing of a train of 20 action potentials. (b) Representative voltage recording of action potentials evoked once every 30 s in a DRG cell by a train of 4 ms pulses (20 APs, 25 Hz). Increases in $[Ca^{2+}]_i$ in response to train of action potentials were reversibly inhibited by both 100 nM NPY (ii) and 100 nM NPY13–36 (iv).

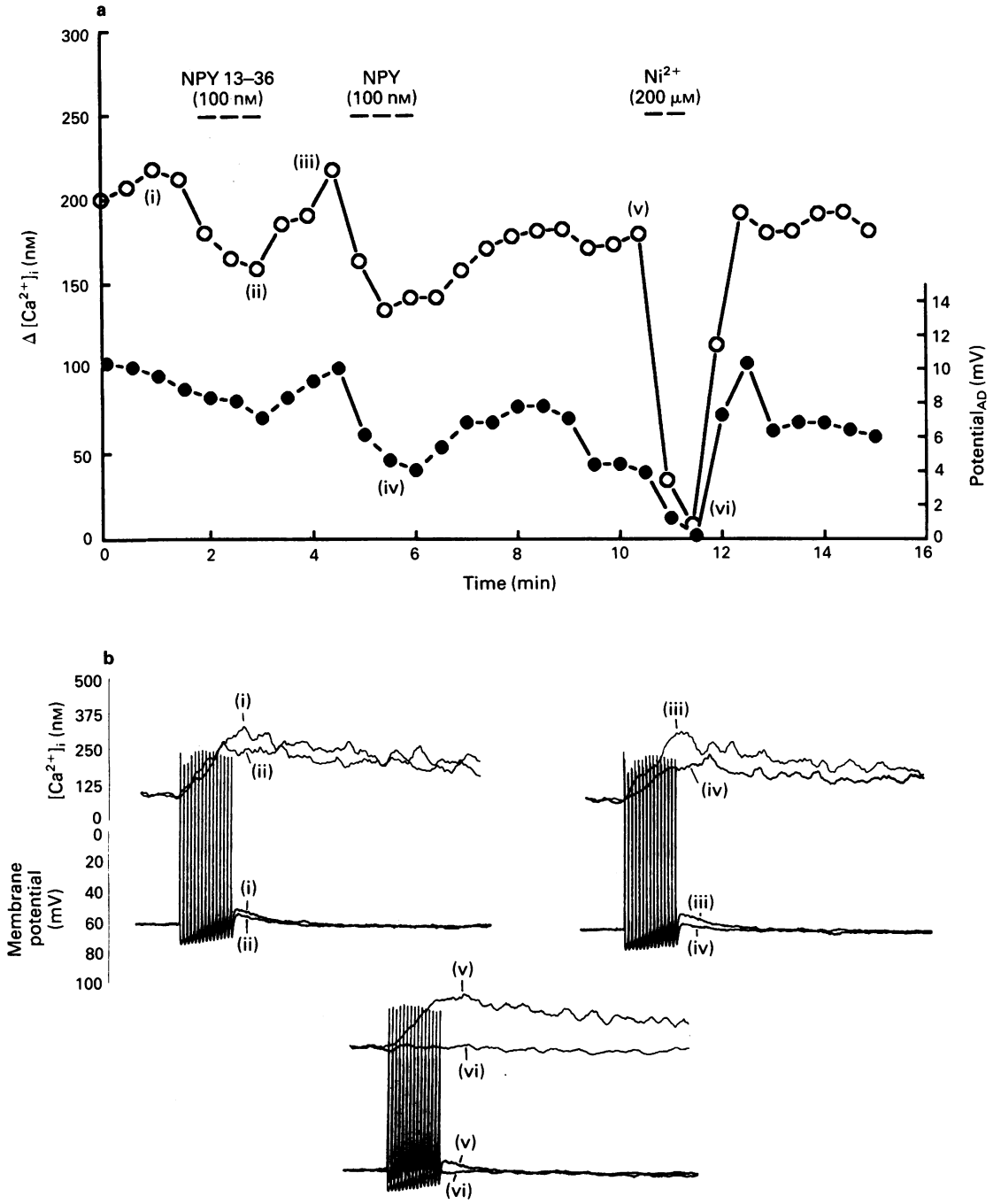


Figure 6 (a) Time course of the rise in $[Ca^{2+}]_i$ due to the firing of 15 action potentials (○) (4 ms, 25 Hz) and the effect of 100 nM neuropeptide Y (NPY), 100 nM NPY13–36 and 200 μM Ni^{2+} on this and on the magnitude of the after-depolarization which resulted. The after-depolarization (AD) (●) was the difference between the resting membrane potential before evoking the train of action potentials and the peak value of the depolarization between the last action potential and 2 s following this point. (b) Individual timepoints of after-depolarizing potentials and their modulation by 100 nM NPY and 100 nM NPY13–36 and 200 μM Ni^{2+} as indicated in (a).

followed by an after-depolarization (Dichter & Fischbach, 1977). In the present experiments, after-depolarizations were also observed which increased in magnitude with longer trains of action potentials and accordingly larger accompanying $[Ca^{2+}]_i$ transients. It is likely that the after-depolarizations are due to activation of a Cl^- conductance by the increase in $[Ca^{2+}]_i$ as described elsewhere (Scott *et al.*, 1988). After-depolarizations were observed in the present series of experiments in 5 of 16 cells and were modulated by agents which reduced Ca^{2+} influx. As can be seen in Figure 6, 100 nM NPY13–36, 100 nM NPY and 200 μM Ni^{2+} reduced the magnitude of the after-depolarization. These changes were always accompanied by decreases in $[Ca^{2+}]_i$.

Under whole-cell voltage clamp conditions the after-depolarization which followed the action potential manifested itself as a slow inward Cl^- tail current ($I_{Cl(Ca)}$) which has previously been described by others (Mayer, 1985; Scott *et al.*, 1988). Tail currents were observed in the DRG cells which lasted between 1 and 4 s following repolarization to −80 mV. Both 100 nM NPY and 100 nM NPY13–36 reduced the magnitude of the tail current and the associated $[Ca^{2+}]_i$ transient (Figure 7). Figure 7c also illustrates the effect of replacing the extracellular Ca^{2+} with Ba^{2+}. Under such conditions the magnitude of the Ca^{2+} activated Cl^- tail current was reduced. A residual fura-2 signal was observed, consistent with the ability of Ba^{2+} to bind to fura-2 (Schilling *et al.*, 1989).

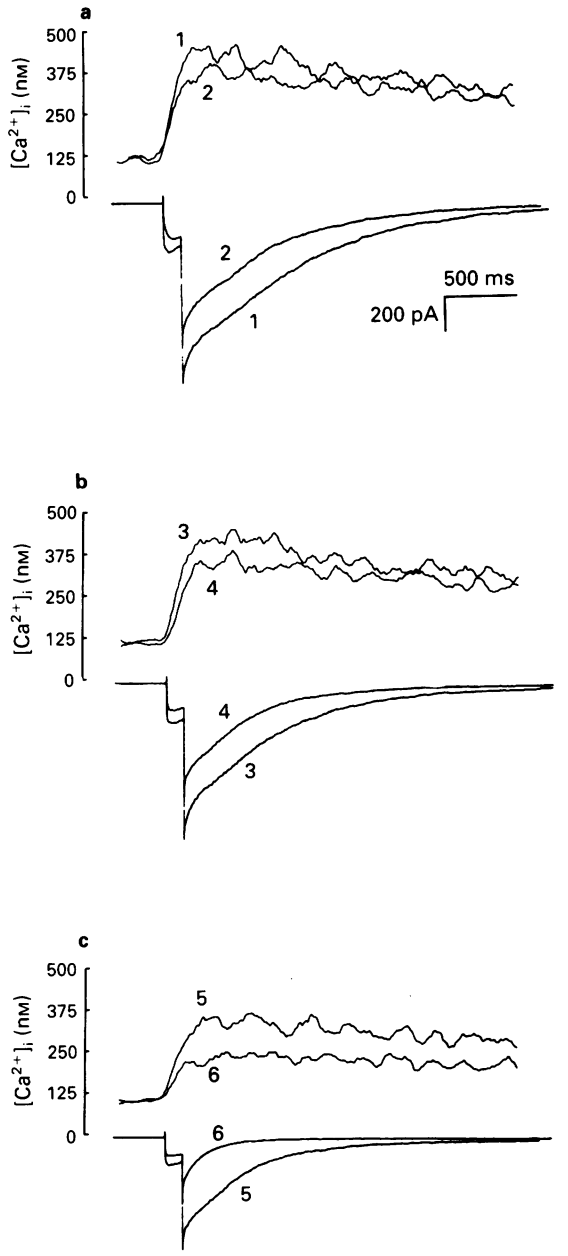


Figure 7 Tail currents and their modulation by 100 nM NPY13–36 ((1) control; (2) NPY13–36) and after recovery from this, 100 nM neuropeptide Y (NPY) ((3) control; (4) NPY). Also shown is the effect of replacement of Ca^{2+} with Ba^{2+} in the same cell as the other traces ((5) 2 mM Ca^{2+}; (6), 2 mM Ba^{2+}).

Discussion

Neuropeptide Y inhibits the influx of Ca^{2+} into rat DRG neurones in culture by inhibition of voltage-operated Ca^{2+} channels (Walker *et al.*, 1988; Ewald *et al.*, 1988). This paper presents evidence that the receptor for NPY on these cells is identical in its agonist profile to the Y_2 receptor present on presynaptic terminals at peripheral sympathetic neuroeffector junctions and on presynaptic glutamatergic terminals in area CA1 of rat hippocampus (Colmers *et al.*, 1987). NPY was without any effect on the holding current or resting membrane potential in the present experiments, and there was no evidence for an effect on cell membrane resistance. Thus the actions of the peptide seem to be manifest only on the Ca^{2+} conductances in these neurones.

The results from three different experimental approaches were congruent. Thus, NPY, PYY and NPY13–36 all inhibited Ba^{2+} influx through voltage-gated Ca^{2+} channels, inhibited Ca^{2+} influx during action potentials and simultaneously inhibited the peak I_{Ca} and the rise in $[Ca^{2+}]_i$ due to the voltage step. In the action potential experiments, the afterdepolarization observed in response to a train of action potentials, which is due to an increase in a Ca^{2+} activated Cl^- conductance (Dichter & Fischbach, 1977; Mayer, 1985) was also reduced by NPY, PYY and NPY13–36 application. In all cases, the short NPY25–36 fragment was without significant activity on any of the parameters measured. Interestingly, the NPY16–36 fragment exhibited clear, but weak, inhibitory effects in all preparations in which it was tested, and the NPY18–36 fragment also weakly inhibited I_{Ba}. A similar, but somewhat smaller inhibitory action of NPY16–36 has been observed on excitatory postsynaptic potentials, but not on population field responses, in area CA1 of rat hippocampal slice *in vitro*; however, unlike the present experiments, no effect of NPY18–36 was seen in this preparation (Colmers *et al.*, 1991).

The Y_2 receptor for NPY has been associated with inhibition of neurotransmitter release from sympathetic (Wahlestedt *et al.*, 1986), parasympathetic (Potter *et al.*, 1989) and sensory neurones (Perney & Miller, 1989). Several second messenger systems have been implicated in mediating the effects of this Y_2 response. For example Y_2 receptors for NPY have been linked to an inhibition of adenylate cyclase (reviewed in McDonald, 1988). However this effect does not appear to be a satisfactory criterion for the subclassification of receptor subtypes for NPY since NPY decreases forskolin-stimulated adenosine 3′ : 5′-cyclic monophosphate (cyclic AMP) levels in both SK-N-MC (Y_1-receptor) and SK-N-BE2 (Y_2 receptor) transfected cell lines (Wahlestedt *et al.*, 1990). In addition, in hippocampal slices, the elevation of intracellular cyclic AMP levels with the membrane soluble cyclic AMP analogue, 8(4-chlorophenylthio) cyclic AMP, does not appear to interfere with Y_2 receptor-mediated inhibition of neurotransmitter release (Klapstein *et al.*, 1990). The actions of NPY at the Y_2 receptor have also been associated with elevations in $[Ca^{2+}]_i$ and the generation of IP_3 following activation of PLC in a subpopulation of DRG neurones (Perney & Miller, 1989). However, NPY also increased $[Ca^{2+}]_i$ in neurones which contain Y_1 receptors (Aakerlund *et al.*, 1990). Thus, the characterization of Y_1 and Y_2 receptors for NPY on the basis of intracellular second messenger systems is equivocal.

In the present experiments it is unlikely that the inhibition of the I_{Ca} is secondary to an increase in $[Ca^{2+}]_i$ since inhibition of the I_{Ca} was observed even when the $[Ca^{2+}]_i$ was buffered with BAPTA in the patch pipette. Inhibition of the I_{Ca} by NPY has also been observed in acutely dissociated nodose ganglion cells (Wiley *et al.*, 1990) and in myenteric plexus neurones (Hirning *et al.*, 1990) in both studies the inhibition of the I_{Ca} was found to be sensitive to the action of pertussis toxin (PTX) in agreement with earlier studies on DRG cells in culture (Ewald *et al.*, 1988). However this may not be a universal mechanism for coupling NPY responses since in hippocampal slices the effect of NPY activation on transmitter release, which may be associated with inhibition of the I_{Ca} (Colmers *et al.*, 1987), is insensitive to pretreatment with PTX (Colmers & Pittman, 1989). This suggests that a PTX-insensitive G-protein may be involved in coupling NPY receptors to Ca^{2+} channels in this case. It is interesting to note that the receptor in hippocampal neurones also appears to be of the Y_2 type (Colmers *et al.*, 1991).

Thus the present study provides the first clear evidence that Y_2 receptors are coupled to the inhibition of Ca^{2+} influx by an effect on voltage-gated Ca^{2+} channels. To date there is no evidence that the Y_1 receptor in neurones can be coupled to this response.

D.B. was supported by a Fulbright Travel Fellowship. This work was funded by grants DA 02121, MH-40165 and a Digestive Diseases Research Centre Core Grant IP30-DK42086 to R.J.M. W.F.C. is an Alberta Heritage Foundation for Medical Research Scholar and was supported by an MRC Canada grant MT 10520.

References

AAKERLUND, L., GETHER, U., FUHLENDORFF, J., SCHWARTZ, T.W. & THASTRUP, O. (1990). Y1 receptors for neuropeptide Y are coupled to mobilization of intracellular calcium and inhibition of adenylate cyclase. *FEBS Lett.*, **260**, 73–78.

BEAN, B.P. (1989). Neurotransmitters inhibit neuronal calcium currents by changes in channel voltage dependence. *Nature*, **340**, 153–156.

BLEAKMAN, D., BRORSON, J.R. & MILLER, R.J. (1990). The effect of capsaicin on voltage-gated calcium currents and calcium signals in cultured dorsal root ganglion cells. *Br. J. Pharmacol.*, **101**, 423–431.

COLMERS, W.F., KLAPSTEIN, G.J., FOURNIER, A., ST.-PIERRE, S. & TREHERNE, K.A. (1991). Presynaptic inhibition by neuropeptide Y (NPY) in rat hippocampal slice *in vitro* is mediated by a Y_2 receptor. *Br. J. Pharmacol.*, **102**, 41–44.

COLMERS, W.F., LUKOWIAK, K.D. & PITTMAN, Q.J. (1988). Neuropeptide Y action in the rat hippocampal slice: site and mechanism of presynaptic action. *J. Neurosci.*, **8** 3827–3837.

COLMERS, W.F., LUKOWIAK, K.D. & PITTMAN, Q.J. (1987). Presynaptic action of neuropeptide Y in area CA1 of the rat hippocampal slice. *J. Physiol.*, **383**, 285–299.

COLMERS, W.F. & PITTMAN, Q.J. (1989). Presynaptic inhibition by neuropeptide Y and baclofen in hippocampus; insensitivity to pertussis toxin treatment. *Brain Res.*, **498**, 99–104.

DICHTER. M.A. & FISHBACH, G.D. (1977). The action potential of chick dorsal root ganglion neurons in cell culture. *J. Physiol.*, **267**, 281–298.

EWALD, D.A., MATTHIES, H.J.G., PERNEY, T.M., WALKER, T.M. & MILLER, R.J. (1988). The effect of down regulation of protein kinase C on the inhibitory modulation of dorsal root ganglion neurone Ca currents by neuropeptide Y. *J. Neurosci.*, **8**, 2447–2451.

EWALD, D.A., PANG, I.-H., STERNWEIS, P.C. & MILLER, R.J. (1989). Differential G-protein mediated coupling of neurotransmitter receptors to Ca channels in rat dorsal ganglion neurons *in vitro*. *Neuron*, **2**, 1185–1193.

FABATIO, A. & FABATIO, F. (1979). Calculator programs for computing the composition of the solutions containing multiple metals and ligands used for experiments in skinned muscle cells. *J. Physiol. (Paris)*, **75**, 463–505.

FOREST, M. & FOURNIER, A. (1990). BOP reagent for the coupling of pGlu and BocHis(Tos) in solid phase peptide synthesis. *Int. J. Pept. Res.*, **35**, 89–94.

FOURNIER, A., WANG, C.T. & FELIX, A.M. (1988). Applications of BOP reagent in solid phase synthesis. Advantages of BOP reagent for difficult couplings exemplified by a synthesis of [Ala^{15}]-GRF(1-29)NH_2. *Int. J. Pept. Res.*, **31**, 86–97.

GRYNKIEWICZ, G., PEONIE, M. & TSIEN, R.Y. (1985). A new generation of Ca indicators with greatly improved fluorescent properties. *J. Biol. Chem.*, 260, 3440–3450.

HAMILL, O.P., MARTY, A., NEHER, E., SAKMANN, B. & SIGWORTH, F. (1981). Improved patch-clamp technique for high resolution current recording from cells and cell free membrane patches. *Pflügers Arch.*, **391**, 85–100.

HIRNING, L.D., FOX. A.P. & MILLER, R.J. (1990). Inhibition of calcium currents in cultured myenteric neurons by neuropeptide Y: evidence for a direct receptor/channel coupling. *Brain Res.*, **532**, 120–130.

KLAPSTEIN, G.L., TREHERNE, K.A. & COLMERS, W.F. (1990). Neuropeptide Y presynaptic effects in hippocampal slice *in vitro* are Y2 receptor mediated but not via adenylate cyclase. *Proc. N.Y. Acad. Sci.*, **611**, 457–458.

MAYER, M.L. (1985). A calcium dependent chloride current generated after depolarization of rat sensory neurons in culture. *J. Physiol.* (London), **364**, 217–239.

MCDONALD, J.K. (1988). NPY and related substances. *Crit. Rev. Neurobiol.*, **4**, 97–135.

PERNEY, T.M. & MILLER, R.J. (1989). Two different G-proteins mediate Neuropeptide Y and bradykinin-stimulated phospholipid breakdown in cultured rat sensory neurons. *J. Biol. Chem.*, **264**, 7317–7327.

PIETTA, P.G., CAVALLO, P.F., TAKAHASSHI, K. & MARSHALL, G.R. (1974). Preparation and use of benzhydrylamine polymers in peptide synthesis. II. Synthesis of thyrotropin releasing hormone, thyrocalcitonin 26–32 and eledoisin. *J. Org. Chem.*, **39**, 44–48.

POTTER, E.K., MITCHELL, L., MCCLOSKEY, M.J.D., TSENG, A., GOODMAN, A.E., SHINE, J. & MCCLOSKEY, D.I. (1989). Pre- and post-junctional actions of NPY and related substances. *Regul. Pept.*, **25**, 167–177.

SCOTT, R.H., MCGUIRK, S.M. & DOLPHIN, A.C. (1988). Modulation of divalent cation-activated chloride ion currents. *Br. J. Pharmacol.*, **94**, 653–662.

SCHILLING, W.P., RAJAN, L. & STROBL-JAGER, E. (1989). Characterization of the bradykinin-stimulated calcium influx pathway of cultured vascular endothelial cells. *J. Biol. Chem.*, **264**, 12838–12848.

THAYER, S.A., STUREK, M. & MILLER, R.J. (1988). Measurement of neuronal calcium transients using simultaneous microfluorimetry and electrophysiology. *Pflügers Arch.*, **415**, 216–233.

WAHLESTEDT, C. (1987). Neuropeptide Y (NPY): actions and interactions in neurotransmission. *Thesis, University of Lund*, pp. 1–226.

WAHLESTEDT, C., YANAIHARA, N. & HÅKANSON, R. (1986). Evidence for different pre- and post-junctional receptors for neuropeptide Y and related peptides. *Reg. Pept.*, **13**, 307–318.

WAHLESTEDT, C., GRUNDEMAR, L., HÅKANSON, R., HEILEG, M., SHEN, G.H., ZUKOWSKA-GROJEK, Z. & REIS, D.J. (1990) Neuropeptide Y receptor subtypes, Y1 and Y2. *Ann. N.Y. Acad. of Sci.*, **611**, 7–26.

WALKER, M.W., EWALD, D.A., PERNEY, T.M. & MILLER, R.J. (1988). Neuropeptide Y modulates neurotransmitter release and calcium currents in rat sensory neurons. *J. Neurosci.*, **8**, 2438–2446.

WILEY, J.W., GROSS, R.A., LU, Y. & MACDONALD, R.L. (1990). Neuropeptide Y reduces calcium current and inhibits acetylcholine release in nodose neurones via a pertussis toxin-sensitive mechanism. *J. Neurosci.*, **63**, 1499–1507.

(Received November 9, 1990
Revised February 25, 1991
Accepted March 11, 1991)

Br. J. Pharmacol. (1991), **103**, 1790–1794 © Macmillan Press Ltd, 1991

Cholecystokinin release mediated by 5-HT_3 receptors in rat cerebral cortex and nucleus accumbens

Paolo Paudice & [1]Maurizio Raiteri

Institute of Pharmacology and Pharmacognosy, University of Genoa, Viale Cembrano 4, 16148 Genoa, Italy

1 The effects of 5-hydroxytryptamine (5-HT) on the release of cholecystokinin-like immunoreactivity (CCK-LI) were examined in synaptosomes prepared from rat cerebral cortex and nucleus accumbens and depolarized by superfusion with 15 mM KCl.

2 In both areas 5-HT, tested between 0.1 and 100 nM, increased the calcium-dependent, depolarization-evoked CCK-LI release in a concentration-related manner. The concentration-response curves did not differ significantly between the two brain areas (EC_{50}: 0.4 ± 0.045 nM and 0.48 ± 0.053 nM, respectively, in cortical and n. accumbens synaptosomes; maximal effect: about 60% at 10 nM 5-HT).

3 The 5-HT_1/5-HT_2 receptor antagonist methiothepin (300 nM) did not affect the CCK-LI release elicited by 10 nM 5-HT. However, the effects of 10 nM 5-HT were antagonized in a concentration-dependent manner by the 5-HT_3 receptor antagonists (3α-tropanyl)-1H-indole-3-carboxylic acid ester (ICS 205-930; 0.1–100 nM; IC_{50}: 3.56 ± 0.42 nM in the cortex and 3.90 ± 0.50 nM in the n. accumbens) and ondasetron (IC_{50}: 8.15 ± 0.73 nM in the cerebral cortex). 5-HT (10 nM) was also strongly antagonized by 100 nM 1αH, 3α5αH-tropan-3-yl-3,5-dichlorobenzoate (MDL 72222) another blocker of the 5-HT_3 receptor. Moreover, the 5-HT_3 receptor agonist 1-phenylbiguanide (tested in the cerebral cortex between 0.1 and 100 nM) enhanced CCK-LI release in a manner almost identical to that of 5-HT (EC_{50} = 0.64 ± 0.071 nM).

4 It is concluded that 5-HT can act as a potent releaser of CCK-LI in rat cerebrocortex and nucleus accumbens through the activation of receptors of the 5-HT_3 type situated on the CCK-releasing terminals. This interaction may provide a rationale for the clinical development of both 5-HT_3 and CCK receptor antagonists as novel anxiolytic drugs.

Keywords: 5-Hydroxytryptamine; cholecystokinin release; 5-HT_3 presynaptic receptors; cerebrocortex; nucleus accumbens; 1-phenylbiguanide; ICS 205-930; MDL 72222; ondasetron; anxiety

Introduction

5-Hydroxytryptamine (5-HT) has long been implicated in the control of anxiety (Iversen, 1984; Chopin & Briley, 1987). In general, it seems that stimulation of the 5-HT system results in an anxiogenic effect, while a reduction in inappropriately elevated 5-HT neuronal activity leads to anxiolysis. Accordingly anxiolytic activity has recently been reported for 5-HT_3 receptor antagonists (Jones *et al.*, 1988; Lecrubier *et al.*, 1990).

Administration of cholecystokinin (CCK), a major neuropeptide in the central nervous system (Vanderhaeghen *et al.*, 1975; Dockray, 1976) has been found to induce anxiety both in the experimental animal and in man and CCK receptor antagonists have been shown to display anxiolytic activity (see review by Ravard & Dourish, 1990, and references therein).

This similarity between 5-HT and CCK prompted us to investigate whether the two systems could interact in the brain. The question was approached by examining the action of 5-HT on the release of cholecystokinin-like immunoreactivity (CCK-LI) from cerebral tissue. It is known that CCK is widely distributed throughout the brain (Beinfeld *et al.*, 1981; Emson & Marley, 1983), the highest amounts being found in the cerebral cortex and in limbic areas possibly involved in the expression of anxiety.

The peptide is concentrated in nerve endings from which it can be released upon depolarization (Pinget *et al.*, 1979). Thus we have used synaptosomal preparations obtained from rat cerebral cortex or nucleus accumbens which were exposed to 5-HT during depolarization. The data show that the release of CCK-LI, determined by radioimmunoassay, was potentiated by nanomolar concentrations of 5-HT via the activation of receptors of the 5-HT_3 type.

[1] Author for correspondence.

Methods

Preparation of synaptosomes

Adult male Wistar rats (200–250 g) were used. Crude synaptosomes were prepared from the cortex or from the nucleus accumbens as previously described (Raiteri *et al.*, 1984). Briefly, the tissue was homogenized in 40 vol of 0.32 M sucrose, buffered at pH 7.4 with phosphate. The homogenate was centrifuged (5 min, 1000 *g* at 0–4°C) to remove nuclei and debris and synaptosomes were isolated from the supernatant by centrifugation at 12,000 *g* for 20 min. The synaptosomal pellet was then resuspended in a physiological medium having the following composition (mM): NaCl 125, KCl 3, $MgSO_4$ 1.2, $CaCl_2$ 1.2, NaH_2PO_4 1.0, $NaHCO_3$ 22 and glucose 10 (aeration with 95% O_2 and 5% CO_2 37°C), pH 7.2–7.4.

Protein was measured according to Bradford (1976), with bovine serum albumin used as a standard.

Release experiments

Identical aliquots of the synaptosomal suspension (ranging between 0.8–1 mg protein in the different experiments) were layered at the bottom of a set of parallel superfusion chambers maintained at 37°C (Raiteri *et al.*, 1974). Superfusion was then started with standard medium supplemented with 0.1% gelatine and aerated with 95% O_2 and 5% CO_2, at a rate of 0.6 ml min^{-1}. After 36 min, to equilibrate the system, fractions were collected according to the following scheme: two 3-min samples (basal release) before and after one 6-min sample (evoked release). A 90 s period of depolarization was applied at the end of the first fraction collected. Depolarization of synaptosomes was performed with 15, 25, or 35 mM KCl, substituting an equimolar concentration of NaCl in the superfusion

medium. 5-HT or 1-phenylbiguanide was added to the superfusion medium concomitantly with the depolarizing stimulus. Methiothepin, ICS 205-930, ondansetron or MDL 72222 was added 8 min before 5-HT. The Ca^{2+}-free medium, when used, was substituted for the standard medium 18 min before depolarization. Superfusate fractions were collected into vials containing acetic acid (final concentration 1 M) and boiled to ensure peptidase inactivation. At the end of superfusion, synaptosomes were sonicated in distilled water and the extracts were boiled in 1 M acetic acid. All superfusate fractions and synaptosomal extracts were freeze dried before assay.

Radioimmunoassay

The freeze dried samples were reconstituted in phosphate buffer (50 mM; pH 7.4) and radioimmunoassayed essentially according to Emson *et al.* (1980). The antiserum used (Ab 2609) had been characterized in detail by Rehfeld (1978). The assay sensitivity was 1 pg per tube and the calibration curve was linear between 1.5 and 100 fmol with [^{125}I]-CCK-8 (sulphated) used as a tracer.

Calculation

The amount of CCK-LI released in each fraction and that remaining in the synaptosomes at the end of the superfusion was expressed as fmol mg^{-1} protein. The depolarization-evoked overflow was estimated by subtracting the CCK-LI content of the basal release from the release evoked in the 6-min fraction collected during and after the depolarization period. The drug effects were evaluated as the ratio of the depolarization-evoked overflow calculated in the presence of the drugs vs. that calculated under control conditions. The two-tailed Student's t test was used for statistical comparison of the data.

Drugs

[^{125}I]-cholecystokinin-8 and cholecystokinin-8 were obtained from Amersham Radiochemical Centre (UK) and from NOVA Biochem (Switzerland), respectively. 5-Hydroxytryptamine was purchased from Sigma Chemical Co (St. Louis, MO, U.S.A.) and 1-phenylbiguanide from RBI (Natick, MA, U.S.A.). The following drugs were kindly given from the companies indicated: methiothepin (Hoffman-La Roche, Basel, Switzerland); ICS 205-930 (3α-tropanyl)-1H-indole-3-carboxylic acid ester, Sandoz AG, Basel, Switzerland); MDL 72222 (1αH,3α,5αH-tropan-3yl-3,5-dichlorobenzoate, Merrell Dow Research Institute, Strasbourg, France); ondansetron (Glaxo, Ware, U.K.).

Results

Depolarization-evoked release of cholecystokinin-like immunoreactivity

The basal CCK-LI release from rat cerebrocortical synaptosomes was 2.9 ± 0.13 fmol mg^{-1} protein min^{-1}, corresponding to 0.2 ± 0.01% of the total synaptosomal content (n = 20). Increasing concentrations of KCl in the superfusion medium (from 15 to 35 mM) resulted in a concentration-dependent increase in CCK-LI release (Figure 1). The K^+-stimulated overflow was found to be largely calcium-dependent. Results similar to those shown for the cerebral cortex were obtained with synaptosomes from n. accumbens (data not presented). In the subsequent experiments 15 mM K^+ was chosen as the depolarizing stimulus because this submaximal concentration of KCl allowed for an increase or decrease in release following drug exposure.

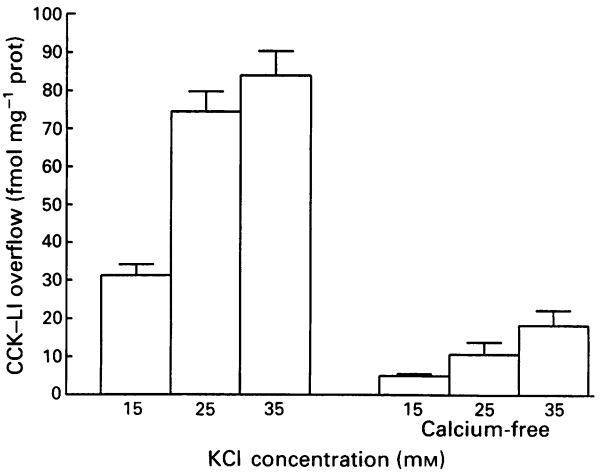


Figure 1 K^+-evoked overflow of cholesystokinin-like immunoreactivity (CCK-LI) from rat brain cortex synaptosomes and its Ca^{2+}-dependence. Synaptosomes were prepared and superfused as described in the Methods section. A 90 s pulse of 15, 25 or 35 mM KCl was applied after 39 min of superfusion. The Ca^{2+}-free medium, when used, was introduced 18 min before the depolarizing stimuli. Shown are means with s.e.mean (vertical bars) of 3 experiments in triplicate.

Effect of 5-hydroxytryptamine

When added to the superfusion medium concomitantly with 15 mM K^+, 5-HT (0.1–100 nM) produced concentration-dependent increases in the depolarization-evoked CCK-LI release (Figure 2). The concentration-response curve for 5-HT obtained with cerebrocortical synaptosomes was superimposable on that obtained with synaptosomes from n. accumbens. The maximal effect (about 60% increase of CCK-LI release) was produced by 10 nM of the indoleamine. The EC_{50} values were 0.40 ± 0.045 nM and 0.48 ± 0.053 nM, respectively, in the cortex and in the n. accumbens.

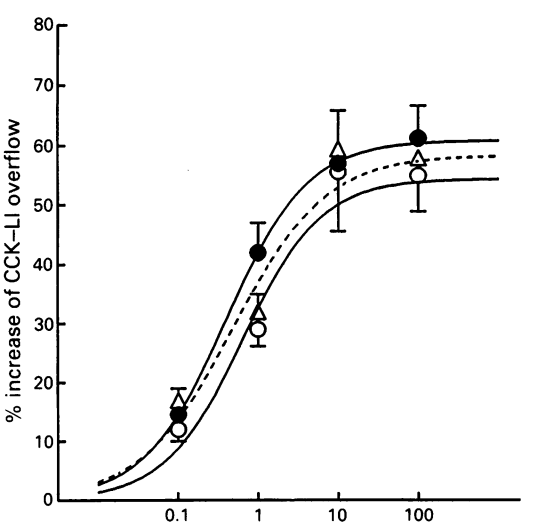


Figure 2 Effect of 5-hydroxytryptamine (5-HT) or 1-phenylbiguanide on the K^+ (15 mM)-evoked overflow of cholecystokinin-like immunoreactivity (CCK-LI) from rat cortical or n. accumbens synaptosomes. 5-HT or 1-phenylbiguanide was added to the superfusion medium concomitantly with the depolarizing stimulus. See Methods for other technical details. Each point represents the mean with s.e.mean (vertical bars) of 3–6 experiments in triplicate: (●) 5-HT (cortex); (△) 5-HT (n. accumbens); (○) 1-phenylbiguanide (cortex).

Characterization of the 5-HT receptor involved

The releasing effect of 5-HT (at the concentration of 10 nM corresponding to the maximal effect) was insensitive to 300 nM methiothepin. In contrast it was antagonized by 100 nM MDL 72222, in both brain regions (Figure 3). Figure 4 shows that the effect of 10 nM 5-HT in cortical synaptosomes was concentration-dependently antagonized by ICS 205-930 ($IC_{50} = 3.56 \pm 0.42$ nM) or by ondansetron ($IC_{50} = 8.15 \pm 0.73$ nM). Data superimposable on those in the cortex were obtained in the n. accumbens with ICS 205-930 ($IC_{50} = 3.90 \pm 0.50$).

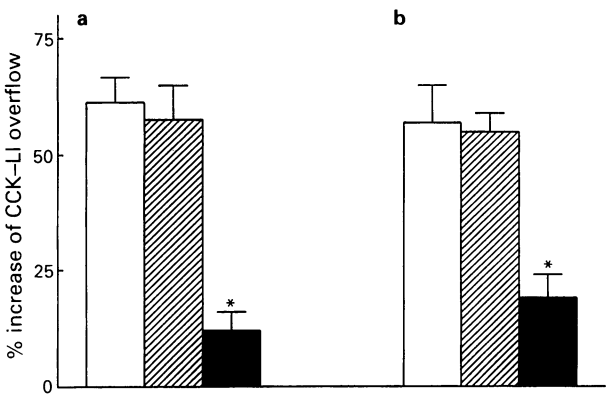


Figure 3 Antagonism by methiothepin or MDL 72222 of the enhancement by 5-hydroxytryptamine (5-HT) of cholecystokinin-like immunoreactivity (CCK-LI) release from cortical (a) or n. accumbens (b), synaptosomes. Synaptosomes were exposed to superfusion with 5-HT at the same time as the depolarizing stimulus; methiothepin or MDL 72222 was added 8 min before 5-HT. See Methods for other technical details. Values represent means with s.e.mean (vertical bars) of 3-4 experiments run in triplicate. Open columns: 10 nM 5-HT; hatched columns: 10 nM 5-HT + 300 nM methiothepin; solid columns: 10 nM 5-HT + 100 nM MDL 72222. * $P < 0.01$ vs. 10 nM 5-HT.

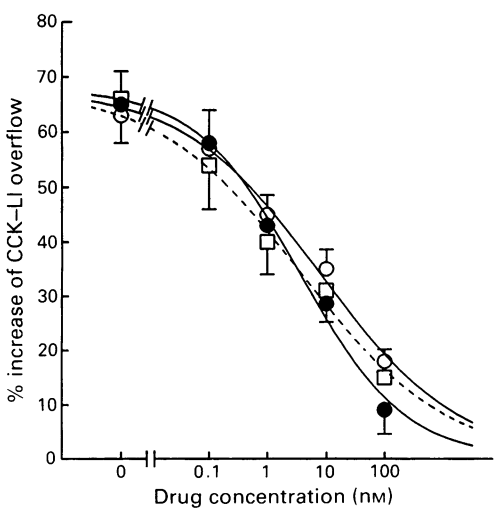


Figure 4 Antagonism by ICS 205-930 or ondansetron of the enhancement by 5-hydroxytryptamine (5-HT) of cholecystokinin-like immunoreactivity (CCK-LI) release from cortical or n. accumbens synaptosomes. 5-HT (10 nM) was added to the superfusion medium at the same time as the depolarizing stimulus was applied; antagonists 8 min before 5-HT. For other technical details see Methods. Each point of the curve represents the mean with s.e.mean (vertical bars) of 3–5 experiments in triplicate. Concentrations of antagonists higher than 0.1 nM antagonized 5-HT significantly ($P < 0.001$): (●) 5-HT plus ICS 205–930 (cortex); (○) 5-HT plus ondansetron (cortex); (□) 5-HT plus ICS 205-930 (n. accumbens).

The effect of 5-HT on the K^+-evoked CCK-LI release from cortical synaptosomes was mimicked by 1-phenylbiguanide (0.1–100 nM). This drug was slightly (although not significantly) less potent than 5-HT ($EC_{50} = 0.64 \pm 0.071$) (Figure 2).

Discussion

The first result of this work shows that nanomolar concentrations of 5-HT enhanced the release of CCK-LI, produced by exposure to high-K^+, from crude synaptosomal preparations of rat cerebral cortex or nucleus accumbens. The data suggest a functional connection between the 5-HT and the CCK systems in the rat brain.

The origin of the released CCK-LI is most probably neuronal since CCK-LI has been reported to be concentrated in CNS nerve terminals (Pinget *et al.*, 1978). Possible 'gliasomal' contamination of our nerve ending preparations should not contribute significantly to the released peptide inasmuch as CCK has not been detected in glial cells (Loren *et al.*, 1979).

The experimental set up employed in this study (a thin layer of synaptosomes up-down superfused; Raiteri *et al.*, 1974) prevents or minimized indirect effects. Thus it can be assumed that the site of action of 5-HT is on the CCK-releasing nerve terminals suggesting that the 5-HT and the CCK systems are directly interconnected in the rat brain.

Mammalian 5-HT receptors are heterogeneous and have been divided into three major types: 5-HT_1-like, 5-HT_2 and 5-HT_3 (Bradley *et al.*, 1986). The CCK-releasing effect of 5-HT was insensitive to methiothepin, a non-selective 5-HT_1/5-HT_2 receptor antagonist, while it was sensitive to nanomolar concentrations of the 5-HT_3 receptor antagonists MDL 72222 (Fozard, 1984), ICS 205-930 (Richardson *et al.*, 1985), and ondansetron (Butler *et al.*, 1988). Moreover, the effect of 5-HT on CCK-LI release was mimicked by 1-phenylbiguanide, a selective 5-HT_3 receptor agonist (Ireland & Tyers, 1987). These results suggest that the enhancement of CCK-LI release by 5-HT is mediated by receptors of the 5-HT_3 type.

Involvement of the recently proposed 5-HT_4 receptor type (Dumuis *et al.*, 1989) seems unlikely for a number of reasons: (a) the 5-HT_4 receptor is totally insensitive to MDL 72222 and to ondansetron; (b) the 5-HT_4 receptor can be blocked by ICS 205-930, but only at micromolar concentrations; (c) 5-HT shows relatively low potency towards the 5-HT_4 receptor while the receptor mediating CCK-LI release seems to be activated by extremely low concentrations of 5-HT.

If the pharmacological characteristics of the 5-HT receptor situated on CCK-releasing terminals are most compatible with its classification as a 5-HT_3 type, it should be noted that the 5-HT_3 receptors classically found in the periphery require micromolar concentrations of 5-HT or 1-phenylbiguanide for activation (Richardson *et al.*, 1985; Richardson & Engel, 1986; Ireland & Tyers, 1987). The present finding that 5-HT and 1-phenylbiguanide were almost 1000 times more potent than expected for a 5-HT_3-mediated effect may have various explanations. In a thin layer of superfused synaptosomes the agonists reach the receptor very rapidly, thus minimizing factors (tissue uptake, metabolism, receptor access etc.) which may influence estimates of agonist potency in more intact tissues. A high 5-HT_3 receptor reserve may be present on CCK-releasing nerve endings. A receptor coupling which is more efficient in brain than in other tissues may also contribute. Finally, the possibility that the central receptor under study represents a subtype of the 5-HT_3 receptor cannot be excluded.

Receptors of the 5-HT_3 type mediate depolarizing actions and are probably coupled to membrane cation channels (Derkach *et al.*, 1989), properties which are particularly well-suited to a release-regulating receptor. Evidence from radioligand binding studies (Kilpatrick *et al.*, 1987; Peroutka & Hamik, 1988; Waeber *et al.*, 1989) and behavioural tests

(Costall *et al.*, 1987; Jones *et al.*, 1988) have shown that 5-HT$_3$ receptors exist not only in the periphery but also in the central nervous system.

5-HT$_3$ receptors appear most promising as targets for novel drugs. Antagonists at these receptors are indeed under clinical development in a variety of important indications including emesis in cancer chemotherapy, schizophrenia and anxiety (for a review see Fozard, 1987). The recent finding that 5-HT$_3$ receptors modulate acetylcholine release in rat entorhinal cortex suggests that 5-HT$_3$ receptor antagonists might also be useful in conditions of impaired cholinergic function (Barnes *et al.*, 1989).

A relationship between central 5-HT$_3$ receptors and anxiety is supported by a wealth of data. As already mentioned, the prevailing view points to a reduction in abnormally elevated 5-HT neuronal activity as the basis of anxiolysis. In keeping with this view, 5-HT$_{1A}$ receptor agonists which cause a generalized depression of impulse flow by activating somatodendritic autoreceptors on raphe neurones (Sprouse & Aghajanian, 1987) are effective novel anxiolytics (Goa & Ward, 1986; Fozard, 1987). However, 5-hydrotytryptaminergic transmission can also be blocked more distally, i.e. at the axon terminal synapses. Considering that 5-HT is released onto a variety of receptor types and subtypes, antagonists at 5-HT$_3$ receptors may be more selective anxiolytics than those acting in a more generalized way.

The finding that the release of CCK can be enhanced by 5-HT$_3$ receptor activation deserves some comments. CCK binding sites are widely distributed throughout the brain (Innis & Snyder, 1980; Saito *et al.*, 1980). It was shown in electrophysiological experiments that CCK was selectively antagonized by low doses of benzodiazepines (Bradwejn & De Montigny, 1984) and it was predicted that CCK receptor activation might induce anxiety. This idea has been supported by experiments in the laboratory animal (Deupree & Hsiao, 1988) and by recent clinical studies (De Montigny, 1989) in which i.v. injection of CCK provoked panic attacks in normal volunteers and reproduced the symptoms of spontaneous panic in anxious patients. On the basis of these observations, CCK receptor antagonists have been tested and found to possess anxiolytic properties in animal models of anxiety (Dourish *et al.*, 1990; Hughes *et al.*, 1990), suggesting that CCK antagonists may be useful anxiolytic drugs (see for review, Ravard & Dourish, 1990).

In conclusion, we would like to propose that 5-HT and CCK may strictly cooperate in the biochemistry of anxiety. According to this idea, in some yet unidentified brain regions, but possibly in the areas examined in the present study, abnormally elevated 5-HT transmission activates release-enhancing 5-HT$_3$ receptors situated on CCK nerve terminals and the released CCK contributes to the expression of anxiety. This picture would represent a rationale for the clinical development of both 5-HT$_3$ and CCK receptor antagonists as novel antianxiety drugs.

This work was supported by grants from the Italian M.U.R.S.T. (40% and 60%) and Italian C.N.R. (Progetto Strategico 'Transmitter release and its regulation'). The authors are very grateful to Dr Piers Emson for his generous gift of the antiserum for cholecystokinin used in this work and to Mrs Maura Agate for her help in preparing the manuscript.

References

BARNES, J.M., BARNES, N.M., COSTALL, B., NAYLOR, R.J. & TYERS, M.B. (1989). 5-HT$_3$ receptors mediate inhibition of acetylcholine release in cortical tissue. *Nature*, **338**, 762–763.

BEINFELD, M.C., MEYER, D.K., ESKAY, R.L., JENSEN, R.T. & BROWNSTEIN, M.J. (1981). The distribution of cholecystokinin in the central nervous system of the rat as determined by RIA. *Brain Res.*, **212**, 51–57.

BRADFORD, M. (1976). A rapid and sensitive method for quantitation of microgram quantities of proteins utilising the principles of protein-dye binding. *Anal. Biochem.*, **72**, 248–254.

BRADLEY, P.B., ENGEL, G., FENIUK, W., FOZARD, J.R., HUMPHREY, P.P.A., MIDDLEMISS, D.N., MY LECHARANE, E.J., RICHARDSON, B.P. & SAXENA, P.R. (1986). Proposals for the classification and nomenclature of functional receptors for 5-hydroxytryptamine. *Neuropharmacology*, **25**, 563–576.

BRADWEJN, J. & DE MONTIGNY, C. (1984). Benzodiazepines antagonize cholecystokinin-induced activation of rat hippocampal neurones. *Nature*, **312**, 363–364.

BUTLER, A., HILL, J.M., IRELAND, S.J., JORDAN, C.C. & TYERS, M.B. (1988). Pharmacological properties of GR38032F, a novel antagonist at 5-HT$_3$ receptors. *Br. J. Pharmacol.*, **94**, 397–412.

CHOPIN, P. & BRILEY, M. (1987). Animal models of anxiety: the effect of compounds that modify 5-HT neurotransmission. *Trends Pharmacol. Sci.*, **8**, 383–388.

COSTALL, B., DOMENEY, A.M., NAYLOR, R.J. & TYERS, M.B. (1987). Effects of the 5-HT$_3$ receptor antagonist GR38032F, on raised dopaminergic activity in the mesolimbic system of the rat and marmoset brain. *Br. J. Pharmacol.*, **92**, 881–894.

DE MONTIGNY, C. (1989). Cholecystokinin tetrapeptide induces panic-like attacks in healthy volunteers. *Arch. Gen. Psychiat.*, **46**, 511–517.

DERKACH, V., SUPRENANT, A. & NORTH, R.A. (1989). 5-HT$_3$ receptors are membrane ion channels. *Nature*, **339**, 706–709.

DEUPREE, D. & HSIAO, S. (1988). Cholecystokinin octapeptide increases passive avoidance latencies in rats. *Physiol. Behav.*, **42**, 203–208.

DOCKRAY, G.J. (1976). Immunochemical evidence of cholecystokinin-like peptides in brain. *Nature*, **264**, 568–570.

DOURISH, C.T., RYCROFT, W., DAWSON, G.R., TATTERSALL, F.D. & IVERSEN, S.D. (1990). Anxiolytic effects of the CCK antagonist devazepide and L-365,260 in a conditioned suppression of drinking model. *Eur. J. Neurosci.*, **2**, suppl. 3, p. 38.

DUMUIS, A., SEBBEN, M. & BOCKAERT, J. (1989). The gastrointestinal prokinetic benzamide derivatives are agonists at the non-classical 5-HT receptor (5-HT$_4$) positively coupled to adenylate cyclase in neurons. *Naunyn-Schmiedebergs Arch. Pharmacol.*, **340**, 403–410.

EMSON, P.C., LEE, C.M. & REHFELD, J.F. (1980). Cholecystokinin octapeptide: vesicular localization and calcium dependent release from rat brain in vitro. *Life Sci.*, **26**, 2157–2163.

EMSON, P.C. & MARLEY, P.D. (1983). Cholecystokinin and vasoactive intestinal polypeptide. In *Handbook of Psychopharmacology*, Vol. 16, pp. 255–306. ed. Iversen, L., Iversen, S.D. & Snyder, S.H. New York: Plenum Publishing Co.

FOZARD, J.R. (1984). MDL 72222: a potent and highly selective antagonist at neuronal 5-hydroxytryptamine receptors. *Naunyn-Schmiedebergs Arch. Pharmacol.*, **326**, 36–44.

FOZARD, J.R. (1987). 5-HT: the enigma variations. *Trends Pharmacol. Sci.*, **8**, 501–506.

GOA, K. & WARD, A. (1986). Buspirone: a preliminary review of its pharmacological properties and therapeutic efficacy as an anxiolytic. *Drugs*, **32**, 114–129.

HUGHES, J., BODEN, P., COSTALL, B., DOMENEY, A., KELLY, E., HORWELL, D.C., HUNTER, J.C., PINNOCK, R.D. & WOODRUFF, G.N. (1990). Development of a class of selective cholecystokinin type B receptor antagonists having potent anxiolytic activity. *Proc. Natl. Acad. Sci. USA*, **87**, 6728–6732.

INNIS, R.B. & SNYDER, S. (1980). Distinct cholecystokinin receptors in brain and pancreas. *Proc. Natl. Acad. Sci. U.S.A.*, **77**, 6917–6921.

IRELAND, S.J. & TYERS, M.B. (1987). Pharmacological characterization of 5-hydroxytryptamine-induced depolarization of the rat isolated vagus nerve. *Br. J. Pharmacol.*, **90**, 229–238.

IVERSEN, S.D. (1984). 5-HT and anxiety. *Neuropharmacology*, **23**, 1553–1560.

JONES, B.J., COSTALL, B., DOMENEY, A.M., KELLY, M.E., NAYLOR, R.G., OAKLEY, N.R. & TYERS, M.B. (1988). The potential anxiolytic activity of GR38032F, a 5-HT$_3$ receptor antagonist. *Br. J. Pharmacol.*, **93**, 985–993.

KILPATRICK, G.J., JONES, B.J. & TYERS, M.B. (1987). The identification and distribution of 5-HT$_3$ receptors in rat brain using radioligand binding. *Nature*, **330**, 746–748.

LECRUBIER, Y., PUECH, A.J. & AZCONA, A. (1990). 5-HT$_3$ receptors in anxiety disorders. *Br. Ass. Psychopharmacol. Meeting*, Abstr. No. 19.

LOREN, I., ALUMETS, J., HAKANSON, R.H. & SUNDLER, F. (1979). Dis-

tribution of gastrin and cholecystokinin-like peptides in rat brain. *Histochemistry*, **59**, 249–257.

PEROUTKA, S.J. & HAMIK, A. (1988). [^{3}H]quipazine labels 5-HT$_3$ recognition sites in rat cortical membranes. *Eur. J. Pharmacol.*, **148**, 297–299.

PINGET, M., STRAUSS, E. & YALOW, R.S. (1978). Localization of cholecystokinin-like immunoreactivity in isolated nerve terminals. *Proc. Natl. Acad. Sci. U.S.A.*, **75**, 6324–6326.

PINGET, M., STRAUSS, E. & YALOW, R.S. (1979). Release of cholecystokinin peptides from synaptosoma-enriched fraction of rat cerebral cortex. *Life Sci.*, **25**, 339–342.

RAITERI, M., ANGELINI, F. & LEVI, G. (1974). A simple apparatus for studying the release of neurotransmitters from synaptosomes. *Eur. J. Pharmacol.*, **25**, 411–414.

RAITERI, M., BONANNO, G., MARCHI, M. & MAURA, G. (1984). Is there a functional linkage between neurotransmitter uptake mechanisms and presynaptic receptors? *J. Pharmacol. Exp. Ther.*, **231**, 671–677.

RAVARD, S. & DOURISH, C.T. (1990). Cholecystokinin and anxiety. *Trends Pharmacol. Sci.*, **11**, 271–273.

REHFELD, J.F. (1978). Immunochemical studies on cholecystokinin. I. Development of sequence-specific radioimmunoassays for porcine triacontatriapeptide cholecystokinin. *J. Biol. Chem.*, **253**, 4016–4021.

RICHARDSON, B.P., ENGEL, G., DONATSCH, P. & STADLER, P.A. (1985). Identification of serotonin M-receptor subtypes and their specific blockade by a new class of drugs. *Nature*, **316**, 126–131.

RICHARDSON, B.P. & ENGEL, G. (1986). The pharmacology and function of 5-HT$_3$ receptors. *Trends Pharmacol. Sci.*, **9**, 424–428.

SAITO, A.H., SANKARAN, H., GOLDINE, I.D. & WILLIAMS, J.A. (1980). Cholecystokinin receptors in the brain: Characterization and distribution. *Science*, **208**, 1155–1156.

SPROUSE, J.S. & AGHAJANIAN, G.K. (1987). Electrophysiological responses of serotonergic dorsal raphe neurones to 5-HT$_{1A}$ and 5-HT$_{1B}$ agonists. *Synapse*, **1**, 3–9.

VANDERHAEGHEN, J.-J., SIGNEAU, J.C. & GEPTS, W. (1975). New peptide in vertebrate CNS reacting with antigastrin antibodies. *Nature*, **257**, 604–605.

WAEBER, C., HOYER, D. & PALACIOS, J.M. (1989). 5-hydroxytryptamine$_3$ receptors in the human brain: autoradiographic visualization using [^{3}H]ICS205-930. *Neuroscience*, **31**, 393–400.

(Received October 22, 1990
Revised January 4, 1991
Accepted March 5, 1991)

Br. J. Pharmacol. (1991), **103**, 1795–1801 © Macmillan Press Ltd, 1991

Alkali cation permeability and caesium blockade of cromakalim-activated current in guinea-pig ventricular myocytes

[1]J.C.R. Randle, [2]S.H.R. Oliet & J.-F. Renaud

FONDAX, Groupe de Recherche Servier, 7, rue Ampère, 92800 Puteaux, France

1 The sensitivity of cromakalim-activated current (I_{crom}) to manipulations of extracellular cationic composition was examined in whole-cell voltage clamp recordings from freshly-dispersed, adult guinea-pig ventricular myocytes. In bathing media with different concentrations of K^+ (1, 2.5, 5.4 and 12 mM) the I_{crom} reversal potential (E_{rev}) varied in strict correspondance with the K^+ equilibrium potential and inward I_{crom} amplitude was proportional to the external K^+ concentration.

2 Replacement of 12 mM K^+ with 12 mM Rb^+ induced a slight positive shift of E_{rev} indicating that $P_{Rb+}/P_{K+} = 1.06$. K^+ replacement with 12 mM Cs^+ reduced or abolished inward I_{crom} and produced a negative shift of E_{rev} by at least 50 mV; an upper limit of P_{Cs+}/P_{K+} was fixed at 0.18.

3 Addition of Rb^+ (1–30 mM) to 2.5 mM K^+-containing medium produced a concentration-dependent increase in inward I_{crom} and positive shift of E_{rev} suggesting that K^+ and Rb^+ have similar permeabilities and conductivities and do not interfere with each other in the channel.

4 Cs^+ (0.01–30 mM), added to medium containing 12 mM Rb^+, induced a potent, voltage-dependent inhibition of inwardly rectifying current (I_{K1}; IC_{50} = 0.2–3 mM). Voltage-dependent inhibition of inward I_{crom} was observed only at considerably higher Cs^+ concentrations (IC_{50} = 4–30 mM). Extracellular Rb^+ and Cs^+ did not substantially alter the amplitude of outward I_{crom}.

5 The results support the contention that the ATP-sensitive K^+ channel is the primary target of cromakalim action in ventricular myocytes.

Keywords: ATP-sensitive K^+ channel; whole-cell patch clamp; inward rectifying K^+ channel I_{K1}, Rb^+; voltage-dependent block

Introduction

Cromakalim is a benzopyran derivative that activates ATP-sensitive K^+ [K(ATP)] channels in cardiac myocytes (Escande *et al.*, 1988; Sanguinetti *et al.*, 1988), arterial smooth muscle cells (Standen *et al.*, 1989) and an insulin-secreting cell line (Dunne *et al.*, 1989). Since the relaxation of smooth muscle and decrease of blood pressure that it induces are inhibited by sulphonylureas such as glibenclamide (Standen *et al.*, 1989; Quast & Cook, 1989a; Winquist *et al.*, 1989; Cavero *et al.*, 1989; Eltze, 1989) which block K(ATP) channels (Schmid-Antomarchi *et al.*, 1987; Sturgess *et al.*, 1988), K(ATP) channel activation may be the primary mechanism of action of cromakalim. A complementary approach to examine this mechanistic link in electrophysiological experiments is to compare membrane permeability changes induced by cromakalim in whole-cell recordings with the permeability of the K(ATP) channel. Single channel studies of the ionic selectivity of K(ATP) channels in heart, skeletal muscle and β-pancreatic cells indicate that they are highly permeable to K^+ and Rb^+ but not to Na^+ (Kakei *et al.*, 1985; Spruce *et al.*, 1987; Ashcroft *et al.*, 1989) and are blocked by Cs^+ (Quayle *et al.*, 1988). In this paper we describe the effects of changes in extracellular alkali cation composition on cromakalim-activated current (I_{crom}) in whole-cell recordings of adult guinea-pig isolated ventricular myocytes.

Methods

Preparation of adult guinea-pig ventricular myocytes

Ventricular myocytes were isolated by a technique adapted from Mitra & Morad (1985). The two principal modifications to the technique were, (a) the use of a peristalic pump to regulate flow perfusion medium at 6–8 ml min^{-1} through the heart and, (b) the gradual reintroduction of $CaCl_2$ to the isolated cell suspension at 5–10 min intervals to intermediate concentrations of 100 μM, 200 μM, 500 μM and 1 mM. Isolated myocytes were stored at 37°C and used within 6 h.

Whole-cell patch clamp experiments

Electrophysiological measurements were made by the whole-cell patch clamp technique (Hamill *et al.*, 1981). The cells were placed in a plexiglas recording chamber maintained at 33–35°C and perifused with medium of composition (in mM): NaCl 143, KCl 2.5, $MgCl_2$ 1, $CaCl_2$ 1.8, NaH_2PO_4 0.33, N-2-hydroxyethyl-piperazine-N'-2-ethanesulphonic acid (HEPES) 10 and glucose 10, at pH 7.35. Recording pipettes were made from 1.2 mm borosilicate glass tubing and filled with a solution containing (in mM): KCl 140, NaCl 1, $MgCl_2$ 2, $CaCl_2$ 3.3, HEPES 10, ethyleneglycol-*bis* (β-aminoethylether) N,N,N',N'-tetraacetic acid (EGTA) 10, diNa^+ adenosine 5'-triphosphate (ATP) 3 and Na^+ adenosine 3':5'-cyclic monophosphate (cyclic AMP) 0.1, adjusted to pH 7.15 with ~3 mM KOH and had tip resistances of 4–8 MΩ. A 4% agar/NaCl bridge was used to connect the Ag/AgCl ground wire to the bath solution and variation of junction potential associated with solution changes was never greater than 1 mV. Membrane currents were recorded by use of a Biologic RK300 amplifier with careful series resistance compensation.

Voltage protocol generation and data acquisition and analysis was achieved by use of an A–D converter (Labmaster DMA, Scientific Solutions) and interface (TL-1, Axon Instruments) and a microcomputer (IBM PC-AT) equipped with an appropriate software package (pCLAMP, Axon Instruments). Data were digitized at 1–2 kHz. Averaged data from several cells were expressed as the mean ± standard error of the mean (s.e.mean). Statistical treatment of data was performed by analysis of variance followed by the Newman-Keuls test.

[1] Author for correspondence.

[2] Present address: Centre for Research in Neuroscience, Montreal General Hospital Research Institute, 1650 Cedar Avenue, Montreal, Quebec, H3G 4A1, Canada.

Cromakalim [(−)-BRL 34915; (−)-6-cyano-3,4-dihydro-2,2-dimethyl-*trans*-4-(2-oxo-1-pyrrolidyl)-2H-benzo [b] pyran-3-ol], synthesized in the chemistry department of the Groupe de Recherche Servier, was prepared as a stock solution (10, 50 or 100 mM) in dimethylsulphoxide (DMSO) stored at +4°C, diluted to 100 μM in the appropriate medium just before use and applied by superfusion. In control experiments, the DMSO vehicle solution (0.1–1%) had no effect on ventricular myocyte membrane currents. Changes in the ionic composition of the perfusion medium were made as follows. Different K^+ concentrations (1–12 mM) were obtained by equimolar replacement of NaCl with KCl. When RbCl or CsCl (12 mM) was added, KCl was omitted and NaCl was reduced from 143 mM to 133 mM. In the remaining experiments, RbCl (1–30 mM) or CsCl (0.001–30 mM) were added to the bathing medium and an equal amount of NaCl was removed from normal medium containing 2.5 mM KCl or 12 mM RbCl.

Results

Cromakalim-activated current (I_{crom}): *dependence upon extracellular potassium concentration* ($[K^+]_o$)

Whole-cell membrane currents were measured during 100–200 ms voltage steps over the range −200 mV to +80 mV. Under control conditions (before application of cromakalim), guinea-pig ventricular myocytes display a prominent inward K^+ current (I_{K1}) that varies in amplitude and voltage-dependence with $[K^+]_o$. The results illustrated in (Figures 1 and 2a) are very similar to those reported previously in cardiac (Sakmann & Trube, 1984; DiFrancesco *et al.*, 1984; Tourneur *et al.*, 1987) and other preparations (Hagiwara & Takahashi, 1974; Leech and Stanfield, 1981). A relatively small outward K^+ current is also evident at positive potentials (see below) and inward Na^+ and Ca^{2+} currents inactivate rapidly and make little contribution to whole-cell current measured at the end of 100–200 ms voltage steps.

Cromakalim-induced current (I_{crom}) was measured as the difference between whole-cell current at the end of 200 ms voltage steps in the absence and presence of cromakalim (100 μM). The most prominent response to cromakalim, observed in each of more than 90 guinea-pig ventricular myocytes, is a very large outward current at potentials positive to the K^+ reversal potential (Figure 1). In the experiments described here, outward current measured at +80 mV in the presence of 100 μM cromakalim (a concentration that induces an effect ~80% of maximal) was 4.4 ± 0.5 nA (range 1.5–12.5 nA, 31 cells) while under control conditions it was 0.65 ± 0.03 nA, in good agreement with previous reports (Escande *et al.*, 1988; Sanguinetti *et al.*, 1988). Mean outward I_{crom} slope conductance (measured between −20 and +20 mV) appeared to increase with $[K^+]_o$ and was: 20.8 ± 2.8 nS for 1 mM K^+ (9 cells), 26.7 ± 6.0 nS for 2.5 mM K^+ (18 cells), 40.0 ± 5.4 nS for 5.4 mM K^+ (14 cells) and 81.9 ± 21.4 nS for 12 mM K^+ (9 cells) as shown in Figures 1 and 2. Only the data from the 12 mM K^+ group were statistically significantly different ($P < 0.01$) from the other groups.

Clear reversal of (inward) I_{crom} was less reliably observed: in 4 of 9 cells in 1 mM K^+, 9 of 18 cells in 2.5 mM K^+, 12 of 14 cells in 5.4 mM K^+, and 7 of 9 cells in 12 mM K^+. Nevertheless, the reversal potential of I_{crom} in cells in which reversal was observed varied with $[K^+]_o$ concentration strictly as predicted by the Nernst equation: 1 mM K^+ = −131.5 ± 1.8 mV, 2.5 mM K^+ = −104.6 ± 6.9 mV, 5.4 mM K^+ = −87.2 ± 1.9 mV, 12 mM K^+ = −65.8 ± 2.2 mV (Figures 2 and 3a). Inward I_{crom} amplitude was roughly proportional to the $[K^+]_o$ (Figure 2b). Mean inward I_{crom} slope conductance was: 5.3 ± 0.9 nS for 1 mM K^+, 5.8 ± 0.9 nS for 2.5 mM K^+, 9.3 ± 1.8 nS for 5.4 mM K^+ and 11.7 ± 4.0 nS for 12 mM K^+ (measured between −150 and −130 mV). In nominally K^+-free medium (all K^+-free replaced by Na^+), no inward I_{crom} was measured in any of 5 cells tested while mean outward current slope conductance measured between −20 mV and +20 mV was 25.8 ± 9.2 nS.

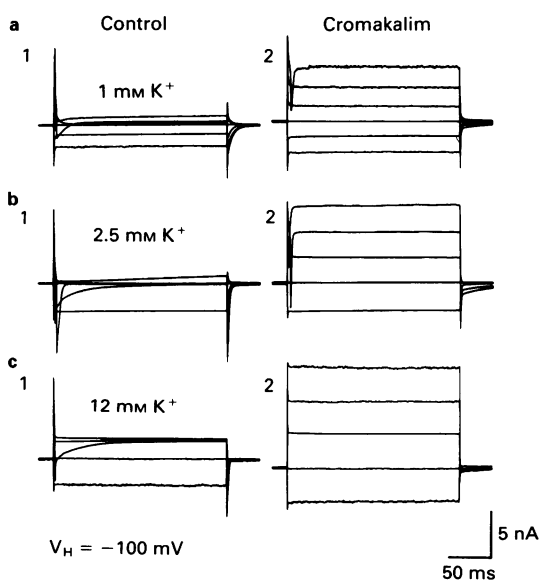


Figure 1 Membrane currents recorded from freshly dispersed adult guinea-pig ventricular myocytes under whole-cell clamp. Voltage steps (200 ms) to −200 mV (a1 and a2, only), −150 mV, −100 mV, −50 mV, 0 mV and +50 mV from a holding potential (V_H) of −100 mV were made under control conditions (column 1) and in the presence of cromakalim (100 μM; column 2) with the external K^+ concentration ($[K^+]_o$) adjusted to 1 mM (a), 2.5 mM (b) or 12 mM (c).

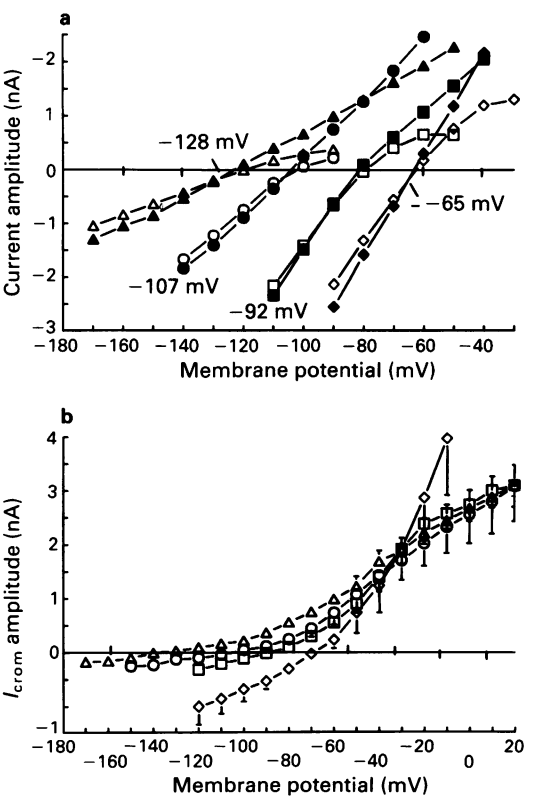


Figure 2 Effects of changes in external K^+ concentration ($[K^+]_o$) on cromakalim-induced current (I_{crom}). (a) Whole-cell current measured at the end of 200 ms voltage steps (in Figure 1) is plotted versus membrane potential under control conditions (open symbols) and in the presence of cromakalim (100 μM; filled symbols) for four $[K^+]_o$: 1 mM (△, ▲), 2.5 mM (○, ●), 5.4 mM (□, ■) and 12 mM (◇, ◆). Data are from the three cells in Figure 1, as well as one not illustrated, in which clear reversal of I_{crom} was evident. (b) I_{crom}, estimated as the difference between whole-cell current measured as in (a) in the absence and presence of cromakalim, is plotted versus membrane potential for the four $[K^+]_o$ (same symbols as in a). Data from 6 to 14 cells.

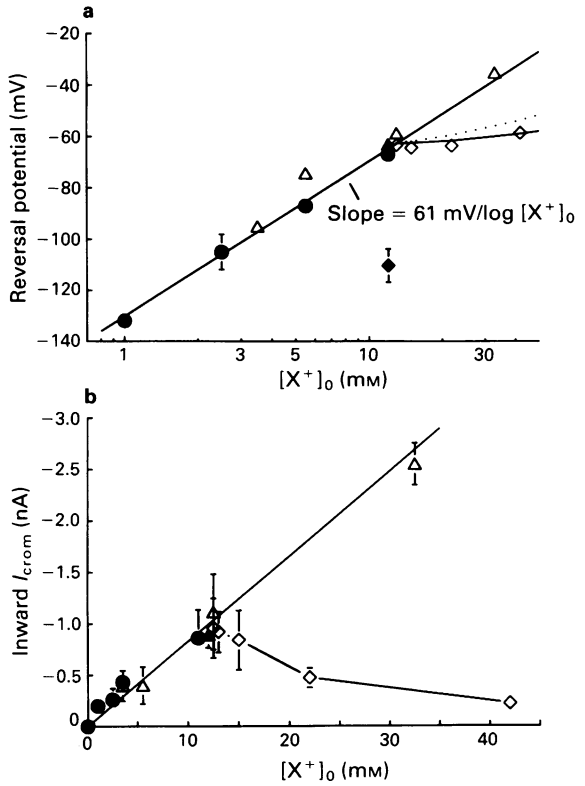


Figure 3 (a) Plot of the reversal potential of I_{crom} with various external cation concentrations ($[X^+]_o$). The data illustrated are for media containing only K^+ (1, 2.5, 5.4 or 12 mM; ●), only Rb^+ (12 mM, ▲), only Cs^+ (12 mM, ◆), K^+ (2.5 mM) plus Rb^+ (1–30 mM; △) and Rb^+ (12 mM) plus Cs^+ (0.1–30 mM, ◇). Strict adherence to values predicted by the Nernst equation (line) were observed for media containing K^+ and/or Rb^+. The dotted line adjacent to the 12 Rb^+/1–30 Cs^+ data illustrates predicted values of I_{crom} reversal potential using the upper limit of $P_{Cs^+}/P_{K^+} = 0.18$ obtained from the reversal of I_{crom} in 12 mM Cs^+ medium. The solid line was drawn using $P_{Cs^+}/P_{K^+} = 0.07$. Data from 4–22 cells. (b) Under the same experimental conditions as in (a), inward I_{crom} amplitude (measured 50 mV negative to E_{rev}) is plotted as a function of $[X^+]_o$. Inward I_{crom} in media containing K^+ and/or Rb^+ showed no sign of saturation over this range of $[X^+]_o$.

Permeabilities of rubidium and caesium

The permeabilities of Rb^+ and Cs^+ relative to K^+ were assessed in terms of their abilities to carry inward cromakalim current and the reversal potential in nominally K^+-free medium containing either 12 mM Rb^+ or 12 mM Cs^+.

In medium containing 12 mM Rb^+ prior to application of cromakalim, Na^+, Ca^{2+} and outward K^+ currents displayed little change in amplitude and voltage-dependence (Figure 4a). I_{K1} was reduced as much as 90% relative to that observed in 12 mM K^+ in a manner consistent with reports of the low Rb^+ permeability of inwardly rectifying K^+ channel of cardiac muscle (Matsuda *et al.*, 1989), skeletal muscle (Standen & Stanfield, 1980) and starfish eggs (Hagiwara & Takahashi, 1974). In the presence of external Rb^+ (12 mM), the average outward I_{crom} amplitude was almost as large as that observed in 12 mM K^+ (Figure 4c and 4d).

However, clear reversal of I_{crom} was observed in all 22 cells recorded in 12 mM Rb^+ and average inward I_{crom} amplitude was virtually identical to that observed in 12 mM K^+ The average reversal potential (-64.2 ± 1.1 mV) was positive to the average value in 12 mM K^+ by 1.6 mV. Using the relationship:

$$\Delta E_{rev} = E_{Rb^+} - E_{K^+} = RT/F \ln (P_{Rb^+}/P_{K^+}) \quad (1)$$

and assuming that intracellular permeant ion concentration is constant and that Rb^+ and K^+ are the only permeant extracellular ions, the permeability of Rb^+ relative to K^+ (P_{Rb^+}/P_{K^+}) is estimated to be 1.06.

In medium containing Cs^+ (12 mM), inward current was reduced to <5% of control at membrane potentials negative to −100 mV (Figure 4b1); Na^+ and Ca^{2+} currents were relatively unaffected. Under these conditions, cromakalim (100 μM) induced outward current at membrane potentials above −100 mV that was of amplitude comparable to that seen in K^+-containing or Rb^+-containing medium at potentials positive to −50 mV (Figure 4). However, in 12 mM Cs^+ medium there was little or no difference in current at membrane potentials below −120 mV in the absence or presence of cromakalim. Clear inward I_{crom} was observed in only 4 of 8 cells. The mean I_{crom} reversal potential in these 4 cells was -110.3 ± 6.6 mV. Using the relationship for Cs^+ permeability analogous to equation (1) an upper limit for the permeability of Cs^+ relative to K^+ (P_{Cs^+}/P_{K^+}) of 0.18 was calculated.

Interactions of Rb^+ and K^+ in the cromakalim-activated channel

Rb^+ (1–30 mM) was added to normal medium containing 2.5 mM K^+ to examine possible interactions between the two permeant cations in the channel activated by cromakalim. Figure 5 illustrates I_{crom} measured under these conditions using the same procedure as in Figures 2b and 4d. Inward I_{crom} amplitude increased with increasing concentrations of Rb^+ (see also Figure 3b), while the slope conductance of outward I_{crom} was unaffected. The I_{crom} reversal potential was shifted to more positive voltages in higher concentrations of Rb^+ in a manner consistent with the relation:

$$E_{rev} = RT/F \ln \{([K^+]_o + P_{Rb^+}/P_{K^+}[Rb^+]_o)/145\}$$

using $P_{Rb^+}/P_{K^+} = 1.06$ obtained above and assuming that the concentration of the intracellular permeant cation, K^+, remains constant at 145 mM.

Effects of Cs^+ on K^+ and Rb^+ current

The experiments illustrated in Figure 4 show that Cs^+ is a poor charge carrier for I_{crom}. To determine if Cs^+ is able to block the I_{crom} carried by K^+ and Rb^+, I_{crom} was measured in medium containing 2.5 mM K^+ or 12 mM Rb^+ to which 0.001–30 mM Cs^+ was added. Most of these experiments were carried out with medium containing Rb^+ because these conditions permitted the most reliable measurement of inward I_{crom}.

It was particularly important in these experiments to control for the potent ($IC_{50} = 0.01$–3 mM), voltage-dependent block of I_{K1} by Cs^+ in order to distinguish it from block of inward I_{crom}. In medium containing 2.5 mM K^+, our results (not shown) were similar to those of previous reports of block by Cs^+ of I_{K1} in cardiomyocytes (Isenberg, 1976; Argibay *et al.*, 1983; Tourneur *et al.*, 1987; Harvey & Ten Eick, 1989) as well as in other tissues (Hagiwara *et al.*, 1976; Gay & Stanfield, 1977). The concentration of Cs^+ inhibiting I_{K1} by 50% (IC_{50}) was strongly voltage-dependent and varied from 12 μM at −200 mV to >3 mM at −90 mV with an *e*-fold change in IC_{50} for a 15 mV change in membrane potential. In medium containing 12 mM Rb^+, Cs^+ was an effective, but slightly less potent, blocker of I_{K1} (Figure 6). IC_{50} varied from 20 μM at −200 mV to 8 mM at −90 mV with an *e*-fold change in IC_{50} for a 27 mV change in membrane potential (Figure 8). The equivalent valence of Cs^+ was estimated using the relation

$$z\delta = RT/F[\ln (IC_{50(E1)}/IC_{50(E2)})/(E1 - E2)]$$

where z is the charge of the blocking cation and δ the fraction of the membrane electrical field that Cs^+ traverses to reach its blocking site. $IC_{50(E1)}$ and $IC_{50(E2)}$ are the half-inhibitory concentrations of the blocking cation at two membrane potentials (E1 and E2) and R, T and F have their usual thermodynamic meanings. In K^+-containing medium $z\delta$ was approximately 1.54 while in Rb^+-containing medium $z\delta$ was 0.82.

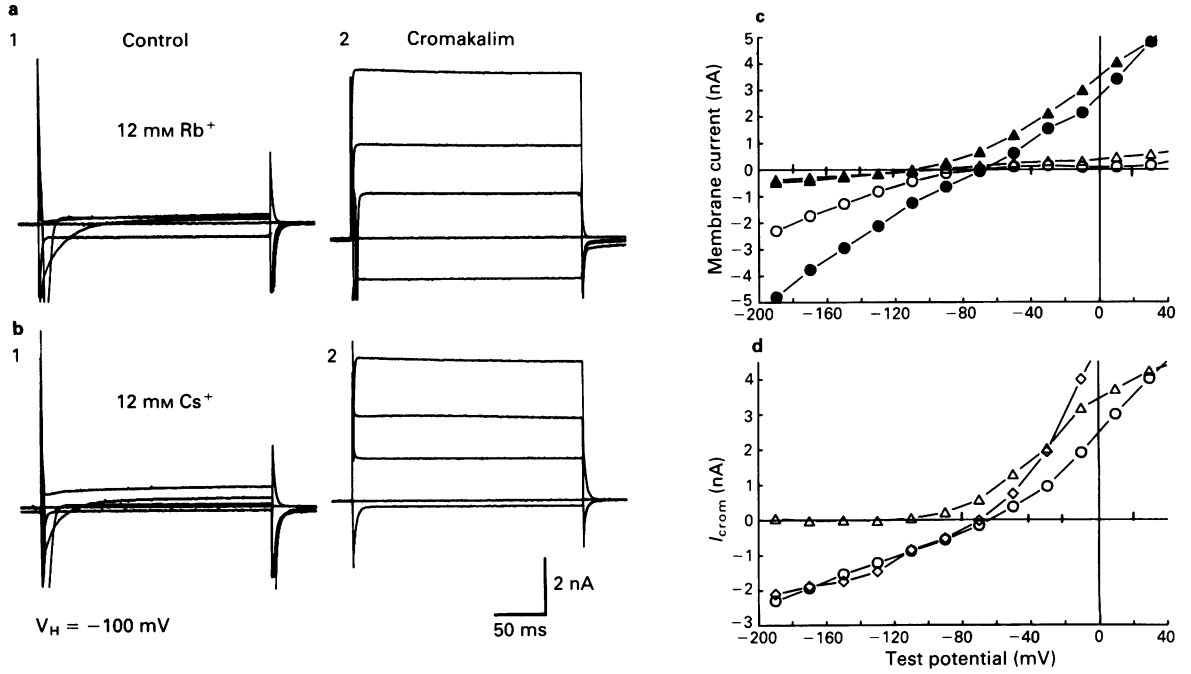


Figure 4 Rb^+ and Cs^+ as charge carriers of cromakalim-induced inward current (I_{crom}). Whole-cell membrane current was measured as in Figures 1 and 2, but in the presence of 12 mM Rb^+ (a) or Cs^+ (b); bathing medium was nominally K^+-free. Holding potential (V_H) was −100 mV; currents for voltage steps from −150 mV to +50 mV at 50 mV intervals are illustrated. (a1) 12 mM Rb^+; (a2) cromakalim (100 μM) in 12 Rb^+; (b1) 12 mM Cs^+; (b2) cromakalin (100 μM) in 12 mM Cs^+. (c) Current-voltage relationship for whole-cell membrane current measured at the end of 200 ms voltage steps in Rb^+-containing (○, ●) and Cs^+-containing (△, ▲) medium under control conditions (open symbols) and in the presence of cromakalim (100 μM; filled symbols). Symbols for current in Cs^+ in the absence and presence of cromakalim overlap at potentials between −200 and −100 mV. (d) Plot of I_{crom} (estimated as in Figure 2) versus membrane potential recorded in 12 mM Rb^+ (○, 22 cells), 12 mM Cs^+ (△, 8 cells) and 12 mM K^+ (◇, 9 cells, same data as in Figure 2b).

Cs^+ also inhibited inward I_{crom} carried by K^+ and Rb^+, but had little effect on outward I_{crom} amplitude at membrane potentials more than 50 mV positive to the I_{crom} reversal potential (Figures 6 and 7). In Rb^+-containing medium with moderate concentrations of Cs^+ (0.1–1 mM, sufficient to inhibit I_{K1}) inward I_{crom} was unchanged, or even slightly increased. Higher concentrations of Cs^+ (3–30 mM) strongly inhibited inward I_{crom}. This inhibition was voltage-dependent; the potency of Cs^+ was greater at more negative membrane potentials such that IC_{50} varied between 4 mM at −200 mV and 20 mM at −120 mV (Figure 8) and Cs^+ was entirely ineffective at membrane potentials positive to the reversal poten-

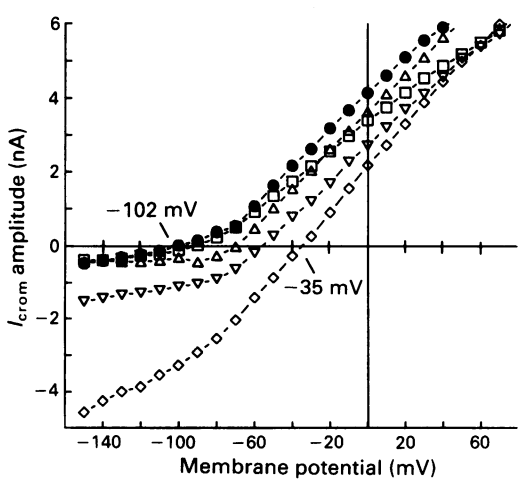


Figure 5 Interactions of K^+ and Rb^+ in the cromakalim-activated channel. With the K^+ concentration ($[K^+]_o$) constant at 2.5 mM, I_{crom} was measured with Rb^+ concentrations ($[Rb^+]_o$) of 0 mM (●), 1 mM (□), 3 mM (△), 10 mM (▽) and 30 mM (◇). Note the positive shift in I_{crom} reversal potential increased inward I_{crom} with increased $[Rb^+]_o$. Data from 4 cells; s.e.mean (not shown) were <20%.

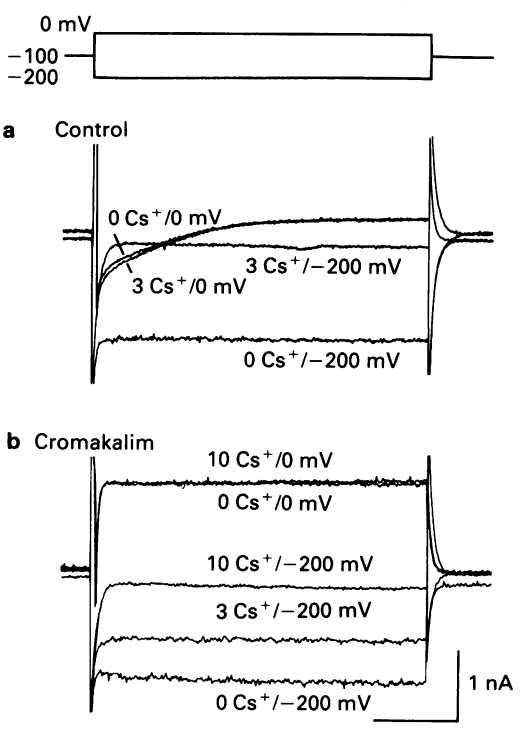


Figure 6 Effects of extracellular Cs^+ on I_{crom}, I_{K1} and other currents in a ventricular myocyte recorded in 12 mM Rb^+-containing medium. Voltage (top) and current traces are illustrated for voltage steps from a holding of −100 mV to test potentials of −200 mV and 0 mV under control conditions (a) and in the presence of 100 μM cromakalim (b). Under control conditions, Cs^+ (3 mM) blocks I_{K1} activated at −200 mV but has no effect on outward current or inward Na and Ca currents activated at 0 mV. In the presence of cromakalim, inward current at −200 mV is reduced by 3 mM Cs^+ and blocked by 10 mM Cs^+. Outward I_{crom} at 0 mV is unaffected by 10 mM Cs^+.

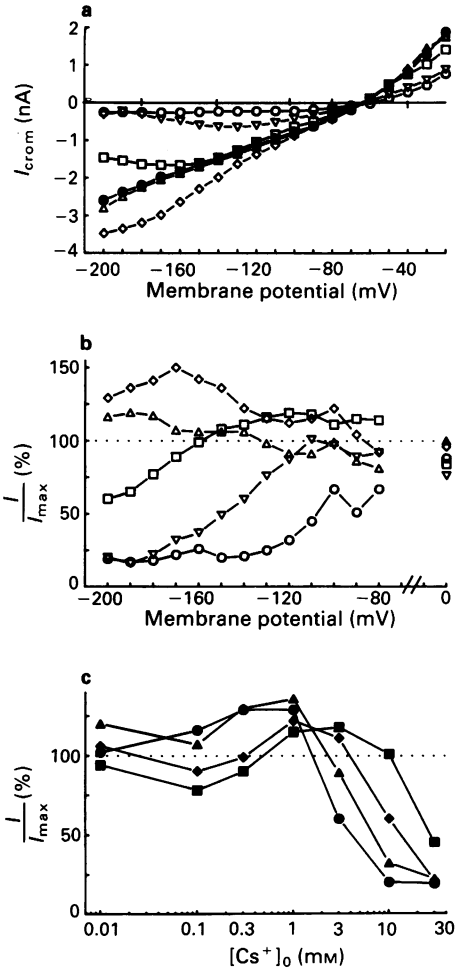


Figure 7 Effects of extracellular Cs^+ on I_{crom} in 12 mM Rb^+. (a) As previously, I_{crom} was estimated as the difference between whole-cell membrane current measured in the absence and presence of cromakalim (100 μM) in bathing solutions containing 0.01–30 mM CsCl ($[Cs^+]_o$: 0 mM, ●; 0.1 mM, △; 1 mM, ◇; 10 mM, ▽; 30 mM, ○). Rb^+ (12 mM) was present throughout as the carrier of inward I_{crom}. In (b) I_{crom} (I) measured in the presence of various $[Cs^+]_o$ is expressed as a percentage of control I_{crom} (I_{max}, $[Cs^+]_o$ = 0 mM) and plotted as a function of membrane potential. Same symbols as in (a). (c) I_{crom} data from (a) for different membrane potentials (−200 mV, ●; −170 mV, ▲; −140 mV, ◆; −110 mV, ■) are plotted as a function of $[Cs^+]_o$. Data from 3–8 cells; s.e.mean of 8–30% are omitted for clarity.

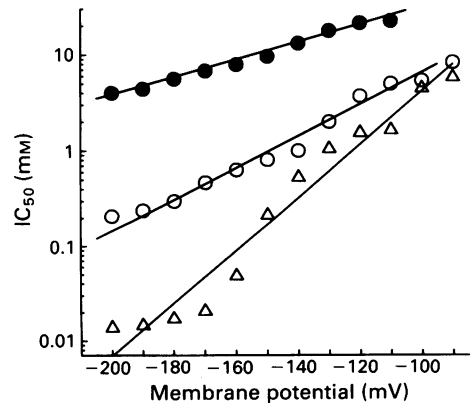


Figure 8 Voltage-dependence of inhibition of I_{K1} and inward I_{crom} by external Cs^+. The concentration of external Cs^+ that reduced the currents by 50% (IC_{50}) is plotted as a function of membrane potential for I_{K1} recorded in medium containing 2.5 mM K^+ (△) and 12 mM Rb^+ (○) and for I_{crom} recorded in 12 mM Rb^+ medium (●). The lines, through the data were drawn by eye and have slopes of 16, 28 and 44 mV/e-fold change in IC_{50}, respectively.

tial. The equivalent valence $z\delta$ for Cs^+ block of I_{crom} over the voltage range −200 mV to −100 mV was estimated to be 0.46. The reversal potential of I_{crom} in solutions containing 12 mM Rb^+ plus 1–30 mM Cs^+ varied in a manner consistent with the estimate of P_{Rb^+}/P_{K^+} (1.06) obtained above and P_{Cs^+}/P_{K^+} equal to 0.07 (Figure 3a).

Discussion

This paper describes the ionic selectivity of whole-cell current activated by cromakalim (I_{crom}) in guinea-pig isolated ventricular myocytes. Cromakalim is known to activate ATP-sensitive K^+ [K(ATP)] channels, and correspondingly the sulphonylurea, glibenclamide, inhibits I_{crom} as it does the K(ATP) channel (Schmid-Antomarchi *et al.*, 1987; Escande *et al.*, 1988; Sanguinetti *et al.*, 1988; Sturgess *et al.*, 1988). Our present data support the contention that the main current response to cromakalim is the activation of K(ATP) channels.

In the majority of cardiomyocytes, there appeared to be a decrease in the amplitude of the voltage-dependent Na^+ and Ca^{2+} currents (I_{Na} and I_{Ca}) and (or) a shift of the activation of these currents to more positive potentials. This effect was extremely variable between cells, but was always reversed by glibenclamide (J.C.R. Randle and S.H.R. Oliet, unpublished observations and see also Liu *et al.*, 1990). We do not have compelling evidence from our current experiments that this phenomenon is a primary effect of cromakalim on cardiomyocytes as suggested in vascular smooth muscle cells (Okabe *et al.*, 1990). Rather, as described recently by Shuba *et al.* (1990), deviations of true membrane potential from command potential under voltage clamp owing to large membrane currents may be responsible for the changes in I_{Na} and I_{Ca} that we observe.

Cation permeabilities

The reversal potential of I_{crom} varied with $[K^+]_o$ strictly as predicted by the Nernst equation and no inward I_{crom} was observed when no K^+ was added to the external medium. Thus, under physiological conditions cromakalim activates a pure K^+ conductance in cardiac myocytes, in agreement with the estimates of relative Na^+ and K^+ permeabilities (P_{Na^+}/P_{K^+}) of the K(ATP) channel in heart (Kakei *et al.*, 1985), in skeletal muscle (0.015; Spruce *et al.*, 1987) and in pancreatic β-cells (0.007; Ashcroft *et al.*, 1989). The reversal potential of I_{crom} activated in the presence of 12 mM Rb^+ or combinations of 2.5 mM K^+ plus 1–30 mM Rb^+ varied in a manner suggesting that Rb^+ and K^+ have similar permeabilities (P_{Rb^+}/P_{K^+} = 1.06). This value is slightly higher than those obtained in single K(ATP) channel recordings in skeletal muscle (0.76; Spruce *et al.*, 1987) and β-cells (0.7; Ashcroft *et al.*, 1989). Similar experiments with Cs^+-containing media indicate that Cs^+ has a low, but measurable permeability with $P_{Cs^+}/P_{K^+} < 0.2$. The estimate of P_{Cs^+}/P_{K^+} = 0.18 from experiments with 12 mM Cs^+ must be considered an upper limit since this value was derived from the I_{crom} reversal potential in four cells in which clear reversal occurred, while in four other cells no I_{crom} reversal was observed even at −200 mV. Thus, a P_{Cs^+}/P_{K^+} = 0.07, which adequately describes the data from experiments in which 1–30 mM Cs^+ was added to 12 mM Rb^+, is probably closer to a 'true' value. The permeability sequence for monovalent alkali metal cations is therefore $K^+ \simeq Rb^+ \gg Cs^+ > Na^+$.

Inward I_{crom}

As illustrated in previous reports (Sanguinetti *et al.*, 1988; Liu *et al.*, 1990), the amplitude of inward I_{crom} for a given $[K^+]_o$ was extremely variable, to the extent that even in high $[K^+]_o$ some cells displayed no inward I_{crom}. This phenomenon is not peculiar to the activation of K(ATP) channels by cromakalim. Activation of K(ATP) channels by depletion of intracellular

ATP in cardiac myocytes can induce a decrease (rather than an increase) in total inward current at negative potentials associated with the appearance of a large outward current at positive potentials (Noma & Shibasaki, 1985).

It is unlikely that the inconsistency in inward I_{crom} observed results from a property of the K(ATP) channel. Single channel studies of K(ATP) indicate that rectification of inward current does not occur. Rather, the inconsistency in the measurement of inward I_{crom} (or $I_{K(ATP)}$) probably results from technical difficulties associated with the very large inwardly rectifying K^+ current, I_{K1}, in ventricular myocytes. I_{K1} amplitude is typically 5 to 10 times that of the mean inward I_{crom}, so small variations in I_{K1} amplitude will interfere significantly with measurement of inward I_{crom}. Second, small series resistance compensation errors may result in significant errors in the measurement of membrane potential over the range where I_{K1} is active. Finally, the large size of these cylindrical (10–20 μm diameter × 70–200 μm long) cells, their complex intracellular organization and their high specific membrane conductivity over the range of voltages where I_{K1} is active may conspire to make space clamp imperfect at voltages negative to E_{K+} (cf. Brown *et al.*, 1981; Shuba *et al.*, 1990). The effects of external Rb^+ and Cs^+ on the amplitudes of inward I_{K1} and I_{crom} also support these conclusions (see below). Furthermore, we have observed consistent reversal of I_{crom} in an insulin-secreting cell line, RIN m5F, which has little active current at voltages negative to E_{K+} and favourable geometry (unpublished observations).

Our experiments suggest that the conductivities of Rb^+ and K^+ in the cromakalim-activated channel [presumably K(ATP)] of cardiomyocytes are similar and that the two ions do not interfere with each other's passage through the channel. Our results are thus in contrast with single channel data for the K(ATP) channel of skeletal muscle (Spruce *et al.*, 1986; 1987) and pancreatic β-cell (Ashcroft *et al.*, 1989). This may reflect differences in the permeability characteristics of K(ATP) channels of various tissues, in addition to their differing sensitivities to cromakalim, sulphonylureas and ATP (for review see Quast & Cook, 1989b).

Caesium block of I_{K1} *and* I_{crom}

Our observations of the voltage-dependent block of I_{K1} by Cs^+ in the presence of 2.5 mM external K^+ are similar to those of previous authors (Isenberg, 1976; Argibay *et al.*, 1983; Tourneur *et al.*, 1987; Harvey & Ten Eick, 1989). Interestingly, the Cs^+ block of I_{K1} in the presence of 12 mM Rb^+ was less potent and the voltage-dependence was considerably less than that observed in 2.5 mM K^+ (Figure 8). The equivalent valence $z\delta$ of 1.54 in 2.5 mM K^+ medium agrees with estimates in the range 1.3 to 1.6 made by the aforementioned authors. Since these estimates are greater than unity, it is proposed that the channel is blocked by two or more Cs^+ ions that traverse a significant portion of the membrane electrical field to reach their blocking sites. The lower equivalent valence of Cs^+ for the block of Rb^+ current through the I_{K1} channel (0.82) may result from differences in interactions between the permeant cations, K^+ and Rb^+, and the blocking cation, Cs^+, at the three binding sites proposed for this channel (cf.: Hille & Schwarz, 1978). Further examination of this question is beyond the scope of this paper.

Cs^+ (0.1–30 mV) had no effect on outward I_{crom}. Cs^+ blocked inward I_{crom} carried by Rb^+ considerably less potently than it did I_{K1}. We observed IC_{50} values of 4–20 mM for membrane potentials between −200 and −100 mV and an effective valence of 0.55. Notably, external Cs^+ at concentrations as great as 30 mM had no consistent effect on outward I_{crom}. Quayle *et al.* (1988) reported somewhat greater potency and voltage-dependence ($z\delta = 1.22$) for the Cs^+ block of single skeletal muscle K(ATP) channel current. This discrepancy may reflect differences in the ability of Cs^+ to block the passage of Rb^+ and K^+ in the channel in a manner analogous to the I_{K1} channel. Another possible explanation is that the technical difficulties associated with large-amplitude I_{K1} discussed above interfered with the precise measurement of I_{crom} in the absence of Cs^+. In fact, moderate concentrations (0.1–1 mM) of Cs^+ that blocked I_{K1} often appeared to increase inward I_{crom}. It seems unlikely that this represents a true increase in I_{crom} since Quayle *et al.* (1988) observed no such increase in single K(ATP) channel current at these concentrations of Cs^+. With I_{K1} blocked in the presence of Cs^+, the improved measurement of I_{crom} would have resulted in the apparent increase in I_{crom} and decreased the apparent potency of Cs^+.

Conclusions

Our results confirm that cromakalim activates a pure K^+ conductance in guinea-pig ventricular myocytes, in support of the contention that K(ATP) channel activation is the major mechanism of action of this benzopyran. The high apparent Rb^+ permeability and conductivity argue that Rb^+ is a good substitute for K^+ in ion flux studies. Rb^+ has also proved to be useful in electrophysiological studies where reliable measurements of inward, as well as outward, I_{crom} are required. Extracellular Cs^+ blocks inward I_{crom} weakly in comparison with its block of the inwardly rectifying current, I_{K1}. Outward I_{crom} is insensitive to extracellular Cs^+.

We would like to thank Dr G.L. Regnier (Chemistry Department, Institut de Recherche Servier) for providing the cromakalim used in this study and Mrs S. Dumoulin for typing the manuscript.

References

ARGIBAY, J.A., DUTEY, P., ILDEFONSE, M., OJEDA, C., ROUGIER, O. & TOURNEUR, Y. (1983). Block by Cs of K current I_{K1} and of carbachol induced K current I_{Cch} in frog atrium. *Pflügers Arch.*, **397**, 295–299.

ASHCROFT, F.M., KAKEI, M. & KELLY, R.P. (1989). Rubidium and sodium permeability of the ATP-sensitive K^+ channel in single rat pancreatic β-cells. *J. Physiol.*, **408**, 413–430.

BROWN, A.M., LEE, K.S. & POWELL, T. (1981). Voltage clamp and internal perfusion of single rat heart muscle cells. *J. Physiol.*, **318**, 455–477.

CAVERO, I., MONDOT, S. & MESTRE, M. (1989). Vasorelaxant effects of cromakalim in rats are mediated by glibenclamide-sensitive potassium channels. *J. Pharmacol. Exp. Ther.*, **248**, 1261–1268.

DIFRANCESCO, D., FERRONI, A. & VISENTIN, S. (1984). Barium-induced blockade of the inward rectifier in calf Purkinje fibres. *Pflügers Arch.*, **402**, 446–453.

DUNNE, M.J., YULE, D.I., GALLACHER, D.V. & PETERSEN, O.H. (1989). Cromakalim (BRL 34915) and diazoxide activate ATP-regulated potassium channels in insulin-secreting cells. *Pflügers Arch.*, **414** (Suppl. 1), S154–S155.

ELTZE, M. (1989). Competitive antagonism by glibenclamide of cromakalim inhibition of twitch contractions in rabbit vas deferens. *Eur. J. Pharmacol.*, **161**, 103–106.

ESCANDE, D., THURINGER, D., LEGUERN, S. & CAVERO, I. (1988). The potassium channel opener cromakalim (BRL 34915) activates ATP-dependent K^+ channels in isolated cardiac myocytes. *Biochem. Biophys. Res. Commun.*, **154**, 620–625.

GAY, L.A. & STANFIELD, P.R. (1977). Cs^+ causes a voltage-dependent block of inward K currents in resting skeletal muscle fibres. *Nature*, **267**, 169–170.

HAGIWARA, S., MIYAZAKI, S. & ROSENTHAL, N.P. (1976). Potassium current and the effect of cesium on this current during anomalous rectification of the egg cell membrane of a starfish. *J. Gen. Physiol.*, **67**, 621–638.

HAGIWARA, S. & TAKAHASHI, K. (1974). The anomalous rectification and cation selectivity of the membrane of a starfish egg cell. *J. Memb. Biol.*, **18**, 61–80.

HAMIL, O.P., MARTY, A., NEHER, E., SAKMANN, B. & SIGWORTH, F.J. (1981). Improved patch-clamp techniques for high-resolution current recording from cells and cell-free membrane patches. *Pflü-*

gers Arch., **391**, 85–100.

HARVEY, R.D. & TEN EICK, R.E. (1989). Voltage-dependent block of cardiac inward-rectifying potassium current by monovalent cations. *J. Gen. Physiol.*, **94**, 349–361.

HILLE, B. & SCHWARZ, W. (1978). Potassium channels as multi-ion single-file pores. *J. Gen. Physiol.*, **72**, 409–442.

ISENBERG, G. (1976). Cardiac purkinje fibers: cesium as a tool to block inward rectifying K^+ currents. *Pflügers Arch.*, **365**, 99–106.

KAKEI, M., NOMA, A. & SHIBASAKI, T. (1985). Properties of adenosine-triphosphate regulated potassium channels in guinea-pig ventricular cells. *J. Physiol.*, **363**, 441–442.

LEECH, C.A. & STANFIELD, P.R. (1981). Inward rectification in frog skeletal muscle fibres and its dependence on membrane potential and external potassium. *J. Physiol.*, **319**, 295–309.

LIU, B., McCULLOUGH, J.R. & VASSALE, M. (1990). On the mechanism of increased potassium conductance by the K^+ channel opener BRL 34915 in isolated ventricular myocytes. *Drug Dev. Res.*, **19**, 409–423.

MATSUDA, H., MATSURA, H. & NOMA, A. (1989). Triple-barrel structure of inwardly rectifying potassium channels revealed by Cs^+ and Rb^+ block in guinea-pig heart cells. *J. Physiol.*, **413**, 139–157.

MITRA, R. & MORAD, M. (1985). A uniform enzymatic method for dissociation of myocytes from hearts and stomachs of vertebrates. *Am. J. Physiol.*, **249**, H1056–H1060.

NOMA, A. & SHIBASAKI, T. (1985). Membrane current through adenosine-triphosphate-regulated potassium channels in guinea-pig ventricular cells. *J. Physiol.*, **363**, 463–480.

OKABE, K., KAJIOKA, S., NAKAO, K., KITAMURA, K., KURIYAMA, H. & WESTON, A.H. (1990). Actions of cromakalim on ionic currents recorded from single smooth muscle cells of the rat portal vein. *J. Pharmacol. Exp. Ther.*, **252**, 832–839.

QUAST, U. & COOK, N.S. (1989a). In vitro and in vivo comparison of two channel openers, diazoxide and cromakalim, and their inhibition by glibenclamide. *J. Pharmacol. Exp. Ther.*, **250**, 261–271.

QUAST, U. & COOK, N.S. (1989b). Moving together: K^+ channel openers and ATP-sensitive K^+ channels. *Trends Pharmacol. Sci.*, **10**, 431–435.

QUAYLE, J.M., STANDEN, N.B. & STANFIELD, P.R. (1988). The voltage-dependent block of ATP-sensitive potassium channels of frog skeletal muscle by caesium and barium ions. *J. Physiol.*, **405**, 677–697.

SANGUINETTI, M.C., SCOTT, A.L., ZINGARO, G.J. & SIEGL, P.K.S. (1988). BRL 34915 (cromakalim) activated ATP-sensitive K^+ current in cardiac muscle. *Proc. Natl. Acad. Sci. U.S.A.*, **85**, 8360–8364.

SAKMANN, B. & TRUBE, G. (1984). Conductance properties of single inwardly rectifying potassium channels in ventricular cells from guinea-pig heart. *J. Physiol.*, **347**, 641–647.

SCHMID-ANTOMARCHI, H., DEWEILLE, J., FOSSET, M. & LAZDUNSKI, M. (1987). The antidiabetic sulfonylurea glibenclamide is a potent blocker of the ATP-modulated K^+ channel in insulin secreting cells. *Biochem. Biophys. Res. Commun.*, **146**, 21–25.

SHUBA, Y.M., HEßLINGER, B., TRAUTWEIN, W., McDONALD, T.F. & PELZER, D. (1990). A dual-pipette technique that permits rapid internal dialysis and membrane potential measurement in voltage-clamped cardiomyocytes. *Pflügers Arch.*, **415**, 767–773.

SPRUCE, A.E., STANDEN, N.B. & STANFIELD, P.R. (1985). Voltage-dependent ATP-sensitive potassium channels of skeletal muscle membrane. *Nature*, **316**, 736–738.

SPRUCE, A.E., STANDEN, N.B. & STANFIELD, P.R. (1986). Rb^+ permeability of ATP-dependent potassium channels of frog skeletal muscle. *J. Physiol.*, **378**, 105P.

SPRUCE, A.E., STANDEN, N.B. & STANFIELD, P.R. (1987). Studies of the unitary properties of adenosine-5′-triphosphate-regulated potassium channels of frog skeletal muscle. *J. Physiol.*, **382**, 213–236.

STANDEN, N.B., QUAYLE, J.M., DAVIES, N.W., BRAYDEN, J.E., HUANG, Y. & NELSON, M.T. (1989). Hyperpolarizing vasodilators activate ATP-sensitive K^+ channels in arterial smooth muscle. *Science*, **245**, 177–180.

STANDEN, N.B. & STANFIELD, P.R. (1980). Rubidium block and rubidium permeability of the inward rectifier of frog skeletal muscle fibres. *J. Physiol.*, **304**, 415–435.

STURGESS, N.C., KOZLOWSKI, R.Z., CARRINGTON, C.A., HALES, C.N. & ASHFORD, M.L.J. (1988). Effects of sulphonylureas and diazoxide on insulin secretion and nucleotide-sensitive channels in an insulin-secreting cell line. *Br. J. Pharmacol.*, **95**, 83–94.

TOURNEUR, Y., MITRA, R., MORAD, M. & ROUGIER, O. (1987). Activation properties of the inward-rectifying potassium channel on mammalian heart cells. *J. Memb. Biol.*, **97**, 127–135.

WINQUIST, R.J., HEANEY, L.A., WALLACE, A.A., BASKIN, E.P., STEIN, R.B., GARCIA, M.L. & KACZOROWSKI, G.J. (1989). Glyburide blocks the relaxation response to BRL 34915 (cromakalim), minoxidil sulfate and diazoxide in vascular smooth muscle. *J. Pharmacol. Exp. Ther.*, **248**, 149–156.

(Received November 13, 1990
Revised March 12, 1991
Accepted March 18, 1991)

Br. J. Pharmacol. (1991), **103**, 1802–1806 © Macmillan Press Ltd, 1991

Age-dependent changes in cardiovascular responses induced by muscimol infused into the nucleus tractus solitarii and nucleus parabrachialis medialis in rats

V. Mollace, *E.A. De Francesco, *G. Fersini & [1]G. Nistico'

Institute of Pharmacology, Faculty of Medicine, University of Reggio Calabria, Policlinico Mater Domini, Via T. Campanella, 88100 Campanella, 88100 Cantanzaro and *FIDIA-GRF Neuropsychopharmacology Centre, USL 19, Girifalco, Italy

1 The effects of muscimol and bicuculline on mean arterial blood pressure (MAP) and heart rate (HR) were studied after their microinfusion into the nucelus tractus solitarii (NTS) and into the nucleus parabrachialis medialis (NPBmed) in 3 and 24 month old rats.

2 In 3 month old rats a dose of 0.01 μg of muscimol given into the NTS increased MAP, whereas higher doses (0.05, 0.1 and 0.25 μg) produced dose-dependent bradycardia with either no change (0.05 and 0.1 μg) or a decrease (0.25 μg) in MAP.

3 On the other hand, in 24 month old rats, the same doses of muscimol given into the NTS failed to change MAP, whereas in comparison to 3 month old rats they produced a significantly lesser bradycardia.

4 The cardiovascular changes elicited by infusion of muscimol into the NTS in 3 and 24 month old rats were prevented by prior microinfusion of bicuculline into the same site.

5 Muscimol given into the NPBmed in doses from 0.05 to 0.25 μg produced, in 3 month old rats dose-dependent decreases in MAP and HR which were prevented by prior administration of bicuculline. These effects were significantly reduced in 24 month old rats.

6 The present experiments show that with aging there is impairment of GABA-ergic mechanisms involved in the regulation of cardiovascular activity in the NTS and NPBmed.

Keywords: GABA; nucleus tractus solitarii; parabrachial medial nucleus; cardiovascular control; aging

Introduction

Evidence exists that γ-aminobutyric acid (GABA)mediated mechanisms play an important role in the control of cardiovascular activity. Classical studies have shown that an intravenous injection of GABA in rabbits produces a marked fall in blood pressure (Takahashi *et al.*, 1955). Hypotension and bradycardia following systemic administration of GABA was suggested to be modulated through the lower brainstem (Bhargava *et al.*, 1964; Bhattacharja *et al.*, 1964). In fact, the intracerebroventricular administration of GABA-mimetic drugs produces, in several animal species, a decrease in blood pressure and heart rate (Sgaragli & Pavan, 1972; Philippu *et al.*, 1973; Persson, 1980; Baum & Becker, 1982). Furthermore, the elevation of GABA levels in the brain following inhibition of GABA transaminase, has been reported to reduce blood pressure (Loscher, 1982).

Several medullary and diencephalic sites have been implicated in mediating the cardiovascular response to drugs acting at GABA receptors (Antonaccio *et al.*, 1978; Bousquet *et al.*, 1981). It has been generally assumed that the cardiovascular depression induced by GABA was mediated via decreased activity of the sympathetic nervous system and probably via increased vagal activity (Persson, 1980). This was confirmed by observation of an increase in the peripheral sympathetic activity and by suppression of vagal excitability of the heart after administration into the lateral cerebral ventricle of antagonists at GABA receptors such as bicuculline and picrotoxin (Di Micco, 1982).

The nucleus tractus solitarii (NTS) is a brainstem nucleus receiving inputs from primary baroreceptor afferents and is involved in cardiovascular regulation. It has been shown that GABA, muscimol and drugs enhancing GABA-ergic transmission microinjected directly into the NTS produce an increase in blood pressure and heart rate both in normotensive and spontaneously hypertensive rats (Kubo & Kihara, 1987; Catelli & Sved, 1987; 1988). We have recently confirmed that muscimol, a $GABA_A$ receptor agonist, is able to affect both mean arterial blood pressure (MAP) and heart rate (HR), when microinfused directly into the NTS. This effect was antagonized by pretreatment with bicuculline, a selective $GABA_A$ receptor antagonist (Mollace *et al.*, 1989a). Another important region involved in cardiovascular regulation, and in modulating afferent inputs to NTS neurones, is represented by the nucleus parabrachialis medialis (NPBmed) (Felder & Mifflin, 1988). In previous experiments, we have shown that during aging there is a decrease in the cardiovascular response to α_2-adrenoceptor agonists administered directly into the NTS (Mollace *et al.*, 1989b). In particular, clonidine, microinfused into the NTS in 24 month old rats, was unable to induce cardiovascular responses when compared to 3 and 12 month old rats. In addition chronic pretreatment with phosphatidylserine restored the decreased cardiovascular response to clonidine microinfused into NTS in 16 but not in 24 month old rats (Mollace *et al.*, 1990). The present study was undertaken in order to compare the cardiovascular effects produced by muscimol when microinfused into the NTS and the NPBmed in 3 and 24 month old rats. This could give some information as to whether, during the aging process, an alteration of GABA-ergic mechanisms occurs in areas of the brain involved in the central cardiovascular regulation and whether the aging process affected the cardiovascular responses to drugs acting on GABA receptors in a similar manner in different nuclei of the brain.

Methods

Adult male Wistar Morini (S. Polo d'Enza, Reggio Emilia, Italy) normotensive rats were divided into two groups: 3 and 24 month old, weighing approx 250 and 600 g respectively. Intracerebral cannulae were implanted in rats under sodium pentobarbitone anaesthesia (55 mg kg^{-1}, i.p.). Each cannula consisted of two concentric stainless steel tubes, a 1.6 cm long 23 gauge outer tube or guide cannula which was implanted

[1] Author for correspondence.

stereotactically (David Kopf Instrument) into the brain, and an inner tube, (o.d. 0.2 mm) used for the infusion. For the implantation of the guide cannulae into the brain, the following coordinates of Paxinos & Watson (1982) were used: AP = 12.8 mm posterior to bregma, L = 1.5 mm lateral to the midline, H = 8 mm ventral to the skull surface, for the NTS; AP = 8 mm posterior to the bregma, L = 1.7 lateral to the midline, H = 7 mm ventral to the skull surface, for the NPBmed. *Post mortem* histological examination of the brain confirmed the exact position of the guide cannula. Catheters (PE 50), filled with heparinized saline (200 u ml^{-1}) were inserted into the left common carotid artery to record blood pressure. After surgery, a stabilization period of 48 h was allowed before the experiments were carried out. In animals maintained under general anaesthesia (pentobarbitone, 55 mg kg^{-1}, i.p.) mean arterial blood pressure (MAP) was recorded by attaching an arterial catheter to a Bentley transducer (Ugo Basile, Comerio Varese, Italy) connected to a Gemini polygraph (Ugo Basile). Heart rate was recorded using a cardiotachograph (Ugo Basile). To quantify drug-induced cardiovascular responses, the area under the curve (AUC) of MAP and HR changes during 120 min was calculated according to the 'trapezoidal rule' (Tallarida & Murray, 1981). In particular, the AUCs for MAP (expressed as mmHg min^{-1}) or HR (expressed as beats min^{-1}) were measured as the area between the top of the curve obtained by calculating the differences (Δ) in MAP or HR produced by drugs, when compared to the basal levels, and the zero line.

In order to verify whether or not the effects of muscimol were due to it acting as an agonist at $GABA_A$ receptors, pretreatment with bicuculline was carried out 10 min before microinjection of muscimol into the NTS or the NPBmed and the percentage changes in their cardiovascular effects were assessed. For statistical evaluation, Student's *t* test for unpaired data was used.

Drugs

Muscimol (Sigma, St. Louis, MO, U.S.A.) was easily dissolved in twice distilled pyrogen-free water. Bicuculline (Sigma) was dissolved in 0.1 N HCl, the pH adjusted to 5.5 with 0.5 N NaOH and the final volume made up of NaCl, according to Persson (1980). Drugs were infused in a volume of 1 μl over 1 min (the maximal volume was 1 μl). For use as the anaesthetic, pentobarbitone sodium salt (Sigma) was dissolved in saline and administered i.p. in a 0.25 ml volume.

Results

Cardiovascular effects of muscimol and bicuculline microinfused into the NTS and NPB med in 3 month old rats

Muscimol (0.01 μg; $n = 5$), microinfused into the NTS of 3 month old rats induced an increase (mean maximal increase of 22 ± 2.2 mmHg; AUC = 875 ± 42) in MAP reaching its peak 20 min after its administration and lasting approximately 45 min. The same dose of muscimol was without effect on HR. Doses of 0.05, 0.1 and 0.25 μg ($n = 5$ for each dose) induced a dose-dependent decrease in HR, whereas no significant changes in MAP were observed with 0.05 and 0.1 μg: a significant ($P < 0.05$) fall occurred only after 0.25 μg of muscimol (Figure 1). Bicuculline (0.5 μg), given into the NTS 10 min before muscimol, was able to antagonize the changes in MAP and HR induced by muscimol (Table 1).

The microinfusion of muscimol (0.05, 0.1 and 0.25 μg; $n = 5$ for each dose) into the NPBmed induced dose-dependent hypotension and bradycardia (Figure 2). No effects were observed when muscimol was infused into the NPBmed in doses smaller than 0.05 μg. These effects were antagonized by pretreatment with bicuculline (0.5 μg) microinfused into the same site 10 min before muscimol (Table 1). No significant

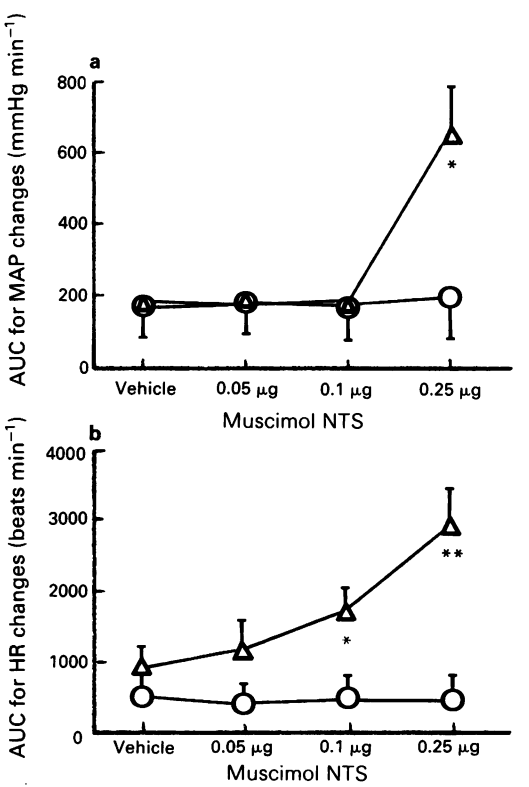


Figure 1 Effects of muscimol (0.05, 0.1 and 0.25 μg) and vehicle (same volume, 1 μl) microinfused into the nucleus tractus solitarii (NTS), on areas under curves (AUCs) for mean arterial blood pressure (a) or heart rate (HR) (b) changes in 3 (Δ) and 24 (○) month old rats. Each point is the mean of AUCs for the changes in 5 rats and the bars show s.e.mean. * $P < 0.05$; ** $P < 0.01$ between 3 and 24 month old rats.

Table 1 Effects of pretreatment with bicuculline (0.5 μg) given into the nucleus tractus solitarii (NTS) on changes of areas under the curves (AUCs) for mean arterial blood pressure (MAP) and heart rate (HR) induced by subsequent (10 min later) microinfusion of vehicle or muscimol (0.05, 0.1 and 0.25 μg) microinjected into the same site in 3 and 24 month old rats

	AUCs for MAP changes (mmHg min^{-1})		*AUC for HR changes* (beats min^{-1})	
Treatment	*3 month old*	*24 month old*	*3 month old*	*24 month old*
Vehicle	200 ± 33.6	220 ± 42.1	750 ± 100	400 ± 51.5
+ bicuculline (0.5 μg)	185 ± 41.0	205 ± 35.4	450 ± 80.1*	400 ± 51.5
Muscimol (0.05 μg)	189 ± 27.8	225 ± 33.3	1050 ± 158	580 ± 81.9
+ bicuculline (0.5 μg)	211 ± 34.1	175 ± 36.0	555 ± 87.9*	472 ± 60.2
Muscimol (0.1 μg)	210 ± 42.7	200 ± 31.5	1547 ± 156	551 ± 68.8
+ bicuculline (0.5 μg)	180 ± 29.4	175 ± 29.3	499 ± 82.1*	599 ± 78.5
Muscimol (0.25 μg)	620 ± 51.2	165 ± 22.7	3100 ± 123	600 ± 54.9
+ bicuculline (0.5 μg)	180 ± 39.3*	189 ± 37.8	599 ± 86.1*	652 ± 73.8

Data are expressed as mean ± s.e.mean of AUC for MAP and HR changes in 5 rats.
* $P < 0.05$ between rats pretreated with bicuculline and rats treated with vehicle or muscimol.

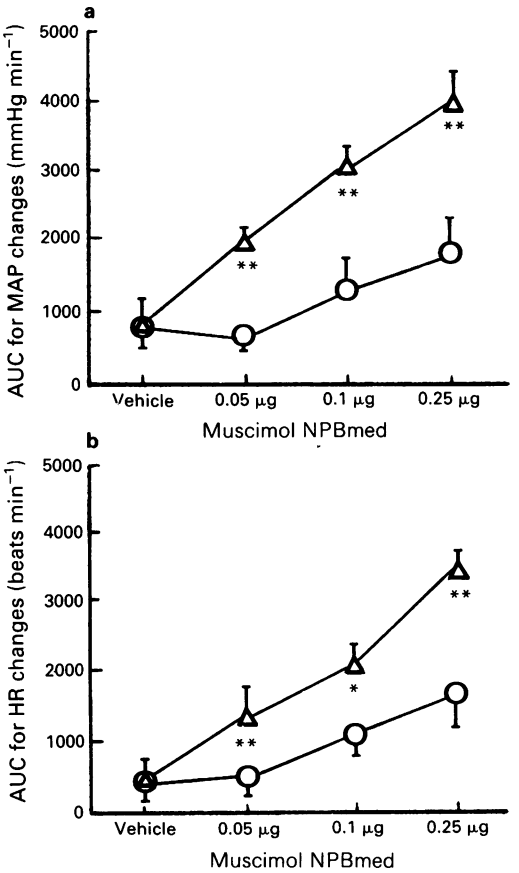


Figure 2 Effects of muscimol (0.05, 0.1 and 0.25 μg) and vehicle (same volume, 1 μl) microinfused into the nucleus parabrachialis medialis (NPBmed) on areas under curves (AUCs) for mean arterial blood pressure (MAP) (a) or heart rate (HR) (b) changes in 3 (△) and 24 (○) month old rats. Each point is the mean of AUCs for the changes in 5 rats and the bars show the s.e.mean. * $P < 0.05$; ** $P < 0.01$ between 3 and 24 month old rats.

changes in HR and MAP were evoked by microinfusion of vehicle (1 μl twice-distilled pyrogen-free water) into the NTS and NPBmed (Tables 1 and 2).

Cardiovascular effects of muscimol and bicuculline microinfused into the NTS and NPBmed in 24 month old rats

In these rats, muscimol did not induce any change in MAP or HR when low (0.01 μg; $n = 5$; data not shown) as well as higher doses (0.05, 0.1 and 0.25 μg; $n = 5$ for each dose; Figure 1) were injected into the NTS. When compared to the effects produced by the microinfusion of the same doses of muscimol into the NTS of 3 month old rats, the MAP (only at 0.25 μg concentration) or HR (at 0.1 and 0.25 μg concentrations) responses were significant smaller (Figure 1). Microinfusion of muscimol (0.05, 0.1 and 0.25 μg; $n = 5$ for each dose) into the NPBmed of 24 month old rats produced decreases in both MAP and HR. However, the AUCs for MAP and HR were significantly less than in 3 month old rats (Figure 2). Pretreatment with bicuculline (0.5 μg) antagonized the cardiovascular effects induced by muscimol both in the NTS and in the NPBmed. Microinfusion of vehicle (1 μl) into the NTS or NPBmed of 24 month old rats did not affect the basal levels of MAP and HR (Tables 1 and 2).

Discussion

The present experiments confirm that GABA-ergic mechanisms in the NTS and in the NPBmed play an important role in the regulation of cardiovascular activity (Kubo & Kihara, 1987; Catelli & Sved, 1987; 1988; Mollace *et al.*, 1989a). In particular we have confirmed that low doses of muscimol given into the NTS produced a hypertensive response, whereas a significant fall occurred only after the highest dose used. This seems to indicate that muscimol at high doses is able to reach, in sufficient amounts, other brainstem nuclei in which the stimulation of $GABA_A$ receptors leads to hypotension. In fact, the microinjection of GABA into an area just below the NTS resulted in a fall in blood pressure (Kubo & Kihara, 1987). In addition, the stimulation of $GABA_A$ receptors in the NTS with muscimol and with nipecotic acid, a GABA re-uptake inhibitor, was found to reduce the hypotension and bradycardia occurring in response to aortic baroreceptor stimulation (Kubo & Kihara, 1988) suggesting that GABA in the NTS plays a modulatory role on the aortic baroreceptor reflex. Taken together these data seem to indicate that GABA receptors in the NTS can exert an inhibitory influence on vagal inhibitory neurones (Gale *et al.*, 1980; Kubo & Kihara, 1987) as well as on nearby adrenergic stimulatory neurones, thus making possible the occurrence of opposite cardiovascular effects.

In comparison to the NTS, the microinjection of muscimol into the NPBmed elicited only hypotensive and bradycardic responses, thus suggesting that neurones in the NPBmed are mainly stimulatory in their actions on the cardiovascular system and that stimulation of $GABA_A$ receptors exerts an inhibitory effect on these neurones, thus leading to hypotension and bradycardia. This is in agreement both with the anatomical and physiological findings that the NPB provides the major source of the descending pontine projections to regions of the ventrolateral medulla (Fulwiler & Saper, 1984), which send the major tonic sympathetic output to the periphery (Dampney *et al.*, 1982; Ross *et al.*, 1984) and with the demonstration that stimulation of parabrachial neurones elicits a sympathetically mediated pressor response in cats (Mraovitch *et al.*, 1982; Hade *et al.*, 1988). It is well know that the NPB is richly interconnected with other areas of the brain,

Table 2 Effects of pretreatment with bicuculline (0.5 μg) given into the nucleus parabrachialis medialis (NPBmed) on changes in areas under the curves (AUCs) for mean arterial blood pressure (MAP) and heart rate (HR) induced by subsequent (10 min later) microinfusion of vehicle or muscimol (0.05, 0.1 and 0.25 μg) into the same site in 3 and 24 month old rats

	AUCs for MAP changes (mmHg min^{-1})		*AUCs for HR changes* (beats min^{-1})	
Treatment	*3 month old*	*24 month old*	*3 month old*	*24 month old*
Vehicle	800 ± 60.9	882 ± 54.5	449 ± 51.0	470 ± 53.3
+ bicuculline (0.5 μg)	862 ± 51.9	740 ± 52.4	826 ± 69.8*	551 ± 44.1*
Muscimol (0.05 μg)	2024 ± 43.7	782 ± 42.8	1447 ± 74.3	680 ± 40.5
+ bicuculline (0.5 μg)	822 ± 59.9*	787 ± 49.0	980 ± 52.1*	859 ± 55.7
Muscimol (0.1 μg)	2880 ± 60.5	1323 ± 100	2091 ± 39.0	1082 ± 52.9
+ bicuculline (0.5 μg)	180 ± 29.4	175 ± 29.3	760 ± 39.9	784 ± 28.3*
Muscimol (0.25 μg)	4166 ± 48.9	1847 ± 84.9	3620 ± 59.4	1650 ± 74.7
+ bicuculline (0.5 μg)	816 ± 42.0*	571 ± 45.1	793 ± 59.3*	734 ± 22.1*

Data are expressed as mean ± s.e.mean of AUC for MAP and HR changes in 5 rats.
* $P < 0.05$ between rats pretreated with bicuculline and rats treated with vehicle or muscimol.

including the hypothalamus and NTS (Norgren, 1976; King, 1980; Saper & Loewy, 1980), which are involved in central cardiovascular regulation. In addition, evidence exists that neurones of the NPBmed respond to haemorrhage, thus indicating that they may play a critical role in processing haemodynamic signals and in the control of sympathetic responses in relation to regulation of blood pressure, blood volume and fluid balance (Ward, 1989). The cardiovascular effects of muscimol were blocked by bicuculline at a dose which, in itself, produced no direct effects on MAP and HR (Di Micco *et al.*, 1979) and this indicates that the central effects of muscimol were mediated by $GABA_A$ receptor stimulation. The present results show that the GABA depressor action on the brainstem noradrenergic sympathetic output neurones (Blessing, 1988) is very likely to be mediated by depression at NPBmed neurones as well as at neurones near the NTS. In other experiments it was shown that baclofen, a selective $GABA_B$ receptor agonist, given into the cerebral ventricles produced a fall in blood pressure (Persson & Henning, 1980), whereas an increase in blood pressure was observed after microinjection into the NTS, this response being greater in spontaneously hypertensive rats (Persson, 1981; Catelli & Sved, 1988). In addition, the cardiovascular responses elicited by muscimol were centrally mediated since the doses required to induce changes after microinfusion into the NTS and NPBmed were much smaller than those required to produce changes after intravenous administration (Persson, 1980).

The present results have also shown that, in older rats, the cardiovascular responses to muscimol microinfused into the NTS or into the NPBmed were significantly reduced. However, whereas no changes in MAP were observed in 24 month old rats after microinfusion of muscimol into the NTS, only a decrease in its hypotensive and bradycardic effects was obtained from the NPBmed suggesting a different vulnerability of the two nuclei during the aging process.

The reasons underlying the lack or the decrease of cardiovascular responses elicited by muscimol on the NTS and NPBmed level are not known. Evidence exists that for other neurotransmitter receptors also, such as α_2-adrenoceptors in the NTS, there is a decreased responsiveness to α_2-adrenoceptor agonists in old rats (Mollace *et al.*, 1989a; 1990). In addition evidence exists that, during aging in some areas of the rat brain, there is a significant decrease in GABA receptor binding (De Blasi *et al.*, 1982) and a more recent study has shown a significant fall of GABA content in the parabrachial nuclei as well as in the NTS of 29 month old rats (Banay-Schwartz *et al.*, 1989). Whether the decreased cardiovascular response to neurotransmitters is due to a decrease in the number of receptors, or in their affinity for agonists and/or to changes in the associated transduction mechanism(s) remains to be demonstrated. An altered coupling between the GABA recognition site and the chloride channel has been suggested to occur in aged rats, since there was a marked decrease of GABA-induced stimulation of chloride uptake in membrane vesicles from aged compared with young adult rats (Concas *et al.*, 1988). But clearly, whatever mechanism is responsible, these changes may contribute to the causes of tonic and phasic cardiovascular dysfunctions occurring in the elderly.

Partial support from the Italian Council for Research and from Consorzio Italiano Tecnologie Farmaci Invecchiamento (CITFI, Bresso, Milan) is gratefully acknowledged. Our thanks to Mrs Marika Nisticó, Giovanni Marra and Giovanni Politi for their skilful technical assistance.

References

ANTONACCIO, M.J., KERWIN, L. & TAYLOR, D.G. (1978). Effects of central GABA receptor agonism and antagonism on evoked diencephalic cardiovascular responses. *Neuropharmacology*, **17**, 597–603.

BANAY-SCHWARTZ, M., LAJTHA, A. & PALKOVITS, M. (1989). Changes with aging in the levels of amino acids in rat CNS structural elements. I. Glutamate and related amino acids. *Neurochem. Res.*, **14**, 555–562.

BAUM, T. & BECKER, F.T. (1982). Hypotensive and postural effects of the gamma-aminobutyric acid agonist muscimol and of clonidine. *J. Cardiovasc. Pharmacol.*, **4**, 165–169.

BHARGAVA, K.P., BHATTACHARJA, S.S. & SRIMAL, R.C. (1964). Central cardiovascular action of gamma-aminobutyric acid. *Br. J. Pharmacol.*, **23**, 383–390.

BHATTACHARJA, S.S., KISHOR, K., SAXENA, P.N. & BHARGAVA, K.P. (1964). Neuropharmacological study of gamma-aminobutyric acid (GABA). *Arch. Int. Pharmacodyn. Ther.*, **150**, 295–305.

BLESSING, W.W. (1988). Depressor neurones in rabbit caudal medulla act via GABA receptors in rostral medulla. *Am. J. Physiol.*, **254**, H686–692.

BOUSQUET, P., FELDMAN, J., BLOCH, R. & SCHWARTZ, J. (1981). The central hypotensive action of baclofen in anesthetized cat. *Eur. J. Pharmacol.*, **76**, 193–201.

CATELLI, J.M. & SVED, A.F. (1987). Enhanced GABA activity within the nucleus tractus solitarius of the spontaneously hypertensive rat. *Fed. Proc.*, **46**, 11541.

CATELLI, J.M. & SVED, A.F. (1988). Enhanced response to GABA in the nucleus tractus solitarii of the spontaneously hypertensive rat. *Eur. J. Pharmacol.*, **151**, 243–248.

CONCAS, R., PEPITONI, S., ATSOGGIU, T., TOFFANO, G. & BIGGIO, G. (1988). Aging reduces the GABA dependent 36Cl-flux in rat brain membrane vesicles. *Life Sci.*, **43**, 1761–1771.

DAMPNEY, R.A.L., GOODCHILD, A.K. & ROBERTSON, L.G. (1982). Role of the ventrolateral medulla in vasomotor regulation: a correlative anatomical and physiological study. *Brain Res.*, **249**, 223–235.

DE BLASI, A., COTECCHIA, S. & MENNINI, T. (1982). Selective changes of receptor binding in brain regions of aged rats. *Life Sci.*, **31**, 335–340.

DI MICCO, J.A. (1982). Blockade of forebrain gamma aminobutyric acid (GABA) receptors and reflex activation of the cardiac vagus in anesthetized cats. *J. Pharmacol. Exp. Ther.*, **233**, 654–661.

DI MICCO, J.A., GALE, K., HAMILTON, B. & GILLIS, R.A. (1979). GABA receptor control of parasympathetic outflow to the heart: characterization and brain-stem localization. *Science*, **204**, 1106–1109.

FELDER, R.B. & MIFFLIN, S.W. (1988). Modulation of carotid sinus afferent input to nucleus tractus solitarius by parabrachial nucleus stimulation. *Circ. Res.*, **63**, 35–49.

FULWILER, C.E. & SAPER, C.B. (1984). Subnuclear organization of the efferent connections of the parabrachial nucleus in the rat. *Brain Res. Rev.*, **7**, 229–239.

GALE, K., HAMILTON, B.L., BROWN, S.C., NORMAN, W.B., SOUZA, J.D. & GILLIS, R.A. (1980). GABA and specific GABA binding site in brain nuclei associated with vagal outflow. *Brain Res. Bull.*, **5**, suppl. 2, 325–328.

HADE, J.S., MIFFLIN, S.W., DONTA, T.S. & FELDER, R.B. (1988). Stimulation of parabrachial neurons elicits a sympathetically mediated pressor response in cats. *Am. J. Physiol.*, **255**, H1349–1358.

KING, G.W. (1980). Topology of ascending brainstem projections to nucleus parabrachialis in the cat. *J. Comp. Neurol.*, **191**, 615–638.

KUBO, T. & KIHARA, M. (1987). Evidence for the presence of GABA-ergic and glycine-like systems responsible for cardiovascular control in the nucleus tractus solitarius of the rat. *Neurosci. Lett.*, **74**, 331–336.

KUBO, T. & KIHARA, M. (1988). Evidence for gamma-aminobutyric acid receptor-mediated modulation of the aortic baroreceptor reflex in the nucleus tractus solitarius of the rat. *Neurosci. Lett.*, **88**, 156–160.

LOSCHER, W. (1982). Cardiovascular effects of GABA, GABA-aminotransferase inhibitors and valproic acid following systemic administration in rats, cats and dogs: pharmacological approach to localize the site of action. *Arch. Int. Pharmacodyn. Ther.*, **257**, 32–58.

MOLLACE, V., DE FRANCESCO, A.E. & NISTICO', G. (1989a). Muscimol induced cardiovascular effects when microinfused into the NTS and NPBmed. *Prev. Cardiol.*, **10**, 23 c.

MOLLACE, V., DONATO DI PAOLA, E., GRATTERI, S. & NISTICO', G. (1989b). Age-related alterations in cardiovascular responsiveness to clonidine infused into the nucleus tractus solitarii in rats. *Neuropharmacology*, **28**, 37–42.

MOLLACE, V., MASUDA, Y., PELAGGI, T. & NISTICO', G. (1990). The effects of phosphatidylserine on the decreased cardiovascular response to clonidine microinfused into the nucelus tractus solitarii of old rats. *Br. J. Pharmacol.*, **100**, 547–551.

MRAOVITCH, S., KUMADA, M. & REIS, D.J. (1982). Role of the nucleus parabrachialis in cardiovascular regulation in cat. *Brain Res.*, **232**, 57–75.

NORGREN, R. (1976). Taste pathways to hypothalamus and amygdala. *J. Comp. Neurol.*, **166**, 17–33.

PAXINOS, G. & WATSON, C. (1982). *The Rat Brain in Stereotaxic Coordinates*. London: Academic Press.

PERSSON, B. (1980). Cardiovascular effects of intracerebroventricular GABA, glycine and muscimol in the rat. *Naunyn-Schmiedebergs Arch. Pharmacol.*, **313**, 225–236.

PERSSON, B. (1981). A hypertensive response to baclofen in the nucleus tractus solitarii in rats. *J. Pharm. Pharmacol.*, **33**, 226–231.

PERSSON, B. & HENNING, M. (1980). Central cardiovascular and biochemical effects of baclofen in the conscious rat. *J. Pharm. Pharmacol.*, **32**, 417–422.

PHILIPPU, A., PRUNTEK, H. & ROENSHERC, W. (1973). Superinfusion of the hypothalamus with gamma-aminobutyric acid. *Naunyn-Schmiedebergs Arch. Pharmacol.*, **276**, 137–143.

ROSS, C.A., RUGGIERO, D.A., PARK, D.H., JOH, T.H., SVED, A.F., FERNANDEZ-PARDAL, J., SAAVEDRA, J.M. & REIS, D.J. (1984). Tonic vasomotor control by the rostral ventrolateral medulla: effects of electrical or chemical stimulation of the area containing C1 adrenergic neurons on arterial pressure, heart rate and plasma catecholamines and vasopressin. *J. Neurosci.*, **4**, 474–494.

SAPER, D.G. & LOEWY, A.D. (1980). Efferent connections of the parabrachial nucleus in the rat. *Brain Res.*, **197**, 291–317.

SGARAGLI, G. & PAVAN, F. (1972). Effect of aminoacid compounds injected into cerebrospinal fluid space on clonic temperature, atrial blood pressure and behaviour of the rat. *Neuropharmacology*, **11**, 44–56.

TAKAHASHI, H., TIBA, M., INO, M. & TAKAYASU, T. (1955). The effects of gamma-aminobutyric acid on blood pressure. *Jpn. J. Physiol.*, **5**, 334–339.

TALLARIDA, R.J. & MURRAY, R.B. (1981). *Manual of Pharmacological Calculation with Computer Programs*. pp. 47–49. Berlin: Springer Verlag.

WARD, D.G. (1989). Neurons in the parabrachial neurons respond to hemorrhage. *Brain Res.*, **491**, 80–92.

(Received October 25, 1990
Revised March 1, 1991
Accepted March 13, 1991)

Br. J. Pharmacol. (1991), **103**, 1807–1813 © Macmillan Press Ltd, 1991

Quinidine-induced inhibition of the fast transient outward K^+ current in rat melanotrophs

S.J. Kehl

Department of Physiology, University of British Columbia, Vancouver, B.C., V6T 1W5, Canada

1 The effect of quinidine on the fast-activating, fast-inactivating potassium current (I_K(f)) in acutely dissociated melanotrophs of the adult rat pituitary was examined. Macroscopic currents were measured by use of the whole-cell configuration of the patch clamp technique.

2 Bath application of quinidine caused a dose-dependent reduction of the peak amplitude of I_K(f). The K_d for blockade of I_K(f) at 0 mV was estimated to be 41 ± 5.6 μM.

3 Quinidine elicited a dose-dependent increase of the rate of the decay of I_K(f) and this effect was enhanced by membrane depolarization. The possibility that this phenomenon reflects an open channel blocking reaction is discussed.

4 Quinidine also caused a 5 mV hyperpolarizing shift of the steady-state inactivation curve and increased the half-time for recovery from inactivation. Quinidine did not affect the onset of inactivation measured at −30 mV.

5 Internal quinidine did not appear substantially to affect either the peak amplitude or kinetics of I_K(f).

6 A study of some structural analogues showed that hydroquinidine and quinacrine had effects similar to those of quinidine. The effect of quinacrine on the amplitude and kinetics of I_K(f) was also pH-dependent. Cinchonine, which bears a close structural resemblance to quinidine, was much less effective as a blocker of I_K(f).

Keywords: Fast transient K^+ current; melanotroph; quinidine; quinacrine

Introduction

Quinidine is a clinical anti-arrythmic drug which affects ionic currents in heart muscle and which has also been shown to be a potent blocker of several classes of K^+ channel in a variety of cell types (e.g., Fishman & Spector, 1981; Hermann & Gorman, 1984; Imaizumi & Giles, 1987; Glavinović & Trifaró, 1988). As part of the pharmacological characterization of the channels subserving the transient outward potassium current (I_K(f)) in rat melanotrophs (Kehl, 1989; 1990) the effects of quinidine and some of its structural analogues were investigated. The results described here show that quinidine blocks I_K(f) and also affects the rate of decay of the current.

Methods

Recordings were made from acutely dissociated melanotrophs. These were obtained following the enzymatic treatment and mechanical disruption of the neuro-intermediate lobe of the pituitary gland of the adult male rat (Wistar, 200–300 g), as described previously (Kehl, 1990). Cells were held in tissue culture medium (Dulbecco's modified Eagle's medium: Ham's F-12 = 1:1) at 35°C in an atmosphere of humidified air for 1–10 h before use.

Macroscopic (whole-cell) currents were recorded at room temperature (20–25°C) by conventional patch electrode techniques. Patch electrodes pulled from Corning No. 7052 glass (A-M Systems, WA, U.S.A.) had a resistance of 3–5 MΩ and were coated at the tip with Sylgard (Dow Corning) to reduce capacitive transients. Unless indicated otherwise the holding potential was −70 mV. Current and voltage signals from a LIST EPC-7 amplifier were stored on video cassette tape and analysed off-line with a Labmaster A/D computer interface (Scientific Solutions, OH) and Indec BASIC-Fastlab routines (Sunnyvale, CA). For the calculation of the current density the membrane capacitance was read from the front panel setting of the amplifier and the specific capacitance was assumed to be 1 $\mu F\,cm^{-2}$.

The control recording solution contained (mM): NaCl 120, KCl 3.5, $MgCl_2$ 1.0, $CaCl_2$ 2, N-2-hydroxyethylpiperazine-N'-2-ethanesulphonic acid (HEPES) 10, glucose 5 and tetraethylammonium (TEA^+) chloride 20 to block the slowly-activating, slowly-inactivating K^+ current (I_K(s)). The Na^+ and Ca^{2+} currents (McBurney & Kehl, 1988) were blocked with $CdCl_2$ 0.3 mM and tetrodotoxin 1–2 μM, respectively. The patch pipette (internal) solution contained (mM): KCl 120, $MgCl_2$ 5, ethyleneglycol-*bis*-(β-aminoethyl ether)-N,N,N',N'-tetraacetic acid (EGTA) 10, HEPES 10 and Na_2ATP 1. The pH of the external and internal solutions was adjusted to 7.4 with NaOH and KOH, respectively.

Drugs were obtained from Sigma or Aldrich. Solutions containing quinidine sulphate or structural analogues of quinidine were prepared fresh from 10 mM stock solutions stored at 4°C. Experiments were performed under dimmed lights to prevent photoinactivation of the test drugs. Solution changes were carried out with a stop-flow system in which the test solution flowed into one end of the recording chamber while at the other end solution was drawn off at a rate sufficient to maintain a constant depth of fluid. Once complete replacement of the bath solution had been achieved the flow was stopped and recordings were made.

Curve fitting was done by non-linear regression routines in BASIC-Fastlab or SYSTAT (Evanston, IL). Values are expressed as mean ± the standard error of the mean (s.e.mean).

Results

Quinidine reduces the peak amplitude of $I_K(f)$

In control medium the threshold for activation of I_K(f) was between −40 and −20 mV and the peak amplitude of the current increased monotonically with membrane depolarization (Figure 1a, circles; see also Kehl, 1989). Bath application of quinidine had two simultaneous effects. The rate of decay of I_K(f) increased and there was a reduction of the peak amplitude of evoked currents. The effect of quinidine on the amplitude of I_K(f) will be described first.

The current/voltage relation of Figure 1a indicates that the block of I_K(f) was concentration-dependent but only weakly voltage-dependent, if at all. For example, in 50 μM quinidine

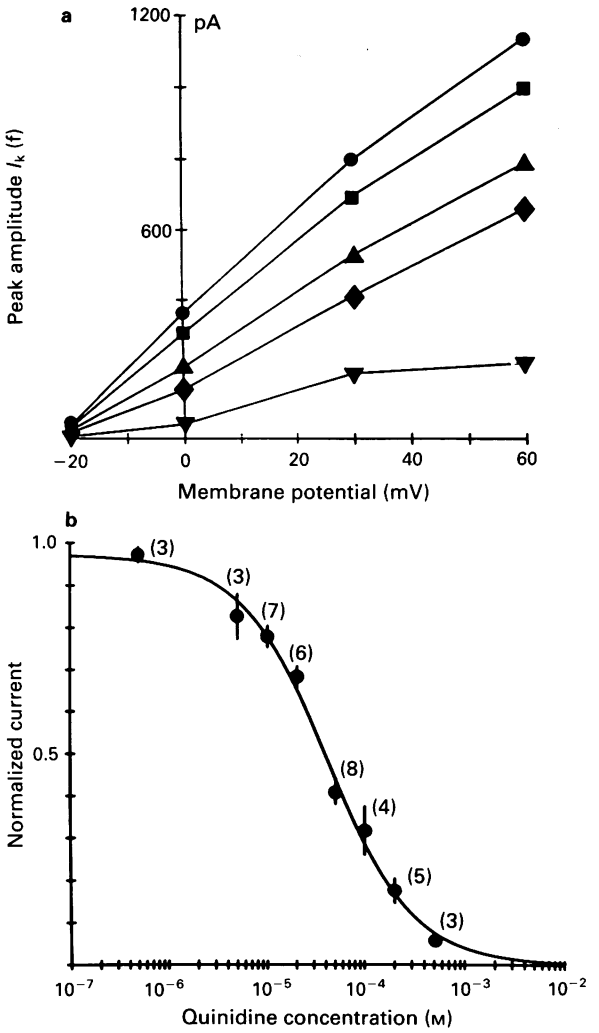


Figure 1 (a) The current/voltage relationship in 0 (●), 5 (■), 25 (▲), 50 (◆) and 250 (▼) μM quinidine. The peak amplitude of I_K(f) is plotted against the membrane potential during the test pulse. (b) The relationship between the peak amplitude of the I_K(f) and the concentration of external quinidine. The graphed points represent the mean with s.e.mean shown by vertical lines; the numbers in parentheses indicate the number of cells tested. The solid line represents the solution for the Hill equation in which K_d is 41 μM and n is 0.99.

(Figure 1a, diamonds) there was approximately a 50% reduction of the current at 0, 30 and 60 mV. The latency of onset for the effect of quinidine was short (<20 s with high concentrations) and a steady-state effect was obtained after a 1–2 min exposure to the drug. This inhibition of I_K(f) by quinidine could not be shown to be use-dependent, i.e., increasing the stimulus frequency to 1 Hz had no effect on the degree of block (not shown).

To quantify the actions of quinidine the amplitude of I_K(f) was measured from the difference current obtained by subtracting conditioned test currents from unconditioned test currents. Test pulses consisted of a step of the membrane potential from −70 mV to 0 mV for 300 ms. Conditioning pulses were applied to inactivate I_K(f) and reveal the leak current and any residual I_K(s). The conditioning pulse consisted of a 500 ms voltage step from −70 mV to −20 mV applied immediately before the test pulse. The cycle length was 4 s. After obtaining the controls the external solution was changed to one containing a known concentration of quinidine. Because the effect of quinidine treatment reversed slowly and was rarely completely reversible (see also Lee *et al.*, 1981; Hermann & Gorman, 1984) no attempt was made to obtain recovery responses before changing to a higher quinidine concentration. The decline of the current amplitude in quinidine did not appear to reflect cell deterioration since I_K(f) in quinidine-treated cells was stable for up to 1 h (the longest period tested) and I_K(f) could be recorded in cells which had been exposed to 50 μM quinidine for up to 5 h. Since quinidine did not alter the reversal potential of I_K(f) (data not shown) the inhibition of the current represents a conductance decrease.

The dose-response curve of Figure 1b was constructed by plotting the normalized amplitude ($I_{quinidine}/I_{control}$) of I_K(f) against the quinidine concentration. The data points were fitted by a least squares regression routine to the Hill equation:

$$I = (1 + (K_d/[Q])^{-n})^{-1}$$

where I is the normalized current, K_d is the apparent equilibrium dissociation constant and n is the order of the binding reaction. The K_d was 41 ± 5.6 μM (95% confidence limits 30.1–52.0 μM). The value for n was 0.985 ± 0.1 (95% C.L. 0.78–1.19) suggesting a first order reaction between quinidine and its binding site.

Quinidine increases the rate of decay of $I_K(f)$

Superimposed traces of control responses and those recorded at different quinidine concentrations showed that the decay of I_K(f) was accelerated while the rising phase of the current was only slightly affected by quinidine (e.g., Figure 4b). This increased rate of decay of I_K(f) in quinidine could arise from two mechanistically distinct (though not mutually exclusive) processes: (1) the blockade of open channels, subsequently referred to as open channel block; and (2) by an increase of the rate of channel inactivation. The possibility that quinidine was affecting inactivation was examined first.

Quinidine causes a hyperpolarizing shift of the steady-state inactivation curve for $I_K(f)$

By use of a two pulse protocol, steady-state inactivation was measured in 5 cells exposed to 100 μM quinidine. The data, when fitted to the Boltzmann equation by a non-linear least squares routine, gave a half-inactivation potential (V′) of −42 ± 0.6 mV and a slope factor (s) of 4.7 ± 0.5 mV (Figure 2a, squares). In control cells V′ and s were −37.5 ± 0.2 mV and 3.8 ± 0.1 mV, respectively (n = 6, Figure 2a, circles). The leftward shift of the inactivation curve in quinidine cannot account for the decline of the peak current shown in Figure 1a, since inactivation in quinidine, at least in 100 μM or lower concentrations, would be completely removed at the holding potential of −70 mV.

Onset of inactivation in quinidine

To determine if quinidine affected the kinetics of the onset of inactivation, a test pulse to 20 mV was preceded by a conditioning pulse to −30 mV lasting for 0–4 s. The rationale for this experimental approach was that at the potential of the conditioning pulse very few of the channels would open so that any change of kinetics would be due to a change of inactivation gating rather than open channel block (this assumes that the channels can inactivate directly from a closed (resting) state). The decline of the peak amplitude of the conditioned test currents both in control and 50 μM quinidine-treated cells was well-fitted by a single exponential with a time constant of 89 ± 16 ms (n = 3) and 94 ± 24 ms (n = 3), respectively. This indicated that inactivation at −30 mV was not affected by quinidine.

Recovery from inactivation in quinidine

Recovery from inactivation was investigated by use of a two pulse protocol in which 300 ms pulses to 10 mV were separated by a 5–2000 ms interval at −70 mV. A plot of the normalized peak current against the interval between pulses

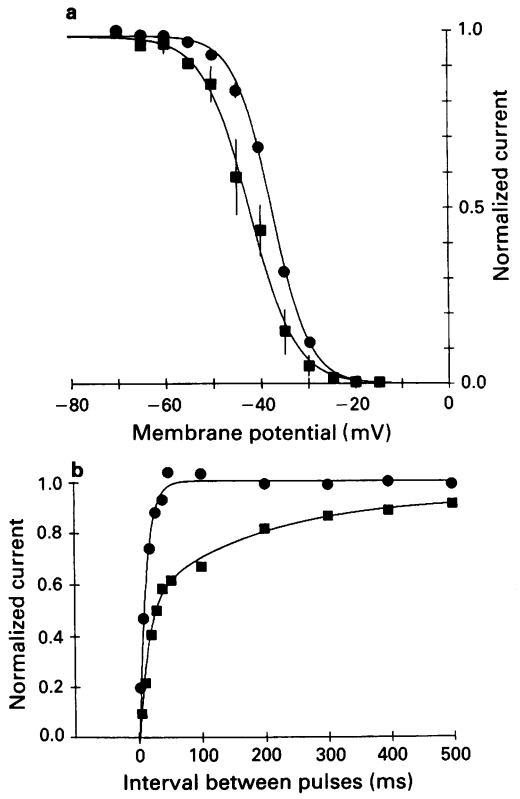


Figure 2 The effects of quinidine on steady-state inactivation and recovery from inactivation. (a) In a two-pulse protocol, a conditioning pulse to the potential indicated on the abcissa scale was applied for 500 ms immediately before the test pulse to 10 mV. Shown are the steady-state inactivation curves in control (●) and, in a separate group of cells, in 50 μM quinidine (■). The solid lines represent solutions to the Boltzmann equation in which V' and s were −37.5 mV and 3.8 mV in control cells ($n = 6$) and −42 mV and 4.7 mV in quinidine-treated cells ($n = 5$). (b) Quinidine slows recovery from inactivation. In control medium recovery from inactivation was well-fitted by a single exponential with a time constant of 12.5 ms (●). After changing to medium containing 50 μM quinidine, recovery was fitted by the sum of two exponentials with time constants of 14.5 and 180 ms (■). The slower component accounted for approximately 40% of the total current. A high room temperature (30°C) probably accounts for the faster than usual recovery from inactivation in the control cell.

showed in control cells that recovery from inactivation followed a single exponential (e.g. Figure 2b, circles) with a mean time constant of 25.7 ± 11.7 ms, $n = 4$ (half-recovery time of 17.9 ± 8.13 ms). In the same cells, after changing to 50 μM quinidine, recovery from inactivation was no longer well-fitted by a single exponential (Figure 2b, squares) and there was a wide variation in the half-recovery time (97.5 ± 68 ms).

Tail currents in quinidine

A common feature of many agents which block open channels is the alteration of tail current kinetics. This arises because the presence of the blocking particle in the channel pore hinders the 'closing' of the activation gate, i.e. the deactivation rate slows. The effect of 50 μM quinidine on the tail currents was examined in 43 mM external K^+ ($E_K \approx -30$ mV) since this allows a large inward tail current to be measured when the membrane potential is stepped to −70 mV from a potential where channels are open. For the traces illustrated in Figure 3 the membrane potential was stepped to 20 mV for 2–60 ms before returning to −70 mV. Note that the envelope of the peak tail currents accurately reflects the time course of $I_K(f)$ during the depolarizing pulse. This indicates that the tail current arises from channels which are open when the potential is suddenly changed to −70 mV and that the channels

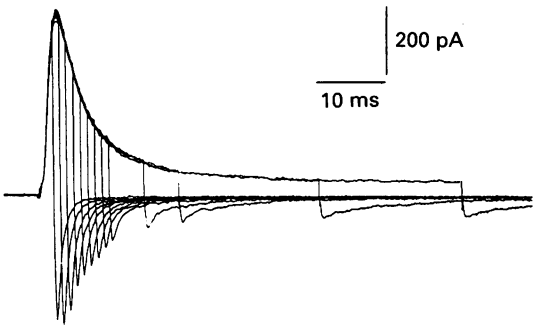


Figure 3 The $I_K(f)$ in 50 μM quinidine and 43 mM external K^+. Test pulses taking the potential from −70 mV to 20 mV lasted for 2–60 ms. Note the parallelism between the envelope of the peak inward tail current and the amplitude of the outward current prior to the end of the test pulse. This suggests that during the tail of current, quinidine-blocked channels do not become conductive prior to closure of the activation gate. The decay of the outward pulse current was well-fitted by a single exponential with a time constant of 4.6 ms. The slow tail current evident at the end of the 60 ms pulse is probably due to a residual $I_K(s)$.

which stopped conducting during the depolarizing pulse, either because of channel block or inactivation, do not re-open to contribute to the peak tail current. The deactivation time constant was not affected by quinidine (data not shown).

Since the results of these experiments indicated that quinidine either did not affect or slowed the onset of inactivation or recovery from inactivation, the simplest conclusion, particularly with the precedent for open channel block of Ca^{2+}-activated K^+ channels by quinidine (Glavinović & Trifaró, 1988), was that the increased rate of decay of $I_K(f)$ was due to an open channel blocking mechanism.

Open channel block by quinidine is concentration- and voltage-dependent

If quinidine blocks open channels then the rate constant for the decay ($1/\tau_{decay}$) of the macroscopic current will reflect the mean open time of the channel which is affected by two events, channel inactivation and open channel block for which the rate constants are, respectively, ($1/\tau_{inactivation}$) and ($1/\tau_{block}$). The relationship between these rate constants is,

$$1/\tau_{decay} = 1/\tau_{block} + 1/\tau_{inactivation}$$

The data shown in Figure 4 were generated from cells in which test pulses to 0, 30 and 60 mV were given in the presence of 5, 10, 50, 100 and 500 μM quinidine. The value of $1/\tau_{block}$ was calculated after fitting the decay of the membrane current to a single exponential to obtain $1/\tau_{decay}$ and using the time constant for inactivation in control medium to obtain $1/\tau_{inactivation}$. It should be emphasized here that although 50 μM quinidine was shown not to affect the onset of inactivation at −30 mV the assumption that the inactivation process is not affected at more depolarized potentials or with higher quinidine concentrations may introduce an unknown degree of error in the analysis. Additionally, the currents evoked in control cells at potentials of 30 mV or greater sometimes contained a second small exponential (which was not fitted) and there was a tendency for the time constant of the fitted exponential to increase slightly with increasing depolarization (e.g., Figure 7c, circles). It has not been possible to determine if this change of the kinetics of the control outward current with strong depolarizations reflects the gating of $I_K(f)$ channels or if there is a contribution from another channel type.

In the graph of Figure 4, which shows the relationship between the quinidine concentration and the blocking rate, the solid lines represent the best fit of a Michaelis-Menten type equation,

$$V = V_{max}/(1 + (K_m/[Q]),$$

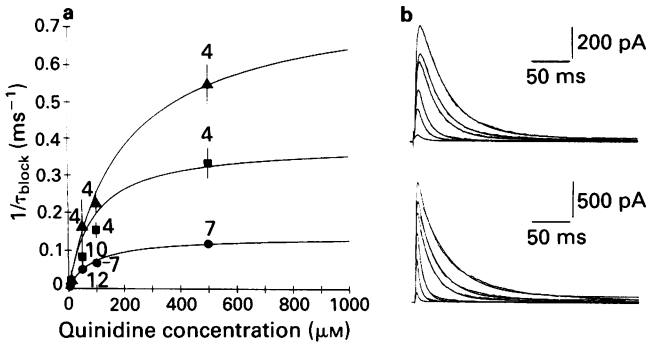


Figure 4 (a) The relationship between the concentration of quinidine and the estimated rate of blocking of open I_K(f) channels (see text for discussion). The solid lines represent the least squares fit to a Michaelis-Menten type equation. The values for V_{max} and K_m of the superimposed line are 0.14 ms^{-1} and 89 μM at 0 mV (●), 0.39 ms^{-1} and 48 μM at 30 mV (■) and 0.78 ms^{-1} and 106 μM at 60 mV (▲). The number adjacent to the symbol (mean with s.e.mean shown by vertical lines) indicates the number of cells tested. (b) Current traces, on which the graph is partially based, show, superimposed, responses in a cell depolarized to 0 mV (upper) and 30 mV (lower) in 0, 5, 10, 50, 100 and 500 μM quinidine. Exponentials superimposed on individual current traces had time constants of 37.8, 28.8, 24.7, 13.7, 10.1 and 7.9 ms (upper traces) and 39.8, 26.6, 20.4, 7.9, 4.9 and 3.1 ms (lower traces).

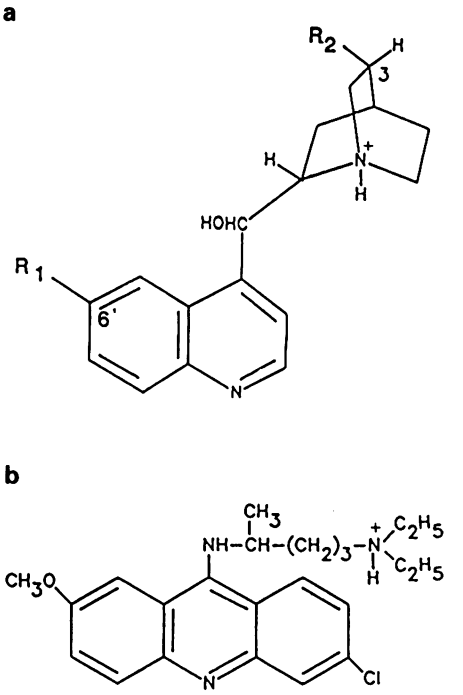


Figure 5 (a) The cinchona alkaloid structure on which quinidine, hydroquinidine and cinchonine are based. R_1 represents the group substituted on C-6' of the quinoline ring. R_2 represents the group substituted on C-3 of the quinuclide ring. For quinidine $R_1 = OCH_3$ and $R_2 = -CH{=}CH_2$; for cinchonine $R_1 = H$ and $R_2 = -CH{=}CH_2$; and for hydroquinidine $R_1 = -OCH_3$ and $R_2 = -CH_2{-}CH_3$. Each of the cinchona alkaloids is the 8S:9R isomer. (b) The structure of quinacrine.

where V_{max} is the maximal blocking rate and K_m is the concentration of quinidine ([Q]) at which the blocking rate ($1/\tau_{block}$) is half-maximal. The estimates of V_{max} and K_m were 0.14 ms^{-1} and 89 ± 16 μM at 0 mV, 0.39 ms^{-1} and 97.4 ± 16 μM at 30 mV, and 0.78 ms^{-1} and 212 ± 58 μM at 60 mV. These results indicate that the blocking rate increases with the concentration of quinidine and that depolarization accelerates the blocking rate.

Internal quinidine does not affect $I_K(f)$

With pK_a values of 8.3 and 4.2 for the nitrogen atoms on the quinuclide and quinoline groups of the quinidine molecule (Roche & Kier, 1981) (Figure 5a), then at pH 7.4 approximately 10% of the molecules exist in the uncharged hydrophobic form and might therefore diffuse through the membrane (Iwatsuki & Petersen, 1985). To assess the possibility that access to the site of action might be gained from the cytoplasmic face of the channel the effect of internal quinidine (at pH 7.4) was studied. With 100 μM quinidine inside the cell the decay of the current at 0 mV was not significantly affected (τ = 28.2 ± 3.9 ms, n = 13, vs. 32.5 ± 3.2 ms in 11 control cells). With 500 μM internal quinidine the decay of the current at 0 mV was still substantially slower (τ = 24.6 ± 1.2 ms, n = 4) than with 100 μM external quinidine (τ = 10.1 ± 0.6 ms, n = 7). The persistence of large outward currents at 0 mV with 500 μM internal quinidine (56.9 ± 13 μA cm^{-2}, n = 4 vs. 82.2 ± 29 μA cm^{-2} in 3 control cells and vs. 4.9 ± 2.2 μA cm^{-2} in 500 μM external quinidine, n = 3) also implied that there was little or no blocking effect of quinidine when it was applied internally.

Effect of structural analogues of quinidine

To gain some insight into the structural requirements for inhibition of I_K(f), the actions of some compounds related to quinidine (Figure 5) were tested.

Quinine, the stereoisomer of quinidine, reduced the amplitude of I_K(f) and accelerated the rate of the current decay. Quinine appeared to be as potent as quinidine but this was not quantified.

Cinchonine, which is identical to quinidine save for the substitution of hydrogen for the methoxy group on C-6' of the quinoline ring (Figure 5a) was, surprisingly, much less potent than quinidine. For example, 100 μM cinchonine reduced the peak amplitude of I_K(f) elicited at 0 mV by only 18 ± 3% (n = 6) and did not significantly affect the rate of the current decay at 0 mV (τ_{decay} = 37.8 ± 2.1 ms and 36.6 ± 1.2 ms in 0 and 100 μM cinchonine, respectively, n = 5). In three of these cells which were subsequently exposed to 100 μM quinidine τ_{decay} decreased to 12.4 ± 1.4 ms and the peak amplitude of I_K(f) decreased by 49 ± 3% (Figure 6a, traces). As with quinidine, with stronger membrane depolarization there was a reduction of τ_{decay}, an effect which may have contributed to the slightly greater inhibition of I_K(f) by cinchonine at positive membrane potentials in the current/voltage relation of Figure 6a.

Hydroquinidine, which differs from quinidine only at C-3 of the quinuclide ring where there is an ethyl group instead of an ethylene group (Figure 5a), affected I_K(f) in the same manner as quinidine and appeared to be of a similar potency. Half-maximal inhibition of I_K(f) at 0 mV occurred with 23 ± 7.8 μM hydroquinidine (95% C.L. 6.9–39.8 μM, n = 8) (traces of Figure 6b). The effect of hydroquinidine on τ_{decay} was identical to that of quinidine: the blocking rate was voltage-dependent and again the relationship between the blocking rate and the drug concentration was hyperbolic. The lines fitted to the data of the graph in Figure 6b represent solutions to the Michaelis-Menten type equation in which K_m at 0, 30 and 60 mV was 81.2 ± 19, 84.6 ± 15 and 81.2 ± 14.7 μM, respectively, and V_{max} was 0.1 ± 0.01, 0.28 ± 0.02 and 0.404 ± 0.03 ms^{-1}.

Quinacrine is an anti-malarial agent based upon the aminoacridine ring structure (Roche & Kier, 1981) (Figure 5b). The ring nitrogen has a pK_a of 8.2 whereas the pK_a of the tertiary amine of the side chain is 10.2. On the premise that the hydrophobicity of the ring might be an important determinant of binding, the actions of quinacrine were tested at pH 6.5 and pH 8.5 where the ratio of charged to neutral aromatic nitrogens would be approximately 50:1 and 1:2, respectively. The results of one of three such experiments are shown in Figure 7. At pH 6.5, 100 μM quinacrine had only a small effect on the amplitude and decay of I_K(f) evoked at 0 mV (Figure 7a, left traces). Switching to control solution with a pH of 8.5 (Figure

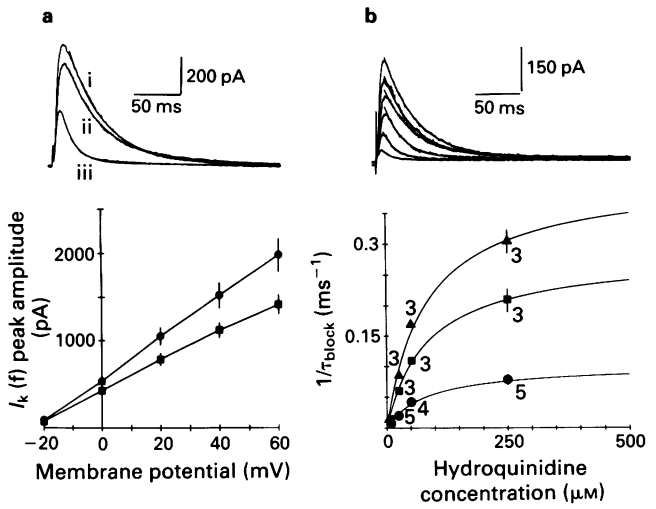


Figure 6 (a) Cinchonine is a poor blocker of I_K(f). The traces show the current evoked at 0 mV in control medium (i) and medium containing 100 μM cinchonine (ii) or 100 μM quinidine (iii). The graph below shows the current/voltage relationship derived from 5 cells in 0 (●) and 100 μM cinchonine (■). (b) Hydroquinidine reduces the peak amplitude of I_K(f) and increases its rate of decay. The traces illustrate the currents evoked at 0 mV in 0, 1, 5, 25, 50 and 250 μM hydroquinidine. The time constants for the superimposed exponentials are 37.9, 34.1, 34.5, 22, 15.4, and 11.7 ms. The lines in the graph were fitted as described in the text and represent solutions to a Michaelis-Menten type equation. The numbers adjacent to the symbols (mean with s.e.mean shown by vertical lines) indicate the number of cells tested.

7a, middle traces) had no discernible effect on either the amplitude or kinetics of I_K(f). At pH 8.5, however, 100 μM quinacrine reduced the amplitude of I_K(f) (205 ± 32 pA vs. 474 ± 6 pA in pH 8.5 control solution) and decreased τ_{decay} (24.2 ± 3 ms vs. 55 ± 6 ms). The effect of quinacrine reversed after returning to control medium at pH 6.5 (Figure 7a, right traces). As with quinidine there was no apparent voltage-dependence for the reduction of the amplitude of I_K(f) by quinacrine (Figure 7b, inverted triangle) but the rate of decay

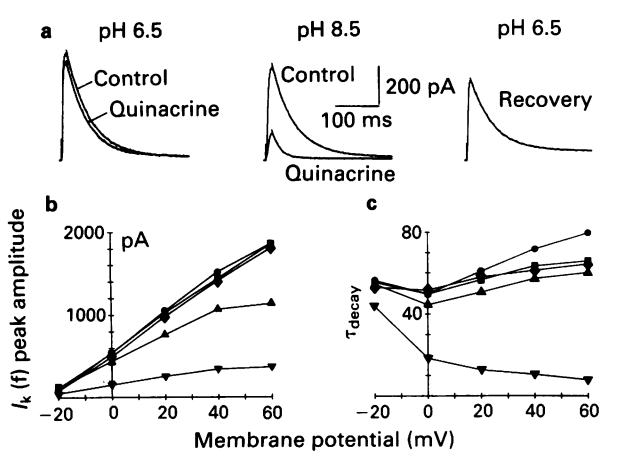


Figure 7 The block of I_K(f) by quinacrine is pH-dependent. (a) The traces show the currents evoked at 0 mV in control medium and 100 μM quinacrine. The time constants of the superimposed exponentials are 49.7 ms (control, pH 6.5), 44.4 ms (100 μM quinacrine, pH 6.5), 49.6 ms (control, pH 8.5), 18.4 ms (100 μM quinacrine, pH 8.5) and 51.5 ms (recovery, pH 6.5). The graphs show the current/voltage relationship (b) and the τ_{decay}/voltage relationship (c) in the control medium at pH 6.5 (●), in 100 μM quinacrine at pH 6.5 (◆), in control solution at pH 8.5 (■), in 100 μM quinacrine at pH 8.5 (▼), and recovery at pH 6.5 (▲). Note that at pH 6.5, quinacrine slightly reduces the amplitude of I_K(f) and slightly decreases τ_{decay}. At pH 8.5, however, there is a large reduction of the current amplitude and τ_{decay} shows a marked voltage-dependence.

of I_K(f) did increase with depolarization (Figure 7c, inverted trian[illegible]).

Discussion

It has been shown that I_K(f) in melanotrophs is blocked by quinidine. Quinidine also causes a small hyperpolarizing shift of the steady-state inactivation curve and slows the recovery of I_K(f) from inactivation. Quinidine exerts similar actions on the Na^+ current (Lee *et al.*, 1981) and the fast outward K^+ current (Imaizumi & Giles, 1987) in cardiac myocytes. Although having no apparent effect on activation or deactivation kinetics, the slowing of recovery from inactivation implies that the occupation by quinidine of its binding site can affect the operation of the inactivation gate.

In addition to reducing the peak amplitude of I_K(f), quinidine accelerated its rate of decay. It is not clear how these two effects are related. It is most unlikely however that the decline of the current amplitude is due solely to the increased rate of current decay. This suggestion is based on the output of computer simulations shown in Figure 8. To generate the traces of Figure 8d quinidine was constrained to bind only to open channels and so cause open channel block (B_{oc}). For the traces of Figure 8c it was assumed that the binding of quinidine to a site on closed (resting) channels would prevent channel opening and thereby reduce the amplitude of I_K(f) in a concentration-dependent manner. This represents the process referred to subsequently as tonic block (B_t). The traces of Figure 8b were derived from a model incorporating both tonic and open channel block. In modelling the current behaviour it was assumed that channel inactivation was coupled to channel opening:

$$\begin{array}{ccccc} & & I & & \\ & & \Downarrow\Uparrow & & \\ B_t & \rightleftharpoons & C & \rightleftharpoons & O \\ & & \Downarrow\Uparrow & & \\ & & B_{oc} & & \end{array}$$

The values for the rate constants for the channel gating reactions were derived from control currents at 0 mV and are given in the legend of Figure 8. The degree of tonic block was calculated from the Hill equation fitted to the data of Figure 1b. The rate constant for the open channel blocking reaction was derived from the data obtained at 0 mV in Figure 4 (circles).

A comparison of the outcome of the different blocking models with experimentally-derived traces (Figure 8a) shows that the model incorporating only an open channel blocking mechanism (Figure 8d) caused the expected increase in the rate of the current decay but produced, at most, only a 20% reduction of the peak amplitude of the current. Because open channel block alone does not reproduce the experimentally observed decline of the peak amplitude it is necessary to invoke an additional blocking mechanism, the tonic block. Indeed in the model incorporating both open channel block and tonic block the output of the simulation (Figure 8b) most closely resembled the experimental responses (Figure 8a). In Figure 8c, which shows the output of the model with tonic but with no open channel block, the amplitudes of the currents are comparable to those in Figure 8a and 8b (which is consistent with the relatively minor effects of open channel block on peak amplitudes in Figure 8d), but the decay of the current in quinidine is slower than that observed experimentally.

Although the data of Figure 8 show clearly that open channel block cannot in itself account for the effects of quinidine on the amplitude of I_K(f), the mechanistic basis for the tonic block remains unknown. Amongst the possibilities are a reduction of the probability of channel opening and/or a decrease of the single channel conductance.

The analysis of I_K(f) in quinidine indicated: (1) that at a given voltage the rate of decay of I_K(f) increased with the

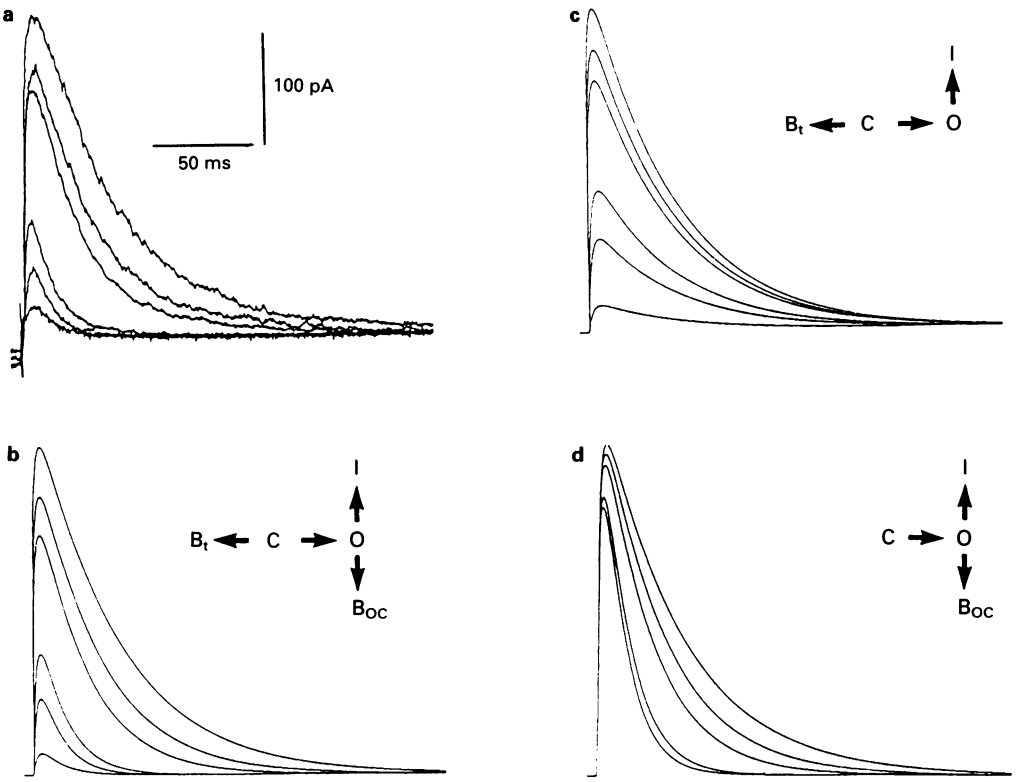


Figure 8 Superimposed traces of $I_K(f)$ obtained experimentally (a) or from a kinetic model in which, in addition to the normal course of channel activation and inactivation, there was: (b) tonic (B_t) and open channel (B_{oc}) block; (c) tonic channel block only; and, (d) open channel block only. The experimental and computer-generated data represent responses at 0 mV in 2.5, 5, 25, 50 and 250 μM quinidine. Although the amplitudes of the traces both in (b) and (c) are comparable to those of the experimentally-derived currents, the rate of decay of the current is better matched when open channel block is incorporated (b). The traces shown in (d) indicate that open channel block by itself has a relatively small effect on the amplitude of $I_K(f)$ despite the increased rate of decay of the current. The values for the forward rate constant for the channel blocking reaction (O–B_{oc}) were calculated from the curve fitted to the data obtained at 0 mV in Figure 4a; the rate constants for channel activation (C–O) and inactivation (O–*I*), estimated from control responses, were 0.5 and 0.033 ms^{-1}, respectively. Tonic channel block (C–B_t), estimated from the curve of Figure 1a, was mimicked by reducing the number of closed (resting) channels available for activation at the beginning of the test pulse. The time scale for the computed traces is the same as in (a); the output of the computer model was scaled so that the amplitude of the control response matched the peak of the control current in (a).

quinidine concentration; and (2) that for a given concentration of quinidine the rate of decay of $I_K(f)$ increased with membrane depolarization. There are a number of schemes which might account for the increase of the decay rate in quinidine. One possibility which cannot be ruled out is that quinidine increases the rate of channel inactivation. However, since the onset of inactivation at −30 mV was not affected by quinidine and since in control cells inactivation is only weakly voltage-dependent above 0 mV (Kehl, 1989) this seems unlikely.

I reported previously that 50 μM quinidine increased the rate of decay of the current at 50 mV but had little effect on the peak amplitude of the current (Kehl, 1989). There is no simple explanation for the failure to detect the tonic block in the previous study. One possibility is that in the previous experiments the quinidine (which was applied with a 'U-tube' tool) was not achieving the expected concentration near the cell, perhaps because of unstirred layer effects. Indeed in this study with 5 μM quinidine it was possible consistently to increase the rate of decay of the current at 50 mV while causing only a small decrease of the peak current.

If the quinidine binding site is situated within the lumen of the channel in such a way that access to the site is normally prevented by a physical barrier (such as the closed 'activation gate'), then once the channel is open quinidine would be able to diffuse through the aqueous phase to its binding site. Since at pH 7.4 most of the quinidine molecules would be positively charged and if the quinidine binding site is within the electric field of the membrane then the rate constants for the binding and unbinding reactions would be expected to be influenced by the membrane potential (Woodhull, 1973). An interaction between positively-charged quinidine and the electric field should be manifest as an inhibition of quinidine binding with membrane depolarization but in fact the opposite is observed: membrane depolarization apparently increases the blocking rate (Figure 4a).

The effects of quinidine on $I_K(f)$ are reminiscent of the actions of local anaesthetics on other types of voltage-gated currents. For example, in the squid axon the block of the Na^+ current by quinidine (Lee *et al.*, 1981) and quaternary lignocaine derivatives appears also to arise from tonic and phasic block possibly by 'different mechanisms [and receptors?]' (Cahalan & Almers, 1979). The basis for the tonic block of the Na^+ current by quinidine and local anaesthetics remains controversial. Phasic block, which for Na^+ currents is evident as a frequency-dependent decline of the current amplitude on successive pulses of depolarizing trains, has been attributed to a state-dependent binding reaction in which the drug binds to open and/or inactivated but not resting channels. It is very likely that part of the effect of quinidine reported here also requires channel opening, the principal differences being, first, that the effect of the drug is evident during each depolarizing pulse and, second, the unbinding reaction at −70 mV is rapid (relative to recovery from inactivation) so that a frequency-dependent decline of the current is not observed. Interestingly, another cardiac anti-arrhythmic agent, tedisamil, has recently been reported to speed the inactivation of the transient potassium current in ventricular myocytes (Dukes & Morad, 1989).

Internal quinidine had little or no effect on either the peak amplitude or the rate of decay of $I_K(f)$. This information may

provide a useful clue regarding the channel dimensions. For example, if quinidine acts by binding to a site within the lumen of the channel then the failure of internal quinidine to affect the rate of decay of I_K(f) implies that the dimensions of the inner mouth of the channel prevent the entry of the quinidine molecule into the pore. A depot site for quinidine in the membrane phase near the channel protein, such as has been proposed to account for the actions of some local anaesthetics (Hille, 1977), also seems unlikely given the ineffectiveness of internal quinidine. The simplest conclusion is that the quinidine binding site is on the external face of the membrane. The short latency of onset with external quinidine is consistent with the latter conclusion and, interestingly, it has been reported that external but not internal quinine blocks open Ca^{2+}-activated K^+ channels in molluscan neurones, chromaffin cells and red blood cells (Hermann & Gorman, 1984; Glavinović & Trifaró, 1988; Reichstein & Rothstein, 1981). This suggests that a quinidine-binding site may be a structural element common to transient and Ca^{2+}-activated K^+ channels.

The quinidine molecule consists of a hydrophobic portion, the aromatic quinoline ring, and a quinuclide ring bearing a nitrogen which would be protonated at pH 7.4. This arrangement in which a hydrophobic group is separated by a carbon chain from a charged nitrogen resembles the optimum configuration for open channel block of delayed rectifier channels in the squid giant axon by quaternary ammonium (QA) ion derivatives (Armstrong, 1971). In Armstrong's model it was proposed that a configuraton in which a hydrophobic benzene ring is separated by a 3 carbon chain from a quaternary nitrogen acts to stabilize the QA-blocking site complex. The influence of the pH on the actions of quinacrine is also consistent with the notion that the aromatic ring plays an important anchoring or stabilizing role at the site to which quinidine and its analogues bind.

The failure of cinchonine to mimic the actions of quinidine was somewhat surprising given the slight structural difference between the two molecules. These results suggest that the methoxy group on C-6′ of the quinoline ring is required for activity but it is not clear why this is so. This substitution at C-6′ would be expected to cause only a slight decrease of hydrophobicity.

The ethylene group on the quinuclide ring of quinidine and indeed the quinoline ring itself does not appear to be critical for the blocking reaction since hydroquinidine and quinacrine are also effective.

Quinidine blocks I_K(f) in melanotrophs but it is not a selective blocker for this channel. The slowly-activating, slowly-inactivating potassium current (I_K(s)) in melanotrophs is also potently blocked by quinidine (Kehl, unpublished observations). Nonetheless quinidine may be a useful tool for discriminating subclasses of fast transient K^+ currents based on the mechanism(s) of channel blockade. In this connection the transient outward K^+ current in cardiac myocytes is blocked by quinidine ($K_d \approx 7\,\mu M$) but there is no clear indication that this effect is accompanied by an increase of the rate of decay of the current (Imaizumi & Giles, 1987).

Supported by a Scholarship from the B.C. Health Care Research Foundation and operating grants from BCHCRF and the Medical Research Council of Canada. I am grateful to Dr P. Vaughan and Dr D. Mathers for comments on the manuscript.

References

ARMSTRONG, C.M. (1971). Interaction of tetraethylammonium ion derivatives with potassium channels of giant axons. *J. Gen. Physiol.*, **58**, 413–437.

CAHALAN, M. & ALMERS, W. (1979). Interactions between quaternary lidocaine, the sodium channel gates, and tetrodotoxin. *J. Gen. Physiol.*, **27**, 39–56.

DUKES, I.D. & MORAD, M. (1989). Tedisamil inactivates transient outward K^+ current in rat ventricular myocytes. *Am. J. Physiol.*, **257**, H1746–H1749.

FISHMAN, M.C. & SPECTOR, I. (1981). Potassium current suppression by quinidine reveals additional calcium currents in neuroblastoma cells. *Proc. Natl. Acad. Sci., U.S.A.*, **78**, 5245–5249.

GLAVINOVIĆ, M.I. & TRIFARÓ, J.M. (1988). Quinine blockade of currents through Ca^{2+}-activated K^+ channels in bovine chromaffin cells. *J. Physiol.*, **399**, 139–152.

HERMANN, A. & GORMAN, A.L.F. (1984). Action of quinidine on ionic currents of molluscan pacemaker neurons. *J. Gen. Physiol.*, **83**, 919–940.

HILLE, B. (1977). Local anaesthetics: hydrophilic and hydrophobic pathways for the drug-receptor reaction. *J. Gen. Physiol.*, **69**, 497–515.

IMAIZUMI, Y. & GILES, W.R. (1987). Quinidine-induced inhibition of transient outward current in cardiac muscle. *Am. J. Physiol.*, **253**, H704–H708.

IWATSUKI, N. & PETERSEN, O.H. (1985). Inhibition of Ca^{2+}-activated K^+ channels in pig pancreatic acinar cells by Ba^{2+}, Ca^{2+}, quinine and quinidine. *Biochem. Biophys. Acta*, **819**, 249–257.

KEHL, S.J. (1989). Cultured melanotrophs of the adult rat pituitary possess a voltage-activated fast transient outward current. *J. Physiol.*, **411**, 457–468.

KEHL, S.J. (1990). 4-Aminopyridine causes a voltage-dependent block of the transient outward K^+ current in rat melanotrophs. *J. Physiol.*, **431**, 515–528.

LEE, K.S., HUME, J.R., GILES, W. & BROWN, A.M. (1981). Sodium current depression by lidocaine and quinidine in isolated ventricular cells. *Nature*, **291**, 325–327.

McBURNEY, R.N. & KEHL, S.J. (1988). Electrophysiology of neurosecretory cells from the pituitary intermediate lobe. *J. Exp. Biol.*, **139**, 317–328.

REICHSTEIN, E. & ROTHSTEIN, A. (1981). Effects of quinidine on Ca^{2+} induced K^+ efflux from human red blood cells. *J. Membr. Biol.*, **59**, 57–63.

ROCHE, E.B. & KIER, L.B. (1981). Parasite chemotherapy. In *Principles of Medicinal Chemistry*. ed. Foye, W.O. pp. 793–807. Philadelphia: Lea & Febiger.

WOODHULL, A.M. (1973). Ionic blockage of sodium channels in nerve. *J. Gen. Physiol.*, **61**, 687–708.

(Received March 8, 1991
Accepted March 19, 1991)

Br. J. Pharmacol. (1991), **103**, 1814–1818 © Macmillan Press Ltd, 1991

Guinea-pig isolated trachealis: the effects of charybdotoxin on mechanical activity, membrane potential changes and the activity of plasmalemmal K^+-channels

M.A. Murray, J.L. Berry, S.J. Cook, R.W. Foster, K.A. Green & [1]R.C. Small

Smooth Muscle Research Group, Department of Physiological Sciences, University of Manchester, Oxford Road, Manchester M13 9PT

1 A study has been made, in guinea-pig isolated trachealis, of the effects of charybdotoxin in modulating (a) the activity of large conductance K^+-channels, (b) the spontaneous electrical activity of intact cells and (c) the mechanical effects of some bronchodilator drugs.

2 Single smooth muscle cells were isolated from guinea-pig trachealis by enzymic digestion and were studied by the patch clamp recording technique. Recordings were made from outside-out plasmalemmal patches when the medium bathing the external surface of the patches contained 1.2 mM Ca^{2+} and 6 mM K^+ while that bathing the cytosolic surface contained 0.1 μM Ca^{2+} and 140 mM K^+. Charybdotoxin (100 nM), applied to the external surface of patches held at 0 mV, abolished the unitary currents associated with the opening of large conductance K^+-channels.

3 Opened segments of guinea-pig trachea were used for the simultaneous recording of membrane potential and tension changes. In these experiments charybdotoxin (100 nM) caused the conversion of spontaneous electrical slow waves into spike-like action potentials. This effect was accompanied by a very small reduction in resting membrane potential.

4 Tissue bath recording showed that charybdotoxin (100 nM) increased the spontaneous mechanical tone of the tissue, antagonized (2.8 fold in each case) the relaxant actions of isoprenaline and theophylline but did not antagonize the relaxant actions of cromakalim or RP 49356.

5 It is concluded that charybdotoxin is an effective inhibitor of large conductance K^+-channels in guinea-pig trachealis cells. The ability of charybdotoxin to convert spontaneous slow waves into spike-like action potentials suggests that the large, charybdotoxin-sensitive, K^+-channels play an important role in determining the strong outward rectifying behaviour of the cells. The ability of charybdotoxin to antagonize isoprenaline and theophylline, but not to antagonize cromakalim and RP 49356, suggests that opening of the large conductance, charybdotoxin-sensitive K^+-channel is implicated in the action of the former but not the latter pair of bronchodilator drugs.

Keywords: Trachealis; charybdotoxin; cromakalim; RP 49356; isoprenaline; theophylline; membrane potential recording; patch clamp recording; large conductance K^+-channels

Introduction

Patch clamp recording techniques have shown that the plasmalemma of trachealis muscle from the dog (McCann & Welsh, 1986), pig (Huang *et al.*, 1987), rabbit (Kume *et al.*, 1990), guinea-pig (Hisada *et al.*, 1990; Small *et al.*, 1990) and ox (Berry *et al.*, 1991; Green *et al.*, 1991) is richly endowed with large, Ca^{2+}-dependent K^+-channels.

Trachealis muscle cells exhibit strong outward rectifying behaviour but this can be suppressed by the K^+-channel inhibitor tetraethylammonium (TEA) (for reviews see Small & Foster, 1988; Small *et al.*, 1990). The relative abundance of the large, Ca^{2+}-dependent K^+-channels, their high specific conductance and their susceptibility to inhibition by externally-applied TEA were among factors which led McCann & Welsh (1986) to suggest that such channels might play a major role in determining the outward rectifying behaviour of the trachealis cell. However, Kotlikoff (1989) has demonstrated, in canine tracheal myocytes, that major components of the outward current induced by a depolarizing voltage step are resistant to charybdotoxin, an agent known to block large, Ca^{2+}-dependent K^+-channels in smooth muscle (Cook & Quast, 1990) including that of the airways (Green *et al.*, 1991). At present, therefore, the role of the large, Ca^{2+}-dependent K^+-channel in determining the strong outward rectifying behaviour of the trachealis cell membrane remains unclear. Kume *et al.* (1989) have suggested that these channels are activated by isoprenaline acting on rabbit tracheal myocytes. These authors proposed that the action of isoprenaline involves the activation of protein kinase A. By phosphorylating the channel or a channel-related protein this enzyme promotes opening of the channel. While the opening of such channels may be implicated in the tracheal relaxant actions of agonists at β-adrenoceptors it does not seem to be necessary for the actions of potassium channel opening drugs such as cromakalim and RP 49356. Tested in bovine trachealis, these two potassium channel opening drugs did not modify P_{open} of the large, Ca^{2+}-dependent K^+-channel (Berry *et al.*, 1991). Furthermore, a recent brief report (Jones & Charette, 1990) has indicated that, in guinea-pig trachealis, charybdotoxin can antagonize the relaxant action of isoprenaline without antagonizing cromakalim or pinacidil. If it can be assumed that charybdotoxin acts specifically to inhibit the large Ca^{2+}-dependent K^+-channel then the work of Jones & Charette (1990) lends support to the idea that the opening of these channels is implicated in the actions of agonists at β-adrenoceptors but not in the actions of cromakalim-like K^+-channel opening drugs.

The experiments of the present study were designed to shed more light on the role of the large Ca^{2+}-dependent K^+-channel in determining the outward rectifying behaviour of the trachealis cell and in mediating the tracheal relaxant actions of agonists at β-adrenoceptors, alkylxanthines and K^+-channel opening drugs such as cromakalim and RP

[1] Author for correspondence.

49356. Charybdotoxin has been used as an analytical tool but the great expense of this agent has necessarily placed some restrictions on the scope of the experimental work.

Methods

Tissue bath studies of mechanical activity

Small segments of trachea were set up for the isometric recording of tension changes essentially as described by Foster *et al.* (1983). At the outset of each experiment, tissues were subjected to an imposed tension of 1.5 g. Approximately 20 min later aminophylline (1 mM) was added in order to determine the recorder pen position at zero tone. The aminophylline was removed from the tissues (initial wash followed by two further washes at 10 min intervals) and when tone subsequently became maximal (40 min after initial wash), study of bronchodilator drugs started.

Cumulative log concentration-effect curves were constructed for all relaxant drugs examined. Half-$\log_{10}$ unit concentration increments were used. Each concentration increment of cromakalim or RP 49356 was allowed 8 min tissue contact. For theophylline the contact time was 5 min and for isoprenaline 4 min. In order to minimize desensitization to cromakalim or RP 49356, a concentration-effect curve for theophylline was always interposed between successive concentration-effect curves of the potassium channel openers. The effects of the various relaxants were measured in terms of the maximal relaxation induced by aminophylline.

Following construction of the initial log concentration-effect curve of the relaxant drug under investigation, test tissues were exposed to Krebs solution containing charybdotoxin (100 nM); 20 min later the log concentration-effect curve of the relaxant drug was reconstructed in the presence of the toxin. In all experiments time-matched control tissues were treated identically to test tissues but were not exposed to charybdotoxin.

The effects of charybdotoxin on spontaneous tone were measured by comparison of the maximal tone observed prior to and ~20 min after toxin administration. In both cases zero tone was identified by the position of the maximal relaxation induced by aminophylline.

Intracellular electrophysiological recording from guinea-pig trachealis

Simultaneous recording of intracellular electrical activity and mechanical changes of a contiguous segment of trachea was performed by use of the technique and tissue holder described by Dixon & Small (1983). In brief, part of the trachealis was immobilized to permit long-term electrical recording while mechanical activity of contiguous muscle bundles was measured under an initial, imposed tension of 1.5 g. The recording microelectrodes were filled with 3 M KCl and were of resistance greater than 40 MΩ.

In these experiments microelectrode impalements of several trachealis cells were attempted prior to tissue treatment with charybdotoxin. Subsequently a trachealis cell was impaled and, during the impalement, charybdotoxin (100 nM) was added to the Krebs solution superfusing the tissue. In this way the onset of the effects of the toxin on electrical and mechanical activity could be recorded. The electrical activity was monitored for as long as the microelectrode tip remained within the impaled cell. Thereafter attempts were made to record the electrical activity of several more trachealis cells in the continued presence of the toxin. The great expense of the toxin made it necessary at this stage in the experiment for the charybdotoxin-containing Krebs solution to be re-cycled through the recording chamber.

Patch clamp recording

Muscle-rich strips of guinea-pig trachea were prepared as previously described (Foster *et al.*, 1983). Each tissue strip was then incubated for 15 min in a Ca^{2+}-free physiological salt solution (Ca^{2+}-free PSS) of the following composition (mM): NaCl 126, KCl 6, Na_2HPO_4 1.2, $MgCl_2$ 1.2, glucose 11, HEPES 10, adjusted to pH 7.4 with NaOH. The tissue was then cut into small segments and subjected to two periods of incubation (30 min at 35°C) in 2 ml Ca^{2+}-free PSS to which had been added 4 mg bovine serum albumin, 1400 μg collagenase (Worthington type 1) and 60 μg elastase (Sigma type IIa). After its removal from the enzymic digestion medium, the tissue was resuspended in 2 ml Ca^{2+}-free PSS. The tissue was then repeatedly aspirated (sucked in and out of a blunt Pasteur pipette) to promote cell shedding. The supernatant fluid was drawn off and examined for its content of isolated smooth muscle cells. The tissue was resuspended in a fresh aliquot of Ca^{2+}-free PSS and aspiration was repeated. Working in this way, several samples of supernatant fluid were collected. Samples containing the greatest cell numbers were pooled and the cells were spun down. The cells were resuspended in the PSS described above but with the addition of $CaCl_2$ (1.2 mM). The cells were plated onto cover slips coated with poly-L-lysine (molecular wt. 500,000 Da). The cells were kept at 4°C and used within 8 h.

Recordings were made (at 22°C) from outside-out patches. The recording pipette contained K^+-rich PSS of the following composition (mM): KCl 126, NaCl 6, $MgCl_2$ 1.2, EGTA 2, glucose 11 and HEPES 10. $CaCl_2$ was added to achieve a free [Ca^{2+}] of 0.1 μM. The pH of this solution was adjusted to 7.4 with KOH solution. The external surface of the patches was bathed by the Ca^{2+}-containing PSS used for plating out the isolated cells.

Recording was performed by use of an Axopatch 1B amplifier (Axon Instruments Inc.). Data were stored on magnetic tape and analysed with a microcomputer and pCLAMP Software (Axon Instruments Inc.). Unitary current amplitudes were measured with a Gould DSO 400 digital storage oscilloscope. Once unitary current recording was established from an outside-out plasmalemmal patch, charybdotoxin (100 nM) was applied to the external surface of the patch by superfusion from a second micropipette positioned in close proximity to the recording pipette.

Drugs and solutions/statistical analysis of results

Drug concentrations are expressed in terms of the molar concentration of the active species. The following substances were used: aminophylline (BDH), purified charybdotoxin (Latoxan), cromakalim (SmithKline Beecham Pharmaceuticals), (−)-isoprenaline hydrochloride (Sigma), RP 49356 ((±)-N-methyl-2-(3-pyridinyl)-tetrahydrothiopyran-2-carbothioamide-1-oxide; Rhone Poulenc-Rorer), theophylline (Sigma).

Stock solutions of most drugs were prepared in twice-distilled water. Those of cromakalim and RP 49356 were prepared in 70% ethanol. Isoprenaline stock solutions were prepared in 0.1 M HCl and dilutions were made with distilled water containing 0.57 mM ascorbic acid. Solutions of charybdotoxin were stored at 4°C and used within 48 h of preparation.

The Krebs solution used in the tissue bath experiments and for the microelectrode recording of membrane potential changes had the following composition (mM): Na^+ 143.5, K^+ 5.9, Ca^{2+} 2.6, Mg^{2+} 1.2, Cl^- 127.6, HCO_3^- 25, SO_4^{2-} 1.2, $H_2PO_4^-$ 1.2 and glucose 11.1. This solution (pH 7.4) was maintained at 37°C and was gassed with a mixture of 95% O_2, 5% CO_2.

The significance of differences between means was assessed by use of a two-tailed, unpaired *t* test. The null hypothesis was rejected when $P < 0.05$.

Results

Tissue bath recording of mechanical activity

Following the construction of the initial log concentration-effect curve of a relaxant drug, test tissues were given two

washes with drug-free Krebs solution before exposure to Krebs solution containing charybdotoxin (100 nM). Exposure of the test tissues to the toxin led to the development (20 min toxin contact) of peak tone greater than that observed in control tissues. The mean (±s.e.mean; $n = 26$) increases in peak tone observed in the test and time-matched control tissues were 17.4 ± 2.8% and 1.2 ± 2.0% respectively ($P < 0.05$; two-tailed unpaired t test). Tone development observed in the presence of the toxin proceeded smoothly (i.e. was not interrupted by phasic tension changes).

Cromakalim (0.1–100 μM), isoprenaline (1 nM–1 μM), RP 49356 (0.1–100 μM) and theophylline (1 μM–1 mM) each caused concentration-dependent suppression of tracheal tone. The maximal effects of cromakalim and RP 49356 were smaller than those of isoprenaline and theophylline (Figure 1). The use of time-matched control tissues showed that log concentration-effect curves for these agents were relatively constant in shape and position during the experimental period.

Tested in the presence of charybdotoxin, each of the bronchodilator drugs retained its ability to suppress tracheal tone. However, in some tissues, determination of the shape of the log concentration-effect curve for the relaxant drug was rendered difficult by the occurrence of phasic mechanical activity. Such tissues could not be used to measure shifts in the log concentration-effect curves of the bronchodilator drugs. Charybdotoxin (100 nM) caused small (2.8 fold in each case) but significant rightward shifts in the log concentration-effect curves of isoprenaline and theophylline without reducing their maximal relaxant effects. In contrast, charybdotoxin failed to antagonize either cromakalim or RP 49356 (Figure 1 and Table 1).

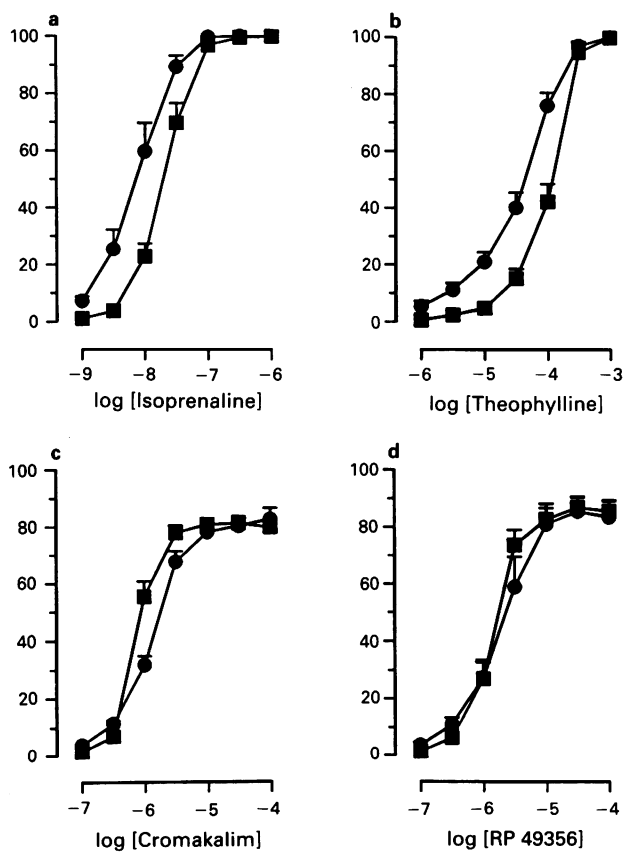


Figure 1 Suppression of the spontaneous tone of guinea-pig isolated trachealis by (a) isoprenaline, (b) theophylline, (c) cromakalim and (d) RP 49356: the effects of charybdotoxin. In each panel (●) indicates the log concentration-effect curve of the relevant bronchodilator drug obtained in the absence of charybdotoxin (time-matched control). (■) indicates the log concentration-effect curve obtained in the presence of charybdotoxin (100 nM). Each point represents the mean (vertical bars show s.e.mean) of values from at least 6 tissues. Note that charybdotoxin antagonized isoprenaline and theophylline but did not antagonize either cromakalim or RP 49356.

Table 1 The effects of charybdotoxin (100 nM) on the actions of some relaxant drugs in guinea-pig isolated trachealis muscle

Relaxant	*Control tissues*	*Test tissues*
Isoprenaline	8.13 ± 0.21	7.69 ± 0.06*
Theophylline	4.38 ± 0.08	3.94 ± 0.06*
Cromakalim	5.89 ± 0.02	6.12 ± 0.07
RP 49356	5.75 ± 0.11	5.84 ± 0.06

Data are mean (± s.e.mean; $n = 6$) values of pD_2 for the tabulated relaxant drugs in time-matched control tissues and in test tissues treated with charybdotoxin. * Indicates a significant difference from the corresponding values in control tissues (two-tailed unpaired t test). Note that charybdotoxin antagonized isoprenaline and theophylline but did not significantly affect the pD_2 values of cromakalim or RP 49356.

Simultaneous recording of membrane potential and mechanical activity

Microelectrode impalement of trachealis cells revealed that, while some cells were electrically quiescent, others exhibited spontaneous oscillations (slow waves) of membrane potential (Figure 2). In this respect the present study has confirmed our earlier findings (Small, 1982; Allen *et al.*, 1986). The addition of charybdotoxin (100 nM) to the Krebs solution superfusing the tissue increased slow wave amplitude and eventually led to the discharge of spike-like action potentials. These changes occurred over a period of 10 minutes and were accompanied by very minor depolarization (mean depolarization measured at 5 min after toxin administration = 2.7 mV; $n = 3$) of the impaled cell and by a small increase in mechanical tone (Figure 2). Charybdotoxin caused changes of this kind in all 7 preparations examined. The very high cost of the toxin precluded more ambitious experimentation.

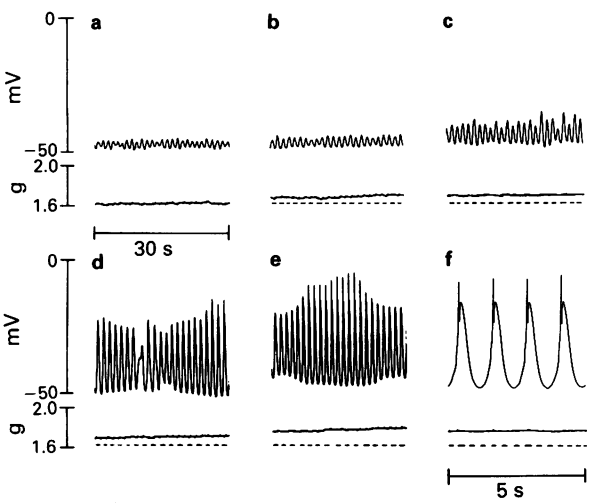


Figure 2 The effects of charybdotoxin (100 nM) on the spontaneous electrical and mechanical activity of guinea-pig isolated trachealis. In each case the upper trace represents membrane potential changes while the lower trace represents the mechanical activity of a contiguous segment of trachea. All electrical recordings are taken from the same cell. Panel (a) indicates control activity recorded immediately prior to the addition of toxin; (b), (c), (d) and (e) activity recorded 2, 4, 6 and 8 min respectively after the addition of charybdotoxin (100 nM) to the Krebs solution superfusing the tissue. Panel (f) is a segment from (e) but run at higher chart speed in order to reveal the waveform of the action potentials. The broken line in panels (b)–(f) indicates the level of mechanical tone prior to toxin administration. Note that charybdotoxin increases slow wave amplitude and eventually causes the discharge of spike-like action potentials. These effects are accompanied by very minor depolarization of the impaled cell and by a small increase in mechanical tone.

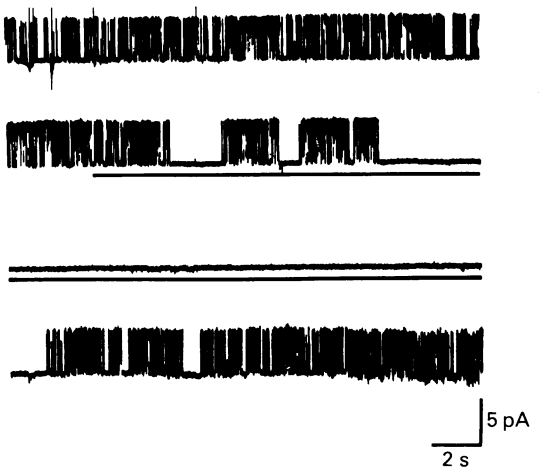


Figure 3 Continuous unitary current recording from an outside-out plasmalemmal patch from guinea-pig trachealis. The holding potential was 0 mV. The solution bathing the external surface of the patch contained 1.2 mM Ca^{2+} and 6 mM K^+ while that bathing the cytosolic surface contained 0.1 μM Ca^{2+} and 140 mM K^+. The bar underneath the trace indicates the local perfusion of 100 nM charybdotoxin by positioning a separate pipette near the patch. The upper three sweeps are continuous recordings. A 5 min period of superfusion with toxin-free PSS separates the third and fourth sweeps. Note that the toxin abolished the unitary current activity but that recovery occurred following the removal of the charybdotoxin from the superfusate.

Patch clamp recording of ion channel activity

Outside-out plasmalemmal patches were set up for recording under conditions where the solution bathing the external surface of the patch contained 1.2 mM Ca^{2+} and 6 mM K^+, while that bathing the cytosolic surface contained 0.1 μM Ca^{2+} and 140 mM K^+. These plasmalemmal patches exhibited large, outwardly-directed unitary currents when held at potentials in the range 0 to +60 mV. Unitary current activity increased (i.e. channel openings occurred more frequently and the incidence of multiple openings increased) as membrane potential was changed from 0 mV to more positive values. The extrapolated reversal potential of the unitary currents was more negative than −40 mV. The slope of the unitary current amplitude/membrane potential relationship measured over the range 0 to +40 mV indicated that the conductance of the ion channels carrying the large unitary currents was 130 ± 7 pS (mean ± s.e.mean; $n = 4$). The voltage-dependence of the unitary currents, the reversal potential of the unitary currents, the conductance of the channels carrying the currents and the abundance of the channels collectively suggested that we were recording the activity of large Ca^{2+}-dependent K^+-channels. This notion was substantiated when we tested the susceptibility of the unitary currents to blockade by charybdotoxin.

Charybdotoxin (100 nM) applied by local superfusion reduced the number of large unitary currents recorded from outside-out plasmalemmal patches held at 0 mV without affecting unitary current amplitude. The inhibitory effects of charybdotoxin were reversible (Figure 3). Charybdotoxin (100 nM) produced similar effects in all preparations ($n = 4$) examined.

Discussion

Role of large, Ca^{2+}-dependent, charybdotoxin-sensitive K^+-channels in determining the strong outward rectifying behaviour of trachealis cells

McCann & Welsh (1986) observed that canine trachealis cells were richly endowed with large, Ca^{2+}-dependent K^+-channels. The abundance of these channels, their high conductance and their susceptibility to inhibition by externally-applied TEA were among factors which led these authors to suggest that such channels play an important role in determining the strong outward rectifying behaviour of the trachealis cells.

Charybdotoxin is a relatively specific inhibitor of large Ca^{2+}-dependent K^+-channels (Cook & Quast, 1990). Accordingly, it might be expected to suppress the outward rectifying properties of trachealis cells. However, Kotlikoff (1989) measured outward current induced by a depolarizing voltage step in canine tracheal myocytes and observed that it was resistant both to substitution of extracellular Ca^{2+} by Mn^{2+} and to charybdotoxin (40 nM). Kotlikoff (1989) concluded that such current was carried by charybdotoxin-insensitive, Ca^{2+}-independent (delayed rectifier) K^+-channels and that the delayed rectifier K^+-channels were the major determinant of the outward rectifying behaviour of trachealis cells. In contrast to Kotlikoff's observations in canine tissue, Green *et al.* (1991) observed in bovine trachealis that charybdotoxin (0.01–1 μM) suppressed the greater part of the outward current induced by a depolarizing voltage ramp. The findings of Green *et al.* (1991), together with the present observations in guinea-pig trachealis that charybdotoxin causes an increase in the amplitude of spontaneous slow waves and their conversion into spike-like action potentials (Figure 3), prompt us to endorse the view of McCann & Welsh (1986) that the large Ca^{2+}-dependent K^+-channel plays a major role in determining the outward rectifying behaviour of trachealis cells.

Role of the large, Ca^{2+}-dependent K^+-channel in the relaxant actions of isoprenaline and theophylline

As mentioned above, Kume *et al.* (1989) have observed that isoprenaline opens large Ca^{2+}-dependent K^+-channels in the plasmalemma of trachealis cells by activating protein kinase A. If this action depends on the intracellular accumulation of adenosine 3':5'-cyclic monophosphate (cyclic AMP), then we should expect cyclic nucleotide phosphodiesterase inhibitors such as theophylline to share the ability of isoprenaline to open the large Ca^{2+}-dependent K^+-channel. This expectation is borne out by the finding (Jones & Charette, 1990; present study) that charybdotoxin antagonizes the tracheal relaxant actions of both isoprenaline and theophylline.

It must be admitted that the single concentration (100 nM) of charybdotoxin used in the present study provided quite minor (2.8 fold) rightward shifts in the log concentration-effect curves of isoprenaline and theophylline. While Jones & Charette (1990) were able to demonstrate greater antagonism by the use of higher toxin concentrations, considerations of cost prevented similar experimentation in our laboratories.

The antagonism of charybdotoxin to actions of isoprenaline and theophylline was not a simple reflection of the ability of the toxin to raise tracheal tone because the toxin failed to antagonize cromakalim, pinacidil and RP 49356 (Jones & Charette, 1990; present study). Accordingly, it may be suggested that opening of large, Ca^{2+}-dependent K^+-channels forms part of the relaxant actions of isoprenaline and theophylline. It should be appreciated, however, that the opening of plasmalemmal K^+-channels with the consequential cellular hyperpolarization and inhibition of Ca^{2+} influx is not crucial to the relaxant actions of these drugs. The relaxant activity of β-adrenoceptor agonists and alkylxanthines is largely retained when these agents are tested against the spasm induced by a medium which is K^+-rich (100–120 mM) yet of osmolality equal to that of normal Krebs solution (Kumar, 1978; Allen *et al.*, 1985; 1986; Small *et al.*, 1989). In this circumstance the potassium equilibrium potential and the resting membrane potential of the cell are so closely apposed that K^+-channel opening cannot evoke sufficient hyperpolarization to ensure closure of voltage-operated Ca^{2+}-channels in the plasmalemma. We conclude, therefore, that the opening of plasmalemmal K^+-channels plays a supportive though not a crucial role in the relaxant actions of isoprenaline and theophylline.

Role of the large, Ca^{2+}-dependent K^+-channel in the relaxant actions of cromakalim-like potassium channel opening drugs

Our observation that charybdotoxin does not antagonize the tracheal relaxant actions of cromakalim and RP 49356 confirms and extends the earlier findings of Jones & Charette (1990) who reported that charybdotoxin failed to antagonize the tracheal relaxant actions of cromakalim and pinacidil. The failure of charybdotoxin to antagonize the cromakalim-like K^+-channel opening drugs suggests that the tracheal relaxant action of such drugs does not involve the opening of large, Ca^{2+}-dependent K^+-channels. This suggestion receives support from the observation (Berry *et al.*, 1991) that P_{open} for the large Ca^{2+}-dependent K^+-channel of bovine trachealis is unaffected by cromakalim, RP 49356 and putative inhibitors (i.e. glibenclamide and phentolamine; for review see Small *et al.*, 1991) of the K^+-channel opened by cromakalim-like drugs.

The authors wish to thank ICI Pharmaceuticals, the Napp Research Center, Pfizer Ltd., Rhone Poulenc-Rorer Ltd. and SmithKline Beecham Pharmaceuticals for assistance with the costs of purchasing the charybdotoxin. M.A.M. is supported by SERC and Rhone Poulenc-Rorer Ltd.; S.J.C. by Glaxo Group Research Ltd. R.W.F. and R.C.S. gratefully acknowledge the support of the National Asthma Campaign, Sandoz Pharma Ltd. and the Wellcome Trust.

References

ALLEN, S.L., BEECH, D.J., FOSTER, R.W., MORGAN, G.P. & SMALL, R.C. (1985). Electrophysiological and other aspects of the relaxant action of isoprenaline in guinea-pig isolated trachealis. *Br. J. Pharmacol.*, **86**, 843–854.

ALLEN, S.L., BOYLE, J.P., CORTIJO, J., FOSTER, R.W., MORGAN, G.P. & SMALL, R.C. (1986). Electrical and mechanical effects of BRL 34915 in guinea-pig isolated trachealis. *Br. J. Pharmacol.*, **89**, 395–405.

BERRY, J.L., ELLIOTT, K.R.F., FOSTER, R.W., GREEN, K.A., MURRAY, M.A. & SMALL, R.C. (1991). Mechanical, biochemical and electrophysiological studies of RP 49356 and cromakalim in guinea-pig and bovine trachealis muscle. *Pulmonary Pharmacol.*, **4**, 91–98.

COOK, N.S. & QUAST, U. (1990). Potassium Channel Pharmacology. In *Potassium Channels: Structure, Classification, Function and Therapeutic Potential.* ed. Cook, N.S. pp. 181–231. Chichester: Ellis Horwood Ltd.

DIXON, J.S. & SMALL, R.C. (1983). Evidence of poor conduction of muscle excitation in the longitudinal axis of guinea-pig isolated trachea. *Br. J. Pharmacol.*, **79**, 75–83.

FOSTER, R.W., SMALL, R.C. & WESTON, A.H. (1983). Evidence that the spasmogenic action of tetraethylammonium in guinea-pig trachealis is both direct and dependent on the cellular influx of Ca^{2+} ion. *Br. J. Pharmacol.*, **79**, 255–263.

GREEN, K.A., FOSTER, R.W. & SMALL, R.C. (1991). A patch-clamp study of K^+-channel activity in bovine isolated tracheal smooth muscle cells. *Br. J. Pharmacol.*, **102**, 871–878.

HISADA, T., KURACHI, Y. & SUGIMOTO, T. (1990). Properties of membrane currents in isolated smooth muscle cells from guinea-pig trachea. *Pflügers Arch.*, **416**, 151–161.

HUANG, H.M., DWYER, T.M. & FARLEY, J.M. (1987). Patch-clamp recording of single Ca^{2+}-activated K^+-channels in tracheal smooth muscle from swine. *Biophys. J.*, **51**, 50a.

JONES, T.R. & CHARETTE, L. (1990). Inhibition of relaxation of guinea-pig trachea by the K^+-channel antagonist, charybdotoxin (CHTX). In Proceedings of XI International Congress of Pharmacology, Amsterdam. *Eur. J. Pharmacol.*, **183**, 2131–2132.

KOTLIKOFF, M.I. (1989). Ion channels in airway smooth muscle. In *Airway Smooth Muscle in Health and Disease.* ed. Coburn, R.F. pp. 169–182. New York: Plenum Press.

KUMAR, M.A. (1978). The basis of β-adrenergic bronchodilation. *J. Pharmacol. Exp. Ther.*, **206**, 528–534.

KUME, H., TAKAGI, K., SATAKE, T., TOKUNO, H. & TOMITA, T. (1990). Effects of intracellular pH on calcium-activated potassium channels in rabbit tracheal smooth muscle. *J. Physiol.*, **424**, 445–457.

KUME, H., TAKAI, A., TOKUNO, H. & TOMITA, T. (1989). Regulation of Ca^{2+}-dependent K^+-channel activity in tracheal myocytes by phosphorylation. *Nature*, **341**, 152–154.

McCANN, J.D. & WELSH, M.J. (1986). Calcium-activated potassium channels in canine airways smooth muscle. *J. Physiol.*, **372**, 113–127.

SMALL, R.C. (1982). Electrical slow waves and tone of guinea-pig isolated trachealis muscle: effects of drugs and temperature changes. *Br. J. Pharmacol.*, **77**, 45–54.

SMALL, R.C., BOYLE, J.P., DUTY, S., ELLIOTT, K.R.F., FOSTER, R.W. & WATT, A.J. (1989). Analysis of the relaxant effects of AH 21-132 in guinea-pig isolated trachealis. *Br. J. Pharmacol.*, **97**, 1165–1173.

SMALL, R.C., BOYLE, J.P., FOSTER, R.W. & GOOD, D.M. (1990). Airways smooth muscle: electrophysiological properties and behaviour. In *Airway Smooth Muscle: Modulation of Receptors and Response.* ed. Agrawal, D.K. & Townley, R.G. pp. 69–94. Boca Raton: CRC Press.

SMALL, R.C. & FOSTER, R.W. (1988). Electrophysiology of the airways smooth muscle cell. In *Asthma: Basic Mechanisms and Clinical Management.* ed. Barnes, P.J., Rodger, I.W. & Thompson, N.C. pp. 35–56. London: Academic Press.

SMALL, R.C., BERRY, J.L., FOSTER, R.W., GREEN, K.A. & MURRAY, M.A. (1991). The Pharmacology of K^+-channel modulators in airway smooth muscle: relevance to airway disease. In *Potassium Channel Modulators: Pharmacological, Molecular and Clinical Aspects.* ed. Weston, A.H. & Hamilton, T.C. Oxford: Blackwell Scientific.

(Received December 21, 1990
Revised March 8, 1991
Accepted March 18, 1991)

Br. J. Pharmacol. (1991), **103**, 1819–1823 © Macmillan Press Ltd, 1991

Neuroprotective actions of GR89696, a highly potent and selective κ-opioid receptor agonist

[1]P.J. Birch, H. Rogers, A.G. Hayes, [2]N.J. Hayward, M.B. Tyers, *D.I.C. Scopes, *A. Naylor & *D.B. Judd

Department of Neuropharmacology and *Medicinal Chemistry, Glaxo Group Research Ltd., Ware, Hertfordshire, SG12 0DP

1 The effect of a novel, highly potent and selective κ-opioid receptor agonist, GR89696, has been evaluated in two animal models of cerebral ischaemia: transient bilateral carotid artery occlusion in the Mongolian gerbil and permanent, unilateral middle cerebral artery occlusion in the mouse.

2 In the Mongolian gerbil model, administration of GR89696 (3 to 30 $\mu g\,kg^{-1}$, s.c.), immediately before and at 4 h after insult, produced a dose-dependent reduction in the hippocampal CA_1 neuronal cell loss resulting from a 7-min bilateral carotid occlusion. Similar effects were obtained with two other κ-agonists, GR86014 (1 $mg\,kg^{-1}$, s.c.) and GR91272 (1 $mg\,kg^{-1}$, s.c.). The neuroprotective effect of GR89696 was completely blocked by prior administration of the opioid receptor antagonist, naltrexone, at 10 $mg\,kg^{-1}$, s.c. Repeated post-treatment with GR89696 (100 $\mu g\,kg^{-1}$, s.c.) or GR44821 (10 $mg\,kg^{-1}$, s.c.) was also effective in protecting completely the hippocampal CA_1 neurones from ischaemia-induced neurodegeneration.

3 In the permanent, unilateral middle cerebral artery occlusion model in the mouse, repeated administration of GR89696 at 300 $\mu g\,kg^{-1}$, s.c. produced a 50% reduction in cerebrocortical infarct volume. In these experiments GR89696 was dosed 5 min, 4, 8, 12, 16, 20 and 24 h after occlusion on the first day and then three times daily for the next three days. GR89696 (300 $\mu g\,kg^{-1}$) also produced a significant 35% reduction in infarct volume in this model when the initiation of dosing was delayed for 6 h after the insult.

4 The results indicate that the potent κ-opioid receptor agonist, GR89696, is neuroprotective in both global and focal cerebral ischaemia models and suggest that, with this class of compound, there may be a considerable time window for pharmacological intervention.

Keywords: κ-opioid agonists; neuroprotection; cerebral ischaemia; GR89696; naltrexone

Introduction

Opioid receptors have been divided into three subtypes: mu (μ), kappa (κ) and delta (δ) and it is well established that activation of each of these receptors can produce antinociceptive effects in a variety of animal models (Hayes *et al.*, 1987; Dickenson *et al.*, 1988; Rodriguez *et al.*, 1986). Within the last decade a number of compounds with enhanced selectivity for the κ-opioid receptor have been described: U50488H (Vonvoigtlander *et al.*, 1983), U62066E (Peters *et al.*, 1987), PD117302 (Leighton *et al.*, 1987), ICI199441 (Costello *et al.*, 1988) and CI-977 (Hunter *et al.*, 1990). It has been suggested that agonists selective for the κ-opioid receptor, while producing good analgesic activity, will lack many of the side-effects associated with μ-opioid receptor agonists.

In addition to playing a role in antinociception, it has been suggested that activation of the κ-opioid receptor can produce neuroprotective effects in certain animal models of cerebral ischaemia. For instance, Tang (1985) and Hall & Pazara (1988) reported that U50488H and U62066E reduced the hippocampal CA_1 neuronal necrosis resulting from transient (7 or 10 min) bilateral carotid occlusion in the Mongolian gerbil. Further studies showed that U50488H also reduced the cerebral oedema and mortality resulting from a 4 h bilateral carotid occlusion in Fischer 344 rats (Silvia & Tang, 1986; Silvia *et al.*, 1987) and the cerebral oedema, cerebrocortical and striatal neuronal cell loss and the mortality resulting from transient (1 h) or permanent middle cerebral artery occlusion in the cat (Silvia & Tang, 1986; Tang & Silvia, 1986). Similarly, CI-977 has been shown recently to reduce infarct volume in a rat middle cerebral artery occlusion model (Cordon *et al.*, 1990). Thus, clinical use of κ-opioid receptor agonists may provide a novel approach for the treatment of stroke.

Recently, our own laboratory has described the chemistry and pharmacology of a series of highly potent and selective κ-opioid receptor agonists (Hayes *et al.*, 1990; Naylor *et al.*, 1990; Scopes *et al.*, 1990). The aim of the present study was to evaluate the efficacy of these compounds in two animal models of cerebral ischaemia: transient bilateral carotid artery occlusion (BCO) in the Mongolian gerbil (Kirino, 1983) and permanent unilateral middle cerebral artery occlusion in the mouse (Gotti *et al.*, 1989). Some of these data have appeared in abstract form (Birch *et al.*, 1990).

Methods

Transient bilateral carotid artery occlusion in the Mongolian gerbil

Mongolian gerbils, of either sex, weighing 60–100 g were anaesthetized with a mixture of isoflurane (5% induction; 2% maintenance), 70% nitrous oxide and 30% oxygen. A 1–2 cm midline cervical incision was made to expose both carotid arteries lying lateral to the trachea. Each carotid artery was carefully isolated from the vagus nerve and a length of cotton thread was placed loosely around it. Once both carotid arteries had been dissected free from accompanying structures, they were occluded for 7 min by the use of microaneursym clips. At the end of the occlusion period, the clips were removed, the patency of the arteries assured by visual inspection and the incision was closed with two wound clips. Sham-operated animals underwent anaesthesia and surgery but the arteries were not occluded. Seven days later, animals were killed by cervical dislocation and the brains removed and rapidly frozen. Coronal sections (20 μm), containing the dorsal hippocampus (1 to 3 mm posterior to Bregma), were then cut

[1] Author for correspondence.
[2] Present address: Parke-Davis Research Unit, Addenbrookes Hospital Site, Hills Road, Cambridge, CB2 2QB.

on a cryostat at 80 to 120 μm intervals. Sections were placed on a microscope slide, fixed in buffered 10% formalin for 10 min and then stained with haematoxylin. Slides were then coded and the area of staining of the CA_1 hippocampal neuronal cell layer was determined with an image analyser (Quantimet 970). Results are expressed as the mean area (μm^2) of staining $\pm$ s.e.mean.

Permanent unilateral middle cerebral artery occlusion in the mouse

Male mice (Glaxo-bred CRH) weighing 18–22 g were anaesthetized with a mixture of isoflurane (5% induction; 2% maintenance), 70% nitrous oxide and 30% oxygen. Under a dissecting microscope (20 × magnification) a skin incision was made on one side between the eye and ear. The underlying muscle was retracted down, exposing the semi-translucent skull through which the middle cerebral artery was visible. The middle cerebral artery was exposed by means of a burr-hole craniectomy with removal of underlying dura using a fine curved forceps and then electrocoagulated by bipolar diathermy (Gotti *et al.*, 1989; Welsh *et al.*, 1987). The burr-hole was then filled with bone wax, the area of surgery dusted with Acramide antibiotic and the wound sutured. Animals were allowed to recover from anaesthesia before being returned to holding rooms. Four days later animals were anaesthetized with Saffan (0.9% alphaxolone, 0.3% alphadolone acetate; 300 mg kg^{-1}, i.v.) and the brains fixed via transcardiac perfusion with 10% formalin. Immediately following perfusion, the brains were removed and placed in 10% formalin solution for 48 h. Brains were then processed by successive immersion in 70% (30 min), 90% (2 h) and 100% ethanol (4 × 1.5 h) followed by CNP30 (3 × 1 h) and finally embedded in molten paraffin wax. Coronal sections (3 μm) were cut on a microtome at 300 μm intervals throughout the length of the brain. Sections were dried overnight at 35°C and then stained with haematoxylin and eosin. Slides were coded and the area of infarction (mm^2) in adjacent coronal sections was measured with the image analyser. The volume of infarction (mm^3) was then computed with the trapezoidal rule. In this model the area of infarction is confined mainly to the tempero-parietal cortex and no gross behavioural changes are observed in animals which had undergone permanent unilateral middle cerebral artery occlusion.

Dosing regimens

Gerbil model In one set of animals, GR89696 (3 to 30 μg kg^{-1}, s.c.), GR86014 (1 mg kg^{-1}, s.c.) or GR91272 (1 mg kg^{-1}, s.c.), were administered in two injections immediately before and at 4 h after the 7 min BCO. The ED_{50} value for GR89696 (defined as the dose reducing the neuronal damage by 50%) was determined by the method of Finney (1964). In a second set of animals, GR89696 (100 μg kg^{-1}, s.c.) was administered in three injections 0.5, 4.5 and 8.5 h after the 7 min BCO and GR44821 (10 mg kg^{-1}, s.c.) in three injections 1, 4.5 and 8 h after the 7 min BCO. Saline-injected animals were used as controls. The frequency of dosing was determined by the duration of the sedation produced by these κ-agonists in the gerbil: GR89696 (3 to 300 μg kg^{-1}, s.c.) and GR44821 (10 mg kg^{-1}, s.c.) produced mild to marked sedation which lasted 4 to 5.5 h and 3.5 to 5 h, respectively. GR86014 (1 mg kg^{-1}, s.c.) and GR91272 (1 mg kg^{-1}, s.c.) both produced marked sedation which lasted for 4 to 5 h. In experiments investigating the actions of the opioid antagonist, naltrexone (10 mg kg^{-1}, s.c.), this drug was administered 30 min prior to each injection of GR89696.

Mouse model GR89696 was administered at 300 μg kg^{-1}, s.c. every 4 h after occlusion for the first 24 h and then three times daily for the next three days. In some studies the initial dose was given at 5 min after occlusion and in other experiments at 6 h after occlusion. The frequency of dosing was determined by the duration of the sedation produced in this species: GR89696 (300 μg kg^{-1}, s.c.) produced marked sedation which lasted for 4 h. MK801 was administered at 300 μg kg^{-1}, s.c. at 5 min, 6 h and 18 h after occlusion on the first day and then twice daily for the next three days (Benavides *et al.*, 1989). Saline-injected animals served as controls and underwent middle cerebral artery occlusion.

Drugs

GR44821 (1-[(3,4-dichlorophenyl) acetyl]-2-[(3-oxo-1-pyrrolidinyl)methyl]piperidine maleate), GR86014 (2-[(3,4-dichlorophenyl) acetyl]-1,2,3,4-tetrahydro-1-(1-pyrrolidinyl-methyl)-5-isoquinolinol maleate)), GR89696 (methyl 4-[(3,4-dichlorophenyl)acetyl]-3-(1-pyrrolidinylmethyl)-1-piperazinecarboxylate fumarate), GR91272 (5-[3,4-dichlorophenyl)-acetyl]-4,5,6,7-tetrahydro-4-[(3-hydroxy-1-pyrrolidinyl)-methyl]furo[3,2-c]pyridine hydrochloride) and MK801 ((+)-5-methyl-10,11-dihyro-5H-dibenzo[a,d]-cycloheptene-5,10-imine maleate) were synthesized in the Department of Medicinal Chemistry, Glaxo Group Research. Naltrexone hydrochloride was purchased from the Sigma Chemical Company.

Results

Transient bilateral carotid artery occlusion in the Mongolian gerbil

In the Mongolian gerbil model, administration of GR89696 (3 to 30 μg kg^{-1}, s.c., n = 11–29), immediately before and at 4 h after insult, produced a dose-dependent reduction in the hippocampal CA_1 neuronal necrosis resulting from a 7 min BCO (Figure 1); the ED_{50} value (95% confidence limits) for GR89696 was 11 (7–18) μg kg^{-1}, s.c. Similar results were obtained by pretreatment with two other κ-agonists, GR86014 (1 mg kg^{-1}, s.c.) and GR91272 (1 mg kg^{-1}, s.c.); hippocampal CA_1 neuronal cell areas (mean $\pm$ s.e.mean) were: sham-operated, 336 $\pm$ 12 μm^2 (n = 22); BCO, 210 $\pm$ 28 μm^2 (n = 22); BCO + GR86014, 354 $\pm$ 8 μm^2 (n = 10; $P < 0.05$ compared to BCO group); BCO + GR91272, 303 $\pm$ 14 μm^2 (n = 12; $P < 0.05$ compared to BCO group). The opioid receptor antagonist, naltrexone (10 mg kg^{-1}, s.c.) had no significant neuroprotective effect on its own (n = 13) but completely prevented the action of GR89696 (n = 13; Figure 2).

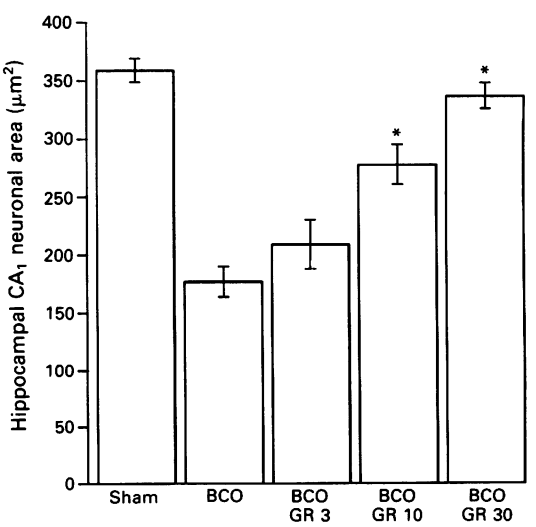


Figure 1 Dose-dependent neuroprotective effects of the κ-opioid receptor agonist GR89696 (GR) in the Mongolian gerbil model of cerebral ischaemia. Gerbils were subjected to a 7 min bilateral carotid occlusion (BCO). Drugs were administered immediately before and at 4 h after occlusion. Doses given are in μg kg^{-1}, s.c. Columns show mean values and s.e.mean indicated by vertical bars. * $P < 0.05$, significantly different from the BCO group (Mann-Whitney test).

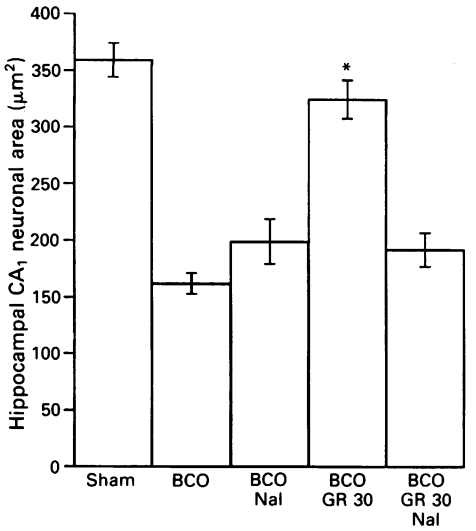


Figure 2 Antagonism by naltrexone (Nal) of the neuroprotective effect of GR89696 (GR) in the Mongolian gerbil model of cerebral ischaemia. GR89696 (30 $\mu g\,kg^{-1}$, s.c.) was administered immediately before and at 4 h after a 7 min bilateral carotid occlusion (BCO). Naltrexone (10 $mg\,kg^{-1}$, s.c.) was administered 30 min prior to each injection of GR89696. Columns show mean values and s.e.mean indicated by vertical bars. * $P < 0.05$, significantly different from the BCO group (Mann-Whitney test).

In a second group of animals, repeated post-treatment, initiated at 30 min post-insult with GR89696 (100 $\mu g\,kg^{-1}$, s.c.; $n = 13$), or initiated at 1 h post-insult with GR44821 (10 $mg\,kg^{-1}$, s.c.; $n = 20$), produced complete protection against the neuronal cell loss resulting from a 7 min BCO (Figure 3).

Permanent unilateral middle cerebral artery occlusion in the mouse

In the mouse middle cerebral artery occlusion model, repeated dosing with GR89696 (300 $\mu g\,kg^{-1}$, s.c.), administered at 5 min, 4, 8, 12, 16, 20, 24 h after occlusion on the first day and then three times daily for the next three days produced a 50% reduction in cerebrocortical infarct volume (infarct volumes were: $8.7 \pm 0.6\,mm^3$, $n = 26$ and $4.3 \pm 0.5\,mm^3$, $n = 30$, for the saline- and GR89696-treated groups, respectively; Figure 4a). Prolonged administration of GR89696 was essential for neuroprotection, as GR89696 produced only a 5% reduction in infarct volume when the dosing covered only the first 16 h ($n = 9$). The neuroprotective effect of GR89696 was slightly greater than that produced by repeated administration of the N-methyl-D-aspartate (NMDA) receptor antagonist MK801 (39% reduction in infarct volume; infarct volumes were: $7.7 \pm 0.6\,mm^3$, $n = 45$ and $4.7 \pm 0.6\,mm^3$, $n = 44$, for the saline- and MK801-treated groups, respectively; Figure 4b).

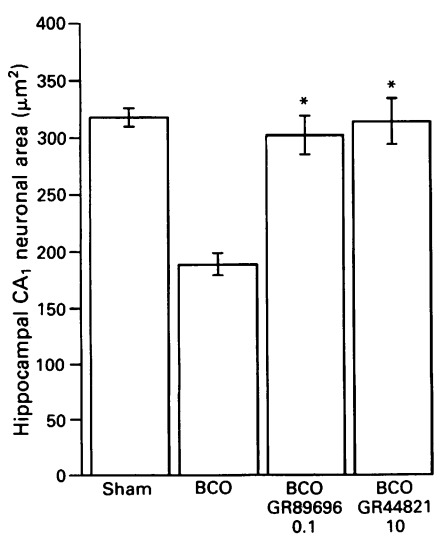


Figure 3 Effect of post-treatment with GR89696 (100 $\mu g\,kg^{-1}$, s.c.) and GR44821 (10 $mg\,kg^{-1}$, s.c.) in the Mongolian gerbil model of cerebral ischaemia. Drugs were administered in three injections at 0.5, 4.5 and 8.5 h (GR89696) or at 1.0, 4.5 and 8.0 h (GR44821) after a 7 min bilateral carotid occlusion (BCO). Columns show mean values and s.e.mean indicated by vertical bars. * $P < 0.05$, significantly different from the BCO group (Mann-Whitney test).

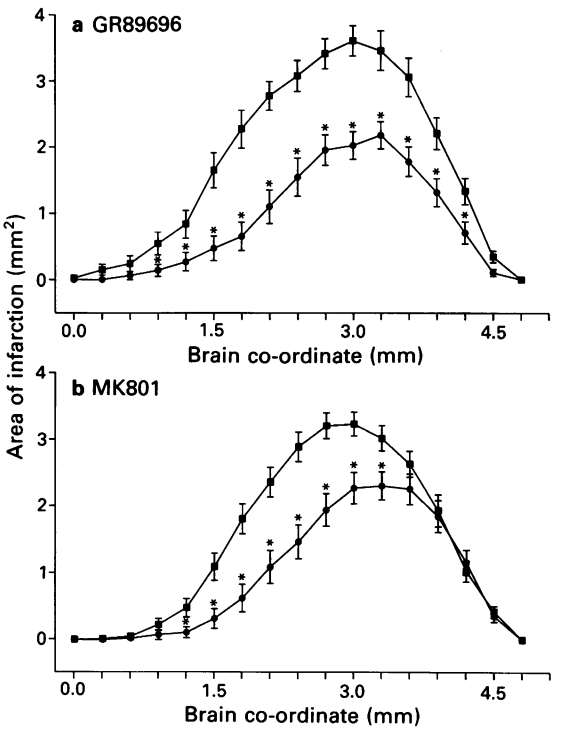


Figure 4 Neuroprotective effect of GR89696 (a) and MK801 (b) in the mouse middle cerebral artery occlusion model. GR89696 (300 $\mu g\,kg^{-1}$, s.c.) was administered at 4 h intervals for the first 24 h and then three times daily for the next three days. Dosing started at 5 min after occlusion. MK801 (300 $\mu g\,kg^{-1}$, s.c.) was administered at 5 min, 6 and 18 h after occlusion on the first day and then twice daily for the next three days. Data points represent area of infarct (mm^2) in adjacent brain sections for saline-treated animals (■) and drug-treated animals (●); s.e.mean indicated by vertical bars. * $P < 0.05$, significantly different from the saline-treated group (Mann-Whitney test).

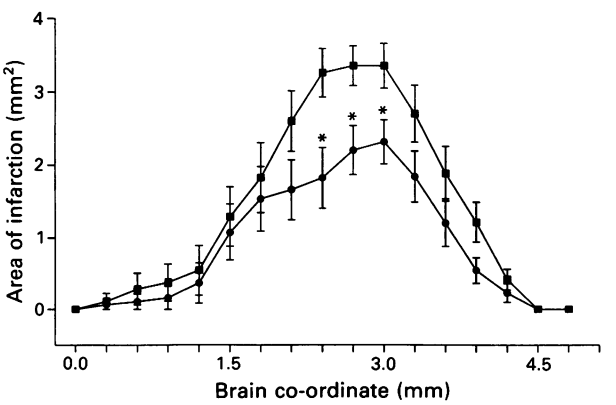


Figure 5 Neuroprotective effect of GR89696 (300 $\mu g\,kg^{-1}$, s.c.) in the mouse middle cerebral artery occlusion model when the initiation of dosing on the first day is delayed for 6 h. Data points represent area of infarct (mm^2) in adjacent brain sections for saline-treated animals (■) and drug-treated animals (●); s.e.mean indicated by vertical bars. * $P < 0.05$, significantly different from the saline-treated group (Mann-Whitney test).

Importantly, GR89696 produced a significant 35% reduction in infarct volume when the initiation of dosing on the first day was delayed for 6 h; infarct volumes were: $7.0 \pm 1.0\,mm^3$, $n = 17$ and $4.6 \pm 0.9\,mm^3$, $n = 18$, for the saline- and GR89696-treated groups, respectively (Figure 5).

Discussion

The results indicate that κ-agonists exert neuroprotective effects in both global and focal models of cerebral ischaemia. More importantly, in both models the compounds are effective when administered post-insult. In the Mongolian gerbil model, the κ-agonists were effective when the start of dosing was delayed for 30 min or 1 h. Interestingly, the non-competitive NMDA receptor antagonist, MK801, has been reported to be neuroprotective when dosing is delayed for 24 h after occlusion in this model (Foster *et al.*, 1987). Experiments with longer post-treatment times were not performed with κ-agonists in the gerbil. In the mouse middle cerebral artery occlusion model, the κ-agonist, GR89696, was efficacious when the start of dosing was delayed for 6 h after occlusion. Interestingly, the NMDA receptor antagonist SL820715 is only effective at time points up to 3 h post-occlusion in the mouse middle cerebral artery occlusion model (Benavides *et al.*, 1989), suggesting that the time window for therapeutic intervention with κ-agonists in this focal cerebral ischaemia model may be superior to NMDA receptor antagonists, although a direct comparison was not made in the present study. The requirement for prolonged dosing with GR89696 in this model is similar to that of SL820715 which becomes more efficacious as the dosing period is increased to cover the first 36 h (Benavides *et al.*, 1989).

κ-Agonists are effective in the gerbil model at doses approximately 100 fold greater than antinociceptive ED_{50} values as determined in the mouse (Hayes *et al.*, 1990). Unfortunately, an antinociceptive test is not available in the gerbil and thus a direct comparison of potencies in this species cannot be made. However, it is important to stress that the neuroprotective action of GR89696 was prevented by naltrexone, indicating that the effect was mediated by activation of an opioid receptor. In the mouse middle cerebral artery occlusion model, lower doses of GR89696 were not tested and thus again an effective comparison between neuroprotective and antinociceptive doses cannot be made. At the doses which are neuroprotective in both gerbil and mouse, κ-agonists produce mild to marked sedation.

In the gerbil model, the opioid receptor antagonist, naltrexone, had no significant neuroprotective effect when administered on its own. This contrasts with published data where this antagonist has been reported to decrease neurological deficit and enhance survival time in a focal cerebral ischaemia model in the cat (Baskin *et al.*, 1985), although in this latter study an effect on infarct size was not observed. Assessments of neurological function were not made in the present study.

The mechanism of action for the neuroprotective effect of κ-agonists is not fully understood, but both neuronal and non-neuronal effects could be involved. It is well established that the excitatory amino acid neurotransmitter, glutamate, plays an important role in ischaemia-induced neurodegeneration and that during ischaemia, synaptic levels of glutamate increase and activate excitatory amino acid receptors. Activation of these receptors leads to a chain of events which results in excessive calcium entry into the neurone and eventual cell death (Meldrum *et al.*, 1985). κ-Agonists may modulate the action of glutamate at presynaptic sites by inhibiting its release or at postsynaptic sites by reducing excitatory amino acid receptor-evoked excessive calcium entry. Recently, κ-agonists have been shown to inhibit glutamate release from rat cerebrocortical slices (Lambert *et al.*, 1991) and to decrease glutamate-stimulated calcium entry into rat cortical cell cultures (DeCoster *et al.*, 1991). However, in our own studies (P.J. Birch, unpublished observations), GR89696 at concentrations up to 1 μM failed to reduce NMDA-induced or anoxia/hypoglycaemia-induced CA_1 neuronal cell loss in a gerbil hippocampal slice preparation, an *in vitro* system in which MK801 is effective (Harrison *et al.*, 1990). This suggests that κ-agonists do not act directly on hippocampal CA_1 neurones to produce their anti-ischaemic effect in the gerbil. κ-Agonists are known to exert anticonvulsant actions (Vonvoigtlander *et al.*, 1987; Tortella *et al.*, 1990) and it has been reported that this effect may involve an interaction between the κ-receptor and the strychnine-insensitive glycine site allosterically linked to the NMDA receptor (Singh *et al.*, 1990). Interestingly, it has been suggested that the anticonvulsant action of κ-agonists may result from a presynaptic inhibition of excitatory amino acid release (Singh *et al.*, 1990) and this could account for the neuroprotection observed in the gerbil.

It has been suggested recently (Corbett *et al.*, 1990) that the neuroprotective effect of MK801 in the gerbil BCO model is due to a drug-related drop in brain temperature. Although high doses of κ-agonists do not decrease body temperature in the gerbil or mouse (P.J. Birch, unpublished observation), brain temperature was not measured or controlled in the present study. κ-Agonists are known to produce a marked diuresis in rodents and such an effect has been suggested to account for the anti-oedematous action of these compounds in rat and cat cerebral ischaemia models (Silvia & Tang, 1986; Silvia *et al.*, 1987). Although no overt diuresis could be detected in the gerbil with doses of GR89696 up to $100\,\mu g\,kg^{-1}$, s.c., this compound produced diuresis in the mouse in the dose range 1 to $100\,\mu g\,kg^{-1}$, s.c. (P.J. Birch, unpublished observations). Hence, an anti-oedema effect may explain in part the neurprotection observed in the focal ischaemia model, although a neuroprotective action of κ-agonists has been demonstrated in rat cortical cell cultures (De Coster *et al.*, 1990) suggesting a neuronal mechanism could also occur. κ-Agonists may also modulate cerebral blood flow, for instance, U50488H has been reported to attenuate post-ischaemic hypoperfusion in a mouse brain injury model (Hall *et al.*, 1987). This has not been assessed in the present study.

In conclusion, κ-opioid receptor agonists are effective neuroprotective agents in both global and focal cerebral ischaemia models and are active when administered post-insult. Although the mechanism of action is as yet undefined, they represent another class of compound which should be considered for clinical evaluation in stroke.

We wish to thank Mrs R. Sargent, Mrs S.M. Harrison and Mr. L. Fernandez for their excellent technical assistance. We also acknowledge the help provided by Mr B. Read and Mr J. Cook from the Department of Histopathology, Glaxo Group Research.

References

BASKIN, D.S., KURODA, H., HOSOBUCHI, Y. & LEE, N.M. (1985). Treatment of stroke with opiate antagonists – effects of exogenous antagonists and dynorphin 1–13. *Neuropeptides*, **5**, 307–310.

BENAVIDES, J., GOTTI, B., DUBOIS, A., MACKENZIE, E.T., SCATTON, B. & THERALAUZ, M. (1989). Neuroprotective effects of NMDA antagonists in mouse focal cerebral ischaemia. *J. Cereb. Blood Flow Metab.*, **9**, (Suppl 1) S748.

BIRCH, P.J., HAYWARD, N.J., ROGERS, H., HAYES, A.G., NAYLOR, A., SCOPES, D.I.C. & TYERS, M.B. (1990). Neuroprotective effects of a highly potent and selective agonist for the kappa opioid receptor. In *New Leads in Opioid Research*, Excerpta Medica. ed. van Ree, J.M., Mulder, A.H., Wiegant, V.M. & van Wimersma Greidanus, T.B. pp. 188–189. Amsterdam: Elsevier.

CORBETT, D., EVANS, S., THOMAS, C., WANG, D. & JONAS, R.S. (1990). MK801 reduced cerebral ischaemic injury by inducing hypothermia. *Brain Res.*, **514**, 300–304.

CORDON, J.J., BOXER, P.A., DOMINICK, M.A. & MARCOUX, F.W. (1990). CI-977, a novel kappa opioid receptor agonist, reduces

infarct size in a model of focal cerebral ischaemia. *Soc. Neurosci. Abstr.*, **16**, 934.

COSTELLO, G.F., MAIN, B.G., BARLOW, J.J., CARROLL, J.A. & SHAW, J.S. (1988). A novel series of potent and selective agonists at the opioid κ-receptor. *Eur. J. Pharmacol.*, **151**, 475–478.

DECOSTER, M.A., HUNTER, J.C., HUGHES, J. & TORTELLA, F.C. (1990). PD117302 attenuates glutamate neurotoxicity *in vitro*. *Soc. Neurosci. Abstr.*, **16**, 463.

DECOSTER, M.A., HUNTER, J.C., HUGHES, J. & TORTELLA, F.C. (1991). Neuroprotective mechanisms of the novel kappa opioid CI-977. *FASEB J.*, **5**, (in press).

DICKENSON, A.H., SULLIVAN, A.F. & ROQUES, B.P. (1988). Evidence that endogenous enkephalins and a δ opioid receptor agonist have a common site of action in spinal antinociception. *Eur. J. Pharmacol.*, **148**, 437–439.

FINNEY, D.J. (1964). In *Statistical Methods in Biological Assay*, 2nd edition, London: Griffin.

FOSTER, A.C., GILL, R., IVERSEN, L.L. & WOODRUFF, G.N. (1987). Systemic administration of MK-801 protects against ischaemia-induced hippocampal neurodegeneration in the gerbil. *Br. J. Pharmacol.*, **90**, 9P.

GOTTI, B., BENAVIDES, J., DUBOIS, A., MACKENZIE, E.T., SCATTON, B. & THERALAUZ, M. (1989). Quantification of experimental focal ischaemic lesions with an ω_3 site radioligand in mouse brain. *J. Cereb. Blood Flow Metab.*, **9**, (Suppl. 1) S258.

HALL, E.D. & PAZARA, K.E. (1988). Quantitative analysis of effects of kappa-opioid agonists on postischaemic hippocampal CA1 neuronal necrosis in gerbils. *Stroke*, **19**, 1008–1012.

HALL, E.D., WOLF, D.L., ALTHAUS, J.S. & VONVOIGTLANDER, P.F. (1987). Beneficial effects of the κ-opioid receptor agonist U-50488H in experimental acute brain and spinal cord injury. *Brain Res.*, **435**, 174–180.

HARRISON, S.M., ROGERS, H., HAYES, A.G. & BIRCH, P.J. (1990). Anoxia- and hypoglycaemia-induced neurodegeneration in neonatal rat hippocampal slices. *Br. J. Pharmacol.*, **99**, 283P.

HAYES, A.G., BIRCH, P.J., HAYWARD, N.J., SHEEHAN, M.J., ROGERS, H., TYERS, M.B., JUDD, D.B., SCOPES, D.I.C. & NAYLOR, A. (1990). A series of novel, highly potent and selective agonists for the κ-opioid receptor. *Br. J. Pharmacol.*, **101**, 944–948.

HAYES, A.G., SHEEHAN, M.J. & TYERS, M.B. (1987). Differential sensitivity of models of antinociception in rat, mouse and guinea-pig to μ- and κ-opioid receptor agonists. *Br. J. Pharmacol.*, **91**, 823–832.

HUNTER, J.C., LEIGHTON, G.E., MEECHAM, K.G., BOYLE, S.J., HORWELL, D.C., REES, D.C. & HUGHES, J. (1990). CI-977, a novel and selective agonist for the κ-opioid receptor. *Br. J. Pharmacol.*, **101**, 183–189.

KIRINO, T. (1982). Delayed neuronal death in the gerbil hippocampus following ischaemia. *Brain Res.*, **239**, 57–69.

LAMBERT, P.D., BARNES, S., HUGHES, J., WOODRUFF, G.N. & HUNTER, J.C. (1991). The effect of CI-977 on potassium-stimulated glutamate release from rat cortical slices. *Br. J. Pharmacol.*, **102**, 72P.

LEIGHTON, G.E., JOHNSON, M.A., MEECHAM, K.G., HILL, R.G. & HUGHES, J. (1987). Pharmacological profile of PD117302, a selective κ-opioid agonist. *Br. J. Pharmacol.*, **92**, 915–922.

MELDRUM, B., EVANS, M., GRIFFITHS, T. & SIMON, R. (1985). Ischaemic brain damage: the role of excitatory activity and of calcium entry. *Br. J. Anaesth.*, **57**, 44–46.

NAYLOR, A., SCOPES, D.I.C., JUDD, D.B., LLOYD, J.E., HAYES, A.G. & BIRCH, P.J. (1990). Structure-activity studies in a series of benzeneacetamido-piperazine analogues: a potent new class of kappa-receptor agonist. In *New Leads in Opioid Research*, Excerpta Medica. ed. van Ree, J.M., Mulder, A.H., Wiegant, V.M. & van Wimersma Greidanus, T.B. pp. 215–216. Amsterdam: Elsevier.

PETERS, G.R., WARD, N.J., ANTAL, E.G., LAI, P.Y. & DEMAAR, E.W. (1987). Diuretic actions in man of a selective kappa opioid agonist: U-62066E. *J. Pharmacol. Exp. Ther.*, **240**, 128–131.

RODRIGUEZ, R.E., LEIGHTON, G.E., HILL, R.G. & HUGHES, J. (1986). *In-vivo* evidence of spinal delta opiate receptor-operated antinociception. *Neuropeptides*, **8**, 221–242.

SCOPES, D.I.C., NAYLOR, A., JUDD, D.B., BAYS, D.E., BELTON, D., HAYES, A.G. & BIRCH, P.J. (1990). New classes of kappa opioid receptor agonist: spirocyclic 2-alkyl-aminomethylpiperidines and 4-alkylaminomethylfuro[3,2-C]pyridines. In *New Leads in Opioid Research*, Excerpta Medica. ed. van Ree, J.M., Mulder, A.H., Wiegant, V.M. & van Wimersma Greidanus, T.B. pp. 212–214. Amsterdam: Elsevier.

SILVIA, R.C., SLIZGI, G.R., LUDENS, J.H. & TANG, A.H. (1987). Protection from ischaemia-induced cerebral oedema in the rat by U-50488H, a kappa opioid receptor agonist. *Brain Res.*, **403**, 52–57.

SILVIA, R.C. & TANG, A.H. (1986). Protection of ischaemic-induced cerebral oedema by the kappa opioid agonist U-50488. In *Pharmacology of Cerebral Ischaemia*. ed. Kreigelstein, J. pp. 381–384. Amsterdam: Elsevier.

SINGH, L., VASS, C.A., HUNTER, J.C., WOODRUFF, G.N. & HUGHES, J. (1990). The anticonvulsant action of CI-977, a selective κ-opioid receptor agonist: a possible involvement of the glycine/NMDA receptor complex. *Eur. J. Pharmacol.*, **191**, 477–480.

TANG, A.H. (1985). Protection from cerebral ischaemia by U-50,488E, a specific kappa opioid analgesic agent. *Life Sci.*, **37**, 1475–1482.

TANG, A.H. & SILVIA, R.C. (1986). Protection from cerebral ischaemia by U-50488 in cats subjected to occlusion of the middle cerebral artery. *Soc. Neurosci. Abstr.*, **12**, 64.

TORTELLA, F.C., ROBLES, L., ECHEVARRIA, E., HUNTER, J.C. & HUGHES, J. (1990). PD117302, a selective non-peptide opioid kappa agonist protects against NMDA and maximal electroshock convulsions in rats. *Life Sci.*, **46**, 1–7.

VONVOIGTLANDER, P.F., HALL, E.D., OCHOA, M.C., LEWIS, R.A. & TRIEZENBERG, H.J. (1987). U-54494A: A unique anticonvulsant related to kappa opioid agonists. *J. Pharmacol. Exp. Ther.*, **243**, 542–547.

VONVOIGTLANDER, P.F., LAHTI, R.A. & LUDENS, J.H. (1983). U-50, 488: a selective and structurally novel non-mu (kappa) opioid agonist. *J. Pharmacol. Exp. Ther.*, **224**, 7–12.

WELSH, F.A., SAKAMOTO, T., McKEE, A.E. & SIMS, R.E. (1987). Effect of lactacidosis on pyridine nucleotide stability during ischaemia in mouse brain. *J. Neurochem.*, **49**, 846–851.

(Received January 25, 1991
Revised March 13, 1991
Accepted March 18, 1991)

Br. J. Pharmacol. (1991), **103**, 1824–1828 © Macmillan Press Ltd, 1991

Selective stimulation of glucagon secretion by β_2 -adrenoceptors in isolated islets of Langerhans of the rat

Rosemary J. Lacey, Nicholas S. Berrow, *John H.B. Scarpello & [1]Noel G. Morgan

Cellular Pharmacology Group, Department of Biological Sciences, and *Department of Postgraduate Medicine, University of Keele, Keele, Staffordshire ST5 5BG

1 In rat isolated islets of Langerhans the selective β_2-adrenoceptor agonist, clenbuterol (1 to 20 μM), significantly increased the level of adenosine 3':5'-cyclic monophosphate (cyclic AMP) within 2 min of incubation.

2 The cyclic AMP response to clenbuterol was inhibited in the presence of the selective β_2 adrenoceptor antagonist, ICI 118551 (0.1 or 10 μM) but remained unchanged when the β_1-antagonist, atenolol (0.1 μM) was administered.

3 Despite causing an elevation in cyclic AMP, clenbuterol (up to 20 μM) failed to influence insulin secretion at any glucose concentration tested, even in the presence of a phosphodiesterase inhibitor.

4 By contrast, clenbuterol elicited a dose-dependent rise in the rate of glucagon secretion; the maximal agonist-induced increase in secretion was two fold, a response equivalent to that observed with 20 mM L-arginine.

5 ICI 118551 significantly inhibited the rise in glucagon secretion induced by clenbuterol (up to 20 μM).

6 The results indicate that the rat islet A cell population is equipped with functional β_2-adrenoceptors which influence glucagon secretion via the second messenger cyclic AMP, but that the B cells are deficient in functional β-receptors.

Keywords: β_2-adrenoceptor; clenbuterol; cyclic AMP; glucagon secretion; insulin secretion

Introduction

The adrenergic regulation of insulin secretion has been reported to consist of separate components, defined as inhibitory (α_2) and stimulatory (β) (Miller, 1981). It is well established that islet cells possess functional α_2-adrenoceptors (Nakaki *et al.*, 1983; Morgan & Montague, 1985; Schuit & Pipeleers, 1986), however, the role of β-adrenoceptors is controversial. Although it has been reported consistently that β-agonists cause a rise in plasma insulin levels in many species (Porte, 1967; Iversen, 1973; Massara *et al.*, 1975; Miller, 1981), evidence from studies with isolated islet preparations is equivocal (Cherksey *et al.*, 1981; Zielmann *et al.*, 1985; Fyles *et al.*, 1986). This may be due in part to significant species differences in the response of isolated pancreatic islets to β-adrenoceptor agonists (Lacey *et al.*, 1990a). Thus it remains unclear whether responses observed *in vivo* can be attributed to direct interaction with islet cell β-receptors or whether the effects result from indirect mechanisms such as the secondary stimulation of glucagon release. Furthermore, there is still conflicting evidence as to the subtype of β-receptor present in islets, since both β_1 and β_2-receptors have been implicated in the control of hormone secretion (Furman & Tayo, 1974; Miller, 1981).

It is well established that β-receptors of both the β_1 and β_2 subtypes normally mediate their effects via the second messenger adenosine 3':5'-cyclic monophosphate (cyclic AMP) (Lefkowitz & Caron, 1988). The physiological consequences of β-agonism should therefore follow from an increase in intracellular cyclic AMP levels. In order to clarify the situation in the endocrine pancreas, we have studied the effect of the selective β_2 adrenoceptor agonist, clenbuterol, on cyclic AMP levels, insulin and glucagon secretion in rat isolated islets. We have also employed selective β-antagonists to characterize the β-receptor subtype involved. Our data demonstrate that whilst clenbuterol raises cyclic AMP levels and stimulates glucagon secretion from rat islets, it is ineffective on insulin secretion. This indicates that rat islet A cells possess β-adrenoceptors which influence glucagon secretion, but that the insulin-secreting B cells are deficient in functional β-receptors. Part of this work has recently been published in abstract form (Lacey *et al.*, 1990b).

[1] Author for correspondence.

Methods

Islet isolation

Isolation of islets of Langerhans from the pancreata of male Wistar rats was carried out by collagenase digestion, as previously described (Montague & Taylor, 1968). Islets were isolated with a bicarbonate-buffered physiological saline solution (Gey & Gey, 1936), equilibrated to pH 7.4 by gassing with O_2:CO_2 (95:5) and containing glucose (4 mM) and $CaCl_2$ (1 mM). Islets were handpicked under a dissecting microscope and used within 2 h of isolation.

Secretion studies

For insulin and glucagon secretion studies, groups of 3 or 5 islets, respectively, were placed in 0.5 ml of the bicarbonate-buffered medium described above, also containing bovine serum albumin (1 mg ml^{-1}). After incubation at 37°C for 1 h in the presence of the appropriate test reagents, samples of the medium were removed for the measurement of insulin or glucagon content by radioimmunoassay.

Cyclic AMP measurement

Groups of 50 isolated islets were placed in microfuge tubes, to which 0.5 ml of the bicarbonate-buffered medium containing 4 mM glucose, 100 μM 3-isobutyl-1-methylxanthine (IBMX) and the test reagents was added. After an incubation period of 5 min at 37°C, the tubes were centrifuged briefly (9000 *g*) and the supernatant replaced with 200 μl of 80% ethanol. Samples were sonicated for 5 s at low power and then freeze dried. The amount of cyclic AMP in the resultant pellets was initially determined by use of a protein binding assay (Brown *et al.*, 1971). The sensitivity of this assay was such that small changes

in islet cyclic AMP were difficult to quantitate and later experiments made use of a more sensitive commercially obtained [^{125}I]-cyclic AMP radioimmunoassay (RIA) kit. For these experients, fewer islets were required (40/tube), and pellets were reconstituted in sodium acetate buffer (pH 6.2), provided in the RIA kit.

Materials

Clenbuterol, atenolol and ICI 118551 (erythro-d,l-1 (7-methylindan-4-yloxy)-3-isopropylaminobutan-2-ol) were kindly donated by ICI Pharmaceuticals, and crystalline biosynthetic human insulin was a gift from Eli Lilly & Co. Forskolin, 3-isobutyl-1-methylxanthine, L-arginine and collagenase (type XI) were obtained from Sigma Chemical Co. Guinea-pig anti-glucagon serum was a gift from Dr P.M. Jones, Biomedical Sciences Division, King's College, London. [^{125}I]-cyclic AMP RIA kit was from Du Pont (UK) Ltd.

Statistical analysis

All data are presented as mean values ± s.e.mean. Statistical significance was assessed by Student's *t* test for unpaired data.

Results

At a concentration of 1 μM, the β_2-adrenoceptor agonist clenbuterol significantly increased the level of cyclic AMP in rat isolated islets incubated in the presence of 4 mM glucose and the phosphodiesterase inhibitor 3-isobutyl-1-methylxanthine (IBMX; 100 μM; Table 1). It was noted that in different experiments the basal level of cyclic AMP was somewhat variable, but the magnitude of the response to 1 μM clenbuterol was consistent, and the extent of elevation of cyclic AMP was not further increased when 20 μM clenbuterol was used (control: 1.39 ± 0.26; 1 μM clenbuterol: 2.69 ± 0.31; 20 μM clenbuterol: 2.69 ± 0.33 fmol cyclic AMP/islet). The response to clenbuterol (20 μM) was transient, since a three fold increase in cyclic AMP could be detected as early as 2 min but this increase was no longer evident after 15 or 30 min of incubation (Figure 1). The stimulation of cyclic AMP by 1 μM clenbuterol was totally blocked by addition of the β_2-adrenoceptor antagonist, ICI 118551, at both concentrations tested (0.1 and 10 μM), whilst the β_1-antagonist atenolol did not significantly alter the cyclic AMP response to clenbuterol (Table 1). The adenylate cyclase activator forskolin was used as a positive control in these experiments and was able to increase cyclic AMP to levels greater than those observed with clenbuterol alone (Table 1). Neither ICI 118551 nor atenolol altered islet cyclic AMP in the absence of agonist (data not presented).

Whilst raising the glucose concentration from 4 to 20 mM caused a marked rise in the rate of insulin secretion, addition of the β_2-adrenoceptor agonist at 20 μM did not further influence either basal or glucose-induced insulin secretion (Figure 2). Forskolin (10 μM) significantly potentiated insulin secretion induced by 20 mM glucose (Figure 2). Incubation of rat isolated islets in the presence of glucose 8 mM and IBMX 50 μM elicited a large increase in the release of insulin compared to the response observed with 8 mM glucose alone (Figure 3). However, even in the presence of IBMX, clenbuterol (10 μM) failed to raise the insulin secretory rate above that seen with 8 mM glucose and IBMX alone (Figure 3). In contrast, addi-

Table 1 Effects of selective β-adrenoceptor antagonists on clenbuterol-induced changes in cyclic AMP levels in rat isolated islets

Clenbuterol (μM)	*ICI 118551* (μM)	*Atenolol* (μM)	*Forskolin* (μM)	*Cyclic AMP* (fmol/islet)
—	—	—	—	7.59 ± 0.67 (15)
1	—	—	—	11.25 ± 0.77 (23)[a]
1	0.1	—	—	5.60 ± 0.93 (8)[b]
1	10	—	—	7.80 ± 0.67 (19)[c]
1	—	0.1	—	10.74 ± 1.03 (4)[NS]
—	—	—	10	30.80 ± 2.90 (11)[b]

Islets were incubated for 5 min in the presence of 4 mM glucose, 100 μM 3-isobutyl-1-methylxanthine and test reagents as shown, prior to measurement of cyclic AMP levels by RIA. Data are presented as mean values ± s.e.mean. Numbers of observations are shown in parentheses. [a]$P < 0.001$ relative to control; [b]$P < 0.001$ relative to clenbuterol alone; [c]$P < 0.005$ relative to clenbuterol alone. NS, not significant relative to clenbuterol alone.

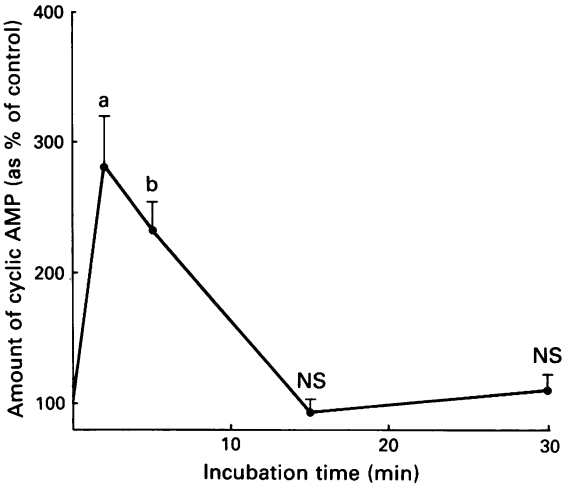


Figure 1 Time course of the effect of the selective β-adrenoceptor agonist, clenbuterol, on cyclic AMP levels in rat isolated islets. Islets were incubated for 2, 5, 15 or 30 min at 37°C, in the presence of 4 mM glucose, 100 μM 3-isobutyl-1-methylxanthine and 20 μM clenbuterol. The amount of cyclic AMP in the resultant pellets was determined by a protein binding assay. Results are expressed as % of control of 6–12 observations; s.e.mean shown by vertical bars. Control values, incubated in the absence of clenbuterol, were as follows: 2 min: 0.71 ± 0.09; 5 min: 1.28 ± 0.15; 15 min: 11.5 ± 0.9; 30 min: 13.2 ± 1.4 fmol cyclic AMP/islet. [a]$P < 0.005$ relative to respective control value; [b]$P < 0.001$ relative to respective control value, NS, not significant relative to respective control value.

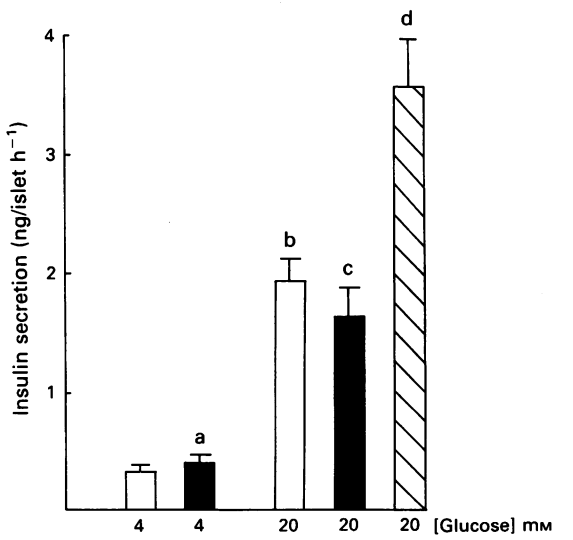


Figure 2 Effect of clenbuterol and forskolin on glucose-induced insulin secretion. Islets were incubated in the presence of 4 or 20 mM glucose and 20 μM clenbuterol (solid columns) or 10 μM forskolin (hatched columns) as shown. After 1 h, samples of the medium were assayed for their insulin contents. Data are presented as mean values for 7–8 observations; vertical bars show s.e.mean. [a]Not significant relative to 4 mM glucose alone. [b]$P < 0.001$ relative to 4 mM glucose alone; [c]not significant relative to 20 mM glucose alone; [d]$P < 0.005$ relative to 20 mM glucose alone.

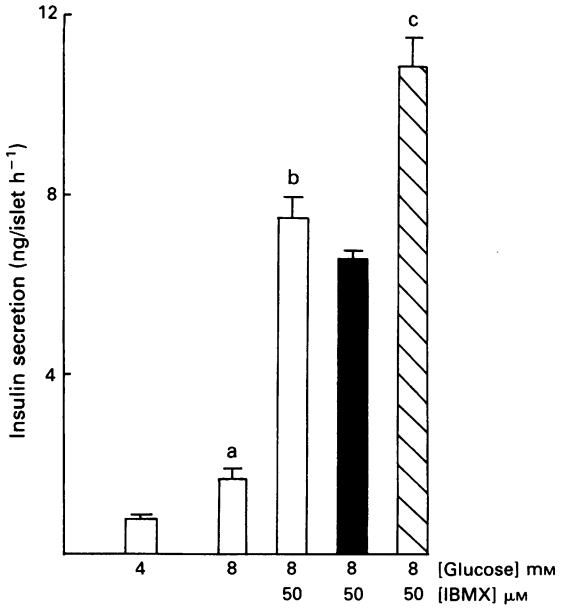


Figure 3 Effect of 3-isobutyl-1-methylxanthine (IBMX), clenbuterol and forskolin on insulin secretion. Rat isolated islets were incubated in the presence of glucose alone, or glucose and IBMX (50 μM) as shown. In addition, the medium containing 8 mM glucose and IBMX was supplemented with either 10 μM clenbuterol (solid columns) or 1 μM forskolin (hatched columns). After 1 h, samples of the medium were removed and their insulin content determined. Data are presented as mean values of 8 observations; s.e.mean shown by vertical bars. $^{a}P < 0.02$ relative to 4 mM glucose; $^{b}P < 0.001$ relative to 8 mM glucose in the absence of IBMX; $^{c}P < 0.01$ relative to 8 mM glucose and IBMX in the absence of forskolin.

tion of forskolin (1 μM), under these conditions, significantly augmented insulin release (Figure 3).

By contrast with its lack of effect on insulin secretion, clenbuterol (20 μM) caused a significant increase in the rate of glucagon release from islets incubated in the presence of 4 mM glucose (Table 2). The maximal extent of stimulation elicited by clenbuterol resulted in a two fold increase in secretion (Tables 2 and 3). Two other reported stimulators of glucagon secretion, L-arginine (20 mM) and forskolin (25 μM) also produced increases in the rate of glucagon release of a similar magnitude (Table 2). The stimulation of glucagon secretion by clenbuterol was dose-dependent (Table 3) with a significant increase observed when islets were incubated with $\geqslant 0.2$ μM clenbuterol.

The β_2-adrenoceptor antagonist ICI 118551 (50 μM) completely inhibited the glucagon secretory response to clenbuterol (1 or 20 μM; Table 4). At a lower concentration (25 μM) ICI 118551 was less effective as an inhibitor of the response induced by 20 μM clenbuterol, but was still able to suppress completely secretion induced by 1 or 10 μM clenbuterol (Table 4).

Table 2 Effects of clenbuterol, arginine and forskolin on glucagon secretion in rat isolated islets

Clenbuterol (20 μM)	*Arginine* (20 mM)	*Forskolin* (25 μM)	*Glucagon secretion* (ng/islet h^{-1})
−	−	−	0.25 ± 0.02 (40)
+	−	−	0.51 ± 0.06 (18)[a]
−	+	−	0.52 ± 0.04 (14)[a]
−	−	+	0.56 ± 0.06 (19)[a]

Islets were incubated for 1 h in the presence of 4 mM glucose and test reagents as shown, prior to measurement of glucagon release by RIA. Data are presented as mean rates of glucagon secretion ± s.e.mean. Numbers of observations are shown in parentheses. $^{a}P < 0.001$ relative to control.

Table 3 Effect of increasing concentrations of clenbuterol on glucagon secretion

Clenbuterol (μM)	*Glucagon secretion* (ng/islet h^{-1})
0	0.48 ± 0.03 (7)
0.002	0.46 ± 0.07 (5)
0.02	0.48 ± 0.08 (8)
0.2	0.70 ± 0.04 (7)[a]
2	0.90 ± 0.07 (7)[a]
20	0.84 ± 0.05 (6)[a]

Islets were incubated as described in Table 2. Data are presented as mean rates of glucagon secretion ± s.e.mean. Numbers of observations are shown in parentheses. $^{a}P < 0.001$ relative to absence of clenbuterol.

Table 4 Effect of the selective β_2-adrenoceptor antagonist, ICI 118551, on clenbuterol-induced glucagon secretion

Clenbuterol (μM)	*ICI 118551* (μM) 0	25	50
0	0.41 ± 0.04 (14)	0.51 ± 0.08 (4)	0.47 ± 0.06 (8)
1	0.82 ± 0.08 (10)	0.49 ± 0.05 (7)[a]	0.43 ± 0.02 (8)[b]
10	0.97 ± 0.10 (6)	0.59 ± 0.09 (5)[a]	ND
20	0.76 ± 0.10 (13)	0.85 ± 0.06 (4)	0.47 ± 0.05 (8)[b]

Islets were incubated under the conditions shown for 1 h, and the medium sampled for assay of glucagon secretion. Data are presented as mean rates of glucagon secretion (ng/islet h^{-1}) ± s.e.mean. Numbers of observations are shown in parentheses. $^{a}P < 0.02$; $^{b}P < 0.001$ relative to clenbuterol in the absence of ICI 118551. ND, not determined.

Discussion

There has been a considerable amount of work investigating the relationships between β- and α-adrenoceptor mechanisms in the regulation of insulin secretion from the endocrine pancreas. Most studies now concur that the α_2-inhibitory mechanism is predominant (Morgan, 1987). However, a substantial body of evidence has also been presented to support a direct role for β-adrenoceptors in the stimulation of insulin secretion in many species (Porte, 1967; Iversen, 1973; Hermann & Deckert, 1977; Fyles *et al.*, 1986). Many of these results have been obtained from *in vivo* studies (Porte, 1967; Iversen, 1973; Ribes *et al.*, 1984; John *et al.*, 1990), where paracrine and other secondary influences may complicate the interpretation of the observed responses.

Studies on the direct effects of β-agonists on isolated islets have been most controversial. Two groups have reported the presence of binding sites having the pharmacological characteristics of β-adrenoceptors in islet preparations (Cherksey *et al.*, 1981; Fyles *et al.*, 1986), whereas others have concluded that islet B cells are totally unresponsive to β-agonism (Schuit & Pipeleers, 1986). Furthermore, it has been suggested that the limited stimulation of insulin secretion by β-adrenoceptor agonists in some reports may reflect a paracrine response to increased glucagon output (Zielmann *et al.*, 1985). In this context, β-agonists have been shown to increase adenylate cyclase activity in islet homogenates (Howell & Montague, 1973; Fyles *et al.*, 1986) suggesting that at least some of the cells present in rat islets do possess β-receptors that are functionally coupled to an intracellular messenger system (cyclic AMP). Our present study aimed to clarify the situation by investigating the effects of a selective β-adenoceptor agonist on cyclic AMP levels, insulin and glucagon secretion in rat isolated islets.

We have shown that in rat islets the β_2-agonist clenbuterol significantly increased the level of cyclic AMP, a response that

was totally inhibited by the β_2-selective antagonist ICI 118551, but remained unaltered in the presence of an equivalent concentration of atenolol (β_1-selective antagonist; Table 1). These results clearly demonstrate the presence of β_2-adrenoceptors on islet cells that are functionally coupled to the adenylate cyclase system. Information as to the cellular distribution of these receptors can be deduced from the insulin and glucagon secretion studies.

We have confirmed our own (Lacey *et al.*, 1990a) and others (Schuit & Pipeleers, 1986) previous findings that rat isolated islets do not respond to β-agonists with a direct increase in insulin release, even in the presence of IBMX (Figures 2 and 3). The inclusion of IBMX would serve to enhance any intracellular rise in cyclic AMP provoked by agonist-induced adenylate cyclase activation. Since in most cells, a physiological response can be induced by a very modest increase in cyclic AMP, our failure to detect any direct effect of the β-agonist on insulin release, despite the ability of isolated islets to respond to a rise in cyclic AMP, indicates that functional β-receptors are not present on islet B cells.

In contrast, clenbuterol induced a significant increase in islet glucagon secretion which was of similar magnitude to that in response to 20 mM arginine, a previously reported stimulator of glucagon release (Faure *et al.*, 1988; Bjaaland *et al.*, 1988). This response was dose-dependent (Table 3) and could be inhibited by inclusion of the β_2-antagonist ICI 118551 (Table 4). The sensitivity of clenbuterol-induced glucagon secretion to inhibition by ICI 118551 appeared to be lower than that of the cyclic AMP response (Table 2). This may reflect the difference in time course of the two processes. Cyclic AMP elevation in response to clenbuterol was transient (Figure 1) and was determined in the islet cell pellet at a single time point (5 min). In contrast, glucagon secretion was estimated by measuring the total hormone release integrated over a 60 min period. Despite these differences, it is clear that both responses were susceptible to inhibition by ICI 118551.

Taken together, our observations support the view that the A cell population is selectively responsive to β-agonists in isolated rat islets and that the observed β-mediated rise in cyclic AMP occurs in the A and not the B cells. It should be emphasised that we cannot conclude from these results that the cyclic AMP response is confined exclusively to the islet A cells, since a number of other cell types are also present in rat islets (Orci, 1985; Miller, 1981) which could express β-receptors. We are confident, however, in drawing the conclusion that the insulin secreting B-cells do not express β_2-receptors that directly control insulin secretion in the rat.

It is also noteworthy that, under the conditions of our experiments, the increase in glucagon output resulting from stimulation by clenbuterol, was insufficient to cause a secondary stimulation of insulin secretion.

Our results support the findings of several other studies, both *in vivo* and *in vitro*, that an increase in glucagon secretion can be elicited via β-adrenoceptor agonism (Iversen, 1973; Gerich *et al.*, 1974; Itoh & Gerich, 1982); we now suggest that this is a β_2-adrenoceptor response. It should be noted that this may not be an exclusive mechanism since *in vivo* studies in the mouse have suggested that glucagon secretion can also be mediated via α_2-adrenoceptors (Ahren & Lundquist, 1987). Samols & Weir (1979) obtained similar results in the isolated perfused pancreas of the dog, but reported only a moderate rise in glucagon release following α-agonism, with a much larger increase due to β-adrenoceptor stimulation. However, the situation is not entirely clear since other studies have shown α-adrenoceptor stimulation to decrease plasma glucagon in man (Gerich *et al.*, 1974). Thus, the receptor-mediated control of glucagon secretion is likely to be very complex. α-Adrenoceptor, β_2-adrenoceptor, muscarinic cholinoceptor and somatostatin receptors may all be present on A cells to control glucagon release (Kaneto *et al.*, 1974; Itoh & Gerich, 1982; Schuit & Pipeleers, 1986; Schuit *et al.*, 1989).

The discrepancies in the findings of different workers indicate to us that there is marked species variation in the adrenergic regulation of pancreatic hormone secretion. Indeed, Loubatières-Mariani *et al.* (1977) observed differential effects of β-agonists on insulin secretion *in vitro* in the dog and the rat. We have also recently shown that β-adrenoceptor agonists stimulate insulin secretion from human isolated islets, which contrasts sharply with the situation in rat (Lacey *et al.*, 1990a). It is not yet clear whether glucagon secretion is also under direct β-adrenoceptor control in man.

In conclusion, our results provide evidence to support the view that direct β-adrenoceptor stimulation of B cells does not occur in rat isolated islets. Our data strongly indicate that it is the A cells which possess functional β_2-adrenoceptors and that the observed rise in glucagon secretion rate is mediated via a concomitant elevation in cyclic AMP levels.

Financial support from the West Midlands Regional Health Authority, Scotia Pharmaceuticals plc and the British Diabetic Association is gratefully acknowledged.

References

AHREN, B. & LUNDQUIST, I. (1987). α-Adrenoceptor blockade by phentolamine inhibits β-adrenergically and cholinergically induced glucagon secretion in the mouse. *Horm. Metab. Res.*, **19**, 600–603.

BJAALAND, T., HII, C.S.T., JONES, P.M. & HOWELL, S.L. (1988). Role of protein kinase C in arginine-induced glucagon secretion from isolated rat islets of Langerhans. *J. Mol. Endocrinol.*, **1**, 105–110.

BROWN, B.L., ALBANO, J.D.M., EKINS, R.P., SGHERZI, A.M. & TAMPION, W. (1971). A simple and sensitive saturation assay method for the measurement of adenosine 3′:5′-cyclic monophosphate. *Biochem. J.*, **121**, 561–562.

CHERKSEY, B., ALTSZULER, N. & ZADUNAISKY, J. (1981). Preponderance of β-adrenergic binding sites in pancreatic islet cells of the rat. *Diabetes*, **30**, 172–174.

FAURE, A., HAOUARI, M. & SUTTER, B.C.J. (1988). Short term and direct influence of oestradiol on glucagon secretion stimulated by arginine. *Diabet. Metab.*, **14**, 452–454.

FURMAN, B.L. & TAYO, F.M. (1974). Effect of some β-adrenoceptor blocking drugs on insulin secretion in the rat. *J. Pharm. Pharmacol.*, **26**, 512–517.

FYLES, J.M., CAWTHORNE, M.A. & HOWELL, S.L. (1986). The characteristics of β-adrenergic binding sites on pancreatic islets of Langerhans. *J. Endocrinol.*, **111**, 263–270.

GERICH, J.E., LANGLOIS, M., NOACCO, C., SCHNEIDER, V. & FORSHAM, P.E. (1974). Adrenergic modulation of pancreatic glucagon secretion in man. *J. Clin. Invest.*, **53**, 1441–1446.

GEY, G.O. & GEY, M.K. (1936). Maintenance of human normal cells in continuous culture: preliminary report; cultivation of mesoblastic tumors and normal cells and notes on methods of cultivation. *Am. J. Cancer*, **27**, 45–76.

HERMANN, L.S. & DECKERT, T. (1977). The effect of epinephrine and isoproterenol on insulin secretion and glucose utilization in isolated islets of Langerhans from mice. *Acta Endocrinol.*, **84**, 105–114.

HOWELL, S.L. & MONTAGUE, W. (1973). Adenylate cyclase activity in isolated rat islets of Langerhans: effects of agents which alter rates of insulin secretion. *Biochim. Biophys. Acta*, **320**, 44–52.

ITOH, M. & GERICH, J.E. (1982). Adrenergic modulation of pancreatic somatostatin, insulin and glucagon secretion: evidence for differential sensitivity of islet A, B and D cells. *Metabolism*, **31**, 715–720.

IVERSEN, J. (1973). Adrenergic receptors and the secretion of glucagon and insulin from the isolated, perfused canine pancreas. *J. Clin. Invest.*, **52**, 2102–2116.

JOHN, G.W., DOXEY, J-C., WALTER, D.S. & REID, J.L. (1990). The role of α- and β-adrenoceptor subtypes in mediating the effects of catecholamines on fasting glucose and insulin concentrations in the rat. *Br. J. Pharmacol.*, **100**, 699–704.

KANETO, A., MIKI, E. & KOSAKA, K. (1974). Effects of vagal stimulation on glucagon and insulin secretion. *Endocrinology*, **95**, 1005–1010.

LACEY, R.J., BERROW, N.S., LONDON, N.J.M., LAKE, S.P., JAMES, R.F.,

SCARPELLO, J.H.B. & MORGAN, N.G. (1990a). Differential effects of β-adrenergic agonists on insulin secretion from pancreatic islets isolated from rat and man. *J. Mol. Endocrinol.*, **5**, 49–54.

LACEY, R.J., BERROW, N.S., SCARPELLO, J.H.B. & MORGAN, N.G. (1990b). Activation of β-adrenoceptors in rat islets of Langerhans leads to enhanced glucagon but not insulin secretion. *Diabetologia*, **33** Suppl., A100.

LEFKOWITZ, R.J. & CARON, M.G. (1988). Adrenergic receptors: models for the study of receptors coupled to guanine nucleotide regulatory proteins. *J. Biol. Chem.*, **263**, 4993–4996.

LOUBATIERES-MARIANI, M.M., CHAPAL, J., RIBES, G. & LOUBATIERES, A.L. (1977). Discrepancies in the response of the insulin secreting cells of the dog and rat to different adrenergic stimulating agents. *Acta Diabet. Latina*, **14**, 144–155.

MASSARA, F., FASSIO, V., CAMANNI, F. & MOLINATT, G.M. (1975). Salbutamol-induced increase in plasma insulin in man. *Horm. Metab. Res.*, **7**, 94–96.

MILLER, R.E. (1981). Pancreatic neuroendocrinology: peripheral neural mechanisms in the regulation of the islets of Langerhans. *Endocrine Rev.*, **2**, 471–494.

MONTAGUE, W. & TAYLOR, K.W. (1968). Pentitols and insulin release by isolated rat islets of Langerhans. *Biochem. J.*, **109**, 333–370.

MORGAN, N.G. (1987). Regulation of insulin secretion by α_2-adrenergic agonists. *Trends Pharmacol. Sci.*, **8**, 369–370.

MORGAN, N.G. & MONTAGUE, W. (1985). Studies on the mechanism of inhibition of glucose-stimulated insulin secretion by noradrenaline in rat islets of Langerhans. *Biochem. J.*, **226**, 571–576.

NAKAKI, T., NAKADATE, T., YAMAMOTO, S. & KATO, R. (1983). Inhibition of dibutyryl cyclic AMP-induced insulin release by α_2-adrenergic stimulation. *Life Sci.*, **32**, 191–195.

ORCI, L. (1985). The insulin factory: a tour of the plant surroundings and a visit to the assembly line. *Diabetologia*, **28**, 528–546.

PORTE, D. (1967). β-Adrenergic stimulation of insulin release in man. *Diabetes*, **16**, 150–155.

RIBES, G., TRIMBLE, E.R., BLAYAC, J.P., WOLLHEIM, C.B. & LOUBATIERES-MARIANI, M.M. (1984). *In vivo* stimulation of pancreatic hormone secretion by norepinephrine infusion in the dog. *Am. J. Physiol.*, **246**, E339–E343.

SAMOLS, E. & WEIR, G.C. (1979). Adrenergic modulation of pancreatic A, B and D cells: α-adrenergic suppression and β-adrenergic stimulation of somatostatin secretion, α-adrenergic stimulation of glucagon secretion in the perfused dog pancreas. *J. Clin. Invest.*, **63**, 230–238.

SCHUIT, F.C. & PIPELEERS, D.G. (1986). Differences in adrenergic recognition by pancreatic A and B cells. *Science*, **232**, 875–877.

SCHUIT, F.C., DERDE, M-P. & PIPELEERS, D.G. (1989). Sensitivity of rat pancreatic A and B cells to somatostatin. *Diabetologia*, **32**, 207–212.

ZIELMANN, S., SCHUTTE, G., LENZEN, S. & PANTEN, U. (1985). Effects of isoprenaline and glucagon on insulin secretion from pancreatic islets. *Naunyn-Schmiedebergs Arch. Pharmacol.*, **329**, 299–304.

(Received March 5, 1991
Accepted March 19, 1991)

Br. J. Pharmacol. (1991), **103**, 1829–1833 © Macmillan Press Ltd, 1991

Effects of bradykinin in the rat isolated perfused heart: role of kinin receptors and endothelium-derived relaxing factor

[1]A.R. Baydoun & [2]B. Woodward

Pharmacology Group, University of Bath, Bath, Avon, BA2 7AY

1 The effects of bradykinin (BK) in the microcirculation of the isolated perfused heart of the rat were examined. The kinin receptors mediating the effects of BK were characterized and the role of endothelium-derived relaxation factor (EDRF) and prostacyclin investigated.

2 The dose-related vasodilator responses elicited by bolus doses of BK (0.001–10.0 nmol) were competitively blocked by the selective kinin B_2 receptor antagonist [D-Arg^0,Hyp^3,Thi^{5,8},D-Phe^7]-bradykinin ($pA_2 = 6.8$). Des-Arg^9-bradykinin, a selective kinin B_1 receptor agonist had no vasodilator activity at doses of up to 10 nmol.

3 L-N^G-nitro arginine (100 μM; L-NOArg), an inhibitor of endothelium-dependent vasodilatation, reduced the duration but not the magnitude of the BK vasodilator response. This action of L-NOArg was not reversed by L-arginine (100 μM).

4 Superoxide dismutase (10 units ml^{-1}), haemoglobin (10 μM) and methylene blue (MB; 1 μM), all known to modify EDRF-mediated responses, failed to alter the vasodilator action of BK.

5 Gossypol (1–15 μM), a presumed inhibitor of EDRF biosynthesis, caused a marked drop in perfusion pressure followed by vasoconstriction. These changes in coronary tone were accompanied by an irreversible depression of cardiac contractility and heart rate. Over the same concentration range gossypol abolished the vasodilator action of BK (1.0 nmol), however it also blocked the endothelium-independent vasodilator response to sodium nitroprusside (30 nmol) and the vasoconstrictor effect of endothelin-1 (10 pmol) which suggests non-specific toxic actions of gossypol.

6 Bolus injections of BK (0.001–1.0 nmol) failed to elevate basal levels of prostacyclin (PGI_2) as shown by assaying for its stable metabolite 6-keto-$PGF_{1\alpha}$. In addition, BK-induced vasodilatation was not blocked by flurbiprofen (2 μM) or BW755C (7.5 μM) which are inhibitors of the arachidonic acid pathway. When added with L-NOArg (100 μM), flurbiprofen (10 μM) did not potentiate the inhibitory action of L-NOArg on the BK response.

7 These results show that the vasodilator action of BK in the rat heart is dependent on the activation of the kinin B_2 receptors but independent of PGI_2 release. Although a conclusive role for EDRF could not be established, this study has questioned the suitability of several agents commonly used as inhibitors of EDRF-mediated responses.

Keywords: EDRF; nitric oxide; prostacyclin; bradykinin; kinin receptors; coronary microcirculation

Introduction

Bradykinin (BK) is a potent vasoactive agent which relaxes different vascular smooth muscle preparations via an endothelium-dependent mechanism (Altura & Chand, 1981; Cherry *et al.*, 1982). Endothelium-dependent relaxation involves the release of an endothelium-derived relaxing factor (EDRF) (Furchgott & Zawadzki, 1980) which has been identified as nitric oxide (NO) (Palmer *et al.*, 1987) with L-arginine as its physiological precursor (Palmer *et al.*, 1988a,b; Schmidt *et al.*, 1988). Although the release of this labile intermediate from many large vessels is well documented (Furchgott, 1984) little is known about its role in the microcirculation. Recent studies have indeed suggested that EDRF/NO mediates the vasodilator action of acetylcholine (ACh) and other drugs in resistance vessels (Cherry & Gillis, 1987; Stewart *et al.*, 1987; Bhardwaj & Moore, 1988; Amezcua *et al.*, 1988) and that BK releases NO from the perfused guinea-pig heart (Kelm & Schrader, 1988). However, other studies could not establish an exclusive role for NO (Aisaka *et al.*, 1989) nor could they rule out an additional direct vasodilator action of the drugs on the vascular smooth muscle (Stewart & Piper, 1988). It is therefore not clear whether the vasodilatation of resistance vessels caused by compounds such as ACh and BK are mediated exclusively by the release of EDRF.

The present study was undertaken to establish the underlying mechanism(s) of action of BK on the resistance vessels in the isolated perfused heart of the rat. The role of EDRF in this model was investigated by use of superoxide dismutase (Gryglewski *et al.*, 1986a,b), methylene blue (Martin *et al.*, 1985), oxyhaemoglobin (Martin *et al.*, 1985, 1986), gossypol (Alheid *et al.*, 1987) and L-N^G-nitro arginine (Moore *et al.*, 1990) which are known to modify EDRF-mediated responses in several different vascular preparations. Characterization of the functional receptors mediating the actions of BK was carried out by use of [D-Arg^0,Hyp^3,Thi^{5,8},D-Phe^7]-bradykinin, a selective antagonist of the kinin B_2 receptors (Vavrek & Stewart, 1985; Regoli *et al.*, 1990) and des-Arg^9-bradykinin, a selective B_1 receptor agonist (Regoli & Barabe, 1980).

In addition to EDRF, BK is also known to release prostacyclin (PGI_2), a potent vasodilator in the rat and guinea-pig perfused heart (Schrör *et al.*, 1978; Belo & Talesnik, 1982). In vascular endothelial cells the BK-induced release of PGI_2 is coupled to that of EDRF and is mediated by the activation of kinin B_2 receptors (de Nucci *et al.*, 1988; D'Orleans-Juste *et al.*, 1989). Thus the possibility of PGI_2 being released by BK in the rat heart has also been investigated. This was carried out by direct radioimmunoassay of its stable metabolite 6-keto-$PGF_{1\alpha}$ and by use of agents known to inhibit its synthesis. Some of our findings have been presented in a preliminary form (Baydoun & Woodward, 1989).

[1] Present address: Department of Physiology, Biomedical Sciences Division, King's College London, Campden Hill Road, Kensington, London, W8 7AH.
[2] Author for correspondence.

Methods

Isolation and perfusion of rat heart

Hearts obtained from male Wistar rats (250–350 g) were perfused by a modified Langendorff technique (Broadley, 1979) at a constant flow rate of 10 ml min^{-1} at 37°C of Krebs-Henseleit solution containing 5.9 mM K^+. The hearts were allowed to equilibrate for 20 min before raising coronary tone with Krebs-Henseleit buffer containing 3.2 mM K^+. Changes in aortic perfusion pressure were used to monitor changes in coronary tone. The force of cardiac contraction was measured with a tension transducer attached to the apex of the heart and this was also used to trigger a heart rate meter. Vasodilator agents (in 10 μl aliquots) were administered to hearts as bolus injections into the perfusate, 3 cm proximal to the aortic cannula. All other compounds were added to the buffer reservoir and perfused through the hearts for a minimum period of 10 min before obtaining responses to the drugs. Commercial haemoglobin was prepared for experimental use according to the method of Martin *et al.* (1985).

Radioimmunoassay of prostacyclin

The release of PGI_2 was monitored by measurement of its stable metabolite, 6-keto-$PGF_{1\alpha}$, present in the cardiac effluent collected at 15 s intervals before, during and after the administration of bradykinin. The amount of 6-keto-$PGF_{1\alpha}$ in the effluent was determined by a standard radioimmunoassay technique using an antibody raised in rabbits (Salmon, 1978). Samples were assayed undiluted without prior extraction or purification (limit of detection was 0.05 ng ml^{-1} in the perfusate).

Materials

Bradykinin (BK), superoxide dismutase (SOD), haemoglobin (HB), gossypol, L-N^G-nitro arginine (L-NOArg) and Des-Arg^9-bradykinin were obtained from Sigma (Poole, Dorset); [D-Arg^0,Hyp^3,$Thi^{5,8}$,D-Phe^7]-bradykinin and endothelin-1 from Novabiochem (Nottingham), sodium nitroprusside (SNP) and methylene blue (MB) from British Drug House (Poole, Dorset); flurbiprofen from Boots (Nottingham) and BW755C (3-amino-1-[*m*-(trifluoromethyl)-phenyl]-2-pyrazoline) from Wellcome Laboratories (Beckenham, Kent).

Statistical analysis

Results are expressed as mean ± s.e.mean for n separate experiments. pA_2 was calculated according to Arunlakshana & Schild (1959).

Results

Effects of bradykinin and Des-Arg^9-bradykinin

Bolus injections of BK (0.001–10.0 nmol) induced a dose-dependent vasodilatation in the perfused rat heart producing a maximum drop in coronary perfusion pressure of 42.8 ± 4.5 mmHg at 1 nmol (n = 10). Over the same dose range, BK had very little effect on the force of contraction but produced a dose-related increase in heart rate in four out of ten experiments. As shown in Figure 1, the initial response on coronary tone was a marked and rapid drop in perfusion pressure which was sustained for over 10 min at higher doses.

In contrast to BK, the selective B_1 receptor agonist, Des-Arg^9-bradykinin (0.001–10 nmol), was completely inactive. This indicates that B_1 receptors are not present in the rat heart and suggests that the effects of BK in this model are mediated via the kinin B_2 receptors.

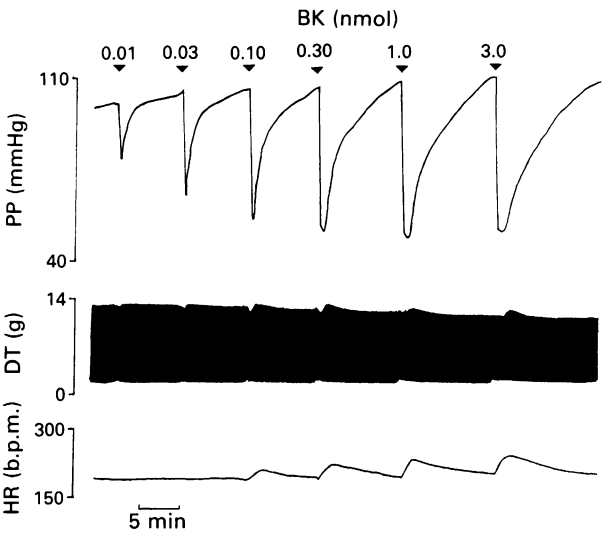


Figure 1 A representative trace of the effects of bradykinin (BK) on perfusion pressure (PP), developed tension (DT) and heart rate (HR, beats per min, b.p.m.) in the isolated perfused heart of the rat. This tracing is one of 10 similar experiments.

Effects of kinin receptor antagonists

The infusion of the selective kinin B_2 receptor antagonist [D-Arg^0,Hyp^3,$Thi^{5,8}$, D-Phe^7]-bradykinin (100 nM and 200 nM) competitively antagonized the vasodilator action of BK (0.001–10.0 nmol) and caused a parallel rightward shift of the BK dose-response curve (Figure 2). A pA_2 value of 6.8 was calculated from these data. This value is comparable to that determined by Vavrek & Stewart (1985) in the rat uterus (pA_2 = 6.4), the guinea-pig ileum (pA_2 = 6.3) and in the dog carotid artery (pA_2 = 6.4).

In addition to reducing the magnitude of the responses, [D-Arg^0,Hyp^3,$Thi^{5,8}$,D-Phe^7]-bradykinin also shortened the duration of the responses to BK. On its own [D-Arg^0,Hyp^3,$Thi^{5,8}$,D-Phe^7]-bradykinin had a transient vasodilator action reducing the basal coronary tone by 7.2 ± 0.3 mmHg (n = 5) and 11.5 ± 2.0 mmHg (n = 4) at 100 nM and 200 nM respectively.

The role of endothelium-derived relaxing factor

Neither the infusion of SOD (10 units ml^{-1}) nor haemoglobin (10 μM) had any effect on the basal coronary tone or on the vasodilator action of BK. Methylene blue (1 μM) elevated basal

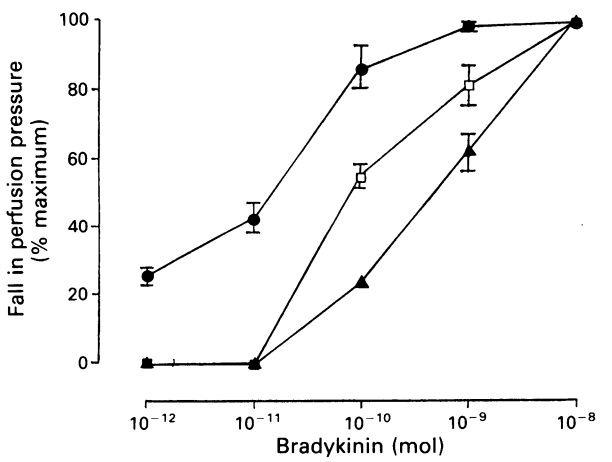


Figure 2 Vasodilator action of bradykinin (BK) in the perfused rat heart in the absence (●) and presence of [D-Arg^0,Hyp^3,$Thi^{5,8}$, D-Phe^7]-bradykinin, 100 nM (□) (n = 5) and 200 nM (▲) (n = 4). The graph shows the mean with s.e.mean indicated by vertical bars.

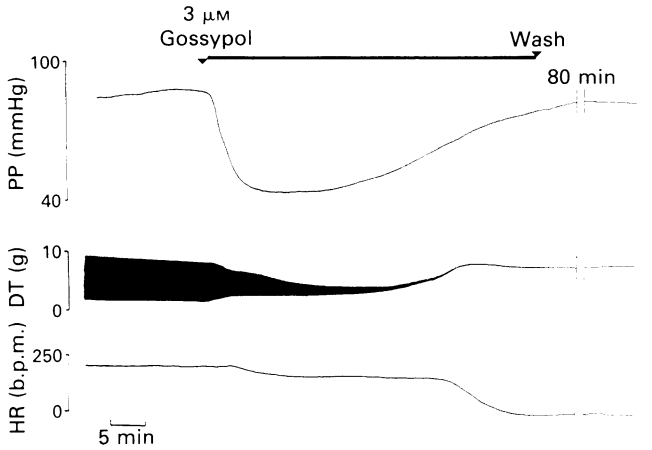


Figure 3 Tracing depicting the effects of gossypol (3 μM) on perfusion pressure (PP), developed tension (DT) and heart rate (HR) in the isolated perfused heart of the rat. This trace is representative of three separate similar experiments.

coronary tone by 14.0 ± 1.7 mmHg (n = 3) but failed to modify the responses to BK (0.01–1.0 nmol). At the same concentration (1 μM), MB did inhibit vascular relaxation induced by ACh in precontracted rat aortic strips (data not shown). Higher concentrations (> 10 μM) of MB could not be used in our studies because of the marked depression in cardiac contractility and vasodilatation produced by the compound itself (Baydoun *et al.*, 1990).

Infusion of gossypol (1–15 μM) caused an initial drop in coronary tone followed by a sustained rise. This effect was accompanied by a depression of contractility and heart rate which was irreversible, even on washing for periods of up to 90 min (Figure 3). At these high concentrations, known to inhibit the actions of EDRF in other vascular preparations (Alheid *et al.*, 1987; Bhardwaj & Moore, 1988), gossypol abolished the vasodilator action of BK (1.0 nmol); however, it also inhibited the endothlium-independent dilator response to sodium nitroprusside (30 nmol) and the response to endothelin-1 (10 pmol) which is a potent vasoconstrictor peptide (Yanagisawa *et al.*, 1988; Baydoun *et al.*, 1989). Lower concentrations (< 0.5 μM) of gossypol had no significant effect on the actions of BK (0.01–1.0 nmol).

Effects of L-nitro arginine

In contrast to the agents used above, the infusion of L-NOArg through the heart elevated coronary tone and induced a positive inotropic action (Figure 4). At 100 μM, L-NOArg increased basal perfusion pressure by 24.0 ± 3.6 mmHg (n = 5) and the developed tension increased from 8.0 ± 0.6 to 9.7 ± 0.5 g (n = 5).

Following L-NOArg (100 μM), bolus injections of BK (0.01–1.0 nmol) produced responses which, although comparable in magnitude to the controls, were less well sustained. This decrease in duration which is expressed as half-recovery time ($t_{1/2}$) in Figure 5 was particularly pronounced at the higher doses of BK.

Infusion of L-arginine (10–100 μM) for 30 min failed to reverse the effects of L-NOArg on the duration of the BK response nor did it modify the vasodilator action of BK in the absence of L-NOArg. When administered as bolus injections, L-arginine (1–30 mmol) produced a drop in basal tone (6.2 ± 0.5 mmHg; n = 3) the magnitude of which was independent of the dose applied.

Release of prostacyclin

Radioimmunoassay of cardiac effluent for PGI_2 release showed that levels of 6-keto-$PGF_{1\alpha}$ (0.061 ± 0.006 ng ml^{-1}; n = 4) detected following bolus injections of 0.1 nmol BK were not significantly different from basal levels (0.063 ± 0.004 ng ml^{-1}; n = 7). In addition to this, the infusion of either flurbiprofen (2 μM) or BW755C (7.5 μM) abolished the basal release of PGI_2 but did not inhibit the vasodilator action of BK. At the concentrations used BW755C however induced a marked drop in perfusion pressure, reducing the basal tone by 26.4 ± 1.9 mmHg (n = 3). A representative trace of the actions of BW755C is shown in Figure 6.

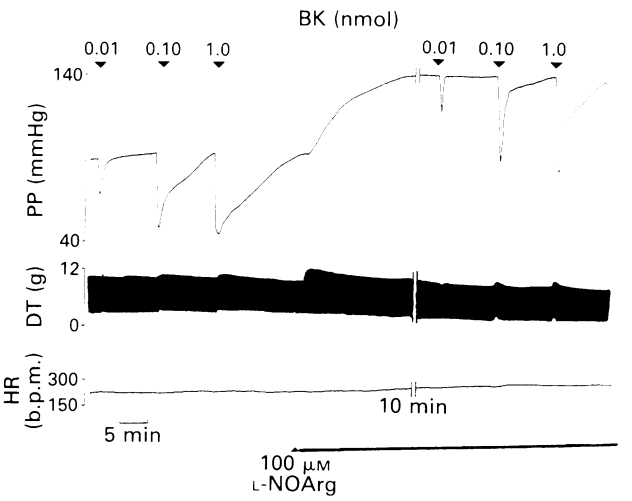


Figure 4 Effect of L-N^G-nitro arginine (L-NOArg) on bradykinin (BK)-induced vasodilatation in the rat isolated perfused heart. This tracing represents one of five separate experiments. PP denotes perfusion pressure, DT developed tension and HR heart rate.

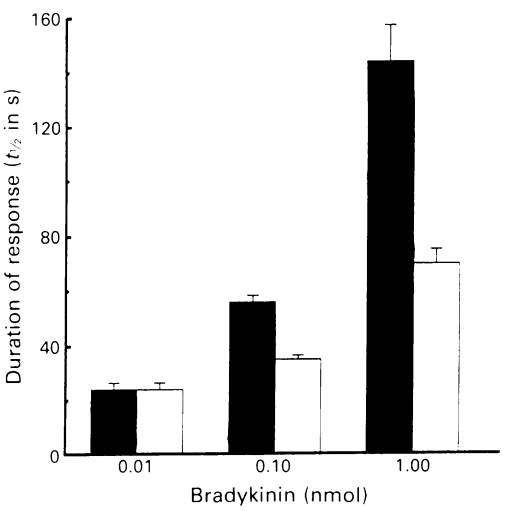


Figure 5 Duration of the vasodilator response to bradykinin under control conditions (solid columns) and in the presence of 100 μM L-N^G-nitro arginine (open columns). Results represent the mean with s.e.mean shown by vertical bars (n = 5) of the time taken for the vasodilator response to return to 50% of its maximum.

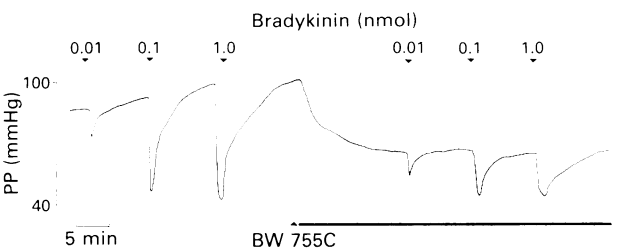


Figure 6 Effect of BW755C (7.5 μM) on the vasodilator action of bradykinin (BK) in the rat isolated perfused heart. This tracing represents one of three separate experiments.

In view of the observation that EDRF and PGI_2 release appear to be coupled in aortic endothelial cells (de Nucci *et al.*, 1988; D'Orleans-Juste *et al.*, 1989) we examined the combined effect of L-NOArg (100 μM) and flurbiprofen (10 μM) on the vasodilator response to BK. This combination, like the action of L-NOArg alone, only reduced the duration of the BK-induced vasodilatation (data not shown). Flurbiprofen therefore did not potentiate the antagonistic action of L-NOArg.

Discussion

The data obtained from this study show that BK is a potent vasodilator of the resistance vessels in the rat isolated perfused heart, mediating its effects via the activation of the kinin B_2 receptors. The role of these receptors was confirmed by the potent competitive inhibition obtained with the kinin B_2 receptor antagonist [D-Arg^0,Hyp^3,$Thi^{5,8}$,D-Phe^7]-bradykinin and by the lack of a vasodilator action with the selective B_1 receptor agonist, Des-Arg^9-bradykinin.

The responses elicited by BK were short-lived at lower doses but longer-lasting at the higher dose-range, indicating that the response consists of more than one component. This is supported by the finding that L-NOArg, a guanidino-substituted analogue of L-arginine (Moore *et al.*, 1990), reduced the duration but not the magnitude of the BK-induced vasodilatation. Since L-NOArg is known to inhibit the biosynthesis of NO (Ishii *et al.*, 1990; Moore *et al.*, 1990), it could imply that NO mediates the later phase of the vasodilator action of BK in the rat isolated heart. However, the inability of L-arginine to reverse the effects of L-NOArg raises the question as to whether L-NOArg is reducing the duration of the BK response by inhibiting the production of NO. It is possible that L-NOArg is having a direct inhibitory action on the later component of the BK response independent of an inhibition of NO synthesis.

The inability of MB (Martin *et al.*, 1985) and haemoglobin (Martin *et al.*, 1985; 1986) to inhibit, and SOD (Gryglewski *et al.*, 1986b) to potentiate the response to BK, adds support to the argument that BK does not produce vasodilatation in the rat heart by releasing NO. However, the lack of effect with haemoglobin and SOD does need to be treated with caution. These are both large molecular weight compounds which may not have access to the subendothelial site of action of NO. In addition if there is a high level of endogenous SOD and/or other superoxide free radical scavengers in the heart, these could mask the effects of exogenous SOD.

In contrast to SOD and haemoglobin, MB is a much smaller molecule which does have access to the extravascular space as indicated by its ability to depress cardiac contractility (Baydoun *et al.*, 1990). Although a low concentration (1 μM) of MB did increase coronary tone, possibly as a result of the inhibition of basal EDRF release, it had no effect on the BK-induced vasodilatation. Several studies have employed higher concentrations of MB (up to 100 μM) to block endothelium-mediated responses in tissues such as rabbit aortic rings (Martin *et al.*, 1985; Warner *et al.*, 1989), and the perfused mesentery of the rat (Bhardwaj & Moore, 1988). However, in the rat heart, high concentrations of MB cause marked coronary dilatation and an irreversible depression of cardiac contractility (Baydoun *et al.*, 1990). As a result of this, these high concentrations of MB could not be used with any confidence in this study as they are probably producing non-specific detrimental effects.

In contrast to SOD, haemoglobin and MB, gossypol an inhibitor of the biosynthesis and/or release of EDRF (Alheid *et al.*, 1987), abolished the vasodilator action of BK. However, cardiac contractility and heart rate were irreversibly depressed and over the same concentration range gossypol also abolished the endothelium-independent dilator responses to sodium nitroprusside and the vasoconstrictor responses to endothelin-1. These findings suggest that in the rat heart the effects of gossypol are nonspecific and they do question the use and selectivity of the compound in inhibiting endothelium-mediated responses.

Finally, our study has shown clearly that metabolites of arachidonic acid, in particular PGI_2, are not involved in mediating the vasodilator action of BK in the rat isolated heart. The action of BK was not associated with an increase in the level of 6-keto-$PGF_{1\alpha}$ in the perfusate, neither was it inhibited by flurbiprofen, or BW755C at concentrations which inhibited the basal release of PGI_2. This finding is consistent with that of Stewart & Piper (1988) who have also concluded that PGI_2 does not mediate the vasodilator action of BK in the perfused guinea-pig heart. In bovine aortic endothelial cells, de Nucci *et al.* (1988) and D'Orleans-Juste *et al.* (1989) showed that BK-induced release of EDRF and PGI_2 synthesis were coupled, and that dual inhibition of EDRF and PGI_2 synthesis were required in order to block the actions of BK. From our data, the combination of flurbiprofen with L-NOArg had no greater inhibitory action on the effects of BK than L-NOArg alone. This shows that the rat coronary circulation behaves differently from bovine aortic endothelial cells in its response to BK.

In conclusion, this study has revealed that the vasodilator action of BK in the rat isolated perfused heart is mediated by the activation of the kinin B_2 receptors. The response appears to be biphasic with the sustained phase possibly involving the release of EDRF by virtue of its sensitivity to L-NOArg inhibition. However, the inability of L-arginine to reverse the inhibition and the lack of specific action by the other agents used, suggests that EDRF may not be the mediator. The suitability of several agents which are commonly used as tools for investigating endothelium-mediated responses is however questioned by some of our findings. It is also evident that extrapolation cannot always be made from studies using large conducting vessels and endothelial cells from these vessels to studies which involve the microvasculature.

We thank Dr John Salmon (Wellcome Laboratories) for the generous gift of the antibody used in the RIA for 6-keto-$PGF_{1\alpha}$. We are also grateful to Dr G. Cirino for his technical assistance and constructive criticisms. This work was supported by the British Heart Foundation.

References

AISAKA, K., GROSS, S.S., GRIFFITH, O.W. & LEVI, R. (1989). L-Arginine availability determines the duration of acetylcholine-induced systemic vasodilation *in vivo*. *Biochem. Biophys. Res. Commun.*, **163**, 710–717.

ALHEID, U., DUDEL, C. & FORSTERMANN, U. (1987). Selective inhibition by gossypol of endothelium-dependent relaxations augments relaxations to glyceryl trinitrate in rabbit coeliac artery. *Br. J. Pharmacol.*, **92**, 237–240.

ALTURA, B.M. & CHAND, N. (1981). Bradykinin-induced relaxation of renal and pulmonary arteries is dependent upon intact endothelial cells. *Br. J. Pharmacol.*, **74**, 10–11.

AMEZCUA, J.L., DUSTING, G.J., PALMER, R.M.J. & MONCADA, S. (1988). Acetylcholine induces vasodilatation in the rabbit isolated heart through the release of nitric oxide, the endogenous nitrovasodilator. *Br. J. Pharmacol.*, **95**, 830–834.

ARUNLAKSHANA, O. & SCHILD, H.O. (1959). Some quantitative uses of drug antagonists. *Br. J. Pharmacol. Chemother.*, **14**, 48–58.

BAYDOUN, A.R., PEERS, S.H., CIRINO, G. & WOODWARD, B. (1989). Effects of endothelin-1 on the rat isolated heart. *J. Cardiovasc. Pharmacol.*, **13**, Suppl. 5, S193–S196.

BAYDOUN, A.R., PEERS, S.H., CIRINO, G. & WOODWARD, B. (1990). Vasodilator action of endothelin-1 in the perfused rat heart. *J. Cardiovasc. Pharmacol.*, **15**, 759–763.

BAYDOUN, A.R. & WOODWARD, B. (1989). Coronary effects of bradykinin in the isolated perfused rat heart are mediated via B_2 bradykinin receptors. *J. Mol. Cell. Cardiol.*, **21**, Suppl. 4, FC77.

BELO, S.E. & TALESNIK, J. (1982). Coronary vasoconstrictor and vasodilator actions of arachidonic acid in the isolated perfused heart of the rat. *Br. J. Pharmacol.*, **75**, 269–286.

BHARDWAJ, R. & MOORE, P.K. (1988). Endothelium-derived relaxing factor and the effects of acetylcholine and histamine on resistance blood vessels. *Br. J. Pharmacol.*, **95**, 835–843.

BROADLEY, K.J. (1979). The Langendorff heart preparation-reappraisal of its role as a research and teaching model for coronary vasoactive drugs. *J. Pharmacol. Methods*, **2**, 143–156.

CHERRY, P.D., FURCHGOTT, R.F., ZAWADZKI, T.V. & JOTHIANANDAN, D. (1982). Role of endothelial cells in relaxation of isolated arteries by bradykinin. *Proc. Natl. Acad. Sci. U.S.A.*, **79**, 2105–2110.

CHERRY, P.D. & GILLIS, C.N. (1987). Evidence for the role of endothelium-derived relaxing factor in acetylcholine induced vasodilatation in the intact lung. *J. Pharmacol. Exp. Ther.*, **241**, 516–520.

DE NUCCI, G., GRYGLEWSKI, R.J., WARNER, T.D. & VANE, J.R. (1988). Receptor-mediated release of endothelium-derived relaxing factor and prostacyclin from bovine aortic endothelial cells is coupled. *Proc. Natl. Acad. Sci., U.S.A.*, **85**, 2334–2338.

D'ORLEANS-JUSTE, P., DE NUCCI, G. & VANE, J.R. (1989). Kinins act on B_1 or B_2-receptors to release conjointly endothelium-derived relaxing factor and prostacyclin from bovine aortic endothelial cells. *Br. J. Pharmacol.*, **96**, 920–926.

FURCHGOTT, R.F. (1984). The role of endothelium in the responses of vascular smooth muscle to drugs. *Annu. Rev. Pharmacol. Toxicol.*, **24**, 175–197.

FURCHGOTT, R.F. & ZAWADZKI, J.V. (1980). The obligatory role of endothelial cells in the relaxation of arterial smooth muscle by acetylcholine. *Nature*, **288**, 373–376.

GRYGLEWSKI, R.J., MONCADA, S. & PALMER, R.M.J. (1986a). Bioassay of prostacyclin and endothelium-derived relaxing factor (EDRF) from porcine aortic endothelial cells. *Br. J. Pharmacol.*, **87**, 685–694.

GRYGLEWSKI, R.J., PALMER, R.M.J. & MONCADA, S. (1986b). Superoxide anion is involved in the breakdown of endothelium-derived vascular relaxing factor. *Nature*, **320**, 454–456.

ISHII, K., CHANG, B., KERWIN, J.F., HUANG, Z-J. & MURAD, F. (1990). N^W-nitro-L-arginine: a potent inhibitor of endothelium-derived relaxing factor formation. *Eur. J. Pharmacol.*, **176**, 219–223.

KELM, M. & SCHRADER, J. (1988). Nitric oxide release from the isolated guinea-pig heart. *Eur. J. Pharmacol.*, **155**, 317–321.

MARTIN, W., VILLANI, G.M., JOTHIANANDAN, D. & FURCHGOTT, R.F. (1985). Selective blockade of endothelium-dependent and glyceryl trinitrate-induced relaxation by hemoglobin and by methylene blue in the rabbit aorta. *J. Pharmacol. Exp. Ther.*, **232**, 708–716.

MARTIN, W., SMITH, J.A. & WHITE, D.G. (1986). The mechanisms by which haemoglobin inhibits the relaxation of rabbit aorta induced by nitrovasodilators, nitric oxide, or bovine retractor penis inhibitory factor. *Br. J. Pharmacol.*, **89**, 563–571.

MOORE, P.K., AL-SWAYEH, O.A., CHONG, N.W.S., EVANS, R.A. & GIBSON, A. (1990). L-N^G-nitro arginine (L-NOARG), a novel, L-arginine-reversible inhibitor of endothelium dependent vasodilation *in vitro*. *Br. J. Pharmacol.*, **99**, 408–412.

PALMER, R.M.J., FERRIGE, A.G. & MONCADA, S. (1987). Nitric oxide release accounts for the biological activity of endothelium-derived relaxing factor. *Nature*, **327**, 524–526.

PALMER, R.M.J., ASHTON, D.S. & MONCADA, S. (1988a). Vascular endothelial cells synthesize nitric oxide from L-arginine. *Nature*, **333**, 664–666.

PALMER, R.M.J., REES, D.D., ASHTON, D.S. & MONCADA, S. (1988b). L-arginine is the physiological precursor for the formation of nitric oxide in endothelium-dependent relaxation. *Biochem. Biophys. Res. Commun.*, **153**, 1251–1256.

REGOLI, D. & BARABE, J. (1980). Pharmacology of bradykinin and related kinins. *Pharmacol. Rev.*, **32**, 1–46.

REGOLI, D., RHALEB, N., DION, S. & DRAPEAU, G. (1990). New selective bradykinin receptor antagonists and bradykinin B_2 receptor characterization. *Trends Pharmacol. Sci.*, **11**, 156–161.

SALMON, J.A. (1978). A radioimmunoassay for 6-keto-prostaglandin-$F_{1\alpha}$. *Prostaglandins*, **15**, 383–397.

SCHMIDT, H.H.H.W., NAU, H., WITTFOTH, W., GERLACH, J., RESCHER, K.-E., KLEIN, M.M., NIROOMAND, F. & BOHME, E. (1988). Arginine is a physiological precursor of endothelium-derived nitric oxide. *Eur. J. Pharmacol.*, **154**, 213–216.

SCHRÖR, K., MONCADA, S., UBATUBA, F. & VANE, J.R. (1978). Transformation of arachidonic acid and prostaglandin endoperoxides by guinea-pig heart. Formation of RCS and prostacyclin. *Eur. J. Pharmacol.*, **47**, 103–114.

STEWART, A.G. & PIPER, P.J. (1988). Vasodilator actions of acetylcholine, A23187 and bradykinin in the guinea-pig isolated perfused heart are independent of prostacyclin. *Br. J. Pharmacol.*, **95**, 379–384.

STEWART, D.J., MUNZEL, T. & BASSENGE, E. (1987). Reversal of acetylcholine induced coronary resistance vessel dilatation by haemoglobin. *Eur. J. Pharmacol.*, **136**, 239–242.

VAVREK, R.J. & STEWART, J.M. (1985). Competitive antagonists of bradykinin. *Peptides*, **6**, 161–164.

WARNER, T.D., MITCHELL, J.A., DE NUCCI, G. & VANE, J.R. (1989). Endothelin-1 and endothelin-3 release EDRF from isolated perfused arterial vessels of the rat and rabbit. *J. Cardiovasc. Pharmacol.*, **13**, Suppl. 5, S85–S88.

YANAGISAWA, M., KURIHARA, H., KIMURA, S., TOMOBE, Y., KOBAYASHI, M., MITSUI, Y., YAZAKI, Y., GOTO, K. & MASAKI, T. (1988). A novel potent vasoconstrictor peptide produced by vascular endothelial cells. *Nature*, **332**, 411–415.

(Received March 11, 1991
Accepted March 20, 1991)

 © Macmillan Press Ltd, 1991

Erratum

Br. J. Pharmacol. (1991), **102**, 865–870.

'Effect of the leukotriene receptor antagonists FPL 55712, LY163443 and MK-571 on the elimination of cysteinyl leukotrienes in the rat'
C. Denzlinger, M. Grimberg, A. Kapp, C. Haberl and W. Wilmanns

In Table 1 of this paper, the values for bolus injections were misaligned from under their headings, and the units for bile flow given under (B) in the footnote were incorrect. The corrected table and its footnote are shown below.

Table 1 Effects of FPL 55712, LY 163443, and MK-571 on (A) the recovery of ^{3}H-leukotriene radioactivity in bile, (B) bile flow, (C) the biliary concentration of ^{3}H-leukotriene radioactivity, and (D) the contribution of [^{3}H]-LTD$_4$ to biliary ^{3}H-leukotriene radioactivity

		FPL 55712		*LY 163443*	*MK-571*
Bolus (μmol kg^{-1})		10	2.5	75	10
Infusion [μmol kg^{-1} h^{-1}]		20	5	25	15
(A) ^{3}H-leukotriene-recovery in bile					
(% of control,	[^{3}H]-LTC$_4$	23.1 ± 9.8^c	ND	ND	110.3 ± 0.2^c
mean ± s.d.)	[^{3}H]-LTD$_4$	35.3 ± 14.9^a	66.9 ± 1.7^c	95.1 ± 7.1	102.4 ± 3.0
	[^{3}H]-LTE$_4$	40.7 ± 16.8^a	ND	91.5 ± 18.4	ND
(B) Bile flow					
(% of control, mean ± s.d.)		75.8 ± 15.8^c	81.8 ± 10.5	97.1 ± 19.5	140.9 ± 9.9^c
(C) ^{3}H-leukotriene-concentration in bile					
(% of control,	[^{3}H]-LTC$_4$	35.1 ± 16.7^b	ND	ND	52.0 ± 6.7^b
mean ± s.d.)	[^{3}H]-LTD$_4$	57.2 ± 14.2^a	78.2 ± 10.6	84.2 ± 9.9	47.3 ± 13.9^a
	[^{3}H]-LTE$_4$	56.0 ± 10.9^a	ND	105.1 ± 35.3	ND
(D) Contribution of [^{3}H]-LTD$_4$ to biliary ^{3}H-leukotrienes					
(% of control, mean ± s.d.]		27.3 ± 14.6^a	ND	55.7 ± 12.2^a	51.7 ± 15.2^a

Experiments were performed as outlined in Figure 1. Leukotriene receptor antagonists were given as continuous infusion following bolus injection.
(A) The total amount of ^{3}H-leukotriene radioactivity recovered in bile within 90 min after the second injection of [^{3}H]-LTC$_4$, D$_4$ or E$_4$ during infusion with leukotriene antagonist was compared to the total amount of ^{3}H-leukotriene radioactivity recovered within 90 min after the first injection of tracer during infusion of the vehicle (control, 100%).
(B) Bile flow during infusion with leukotriene antagonist was compared to bile flow during the preceding control period with vehicle given alone (control, 100%). Under control conditions bile flow was 4.2 ± 0.4 ml kg^{-1} h^{-1} (mean ± s.d.).
(C) The biliary concentration of ^{3}H-leukotriene radioactivity after the second injection of ^{3}H-leukotriene during infusion with leukotriene antagonist was compared to the biliary concentration of ^{3}H-leukotriene radioactivity after the first injection of tracer during infusion of vehicle (control, 100%).
(D) The contribution of [^{3}H]-LTD$_4$ to the total of biliary ^{3}H-leukotriene metabolites obtained 0–10 min after the second injection of [^{3}H]-LTD$_4$ during infusion of leukotriene antagonist was compared to the proportions within the 0–10 min interval after the first injection of tracer during infusion of vehicle (control, 100%).
Mean values ± s.d. from at least 3 animals are indicated. ^{a,b,c} indicate a statistically significant difference from control by $P < 0.05$, $P < 0.01$, $P < 0.001$ respectively, as determined by the t test for paired events. ND: not determined.

British Journal of Pharmacology

VOLUME 103 (3) JULY 1991

SPECIAL REPORT

J.A. Peters, H.M. Malone & J.J. Lambert. Ketamine potentiates 5-HT_3 receptor-mediated currents in rabbit nodose ganglion neurones 1623

PAPERS

H. Sinzinger, I. Virgolini, G. Lupattelli, E. Molinari, A. Gerakakis & P. Angelberger. Prostaglandin E_1 decreases the low-density-lipoprotein entry into rabbit arterial wall 1626

M. Gu, D.A. Elliott, B.Y. Ong & D. Bose. Possible role of leukotrienes in hypoxic contraction of canine isolated basilar artery 1629

J.G. Filep, B. Battistini & P. Sirois. Pharmacological modulation of endothelin-induced contraction of guinea-pig isolated airways and thromboxane release 1633

K. Nakayama, Z. Fan, F. Marumo, T. Sawanobori & M. Hiraoka. Action of nicorandil on ATP-sensitive K^+ channel in guinea-pig ventricular myocytes 1641

S.J. Mason, A.M. Paradiso & R.C. Boucher. Regulation of transepithelial ion transport and intracellular calcium by extracellular ATP in human normal and cystic fibrosis airway epithelium 1649

G.N. Luheshi & M.A. Zar. The effect of streptozotocin-induced diabetes on cholinergic motor transmission in the rat urinary bladder 1657

P.S. Ward, R.W. Fuller, J.M. Ritter, S.J. Cashman, A.J. Rees & C.T. Dollery. Excretion of metabolites of prostacyclin and thromboxane by rats with nephrotoxic nephritis: effects of interleukin-1 1663

M.A. Whittington, S.J. Dolin, T.L. Patch, R.J. Siarey, A.R. Butterworth & H.J. Little. Chronic dihydropyridine treatment can reverse the behavioural consequences of, and prevent adaptations to, chronic ethanol treatment 1669

M.A. Whittington & H.J. Little. Nitrendipine, given during drinking, decreases the electrophysiological changes in the isolated hippocampal slice, seen during ethanol withdrawal 1677

J.M. Bulloch, A. MacDonald & J.C. McGrath. Different sensitivities of rabbit isolated blood vessels exhibiting co-transmission to the slow calcium channel blocker, nifedipine 1685

B.A. Finegan & A.S. Clanachan. Comparison of the haemodynamic effects of adenosine monophosphate with sodium nitroprusside in a canine model of acute global left ventricular dysfunction 1691

T. Itoh, S. Suzuki & H. Kuriyama. Effects of pinacidil on contractile proteins in high K^+-treated intact, and in β-escin-treated skinned smooth muscle of the rabbit mesenteric artery 1697

D. Prieto, M.J. Mulvany & N.C.B. Nyborg. (+)-S-12967 and (−)-S-12968: 1,4-dihydropyridine stereoisomers with calcium channel agonistic and antagonistic properties in rat resistance arteries 1703

D.J. Freeman, D.R. Grant & S.G. Carruthers. The cyclosporin-erythromycin interaction: impaired first pass metabolism in the pig 1709

H. Yamada, F. Yoneyama, K. Satoh & N. Taira. Comparison of the effects of the novel vasodilator FK409 with those of nitroglycerin in isolated coronary artery of the dog 1713

C.-M. Lee, L.-M. Jiang, H.-S. Shang, P.-M. Hon, Y. He & H.N.C. Wong. Prehispanolone, a novel platelet activating factor receptor antagonist from *Leonurus heterophyllus* 1719

S.M. Gardiner, P.A. Kemp & T. Bennett. Effects of N^G-nitro-L-arginine methyl ester on vasodilator responses to acetylcholine, 5'-N-ethylcarboxamidoadenosine or salbutamol in conscious rats 1725

A.L. Horne & J.A. Kemp. The effect of ω-conotoxin GVIA on synaptic transmission within the nucleus accumbens and hippocampus of the rat *in vitro* 1733

D.R. Corfield, S.E. Webber & J.G. Widdicombe. Mechanisms of platelet activating factor-induced changes in sheep tracheal blood flow 1740

J.M. Treherne, J.S. Stern, W.J. Flack & J.M. Young. Inhibition by cations of antagonist binding to histamine H_1-receptors: differential effect of sodium ions on the binding of two radioligands 1745

J.L. Field & N.R. Newberry. On the histamine-induced depolarization of the isolated superior cervical ganglion of the rat 1752

H. Kilbinger, R. Schneider, H. Siefken, D. Wolf & G. D'Agostino. Characterization of prejunctional muscarinic autoreceptors in the guinea-pig trachea 1757

D. Prieto, S. Benedito & N.C.B. Nyborg. Heterogeneous involvement of endothelium in calcitonin gene-related peptide-induced relaxation in coronary arteries from rat 1764

H. Crick & D.I. Wallis. Inhibition of reflex responses of neonate rat lumbar spinal cord by 5-hydroxytryptamine 1769

C.N. May, C.J. Whitehead & C.J. Mathias. The effects of naloxone on the cardiovascular and respiratory effects of centrally administered corticotrophin releasing factor in conscious rabbits 1776

D. Bleakman, W.F. Colmers, A. Fournier & R.J. Miller. Neuropeptide Y inhibits Ca^{2+} influx into cultured dorsal root ganglion neurones of the rat via a Y_2 receptor 1781

P. Paudice & M. Raiteri. Cholecystokinin release mediated by 5-HT_3 receptors in rat cerebral cortex and nucleus accumbens 1790

J.C.R. Randle, S.H.R. Oliet & J.-F. Renaud. Alkali cation permeability and caesium blockade of cromakalim-activated current in guinea-pig ventricular myocytes 1795

V. Mollace, E.A. De Francesco, G. Fersini & G. Nistico. Age-dependent changes in cardiovascular responses induced by muscimol infused into the nucleus tractus solitarii and nucleus parabrachialis medialis in rats 1802

S.J. Kehl. Quinidine-induced inhibition of the fast transient outward K^+ current in rat melanotrophs 1807

M.A. Murray, J.L. Berry, S.J. Cook, R.W. Foster, K.A. Green & R.C. Small. Guinea-pig isolated trachealis: the effects of charybdotoxin on mechanical activity, membrane potential changes and the activity of plasmalemmal K^+-channels 1814

P.J. Birch, H. Rogers, A.G. Hayes, N.J. Hayward, M.B. Tyers, D.I.C. Scopes, A. Naylor & D.B. Judd. Neuroprotective actions of GR89696, a highly potent and selective κ-opioid receptor agonist 1819

R.J. Lacey, N.S. Berrow, J.H.B. Scarpello & N.G. Morgan. Selective stimulation of glucagon secretion by β_2-adrenoceptors in isolated islets of Langerhans of the rat 1824

A.R. Baydoun & B. Woodward. Effects of bradykinin in the rat isolated perfused heart: role of kinin receptors and endothelium-derived relaxing factor 1829

ERRATUM 1834

Edited for the British Pharmacological Society by

A.T. Birmingham *(Chairman)*
R.W. Horton *(Secretary)*
W.A. Large *(Secretary)*

EDITORIAL BOARD

J.A. Angus Prahran, Australia
M.L.J. Ashford Cambridge
G.W. Bennett Nottingham
T. Bennett Nottingham
W.C. Bowman Glasgow
Alison F. Brading Oxford
S.D. Brain London
K.T. Bunce Ware
G. Burnstock London
K.D. Butler Horsham
M. Caulfield London
M.K. Church Southampton
S.J. Coker Liverpool
R.A. Coleman Ware
M.G. Collis Macclesfield
G.A. Cottrell St Andrews
A.J. Cross London
V. Crunelli London
T.C. Cunnane Oxford
A.C. Dolphin London
A. Dray London
J.M. Edwardson Cambridge
W. Feniuk Ware
J.R. Fozard Basle, Switzerland
L.G. Garland Beckenham
A. Gibson London
A.R. Green London
P.E. Hicks Leuville-sur-Orge, France
S.J. Hill Nottingham
J.C. Hunter Cambridge
K.A. Kane Glasgow
P. Keen Bristol
P. Leff Loughborough
D. Lodge London
J.C. McGrath Glasgow
R. McMillan Macclesfield
J. Maclagan London
W. Martin Glasgow
D.N. Middlemiss Harlow
R.C. Miller Strasbourg, France
R.J. Naylor Bradford
C.D. Nicholson Newhouse
D.A.A. Owen London
C.P. Page London
B.K. Park Liverpool
A.N. Payne Milan
F.L. Pearce London
F.F. Roberts Greenford
M.H.T. Roberts Cardiff
P.J. Roberts Southampton
C. Robinson Southampton
G.J. Sanger Harlow
M.A. Simmonds London
J.M. Sneddon Sunderland
M. Spedding Edinburgh
I.P. Stolerman London
P.V. Taberner Bristol
D.A. Terrar Oxford
M.B. Tyers Ware
S.P. Watson Oxford
A.H. Weston Manchester
B.J.R. Whittle Beckenham
T.J. Williams London
J.M. Young Cambridge

CORRESPONDING EDITORS

P.R. Adams Stony Brook, U.S.A.
C. Bell Melbourne, Australia
K.P. Bhargava Lucknow, India
F.E. Bloom La Jolla, U.S.A.
A.L.A. Boura Clayton, Australia
N.J. Dun Toledo, U.S.A.
R.F. Furchgott New York, U.S.A.
T. Godfraind Brussels, Belgium
S.Z. Langer Paris, France
R.J. Miller Chicago, U.S.A.
R.C. Murphy Denver, U.S.A.
E. Muscholl Mainz, F.R.G.
R.A. North Portland, U.S.A.
M. Otsuka Tokyo, Japan
M.J. Rand Melbourne, Australia
S. Rosell Södertalje, Sweden
P. Seeman Toronto, Canada
L. Szekeres Szeged, Hungary
B. Uvnas Stockholm, Sweden
P.A. Van Zwieten Amsterdam, Netherlands
V.M. Varagić Belgrade, Yugoslavia
G. Velo Verona, Italy
Wang Zhen Gang Beijing, China
M.B.H. Youdim Haifa, Israel

Papers will be considered for publication on all aspects of pharmacology, including chemotherapy.

Manuscripts (two copies) should be sent to Editorial Office, British Journal of Pharmacology, St. George's Hospital Medical School, Cranmer Terrace, London SW17 0RE. Authors should consult the Instructions to Authors in Vol. 102, 553–559 (1991) and the Nomenclature Guidelines for Authors in Vol. 102, 560–561 (1991). These Instructions and Guidelines also appear with the journal Index for volumes 99–101, 1990.

The *British Journal of Pharmacology* is published monthly by the Scientific & Medical Division, Macmillan Press Ltd.

The journal is covered by *Current Contents*, *Excerpta Medica* and *Index Medicus*.

All business correspondence and reprint requests should be addressed to the Scientific & Medical Division, Macmillan Press Ltd., Houndmills, Basingstoke, Hampshire RG21 2XS, UK. Telephone: (0256) 29242; Fax: (0256) 810526.

Annual subscription prices for 1991 EEC £375, elsewhere £415/US$750 (sterling rate is definitive). Orders must be accompanied by remittance. Cheques should be made payable to Macmillan Press, and sent to: Macmillan Press Ltd., Subscription Department, Brunel Road, Houndmills, Basingstoke, Hampshire RG21 2XS, UK.

Overseas subscribers may make payments into UK Post Office Giro Account No. 5192455. Full details must accompany the payment.

Second Class postage paid at Rahway NJ. US Mailing Agent: Mercury Airfreight International Ltd, Inc., 2323 Randolph Avenue, Avenel, New Jersey, NJ 07001, USA.

Enquiries concerning advertising space or rates should be addressed to: Michael Rowley, Advertisement Manager, Macmillan Press Ltd., 4 Little Essex Street, London WC2R 3LF. Telephone: 071 836 6633; Fax: 071 379 4204.

All rights of reproduction are reserved in respect of all papers, articles, illustrations, etc., published in this journal in all countries of the world.

Authorization to photocopy items for internal or personal use, or the internal or personal use of specific clients, is granted by Macmillan Press Ltd for libraries and other users registered with the Copyright Clearance Center (CCC) Transactional Reporting Service, provided that the base fee of $3.50 per copy is paid directly to CCC, 21 Congress St., Salem, MA 01970, USA.

© The British Pharmacological Society & Macmillan Press Ltd, 1991.
ISSN 0007–1188

0007–1188/91 $3.50 + $0.00

SPECIAL REPORTS

The purpose of *Special Reports*, which are superseding 'Short Communications', is to provide rapid publication for **new** and **important** results which the Editorial Board considers are likely to be of special pharmacological significance. (Please note that Short Communications are no longer acceptable for publication.) *Special Reports* will have publication priority over all other material and so authors are asked to consider carefully the status of their work before submission.

In order to speed publication there is normally no revision allowed beyond very minor typographical or grammatical corrections. If significant revision is required, the Board may either invite rapid re-submission or, more probably, propose that it be re-written as a Full Paper and be re-submitted for consideration. In order to reduce delays, proofs of *Special Reports* will be sent to authors but **essential corrections must reach the Production Office within 48 hours of receipt.** Authors should ensure that their submitted material conforms exactly to the following requirements.

Special Reports should normally occupy no more than two printed pages of the Journal; two illustrations (Figures or Tables, with legends) are permitted. As a guideline, with type face of 12 pitch and double-line spacing, a page of A4 paper could contain about 400 words. The absolute maximum length of the *Special Report* is 1700 words. For each Figure or Table, please deduct 200 words. The manuscript should comprise a Title page with key words (maximum of 10), a Summary consisting of a single short paragraph, followed by Introduction, Methods, Results, Discussion and References (maximum of 10). In all other respects, the requirements are the same as for Full Papers (see current 'Instructions to Authors').

PREPARATION OF MANUSCRIPTS

Authors are strongly recommended to read the full *Instructions to Authors* and *Nomenclature Guidelines for Authors* (*Br. J. Pharmacol.* 1991, **102,** 553–561) before submitting a manuscript for publication in the *British Journal of Pharmacology*. The manuscript and cover letter should be checked against the following list before mailing.

The original and one copy of the manuscript must be supplied. Manuscripts must be typed in double-line spacing on one side of A4 paper, in type not smaller than 12 characters per inch or 10 point. Both copies to include Tables and a set of labelled Figures. One set of Figures without numbers or letters is also to be included. The text to be arranged in the following subsections:

1. **Title**—To have no more than 150 characters on a separate page, which should also include a Short Title (50 characters maximum) and the name and address of the author for correspondence.
2. **Summary**—To be arranged in numbered paragraphs (Full Papers) or a single paragraph (Special Reports).
   —to include aims, principal results and conclusions.
   —to include Key words (10 maximum) at end of summary.
3. **Introduction**—To contain concise statements of the problem and the aims of the investigation.
4. **Methods**—To have brief but adequate account of the procedures; *full names of drugs (including those referred to by manufacturer's code)*, sources of drugs and statistical tests to be stated.
5. **Results**—To have no repetition of data in Figures, Tables and text.
6. **Discussion**—Findings and conclusions to be placed in context of other relevant work.
   NB Simple repetition of results and unwarranted speculation are not acceptable.
7. **Acknowledgments**—Sources of support. Sources of drugs not widely available commercially.
8. **References**—All references in the text to be included in the Reference List and *vice versa*. References in alphabetical order with complete citations; Journals publishing 'in press' papers identified.
   References to manuscripts submitted to other journals but not yet accepted are not allowed.
9. **Tables**—Each on a separate page and prepared in accordance with current requirements of the Journal.
10. **Figures**—Both labelled and non-labelled Figures to be prepared in accordance with current requirements of the Journal (see *Instructions to Authors*, 1991, vol. **102,** 553–559) and provided with Figure Number and Authors' names on back (*in pencil*)
    —each legend to be typed on a separate page and carrying keys to symbols
11. **Manuscripts**—To be accompanied by a declaration signed by each author that
    (a) results are original
    (b) approval of all persons concerned has been given to submit manuscripts for consideration (see also 12b)
    (c) the same material is neither 'in press' (i.e. is in proof or has definitely been accepted for publication) nor under consideration elsewhere. Furthermore it will not be submitted or published elsewhere before a decision has been reached by the Editorial Board of the *British Journal of Pharmacology* and will not be submitted elsewhere if accepted by the *British Journal of Pharmacology*.
    (d) Copyright assignment is included
12. **Cover letter**—To state clearly
    (a) Corresponding author's full postal address, telephone, telex or Fax number
    (b) where appropriate, that *either* ethical approval has been given for investigation *or* Company or Institutional permission to publish work has been received.
13. **Reminder**—Packaging to be sufficiently robust to protect Figures and to withstand mailing.

Failure to comply with *Instructions to Authors* may lead to substantial delays in processing, review and publication and may even jeopardize acceptance of the manuscript.

BRITISH JOURNAL OF PHARMACOLOGY VOLUME 103 (3) 1991

SPECIAL REPORT

J.A. Peters, H.M. Malone & J.J. Lambert. Ketamine potentiates 5-HT_3 receptor-mediated currents in rabbit nodose ganglion neurones 1623

PAPERS

H. Sinzinger, I. Virgolini, G. Lupattelli, E. Molinari, A. Gerakakis & P. Angelberger. Prostaglandin E_1 decreases the low-density-lipoprotein entry into rabbit arterial wall 1626

M. Gu, D.A. Elliott, B.Y. Ong & D. Bose. Possible role of leukotrienes in hypoxic contraction of canine isolated basilar artery 1629

J.G. Filep, B. Battistini & P. Sirois. Pharmacological modulation of endothelin-induced contraction of guinea-pig isolated airways and thromboxane release 1633

K. Nakayama, Z. Fan, F. Marumo, T. Sawanobori & M. Hiraoka. Action of nicorandil on ATP-sensitive K^+ channel in guinea-pig ventricular myocytes 1641

S.J. Mason, A.M. Paradiso & R.C. Boucher. Regulation of transepithelial ion transport and intracellular calcium by extracellular ATP in human normal and cystic fibrosis airway epithelium 1649

G.N. Luheshi & M.A. Zar. The effect of streptozotocin-induced diabetes on cholinergic motor transmission in the rat urinary bladder 1657

P.S. Ward, R.W. Fuller, J.M. Ritter, S.J. Cashman, A.J. Rees & C.T. Dollery. Excretion of metabolites of prostacyclin and thromboxane by rats with nephrotoxic nephritis: effects of interleukin-1 1663

M.A. Whittington, S.J. Dolin, T.L. Patch, R.J. Siarey, A.R. Butterworth & H.J. Little. Chronic dihydropyridine treatment can reverse the behavioural consequences of, and prevent adaptations to, chronic ethanol treatment 1669

M.A. Whittington & H.J. Little. Nitrendipine, given during drinking, decreases the electrophysiological changes in the isolated hippocampal slice, seen during ethanol withdrawal 1677

J.M. Bulloch, A. MacDonald & J.C. McGrath. Different sensitivities of rabbit isolated blood vessels exhibiting co-transmission to the slow calcium channel blocker, nifedipine 1685

B.A. Finegan & A.S. Clanachan. Comparison of the haemodynamic effects of adenosine monophosphate with sodium nitroprusside in a canine model of acute global left ventricular dysfunction 1691

T. Itoh, S. Suzuki & H. Kuriyama. Effects of pinacidil on contractile proteins in high K^+-treated intact, and in β-escin-treated skinned smooth muscle of the rabbit mesenteric artery 1697

D. Prieto, M.J. Mulvany & N.C.B. Nyborg. (+)-S-12967 and (−)-S-12968: 1,4-dihydropyridine stereoisomers with calcium channel agonistic and antagonistic properties in rat resistance arteries 1703

D.J. Freeman, D.R. Grant & S.G. Carruthers. The cyclosporin-erythromycin interaction: impaired first pass metabolism in the pig 1709

H. Yamada, F. Yoneyama, K. Satoh & N. Taira. Comparison of the effects of the novel vasodilator FK409 with those of nitroglycerin in isolated coronary artery of the dog 1713

C.-M. Lee, L.-M. Jiang, H.-S. Shang, P.-M. Hon, Y. He & H.N.C. Wong. Prehispanolone, a novel platelet activating factor receptor antagonist from *Leonurus heterophyllus* 1719

S.M. Gardiner, P.A. Kemp & T. Bennett. Effects of N^G-nitro-L-arginine methyl ester on vasodilator responses to acetylcholine, 5'-N-ethylcarboxamidoadenosine or salbutamol in conscious rats 1725

A.L. Horne & J.A. Kemp. The effect of ω-conotoxin GVIA on synaptic transmission within the nucleus accumbens and hippocampus of the rat *in vitro* 1733

D.R. Corfield, S.E. Webber & J.G. Widdicombe. Mechanisms of platelet activating factor-induced changes in sheep tracheal blood flow 1740

J.M. Treherne, J.S. Stern, W.J. Flack & J.M. Young. Inhibition by cations of antagonist binding to histamine H_1-receptors: differential effect of sodium ions on the binding of two radioligands 1745

J.L. Field & N.R. Newberry. On the histamine-induced depolarization of the isolated superior cervical ganglion of the rat 1752

H. Kilbinger, R. Schneider, H. Siefken, D. Wolf & G. D'Agostino. Characterization of prejunctional muscarinic autoreceptors in the guinea-pig trachea 1757

D. Prieto, S. Benedito & N.C.B. Nyborg. Heterogeneous involvement of endothelium in calcitonin gene-related peptide-induced relaxation in coronary arteries from rat 1764

H. Crick & D.I. Wallis. Inhibition of reflex responses of neonate rat lumbar spinal cord by 5-hydroxytryptamine 1769

C.N. May, C.J. Whitehead & C.J. Mathias. The effects of naloxone on the cardiovascular and respiratory effects of centrally administered corticotrophin releasing factor in conscious rabbits 1776

D. Bleakman, W.F. Colmers, A. Fournier & R.J. Miller. Neuropeptide Y inhibits Ca^{2+} influx into cultured dorsal root ganglion neurones of the rat via a Y_2 receptor 1781

P. Paudice & M. Raiteri. Cholecystokinin release mediated by 5-HT_3 receptors in rat cerebral cortex and nucleus accumbens 1790

J.C.R. Randle, S.H.R. Oliet & J.-F. Renaud. Alkali cation permeability and caesium blockade of cromakalim-activated current in guinea-pig ventricular myocytes 1795

V. Mollace, E.A. De Francesco, G. Fersini & G. Nistico. Age-dependent changes in cardiovascular responses induced by muscimol infused into the nucleus tractus solitarii and nucleus parabrachialis medialis in rats 1802

S.J. Kehl. Quinidine-induced inhibition of the fast transient outward K^+ current in rat melanotrophs 1807

M.A. Murray, J.L. Berry, S.J. Cook, R.W. Foster, K.A. Green & R.C. Small. Guinea-pig isolated trachealis: the effects of charybdotoxin on mechanical activity, membrane potential changes and the activity of plasmalemmal K^+-channels 1814

P.J. Birch, H. Rogers, A.G. Hayes, N.J. Hayward, M.B. Tyers, D.I.C. Scopes, A. Naylor & D.B. Judd. Neuroprotective actions of GR89696, a highly potent and selective κ-opioid receptor agonist 1819

R.J. Lacey, N.S. Berrow, J.H.B. Scarpello & N.G. Morgan. Selective stimulation of glucagon secretion by β_2-adrenoceptors in isolated islets of Langerhans of the rat 1824

A.R. Baydoun & B. Woodward. Effects of bradykinin in the rat isolated perfused heart: role of kinin receptors and endothelium-derived relaxing factor 1829

ERRATUM 1834

Filmsetting by Santype International Limited, Salisbury, Wiltshire
and printed in Great Britain by Unwin Brothers Ltd., The Gresham Press, Old Woking, Surrey